

Advances

in Clinical and Experimental Medicine

MONTHLY ISSN 1899-5276 (PRINT) ISSN 2451-2680 (ONLINE)

advances.umw.edu.pl

2025, Vol. 34, No. 4 (April)

Impact Factor (IF) – 2.1
Ministry of Science and Higher Education – 70 pts
Index Copernicus (ICV) – 171.00 pts



WROCLAW
MEDICAL UNIVERSITY

Advances
in Clinical and Experimental
Medicine



Advances in Clinical and Experimental Medicine

ISSN 1899-5276 (PRINT)

ISSN 2451-2680 (ONLINE)

advances.umw.edu.pl

MONTHLY 2025

Vol. 34, No. 4

(April)

Advances in Clinical and Experimental Medicine (*Adv Clin Exp Med*) publishes high-quality original articles, research-in-progress, research letters and systematic reviews and meta-analyses of recognized scientists that deal with all clinical and experimental medicine.

Editorial Office

ul. Marcinkowskiego 2–6
50-368 Wrocław, Poland
Tel.: +48 71 784 12 05
E-mail: redakcja@umw.edu.pl

Editor-in-Chief

Prof. Donata Kurpas

Deputy Editor

Prof. Robert Śmigiel

Managing Editor

Marek Misiak, MA

Statistical Editors

Wojciech Bombała, MSc

Anna Kopszak, MSc

Dr. Krzysztof Kujawa

Jakub Wronowicz, MSc

Maciej Wuczyński, MSc

Manuscript editing

Marek Misiak, MA

Paulina Piątkowska, MA

Publisher

Wrocław Medical University
Wybrzeże L. Pasteura 1
50-367 Wrocław, Poland

Online edition is the original version
of the journal

Scientific Committee

Prof. Sandra Maria Barbalho

Prof. Antonio Cano

Prof. Chong Chen

Prof. Breno Diniz

Prof. Erwan Donal

Prof. Chris Fox

Prof. Yuko Hakamata

Prof. Carol Holland

Prof. Sabine Bährer-Köhler

Prof. Markku Kurkinen

Prof. Christopher S. Lee

Prof. Christos Lionis

Prof. Raimundo Mateos

Prof. Zbigniew W. Raś

Prof. Jerzy W. Rozenblit

Prof. Silvina Santana

Prof. Sajee Sattayut

Prof. James Sharman

Prof. Jamil Shibli

Prof. Michał J. Toborek

Prof. László Vécsei

Prof. Cristiana Vitale

Prof. Hao Zhang

Section Editors

Basic Sciences

Prof. Iwona Bil-Lula
Prof. Dorota Danuta Diakowska
Prof. Paweł Andrzej Karpiński
Prof. Bartosz Kempisty
Dr. Wiesława Kranc
Dr. Anna Lebedeva
Dr. Piotr Chmielewski
Dr. Sławomir Woźniak

Clinical Anatomy, Legal Medicine, Innovative Technologies

Prof. Rafael Boscolo-Berto

Dentistry

Prof. Marzena Dominiak
Prof. Tomasz Gedrange
Prof. Jamil Shibli

Laser Dentistry

Prof. Kinga Grzech-Leśniak

Dermatology

Prof. Jacek Szepietowski
Assoc. Prof. Marek Konop

Emergency Medicine, Innovative Technologies

Prof. Jacek Smereka

Evidence-Based Healthcare

Assoc. Prof. Aleksandra Królikowska
Dr. Robert Prill

Gynecology and Obstetrics

Assoc. Prof. Tomasz Fuchs
Dr. Christopher Kobierzycki
Dr. Jakub Staniczek

Histology and Embryology

Dr. Mateusz Olbromski

Internal Medicine

Angiology

Dr. Angelika Chachaj

Cardiology

Dr. Daniel Morris
Assoc. Prof. Joanna Popiołek-Kalisz
Prof. Pierre François Sabouret

Endocrinology

Prof. Marek Bolanowski

Gastroenterology

Assoc. Prof. Katarzyna Neubauer

Hematology

Prof. Andrzej Deptała
Prof. Dariusz Wołowicz

Nephrology and Transplantology

Prof. Mirosław Banasik
Prof. Krzysztof Letachowicz

Rheumatology

Assoc. Prof. Agata Sebastian
Dr. Sylwia Szafraniec-Buryło

Lifestyle Medicine, Nutrition and Health Promotion

Assoc. Prof. Michał Czapla
Prof. Raúl Juárez-Vela
Dr. Anthony Dissen

Microbiology

Assoc. Prof. Adam Junka

Molecular Biology

Dr. Monika Bielecka

Neurology

Assoc. Prof. Magdalena Koszewicz
Assoc. Prof. Anna Pokryszko-Dragan
Dr. Masaru Tanaka

Neuroscience

Dr. Simone Battaglia
Dr. Francesco Di Gregorio

Omics

Prof. Mariusz Fleszar
Prof. Paweł Andrzej Karpiński

Oncology

Prof. Andrzej Deptała
Prof. Adam Maciejczyk
Prof. Hao Zhang

Gynecological Oncology

Dr. Marcin Jędryka

Ophthalmology

Dr. Małgorzata Gajdzis

Orthopedics

Prof. Paweł Reichert

Otolaryngology

Prof. Tomasz Zatoński

Pediatrics

Pediatrics, Metabolic Pediatrics, Clinical Genetics, Neonatology, Rare Disorders

Prof. Robert Śmigiel

Pediatric Nephrology

Prof. Katarzyna Kiliś-Pstrusińska

Pediatric Oncology and Hematology

Assoc. Prof. Marek Ussowicz

Pharmaceutical Sciences

Assoc. Prof. Marta Kepinska
Prof. Adam Matkowski

Pharmacoeconomics

Dr. Sylwia Szafraniec-Buryło

Psychiatry

Dr. Melike Küçükkarapınar
Prof. Jerzy Leszek
Assoc. Prof. Bartłomiej Stańczykiewicz

Public Health

Prof. Monika Sawhney
Prof. Izabella Uchmanowicz

Pulmonology

Prof. Anna Brzecka

Qualitative Studies, Quality of Care

Prof. Ludmiła Marcinowicz

Radiology

Prof. Paweł Gać

Rehabilitation

Assoc. Prof. Aleksandra Królikowska
Dr. Robert Prill

Surgery

Assoc. Prof. Mariusz Chabowski

Telemedicine, Geriatrics, Multimorbidity

Assoc. Prof. Maria Magdalena
Bujnowska-Fedak
Prof. Ferdinando Petrazzuoli

Editorial Policy

Advances in Clinical and Experimental Medicine (Adv Clin Exp Med) is an independent multidisciplinary forum for exchange of scientific and clinical information, publishing original research and news encompassing all aspects of medicine, including molecular biology, biochemistry, genetics, biotechnology and other areas. During the review process, the Editorial Board conforms to the "Uniform Requirements for Manuscripts Submitted to Biomedical Journals: Writing and Editing for Biomedical Publication" approved by the International Committee of Medical Journal Editors (www.ICMJE.org). The journal publishes (in English only) original papers and reviews. Short works considered original, novel and significant are given priority. Experimental studies must include a statement that the experimental protocol and informed consent procedure were in compliance with the Helsinki Convention and were approved by an ethics committee.

For all subscription-related queries please contact our Editorial Office: redakcja@umw.edu.pl

For more information visit the journal's website: advances.umw.edu.pl

Pursuant to the ordinance of the Rector of Wrocław Medical University No. 37/XVI R/2024, from March 1, 2024, authors are required to pay a fee for each manuscript accepted for publication in the journal Advances in Clinical and Experimental Medicine. The fee amounts to 1600 EUR for all types of papers.

Indexed in: MEDLINE, Science Citation Index Expanded, Journal Citation Reports/Science Edition, Scopus, EMBASE/Excerpta Medica, Ulrich's™ International Periodicals Directory, Index Copernicus

Typographic design: Piotr Gil, Monika Kolęda

DTP: Wydawnictwo UMW

Cover: Monika Kolęda

Printing and binding: Drukarnia I-BiS Bierońscy Sp.k.

Contents

Editorials

- 473 Anthony Dissen, Izabella Uchmanowicz, Michał Czapla

Obesity: A call to action

Meta-analysis

- 479 Shuyin Liang, Huiling Xie, Lili Ye, Caifang Huang, Fengying Yuan, Yanping Tang

Supported transitional care applied to stroke survivors: A meta-analysis

Original papers

- 487 Ferdinando Petrazzuoli, Ozden Gokdemir, Maria Antonopoulou, Beata Blahová, Natasa Mrduljaš-Đujić, Gindrovel G. Dumitra, Rosario Falanga, Mercedes Ferreira, Sandra Gintere, Sehnaz Hatipoglu, Jean-Pierre Jacquet, Kateřina Javorská, Ana Kareli, András Mohos, Sody Naimer, Victoria Tkachenko, Angela Tomacinschii, Jane Randall-Smith, Krzysztof Kujawa, Donata Kurpas
Resilience of primary healthcare facilities: Experiences from 16 European countries during the COVID-19 pandemic. A mixed-methods study conducted by EURIPA
- 507 Wadi B. Alonazi, Sahar Alkhawtani
An equity-based financial framework for a sustainable healthcare system in Arab countries
- 529 Weeratian Tawanwongsri, Doungkamol Siri-Archawawat, Sasipaka Sindhusen, Chime Eden
Therapeutic efficiency and safety assessment of intradermal platelet-rich plasma combined with oral tranexamic acid in patients with facial melasma
- 539 Şule Göktürk, Yasin Göktürk, Ali Koç, Ahmet Payas
Comparison of median nerve area measurement between MRI and electromyography in patients diagnosed with carpal tunnel syndrome
- 549 Sijie Yang, Kaixiang Pan, Qikai Hua, Hongjie Su, Jun Hou, Kaibing Liu, Jinmin Zhao
Correlation analysis of patients with diabetic foot ulcers treated with tibial cortex transverse transport surgery and platelet-to-lymphocyte ratio and monocyte-to-neutrophil ratio
- 561 Li Ai, Ran Li, Xixian Teng, Jing Li, Bing Hai
Association of oxygen saturation and mortality in patients with acute respiratory failure
- 573 Weidong Yuan, Hewei Zhao, Shaochuang Wang
Association between preoperative advanced lung cancer inflammation index and recurrence of hepatocellular carcinoma after curative resection
- 585 Shaohua Xu, Guoxu Fang
Identification of a pyroptosis-related long noncoding RNA signature for determining the prognosis and immune status of hepatocellular carcinoma patients
- 597 Mateusz Ulman, Krzysztof Boczar, Katarzyna Holcman, Magdalena Ziąbka, Maciej Dębski, Jacek Lelakowski, Andrzej Ząbek
Endocardial lead insulation wear in a scanning and optical microscope
- 605 Bartosz Karolak, Marta Skowrońska, Michał Machowski, Olga Dzikowska-Diduch, Piotr Bienias, Martyna Kuryła, Małgorzata Wiśniewska, Marek Gołębiowski, Piotr Pruszczyk, Michał Ciurzyński
Plasma N-terminal pro-brain natriuretic peptide concentrations may help to identify patients with very low-risk acute pulmonary embolism: A preliminary study

- 613 Michał Kułakowski, Karol Elster, Wojciech Piotrowski, Paweł Ślęczka, Aleksandra Królikowska, Jarosław Witkowski, Łukasz Oleksy, Dariusz Janczak, Paweł Reichert
Determination of the best point of entry of percutaneous insertion of sacroiliac screws depending on patient positioning for surgery: A cadaveric study
- 623 Chaogang Huang, Ziqi Duan, Baojie Chen, Hailiang Xia, Guangxin Wang
LncRNA *LINC00969* modified by *METTL3* attenuates papillary thyroid cancer progression in an m⁶A-dependent manner

Reviews

- 633 Jin Wang, Yunqing Chen, Chengqin Wang, Keyu Ren
Research status and controversy on non-small cell lung cancer stem cells
- 641 Xuejing Qiao, Haosheng Zhang, Lianmei Shan
Probiotic interventions and quality of life in patients with gastrointestinal diseases: A comprehensive review

Obesity: A call to action

Anthony Disen^{1,A,D–F}, Izabella Uchmanowicz^{2,3,A,D–F}, Michał Czapla^{4,5,A,D–F}

¹ School of Health Sciences, Stockton University, Galloway, USA

² Division of Research Methodology, Department of Nursing, Faculty of Nursing and Midwifery, Wrocław Medical University, Poland

³ Centre for Cardiovascular Health, Edinburgh Napier University, Sighthill Campus, UK

⁴ Division of Scientific Research and Innovation in Emergency Medical Service, Department of Emergency Medical Service, Faculty of Nursing and Midwifery, Wrocław Medical University, Poland

⁵ Group of Research in Care (GRUPAC), Faculty of Health Sciences, University of La Rioja, Logroño, Spain

A – research concept and design; B – collection and/or assembly of data; C – data analysis and interpretation;

D – writing the article; E – critical revision of the article; F – final approval of the article

Advances in Clinical and Experimental Medicine, ISSN 1899–5276 (print), ISSN 2451–2680 (online)

Adv Clin Exp Med. 2025;34(4):473–477

Address for correspondence

Michał Czapla

Email: michal.czapla@umw.edu.pl

Funding sources

None declared

Conflict of interest

None declared

Received on January 30, 2025

Reviewed on March 23, 2025

Accepted on March 23, 2025

Published online on April 8, 2025

Abstract

Obesity has emerged as one of the most pressing public health challenges of the 21st century, impacting millions worldwide and contributing to serious health complications such as type 2 diabetes and cardiovascular diseases, as well as a diminished quality of life. This editorial explores the multifaceted nature of obesity, emphasizing the interplay between genetic predisposition, environmental constraints and behavioral drivers. Key contributors, such as the rising consumption of ultra-processed foods, increasingly sedentary lifestyles and psychosocial stressors, are explored in detail, along with their combined impact on the escalating global obesity rates. The editorial highlights the far-reaching consequences of obesity, including its economic burden, societal implications and the ripple effects on healthcare systems. Priority areas for action are proposed, including public health policies, education and the creation of environments that support active lifestyles. The importance of clinical interventions, such as early screening, personalized treatment strategies and the inclusion of dietitians within multidisciplinary care teams, is emphasized as vital for enhancing patient outcomes and managing obesity effectively. This editorial calls for a comprehensive, systemic response to address the global obesity epidemic, advocating for evidence-based interventions that are tailored to individual needs while addressing societal and environmental determinants. By fostering collaboration across sectors and prioritizing prevention and treatment, meaningful progress can be made in combating this escalating crisis.

Key words: lifestyle, BMI, overweight, obesity, health promotion

Cite as

Disen A, Uchmanowicz I, Czapla M. Obesity:

A call to action. *Adv Clin Exp Med.* 2025;34(4):473–477.

doi:10.17219/acem/203269

DOI

10.17219/acem/203269

Copyright

Copyright by Author(s)

This is an article distributed under the terms of the

Creative Commons Attribution 3.0 Unported (CC BY 3.0)

(<https://creativecommons.org/licenses/by/3.0/>)

Highlights

- Global obesity prevalence has more than doubled in adults and quadrupled in youth since 1990.
- High intake of ultra-processed foods and physical inactivity are key drivers of the obesity epidemic.
- Obesity significantly increases the risk of cardiometabolic disorders, malignancies and premature mortality.
- Comprehensive, individualized interventions including dietary, behavioral and pharmacological strategies are essential in obesity treatment.
- Policy-level actions and built environment modifications are critical for effective, long-term obesity prevention.

Introduction

Obesity has become one of the most pressing public health challenges of the 21st century. According to the World Health Organization (WHO), over 650 million adults were obese worldwide in 2016, accounting for nearly 13% of the global adult population.¹ More recent estimates suggest that this figure will continue to climb in the following years. The rapid rise in obesity prevalence affects not only high-income countries but also low- and middle-income nations, highlighting a global crisis that demands urgent, coordinated action.²

Key statistics and global context

Obesity has reached unprecedented levels globally, emerging as one of the most critical public health challenges of our time. According to a pooled analysis of global trends from 1990 to 2022, the number of individuals affected by obesity worldwide reached 1 billion in 2022. Compared to 1990, the prevalence of obesity has doubled among adults and quadrupled among children and adolescents (aged 5–19 years). In the same year, 43% of adults were classified as overweight. The burden of obesity has now surpassed underweight in the majority of countries, with significant increases observed across all age groups.³ This dramatic escalation underscores the global “nutrition transition,” driven by population over nourishment due to shifts toward diets that are energy-dense and nutrient-poor, as well as factors such as urbanization and a more sedentary lifestyles.^{2,3}

The health impacts of these shifts are equally concerning. It is estimated that possessing a higher body mass index (BMI) contributed to 4 million deaths globally in 2015, nearly 40% of which occurred among individuals who were not classified as obese but were still overweight. Cardiovascular disease accounted for the majority of these deaths, highlighting the wide-reaching consequences of elevated BMI.² These findings are further supported by analyses of the obesity transition, which demonstrate how the prevalence of obesity initially rises among wealthier groups before becoming more widespread among lower socioeconomic populations as the epidemic matures.⁴

Europe exemplifies this pattern, with Poland offering a case study in the shifting burden of obesity. According

to WHO data and national surveys, over 62% of Polish men and 43% of women are classified as overweight or obese, reflecting broader trends observed across Europe.⁵ Among children aged 7–9 years in Poland, 29% are classified as overweight and 12% as obese, with boys consistently more affected than girls. The COVID-19 pandemic exacerbated these trends, contributing to reduced physical activity, prolonged screen time and unhealthy dietary patterns across all age groups.⁶

Main causes and contributing factors

Several factors have been identified as contributing to the rising prevalence of obesity.

Dietary shifts

The increased consumption of ultra-processed, energy-dense foods is a primary driver of excessive caloric intake.^{7,8} Diets high in sugar-sweetened beverages, refined carbohydrates and saturated fats promote weight gain while offering limited nutritional value.⁹ Notably, data suggest that even relatively small but consistent surpluses in daily caloric intake can lead to significant weight gain over time. For example, the average increase in daily caloric intake between 1971 and 2000 was 168 kcal for men and 335 kcal for women, which theoretically could result in annual weight gains of 8 kg and 16 kg, respectively, without adaptive changes in energy expenditure.¹⁰ These findings underscore the role of both dietary excess and declining physical activity in creating an environment that favors energy imbalance and, consequently, rising obesity rates.

Sedentary lifestyles

Modern life has become increasingly sedentary, marked by prolonged hours in desk-based occupations, reliance on personal vehicles, and reduced physical activity at home. Urban infrastructure in many regions often fails to provide accessible and safe environments for walking, cycling or recreational sports, contributing to a decline in daily energy expenditure and exacerbating the obesity epidemic.^{11,12} Sedentary behavior, defined as activities

with energy expenditure below 1.5 metabolic equivalents, such as sitting or lying down, is associated with significant health risks, including increased rates of abdominal obesity and chronic disease.¹³ Research highlights a combined sedentary behavior prevalence of up to 31% among individuals with obesity, with correlations to reduced physical activity and heightened risk of multi-morbidities.^{12,13} Addressing these challenges through urban planning, workplace interventions and public health initiatives is critical to counteract the detrimental effects of sedentary lifestyles.

Genetic and epigenetic influences

While lifestyle remains the predominant factor, genetics can predispose certain individuals to obesity.¹⁴ Studies estimate that genetic factors may account for approx. 40–70% of obesity cases in the general population.¹⁵ Genome-wide association studies (GWAS) have identified numerous genetic loci associated with obesity, the majority of which are involved in neural pathways that regulate appetite control and energy homeostasis.¹⁵ Research on epigenetics, including the role of gut microbiota, is uncovering additional mechanisms that may influence weight regulation.¹⁶ In addition to genetic factors, epigenetic modifications such as DNA methylation and histone modifications play a crucial role in regulating gene expression related to metabolism.¹⁷ Maternal obesity during pregnancy has been linked to persistent epigenetic changes in offspring, which may contribute to an increased risk of obesity and metabolic disorders in later life. Evidence suggests that epigenetic alterations occurring during the pre- and perinatal period may influence metabolic programming, increasing susceptibility to obesity in adulthood.¹⁸ Experimental studies suggest that prenatal exposure to high-fat diets may lead to altered DNA methylation patterns, predisposing offspring to excessive weight gain and insulin resistance.¹⁷ One such mechanism that has been explored is the ways in which epigenetic modifications influence how DNA is transcribed in spite of no alterations to its sequencing (TBD).¹⁹ However, genetic predisposition alone does not fully account for the rapid rise in obesity rates – environmental and behavioral factors remain critical.

Psychosocial elements

Stress, psychological distress and emotional eating significantly contribute to obesity. Research shows that chronic stress, often exacerbated by stigma or adverse environments, can trigger increased cortisol production, which drives appetite and leads to fat accumulation, particularly in the abdominal region. In high-stress settings with limited mental health support, individuals may rely on maladaptive coping mechanisms such as binge-eating or turning to energy-dense “comfort foods”.²⁰ These behaviors are closely linked to increased obesity risk and its associated complications.

Health and social consequences

Owing to its complex etiology, obesity has far-reaching consequences.

Physical comorbidities

Obesity is closely associated with an increased risk of numerous medical conditions, including, among others, type 2 diabetes, hypertension, dyslipidemia, and various cardiovascular pathologies.^{21–23} Excess body weight also increases the risk of certain cancers, including breast, colon and endometrial cancers.²⁴ The resultant healthcare expenditures can be staggering, putting significant strain on both public and private health systems.

Psychological well-being

The psychological burden of obesity includes depression, anxiety and lower self-esteem, often exacerbated by social stigma and discrimination.²⁵ This may create a vicious cycle where psychological distress complicates efforts to adopt healthier lifestyles.

Community and societal impact

Communities with high obesity rates often see reduced productivity and increased reliance on healthcare and social services.²⁶ The ripple effects include diminished workforce capacity and higher insurance premiums, affecting entire economies.

Priority areas for action: A call to action

Public health policies

Comprehensive policy measures, such as taxes on sugar-sweetened beverages, clear front-of-package labeling and stricter regulations on junk food advertising, particularly to children, can help shape healthier consumer choices.²⁷ Governments can also invest in ensuring that schools and community centers provide balanced meals and opportunities for regular physical activity. Recognizing the urgent need for global action, the WHO has developed key strategies to combat obesity, including the Acceleration Plan to Stop Obesity and the Commission on Ending Childhood Obesity (ECHO). These initiatives advocate for comprehensive policies that include fiscal measures, marketing restrictions, school-based nutrition programs, and improvements in urban infrastructure to promote physical activity.^{28,29} A comprehensive approach to obesity prevention requires coordinated efforts, including fiscal policies such as sugar taxes, stricter regulations on food

marketing, improved food labeling, and public education campaigns promoting healthy lifestyles. Long-term success depends on sustained government commitment and cross-sector collaboration. By integrating these evidence-based strategies into national health policies, governments can strengthen their response to the growing obesity epidemic.

Education and awareness

Initiatives that promote nutrition literacy, home economics, and cooking skills are essential for empowering individuals to make informed, healthier dietary choices and fostering long-term behavioral change.³⁰ Schools should integrate physical education programs that are both engaging and adaptable to different fitness levels.

Environment and infrastructure

Creating safe, walkable neighborhoods and expanding public green spaces encourage daily physical activity. Bicycle lanes, pedestrian-only zones and accessible recreational facilities have the potential to transform sedentary communities into active, health-conscious environments.³¹

Clinical interventions

Healthcare providers should be trained to screen for obesity early using comprehensive and person-centered assessments that go beyond BMI. While BMI remains a useful tool for general categorization, it should be complemented by measurements such as waist circumference, waist-to-hip ratio or waist-to-height ratio to better evaluate fat distribution and associated health risks.^{32,33} These combined metrics allow clinicians to assess obesity-related comorbidities, such as metabolic syndrome or cardiovascular risks, with greater accuracy.

The goal of early screening and assessment is to guide appropriate interventions tailored to individual needs. These interventions include nutritional counseling focused on achieving a sustainable caloric deficit, behavioral therapy to address psychological barriers and, when necessary, pharmacological treatments such as the glucagon-like peptide-1 (GLP-1) receptor agonists or other anti-obesity medications. For individuals with severe obesity or obesity-related complications, metabolic and bariatric surgery should be considered as a viable and effective option.^{32,33} Alongside lifestyle modifications, obesity management strategies should integrate medical and psychological support, ensuring access to multidisciplinary care. Expanding healthcare services to include individualized treatment plans can significantly improve long-term outcomes.

Moreover, effective management of obesity requires a multidisciplinary approach. Teams comprising physicians, dietitians, psychologists, and exercise specialists play a pivotal role in delivering personalized care. This includes developing individualized treatment plans that

integrate dietary modifications, increased physical activity and behavioral strategies, alongside medical or surgical interventions when indicated. The overarching aim is not only to reduce body weight but also to improve overall health, mitigate obesity-related complications and enhance quality of life.^{33–35} Initiatives should also focus on better education medical and healthcare professionals on how they can be sources of education on healthy eating to their patients. Many medical and healthcare professional education programs have incorporated “culinary medicine” into their curriculums to accomplish this goal.³⁶

Conclusions and appeal


Addressing the global obesity epidemic demands a multifaceted approach that acknowledges all factors promoting or contributing to obesity. It is not enough to focus solely on the individual; society at large must rally around policies and programs that make healthy eating and active living the default choices. Researchers, clinicians, educators, and policymakers each play a vital role in this endeavor.


A key component of this effort is the enhancement of multidisciplinary care systems. Healthcare teams must be empowered to integrate diverse expertise, with particular emphasis on the crucial role of dietitians in assessing nutritional needs, creating individualized meal plans, and educating patients on sustainable dietary practices. Enhancing the role of dietitians within multidisciplinary teams – alongside physicians, psychologists, nurses, physiotherapists, health promotion specialists, and other allied professionals – can significantly improve obesity outcomes by ensuring that interventions are individualized, evidence-based and culturally sensitive.

By investing in collaborative, system-wide solutions and expanding access to skilled healthcare professionals, we can dismantle the barriers that perpetuate obesity and work toward a healthier future for all. The time to act is now – if we fail to address obesity, its repercussions will resonate for generations to come. However, there is no single solution that fits all populations. Each country must identify and implement the most effective strategies based on its unique socio-economic, cultural and healthcare landscape. A successful approach requires flexibility, ongoing evaluation and adaptation to local needs while maintaining a strong commitment to evidence-based policies and interventions.

ORCID iDs

Anthony Dissen  <https://orcid.org/0000-0003-0828-387X>

Izabella Uchmanowicz  <https://orcid.org/0000-0001-5452-0210>

Michał Czaplá  <https://orcid.org/0000-0002-4245-5420>

References

1. World Health Organization (WHO). Obesity. Geneva, Switzerland: World Health Organization (WHO); 2024. <https://www.who.int/news-room/facts-in-pictures/detail/6-facts-on-obesity>. Accessed January 26, 2025.

2. The GBD 2015 Obesity Collaborators. Health effects of overweight and obesity in 195 countries over 25 years. *N Engl J Med*. 2017;377(1): 13–27. doi:10.1056/NEJMoa1614362
3. Phelps NH, Singleton RK, Zhou B, et al. Worldwide trends in underweight and obesity from 1990 to 2022: A pooled analysis of 3663 population-representative studies with 222 million children, adolescents, and adults. *Lancet*. 2024;403(10431):1027–1050. doi:10.1016/S0140-6736(23)02750-2
4. Jaacks LM, Vandevijvere S, Pan A, et al. The obesity transition: Stages of the global epidemic. *Lancet Diabetes Endocrinol*. 2019;7(3):231–240. doi:10.1016/S2213-8587(19)30026-9
5. Wojtyński B, Goryński P, eds. *Health Status of Polish Population and Its Determinants: 2020*. Warsaw, Poland: National Institute of Public Health NIH – National Research Institute; 2020. ISBN:978-83-65870-37-7.
6. Gajewska D, Harton A. Current nutritional status of the Polish population: Focus on body weight status. *J Health Inequalities*. 2023;9(2): 154–160. doi:10.5114/jhi.2023.133899
7. Monteiro CA, Cannon G, Levy RB, et al. Ultra-processed foods: What they are and how to identify them. *Public Health Nutr*. 2019;22(5): 936–941. doi:10.1017/S1368980018003762
8. Popkin BM, Ng SW. The nutrition transition to a stage of high obesity and noncommunicable disease prevalence dominated by ultra-processed foods is not inevitable. *Obes Rev*. 2022;23(1):e13366. doi:10.1111/obr.13366
9. Bleich SN, Vercammen KA. The negative impact of sugar-sweetened beverages on children's health: An update of the literature. *BMC Obes*. 2018;5(1):6. doi:10.1186/s40608-017-0178-9
10. Hill JO, Wyatt HR, Peters JC. Energy balance and obesity. *Circulation*. 2012;126(1):126–132. doi:10.1161/CIRCULATIONAHA.111.087213
11. Bora N, Vaishali K, Verma A, Bharti AK, Sinha MK. Physical activity and sedentary behavior perceptions in overweight and obese adults: A systematic review of qualitative study. *F1000Res*. 2024;13:787. doi:10.12688/f1000research.152905.1
12. Curran F, Davis ME, Murphy K, et al. Correlates of physical activity and sedentary behavior in adults living with overweight and obesity: A systematic review. *Obes Rev*. 2023;24(11):e13615. doi:10.1111/obr.13615
13. Silveira EA, Mendonça CR, Delpino FM, et al. Sedentary behavior, physical inactivity, abdominal obesity and obesity in adults and older adults: A systematic review and meta-analysis. *Clin Nutr ESPEN*. 2022; 50:63–73. doi:10.1016/j.clnesp.2022.06.001
14. Albuquerque D, Nóbrega C, Manco L, Padez C. The contribution of genetics and environment to obesity. *Br Med Bull*. 2017;123(1):159–173. doi:10.1093/bmb/ldx022
15. Loos RJF, Yeo GSH. The genetics of obesity: From discovery to biology. *Nat Rev Genet*. 2022;23(2):120–133. doi:10.1038/s41576-021-00414-z
16. Blüher M. Obesity: Global epidemiology and pathogenesis. *Nat Rev Endocrinol*. 2019;15(5):288–298. doi:10.1038/s41574-019-0176-8
17. Reichetzer C. Overweight and obesity in pregnancy: Their impact on epigenetics. *Eur J Clin Nutr*. 2021;75(12):1710–1722. doi:10.1038/s41430-021-00905-6
18. Wu FY, Yin RX. Recent progress in epigenetics of obesity. *Diabetol Metab Syndr*. 2022;14(1):171. doi:10.1186/s13098-022-00947-1
19. Mahmoud AM. An overview of epigenetics in obesity: The role of lifestyle and therapeutic interventions. *Int J Mol Sci*. 2022;23(3):1341. doi:10.3390/ijms23031341
20. Westbury S, Oyebo O, Van Rens T, Barber TM. Obesity stigma: Causes, consequences, and potential solutions. *Curr Obes Rep*. 2023; 12(1):10–23. doi:10.1007/s13679-023-00495-3
21. Aparicio HJ, Himali JJ, Beiser AS, et al. Overweight, obesity, and survival after stroke in the Framingham Heart Study. *J Am Heart Assoc*. 2017;6(6):e004721. doi:10.1161/JAHA.116.004721
22. Piché ME, Tchernof A, Després JP. Obesity phenotypes, diabetes, and cardiovascular diseases. *Circ Res*. 2020;126(11):1477–1500. doi:10.1161/CIRCRESAHA.120.316101
23. The Council of The Obesity Society. Obesity as a disease: The Obesity Society Council Resolution. *Obesity (Silver Spring)*. 2008;16(6):1151–1151. doi:10.1038/oby.2008.246
24. Pati S, Irfan W, Jameel A, Ahmed S, Shahid RK. Obesity and cancer: A current overview of epidemiology, pathogenesis, outcomes, and management. *Cancers (Basel)*. 2023;15(2):485. doi:10.3390/cancers15020485
25. Sarwer DB, Polonsky HM. The psychosocial burden of obesity. *Endocrinol Metab Clin North Am*. 2016;45(3):677–688. doi:10.1016/j.ecl.2016.04.016
26. Okunogbe A, Nugent R, Spencer G, Ralston J, Wilding J. Economic impacts of overweight and obesity: Current and future estimates for eight countries. *BMJ Glob Health*. 2021;6(10):e006351. doi:10.1136/bmjgh-2021-006351
27. Taillie LS, Busey E, Stoltze FM, Dillman Carpentier FR. Governmental policies to reduce unhealthy food marketing to children. *Nutr Rev*. 2019;77(11):787–816. doi:10.1093/nutrit/nuz021
28. World Health Organization (WHO). WHO Acceleration Plan to Stop Obesity. Geneva, Switzerland: World Health Organization (WHO); 2023. <https://www.who.int/publications/i/item/9789240075634>. Accessed January 26, 2025.
29. Swinburn B, Vandevijvere S. WHO report on ending childhood obesity echoes earlier recommendations. *Public Health Nutr*. 2016;19(1):1–2. doi:10.1017/S1368980015003663
30. Silva P, Araújo R, Lopes F, Ray S. Nutrition and food literacy: Framing the challenges to health communication. *Nutrients*. 2023;15(22):4708. doi:10.3390/nu15224708
31. Swinburn BA, Sacks G, Hall KD, et al. The global obesity pandemic: Shaped by global drivers and local environments. *Lancet*. 2011; 378(9793):804–814. doi:10.1016/S0140-6736(11)60813-1
32. American Diabetes Association Professional Practice Committee. 8. Obesity and Weight Management for the Prevention and Treatment of Type 2 Diabetes: Standards of Care in Diabetes–2024. *Diabetes Care*. 2024;47(Suppl 1):S145–S157. doi:10.2337/dc24-S008
33. Rubino F, Cummings DE, Eckel RH, et al. Definition and diagnostic criteria of clinical obesity. *Lancet Diabetes Endocrinol*. 2025;13(3):221–262. doi:10.1016/S2213-8587(24)00316-4
34. Ortell TA. Improving LGBTQ health and well-being. *Am J Nurs*. 2020; 120(6):1–4. doi:10.1097/01.NAJ.0000668780.88139.1c
35. Clark JM, Garvey WT, Niswender KD, et al. Obesity and overweight: Probing causes, consequences, and novel therapeutic approaches through the American Heart Association's Strategically Focused Research Network. *J Am Heart Assoc*. 2023;12(4):e027693. doi:10.1161/JAHA.122.027693
36. Thomas OW, Reilly JM, Wood NI, Albin J. Culinary medicine: Needs and strategies for incorporating nutrition into medical education in the United States. *J Med Educ Curric Dev*. 2024;11:23821205241249379. doi:10.1177/23821205241249379

Supported transitional care applied to stroke survivors: A meta-analysis

Shuyin Liang^{1,A–F}, Huiling Xie^{2,B–F}, Lili Ye^{3,B–F}, Caifang Huang^{1,B–F}, Fengying Yuan^{1,B–F}, Yanping Tang^{4,B–F}

¹ Department of Neurovascular Center, Zhujiang Hospital of Southern Medical University, Guangzhou, China

² Department of Geriatric Medicine, Zhujiang Hospital of Southern Medical University, Guangzhou, China

³ Department of Day Treatment Center, Zhujiang Hospital of Southern Medical University, Guangzhou, China

⁴ Department of Nursing, Zhujiang Hospital of Southern Medical University, Guangzhou, China

A – research concept and design; B – collection and/or assembly of data; C – data analysis and interpretation;

D – writing the article; E – critical revision of the article; F – final approval of the article

Advances in Clinical and Experimental Medicine, ISSN 1899–5276 (print), ISSN 2451–2680 (online)

Adv Clin Exp Med. 2025;34(4):479–486

Address for correspondence

Shuyin Liang
E-mail: lsy0925@126.com

Funding sources

None declared

Conflict of interest

None declared

Received on February 3, 2024

Reviewed on February 26, 2024

Accepted on April 9, 2024

Published online on June 11, 2024

Abstract

Background. This meta-analysis aims to assess the outcomes of supported intervention transitional care compared to traditional care for stroke survivors.

Materials and methods. A systematic literature review was accomplished and 4,437 stroke patients were recruited for the current study; 2,211 of them were treated with transitional care and 2,226 with traditional care. The inclusion criteria of the current study recruited only randomized clinical trials up until November 2023. A random analysis model was used to analyze the continuous and dichotomous models.

Results. Supported intervention transitional care (early supported discharge) for stroke survivors showed a significant ($p = 0.002$) impact regarding the functional status of patients as expressed by the Barthel index (mean difference (MD) = 0.57, 95% confidence interval (95% CI): 0.20–0.94, $I^2 = 93.72\%$). On the other hand, there were no considerable ($p > 0.05$) differences regarding other outcomes such as activities of daily living, the Caregiver Strain Index (CSI), the modified Rankin scale (mRS), and mortality (MD = 0.29, 95% CI: –0.12–0.69, $I^2 = 94.5\%$; MD = –0.13, 95% CI: –0.40–0.14, $I^2 = 68.65\%$; MD = –0.13, 95% CI: –0.49–0.23, $I^2 = 83.33\%$; and MD = –0.19, 95% CI: –0.58–0.17, $I^2 = 0\%$; respectively).

Conclusions. Supported transitional care allowed stroke survivors to succeed in enhancing their functional status outcomes compared with controls, while there was no significant impact regarding mortality rate. Further investigations and multicenter studies are required to enhance the evidence.

Key words: stroke, rehabilitation, transitional care, early supported discharge

Cite as

Liang S, Xie H, Ye L, Huang C, Yuan F, Tang Y. Supported transitional care applied to stroke survivors: A meta-analysis. *Adv Clin Exp Med*. 2025;34(4):479–486. doi:10.17219/acem/186957

DOI

10.17219/acem/186957

Copyright

Copyright by Author(s)

This is an article distributed under the terms of the Creative Commons Attribution 3.0 Unported (CC BY 3.0) (<https://creativecommons.org/licenses/by/3.0/>)

Background

Individuals undergoing recovery after an acute stroke face considerable difficulties in independently managing the transition from hospital to home. The need for these interventions is due to the need to adapt to a change in one's health condition, a new diagnosis and the recognition of ongoing care requirements.¹ Upon discharge from the hospital, numerous stroke survivors require comprehensive and continuous rehabilitation and assistance to regain and develop skills and capacities, adjust to the limits resulting from the stroke, and address their emotional, social and practical needs both in the community and at home. Interventions to achieve these goals, like early supported discharge (ESD), provided to the stroke survivor during the transition to home from the hospital, decrease the duration of hospitalization in addition to reducing the healthcare costs of stroke care.²

The transition of care as an expression is intricate, difficult to define, and is frequently used in several studies and guidance interchangeably with other concepts such as care navigation, care coordination and care continuity. Transitional care includes both the medical component of transferring care and the needs of the stroke patient and their carer.³ The expression "transition of care" can be defined as a series of measures aimed at ensuring the coordination and continuousness of healthcare when patients move from one site to another or to different levels of care. Rehabilitation interventions during care transitions are recognized as crucial for coordinating care and have an impact on the quality of care and the occurrence of hazardous episodes.^{4,5}

Stroke survivors can be offered support interventions, such as educational programs and personalized discharge plans, as they move from organized stroke care to their homes. These interventions seek to promote the consistency and excellence of healthcare, improve functional results, decrease healthcare expenses, and enhance the overall user experience.⁶ Nevertheless, there is a dearth of understanding regarding effective support treatments to optimally handle transitions for this intricate health condition.

Assessment of the impact of transitional care can be evaluated using different parameters such as the Barthel index, activities of daily living, the Caregiver Strain Index (CSI), the modified Rankin scale (mRS), and mortality rate. The objective of these parameters is to assess the patient's ability to perform daily activities and the necessity of nursing care.

The national stroke recommendations of Canada,⁷ USA⁸ and Scotland⁹ utilize ESD as a rehabilitation technique for post-acute care. Early supported discharge is a crucial element of the stroke care system in the UK. The manuals clearly identify the target group, aim, scope, and methodology of ESD.^{10,11}

Objectives

The purpose of this study was to evaluate the effects of transitional care with supported intervention in comparison to traditional care when it is applied to stroke survivors in terms of functional status, physical activity and mortality.

Materials and methods

Study design

The epidemiological declaration¹² was the subject of the present meta-analysis, which encompassed studies that tracked a prearranged study technique.¹³ Data gathering and analysis of recruited studies were conducted using several scientific databases in accordance with the specified inclusion criteria. The study inclusion sequence is illustrated in Fig. 1.

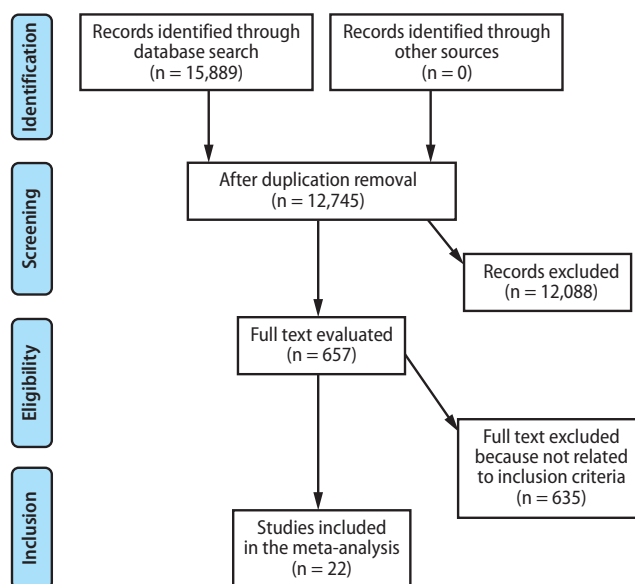


Fig. 1. Diagram representing the study inclusion procedure

Eligibility and inclusion

This study was conducted to assess the impact of assisted intervention transitional care compared to traditional care in individuals who have experienced a stroke. The sensitivity study exclusively encompassed publications that examined the impact of interventions on mortality rate, functional status, validity of daily activity, and the CSI score. To conduct subclass and sensitivity analyses, several patient types were compared to the medical intervention groups.

Inclusion criteria

1. The acceptable study design included in the current study is randomized clinical trials published before November 2023.
2. The study included patients who experienced a stroke (stroke survivors) and are receiving post-stroke care.
3. The design of the study method must be a comparison, comparing outcomes of 2 different interventions (supported transitional care compared to traditional care).

Exclusion criteria

1. Articles that did not present results of the comparison between different interventions in an acceptable form, such as interquartile ranges (IQRs) or medians. The results of different outcomes should be expressed in the form of a mean (\pm standard deviation (\pm SD)) or event/total.
2. Studies in the form of letters, review articles, books, or book chapters.

Identification

We carried out a search concerning papers published up until November 2023 using a combination of several keywords and comparable words for transitional care, rehabilitation, stroke, stroke survivors, supported early discharge, functional status, Barthel index, CSI, and supported nursing intervention.¹⁴ A protocol of our search strategies was defined in accordance with the PICOS principle as follows: P (population) – stroke survivors, I (intervention/exposure) – ESD care (supported transitional care), C (comparison) – transitional care compared to traditional care, O (outcome) – Barthel index, mortality, CSI, mRS, and activity of daily living, and S (study design) – randomized clinical studies (RCTs).

The authors performed a thorough search of the PubMed, Cochrane Library, Embase, Ovid, and Google Scholar databases until November 2023 using the keywords and related terms. Any article that did not discuss and evaluate the role of ESD compared to traditional care was disregarded after an evaluation of the titles and abstracts of the articles that had been collected into a reference managing program. Two authors served as reviewers to find pertinent studies.

Screening

The data were filtered based on specific criteria, including the first author's surname, publication year, country of study, study design, recruited population type, study duration, demographic information, clinical and treatment characteristics, total number of participants, standardized presentation of study-related features, information source, and outcome. Each study was assessed for potential bias, and the methodological quality of the chosen publications was analyzed independently by 2 authors in a blinded manner.

The presence of bias in each of the included studies was assessed using Review Manager v. 5.3 software (The Nordic Cochrane Centre, The Cochrane Collaboration, Copenhagen, Denmark), and the findings were categorized into 3 levels: low, moderate or high potential for bias. Two of the authors conducted a methodological evaluation of each study.

Statistical analyses

The mean difference (MD) with a 95% confidence interval (95% CI) was calculated using random dichotomous (mortality rate) and continuous models (Barthel index, activities of daily living, mRS, and CSI).¹⁵ All p-values were calculated using 2-tailed tests. We used a random model based on the high level of differences between the included studies and the absence of high similarity regarding study parameters between all studies included for analysis of the model. The selection of the analysis model was determined after an accurate assessment of all included studies and comparisons of these papers to each other. According to the data, a random-effects model was fitted. Using a constrained maximum-likelihood estimator, the level of heterogeneity (Tau^2) was calculated. The I^2 index, which is a numerical number ranging from 0 to 100, was obtained using Jamovi software (<https://www.jamovi.org>). The heterogeneity level was shown with percentages ranging from 0% to 100%, and it was also expressed with percentages indicating low, moderate and high levels of heterogeneity. Begg's and Egger's tests were used to conduct quantitative research on publication bias, and the presence of publication bias was deemed to be present if the p-value was >0.05 .

Results

After reviewing 15,889 pertinent studies, 22 research papers meeting the inclusion criteria from the period of 1997 to 2022 were included in the meta-analysis.^{16–37} The results of these investigations are compiled in Table 1 (characteristics of included research including year, country, subject count, and study design).

Barthel index

A total of 13 studies were included in the analysis of the impact of intervention (transitional care) compared to control (traditional care) for stroke survivors. The analysis of this model showed a significantly ($p = 0.002$) higher impact of transitional care on functional status outcomes compared to the controls (MD = 0.57, 95% CI: 0.20–0.94, $I^2 = 93.72\%$). Both the Begg's and Egger's tests did not show significant evidence of publication bias, with p-values of 0.1289 and 0.1602, respectively (Fig. 2A). Subgroup analysis of these models consisted of 2 subgroups, 1st evaluating the impact of the interventions for up to 3 months (7 studies) and a 2nd subgroup evaluating the impact

Table 1. Characteristics of included studies

Study	Year	Country	Type of study	Intervention group	Control group	Total	Duration
Rudd et al. ¹⁶	1997	UK	RCT	167	164	331	up to 12 month
Andersen et al. ¹⁷	2002	Denmark	RCT	51	44	95	up to 6 months
Allen et al. ¹⁸	2002	USA	RCT	47	46	93	≤3 months
Clark et al. ¹⁹	2003	Australia	RCT	35	33	68	up to 6 months
Lincoln et al. ²⁰	2003	UK	RCT	126	124	250	up to 6 months
Askim et al. ²¹	2004	Norway	RCT	29	29	58	≤3 months
Boter ²²	2004	Netherlands	RCT	263	273	536	up to 6 months
Donnelly et al. ²³	2004	UK	RCT	51	46	97	up to 12 month
Fjaertoft et al. ²⁴	2003	Norway	RCT	160	160	320	up to 12 month
Mayo et al. ²⁵	2008	Canada	RCT	96	94	190	≤3 months
Allen et al. ²⁶	2009	USA	RCT	190	190	380	up to 6 months
Chalermwannapong et al. ²⁷	2010	Thailand	RCT	45	47	92	≤3 months
Hofstad et al. ²⁸	2014	Norway	RCT	104	99	203	up to 6 months
Wong and Yeung ²⁹	2015	China	RCT	54	54	108	≤3 months
Rasmussen et al. ³⁰	2016	Denmark	RCT	31	30	61	≤3 months
Santana et al. ³¹	2017	Portugal	RCT	95	95	190	up to 6 months
Geng et al. ³²	2019	China	quasi-randomization	30	30	60	up to 6 months
Rafsten et al. ³³	2019	Sweden	RCT	63	71	134	up to 12 month
Deng et al. ³⁴	2020	China	RCT	49	49	98	≤3 months
Duncan et al. ³⁵	2020	USA	RCT	407	430	837	4 months
Feng et al. ³⁶	2021	China	RCT	60	60	120	≤3 months
Wong et al. ³⁷	2022	China	RCT	58	58	116	≤3 months

RCT – randomized clinical trial.

of the interventions for up to 6 months. A total of 7 studies comparing the impact of transitional care intervention with a control for up to 90 days after stroke survival were included in the analysis. The finding of this analysis showed a significant difference ($p = 0.001$) between the intervention and control groups, reflecting a higher impact of transitional care ($MD = 0.90$, 95% CI: 0.35–1.46, $I^2 = 92.4\%$). Both the Begg's and Egger's tests did not show significant evidence of publication bias, with p -values of 0.56 and 0.52, respectively. (Fig. 2B). On the other hand, 6 studies were analyzed to evaluate the effects over a longer period (6 months). Findings of this model, in contrast with previous models, showed a nonsignificant ($p = 0.26$) impact between the intervention and control ($MD = 0.14$, 95% CI: -0.11 – 0.39 , $I^2 = 94.6\%$) (Fig. 2C). The Egger's test revealed the presence of funnel plot asymmetry ($p = 0.045$), whereas the Begg's test did not show any significant results ($p = 0.27$).

Activities of daily living

A total of 11 studies were included in the analysis of the impact of the intervention compared to controls on activities of daily living (ADL) for stroke survivors. The analysis of this model showed a nonsignificant ($p = 0.16$) impact of transitional care compared to controls

($MD = 0.29$, 95% CI: -0.12 – 0.69 , $I^2 = 94.5\%$) (Fig. 3). The Begg's test revealed significant funnel plot asymmetry ($p = 0.026$), whereas the Egger's test did not provide significant results ($p = 0.053$).

Modified Rankin scale

A total of 4 studies were included in the analysis of the impact of intervention compared to control on the mRS for stroke survivors. The analysis of this model showed a nonsignificant ($p = 0.47$) impact of transitional care compared to controls ($MD = -0.13$, 95% CI: -0.49 – 0.23 , $I^2 = 83.33\%$) (Fig. 4). Both the Begg's and Egger's tests did not show significant evidence of publication bias ($p = 0.33$ and $p = 0.11$, respectively).

Caregiver Strain Index

A total of 5 studies were included in the analysis of the impact of the intervention compared to controls on the CSI for stroke survivors. The analysis of this model showed a nonsignificant ($p = 0.33$) impact of transitional care compared to controls ($MD = -0.13$, 95% CI: -0.40 – 0.14 , $I^2 = 68.65\%$) (Fig. 5). Both the Begg's and Egger's tests showed no significant evidence of publication bias ($p = 0.82$ and $p = 0.60$, respectively).

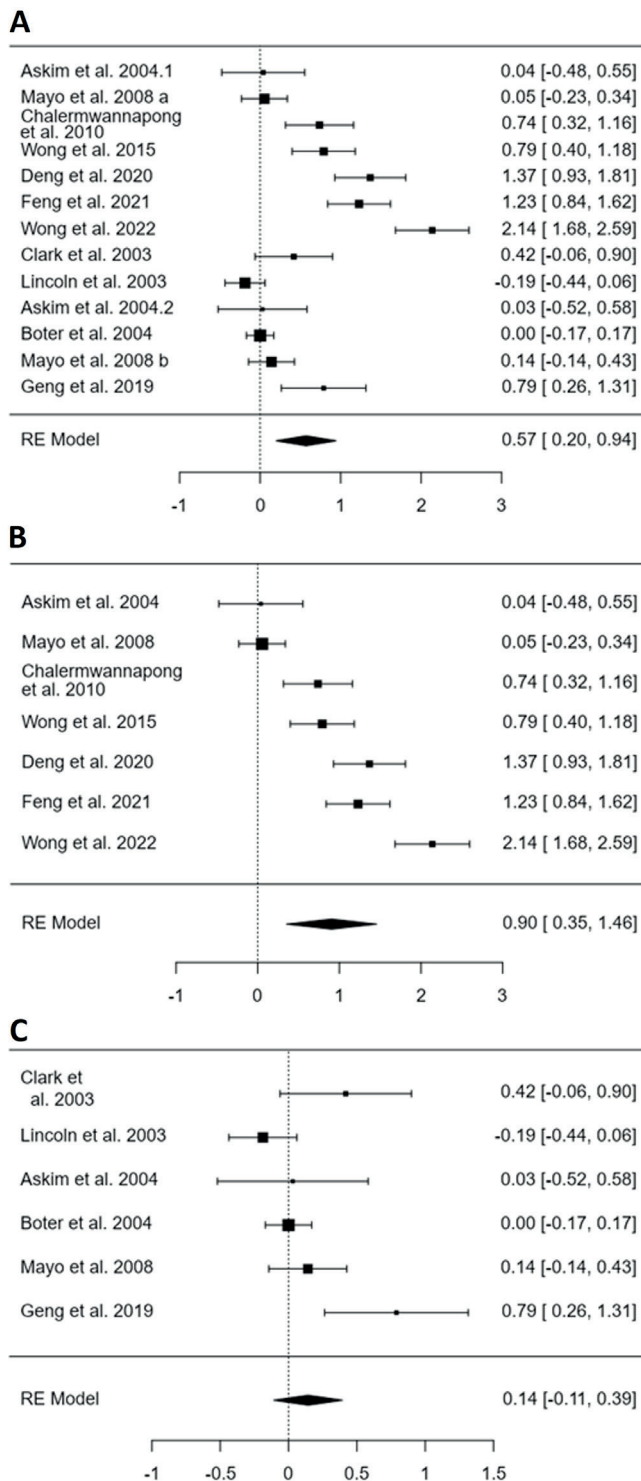


Fig. 2. Forest plot indicating the influence of supported transitional care on the Barthel index compared to controls for all studies (A), studies assessed after 3 months (B) and up to 6 months (C)

Mortality

A total of 8 studies were included in the analysis of the impact of the intervention compared to controls on the mortality rate of stroke survivors. The analysis of this model showed a nonsignificant ($p = 0.30$) impact of transitional care compared to control (MD = -0.19 ,

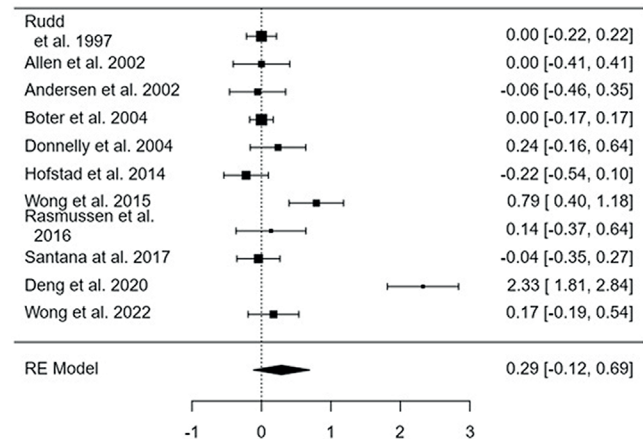


Fig. 3. Forest plot indicating the influence of supported transitional care on the activities of daily living compared to controls

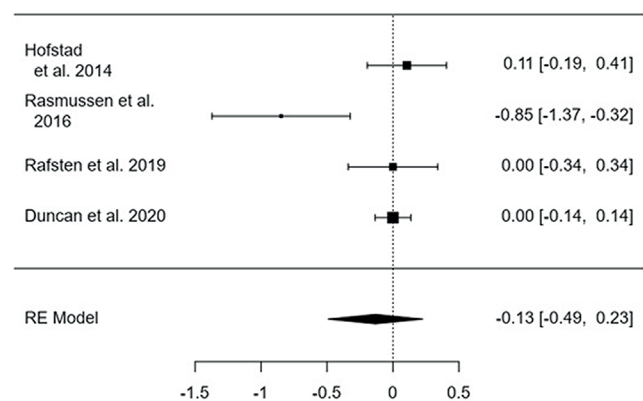


Fig. 4. Forest plot indicating the influence of supported transitional care on the modified Rankin scale compared to controls

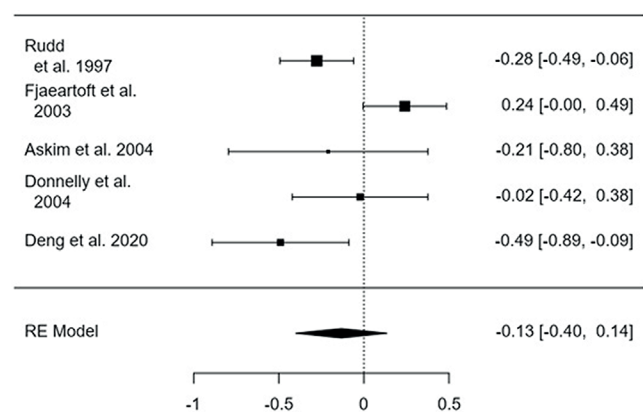


Fig. 5. Forest plot indicating the influence of supported transitional care on the Caregiver Strain Index compared to controls

95% CI: -0.58 – 0.17 , $I^2 = 0\%$ (Fig. 6). Both the Begg's and Egger's tests did not show significant evidence of publication bias ($p = 0.27$ and $p = 0.47$, respectively).

However, the Begg's and Egger's tests determine publication bias statistically, but also visual evaluation of funnel plot symmetry provides supporting evidence. The funnel plots for 6 models showed a different degree of asymmetry (Supplementary Fig. 1), reflecting the presence

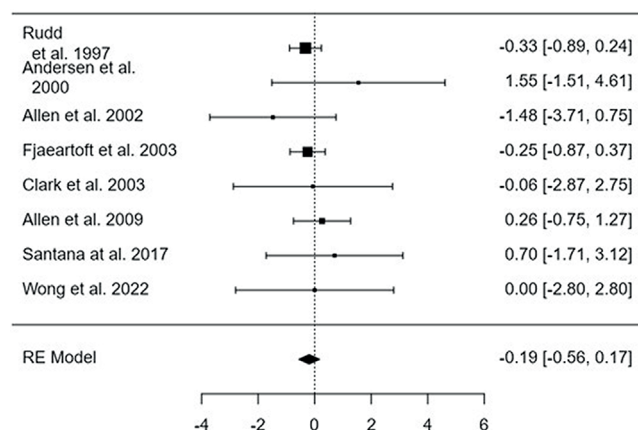


Fig. 6. Forest plot indicating the influence of supported transitional care on mortality rates compared to controls

of publication bias, while the funnel plot for the mortality rate model showed a higher degree of plot symmetry (Supplementary Fig. 2).

Discussion

Twenty-two randomized clinical trials published between 1997 to 2022 were included in the meta-analysis as they met the inclusion criteria.^{16–37} Interventions evaluated using the Barthel index, displaying a mean value of 0.57 and a 95% CI ranging from 0.20 to 0.94, demonstrated that transitional care, also known as ESD, had a substantial influence ($p = 0.002$) on the functional state of stroke survivors. However, it is worth mentioning that there were no noteworthy differences ($p < 0.05$) in relation to the other outcomes, including activities of daily living, mRS, CSI, and death.

Although there have been advancements in acute stroke care on a global scale, deficiencies are still observed in the process of reintegrating stroke patients into their communities and in their ability to manage their own care following a stroke.⁶ Our research indicates that interventions involving multiple components improve short-term functionality. Nevertheless, these interventions seem to have a diminished effect on functional status 6 months following the transition phase. Research indicates that it is challenging to maintain the results attained by self-management tactics. However, it has been found that increased self-efficacy plays a crucial role in the successful and long-lasting benefits of self-management programs.³⁸ This suggests that self-efficacy should be a deliberate goal of self-management programs. There is a need for a deeper comprehension of the tactics that promote long-term self-confidence. Contemporary research explains that healthcare practitioners and healthcare systems must go beyond traditional self-management strategies and customize self-management support to suit the unique needs of each individual, taking into account their life circumstances and the progression of their condition.³⁹

There are several scales to evaluate stroke and other critical care survivors, such as the Barthel index.⁴⁰ It gauges a person's ability to move around and operate independently in daily living tasks, including eating, washing, grooming, dressing, using the restroom, chair transfer, ambulating, and climbing stairs. The scale lists 10 tasks and assigns a grade based on how much time or help the patient needs. The total score ranges from 0 to 100, where lower numbers denote a higher degree of nursing need.⁴¹

A previous study conducted by Langhorne et al. resembled our study.² They carried out a systematic literature review and meta-analysis of 17 randomized controlled trials that involved a total of 2,422 patients. The study found that ESD shortened the duration of hospitalization by approx. 6 days and decreased long-term reliance on assistance for daily activities. Our investigation observed a limited number of instances where ESD resulted in notable disparities in the results. This can be linked to the uniform nature of therapies, which do not include patient-led, family-led or telerehabilitation methods. In contrast, Cochrane's study intentionally included a wide range of criteria for intervention. These disparities resulted in the deletion of several research studies, potentially leading to a decrease in the number of situations where ESD had a significant positive impact on the study results.² Langhorne et al. discovered that the implementation of an ESD program, which includes a multidisciplinary team of specialists, led to reduced long-term functional dependency and readmission rates in stroke patients. Furthermore, the duration of hospitalization was significantly shortened in comparison to the previous service.² Specifically, the overall mean duration of hospitalization decreased to 6 days, and the occurrence of adverse outcomes, such as mortality or readmission, decreased by around 5%. Previous studies did not find any significant variations in the reported outcomes. However, the cost of the ESD program was 15–23% lower compared to traditional treatment.¹⁰

In a comprehensive review of the extant literature on transitional management in Germany, Hempler et al. employed a systematic approach to identify and analyze the current research on this topic.⁴² The literature analysis included a total of 18 studies. However, all of these studies lacked sufficient quality regarding standardized transition management systems. The study findings suggested that Germany requires standardized discharge management services, such as ESD programs. However, countries other than Germany are making efforts to offer alternative services, and these services are gradually being implemented in Asian countries, as reflected by the growing demand for such services in, e.g., South Korea. In contrast to the review study conducted in Germany,⁴² our work holds significance as it involved 2 researchers who independently chose and assessed the papers for meta-analysis.

Limitations

There are a few limitations that apply to this review. In the first place, the quality of the trials, which are fraught with a high risk of bias, inconsistency and imprecision, limits the certainty of the findings. Additionally, there were not many studies that reported on outcomes such as cognition and exhaustion, both of which have the potential to significantly impact functional performance and are essential to stroke survivors. A considerable number of research studies on transitional care did not incorporate outcomes for caregivers, which can influence the utilization of resources and the costs incurred by the healthcare system. Furthermore, there was a limited amount of reporting of adverse occurrences.

Conclusions

The provision of supported transitional care to stroke survivors was found to be effective in enhancing functional status outcomes when compared with a control group. However, there was no discernible impact on mortality rates. To strengthen the evidence, additional research and studies involving multiple centers are required.

Supplementary data

The Supplementary materials are available at <https://doi.org/10.5281/zenodo.10843219>. The package includes the following files:

Supplementary Fig. 1. Funnel plots for assessment of publication bias regarding Barthel index compared to control for all studies (A), studies assessed after 3 months (B) and up to 6 months (C), the activity of daily living compared to control (D), mRS compared to control (E), and the CSI compared to control (F).

Supplementary Fig. 2. Funnel plots for assessment of publication bias regarding mortality rate.

Data availability

The datasets generated and/or analyzed during the current study are available from the corresponding author on reasonable request.

Consent for publication


Not applicable.


ORCID iDs


Shuyin Liang  <https://orcid.org/0009-0003-5365-1114>

Huiling Xie  <https://orcid.org/0009-0009-6326-7259>

Lili Ye  <https://orcid.org/0000-0002-4257-5561>

Caifang Huang  <https://orcid.org/0009-0003-3332-8889>

Fengying Yuan  <https://orcid.org/0009-0000-5846-2476>

Yanping Tang  <https://orcid.org/0000-0003-1446-3199>

References

- Chen L, Xiao LD, Chamberlain D. An integrative review: Challenges and opportunities for stroke survivors and caregivers in hospital to home transition care. *J Adv Nurs*. 2020;76(9):2253–2265. doi:10.1111/jan.14446
- Langhorne P, Baylan S; Early Supported Discharge Trialists. Early supported discharge services for people with acute stroke. *Cochrane Database Syst Rev*. 2017;2017(7):CD000443. doi:10.1002/14651858.CD000443.pub4
- Coleman EA, Boulton C. Improving the quality of transitional care for persons with complex care needs: Position Statement of The American Geriatrics Society Health Care Systems Committee. *J Am Geriatr Soc*. 2003;51(4):556–557. doi:10.1046/j.1532-5415.2003.51186.x
- Reeves MJ. COMPASS trial in transitional stroke care: Navigating towards true north. *Circ Cardiovasc Qual Outcomes*. 2020;13(6):e006745. doi:10.1161/CIRCOUTCOMES.120.006745
- Miller KK, Lin SH, Neville M. From hospital to home to participation: A position paper on transition planning poststroke. *Arch Phys Med Rehabil*. 2019;100(6):1162–1175. doi:10.1016/j.apmr.2018.10.017
- Norring B, Barrick J, Davalos A, et al. Action plan for stroke in Europe 2018–2030. *Eur Stroke J*. 2018;3(4):309–336. doi:10.1177/2396987318808719
- Mountain A, Patrice Lindsay M, Teasell R, et al. Canadian Stroke Best Practice Recommendations: Rehabilitation, recovery, and community participation following stroke. Part Two: Transitions and community participation following stroke. *Int J Stroke*. 2020;15(7):789–806. doi:10.1177/1747493019897847
- Sall J, Eapen BC, Tran JE, Bowles AO, Bursaw A, Rodgers ME. The management of stroke rehabilitation: A synopsis of the 2019 U.S. Department of Veterans Affairs and U.S. Department of Defense Clinical Practice Guideline. *Ann Intern Med*. 2019;171(12):916. doi:10.7326/M19-1695
- Smith LN, James R, Barber M, et al; Guideline Development Group. Rehabilitation of patients with stroke: Summary of SIGN guidance. *BMJ*. 2010;340:c2845. doi:10.1136/bmj.c2845
- Langhorne P, Holmqvist L. Early supported discharge after stroke. *Acta Derm Venereol*. 2007;39(2):103–108. doi:10.2340/16501977-0042
- Langhorne P, Taylor G, Murray G, et al. Early supported discharge services for stroke patients: A meta-analysis of individual patients' data. *Lancet*. 2005;365(9458):501–506. doi:10.1016/S0140-6736(05)17868-4
- Stroup DF, Beach JA, Morton SC, et al. Meta-analysis of observational studies in epidemiology: A proposal for reporting. *JAMA*. 2000;283(15):2008. doi:10.1001/jama.283.15.2008
- Higgins JPT, Thompson SG, Deeks JJ, Altman DG. Measuring inconsistency in meta-analyses. *BMJ*. 2003;327(7414):557–560. doi:10.1136/bmj.327.7414.557
- Liberati A, Altman DG, Tetzlaff J, et al. The PRISMA statement for reporting systematic reviews and meta-analyses of studies that evaluate health care interventions: Explanation and elaboration. *J Clin Epidemiol*. 2009;62(10):e1–e34. doi:10.1016/j.jclinepi.2009.06.006
- Sheikhabahe S, Trahan TJ, Xiao J, et al. FDG-PET/CT and MRI for evaluation of pathologic response to neoadjuvant chemotherapy in patients with breast cancer: A meta-analysis of diagnostic accuracy studies. *Oncologist*. 2016;21(8):931–939. doi:10.1634/theoncologist.2015-0353
- Rudd AG, Wolfe CDA, Tilling K, Beech R. Randomised controlled trial to evaluate early discharge scheme for patients with stroke. *BMJ*. 1997;315(7115):1039–1044. doi:10.1136/bmj.315.7115.1039
- Andersen HE, Schultz-Larsen K, Kreiner S, Forchhammer BH, Eriksen K, Brown A. Can readmission after stroke be prevented? Results of a randomized clinical study: A postdischarge follow-up service for stroke survivors. *Stroke*. 2000;31(5):1038–1045. doi:10.1161/01.STR.31.5.1038
- Allen KR, Hazelett S, Jarjoura D, et al. Effectiveness of a postdischarge care management model for stroke and transient ischemic attack: A randomized trial. *J Stroke Cerebrovasc Dis*. 2002;11(2):88–98. doi:10.1053/jscd.2002.127106
- Clark MS, Rubenach S, Winsor A. A randomized controlled trial of an education and counselling intervention for families after stroke. *Clin Rehabil*. 2003;17(7):703–712. doi:10.1191/0269215503cr6810a
- Lincoln NB, Francis VM, Lilley SA, Sharma JC, Summerfield M. Evaluation of a stroke family support organiser: A randomized controlled trial. *Stroke*. 2003;34(1):116–121. doi:10.1161/01.STR.0000047850.33686.32

21. Askim T, Rohweder G, Lydersen S, Indredavik B. Evaluation of an extended stroke unit service with early supported discharge for patients living in a rural community: A randomized controlled trial. *Clin Rehabil.* 2004;18(3):238–248. doi:10.1191/0269215504cr752oa
22. Boter H. Multicenter randomized controlled trial of an outreach nursing support program for recently discharged stroke patients. *Stroke.* 2004;35(12):2867–2872. doi:10.1161/01.STR.0000147717.57531.e5
23. Donnelly M, Power M, Russell M, Fullerton K. Randomized controlled trial of an early discharge rehabilitation service: The Belfast Community Stroke Trial. *Stroke.* 2004;35(1):127–133. doi:10.1161/01.STR.0000106911.96026.8F
24. Fjærtøft H, Indredavik B, Johnsen R, Lydersen S. Acute stroke unit care combined with early supported discharge: Long-term effects on quality of life. A randomized controlled trial. *Clin Rehabil.* 2004;18(5):580–586. doi:10.1191/0269215504cr773oa
25. Mayo NE, Nadeau L, Ahmed S, et al. Bridging the gap: The effectiveness of teaming a stroke coordinator with patient's personal physician on the outcome of stroke. *Age Ageing.* 2007;37(1):32–38. doi:10.1093/ageing/afm133
26. Allen K, Hazelett S, Jarjoura D, et al. A randomized trial testing the superiority of a postdischarge care management model for stroke survivors. *J Stroke Cerebrovasc Dis.* 2009;18(6):443–452. doi:10.1016/j.jstrokecerebrovasdis.2009.02.002
27. Chalermwannapong S, Panuthai S, Srisuphan W, Panya P, Ostwald SK. Effects of the transitional care program on functional ability and quality of life of stroke survivors. *CMU J Nat Sci.* 2010;9(1):49–66. <https://www.thaiscience.info/Journals/Article/CMUJ/10613602.pdf>. Accessed March 1, 2024.
28. Hofstad H, Gjelsvik BEB, Næss H, Eide GE, Skouen JS. Early supported discharge after stroke in Bergen (ESD Stroke Bergen): Three and six months results of a randomised controlled trial comparing two early supported discharge schemes with treatment as usual. *BMC Neurol.* 2014;14(1):239. doi:10.1186/s12883-014-0239-3
29. Wong FKY, Yeung SM. Effects of a 4-week transitional care programme for discharged stroke survivors in Hong Kong: A randomised controlled trial. *Health Soc Care Community.* 2015;23(6):619–631. doi:10.1111/hsc.12177
30. Rasmussen RS, Østergaard A, Kjær P, et al. Stroke rehabilitation at home before and after discharge reduced disability and improved quality of life: A randomised controlled trial. *Clin Rehabil.* 2016;30(3):225–236. doi:10.1177/0269215515575165
31. Santana S, Rente J, Neves C, et al. Early home-supported discharge for patients with stroke in Portugal: A randomised controlled trial. *Clin Rehabil.* 2017;31(2):197–206. doi:10.1177/0269215515627282
32. Geng G, He W, Ding L, Klug D, Xiao Y. Impact of transitional care for discharged elderly stroke patients in China: An application of the Integrated Behavioral Model. *Top Stroke Rehabil.* 2019;26(8):621–629. doi:10.1080/10749357.2019.1647650
33. Rafsten L, Danielsson A, Nordin A, et al. Gothenburg Very Early Supported Discharge study (GOTVED): A randomised controlled trial investigating anxiety and overall disability in the first year after stroke. *BMC Neurol.* 2019;19(1):277. doi:10.1186/s12883-019-1503-3
34. Deng A, Yang S, Xiong R. Effects of an integrated transitional care program for stroke survivors living in a rural community: A randomized controlled trial. *Clin Rehabil.* 2020;34(4):524–532. doi:10.1177/0269215520905041
35. Duncan PW, Bushnell CD, Jones SB, et al. Randomized pragmatic trial of stroke transitional care: The COMPASS study. *Circ Cardiovasc Qual Outcomes.* 2020;13(6):e006285. doi:10.1161/CIRCOUTCOMES.119.006285
36. Feng W, Yu H, Wang J, Xia J. Application effect of the hospital-community integrated service model in home rehabilitation of stroke in disabled elderly: A randomised trial. *Ann Palliat Med.* 2021;10(4):4670–4677. doi:10.21037/apm-21-602
37. Kam Yuet Wong F, Wang SL, Ng SSM, et al. Effects of a transitional home-based care program for stroke survivors in Harbin, China: A randomized controlled trial. *Age Ageing.* 2022;51(2):afac027. doi:10.1093/ageing/afac027
38. Jones F, Riazi A, Norris M. Self-management after stroke: Time for some more questions? *Disabil Rehabil.* 2013;35(3):257–264. doi:10.3109/09638288.2012.691938
39. Audulv Å, Hutchinson S, Warner G, Kephart G, Versnel J, Packer TL. Managing everyday life: Self-management strategies people use to live well with neurological conditions. *Patient Educ Couns.* 2021;104(2):413–421. doi:10.1016/j.pec.2020.07.025
40. Sundaresan A. Wound complications frequency in minor technique gastrectomy compared to open gastrectomy for gastric cancer: A meta-analysis. *Int J Clin Med Res.* 2023;1(3):37–48. doi:10.61466/ijcmr1030012
41. Quinn TJ, Langhorne P, Stott DJ. Barthel Index for stroke trials: Development, properties, and application. *Stroke.* 2011;42(4):1146–1151. doi:10.1161/STROKEAHA.110.598540
42. Hempler I, Woitha K, Thielhorn U, Farin E. Post-stroke care after medical rehabilitation in Germany: A systematic literature review of the current provision of stroke patients. *BMC Health Serv Res.* 2018;18(1):468. doi:10.1186/s12913-018-3235-2

Resilience of primary healthcare facilities: Experiences from 16 European countries during the COVID-19 pandemic. A mixed-methods study conducted by EURIPA

Ferdinando Petrazzuoli^{1,2,A–F}, Ozden Gokdemir^{2,3,A–F}, Maria Antonopoulou^{2,4,B,D–F}, Beata Blahová^{2,5,B,D–F}, Natasa Mrduljaš-Dujic^{2,6,A–F}, Gindrovel G. Dumitra^{2,7,B–F}, Rosario Falanga^{2,8,A–C,E,F}, Mercedes Ferreira^{2,9,B,E,F}, Sandra Gintere^{2,10,B,E,F}, Sehnaz Hatipoglu^{2,11,B,E,F}, Jean-Pierre Jacquet^{2,12,B,E,F}, Kateřina Javorská^{2,13,B,E,F}, Ana Kareli^{2,14,B,E,F}, András Mohos^{2,15,B,E,F}, Sody Naimer^{2,16,B,E,F}, Victoria Tkachenko^{2,17,B,E,F}, Angela Tomacinschi^{2,18,B,E,F}, Jane Randall-Smith^{2,A,B,D–F}, Krzysztof Kujawa^{19,C,E,F}, Donata Kurpas^{2,20,A–F}

¹ Department of Clinical Sciences, Centre for Primary Healthcare Research, Lund University, Malmö, Sweden

² European Rural and Isolated Practitioners Association (EURIPA), Paris, France

³ Department of Family Medicine, Faculty of Medicine, Izmir University of Economics, Balçova, Turkey

⁴ Spili Primary Care Center, Regional Health System of Crete, Greece

⁵ Department of Public Health, Slovak Medical University, Bratislava, Slovakia

⁶ Department of Family Medicine, School of Medicine, University of Split, Croatia

⁷ Department of Family Medicine, University of Medicine and Pharmacy, Craiova, Romania

⁸ Department of Primary Care, Western Friuli Health Authority, Pordenone, Italy

⁹ Department of Primary Care, Ferrol Health Area, Sergas, Spain

¹⁰ Department of Family Medicine, Faculty of Medicine, Riga Stradiņš University, Latvia

¹¹ Turkish Association of Family Physicians, Primary Care Center, Izmir, Turkey

¹² French College of General Practice, Paris, France

¹³ Department of Preventive Medicine, Faculty of Medicine in Hradec Kralove, Charles University, Czech Republic

¹⁴ Georgian Family Medicine Association, Tbilisi State Medical University, Georgia

¹⁵ Department of Family Medicine, Albert Szent-Györgyi Medical School, University of Szeged, Hungary

¹⁶ Department of Family Medicine, Sial Family Medicine and Primary Care Research Center, Faculty of Health Sciences, Ben-Gurion University of the Negev, Be'er Sheva, Israel

¹⁷ Department of Family Medicine, Shupyk National Healthcare University of Ukraine, Kyiv, Ukraine

¹⁸ University Clinic of Primary Medical Assistance, Nicolae Testemițanu State University of Medicine and Pharmacy, Chișinău, Moldova

¹⁹ Statistical Analysis Centre, Wrocław Medical University, Poland

²⁰ Division of Research Methodology, Department of Nursing, Faculty of Nursing and Midwifery, Wrocław Medical University, Poland

A – research concept and design; B – collection and/or assembly of data; C – data analysis and interpretation;

D – writing the article; E – critical revision of the article; F – final approval of the article

Advances in Clinical and Experimental Medicine, ISSN 1899–5276 (print), ISSN 2451–2680 (online)

Adv Clin Exp Med. 2025;34(4):487–505

Address for correspondence

Ferdinando Petrazzuoli

E-mail: ferdinando.petrazuoli@gmail.com

Cite as

Petrazuoli F, Gokdemir O, Antonopoulou M, et al.

Resilience of primary healthcare facilities: Experiences from 16 European countries during the COVID-19 pandemic. A mixed-methods study conducted by EURIPA.

Adv Clin Exp Med. 2025;34(4):487–505.
doi:10.17219/acem/194212

DOI

10.17219/acem/194212

Copyright

Copyright by Author(s)

This is an article distributed under the terms of the Creative Commons Attribution 3.0 Unported (CC BY 3.0) (<https://creativecommons.org/licenses/by/3.0/>)

Abstract

Background. The role of primary healthcare (PHC) during a pandemic varies across European countries. The coronavirus disease 2019 (COVID-19) pandemic has altered the working practices of family medicine doctors and impacted the resilience of healthcare systems.

Objectives. This study aimed to examine European healthcare system responses to the pandemic, focusing on rural and urban differences.

Materials and methods. This cross-sectional, mixed-methods study used a semi-structured online questionnaire with 68 questions, including 21 free-text comments. Data were collected from May 2020 to January 2021. Key informants from 16 European Rural and Isolated Practitioners Association (EURIPA) member countries distributed questionnaires to 406 PHC doctors. Data were analyzed using descriptive statistics and nonparametric tests (χ^2 , Kruskal–Wallis, Mann–Whitney U) with a significance threshold of 0.05.

Results. A statistically significant difference was found between rural (36.4%, 55/151), semirural (19.4%, 24/124) and urban populations (29.8%, 39/131) regarding medicine shortages ($\chi^2 = 9.91$, degrees of freedom (df) = 4, $p = 0.042$). The semirural setting showed a statistically significant difference from the other settings

Funding sources

None declared

Conflict of interest

None declared

Acknowledgements

We would like to thank primary care physicians across Europe who have actively collaborated in responding to this survey.

Received on June 2, 2024

Reviewed on September 15, 2024

Accepted on October 7, 2024

Published online on December 16, 2024

($p = 0.004$ in post hoc χ^2 test). Significant differences were found between countries in resilience features including, effectiveness of triage, adapting to the rapidly changing requirements, government help, existence of a community resilience group, improved interprofessional collaboration, medicine shortage, and general practitioners (GPs) involvement in palliative care.

Conclusions. Medicine shortage was more prevalent in rural and urban areas compared to semirural areas. Differences were observed between countries in their responses to the pandemic, particularly in adapting to the rapidly changing requirements, effectiveness of triage, government help, and the existence of a community resilience group. These differences were confirmed with qualitative analysis. The results emphasize the need for tailored approaches considering diverse contexts in shaping effective healthcare system resilience.

Key words: rural health, COVID-19, resilience, primary care

Background

Caring for patients with novel coronavirus infections has placed an immense burden on healthcare systems and healthcare workers worldwide. The COVID-19 pandemic, unlike any previous health crisis, has demanded a prolonged and sustained response, akin to a marathon rather than a sprint. This has necessitated that leaders and managers within healthcare organizations carefully pace their strategies and responses to ensure long-term efficacy and sustainability of the healthcare systems.¹

Rural areas tend to have a higher proportion of elderly patients and patients with multiple medical comorbidities.² The shortage of medical specialists, hospital beds and intensive care unit (ICU) beds, as well as the financial problems of many rural hospitals, is a widespread problem worldwide, made more apparent by the COVID-19 pandemic.^{3,4} The lack of personal protective equipment and medications further exacerbates such difficulties. Rural areas are particularly vulnerable during such pandemics due to a higher proportion of elderly patients and individuals with multiple comorbidities.⁵ The chronic shortage of medical specialists, hospital beds and ICU beds, compounded by the financial struggles of many rural hospitals, has been starkly highlighted by the COVID-19 crisis.⁴ Furthermore, the lack of essential resources such as personal protective equipment (PPE) and medications has exacerbated the situation.³ Since February 2020, when COVID-19 began to spread rapidly in Italy, general practitioners (GPs) worldwide have faced the daunting task of managing an unexpected and severe public health challenge.⁶ In the initial stages, health services struggled to recognize and treat suspected cases promptly, leading to increased infection rates and overwhelming healthcare systems. Over time, primary care physicians adapted to the new reality, incorporating teleconsultations, reducing face-to-face interactions and meeting the new demands imposed by the pandemic.^{7,8} Training programs also underwent significant changes, with distance learning being rapidly and successfully implemented across Europe, even in rural areas.⁹

The pandemic has also exposed significant gaps in healthcare infrastructure and support systems. In countries like the UK, the inadequate provision of PPE to healthcare and social care workers during the pandemic was perceived as a betrayal by the government and National Health Service (NHS), undermining the culture of integrity, transparency and support essential for healthcare workers.¹⁰ It is important to recognize that epidemics have a significant impact on daily life, even for those who are not infected. Some recent studies have shown that community volunteers can help provide social distance and minimize disease transmission.¹¹ The role of primary healthcare (PHC) in a pandemic varies across Europe.¹² For example, in the UK, PHC has been effectively involved in managing post-acute COVID-19 conditions, often providing care remotely via telephone or video consultations.^{13,14}

Palliative care presents another critical opportunity for PHC during pandemics. According to Prof. Scott Murray and in line with the World Health Organization's (WHO) statement, the COVID-19 pandemic has underscored the need to integrate palliative care into national healthcare services to enhance quality of life and alleviate suffering in the final stages of life.¹⁵

The COVID-19 pandemic has necessitated rapid innovation across healthcare systems. Family medicine practices, in particular, have faced unique challenges in maintaining care for medically complex older populations. They have had to adapt their traditionally hands-on model of care to accommodate the limitations on face-to-face contact while ensuring the safety of older, medically complex patients in their homes. This required significant flexibility, transparency, teamwork, and partnerships with external providers.^{16,17}

Objectives

This study aimed to examine the attitude of European healthcare systems in responding to the pandemic, with particular attention to PHC and the difference between

rural and urban areas. Searching and understanding the specificity of differences in PHC between European countries, considering urban and rural settings, is essential for creating a more resilient, inclusive and effective health-care system that can better withstand future challenges and emergencies.

Methods

Study design and setting

This study is based on a survey of key informants from 16 member countries of the European Rural and Isolated Practitioners Association (EURIPA) that operate under the umbrella of the World Organization of National Colleges, Academies and Academic Associations of General Practitioners/Family Physicians (WONCA Europe). More details on the study design and setting are described elsewhere.¹⁸

Procedure

The steering committee of this project, called the EURIPA COVID-19 study, developed a semi-structured questionnaire with 68 questions, 21 of these including free-text comments. The open-ended (free-text) responses to some questions were included to explore the issues pragmatically and at a deeper level, considering the complexity of COVID-19 pandemic management.¹⁹ The 1st draft of the questionnaire was based on the research objectives through an extensive literature review. Subsequently, a panel of PHC experts and 1 methodology expert used a Delphi method to evaluate the validity of the items and the length of the questionnaire, formulated suggested changes and identified missing items. The research team then discussed all feedback until consensus was reached, and a 2nd version of the questionnaire was developed. Data were collected between May 2020 and January 2021 using Google's online survey tool – Google Forms.

Validity

The psychometric properties of the questionnaire were assessed, focusing on validity as a theoretical and an empirical construct. During the development of the questionnaire, face validity (whether the questionnaire measures at first glance what it purports to measure) and content validity (whether the items adequately represent the entire domain that the questionnaire attempts to measure) were tested. In each case, this was done by EURIPA PHC experts, who are all international authorities in the field of rural healthcare. The informants were contacted directly via email by the national coordinators, and the response rates were all above 50%.

Participants

The EURIPA, which currently includes 31 member countries, is a representative network organization founded by family doctors to address the health and well-being needs of rural communities and the professional needs of those serving them across Europe (<https://www.euripa.org/page/home>). Although there are several official definitions of rurality for example those developed by WHO and EU, all of them based on solid objective data but with severe limitations in capturing the difference in the mentality between urban and rural setting, for the purpose of our study we have preferred a self-reported statement of the respondents, who characterized the place of their practice as rural, semirural and urban, and this kind of procedure has been repeatedly used in other international studies in PHC.²⁰

The informants were contacted directly by the national coordinators; they were required to be primary care practitioners (PCPs, i.e., any professional working in PHC such as a doctor, nurse, physiotherapist, or assistant) with a good command of English, as the survey was written in English and was not translated into other languages. The baseline characteristics of the informants, broken down by country, and some descriptive statistics are shown in Table 1.

Because a convenience sample of informants was used, the PCPs for each country may not be representative, although there was an attempt to achieve geographical variation.

Study size

When the number of respondents reached or exceeded 30 for countries with a population of 35 million or more, and 20 for countries with a population of less than 35 million, data collection for that country was terminated.

Main outcome measures

The questionnaire consisted of 68 questions including sociodemographic variables, length of clinical experience and experience in dealing with the COVID-19 pandemic, and geographic location (see Supplementary data). The questionnaire was divided into several sections. In this paper, we analyzed the questions related to healthcare system resilience. The other sections of the questionnaire will be analyzed in separate papers.

Participants with complete data could not be distinguished from the less than 10% of participants with incomplete or missing data, which were then considered “Missing Completely at Random” (MCAR) data. We used the “Complete Case Analysis” method in IBM SPSS v. 29.0 (IBM Corp., Armonk, USA) and removed all participants with incomplete data from the analysis.

Table 1. Characteristics of the respondents

Country	Respondents n (%)	Age mean (SD)	Seniority mean (SD)	Male gender n (%)	Location of practice		
					urban n (%)	semirural n (%)	rural n (%)
Croatia	20 (5)	52.9 (8.5)	26.3 (9.8)	6 (30)	6 (30)	6 (30.0)	8 (40)
Czech Republic	22 (5)	36.3 (5.5)	9.0 (5.4)	14 (60)	9 (40)	8 (36.3)	5 (23)
France	30 (7)	45.8 (12.5)	16.8 (12.5)	12 (40)	4 (13)	11 (36.7)	15 (50)
Georgia	31 (8)	45.0 (8.3)	13.6 (8.0)	3 (10)	12 (39)	7 (22.6)	12 (39)
Greece	20 (5)	49.5 (7.2)	20.1 (7.6)	11 (55)	1 (5)	3 (15.0)	16 (80)
Hungary	20 (5)	47.8 (12.2)	19.3 (12.3)	13 (65)	5 (25)	2 (10.0)	13 (65)
Israel	22 (5)	51.1 (11.9)	22.1 (11.3)	15 (68)	5 (23)	12 (54.6)	5 (23)
Italy	31 (8)	53.6 (14.2)	25.4 (14.7)	22 (71)	13 (42)	11 (35.5)	7 (23)
Latvia	25 (6)	49.3 (12.3)	22.9 (15.7)	3 (12)	10 (40)	10 (40)	5 (20)
Moldova	21 (5)	40.3 (11.2)	14.0 (10.9)	2 (11)	14 (67)	3 (14)	4 (19)
Poland	34 (8)	45.6 (10.9)	17.8 (10.8)	13 (37)	17 (50)	8 (24)	9 (7)
Romania	20 (5)	49.9 (7.8)	22.0 (10.0)	5 (25)	6 (30)	1 (5)	13 (65)
Slovakia	20 (5)	46.0 (8.9)	15.9 (12.6)	6 (30)	6 (30)	7 (35)	7 (35)
Spain	28 (7)	47.7 (9.3)	21.2 (8.9)	12 (43)	0 (0)	7 (25)	21 (75)
Turkey	31 (8)	39.3 (8.7)	13.2 (8.2)	14 (45)	10 (32)	14 (45)	7 (23)
Ukraine	31 (8)	38.4 (9.4)	13.4 (8.1)	9 (29)	12 (39)	14 (45)	5 (16)
Total	406 (100)	46 (11.3)	18.2 (11.6)	160 (40)	130 (32)	124 (30.5)	152 (37.5)

SD – standard deviation.

Analyses

To describe baseline characteristics, proportions were calculated for dichotomized or categorized data and means for numeric variables. We used the mean also for non-normally distributed data to show some slight differences between countries.

Pearson's χ^2 test of independence was used to measure the association between categorical variables, followed by the post hoc χ^2 test based on comparing of response frequencies between a given country and all the other countries together. To control the false discovery rate, the Benjamini–Hochberg correction was used with the aid of the R package 'base' (the command 'p.adjust'). As the numeric data were not normally distributed, when comparing the scores between the groups, we used non-parametric tests such as the Kruskal–Wallis test with the post hoc Dunn's test (with the Bonferroni correction) and the Mann–Whitney U test. The statistical significance threshold was set at 0.05.

Statistical package: statistics were obtained using IBM SPSS Statistics for Windows v. 29 (IBM Corp.), Microsoft Excel 2013 (Microsoft Corp., Redmond, USA) and the R environment v. 4.3.2 (R Foundation for Statistical Computing, Vienna, Austria).

Because responses were limited to short sentences for the open-ended questions, a brief conceptual qualitative content analysis was conducted. Responses (direct quotes)

from PCPs were independently reviewed by 2 members of the research team (D.K. and O.G.).

Ethical issues

Respondents' answers were collected anonymously; no formal approval from an ethics committee was required in the countries participating in the survey. Informants were aware that they could stop the survey at any time. Informed consent was obtained. Confidentiality and anonymity were assured. The study was conducted in accordance with the principles of the Declaration of Helsinki.

The questions analyzed in Table 2 are as follows:

- Have you been able to receive help from community volunteers in this pandemic?
Yes, Maybe, No
- How is the triage of patients with suspected COVID-19 working in your rural area?
(5-point Likert scale)
- How easy have you found it to keep up to date with rapidly changing requirements?
(5-point Likert scale)
- How is your government addressing the needs of clinicians and patients in rural and remote areas?
(5-point Likert scale)
- Is there a community resilience group meeting to coordinate access to essential services including transport?
Yes, Maybe, No

Table 2. Resilience features

Country	Community volunteers' help n/total (%)	Effectiveness of triage (5-point Likert scale) mean (SD)	Adapting to the rapidly changing requirements (5-point Likert scale) mean (SD)	Government help (5-point Likert scale) mean (SD)	Existence of a community resilience group n/total (%)
Croatia	8/20 (40.0)	3.20 (1.1)	3.05 (0.8)	2.75 (1.0)	12/20 (60.0)
Czech Republic	12/22 (52.2)	2.68 (1.0)	3.00 (1.1)	1.96 (0.8)	8/23 (34.8)
France	8/30 (26.7)	2.76 (1.0)	2.93 (1.2)	2.72 (1.2)	5/30 (16.7)
Georgia	13/31 (41.9)	3.81 (1.0)	3.48 (0.9)	3.48 (0.8)	6/31 (19.4)
Greece	10/20 (50.0)	3.00 (1.3)	3.15 (0.9)	3.15 (1.1)	3/20 (15.0)
Hungary	6/20 (30.0)	3.45 (1.0)	2.35 (0.9)	2.15 (0.9)	2/20 (10.0)
Israel	10/22 (45.5)	3.36 (1.2)	3.41 (1.0)	2.95 (1.2)	5/22 (22.7)
Italy	11/31 (35.5)	3.10 (1.1)	2.59 (0.8)	2.31 (1.1)	4/31 (12.9)
Latvia	8/25 (32.0)	3.32 (1.0)	3.04 (0.7)	2.88 (0.8)	10/25 (40.0)
Moldova	4/19 (21.1)	3.05 (1.4)	3.37 (0.8)	2.42 (1.1)	13/19 (68.4)
Poland	10/35 (28.6)	3.18 (1.0)	3.35 (1.0)	2.50 (1.1)	12/35 (34.3)
Romania	2/20 (10.0)	3.74 (1.0)	2.60 (0.9)	1.70 (0.9)	5/20 (25.0)
Slovakia	4/20 (20.0)	2.50 (1.4)	2.95 (1.1)	2.45 (1.4)	10/20 (50.0)
Spain	9/28 (32.1)	3.11 (1.2)	3.21 (1.1)	2.61 (1.2)	12/28 (42.9)
Turkey	11/31 (35.5)	3.35 (1.3)	3.40 (1.0)	2.93 (1.1)	8/31 (25.8)
Ukraine	5/31 (16.1)	3.27 (1.1)	3.29 (0.8)	2.97 (1.1)	9/31 (29.0)
Statistics	$\chi^2 = 34.62$, df = 15, p = 0.256	Kruskal–Wallis test = 33.68 (df = 15) p = 0.004	Kruskal–Wallis test = 42.77 (df = 15) p < 0.001	Kruskal–Wallis test = 61.98 (df = 15) p < 0.001	χ^2 (15, n = 406) = 69.80, p < 0.001

SD – standard deviation; df – degrees of freedom; bold font indicates statistical significance.

Table 3. Improved interprofessional collaboration

Country	Yes n/total (%)	Maybe n/total (%)	No n/total (%)
Croatia	12/20 (60.0)	5/20 (25.0)	3/20 (15.0)
Czech Republic	11/23 (47.8)	4/23 (17.4)	8/23 (34.8)
France	14/30 (46.7)	6/30 (20.0)	10/30 (33.3)
Georgia	14/31 (45.2)	7/31 (22.6)	10/31 (32.3)
Greece	3/20 (15.0)	6/20 (30.0)	11/20 (55.0)
Hungary	12/20 (60.0)	5/20 (25.0)	3/20 (15.00)
Israel	7/22 (31.8)	2/22 (9.1)	13/22 (59.1)
Italy	14/31 (45.2)	7/31 (22.5)	10/31 (32.3)
Latvia	12/25 (48.0)	11/25 (44.0)	2/25 (8.0)
Moldova	14/19 (73.7)	5/19 (26.3)	0.0 (0.0)
Poland	17/35 (48.6)	9 (35) (25.7)	9/35 (25.7)
Romania	10/20 (50.0)	4/20 (20.0)	6/20 (30.0)
Slovakia	15/20 (75.0)	2/20 (10.0)	3/20 (15.0)
Spain	17/28 (60.7)	3/28 (10.7)	8/28 (28.6)
Turkey	8/31 (25.8)	9/31 (29.0)	14/31 (45.2)
Ukraine	13/31 (41.9)	8/31 (25.8)	10/31 (32.3)

$\chi^2 = 72.88$; degrees of freedom (df) = 45; p < 0.005.

The question analyzed in Table 3 is as follows: Did the cooperation and collaboration with other disciplines/ services change during this pandemic?

Yes, Maybe, No

Table 4. Medicine shortage

Country	Yes n/total (%)	Maybe n/total (%)	No n/total (%)
Croatia	6/20 (30.0)	2/20 (10.0)	12/20 (60.0)
Czech Republic	6/23 (26.1)	3/23 (13.0)	14/23 (60.9)
France	8/30 (26.7)	6/30 (20.0)	16/30 (53.3)
Georgia	2/31 (6.5)	0/0 (0.0)	29/31 (93.5)
Greece	2/20 (10.0)	2/20 (10.0)	16/20 (80.0)
Hungary	9/20 (45.0)	3/20 (15.0)	8/20 (40.0)
Israel	1/22 (4.5)	1/22 (4.5)	20/22 (90.9)
Italy	15/31 (48.4)	1/31 (3.2)	15/31 (48.4)
Latvia	5/25 (20.0)	9/25 (36.0)	11/25 (44.0)
Moldova	5/19 (26.3)	3/19 (15.8)	11/19 (57.9)
Poland	16/35 (45.7)	6/35 (17.2)	13/35 (37.1)
Romania	12/20 (60.0)	2/20 (10.0)	6/20 (30.0)
Slovakia	7/20 (35.0)	4/20 (20.0)	9/20 (45.0)
Spain	9/28 (32.1)	26/28 (7.2)	17/28 (60.7)
Turkey	7/31 (22.6)	4/31 (12.9)	20/31 (64.5)
Ukraine	8/31 (25.8)	5/31 (16.1)	18/31 (58.1)

$\chi^2 = 72.82$; degrees of freedom (df) = 30; p < 0.001.

The question analyzed in Table 4 is as follows: Have you and your patients had any issues with access to supply of certain medicines during this pandemic?

Yes, Maybe, No

Table 5. General practitioners involvement in palliative care

Country	Yes n/total (%)	No n/total (%)	Other n/total (%)
Croatia	7/20 (35.0)	12/60 (60.0)	1/20 (5.0)
Czech Republic	9/23 (40.9)	12/23 (50.0)	2/23 (9.1)
France	17/30 (56.7)	12/30 (40.0)	1/30 (0.3)
Georgia	12/31 (38.7)	18/31 (58.1)	1/31 (3.2)
Greece	11/20 (55.0)	8/20 (40.0)	1/20 (5.0)
Hungary	10/20 (50.0)	10/20 (50.0)	0/20 (0.0)
Israel	4/22 (18.2)	15/22 (62.8)	3/22 (16.0)
Italy	11/31 (35.5)	18/31 (58.1)	2/31 (6.4)
Latvia	12/25 (48.0)	12/25 (48.0)	1/25 (4.0)
Moldova	13/19 (68.4)	6/19 (31.6)	0/0 (0.0)
Poland	11/35 (31.4)	24/35 (68.6)	0/0 (0.0)
Romania	7/20 (35.0)	13/20 (65.0)	0/0 (0.0)
Slovakia	2/20 (10.0)	16/20 (80.0)	2/20 (10.0)
Spain	19/28 (67.9)	8/28 (28.6)	1/28 (3.5)
Turkey	9/31 (29.0)	21/31 (67.7)	1/31 (3.3)
Ukraine	8/31 (25.8)	23/31 (74.2)	0/0 (0.0)

n – number; $\chi^2 = 72.86$; degrees of freedom (df) = 45; $p < 0.005$.

The question analyzed in Table 5 is as follows: Do you administer supportive and palliative care on your own in COVID-19 patients?

Yes, No, Other

Results

Participants

A total of 406 PHC informants from 16 European countries completed the questionnaires. Of these, 245 (60.5%) were female and 160 (39.5%) were male. Regarding practice location, 152 PHC informants were rural (37.5%), 124 were semirural (30.5%) and 130 were urban (32.0%).

Descriptive data

The mean age of respondents was 45.9 years (standard deviation (SD) 11.30) and the mean length of service was 18.2 years (SD 11.6). Three hundred and eighty-one (93.8%) of the respondents were GPs/family doctors. The remaining 24 respondents (6%) represented a range of other medical specialties, including nurses, doctors, managers, social workers, midwives, dentists, and physical therapists.

Main results

The baseline characteristics of the informants, broken down by country, and some descriptive statistics are shown

in Table 1. The countries involved in the study are illustrated in Fig. 1.

Community volunteers' help

There were differences between countries on the questions related to community volunteer assistance. According to our informants, the percentage of those who stated that they have received community volunteers' help varied from 10% (2/20) in Romania to 52.2% (12/22) in the Czech Republic (Table 2). The relationship between the variables "country" and "community volunteers' help" was statistically insignificant ($\chi^2 = 34.627$, degrees of freedom (df) = 30, $p < 0.256$).

Qualitative analysis

Community help was differentiated within a country and organized locally. Negative comments dominated: "Nobody offers any kind of help. They run away from it" [Croatia_1]; "There are no volunteers in our region" [Greece_3; Romania_2; Slovakia_3,4]. The assistance was mainly related to volunteer support for patients staying at home: "We had sewing masks for patients in the first wave of COVID" [Czech Republic_7]; "PSAs from volunteers, companies or friends" [France_1; Slovakia_2,5; Ukraine_1,3]; "They delivered food and medicines to patients' homes" [Georgia_1,2,3,4; Israel_2]; "Civil Protection and other volunteers delivered free drug prescriptions and medicines to patients with chronic diseases. They also distributed face masks to patients" [Italy_1].

Effectiveness of triage

In our study, most respondents stated that triage worked well, with an average score above 3 on the Likert scale, while only 3 countries, Slovakia, France and the Czech Republic, scored below 3. Respondents indicated that guidelines on clinical management of COVID-19 existed in all countries and that triage was organized similarly.

The lowest score was obtained in Slovakia (2.50, SD 1.40) and the highest score in Georgia (3.81, SD 1.00), but we must point out that this is the "subjective" perception of the success of the triage by the respondents and not an objective evaluation (Table 2, Fig. 2). There was a significant difference across the 16 European countries (Kruskal–Wallis test: $H(15, 400) = 33.683$, $p = 0.004$). Post hoc Dunn's test of the differences in the effectiveness of triage between the countries is illustrated in Table 6.

Qualitative analysis

Guidelines existed in all countries, and triage was organized similarly: "We have algorithms for this" [Croatia_5]; "We follow the described symptoms. If it is necessary,

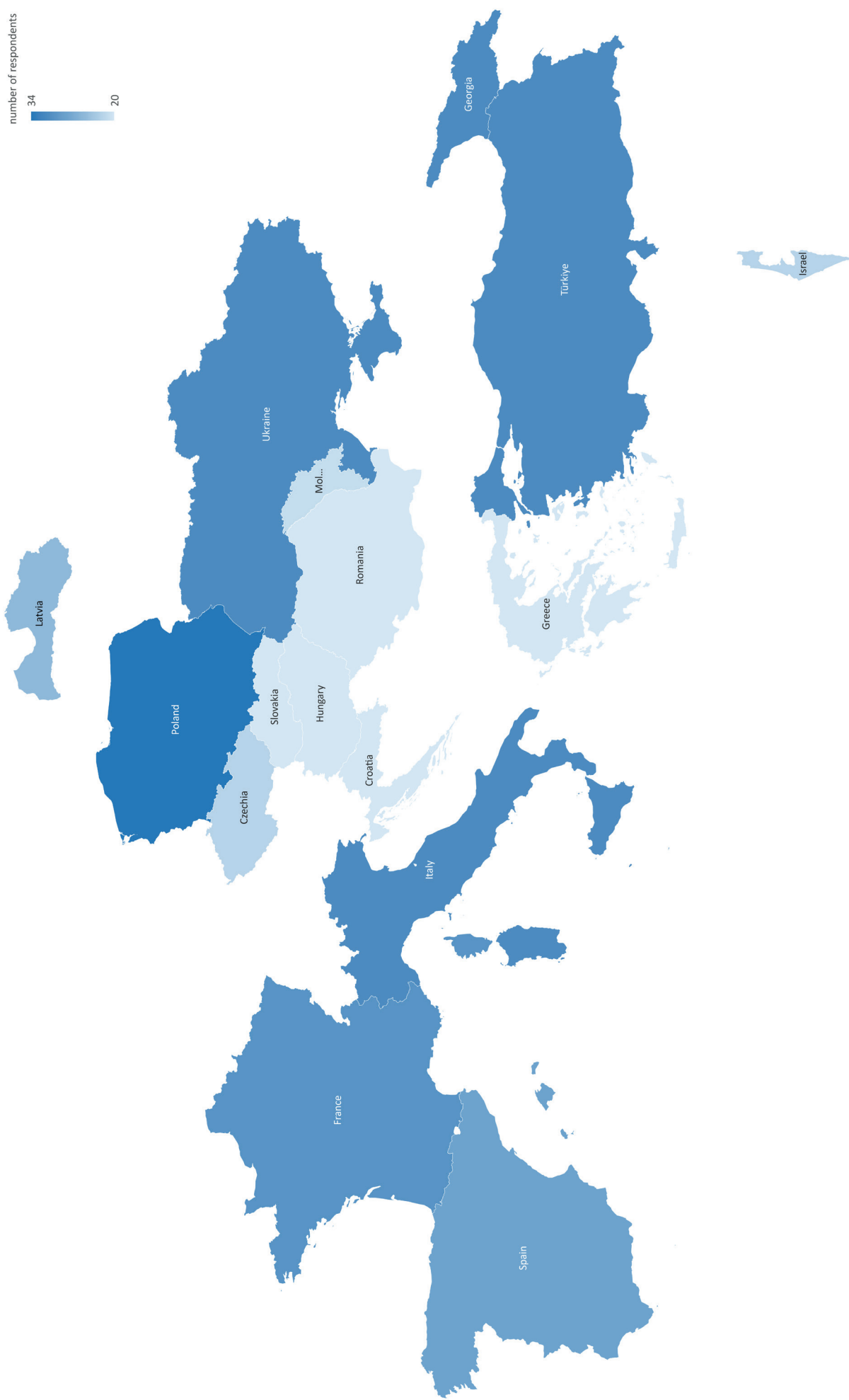


Fig. 1. Countries involved in the study

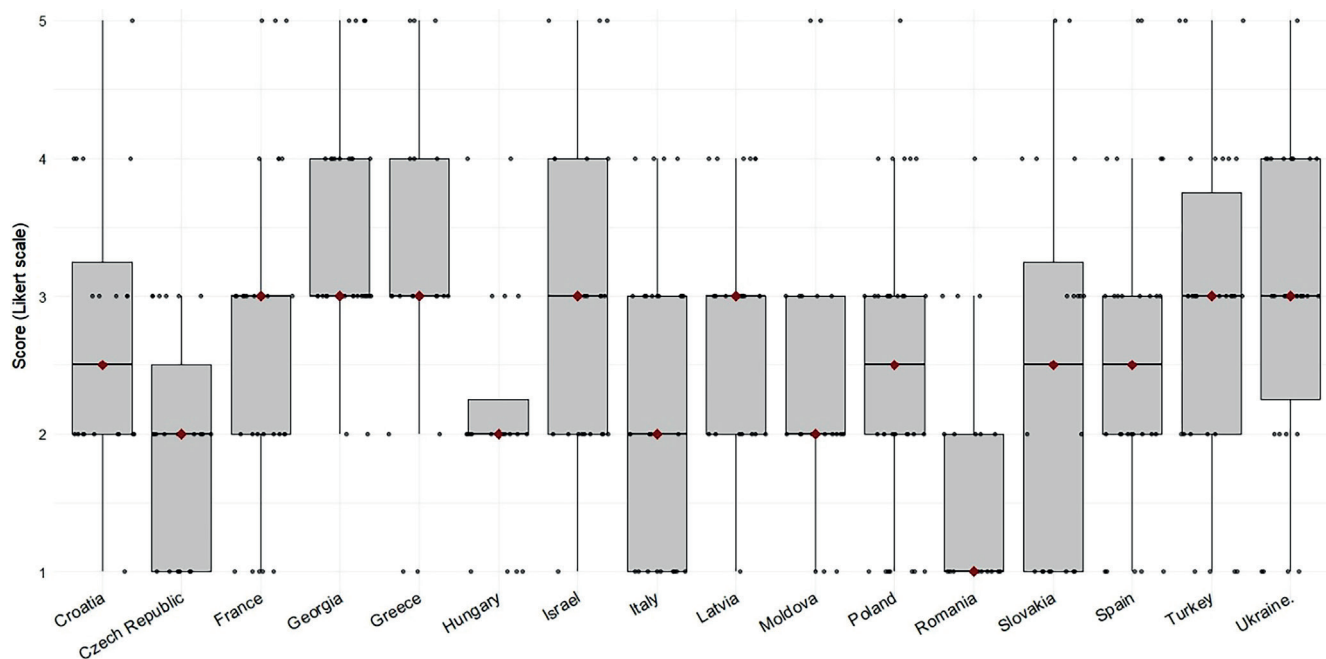


Fig. 2. Effectiveness of triage. Boxplots show the distribution of effectiveness of triage score. The horizontal line in each box indicates the median. Vertical lines extending from the top and bottom of each box end at the max and min values. Upper and lower margins of the boxplot represent the 25th and 75th percentiles

patients have to call the ambulance” [Czech Republic_8]; “Special places for those with suspicious symptoms, organization of remote consultations, for those with high suspicion of COVID-testing and isolation measures, contact tracing in coordination with health authorities via a special online application” [France_1; Greece_4; Hungary_2,3; Moldova_1; Poland_1; Romania_1,3; Turkey_1,3]; “Telephone interview before ordering an appointment, triage at the entrance of the clinic” [Israel_2]. However, “inadequate communication between GPs and hospitals was noted” [Czech Republic_9].

Adapting to the rapidly changing requirements

In our survey, responses on a 5-point Likert scale showed that the majority of our informants found it relatively easy to adapt to the rapidly changing requirements (score above 3). Only in France, Hungary, Italy, Romania, and Slovakia the average score was below 3. The free-text responses showed that GPs were rather confused by the “too many sources, too many changes.” The lowest average score was obtained in Hungary (2.35, SD 0.88 and the highest in Georgia (3.48, SD 0.85, Table 2, Fig. 3. There was a significant difference in the responses to this question across the 16 European countries (Kruskal–Wallis test: $H(15, 402) = 42.772, p < 0.001$).

Post hoc Dunn’s test results of the differences in “adapting to the rapidly changing requirements” between the countries are provided in Table 7.

Qualitative analysis

The most common response from participants was “too many sources, too many changes” [Latvia_9,17; Slovakia_1,4,13,15,20; Poland_5; Romania_1,14; Czech Republic_1,7,18,21; Spain_16,17; France_1,3,10,19,25; Greece_10; Italy_14,28,29; Israel_9]), although in some countries, the problem was “not to be informed” or “late information” [Hungary_1,4,6,16,18,20; Latvia_19,21; Ukraine_15]. Through evidence-based practices, guidelines and patient education, the information storm has both negative and positive effects. While governments published “conflicting statements”, [Czech Republic_18,21], physicians sought to ease the burden for themselves and colleagues through webinars [Greece_12; Israel_10; Italy_2; Spain_3; Poland_12,13,23], professional associations [Poland_11; Romania_11], family medicine department websites [France_1], local hospital email groups [France_9], Facebook groups [Czech Republic_11], and WhatsApp groups [Italy_19]. Only [Slovakia_12,19] reported that “the ministry has established a crisis team that issues guidelines and distributes them via app”, while [Latvia_11; Spain_3,13; Turkey_30] reported that “... daily information was provided via email.”

Government help

Most respondents (except in Greece) rated their answers less than 3 on the 5-point Likert scale, indicating a high level of dissatisfaction among GPs with their respective governments. General practitioners felt neglected and undervalued compared with hospital staff.

Table 6. Post hoc Dunn's test of the differences in the effectiveness of triage between the countries

Country	Czech Republic	France	Georgia	Greece	Hungary	Israel	Italy	Latvia	Moldova	Poland	Romania	Slovakia	Spain	Turkey	Ukraine
Croatia	1	1	1	1	1	1	1	1	1	1	1	1	1	1	1
Czech Republic	–	1	0.040	1	1	1	1	1	1	1	0.429	1	1	1	1
France	1	–	0.044	1	1	1	1	1	1	1	0.573	1	1	1	1
Georgia	0.040	0.044	–	1	1	1	1	1	1	1	1	0.022	1	1	1
Greece	1	1	1	–	1	1	1	1	1	1	1	1	1	1	1
Hungary	1	1	1	1	–	1	1	1	1	1	1	1	1	1	1
Israel	1	1	1	1	1	–	1	1	1	1	1	1	1	1	1
Italy	1	1	1	1	1	1	–	1	1	1	1	1	1	1	1
Latvia	1	1	1	1	1	1	1	–	1	1	1	1	1	1	1
Moldova	1	1	1	1	1	1	1	1	–	1	1	1	1	1	1
Poland	1	1	1	1	1	1	1	1	1	–	1	1	1	1	1
Romania	0.429	0.573	1	1	1	1	1	1	1	1	–	0.247	1	1	1
Slovakia	1	1	0.021	1	1	1	1	1	1	1	0.247	–	1	1	1
Spain	1	1	1	1	1	1	1	1	1	1	1	1	–	1	1
Turkey	1	1	1	1	1	1	1	1	1	1	1	1	1	–	1

Bold font indicates statistical significance; “1” is an abbreviation of p-values >0.999.

Table 7. Post hoc Dunn's test of the differences in adapting to the rapidly changing requirements between the countries

Country	Czech Republic	France	Georgia	Greece	Hungary	Israel	Italy	Latvia	Moldova	Poland	Romania	Slovakia	Spain	Turkey	Ukraine
Croatia	1	1	1	1	1	1	1	1	1	1	1	1	1	1	1
Czech Republic	–	1	1	1	1	1	1	1	1	1	1	1	1	1	1
France	1	–	1	1	1	1	1	1	1	1	1	1	1	1	1
Georgia	1	1	–	1	0.019	1	0.042	1	1	1	0.511	0.022	1	1	1
Greece	1	1	1	–	1	1	1	1	1	1	1	1	1	1	1
Hungary	1	1	0.019	1	–	0.141	1	1	0.223	0.055	1	1	1	1	1
Israel	1	1	1	1	0.141	–	0.353	1	1	1	1	1	1	1	1
Italy	1	1	0.042	1	1	0.353	–	1	0.560	0.131	1	1	1	1	1
Latvia	1	1	1	1	1	1	1	–	1	1	1	1	1	1	1
Moldova	1	1	1	1	0.223	1	0.560	1	–	1	1	1	1	1	1
Poland	1	1	1	1	0.055	1	0.131	1	1	–	1	1	1	1	1
Romania	1	1	0.511	1	1	1	1	1	1	1	–	0.247	1	1	1
Slovakia	1	1	1	1	1	1	1	1	1	1	1	–	1	1	1
Spain	1	1	1	1	0.552	1	1	1	1	1	1	1	–	1	1
Turkey	1	1	1	1	0.054	1	0.130	1	1	1	1	1	1	–	1

Bold font indicates statistical significance; “1” is an abbreviation of p-values >0.999.

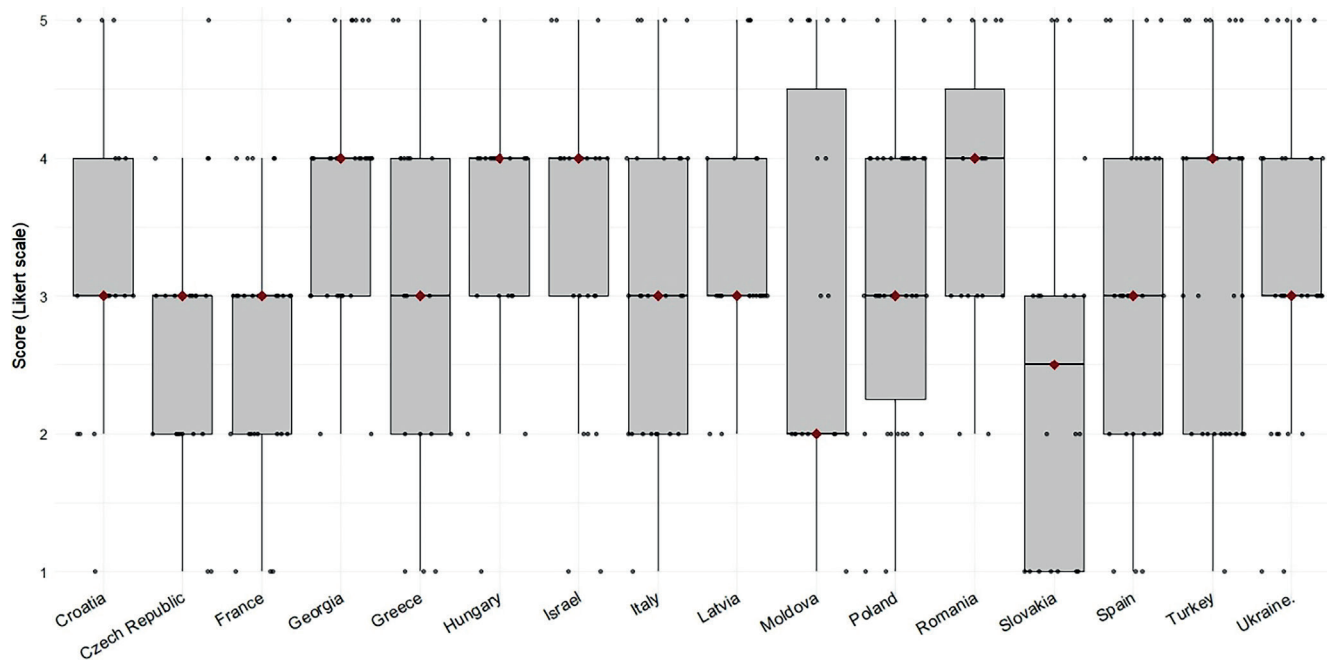


Fig. 3. Adapting to the rapidly changed requirements. Boxplots show the distribution of effectiveness of triage score. The horizontal line in each box indicates the median. Vertical lines extending from the top and bottom of each box end at the max and min values. Upper and lower margins of the boxplot represent the 25th and 75th percentiles

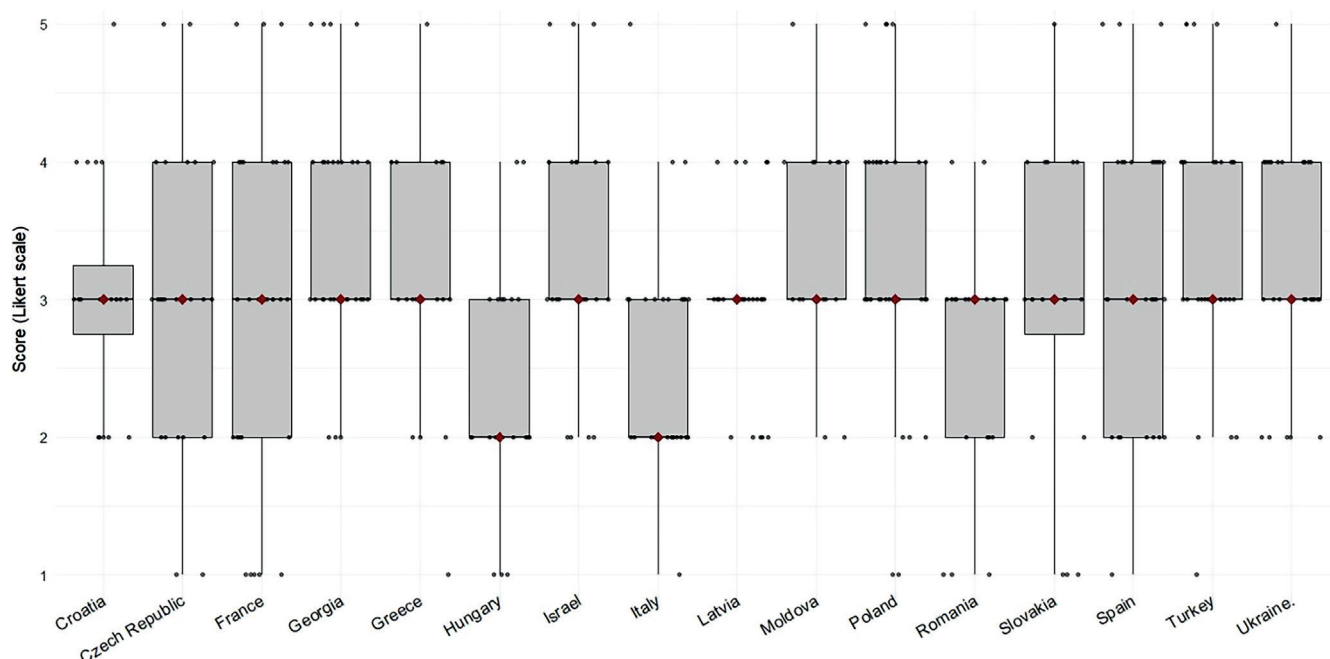


Fig. 4. Adapting to the rapidly changed requirements. Boxplots show the distribution of effectiveness of triage score. The horizontal line in each box indicates the median. Vertical lines extending from the top and bottom of each box end at the max and min values. Upper and lower margins of the boxplot represent the 25th and 75th percentiles

Our respondents seemed disappointed with the official help they received, and the average score above 3 was achieved only in Greece (3.15, SD 1.1) and Georgia (3.48, SD 0.8). All other countries were below 3, with the minimum in Romania (1.70, SD 0.9; Table 2, Fig. 4). The differences between the countries were statistically significant in Kruskal–Wallis test ($H(15, 400) = 61.981, p < 0.001$). The results of the post hoc test for pairwise comparisons are shown in Table 8.

Qualitative analysis

Many GPs seemed dissatisfied with the help they received from their government: “They did not even answer my questions”; “Often we hear some information in the news rather than getting it officially”; “they did not take us important” [Croatia_2; Hungary_3; Spain_4]; “We often have to help ourselves”, “They do not think

Table 8. Post hoc Dunn's test of the differences in government help in rural areas between the countries

Country	Czech Republic	France	Georgia	Greece	Hungary	Israel	Italy	Latvia	Moldova	Poland	Romania	Slovakia	Spain	Turkey	Ukraine
Croatia	1	1	1	1	1	1	1	1	1	1	0.596	1	1	1	1
Czech Republic	–	1	<0.001	0.092	1	0.737	1	0.422	1	1	1	1	1	1	1
France	1	–	0.883	1	1	1	1	1	1	1	0.372	1	1	1	1
Georgia	<0.001	0.883	–	1	0.004	1	0.014	1	0.086	0.069	<0.001	0.022	1	1	1
Greece	0.092	1	1	–	0.683	1	1	1	1	1	0.010	1	1	1	1
Hungary	1	1	0.004	0.683	–	1	1	1	1	1	1	1	1	1	1
Israel	0.737	1	1	1	1	–	1	1	1	1	0.104	1	1	1	1
Italy	1	1	0.014	1	1	1	–	1	1	1	1	1	1	1	1
Latvia	0.422	1	1	1	1	1	1	–	1	1	0.052	1	1	1	1
Moldova	1	1	0.086	1	1	1	1	1	–	1	1	1	1	1	1
Poland	1	1	0.069	1	1	1	1	1	1	–	1	1	1	1	1
Romania	1	0.372	<0.001	0.010	1	0.104	1	0.052	1	1	–	0.247	1	1	1
Slovakia	1	1	0.166	1	1	1	1	1	1	1	1	–	1	1	1
Spain	1	1	0.309	1	1	1	1	1	1	1	1	1	–	1	1
Turkey	0.2538	1	1	1	1	1	1	1	1	1	0.027	1	1	–	1

Bold font indicates statistical significance, "1" is an abbreviation of p-values >0.999.

at all"; "The doctors are left to their own devices"; "It was chaotic"; "We need more staff"; "The health centers were closed and all appointments were centralized in one village. Three months later, the remaining health centers are still closed and patients have to travel several kilometers to reach a nurse/doctor when needed" [Czech Republic_2,3; Italy_4; Slovakia_4, Spain_5,6]; "It all depends on the financial possibilities of the office itself"; "Poor (you have to buy almost everything out of your own pocket)" [Croatia_2; Ukraine_2]; "Pandemic or not, the problems are the same" [France_9]; "Where is the government?", "They have their heads in the clouds, they have no idea what is real!" [France_10; Romania_1]. "Not fast sometimes"; "slow"; "information, medical equipment and security for employees provides a long time"; "sometimes a small delay, also depends on the personal efforts of a particular worker, a pretty good situation" [Greece_1; Latvia_2; Poland_1; Slovakia_2]; "The government only cares about fines and restricts people" [Greece_2]; "I think they just issue some guidelines on a website and do not really know if we have read or understood them" [Greece_3].

Some respondents indicated that the situation is much worse in rural areas than in urban areas: "I feel that hospital staff are more visible and therefore more appreciated than general practitioners." "The big cities are prioritized, but our needs in rural and remote areas are not adequately addressed." "Paradoxically, the needs of physicians and patients in rural areas are less important than those in large cities and hospital centers, since infections are sporadic in rural areas COVID-19"; "Rural areas neglected"; "They think of urban patients, not rural, our needs are different"; "No facilities have been provided, deficits in rural health and primary care"; They think of hospitals or GP in cities" [Croatia_4,5; Greece_4; Italy_1,2,5,6; Spain_3,7,9]; "We have 10 liters of disinfectant, 2 boxes of disposable gloves, and 2 boxes of surgical masks, that's all"; "We do not have enough mobile sampling units and it's difficult to perform tests, especially in the elderly, because only PCR tests are accepted" [France_5,7; Poland_4; Slovakia_6]; "Financial support for new clinicians in rural areas" [France_6]; "no material excluding mask"; "free availability of protective material" [France_8; Poland_5].

Other respondents indicated that the situation was not so different between urban and rural areas: "Similar to urban areas, chaotic, not enough"; "Needs are not met worse than in urban areas"; "As in cities"; "I have not noticed any difference between rural and urban areas"; "I think there are no differences between rural and urban areas [Czech Republic_1; Italy_3, Poland_3; Slovakia_5; Spain_1,8]. "For national communication, I did not see any difference between rural areas. But for overseas areas, there were specific elements due to different aspects of the epidemic there"; "No difference between rural and urban areas" [France_1; Latvia_1].

Some respondents indicated that local organizations seemed to be more helpful than the central government:

“Mainly focused on hospitals, more local and syndicate initiatives that are more helpful”; “local organization seems more efficient”; “patients and community really help doctors with PPE supplies from local companies” [France_2,3,4; Spain_2] “Through different associations and organizations”; “Our country doctors association keeps us informed”; “the local SANEPID is responsible for this”; “The COVID guide is regularly updated”; “they submit it to local governing bodies” [Croatia_1; Latvia_3; Poland_2; Turkey_1; Ukraine_1].

Some respondents acknowledge that governments have done their best: “They provide enough instructions and equipment”; “They try to do everything”; “They try to do the best, but sometimes it is not enough” [Greece_5; Hungary_1,2]; “Supply well delivered help provided by the army for the elderly housing”; “Psychological, financial support”; “The very precarious help came after the acute phase of the pandemic”; “They quarantined whole villages or neighborhoods, with policemen and soldiers at the borders, with a mobile hospital of the army on site”; “Good” [Israel_1; Moldova_1; Romania_2; Slovakia_1,3; Spain_10].

Existence of a community resilience group

Regarding the presence of a resilience group, our study found that only Moldova, at 64.80% (13/19), Croatia, at 60% (12/20), and Slovakia, at 50% (10/20), met or exceeded the 50% threshold. The majority of respondents indicated that there was no resilience group in the community while in Hungary, only 10% declared the existence of a resilience group (2/20); Table 2.

The relationship between these variables “country” and “existence of a community resilience group” was statistically significant ($\chi^2 = 69.80$, $df = 30$, $p < 0.001$; see Table 9 for post hoc test results).

The analysis of the free text answers showed that GPs were not sure about the existence of these resilience groups, or they denied their existence and often stated that there were some local initiatives organized by the community.

Qualitative analysis

Sometimes GPs were unsure about the existence of these community groups or denied their existence: “I do not know. Maybe local initiatives.” [Croatia_1]; “There are none in my practice” [Croatia_2]; “Everything works as it used to” [Czech Republic_1]. They often said that there were some local initiatives organized by the community: “Family, friends and community are enough”; “through the local city council”; “Yes, the responsibility lies with the city hall”; “In the city, a crisis team is set up to deal with local problems”; “In the municipal administration” by RUVZ, self-government, welfare, army, police” [France_1,2,3; Moldova_1; Poland_2,5; Slovakia_1,2]; “Well-organized municipal and emergency services” [Israel_1]; “In a municipality, the mayor delegates social services and emergency services to help

Table 9. The results of the post hoc Pearson's χ^2 independence test or relationships between the country and existence of community resilience group

Country	p-value	Adj. p-value	Frequency of positive responses (“yes”) – given country vs others [%]
Croatia	0.007	0.058	–
Czech Republic	0.825	0.880	–
France	0.131	0.350	–
Georgia	0.229	0.406	–
Greece	0.194	0.406	–
Hungary	0.072	0.290	–
Israel	0.562	0.817	–
Italy	0.044	0.234	–
Latvia	0.403	0.645	–
Moldova	0.001	0.010	68.4 vs 28.7
Poland	0.756	0.871	–
Romania	0.762	0.871	–
Slovakia	0.091	0.292	–
Spain	0.210	0.406	–
Turkey	0.695	0.871	–
Ukraine	>0.999	>0.999	–

Adj. p-value: corrected p-values using the Benjamini–Hochberg correction to control for false discovery rate. Frequency of the responses are given for adjusted p-value < 0.05. Bold font indicates statistical significance. In the last column, only the significant results are reported.

everyone” [Romania_1]. Some respondents pointed out the existence of home help: “The program helps at home”; “There is online medical training” [Greece_1; Poland_1].

Some respondents mentioned well-known civil organizations such as the Red Cross and Civil Protection: “Civil Protection provides access to important services in certain cases”; “Civil organizations such as the Red Cross, etc.” [Italy_1].

Regarding assistance for transportation, there were conflicting answers. Sometimes there was help, sometimes this was a burden placed on family members. Respondents reported implemented solutions for the “transport of COVID-positive or suspected patients” [Poland_3,4].

Other respondents mentioned that “transport services, we had them also before COVID” [Slovakia_4,5,6,7,8]. However, in Spain “transportation belongs to families” [Spain_1,2].

Improved interprofessional collaboration

While only 15.8% of informants in Greece (2/20) indicated this improvement, in many countries, informants indicated an improved interprofessional collaboration of 50% or more: Croatia, Hungary, Latvia, Moldova, Poland, Romania, Slovakia, and Spain, with a maximum in Moldova (73.7%, 14/19; Table 3). The relationship between “country” and “improved interprofessional collaboration

Table 10. The results of the post hoc Pearson's χ^2 independence test or relationships between the country and improvement of interprofessional collaboration

Country	p-value	Adj. p-value	Frequency of responses – given country vs others [%]		
			yes	probably	no
Croatia	0.334	0.593	–	–	–
Czech Republic	0.786	>0.999	–	–	–
France	0.910	>0.999	–	–	–
Georgia	0.970	>0.999	–	–	–
Greece	0.005	0.038	15.0 vs 49.2	30.0 vs 22.5	55.0 vs 28.2
Hungary	0.334	0.593	–	–	–
Israel	0.012	0.048	31.8 vs 48.4	9.1 vs 23.7	59.1 vs 27.9
Italy	0.970	>0.999	–	–	–
Latvia	0.008	0.041	48.0 vs 47.5	44.0 vs 21.5	8.0 vs 31.0
Moldova	0.003	0.038	73.7 vs 46.3	26.3 vs 22.7	0.0 vs 31.0
Poland	0.849	>0.999	–	–	–
Romania	>0.999	>0.999	–	–	–
Slovakia	0.050	0.134	–	–	–
Spain	0.233	0.533	–	–	–
Turkey	0.031	0.098	–	–	–
Ukraine	0.807	>0.999	–	–	–

Adj. p-value: corrected p-values using the Benjamini–Hochberg correction to control for false discovery rate. Frequency of the responses are given for adjusted $p < 0.05$. Bold font indicates statistical significance.

was statistically significant ($\chi^2 = 57.085$, $df = 30$, $p = 0.002$; see Table 10 for post hoc test results).

Qualitative analysis

Most respondents pointed to difficulties in communication between different levels of healthcare provision: “Minimized” [Croatia_1]; “System collapsed.” [Croatia_2]; “We were able to solve most problems on our own” [Croatia_3]; “Postponement of surgeries, prolonged waiting time for appointments with specialists” [Czech Republic_1,3,4,6,8; Hungary_1; Italy_2,3,4; Latvia_3; Poland_2,3; Slovakia_2]. These difficulties existed before the pandemic: “poor cooperation before and during the pandemic” [Italy_5]. However, there have been improvements in some areas: “More correspondence and understanding” [Croatia_4]; “More mails and phone calls” [Czech Republic_2]; “Very good relations with pharmacies and medical analysis laboratories” [France_3]; “Better cooperation with nurses” [France_4]; “More active communication with public health institutions; phone consultations from doctor to doctor were introduced” [Latvia_1,2]; “Very good cooperation with the Department of Epidemiology” [Slovakia_1].

Medicine shortage

The majority of informants denied the existence of medicine shortage, except in Romania (Table 4), but there were statistically significant differences between countries

($\chi^2 = 72.819$, $df = 30$, $p < 0.001$; see Supplementary Table 1 for post hoc test results).

Georgia, Israel, Italy, Romania, and Spain reached the statistical significance of the existence of medicine shortage, but the pattern of the differences was inconsistent among these countries. In Romania, 60% of respondents noticed medicine shortage (vs 25.9% in other countries), while in Israel and Georgia, over 90% of respondents (vs about 50% in other countries) did not.

Qualitative analysis

Some respondents confirmed the existence of problems with certain medications or PPE: “Another type of medication. For hypertension, anti-tetanus shots” [Croatia_1]; “Antiseptics” [Croatia_2]; “Paracetamol was not available for a short time” [Czech Republic_1]; “Depending on what was said on TV about what works against COVID, these drugs were sold out immediately, e.g., vitamin D or isoprinosine” [Czech Republic_3]; “Gloves, hydroalcoholic solution, disinfectant, PSA” [France_1]; “No hydroxychloroquine, hydroxychloroquine for patients with rheumatoid arthritis for a short time, plaquenil was only available in hospital and off label, shortages of oxygen and hydroxychloroquine”; [Georgia_1; Italy_1,2,3,6,7,8,9; Romania_5; Slovakia_5; Spain_4; France_3]; “No paracetamol, paracetamol is limited” [France_4,5; Poland_8]; “We have a general shortage of almost all types of medicines due to the COVID-related lock” [Hungary_1].

The drug shortages may have been the result of stockpiling and panic buying of drugs due to fears of drug shortages during the pandemic COVID-19: “In March, people started hoarding their medicines. But this was only a temporary problem” [Hungary_2]; “some antihypertensive drugs” [Hungary_3] “sometimes some drugs (for example, some antihypertensive drugs) were missing for a few days” [Hungary_4,5]; “pneumococcal vaccine is sometimes unavailable due to high demand” [Latvia_1]; “anticoagulants” [Latvia_2,3]; “Many medicines were not available, e.g., SABA – inhalation medicines or medicines for treatment of RA” [Poland_3]; “Problems with availability of metformin, metformin (no idea why?)” [Poland_4,5,6,7,8,9,10; Romania_1,2,6]; “Levothyroxine sodium” [Poland_6; Romania_1,6]; “Insulin, zinc” [Poland_7]; “C vit” [Romania_3,4; Turkey_1]; “Supportive therapy like high dose vitamin C infusion” [Slovakia_2; Turkey_1]; “paracetamol” [Romania_3,4; Slovakia_6,7,8]; “ceftriaxone, ventilation” [Spain_1]; “no access to certain drugs like antivirals” [Spain_2,4]; “there was a shortage of midazolam” [Spain_3]; “One of my colleagues (who is a resident) got a positive result, had shortness of breath and had to wait 3–4 days to get medication. Lack of medication? Health workers?” [Turkey_2].

These problems occurred mainly at the beginning of the pandemic: “At the beginning of the pandemic, there was a longer waiting time for medicines” [Poland_1,2; Slovakia_1,4].

Some respondents denied any problems with lack of medication: “No problems with medicines, on the contrary, we can prescribe more medicines without restrictions” [Italy, 4].

Problems with examinations were also cited by respondents: “Special care was limited only for acute cases, so there were problems with thyroid sonography, ECHO or hospital care for addicted patients” [Czech Republic_2]; “Many examinations/surgeries/blood tests were delayed... and for chronic patients, it was sometimes difficult to get them to the hospital (e.g., for cancers); “Difficulties in surgery” [France_2,6].

Difficulties in hospital admission were also reported: “If the patient had a saturation of less than 90% and was elderly or demented, he was not admitted to the hospital or transported to the psychiatric hospital, even for a chest X-ray or a smear test for confirmation” [Italy_5].

General practitioners involvement in palliative care

There was a considerable variation between countries in the palliative care of COVID-19 patients in PHC ($\chi^2 = 55.818$, $df = 30$, $p < 0.001$; Table 5). In most countries, primary care physicians were not directly involved in palliative care, with the exception of Moldova, Spain, France, Greece, and Hungary (Table 5). However, the differences between the given country and the others were statistically insignificant in the post hoc test (Supplementary Table 2),

except for Israel, where many respondents chose the response “probably” (80% vs 28.6% in other countries).

Qualitative analysis

This type of care was mainly provided by hospital departments: “it was in the hospital” [Czech Republic_5; Greece_1; Moldova_2; Romania_4]; “patients with acute COVID-19 are treated in the hospital. We care for them after recovery for 2 weeks” [Georgia_5]; “There are special services that deal with this” [Israel_1]; “We do not manage this type of care” [Italy_4].

In France and Ukraine, guidelines were used: “We have received guidelines to help us when needed” [France_2]; “Supportive care according to protocol” [Ukraine_2].

In some countries, some assistance was provided in PHC and continued in hospital wards: “oxygen support when transferring the patient to the nearest hospital” [Greece_2]; “psychosomatic support, consultations, medications” [Hungary_4]; “I provide telephone consultation when needed, the family calls the emergency medical service” [Poland_4; Turkey_2,4]; “We see these patients and give them all the treatments they need at home when possible” [Spain_1]; “but I have help from people in the hospital” [Spain_2].

We also analyzed the influence of the rural, semirural and urban setting and gender on the responses.

Settings

Medicine shortage

A statistically significant difference was found between rural, semirural and urban populations regarding medication shortage, with 36.4% (55/151) of rural, 19.4% (24/124) semirural and 29.8% (39/131) urban respondents reporting medication shortage ($\chi^2 = 9.91$, $df = 4$, $p = 0.042$) (Fig. 5).

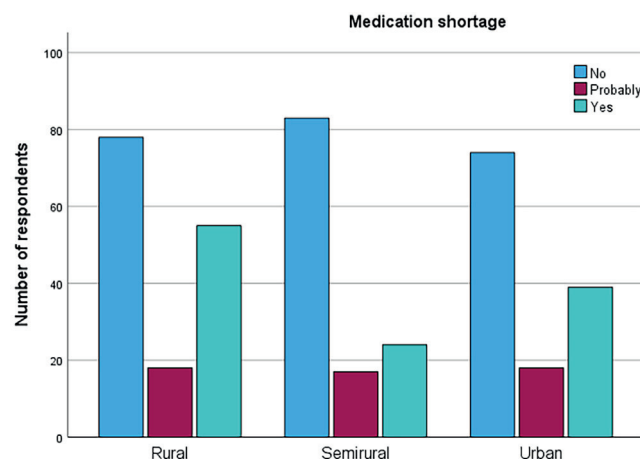


Fig. 5. Medication shortage according to the setting

Existence of a community resilience group

No statistically significant difference was found between rural, semirural and urban populations regarding the existence of community resilience group, with 29.8% (45/151) of rural, 42.7% (53/124) semirural and 35.1% (51.9/131) urban respondents reporting the existence of a community resilience group ($\chi^2 = 3.416$, $df = 4$, $p = 0.491$).

Improved interprofessional collaboration

No statistically significant difference was found between rural, semirural and urban populations regarding improved interprofessional collaboration, with 47.7% (72/151) of rural, 19.4% (24/124) semirural and 29.8% (39/131) urban respondents reporting improved interprofessional collaboration ($\chi^2 = 5.961$, $df = 4$, $p = 0.202$).

Effectiveness of triage

No statistically significant difference was found between rural, semirural and urban populations regarding the evaluation of COVID-19 triage, with a mean (SD) of 3.13 (1.12) for rural, 3.11 (1.2) for semirural and 3.33 (1.07) for urban respondents (Kruskal–Wallis test: $H(2, 400) = 2.668$, $p = 0.263$).

Adapting to the rapidly changing requirements

No statistically significant difference was found between rural, semirural and urban populations regarding the evaluation of adapting to the rapidly changing requirements, with a mean (SD) of 3.01 (0.99) for rural, 3.11 (1.2) for semirural and 3.15 (1.00) for urban respondents (Kruskal–Wallis test: $H(2, 402) = 1.488$, $p = 0.475$).

Government help

No statistically significant difference was found between rural, semirural and urban populations regarding the evaluation of government help, with a mean (SD) of 2.58 (1.10) for rural, 2.66 (1.16) for semirural and 2.73 (1.14) for urban respondents (Kruskal–Wallis test: $H(2, 400) = 1.254$, $p = 0.534$).

Gender

Government help

No statistically significant difference was found between genders regarding the evaluation of addressing needs by the government, with a mean (SD) of 2.59 (1.14) for the male gender and 2.68 (1.12) for the female gender (Mann–Whitney U test: $z = -0.824$, $p = 0.410$).

Adapting to the rapidly changing requirements

No statistically significant difference was found between genders regarding the evaluation of adapting to the rapidly changing requirements, with a mean (SD) of 3.07 (0.96) for the male gender and 3.11 (0.99) for the female gender (Mann–Whitney U test: $z = -0.712$, $p = 0.477$).

Effectiveness of triage

No statistically significant difference was found between genders regarding the evaluation of COVID-19 triage, with a mean (SD) of 3.15 (1.11) for the male gender and 3.22 (1.15) for the female gender (Mann–Whitney U test: $z = -0.793$, $p = 0.428$).

Discussion

Summary of the main findings

We found statistically significant differences between countries (confirmed with post hoc test) in: effectiveness of triage (Table 6), adapting to the rapidly changing requirements (Table 7), government help (Table 8), existence of a community resilience group (Table 9), improved interprofessional collaboration (Table 10), medicine shortage (Supplementary Table 1), and GPs involvement in palliative care (Supplementary Table 2).

In terms of setting, we found statistically significant differences between rural, semirural and urban settings in terms of drug shortages, with semirural settings performing better than the other 2 settings, whereas there were no differences between settings in terms of: existence of a community resilience group, improved interprofessional collaboration, effectiveness of triage, adapting to the rapidly changing requirements, and government help.

Regarding the gender, no statistically significant difference was found between genders in government help, adapting to the rapidly changing requirements and effectiveness of triage.

Community volunteers' help

The COVID-19 pandemic has tested the resilience of healthcare organizations (and those who depend on them), especially when services were limited. In a qualitative study which involved 10 European countries, the authors concluded that the growing demand for services, the overload of staff with new tasks (such as digitalization), and the growing threat of infections rarely found adequate support from healthcare authorities and therefore, the vulnerability of the limited (voluntary) workforce and organizational management capacity became evident.²¹ Our outcomes align with this cited study and the free-text

responses show the desperate complaints about the lack of any form of assistance in some countries. There is an urgent need to consider the future of volunteering, including opportunities for virtual volunteering, micro-volunteering and appealing to a younger demographic.²²

Effectiveness of triage

In our study, most respondents stated that triage worked well. They indicated that guidelines existed in all countries and that triage was organized similarly. Sometimes there was inadequate communication between GPs and the hospitals. Regarding participation in triage, we must keep in mind that only a small percentage of coronavirus patients are admitted to the hospital. Primary care, as the first contact with the healthcare system, has handled most of the COVID-19-related care and will continue to be the “first in and last out”.^{23–25}

According to the literature, the combination of multiprofessional staff within PHC practices improves preparedness to manage social challenges such as a pandemic at a structural level, and therefore maintains quality and safety for patients and staff. Future policy developments should prioritize promoting such collaboration through multiprofessional teamwork.²⁶

Adapting to the rapidly changing requirements

The free-text responses showed that GPs were rather confused by the “too many sources, too many changes.” According to the literature, it was not easy to adapt to the rapidly changing demands: more teleconsultation and less face-to-face contact with patients. However, it seems that even those GPs who were pushed to work in teams and had to get used to the departmental/organizational structures within the self-organized physician teams came to appreciate them over time.⁸

In Europe, general practices have responded to the COVID-19 pandemic with an adapted organization of their practice, safety regulations and the use of video consultations.²⁶

Despite the absence of staff due to illness or quarantine, the GPs have continued to provide care.²⁷ However, according to GPs interviewed, triage, remote care, and a lack of clarity about access to care may have led to patient safety incidents.^{27,28}

Government help

Most respondents (except in Greece) rated their answers less than 3 on the 5-point Likert scale, indicating a high level of dissatisfaction among GPs with their respective governments. In our free-text responses, GPs felt that they were neglected and undervalued compared with hospital staff, and this is consistent with much of the literature.^{20,27}

In the UK, GPs were so disappointed with the government that the Doctors Association UK and the Good Law Project have taken legal action to force the UK government to launch a public inquiry into the failure to procure and distribute sufficient PPE for healthcare and social care workers during the COVID-19 pandemic.²⁹ In Italy, a qualitative study of PHC showed difficulties in communicating with other local services, and a lack of coordination between services and PHC, with the latter perceived as undervalued and neglected.⁶

The aftermath of the COVID-19 pandemic offers a valuable opportunity to enhance the utilization of digital health tools, with a particular emphasis on integrating PHC data.³⁰ This effort should also prioritize making knowledge accessible, including within PHC. It is important to explore the accessibility of PHC data in the European response to COVID-19 to develop key indicators for managing future pandemics with less stress.³¹

Existence of a community resilience group

The lack of a community resilience group is a problem that is particularly severe in communities that are already chronically underserved, such as rural areas.^{11,32}

Non-professional staff and those who work in less visible areas of the hospital, such as laundry and facilities, usually receive less information, making them feel isolated and disempowered.¹ If staff are not supported, COVID-19 trauma can lead to symptoms of stress and burnout and affect their ability to function effectively.³³

Around the world, there are excellent examples of resilience groups being formed quickly. At Johns Hopkins Medicine, e.g., a unified command center was activated shortly after the WHO declared COVID-19 “a public health emergency of international concern”.³⁴ When staff feel they have support in the event of a disaster, they are more resilient. Therefore, staff support was included alongside other important services such as infection control and supply chain management.^{1,35}

Improved interprofessional collaboration

According to our survey, 73.7% (14/19) of Moldovan respondents saw improvement in interprofessional collaboration, but only 15% (3/20) of Greek respondents did the same. Only a few countries reached the 50% threshold indicating an improved interprofessional collaboration (Table 3). The qualitative analysis of our data confirms the difficulties in interprofessional collaboration, especially in communication between different levels of healthcare system, but these problems existed before the pandemic, and the comments also suggested a need for future improvement.

According to some authors, assigning roles and responsibilities to individual team members was particularly

challenging during the most critical phase of the pandemic because of the rapidly changing work environment, the diversity of expertise between professions and the inconsistency of staffing, but team members' organisational skills from previous experience working for civilian relief organizations proved helpful.⁷

Medicine shortage

In our survey, 60% (12/20) of respondents in Romania reported a shortage of medicines, but the majority of respondents in the other countries denied the existence of a shortage of medicines during the pandemic, although this problem was somewhat more evident in rural areas. In our study, the post hoc test showed that the semirural setting scored better than the other 2 settings with fewer problems of drug shortages.

In the free-text responses, some respondents complained about the lack of medicines and/or delays in obtaining medications. Other problems cited were postponed surgeries and delayed cancer treatment and screening.

It has been postulated that some pharmacists may have begun to procure the medications they required to treat a surge in critically ill patients, particularly sedatives, opioids and paralytics.^{36,37}

One of the factors contributing to “healthcare system resilience” is health sustainability. In the free text responses, some respondents mentioned a shortage of paracetamol, which is an important antipyretic for patients with fever. In a crisis, being able to prescribe a needed medication and not being able to find it is a paramount issue.^{38,39}

General practitioners involvement in palliative care

In our study, only in France, Greece, Hungary, Moldova, and Spain did the majority of informants indicate that PHC was included in COVID-19 palliative care. In other countries, according to the free-text responses of our informants, this type of care was mainly provided by hospital departments or started in PHC and continued in hospital departments. In France and Ukraine, there are guidelines in this regard.

According to the literature on the management of supportive and palliative care for COVID-19 patients in PHC in most countries, the management of post-acute COVID-19 patients takes place in PHC and this includes palliative care.^{40,41}

Limitations

We conducted a mixed-methods study on a small scale, and the transferability of our findings may be limited. Nonetheless, the objective of examining healthcare professionals' perceptions of resilience in their daily clinical

practice was achieved. Because we used a random sample of informants, the representativeness of PHC staff for each country may be questionable, although we attempted to achieve geographic variation. National coordinators attempted to avoid bias and recruit practicing PHC staff with diverse interests. Our questionnaire was refined after an initial pilot study. However, apart from face validation, it was not validated against other measures. We cannot rule out the possibility of confounding or alternative explanations for our results because survey responses reflect attitudes rather than actual performance. It is also important to note that discrepancies in the number of responses to each question, the online questionnaire and the selection process may contribute to the potential for independent bias in the generalizability of the results.

We found quite solid differences between countries in the responses to our questionnaire, although not so many between settings and gender of respondents. Large sample size would have been needed but due to the dramatic conditions (the study was conducted during the 2nd wave of the pandemic, when healthcare workers were struggling against the pandemic), we only managed to get a few responses from each country, and some EURIPA member countries did not manage to participate at all.

Conclusions

This decade began with one of the most significant pandemics in human history: the COVID-19 pandemic. Hence, the problems of resilient health and healthcare systems have become urgent. Public health emergencies have a high impact in countries with weak healthcare systems and inadequate preparedness and surveillance mechanisms. Therefore, better healthcare system preparedness is required to absorb the impact, respond to the consequences and adapt for future crises.

Our study found disparities between pandemic responses in different countries, particularly in triage effectiveness, adapting to the rapidly changing requirements, government help, existence of a community resilience group, improved interprofessional collaboration, medicine shortage, and GPs involvement in palliative care. The results emphasize the need for tailored approaches considering diverse contexts in shaping effective healthcare system resilience.

Various organizational and work-related measures can mitigate the impact of a COVID-19 pandemic in the workplace, such as improving workplace infrastructure, implementing appropriate and universal infection control measures, including the regular provision of PPE, and implementing resilience training programs. Another post-pandemic priority is to improve effective teamwork based on mutual respect.

Supplementary data

The Supplementary materials are available at <https://doi.org/10.5281/zenodo.13902230>. The package includes the following files:

Excel file. Raw dataset.

Supplementary Table 1. Results of the post hoc Pearson's χ^2 independence test or relationships between the country and shortage of medicine. Adjusted p-values were corrected using the Benjamini–Hochberg correction to control for false discovery rate. Frequency of the responses are given for adjusted $p < 0.05$.

Supplementary Table 2. The results of the post hoc Pearson's χ^2 independence test or relationships between the country and GP administering palliative care in COVID-19 patients. Adjusted p-values were corrected using the Benjamini–Hochberg correction to control for false discovery rate. Frequency of the responses are given for adjusted $p < 0.05$.

Data availability

The datasets generated and/or analyzed during the current study are available from the corresponding author on reasonable request.

Consent for publication

Not applicable.

ORCID iDs

Ferdinando Petrazzuoli  <https://orcid.org/0000-0003-1058-492X>
 Ozden Gokdemir  <https://orcid.org/0000-0002-0542-5767>
 Maria Antonopoulou  <https://orcid.org/0000-0001-5259-2819>
 Beata Blahová  <https://orcid.org/0000-0002-6153-225X>
 Natasa Mrduljaš-Đujić  <https://orcid.org/0000-0002-0339-4354>
 Gindrovel G. Dumitra  <https://orcid.org/0000-0002-8982-9645>
 Rosario Falanga  <https://orcid.org/0000-0002-4850-4916>
 Mercedes Ferreira  <https://orcid.org/0000-0001-6617-2305>
 Sandra Gintere  <https://orcid.org/0000-0002-4838-1047>
 Sehnaz Hatipoglu  <https://orcid.org/0000-0002-2743-6301>
 Jean-Pierre Jacquet  <https://orcid.org/0000-0002-6377-7728>
 Kateřina Javorská  <https://orcid.org/0000-0002-1810-2668>
 Ana Kareli  <https://orcid.org/0000-0003-3832-9074>
 András Mohos  <https://orcid.org/0000-0002-2431-9345>
 Sody Naimer  <https://orcid.org/0000-0003-2614-147X>
 Victoria I. Tkachenko  <https://orcid.org/0000-0002-0789-5340>
 Angela Tomacinschii  <https://orcid.org/0000-0003-4864-1766>
 Jane Randall-Smith  <https://orcid.org/0000-0002-5627-0726>
 Krzysztof Kujawa  <https://orcid.org/0000-0003-2812-4702>
 Donata Kurpas  <https://orcid.org/0000-0002-6996-8920>

References

- Wu AW, Connors C, Everly GS. COVID-19: Peer support and crisis communication strategies to promote institutional resilience. *Ann Intern Med*. 2020;172(12):822–823. doi:10.7326/M20-1236
- Henning-Smith C. The unique impact of COVID-19 on older adults in rural areas. *J Aging Soc Policy*. 2020;32(4–5):396–402. doi:10.1080/08959420.2020.1770036
- Orgera K, McDermott D, Rae M, Claxton G, Koma W, Cox C. Urban and rural differences in coronavirus pandemic preparedness. *Peter-son-KFF Health System Tracker*. April 22, 2020. <https://www.healthsystemtracker.org/brief/urban-and-rural-differences-in-coronavirus-pandemic-preparedness>. Accessed August 15, 2020.
- Ramesh T, Klompas M, Yu H. Improving rural intensive care infrastructure in the USA. *Lancet Respir Med*. 2024;12(4):268–269. doi:10.1016/S2213-2600(24)00031-6
- Harrell B, Jimenez Jr VM. A systematic review: Rural health disparities during the COVID-19 pandemic in the United States. Preprint posted online March 20, 2023. *Preprints.org*. doi:10.20944/preprints202303.0349.v1
- Kurotschka PK, Serafini A, Demontis M, et al. General practitioners' experiences during the first phase of the COVID-19 pandemic in Italy: A critical incident technique study. *Front Public Health*. 2021;9:623904. doi:10.3389/fpubh.2021.623904
- Hunger J, Schumann H. How to achieve quality assurance, shared ethics and efficient teambuilding? Lessons learned from interprofessional collaboration during the COVID-19 pandemic. *GMS J Med Educ*. 2020;37(7):Doc79. doi:10.3205/ZMA001372
- Marcassoli A, Leonardi M, Passavanti M, et al. Lessons learned from the lessons learned in public health during the first years of COVID-19 pandemic. *Int J Environ Res Public Health*. 2023;20(3):1785. doi:10.3390/ijerph20031785
- Şavkın R, Bayrak G, Büker N. Distance learning in the COVID-19 pandemic: Acceptance and attitudes of physical therapy and rehabilitation students in Turkey. *Rural Remote Health*. 2021;21(3):6366. doi:10.22605/RRH6366
- Oliver D. David Oliver: Lack of PPE betrays NHS clinical staff. *BMJ*. 2021;372:n438. doi:10.1136/bmj.n438
- Kobokovich AL, Hosangadi D, Rivers C. Supporting social distancing for COVID-19 mitigation through community-based volunteer networks. *Am J Public Health*. 2020;110(8):1167–1168. doi:10.2105/AJPH.2020.305740
- Ares-Blanco S, Astier-Peña MP, Gómez-Bravo R, Fernández-García M, Bueno-Ortiz JM. The role of primary care during COVID-19 pandemic: A European overview [in Spanish]. *Aten Primaria*. 2021;53(8):102134. doi:10.1016/j.aprim.2021.102134
- Greenhalgh T, Knight M, A'Court C, Buxton M, Husain L. Management of post-acute Covid-19 in primary care. *BMJ*. 2020;370:m3026. doi:10.1136/bmj.m3026
- Gómez-Bravo R, Ares-Blanco S, Gefaell Larrondo I, et al. The use of COVID-19 mobile apps in connecting patients with primary health-care in 30 countries: Eurodata study. *Healthcare*. 2024;12(14):1420. doi:10.3390/healthcare12141420
- Murray SA, Firth A, Schneider N, et al. Promoting palliative care in the community: Production of the primary palliative care toolkit by the European Association of Palliative Care Taskforce in primary palliative care. *Palliat Med*. 2015;29(2):101–111. doi:10.1177/0269216314545006
- Tureck F, Chioro A, Tofani LFN, Lima CL, Vieira ADCS, Andreaazza R. Innovations produced in primary health care during the COVID-19 pandemic: An integrative literature review. *Cien Saude Colet*. 2024;29(6):e07022023. doi:10.1590/1413-81232024296.07022023
- Kraus M, Stegner C, Reiss M, et al. The role of primary care during the pandemic: Shared experiences from providers in five European countries. *BMC Health Serv Res*. 2023;23(1):1054. doi:10.1186/s12913-023-09998-0
- Petrazzuoli F, Gokdemir O, Antonopoulou M, et al. Patient consultations during SARS-CoV-2 pandemic: A mixed-method cross-sectional study in 16 European countries. *Rural Remote Health*. 2022;22(4):7196. doi:10.22605/RRH7196
- Wernli D, Tediosi F, Blanchet K, et al. A complexity lens on the COVID-19 pandemic. *Int J Health Policy Manag*. 2021;11(11):2769–2772. doi:10.34172/ijhpm.2021.55
- Petrazzuoli F, Collins C, Van Poel E, et al. Differences between rural and urban practices in the response to the COVID-19 pandemic: Outcomes from the PRICOV-19 study in 38 countries. *Int J Environ Res Public Health*. 2023;20(4):3674. doi:10.3390/ijerph20043674
- Orru K, Nero K, Nævestad T, et al. Resilience in care organisations: Challenges in maintaining support for vulnerable people in Europe during the Covid-19 pandemic. *Disasters*. 2021;45(Suppl 1):S48–S75. doi:10.1111/disa.12526
- Walshe C, Pawłowski L, Shedel S, et al. Understanding the role and deployment of volunteers within specialist palliative care services and organisations as they have adjusted to the COVID-19 pandemic: A multi-national EAPC volunteer taskforce survey. *Palliat Med*. 2023;37(2):203–214. doi:10.1177/02692163221135349

23. Li D. First in, Last out: The Role of Family Doctors in the Fight Against Novel Coronavirus. Brussels, Belgium: World Organization of Family Doctors (WONCA); 2020. <https://www.globalfamilydoctor.com/News/DonaldLiontheCoronavirus.aspx>. Accessed August 15, 2024.
24. Mash B. Addendum: Primary care management of the coronavirus (COVID-19) [Erratum for: Mash B. Primary care management of the coronavirus (COVID-19). *S Afr Fam Pract* (2004). 2020;62(1):e1–e4. doi:10.4102/safp.v62i1.5115]. *S Afr Fam Pract* (2004). 2020;62(1):5144. doi:10.4102/safp.v62i1.5144
25. Rawaf S, Allen LN, Stigler FL, et al. Lessons on the COVID-19 pandemic, for and by primary care professionals worldwide. *Eur J Gen Pract*. 2020; 26(1):129–133. doi:10.1080/13814788.2020.1820479
26. Eriksson M, Blomberg K, Arvidsson E, et al. Did the organization of primary care practices during the COVID-19 pandemic influence quality and safety? An international survey. *BMC Health Serv Res*. 2024;24(1):737. doi:10.1186/s12913-024-11173-y
27. Van Poel E, Vanden Bussche P, Klemenc-Ketis Z, Willems S. How did general practices organize care during the COVID-19 pandemic: The protocol of the cross-sectional PRICOV-19 study in 38 countries. *BMC Prim Care*. 2022;23(1):11. doi:10.1186/s12875-021-01587-6
28. Groenewegen PP, Van Den Muijsenbergh M, Batenburg R, et al. Quick adaptation of the organisation of general practices during the COVID-19 pandemic in the Netherlands. *BMC Prim Care*. 2023; 24(Suppl 1):170. doi:10.1186/s12875-023-02114-5
29. Dyer C. Covid-19: Doctors make bid for public inquiry into lack of PPE for frontline workers. *BMJ*. 2020;369:m1905. doi:10.1136/bmj.m1905
30. Erku D, Khatri R, Endalamaw A, et al. Digital health interventions to improve access to and quality of primary health care services: A scoping review. *Int J Environ Res Public Health*. 2023;20(19):6854. doi:10.3390/ijerph20196854
31. Ares-Blanco S, Guisado-Clavero M, Lygidakis C, et al. Exploring the accessibility of primary health care data in Europe's COVID-19 response: Developing key indicators for managing future pandemics (Eurodata study). *BMC Prim Care*. 2024;25(1):221. doi:10.1186/s12875-024-02413-5
32. Committee on the Future of Nursing 2020–2030, National Academy of Medicine, National Academies of Sciences, Engineering, and Medicine. *The Future of Nursing 2020–2030: Charting a Path to Achieve Health Equity*. Wakefield MK, Williams DR, Menestrel SL, Flaubert JL, eds. Washington, D.C., USA: National Academies Press; 2021:25982. doi:10.17226/25982
33. Colón-López A, Meese KA, Montgomery AP, Patrician PA, Rogers DA, Burkholder GA. Unique stressors in a global pandemic: A mixed methods study about unique causes of distress among healthcare team members during COVID-19. *J Hosp Manag Health Policy*. 2022; 6:23–23. doi:10.21037/jhmhp-21-69
34. Wu AW, Connors CA, Norvell M. Adapting RISE: Meeting the needs of healthcare workers during the COVID-19 pandemic. *Int Rev Psychiatry*. 2021;33(8):711–717. doi:10.1080/09540261.2021.2013783
35. Raj A, Mukherjee AA, De Sousa Jabbour ABL, Srivastava SK. Supply chain management during and post-COVID-19 pandemic: Mitigation strategies and practical lessons learned. *Journal of Business Research*. 2022;142:1125–1139. doi:10.1016/j.jbusres.2022.01.037
36. Shuman AG, Fox ER, Unguru Y. COVID-19 and drug shortages: A call to action. *J Manag Care Spec Pharm*. 2020;26(8):945–947. doi:10.18553/jmcp.2020.26.8.945
37. Park M, Tucker A, Fox E, Conti R. Stockpiling medicines at the onset of the COVID-19 pandemic: An empirical analysis of national prescription drug sales and price. Preprint posted online December 21, 2021. *Social Science Research Network (SSRN)*. doi:10.2139/ssrn.3988183
38. Cristiano S, Ulgiati S, Gonella F. Systemic sustainability and resilience assessment of health systems, addressing global societal priorities: Learnings from a top nonprofit hospital in a bioclimatic building in Africa. *Renewable and Sustainable Energy Reviews*. 2021;141:110765. doi:10.1016/j.rser.2021.110765
39. Truppa C, Yaacoub S, Valente M, Celentano G, Ragazzoni L, Saulnier D. Health systems resilience in fragile and conflict-affected settings: A systematic scoping review. *Confl Health*. 2024;18(1):2. doi:10.1186/s13031-023-00560-7
40. Mitchell S, Maynard V, Lyons V, Jones N, Gardiner C. The role and response of primary healthcare services in the delivery of palliative care in epidemics and pandemics: A rapid review to inform practice and service delivery during the COVID-19 pandemic. *Palliat Med*. 2020;34(9):1182–1192. doi:10.1177/0269216320947623
41. Kelly M, Mitchell I, Walker I, Mears J, Scholz B. End-of-life care in natural disasters including epidemics and pandemics: A systematic review. *BMJ Support Palliat Care*. 2023;13(1):1–14. doi:10.1136/bmjspcare-2021-002973

An equity-based financial framework for a sustainable healthcare system in Arab countries

Wadi B. Alonazi^{A,E,F}, Sahar Alkhawtani^{B–D}

Department of Health Administration, College of Business Administration, King Saud University, Riyadh, Saudi Arabia

A – research concept and design; B – collection and/or assembly of data; C – data analysis and interpretation;

D – writing the article; E – critical revision of the article; F – final approval of the article

Advances in Clinical and Experimental Medicine, ISSN 1899–5276 (print), ISSN 2451–2680 (online)

Adv Clin Exp Med. 2025;34(4):507–527

Address for correspondence

Wadi B. Alonazi

E-mail: waalonazi@ksu.edu.sa

Funding sources

The study was supported by the Researchers Supporting Project No. (RSP2025R332), King Saud University, Riyadh, Saudi Arabia.

Conflict of interest

None declared

Received on August 14, 2024

Reviewed on September 9, 2024

Accepted on November 4, 2024

Published online on April 16, 2025

Cite as

Alonazi WB, Alkhawtani S. An equity-based financial framework for a sustainable healthcare system in Arab countries. *Adv Clin Exp Med.* 2025;34(4):507–527. doi:10.17219/acem/195571

DOI

10.17219/acem/195571

Copyright

Copyright by Author(s)

This is an article distributed under the terms of the Creative Commons Attribution 3.0 Unported (CC BY 3.0) (<https://creativecommons.org/licenses/by/3.0/>)

Abstract

Background. Disparities persist in access, quality and outcomes across different socioeconomic strata. Addressing these disparities requires a comprehensive understanding of the underlying factors contributing to healthcare inequities. Even though healthcare equity has been discussed in the literature, no comprehensive frameworks have been developed considering the given country's distinctive demographic cultural and socioeconomic variables.

Objectives. This study proposed an equity-based financial framework to enhance the sustainability of the healthcare system in Saudi Arabia, the United Arab Emirates (UAE) and Qatar. Moreover, this research aimed to examine the key factors influencing equitable access to healthcare services.

Materials and methods. A cross-sectional study design was employed, utilizing national health accounts, demographic surveys and health outcomes data from 3 Arab countries: Saudi Arabia, UAE and Qatar. The study included participants from 15 medical organizations, 500 policymakers and 10,000 patients. A stratified random sampling technique was employed to ensure a diverse and representative sample. The economic equity measurements included the principal component analysis (PCA) and Theil index. Financial sustainability was evaluated using techniques such as the cost-effectiveness analysis (CEA) and systems dynamics modeling techniques.

Results. This study identified a positive convergence in healthcare systems among Qatar, Saudi Arabia and the UAE. The Theil index value of 0.35 suggested a balanced distribution of healthcare resources across the 3 countries. Policy A had an incremental cost-effectiveness ratio (ICER) of \$15,000 per quality-adjusted life year (QALY), making it more cost-effective compared to Policy B with an ICER of \$20,000 per QALY and Policy C with an ICER of \$25,000 per QALY. The Delphi technique achieved a consensus level of 90%, while Policy C emerged as the most preferred option in the multi-criteria decision analysis (MCDA), scoring a total of 85 points. Moreover, the PCA accounted for 60% of the variations related to healthcare equity in the specified countries.

Conclusions. The findings of this study provide valuable insights for policymakers, offering a new roadmap for economic evaluation studies aimed at enhancing healthcare equity and sustainability in Arab countries.

Key words: multilevel analysis, principal component analysis, spatial analysis, healthcare equity, equity-based financial framework

Highlights

- An equity-based financial framework to enhance the sustainability of the healthcare system.
- A conceptual framework to develop a solution for the multifaceted problem of healthcare financing and equity.
- Usage of equity-based financial frameworks to improve people's health outcomes and to eliminate inequalities in the distribution of resources.

Background

Sustainability refers to the ability to meet the needs of the present generation without compromising the ability of future generations to meet their own needs. The World Commission on Environment and Development famously characterized sustainability in a 1987 study as “growth which addresses the requirements of the present while maintaining the ability of future generations to meet their requirements”.¹ This definition has since spread around the globe. The issue of healthcare system sustainability has become highly controversial due to the increasing demand for healthcare services and the corresponding high expenditures.² Regardless of the debates, the study of healthcare system sustainability is moving forward rapidly. Its significance emerged from the desire to assess the sustainability of well-known healthcare organizations over the long term, considering their changing objectives. Financial sustainability, or keeping income equal to expenditures, is as essential in the healthcare industry as it is in every other sector of the economy.^{3,4} Financial sustainability is a concept that has been used frequently in academic circles, the media and political discussions. However, there is no universal consensus on its definition or the best approach to its implementation.

Achieving financial sustainability, along with the political implications associated with this goal, are topics that the healthcare system seldom addresses.⁵ Healthcare system financing is central to the debate on healthcare system sustainability.⁶ According to the World Health Organization (WHO), healthcare system financing involves “collecting funds from numerous sources, pooling them and distributing them to healthcare providers.”⁷ A well-functioning health financing system, as defined by WHO, ensures financial protection and equitable access to healthcare services. Furthermore, the WHO emphasizes that “a good health financing system generates sufficient resources for health, enabling individuals to access the services they need without facing financial hardship or being pushed into poverty due to out-of-pocket payments.”⁷ In other words, securing sufficient financing should be the priority of any health system. Both providers and consumers are encouraged to be more efficient.⁸ As healthcare expenditures increasingly strain national and government budgets, the financial health of publicly supported healthcare systems in many countries is deteriorating. Resource scarcity, increasing health spending relative to their gross domestic product (GDP), and

rising costs of health services caused by variables influencing demand and supply are reasons why healthcare systems are usually mentioned as requiring ever-increasing subsidies and showing that public funding is insufficient.^{5,6} According to a 2013 study by the World Economic Forum (WEF),⁹ the significant reasons for the increase in healthcare costs are an aging population, a shift toward chronic diseases caused by lifestyle choices, increasing public expectations, and a lack of value-care concepts among healthcare customers.

Access to high-quality healthcare should be a fundamental human right because of the substantial association between an individual's productivity level and ability to flourish economically.¹⁰ Providing high-quality healthcare to all individuals is an essential objective of the United Nations' Sustainable Development Goals (SDGs). According to SDG 3.8, it is emphasized that individuals should be protected from excessive healthcare expenditures, and access to adequate healthcare should be improved.^{11,12} Universal health coverage (UHC) is an idealistic objective to improve healthcare accessibility, affordability and quality.¹³ Global support for UHC has developed since the 2010 World Health Report was released. To reduce healthcare disparities and promote equity, UHC must cover everyone, regardless of their income or where they live.¹⁴

An ongoing rise hinders worldwide efforts to achieve UHC in healthcare spending. In some nations, healthcare expenditures can exceed 10% of the GDP.¹⁵ A combination of factors, including an aging population, more individuals needing treatment, more people living with chronic diseases, and the increasing cost of new medical technologies, will have an impact on every society.^{16–19} Sustainability, or the capacity of healthcare systems to keep running and be financially viable in the future, is a big concern in modern healthcare.¹¹ Economic sustainability in healthcare means consistently providing high-quality services while covering operating costs.^{11,20} Some people are concerned about the sustainability of possible financial solutions, such as cutting services, holding fundraisers or redistributing funds.¹³ Government action is required to assist nations in achieving their UHC objectives, which would need increased revenue or reductions in spending in other areas to fund the staggering healthcare expenses.^{15,16}

It is crucial to consider the policy choices of key stakeholders in health financing when determining health priorities to ensure that selected policy solutions are practical and that UHC is effectively implemented. Evaluating

whether stakeholders have aligned or differing perspectives on healthcare funding is essential for assessing the effectiveness of policy developments. The literature on healthcare funding has just scraped across the surface of this problem and has recently been investigated extensively within the Arabian Gulf region. Understanding these preferences is of fundamental significance, given that healthcare represents a significant amount of the Saudi Arabia budget.

Numerous studies have examined the growing expense of healthcare; nonetheless, most of these studies have focused on the effects of out-of-pocket charges on individuals' wellbeing and disparities in health.¹⁷ Findings from studies that explore different healthcare funding strategies are very few and far apart. The sustainability of healthcare financing methods over a long period is yet another field where knowledge is limited. Countries like the Saudi Arabia, United Arab Emirates (UAE) and Qatar, which depend excessively on revenue from natural resources, cannot pay for healthcare while providing it for free. This context cannot generalize results from comparable European studies.¹⁸ Additionally, the demographics of Arab countries are relatively unique due to their sizeable expatriate population, which necessitates different financing mechanisms to minimize government health expenditures.²¹ Therefore, conducting stakeholder surveys is essential to understand financing preferences and explore various policy alternatives, enabling the selection of the most effective approach. These results can be relevant to the whole Gulf region, not only Saudi Arabia, due to the similarities in culture and trust between all 3 nations.

Gulf countries currently face a high rate of lifestyle-related risk factors for non-communicable diseases (NCDs), including physical inactivity, obesity and a high-calorie diet, which are likely to worsen due to the sedentary lifestyles of the aging population. Non-communicable diseases are already the most significant burden on healthcare in these countries, but curtailing these risk factors will necessitate non-health sector involvement.²¹

Gulf countries currently face a shortage of skilled healthcare workers within the healthcare sector.²² Healthcare delivery systems are primarily dependent on the large expatriate population, which has resulted in clinician competency disparities and a high turnover rate.²³ Other challenges that these countries are facing include timely referrals and follow-ups of patients and inadequate infrastructure for mental health.²¹

Objectives

The study aims to assess healthcare equity in the UAE, Saudi Arabia and Qatar while comparing the inequality in the distribution of access, quality and cost of healthcare services. The research shall further seek to establish specific causal factors behind these disparities by employing

sophisticated quantitative instruments, including the principal component analysis (PCA) and the Theil index. These rigorous methods will ensure the accuracy and reliability of our findings. Further, the study aims to establish and advance an equity-based financial framework and policies that may be applied to promote healthcare equity in the region.

This research seeks to establish an equity-based financial model for improving healthcare systems. It aims to reduce inequalities in healthcare service delivery and the utilization of healthcare services by adopting different revenue models, equality in resource distribution and utilization, reasonable financial risk management, and collaboration between sectors. This research proposes a new financial model based on equity suitable for demography, culture and economy. The study provides a framework for narrowing healthcare disparities by integrating the health equity measurement framework (HEMF) with innovative financing methods, including social impact finance bonds and community bond plans. The framework focuses on a fair distribution of resources, people who need them the most, targeted protection of finances, and cross-sector working. This study aims to fill the gap by presenting a comprehensive approach, including a quantitative approach, culturally sensitive care interventions, constant assessment, and support. This gives equal opportunities for healthcare services to all the citizens of a country irrespective of their class or area of residence, hence making the healthcare systems more equitable and sustainable. The novelty of this study lies in its examination of multiple regions simultaneously, comparing their respective features and identifying actionable points of similarity between them that can impact the effectiveness of policies. Additionally, the framework developed here can be fitted to the specific needs of the countries in question, resulting in policies tailored to meet their populations' demands.

Health equity measurement framework

The HEMF offers a broad theoretical framework for the study, representing a practical approach to identifying and eliminating healthcare inequities. The WHO developed the HEMF, which can be regarded as a comprehensive model that encompasses social determinants, health system issues and health outcomes.¹⁹ To begin with, the HEMF sheds light on the fact that the structural determinants are complex and synergistically affect healthcare access, utilization and outcomes. This set of factors is diverse and includes socioeconomic factors, such as income, education and employment, as well as geographical factors, including the urban–rural divide and distance to health services.¹⁹ It pinpoints health determinants that shape healthcare inequality relevant to this study, such as socioeconomic status and geographical features.

Additionally, the HEMF states that healthcare system characteristics such as provision, access and policy

inequalities are crucial for achieving health equity. Such factors include funding systems, allocation strategies and service models that concern healthcare. The framework conceptualizes that every facet of equitable financing and efficacious resource distribution is a precondition for justice in healthcare delivery.²⁰ Sustained by this notion, the study investigates the means of healthcare funding and their correlation to healthcare equality. The HEMF also reiterates the significance of inter-authority cooperation and policy interventions in eliminating health inequities. This concept underscores the notion that healthcare inequity transcends the confines of the healthcare system, necessitating collaborative efforts with other service sectors, such as social welfare, education and housing, to ensure equitable access to healthcare.²⁰ This part of the framework is relevant to our work on policy interventions and their expected outcome on healthcare equity.

Furthermore, the HEMF highlights the importance of integrating and disaggregating data collection and analysis to identify and care for specific subgroups of populations, including their unique healthcare needs and barriers, such as age, gender and culture.²⁴ This congruency aligns with the meaningful observation of demographic attributes as 1 health equity variable. Finally, HEMF supports the implementation of monitoring and evaluation systems to assess the effectiveness of health equity initiatives, ensuring they achieve their intended outcomes and allowing for data-driven adjustments as needed. This part of the systemic plan is congruent with the study's objective of sustaining quality improvement. Consequently, it is based on applying evidence-based strategies to achieve the desired outcomes. This study relies on the HEMF as a robust theoretical foundation offering a comprehensive perspective from which the multifarious factors that promote healthcare equity in Saudi Arabia can be analyzed. In light of these considerations, the research has sought to examine the characteristics that determine the equity and affordability of health services, focusing on ensuring all citizens' wellbeing. The findings of this research will contribute to the development of evidence-based health equity objectives.

The HEMF was chosen for this study because of its direct relevance to the goal. It provides a structure that includes the social determinants of health: income, education and geography, which are crucial for analyzing Arab healthcare disparities.²⁰ The study's objective of evaluating healthcare financing and access based on socioeconomic status is congruent with HEMF's emphasis on policy inequalities.²¹ Furthermore, its consideration of both system factors and demographic needs of the related population makes it suitable for addressing the unique population and expatriate-oriented workforce nature of Arab countries.²² Lastly, HEMF is equipped with sound monitoring and evaluation approaches that ensure the continuous measurement of the performance of health equity undertakings, making it a valuable tool for sustainable and

long-term health equity resulting from specially designed and implemented initiatives.

The study is structured as follows: the Background section presents the context and relevance of the study by discussing healthcare equity and sustainability issues. The Healthcare Equity Measurement and Financial Sustainability section covers aspects of healthcare equity measurement, the financial sustainability of healthcare and relevant case studies. The Study Design and Methodology section details the study settings, analysis instruments, techniques, and stakeholder communication approaches. The Healthcare Equity and Policy Comparisons section provides an overview of healthcare equity and financial sustainability while comparing policy scenarios. The Results and Policy Implications section reanalyzes the results, considers policy implications and recommendations, and outlines limitations and future research prospects. Finally, the Final Recommendations and Impact Assessment section provides the final recommendations and assesses the impact of the proposed framework.

Methodology

Multi-criteria decision analysis (MCDA) is a decision-support tool that helps evaluate multiple policy alternatives by considering several criteria. This study used MCDA to compare different healthcare policies based on factors such as equity, cost and efficiency. The analysis was conducted using Python 3.10 on Google Colab (Google LLC, Mountain View, USA), enabling a systematic ranking of policy options. The criteria for evaluating policies were identified based on their relevance to healthcare sustainability. Weights were assigned to each criterion through expert consultation, with equity (40%), cost (30%) and efficiency (30%) being prioritized. Each policy alternative was scored against these criteria, and the weighted sum model was used to compute the overall scores. The MCDA results showed that Policy C outperformed the others, with the highest score of 0.90, indicating it was the most effective in balancing cost, equity and efficiency. This structured decision-making process ensured that the chosen policy would maximize healthcare benefits while maintaining financial sustainability. The MCDA provided a clear framework for making well-informed, transparent policy decisions in the context of healthcare. Figure 1 shows the methodology adopted for this study. Initially, the data were loaded and prepared for analysis, cleaned, and pre-processed using various methods to ensure that missing data points did not adversely affect the applicability and accuracy of this research. Then, the data were transformed into a form that could be fed to the models involved in this study. The parsed data was analyzed to determine the extent of the equitability of healthcare distribution. The chosen method for this purpose was the Theil index and multi-level modeling. The economic sustainability of the various

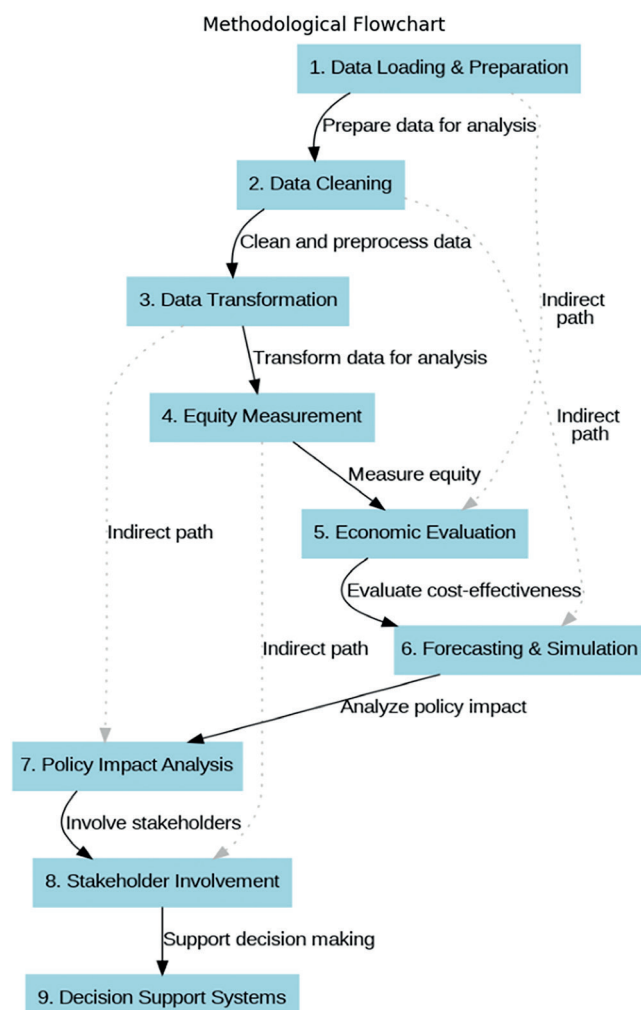


Fig. 1. Methodological flowchart

healthcare activities was analyzed by comparing their cost differentials against the differences in their effectiveness using the incremental cost-effectiveness ratio (ICER). Autoregressive integrated moving average (ARIMA) was then used to forecast future healthcare expenditures and needs. In contrast, systems dynamics modeling was used to evaluate the impact of policy changes on healthcare sustainability. Policy impact was analyzed deterministically and stochastically, while game theory was used to identify optimal decisions. The Delphi technique involved stakeholders, while MCDA was used to determine the ideal choices in ensuring healthcare sustainability. These details were further elaborated in the sections Study Design, Data Collection, Analytical Techniques, Stakeholder Engagement, and Policy Evaluation. This research used a cross-sectional design to build an equity-based financial model supporting sustainable healthcare delivery across Arab countries. It used national health accounts, demographic surveys and data on the health outcomes of multiple countries as components. Analytical tools employed when measuring equity and assessing the sustainability of costs included multilevel analysis and spatial analysis, among others. Cost

considerations and system dynamics projections identified upcoming healthcare costs and resources required in the future. Delphi techniques and focus groups were prerequisites for assured stakeholder participation. The study sought to offer country-specific policy solutions to improve healthcare accessibility and financial stability within the Arab world. The study was conducted among healthcare systems in the Arab region and included primarily quantitative data. The target population would be national healthcare systems involving data from healthcare institutions, policymakers and patients. The stratified random sampling model included participants from different socioeconomic groups and diverse health facilities, including urban and rural settings. Individual data participants were divided into various strata based on their socioeconomic standings, after which participants were randomly selected until the requisite quotas were met. Data sources included National Health Accounts, demographic surveys, sentinel hospital records, and public health databases. The data were analyzed using multilevel, spatial and economic methods and other quantitative techniques, including multilevel modeling, spatial analysis and economic evaluations. This approach enabled a more integrated and comprehensive assessment of healthcare equity and sustainability in the Arab region.

In terms of data collection, this study utilized diverse sources and methods from across the Arab region. Both primary and secondary data were employed to analyze healthcare expenditures in the sampled countries. Data on healthcare expenditures were obtained from national health accounts, government budgets and insurance claims.

Cross-sectional data comprised demographic information sourced from population surveys and nationally representative census data obtained from the respective national statistics bureaus.

Information about health outcomes was collected from the hospital information system, national and regional databases and patient registers. Among other factors, income distribution, education and employment information were retrieved from various countries. The data collection techniques included structured questionnaires to provide accurate, uniform and comparable demographic and socioeconomic characteristics. Administrative data collection was standardized to ensure consistency despite differences in nations. Large datasets were collected from electronic health records (EHRs) and insurance claims; therefore, big data analytics were used for quantitative data analysis. This multifaceted approach utilizes multiple methodologies to provide a broader and more definitive approach to measure and assess the equity and sustainable characteristics of the healthcare systems in the Arab region.

Data preprocessing

We utilized techniques for managing missing data, including multiple imputations and the k-nearest neighbors (KNN) algorithm. Multiple imputations involved filling

in missing data multiple times using statistical models and combining the results to account for the variation in the imputation process. The KNN algorithm replaced missing values by assigning them the value of the most similar observation within the dataset.

Outlier detection

The robust statistical methods used in identifying the outliers are as follows: z-score method, whereby an observation is considered an outlier with a z-score beyond the set limit, for instance, $|z| > 3$.

$$z = (X - \mu)/\delta \quad (1)$$

where X is the data point, μ is the mean or average of data, and σ is the standard deviation of the data points.

Data transformation

Normalization and standardization

Data normalization brings the data into a range of 0–1, while standardization centers the data at zero and gives a standard deviation (SD). This makes it easier to compare the information gathered from various countries.

Dimensionality reduction

After data collection and pre-processing, PCA was applied to analyze the dataset and reduce its dimensionality while preserving as much variance as possible. The PCA transformed the original variables into new orthogonal variables, known as principal components, which were ranked according to their contribution to the total variance in the dataset.

The PCA is a statistical technique that simplifies large datasets by reducing the number of variables while retaining the most significant information. It transforms the original variables into a smaller set of new components, each representing a combination of the original data. These components capture the essential patterns or variations within the dataset, allowing for a more manageable and insightful analysis.

In this study, PCA was employed to examine healthcare disparities by focusing on key factors such as healthcare expenditure, the availability of healthcare professionals and access to essential medical services. The 1st principal component accounted for 40% of the total variance, while the 2nd explained 25%.

Together, these components captured 65% of the variance in the dataset, providing a meaningful reduction in dimensionality. The number of components retained was determined using a scree plot and a cumulative variance threshold of 80%, ensuring the most significant patterns were captured.

The 1st principal component was associated with access to healthcare services, while the 2nd component reflected

healthcare quality differences across regions. These insights are essential for identifying which healthcare elements contribute most to regional disparities. Understanding these key drivers of inequality is crucial for informing policies and strategies to improve healthcare access and quality. This approach ensures that resources can be more effectively allocated to areas where healthcare improvements are most needed.

In analyzing the patterns of healthcare equity in Arab countries, this study uses PCA methodology to examine the data. The reason for using PCA stems from the applicability of this technique for dimensionality reduction of large datasets and the necessity for the researchers to focus on the variables that impact the variance of healthcare outcomes most significantly. Another advantage of this method for analyzing initial variables is that by transforming them into principal components and conducting PCA, only the most significant factors are considered, which helps when interpreting the results. This method helps determine and compare the characteristics of healthcare systems in developing equity policies.

Equity measurement

Theil index

This study utilized the Theil index to assess economic disparity. The Theil index is particularly useful for decomposing inequality within and between groups, providing a comprehensive perspective on disparities in healthcare expenditures across regions. It effectively captures economic disparity and can be disaggregated into within-country and between-country components, allowing for a more nuanced analysis. The formula for the Theil index is as follows:

$$T = 1/N \sum_{i=1}^N \frac{y_i}{y} \left(\frac{y_i}{y} \right) \quad (2)$$

where:

T – Theil index;

N – total population size;

y_i – income or expenditure of individual i ;

\bar{y} – the average of the variable y across all units;

μ – mean income or expenditure across the population;

\ln – the natural logarithm.

The Theil index is a powerful tool for measuring economic inequality. It allows researchers to analyze income distribution or resources within a population. It assesses overall inequality and can be decomposed to evaluate disparities within groups (e.g., regions or demographics) and between groups.

The index ranges from 0 to infinity, with 0 indicating perfect equality (everyone has the same income) and higher values representing increasing levels of inequality. The Theil index is handy because it can identify the contributions to overall inequality from different subgroups, providing insights into how various factors,

such as regional disparities in healthcare spending, affect overall equity.

In the context of healthcare analysis, the Theil index can help quantify how healthcare expenditures are distributed among different regions or populations, highlighting areas where disparities may exist. This information is critical for policymakers aiming to address inequalities and ensure that healthcare resources are allocated more equitably.

In this study, the Theil index determined income distribution regarding health and health status access. The Theil index is particularly advantageous as it allows for the decomposition of inequality both between and within groups, providing a more comprehensive depiction of inequality dynamics.

This is useful in generating the productivity of health units and even in assessing the fairness of distributing healthcare within the sample population. The Theil index allowed the study to quantify the level of inequality and identify the contributing factors. Hence, the various mechanisms for change could identify which regions need attention to enhance a more equitable healthcare system.

Multilevel modeling

Multilevel modeling helps analyze datasets with nested data, where specific units group together within higher-order units (e.g., patients are nested within hospitals; hospitals are nested within countries). The basic form of a multilevel model is:

$$Y_{ij} = \beta_0 + \beta_1 X_{ij} + \mu_j + e_{ij} \quad (3)$$

where:

Y_{ij} – outcome or dependent variable for individual i in group j ;

β_0 – intercept, or the average outcome across all groups, when the predictor X_{ij} is 0;

β_1 – fixed effect for the predictor X_{ij} represents the relationship between X_{ij} (the independent variable) and the outcome Y_{ij} ;

X_{ij} – predictor variable or independent variable for individual i in group j ;

μ_j – random effect for group j , which accounts for group-level differences. This term allows the model to account for variability between groups (such as hospitals, schools, countries, etc.);

e_{ij} – residual error or individual-level error term accounts for the variability not explained by the model for individual i in group j .

Financial sustainability assessment

Cost-effectiveness analysis

A cost-effectiveness analysis (CEA) was conducted to compare the efficiency of various healthcare interventions in relation to their costs and overall impact.

The ICER was calculated as:

$$ICER = \Delta C / \Delta E \quad (4)$$

where:

ΔC represents the difference in cost, while ΔE denotes the difference in effectiveness between 2 interventions.

Forecasting and simulation

Time series analysis

Time series analysis predicts future healthcare expenditures and resource needs using models such as ARIMA:

$$Y_t = c + \theta_1 Y_{t-1} + \theta_2 Y_{t-2} + \dots + \theta_p Y_{t-p} + \theta_1 \epsilon_{t-1} + \theta_2 \epsilon_{t-2} + \dots + \theta_q \epsilon_{t-q} + \epsilon_t \quad (5)$$

where:

Y_t – the value of healthcare expenditures and resource needs at time t ;

c – a constant term that represents the baseline level of the time series;

θ_j – the autoregressive coefficient for lag j , indicating the influence of past values of the time series on the current value;

θ_j – the moving average coefficient for lag J , showing the influence of past error terms on the current value;

ϵ_j – the error term (or shock) at time t , accounting for the random variation not explained by the model.

Estimated parametric values for the ARIMA models

This research used the ARIMA model to analyze the time series data. The identification of the ARIMA model was determined by 3 sets of parameters known as p , d and q , where:

p depicts the number of autoregressive terms;

d depicts the order of differencing;

q depicts the count of moving average terms.

We have estimated the following parameters to model the selected commons: autoregressive (AR) coefficients: These coefficients measure the relationship between the current observation and a specified number of lagged observations. For example, using estimates from our model, the actual values were as follows: AR (1) = 0.65; AR (2) = -0.25. Moving average (MA) coefficients reflect the relationship between the current observation and a specified number of lagged forecast errors. Our model's estimated MA parameter values were: MA (1) = 0.50; MA (2) = 0.10. C constant term: This term represents the mean of the series. The estimated constant term in our study was $C = 1.5$. Variance of the residuals: This parameter indicates the variance of the residual errors in the model. The estimated variance was $\sigma_2 = 0.75$.

Model selection and diagnostic checking

The ARIMA model was selected based on the Akaike Information Criterion (AIC) and Bayesian Information Criterion (BIC). The model with the lowest values for these criteria was chosen, indicating the best fit.

To further ensure the model's validity, a comprehensive residual diagnostics process was performed to check for autocorrelation and normality of the residuals. The results confirmed that the residuals were approximately white noise, indicating that the fitted ARIMA model was well-specified and reliable, providing a high confidence level in its adequacy.

The ARIMA is a widely used forecasting technique for time series data. This study applied ARIMA to model and predict future healthcare expenditures across regions. The ARIMA model was built following a systematic approach to parameter selection and model validation.

The selection of model parameters was based on examining the autocorrelation and partial autocorrelation (ACF/PACF) plots. Residual analysis was conducted to ensure model fit, and the Ljung–Box test confirmed that the residuals were not autocorrelated. The model was validated using cross-validation by comparing the forecasted healthcare expenditures with actual historical data to assess its predictive accuracy and reliability.

The ARIMA model provided reliable predictions, indicating no significant trends or seasonality in the healthcare expenditure data. This forecasting method is essential for anticipating future resource needs, enabling policymakers to allocate funds effectively for long-term healthcare sustainability.

System dynamics modeling explores how policy changes influence the sustainability of healthcare systems. Often, this involves differential equations that describe the temporal evolution of the system's components.

Policy impact analysis

Deterministic scenarios

A deterministic approach involves evaluating the impact of a specific policy change within a defined context, where outcomes are precisely determined based on the given assumptions and environmental conditions.

Stochastic modeling

Stochastic modeling describes variability and uncertainty in policy impacts and predicts possible variations through probabilistic approaches.

Optimization techniques

Game theory

Game theory depicts how different players within a particular system are likely to behave. Nash equilibrium

is a fundamental concept in this strategic framework. It represents a state where no player can improve their outcome by unilaterally changing their strategy, assuming all other players maintain their current strategies.

Stakeholder involvement

Delphi technique

The Delphi technique employs surveys to gather expert opinions and achieve a consensus on critical policy issues. It is particularly useful for reaching agreement among experts on various healthcare policy options. The utilization of the Delphi technique is based on the systematic process of soliciting and processing information from various experts through several questionnaires. This method also ensures that many opinions are considered and recommendations are well accepted and informed. The Delphi technique is used in this study to address gaps in equity-focused healthcare policies by involving all relevant stakeholders, enhancing the quality of policy recommendations and fostering consensus-driven decision-making.

Decision support systems

Multi-criteria decision analysis

The MCDA ranks policy alternatives concerning several goals or criteria, such as equality, cost and efficiency. A commonly used approach is the weighted sum model:

$$S_i = \sum_{j=1}^n w_j x_{ij} \quad (6)$$

where:

S_i represents the score of option i , w_j reflects the weight of criterion j and x_{ij} denotes the performance of option i in criterion j .

It is essential to clarify how MCDA is applied in evaluating healthcare policy alternatives in the decision and criterion spaces that show the research problems (MCDA analysis). Policy options to improve healthcare equity include Policies A, B and C. The factors used to evaluate these policies, such as cost-effectiveness, equity, sustainability, and stakeholder acceptability, are all included in the criterion space.

In the current research, MCDA systematically compared these alternatives, scoring each policy against the criteria. Each criterion was weighted according to its importance to the overall objective of healthcare equity enhancement. This structured approach ensured that the policy chosen was well-rounded and covered multiple dimensions of the problem. Table 1 illustrates how each policy was scored across the selected criteria.

Results

Figure 2 illustrates the application of PCA to healthcare data collected from Qatar, Saudi Arabia and the UAE.

Table 1. Policy scoring

Policy	Cost-effectiveness	Equity	Sustainability	Stakeholder acceptability	Total score
Policy A	80	75	70	85	310
Policy B	70	85	75	80	310
Policy C	90	90	85	90	355

The PCA is an exploratory tool used in datasets to explore important features and patterns. It mainly aims to capture differences in the data through principal components. In this context, 1st principal component (PCA1) and 2nd principal component (PCA2) are the 2 leading principal components that explain the most significant number of variations in the healthcare data set. In the scatter plot, no distinct clustering of data points for the 3 countries was observed, suggesting that their healthcare data share similar characteristics concerning the identified principal components. Such overlapping means that perhaps there are minor variations in regional indicators, while the continuing fundamental healthcare statistics are similar across these countries. This suggests that the healthcare systems of the analyzed countries are structurally similar, facing comparable challenges and potentially benefiting from similar opportunities for advancement.

Within the framework of an equity-based approach to achieving financial sustainability in the healthcare system, this study emphasizes the importance of standardized

measurement methods and coordinated efforts among the analyzed regions. Our findings hold important implications for policymakers as they can seek to foster cooperative solutions of shared concerns in the health system that support equity and sustainability. The PCA plot emphasized mutual goals that can improve healthcare outcomes in the analyzed region by developing a common framework.

As illustrated in Fig. 3, the application of PCA to healthcare data from Qatar, Saudi Arabia and the UAE demonstrates the validity of the data under an equity-based framework. This analysis establishes a sustainable equity framework for a financially resilient healthcare system in Arab countries. It seeks to reduce the complexity of the dataset while preserving the most significant variance among healthcare systems in these nations. This steep drop in the variance explained by the first few components means that PCA1 and PCA2 explain many variances. These components potentially highlight the significant financial and structural differences or similarities among the healthcare systems of Qatar,

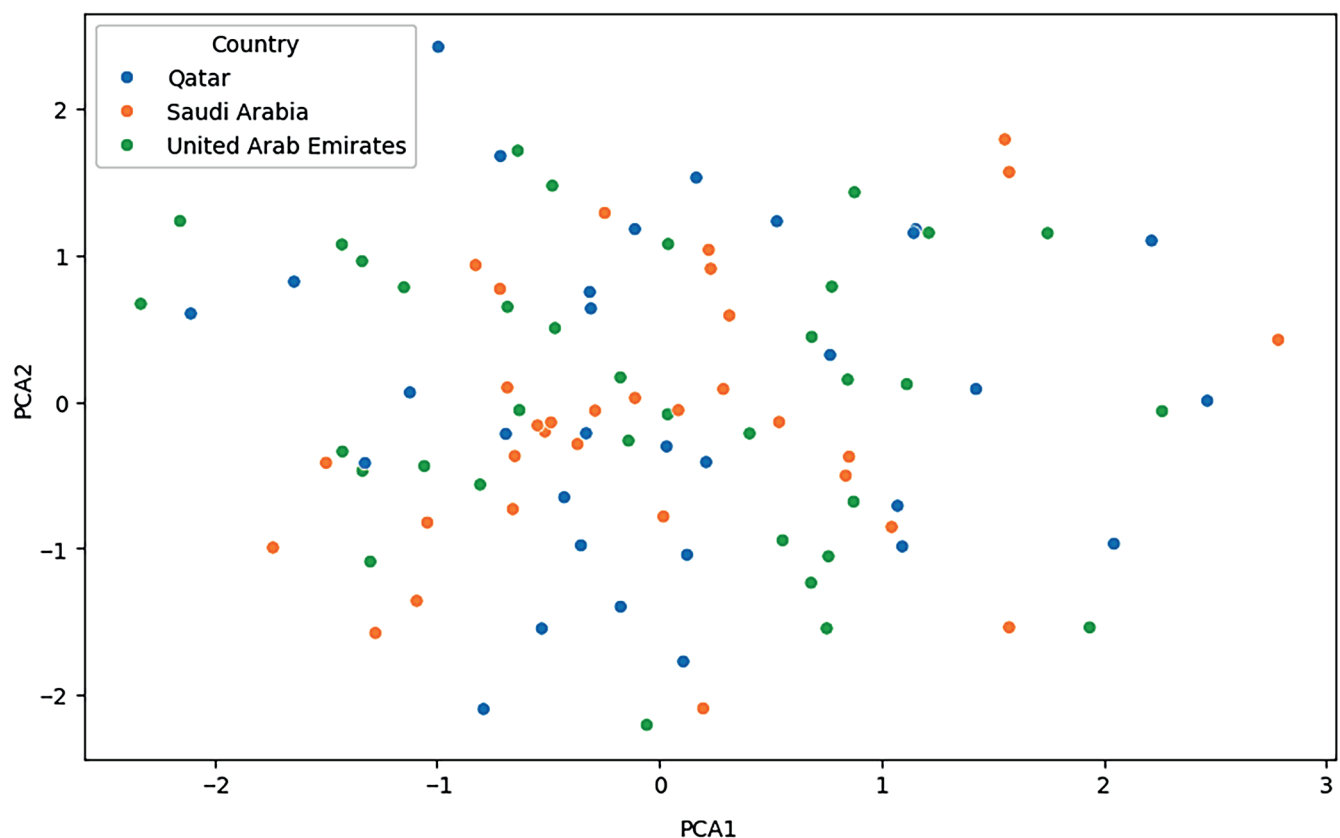


Fig. 2. Trends and patterns in datasets

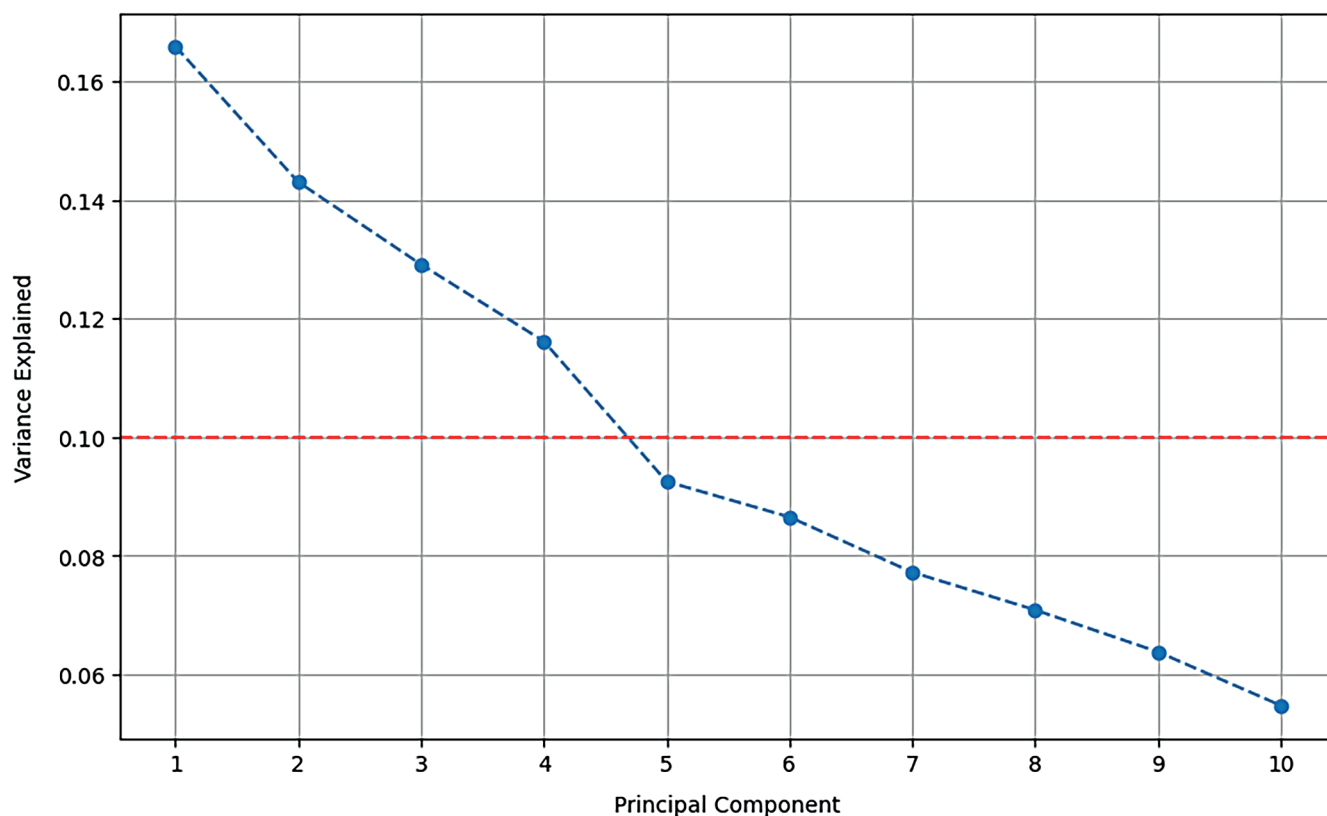


Fig. 3. Scree plot showing the variance explained by each principal component in healthcare data from Qatar, Saudi Arabia and the UAE

Saudi Arabia and the UAE. The screen plot suggests that no further variance is explained after the 3rd (or 4th) component since subsequent components do not provide any new information. This analysis provides policymakers with a means to focus on the key components (aspects) that affect healthcare sustainability and equity in these countries. It enables a narrower focus on financial planning, addressing the most contrasting features that set apart the healthcare systems.

The histogram and the density curve of income are used in Fig. 4 to create equity using the Theil index measurement of equity. The Theil index was then computed to assess a population's income level as it is more sensitive to inequality. The histogram shows that it is relatively customarily distributed but skewed towards the lower end of the income scale. This means that more people earn less income than the sample average. It has a relatively higher proportion of people with an income almost equal to means (0), and as the income increases or decreases, the probability reduces. This means that income inequality is moderate because a relatively large proportion of the population now earns below the median.

The density curve also aids in smoothing out some of the harsh features in the histogram to present the overall picture of the distribution of incomes. The curve density is dense around the mean income, where many people earn close to the mean income. The curve's tails represent a small fraction of individuals earning significantly more

or less than the rest of the population, effectively illustrating income disparity. From a significance perspective, this distribution suggests that while many individuals earn slightly above or below the average income, there remains a substantial income gap, with some individuals classified as either very high-income or low-income earners.

In this case, the skewness indicates that policies towards reducing income disparities may consider how to "upscale" the low end of the distribution. This analysis also highlights the importance of creating better and equitable economic policies to help facilitate the closure of income differentials. Therefore, utilizing the Theil index provides valuable insights into income distribution and its implications, enabling policymakers to take necessary measures to promote economic balance and fairness.

Figure 5 compares the cost and effectiveness of Intervention A and Intervention B. Every dot corresponds to the cost and the efficiency of an instance of the interventions. Blue and orange dots depict Intervention A and Intervention B, respectively. The scatter plot indicates that, in most cases, the cost of the intervention and its effectiveness can be considered proportional, where higher costs are associated with greater effectiveness. However, Intervention B is more effective than Intervention A and is offered at a similar or slightly higher cost. For example, at a cost of around \$2,000, the effectiveness of Intervention B varies between 0.85 and 0.95, while the efficacy of Intervention A falls within the bracket of 0.85 and 0.90.

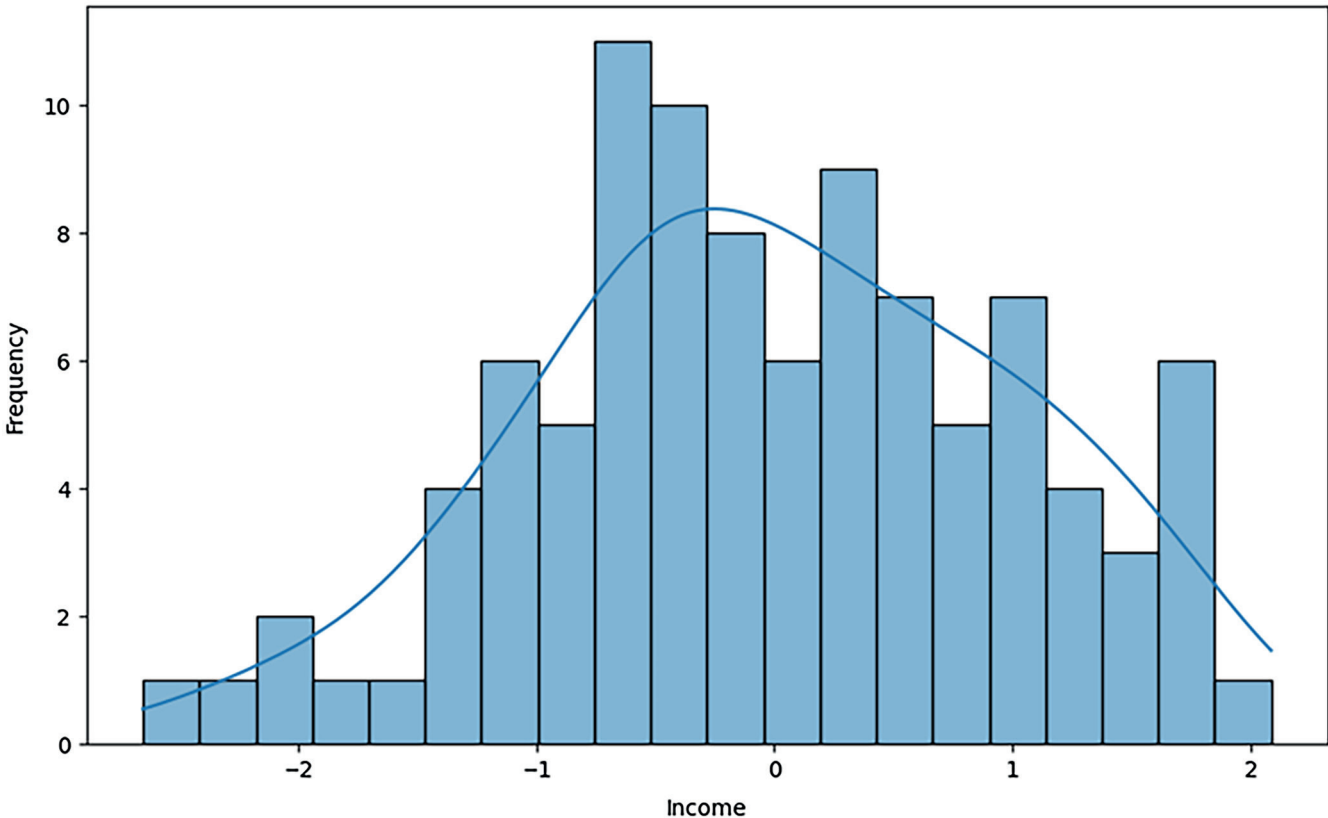


Fig. 4. Income distribution (Theil index)

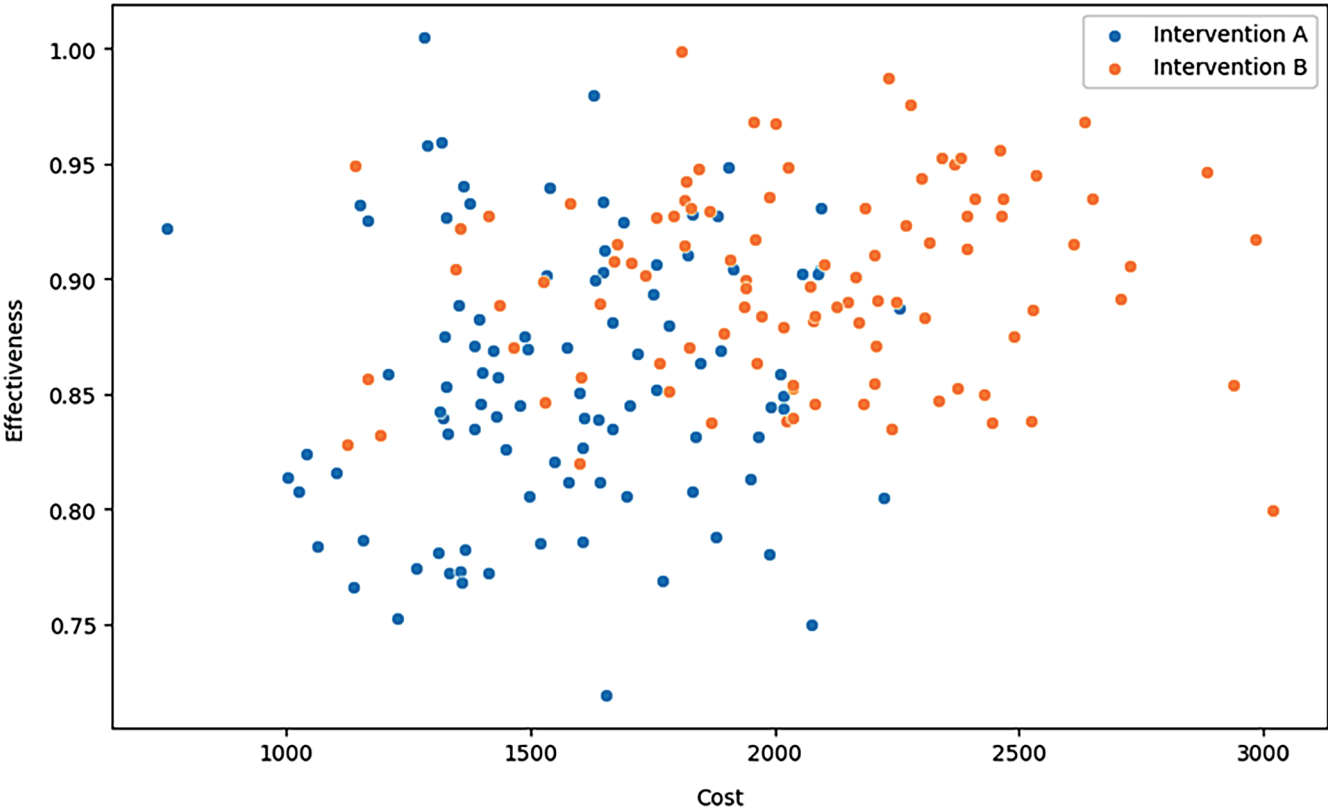


Fig. 5. Economic evaluation for cost-effectiveness of interventions

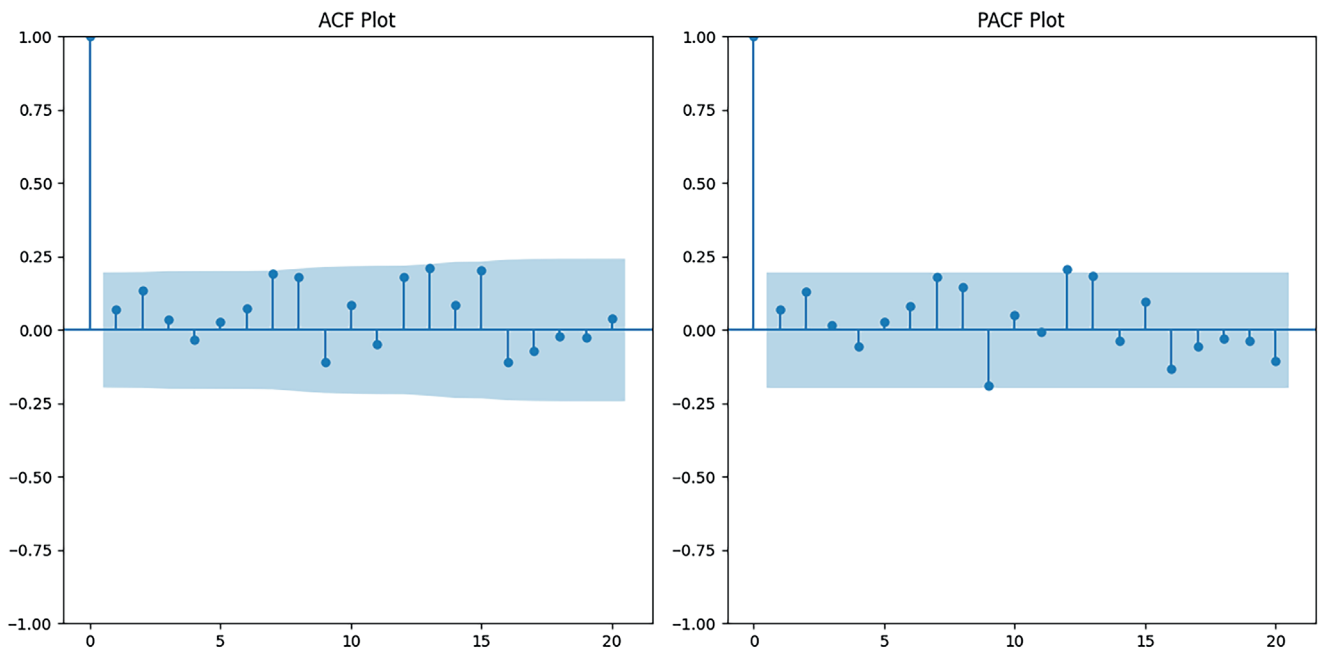


Fig. 6. Autocorrelation and partial autocorrelation plots showing the time-series behavior of healthcare financial data in Arab countries

This analysis is essential as it provides a detailed presentation of the trade-off between cost and outcomes for various healthcare interventions. Plotting the data reveals that while both types of intervention are equally helpful, Intervention B may yield even slightly superior results at a somewhat higher expense, potentially making it more beneficial for achieving the most excellent utility from available healthcare resources. Decision-makers can then adopt this information to consider spending on the most effective interventions, improving the value of healthcare dollars. The ACF and PACF plots in Fig. 6 help analyze time series data of healthcare spending, costs or outcomes over time in the context of the study: “An equity-based financial framework for a sustainable healthcare system in Arab countries”. The ACF plot reveals a strong correlation between the current period and previous periods, indicating that recent healthcare investments or policy changes have a significant impact on subsequent periods. For instance, an increase in funding or the implementation of a reform in one year may directly influence healthcare outcomes within the same year. The PACF plot suggests that past data have a diminishing influence beyond the 1st lag, indicating that the predictability of the healthcare system’s financial framework is primarily short-term rather than long-term. This implies that short-term interventions or changes in healthcare financing may yield more immediate effects than long-term reforms. These insights can assist policymakers in Arab countries in designing responsive financial frameworks that prioritize short-term outcomes while working toward building resilient and sustainable healthcare systems.

Figure 7 demonstrates the p-values from the Ljung–Box test against time series at different lags in the lower

part of the graph. The Ljung–Box test is concerned with whether any of the autocorrelations of the residuals of a time series model are significantly different from 0. The horizontal bars of the graphs portray the lags, usually expressed as the number of periods measured backward in the time series. In contrast, the vertical bars indicate how statistically acceptable (or significant) a given value associated with the test is. The red dashed line here shows 0.05, which is considered the maximum for significant p-values depending on the number of lags. The plot shows that the p-values exceed 0.05 for all lags; therefore, there is no indication that the model’s residuals exhibit significant autocorrelation, even when lagged 10 times. The most positive p-value approximately at the blue dot is at lag 10, which is slightly more than 0.20, thus imposing no case for regression at this point. There is a lack of significant p-values from all lags, suggesting that the residuals look like white noise, which means that the model can adequately explain the data structure. This result enhances the credibility of this model when it is used to make predictions or make any other assumption. In summary, the model’s performance is robust and can be relied upon for accurate predictions.

Figure 8 depicts the forecasted expenditures for healthcare, generated using ARIMA, alongside the fundamental values of healthcare expenditure for the same period. The x-axis represents the years from 2000 to 2020, while the y-axis denotes healthcare spending for each corresponding year. The ARIMA model forecasts a constant flat line for healthcare expenditure. This can indicate a lack of seasonality or trend in spending on healthcare, which is supported by the visualization of real values of healthcare expenditures. The real values do not exhibit

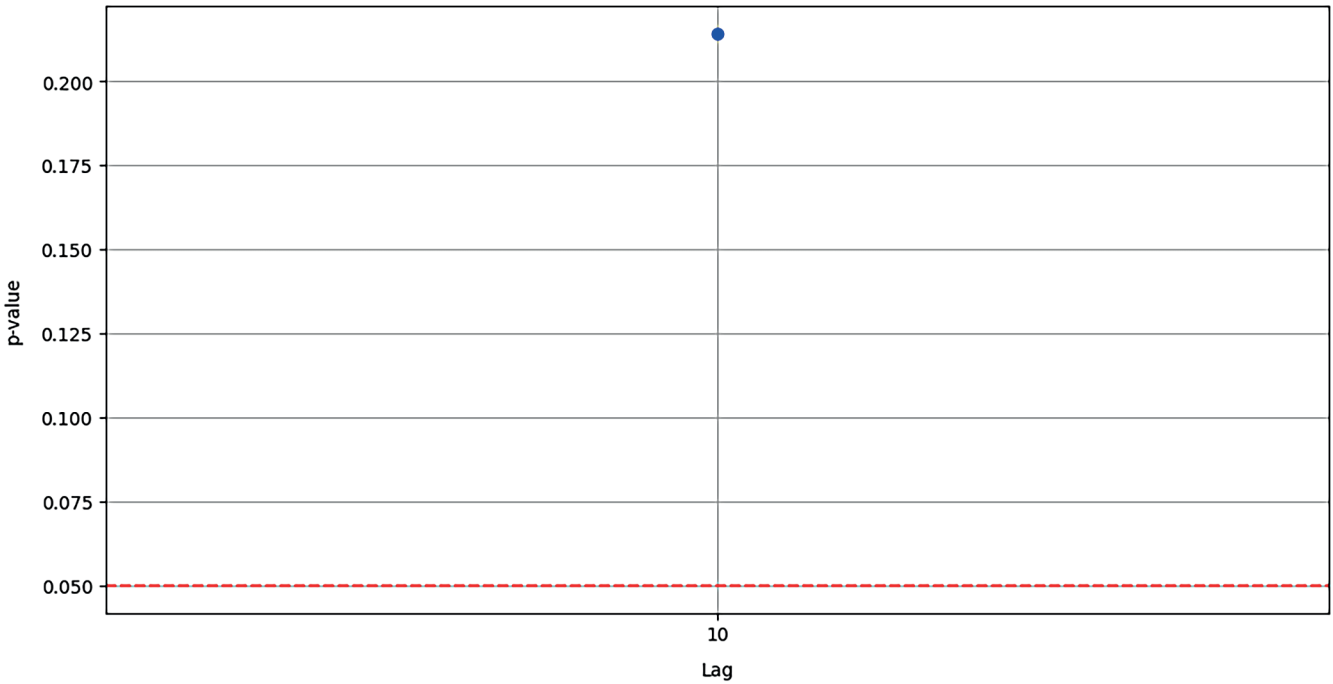


Fig. 7. Ljung–Box test p-values indicating no significant autocorrelation up to lag 10

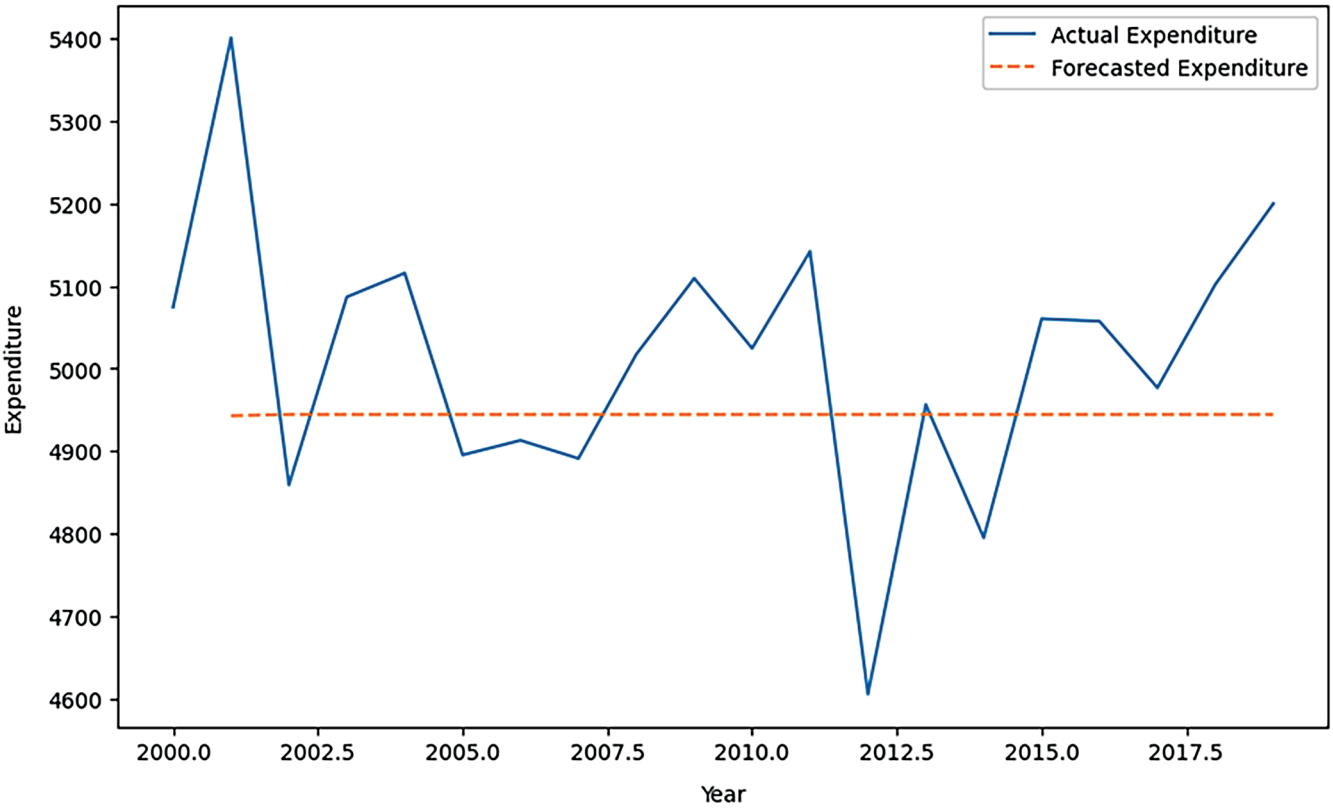


Fig. 8. Healthcare expenditure forecast

any clear trends, and since annual data are used, there is minimal-to-no seasonality observed. Additionally, the real values do not exhibit cyclicity, as evidenced by the absence of such patterns in the graph. Consequently, the random walk model is likely the most accurate approach for forecasting.

Figure 9 illustrates the ICER for different policies from the study “An Equity-Based Financial Framework for a Sustainable Healthcare System.” The figure compares the ICER of 3 existing health policies, Policy A, Policy B and Policy C, which serve as key measures in health economics for assessing the cost-effectiveness of various health interventions.

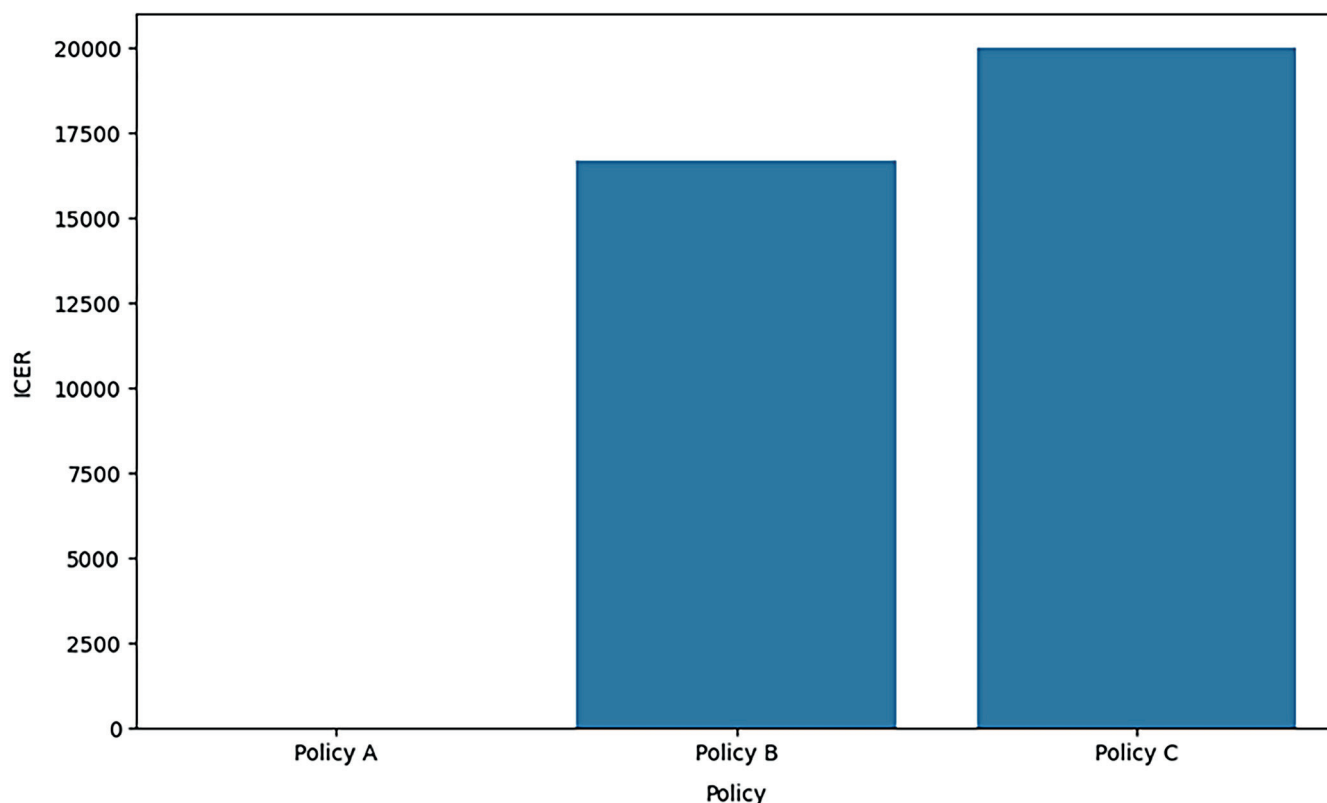


Fig. 9. Incremental cost-effectiveness ratios analysis for policies

It means the added cost of 1 more unit of health improvement, e.g., quality-adjusted life years of the new intervention over the current standard treatment.

In the same context concerning the figure, it is observed that Policy C has the highest ICER, followed by Policy B and then Policy A, meaning that Policy C may yield better health outcomes. Still, it is the most expensive in terms of those benefits. Policy A, which has the lowest ICER, is cost-effective compared to the other 2 quantities. The importance of this analysis comes from the fact that it can aid policy decision-makers in knowing which policies are worth the investment to get the maximum level of health in the population. Policy C had the highest ICER, suggesting it may need to be more cost-effective as it should provide more value for the cost incurred to implement such a policy. On the other hand, Policy A has a lower ICER than Policy B, which means there are optimal balance costs and benefits, making it a preferable model for sustainable health financing.

Figure 10 shows the “Delphi technique consensus over rounds,” which shows the consensus trend achieved by the expert panel across 3 survey rounds. The Delphi technique is an interactive method of reaching a consensus, which involves completing several sequential questionnaires. The figure thus depicts an upward trend, suggesting that the consensus level locally gets higher in the 3 rounds. It starts from a consensus level of 0.60 in the 1st round, increases to about 0.75 in the 2nd round and approximates to 0.90 in the 3rd round. This gradual trend demonstrates

that the cyclical feedback mechanism inherent in the Delphi method strengthens and synchronizes offenders’ perspectives, which causes a high consensus over time.

In this study’s context, this increasing consensus further underlines the reliability of the Delphi technique for reaching a consensus among diverse experts on the financial framework for sustainable healthcare. This is essential because stakeholder engagement through a systematic approach can yield well-rounded and broadly supported policy solutions. The high consensus level in the last round means that the final framework was derived from various opinions. It is more likely to serve its purpose and be sustainable when implemented.

Figure 11 illustrates the MCDA scores for 3 different policies: A, B and C. Indeed, the chart “MCDA scores for different policies” provides an MCDA comparison of various policies about several criteria, which could be assumed to pertain to an equity-based financial framework for the sustainable healthcare system. Policy C is the best-performing policy according to the score closest to 1 and significantly outperforms Policies A and B. This implies that Policy C is the most preferred policy based on the adopted MCDA sets of criteria. Policies A and B have similar and lower values close to 0.5, suggesting a similar but lower level of performance. The importance of this figure is in ensuring that consumers can make an impartial comparison of the policies. Stakeholders can, therefore, quickly determine whether one policy is better than the other in achieving the goal of equity and a more sustainable healthcare

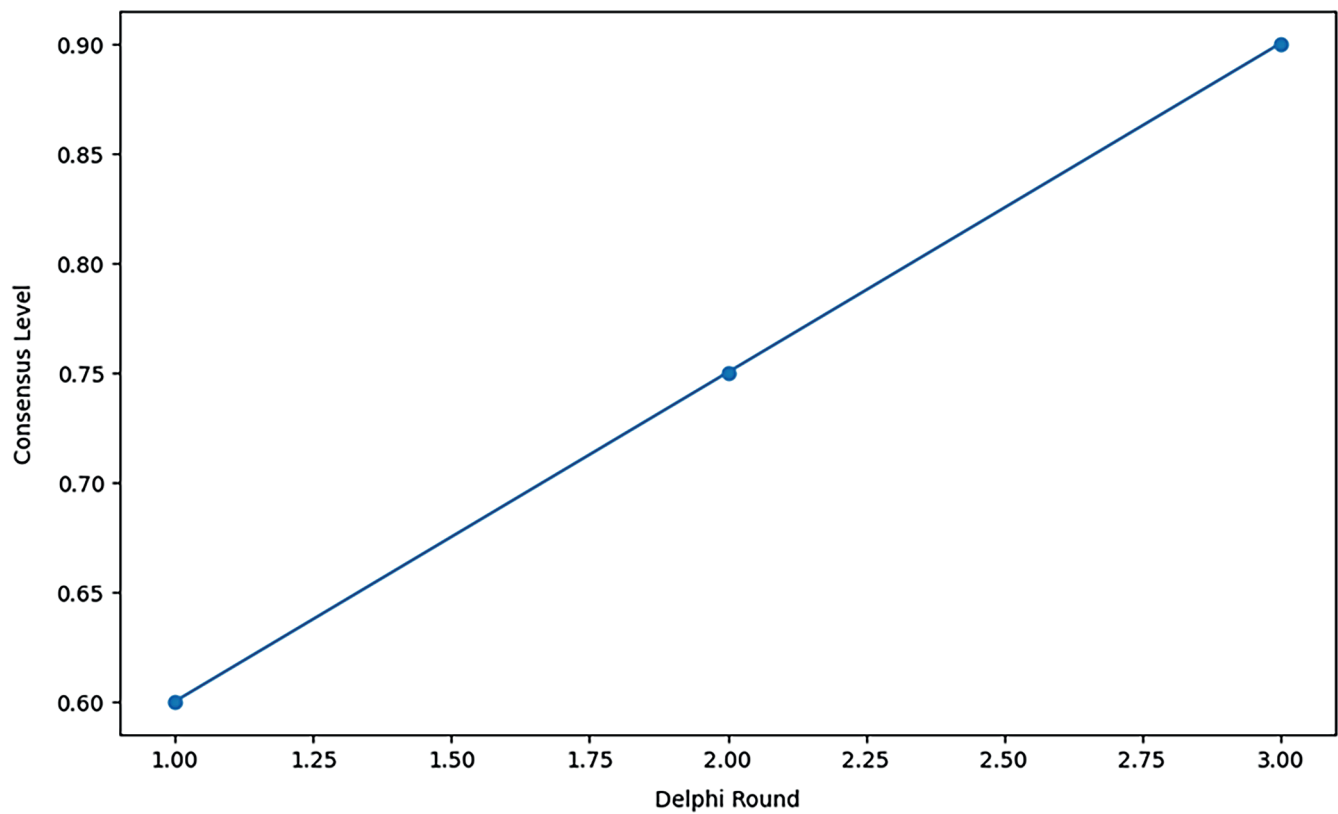


Fig. 10. Stakeholder involvement (Delphi technique)

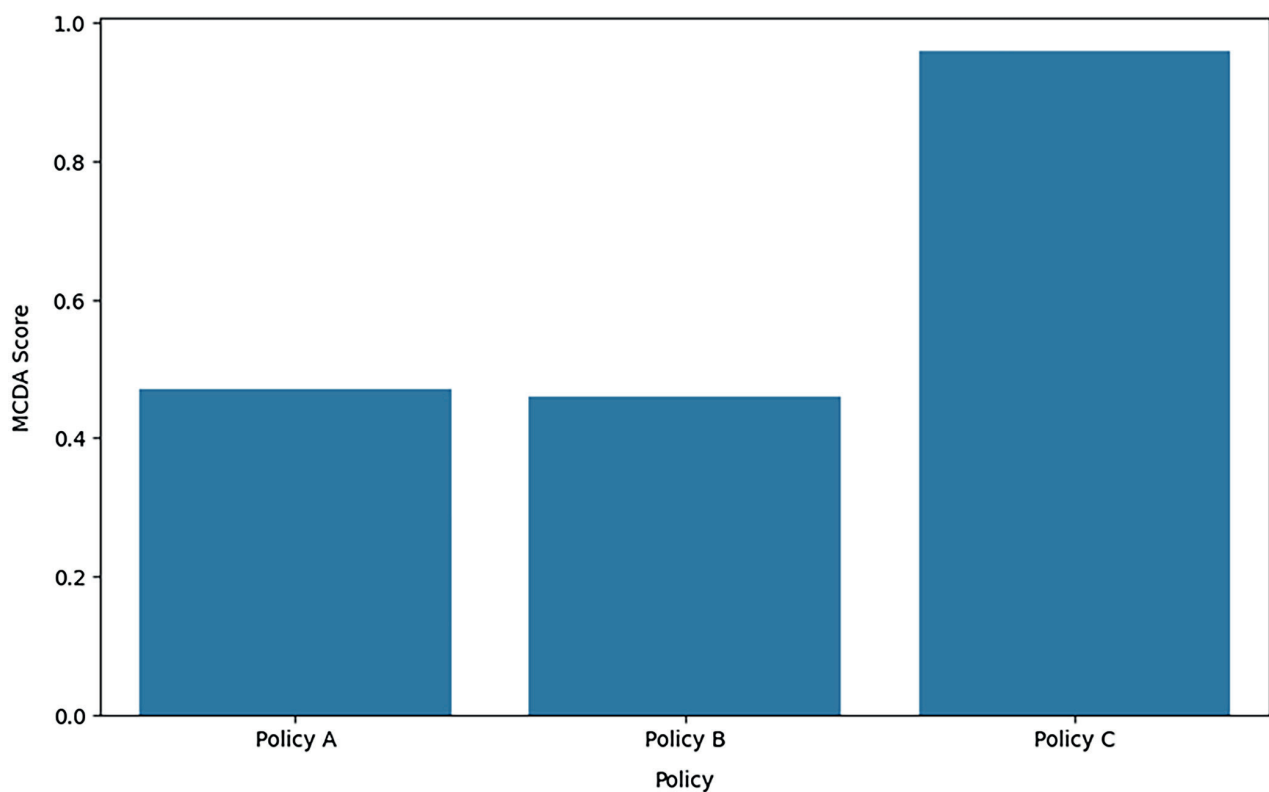


Fig. 11. Decision support systems for policies

system framework. The conclusion that can be made based on the figure is that Policy C is the best option as it holds the greatest likelihood of realizing the set objectives.

Figure 12 is the “Residuals of autoregressive integrated moving average (ARIMA) model.” The plotting factors show the residuals as a time series, where the residuals

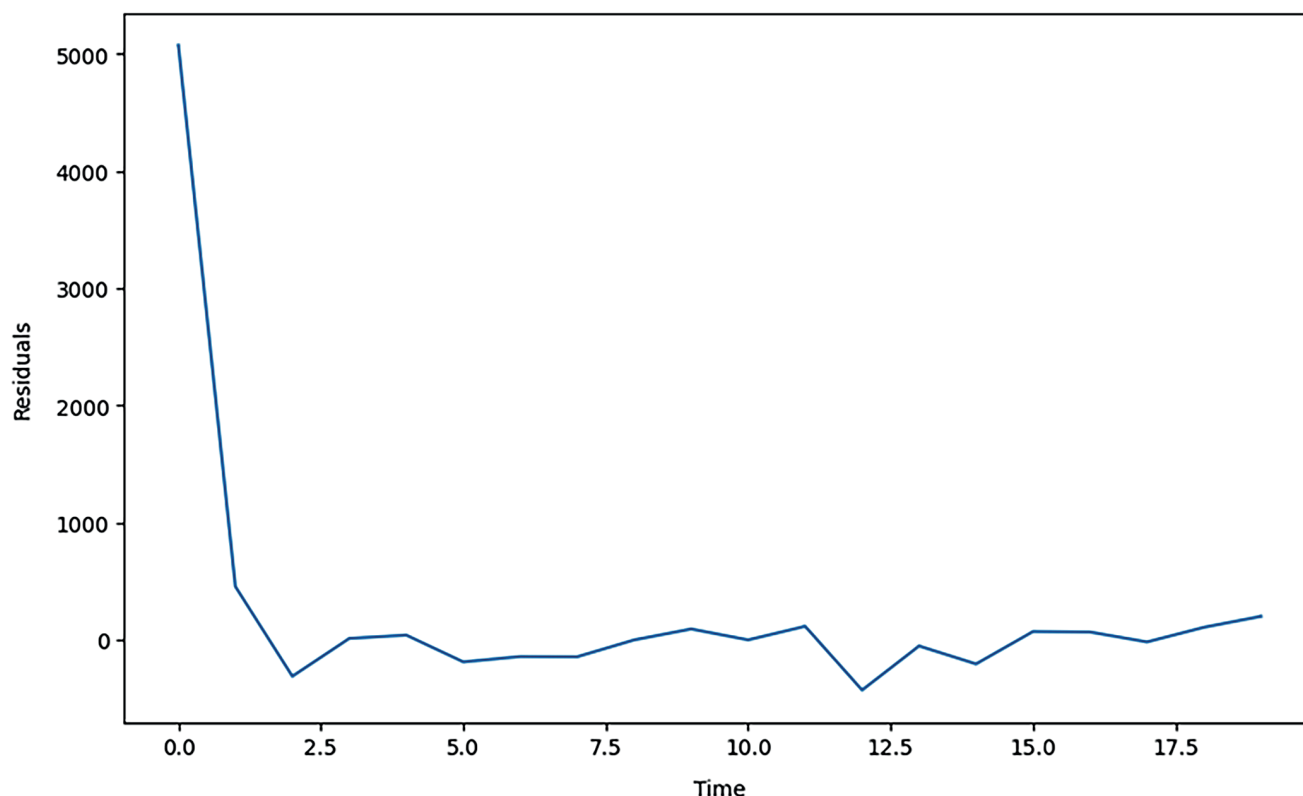


Fig. 12. Residual plot of ARIMA model

are calculated as the difference between the observed and the fitted values. First, the residuals are observed to be relatively large, with a maximum of over 5,000; however, they reduce sharply and oscillate around 0 periodically. This pattern suggests that after a certain period, the data-generating process is well captured by the ARIMA model. The high initial residuals imply that the model takes some time before stabilizing to fit the dataset. Over time, the residuals reach a pattern of randomness, thus suggesting that the model's forecasts are improving and becoming more coherent. In essence, this figure is essential in verifying the reliability of the selected ARIMA model. The fluctuation of residuals around 0 indicates that the residual values are centered along the 0 line, suggesting that the model has accurately captured the data pattern and provides a good fit. The conclusion that can be derived from this analysis is that ARIMA is an effective forecasting model whose ability to predict accurately can be established from the residuals, which are low and constant after the initial adjustment period.

Discussion

The findings of this study on equity-based financial models for universal and sustainable healthcare systems in Arab countries can serve as applicable theoretical and practical guidelines for healthcare equity, financing and

polymaking. The study reveals a multifaceted relationship between healthcare fairness and durability in the region.

The PCA results indicate a high degree of similarity between Qatar, Saudi Arabia and the UAE, aligning with previous studies that suggest the healthcare systems in the Gulf Cooperation Council (GCC) countries share common challenges and opportunities.²⁴ Such overlapping may serve as a foundation for regional cooperation in addressing healthcare trends, stating that the need for common strategies in enhancing healthcare in Arab countries should be coordinated.^{24–26}

The findings of the Theil index depicting incomes of different groups for income distribution indicate relatively low levels of inequality but more concentration of income in the lower end of the bell curve.²⁷ This finding aligns with previous research on income distribution in the Middle East and North Africa (MENA) region, where income inequality has persisted at high levels despite economic growth.²⁸ This pattern of income distribution underscores the need for policy measures to address economic disparities, which are widely recognized as contributing to adverse health outcomes and disparities in healthcare access and utilization.²⁹ The comparison of Interventions A and B in the context of cost analysis has proven that CEA plays a significant role in managing and delivering healthcare.³⁰ This increased cost per patient is still associated with better effectiveness of Intervention B, which is consistent with the literature calling for more comparative effectiveness research in using available resources

efficiently in the healthcare system.³¹ This result aligns with the general direction towards the increased utilization of research findings in formulating health policies.³²

The ICER analysis of policies A, B and C shows that evaluating healthcare policies is not straightforward. The conclusion is that Policy A has the lowest ICER, indicating that it is the most cost-effective option for implementing the identified policy while aligning with the overall objectives of the study. Moreover, the ICER analysis highlights the importance of considering both costs and outcomes in health policymaking to ensure efficient resource allocation and improved healthcare effectiveness.³³ This approach to policy evaluation is relevant within the constraints of scarce resources in healthcare system and the drive to attain UHC in many Arab states.³⁴

The results obtained using the Delphi technique, illustrated by the increasing level of consensus in the responses from participants over 3 rounds, support the applicability and effectiveness of the structured approach to stakeholder involvement in the development of healthcare policy.³⁵ This finding is consistent with the literature pointing to the need for community engagement to develop context-responsive and long-term health policy solutions.³⁶ Therefore, the 3rd-round results show a high degree of consensus concerning the proposed framework, and it can be assumed that the final framework will be supported by various stakeholders who are significant to the success of the implementation.

In addition, the MCDA scores of various policies present an extensive assessment model encompassing numerous criteria. Policy C has demonstrated superior performance in this assessment, emphasizing the effectiveness of MCDA in multi-criteria decision-making within healthcare policymaking, as observed in earlier studies.³⁷ This enables the consideration of policy impacts in a way that goes beyond mere cost-benefit and efficiency calculations and encompasses social and ethical concerns.

Regarding the evaluation of the framework's performance under different economic conditions and policy shifts, a comparative analysis was carried out to identify the framework's applicability and resilience. The impact of different financial conditions, such as economic growth, recession and inflation, on healthcare financing and resource mobilization was assessed using systems dynamics modeling.⁴ For example, in an economic downturn, lower revenues limit spending and require priorities such as public investment in basic infrastructure and social safety nets. Instead, economic growth can create conditions for service extension and investigation of various additional financing models, such as social impact bonds and government subsidizing for the permanent development of the service.¹⁰

Moreover, policy changes were evaluated using stochastic analysis to compare the variability of the impacts resulting from taxation alteration, healthcare subsidies and insurance premiums.⁵ The study illustrated that raising the tax revenue to finance healthcare enhanced equity

and utilization but presented difficulties regarding the financial risk protection of the poorer sectors of society. On the other hand, extending healthcare subsidies led to improving UHC, but questions arose regarding financial feasibility issues, especially during the economic downturn.¹⁸ Based on these findings, it becomes clear that policy interventions should be adapted to changes in the economic environment to ensure that policies promoting equity do not compromise fiscal sustainability.

Therefore, this study's findings help enrich knowledge about healthcare equity and sustainability issues in Arab countries. From economic evaluations to stakeholder engagement, the study offers a conceptual framework to develop a solution for the multifaceted problem of healthcare financing and equity. These findings validate the role of involving stakeholders to form evidence-based policies and reflect on the potential of regions to come up with united solutions to healthcare issues.

Proposed equity-based financial framework for the sustainable and equitable healthcare system

This research suggests the following equity-based financial framework, constructed around the fundamentals of the HEMF and visualized in Fig. 13, for assisting Saudi Arabia in developing a sustainable and equitable healthcare system:

Diversified healthcare financing mechanisms

A diverse range of financing options should be utilized, incorporating government grants, business insurance and innovative methods such as social impact bonds and community bond plans. Moreover, healthcare financing needs to be structured to effectively tackle socioeconomic disparities and geographical variations in access to and consumption of healthcare services.

Resource allocation based on equity and need

The distribution of resources should be based on the population's needs, considering factors such as population size, disease load and socioeconomic status. It is essential to prioritize resource allocation to underserved and rural areas to ensure that everyone has equitable access to healthcare. By doing so, we can address disparities in health outcomes and promote a more fair and just healthcare system for all individuals, regardless of their circumstances.

Targeted financial protection measures

Implementing UHC plans or subsidized healthcare services is essential for making healthcare accessible to low-income and marginalized groups. By doing so, we can ensure that essential healthcare services reach a broader

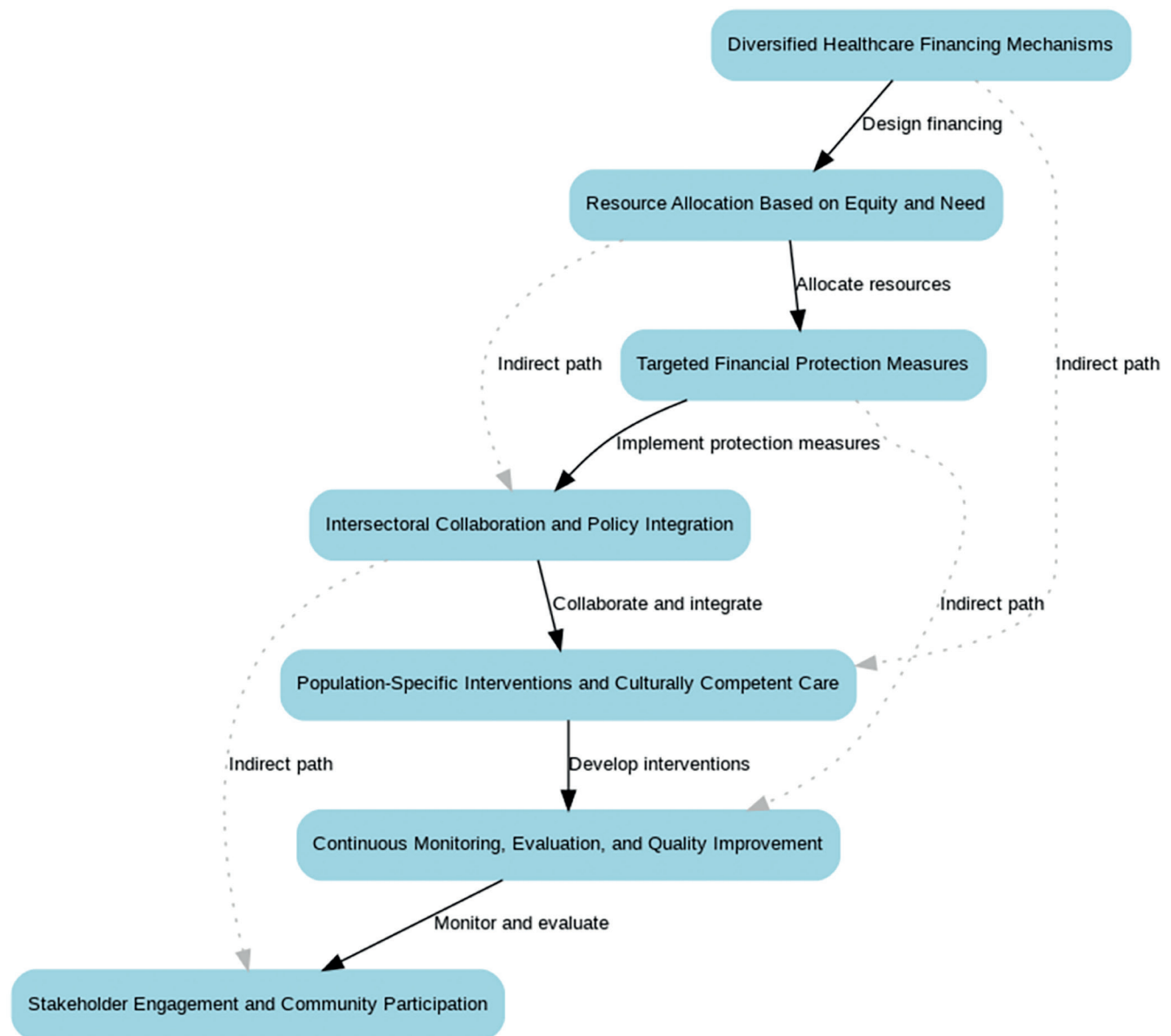


Fig. 13. Equity-based financial framework for the sustainable and equitable healthcare system

segment of the population. Additionally, it is important to explore sliding-scale pricing and allowances, which can further enhance access to healthcare for those in need. These strategies work together to create a more equitable healthcare system that meets the needs of all individuals, regardless of their financial situation.

Intersectoral collaboration and policy integration

To create effective healthcare policies, it's essential for healthcare officials, social welfare organizations, and other key stakeholders to collaborate closely. This collaboration will help in developing appropriate strategies that address the diverse needs of the community. Additionally, it is crucial to consider socioeconomic determinants of health, such as housing, education and employment, within the framework of broader healthcare financing

plans. Addressing these factors is vital for ensuring holistic improvement in health outcomes and fostering a healthier society overall.

Population-specific interventions and culturally competent care

Gathering and analyzing de-identified data is essential for gaining a better understanding of the healthcare requirements and challenges faced by various demographic groups. By leveraging this information, specialized programs can be developed to address the educational, occupational and social needs of underserved communities. Additionally, it is vital for healthcare providers to receive training in patient-centered care techniques, cultural understanding and effective communication methods to enhance the overall quality of care and support these diverse populations.

Continuous monitoring, evaluation and quality improvement

The development of reliable data tracking and analysis tools is essential for measuring the success of healthcare financing strategies and equality measures. By utilizing these tools, organizations can regularly enhance healthcare equity results through informed modifications based on data-driven decision-making and evidence-based approaches. This continuous improvement ensures that healthcare systems can adapt and respond effectively to the evolving needs of the population, ultimately fostering greater equity and access to care.

Stakeholder engagement and community participation

Legislators, healthcare providers, patient advocates, and community leaders are all essential stakeholders in the planning and implementation of an equity-based financial aid system. Their involvement is crucial for the success of this initiative, which aims to address the diverse needs of the community. It is important to drive local participation and gauge the area's sentiment to ensure that the plan effectively incorporates the community's objectives and goals. By engaging these key stakeholders, the system can be designed to reflect the priorities and aspirations of those it intends to serve.

Equity-based financial framework for sustainable healthcare

This equity-based financial scheme, proposed to the authorities, aims to address the various factors contributing to healthcare disparities in the Arab region. It seeks to ensure equal access to healthcare for all citizens, regardless of socioeconomic status, geographic location or family history, ultimately improving health outcomes across the population. This framework outlines the implementation strategy that promotes sustainability goals, reduces health inequalities and creates a healthcare system that satisfies the various needs of Arabs.

Practical implications of the study

The study recommendations for policymakers include implementing evidence-based primary healthcare equity initiatives for each Arab country. This entails employing PCA to ascertain factors that need policy reforms to reduce healthcare disparities. Another measure that policymakers should use is the Theil index, which measures disparities concerning income with a view of directing resources towards the less privileged groups. Therefore, the study indicated that equity-based financial frameworks should be used to improve people's health outcomes because they eliminate inequalities in the distribution of resources.

Policymakers should seek active interaction with relevant stakeholders and use the Delphi technique to enhance and mutually define policies.

Second, it is vital to develop ways of updating and reviewing the healthcare equity data routinely to fit in the ever-shifting socioeconomic framework. These steps will ensure that the policies to be implemented are informed by research and are specific and appropriate for the long-term change desired in the region's healthcare system.

The most pressing challenge to implementing the framework in healthcare within the analyzed regions is the lack of sufficiently skilled healthcare workers. Unfortunately, there is no clear-cut solution for resolving healthcare shortages.³⁸

Healthcare labor can be increased in the short run by raising the wage rates. However, this temporary and unsustainable solution only incentivizes retired and foreign healthcare workers to enter the labor market. Longer-term healthcare labor markets face substantial time lags when reacting to labor shortages due to the long training period needed. Additionally, regulatory constraints and other barriers to entry restrict the number of licensed healthcare professionals. However, loosening regulations is not advisable, as they play a crucial role in maintaining the quality of healthcare services and ensuring standardized care across the system. Therefore, addressing the healthcare labor shortage requires more than just wage adjustments.³⁹

While raising the retirement age for healthcare workers and incentivizing the migration of foreign healthcare professionals can help mitigate short-term labor shortages, bolstering the domestic healthcare workforce will be essential for ensuring the long-term sustainability of the healthcare sector.³⁹

The proposed framework can provide a foundation for identifying the needs of heterogeneous regions. Governments should collaborate with regional stakeholders to comprehensively understand the financial and non-financial factors affecting the healthcare labor supply.

Expanding the number of seats in medical and nursing schools is a valuable policy initiative to consider. Additionally, integrating technological advancements, a trend already being adopted by many Gulf countries, can help alleviate the burden on healthcare workers and enhance efficiency in healthcare delivery.

Limitations

It should be noted that this study has several limitations. The emphasis placed on Arab countries may mandate caution when generalizing the conclusions to other areas of the world. The use of available data may have introduced biases or gaps within the datasets, potentially affecting the accuracy and completeness of the analysis. One of the key limitations of this research is its cross-sectional design, which does not capture temporal effects, making it impossible to establish trends or determine

causality. Finally, the rapidly evolving healthcare systems and the changing socioeconomic dynamics of the studied area may impact the long-term relevance of the proposed framework. Future research should strive to use longitudinal designs to assess the effects of healthcare equity policies, with the potential to encourage significant changes in the field. By comparing countries or regions, we can reveal common trends and irregularities, exploding a sense of shared purpose in achieving equal access to healthcare services. To gain a deeper understanding of the mechanisms driving inequity, future studies should incorporate more detailed socioeconomic characteristics, offering a more comprehensive perspective on the issue. Moreover, future research should also analyze the outcomes of identified specific prevention and treatment measures developed through PCA and the Theil index methods, offering practical insights for policy implementation. These insights could transform the way we approach healthcare equity. Lastly, refining the Delphi technique could improve consensus-building efforts, fostering collaboration among healthcare stakeholders and facilitating decision-making in many different challenging environments.

Conclusions

The contributions of our research are summarized as follows: A survey of Arab countries and their healthcare sector was conducted, which revealed significant deficiencies. A novel framework was presented to address healthcare disparities by integrating equity with innovative financing methods. A comprehensive quantitative approach was presented, incorporating culturally sensitive care interventions, continuous assessment, and support.

This study designed an equity-based financial model to harness sustainable healthcare systems in Arab countries using different analytical tools to solve healthcare equity, financing and policy formulation. The PCA established a significant correlation in the healthcare data of Qatar, Saudi Arabia and the UAE, indicating the similarity of healthcare systems in geographical regions. The analysis of income distribution using the Theil index indicated moderate income inequality, with household incomes skewed toward lower levels. The ICER analysis indicated that Policy A was the most cost-effective among the 3 policies studied. The Delphi technique obtained a satisfactory consensus of 0.90 in the 3rd round with relatively high stakeholder consensus. Lastly, the MCDA analysis revealed that Policy C was the most efficient among the 3 options, achieving the highest score, closer to 1 than Policies A and B.

The study provides a comprehensive framework that integrates various analytical approaches, ranging from economic evaluations to stakeholder engagement strategies. This research is crucial for gaining a holistic understanding of the healthcare landscape in the region and identifying

opportunities for enhanced collaboration and policy development. By utilizing diverse methods, the study can close the gap between theory and policy regarding healthcare financing and equity and strengthen the existing literature as the basis for future theoretical and policy work.

Data availability

The datasets generated and/or analyzed during the current study are available from the corresponding author on reasonable request.

Consent for publication

Not applicable.

Use of AI and AI-assisted technologies

Not applicable.

ORCID iDs

Wadi B. Alonazi  <https://orcid.org/0000-0002-3850-4437>

References

1. Rosen MA. The future of sustainable development: Welcome to the European Journal of Sustainable Development Research. *European Journal of Sustainable Development Research*. 2017;1(1):1–2. doi:10.20897/ejosdr.201701
2. Forum for the Future, Centre for Sustainable Healthcare and NHS Institute for Innovation and Improvement. Sustainable System-Wide Commissioning: How a Whole System Approach Leads to More Sustainable Healthcare. London, UK: NHS Institute for Innovation and Improvement; 2013. <https://climateandhealthalliance.org/wp-content/uploads/2018/02/Sustainable-System-Wide-Commissioning-CSH.pdf>. Accessed August 15, 2023.
3. Almodhen F, Moneir WM. Toward a financially sustainable healthcare system in Saudi Arabia. *Cureus*. 2023;15(10):e46781. doi:10.7759/cureus.46781
4. Giang A, Edwards MR, Fletcher SM, et al. Equity and modeling in sustainability science: Examples and opportunities throughout the process. *Proc Natl Acad Sci U S A*. 2024;121(13):e2215688121. doi:10.1073/pnas.2215688121
5. Thomson S, Foubister T, Figueras J, Kutzin J, Permanand G, Bryndová L. Addressing financial sustainability in health systems. Geneva, Switzerland: World Health Organization (WHO); 2009. <https://iris.who.int/bitstream/handle/10665/107966/Policy-summary-1-2077-1584-eng.pdf?sequence=9&isAllowed=y>. Accessed August 15, 2023.
6. Birch S, Murphy GT, MacKenzie A, Cumming J. In place of fear: Aligning health care planning with system objectives to achieve financial sustainability. *J Health Serv Res Policy*. 2015;20(2):109–114. doi:10.1177/1355819614562053
7. Okonda MO, Bulanda B, Kabasele JYD, Chuga D, Bonganya BI, Kamangu EN. Evaluation of early warning Indicators (EWI) of HIV drug resistance according to the World Health Organization (WHO) in some treatment centers in Kinshasa. *Open Access Library Journal*. 2019;6(7):e5500. doi:10.4236/oalib.1105500
8. Liaropoulos L, Goranitis I. Health care financing and the sustainability of health systems. *Int J Equity Health*. 2015;14(1):80. doi:10.1186/s12939-015-0208-5
9. World Economic Forum (WEF). *Sustainable Health Systems Visions, Strategies, Critical Uncertainties and Scenarios*. Geneva, Switzerland: World Economic Forum (WEF); 2013. https://www3.weforum.org/docs/WEF_SustainableHealthSystems_Report_2013.pdf. Accessed August 15, 2023.

10. Al-Kibsi G, Woetzel J, Isherwood T, Khan J, Mischke J, Noura H. *Saudi Arabia beyond Oil: The Investment and Productivity Transformation*. New York, USA: McKinsey Global Institute; 2015. https://www.mckinsey.com/~/media/mckinsey/featured%20insights/employment%20and%20growth/moving%20saudi%20arabia%20economy%20beyond%20oil/mgi%20saudi%20arabia_executive%20summary_december%202015.pdf. Accessed August 15, 2023.
11. Kennedy EM. Health care as a fundamental human right: Moving from lip service to reality. *Harv Hum Rts J*. 2009;22:165–168. <https://journals.law.harvard.edu/hrj/wp-content/uploads/sites/83/2009/09/kennedy.pdf>.
12. United Nations Department of Economic and Social Affairs. Transforming our world: The 2030 Agenda for Sustainable Development. New York, USA: United Nations (UN), Department of Economic and Social Affairs; 2015. <https://sdgs.un.org/2030agenda>. Accessed August 15, 2023.
13. Smithers D, Waitzkin H. Universal health coverage as hegemonic health policy in low-and middle-income countries: A mixed-methods analysis. *Soc Sci Med*. 2022;302:114961. <https://doi.org/10.1016/j.socscimed.2022.114961>
14. Oraro-Lawrence T, Wyss K. Policy levers and priority-setting in universal health coverage: A qualitative analysis of healthcare financing agenda setting in Kenya. *BMC Health Serv Res*. 2020;20(1):182. doi:10.1186/s12913-020-5041-x
15. Hartwig J. What drives health care expenditure? Baumol's model of 'unbalanced growth' revisited. *J Health Econ*. 2008;27(3):603–623. doi:10.1016/j.jhealeco.2007.05.006
16. Dixon A. Are medical savings accounts a viable option for funding health care? *Croat Med J*. 2002;43(4):408–416. PMID:12187518.
17. Folke C, Carpenter S, Elmqvist T, Gunderson L, Holling CS, Walker B. Resilience and sustainable development: Building adaptive capacity in a world of transformations. *AMBIO J Hum Environ*. 2002;31(5):437–440. doi:10.1579/0044-7447-31.5.437
18. Mathauer I, Vinyals Torres L, Kutzin J, Jakab M, Hanson K. Pooling financial resources for universal health coverage: Options for reform. *Bull World Health Organ*. 2020;98(2):132–139. doi:10.2471/BLT.19.234153
19. Mathauer I, Koch K, Zita S, et al. Revenue-raising potential for universal health coverage in Benin, Mali, Mozambique and Togo. *Bull World Health Organ*. 2019;97(9):620–630. doi:10.2471/BLT.18.222638
20. Hoagland A, Kipping S. Challenges in promoting health equity and reducing disparities in access across new and established technologies. *Can J Cardiol*. 2024;40(6):1154–1167. doi:10.1016/j.cjca.2024.02.014
21. Fadhil I, Ali R, Al-Raisi SS, et al. Review of National Healthcare Systems in the Gulf Cooperation Council Countries for Noncommunicable Diseases Management. *Oman Med J*. 2022;37(3):e370–e370. doi:10.5001/omj.2021.96
22. Albejaidi F, Nair KS. Building the health workforce: Saudi Arabia's challenges in achieving Vision 2030. *Int J Health Plann Manage*. 2019;34(4):e1405–e1416. doi:10.1002/hpm.2861
23. Brownie SM, Hunter LH, Aqtash S, Day GE. Establishing policy foundations and regulatory systems to enhance nursing practice in the United Arab Emirates. *Policy Polit Nurs Pract*. 2015;16(1–2):38–50. doi:10.1177/1527154415583396
24. Mwale ML, Mchenga M, Chirwa GC. A spatial analysis of out-of-pocket payments for healthcare in Malawi. *Health Policy Plan*. 2022;37(1):65–72. doi:10.1093/heapol/czab090
25. Sinha R, Chatterjee K, Nair N, Tripathy P. Determinants of out-of-pocket and catastrophic health expenditure: A cross-sectional study. *Br J Medicine Med Res*. 2016;11(8):1–11. doi:10.9734/BJMMR/2016/21470
26. Mahmoudi MR, Heydari MH, Qasem SN, Mosavi A, Band SS. Principal component analysis to study the relations between the spread rates of COVID-19 in high risks countries. *Alexandria Engineering Journal*. 2021;60(1):457–464. doi:10.1016/j.aej.2020.09.013
27. Husky M, Zgueb Y, Ouali U, et al. Principal component analysis of the Well-being at Work and Respect for Human Rights Questionnaire (WVRRR) in the Mediterranean region. *Clin Pract Epidemiol Mental Health*. 2020;16(1):115–124. doi:10.2174/1745017902016010115
28. Khan MS, Siddique AB. Spatial analysis of regional and income inequality in the United States. *Economies*. 2021;9(4):159. doi:10.3390/economies9040159
29. Andrei T, Oancea B, Richmond P, Dhesi G, Herteliu C. Decomposition of the inequality of income distribution by income types: Application for Romania. *Entropy*. 2017;19(9):430. doi:10.3390/e19090430
30. Tao Y, Wu X, Zhou T, et al. Exponential structure of income inequality: Evidence from 67 countries. Preprint posted online December 6, 2016. *arXiv*. doi:10.48550/ARXIV.1612.01624
31. Wouterse B, Van Baal P, Versteegh M, Brouwer W. The value of health in a cost-effectiveness analysis: Theory versus practice. *Pharmaco-Economics*. 2023;41(6):607–617. doi:10.1007/s40273-023-01265-8
32. Brent RJ. Cost-benefit analysis versus cost-effectiveness analysis from a societal perspective in healthcare. *Int J Environ Res Public Health*. 2023;20(5):4637. doi:10.3390/ijerph20054637
33. Erismann S, Pesantes MA, Beran D, et al. How to bring research evidence into policy? Synthesizing strategies of five research projects in low-and middle-income countries. *Health Res Policy Sys*. 2021;19(1):29. doi:10.1186/s12961-020-00646-1
34. Van Baal P, Morton A, Severens JL. Health care input constraints and cost effectiveness analysis decision rules. *Soc Sci Med*. 2018;200:59–64. doi:10.1016/j.socscimed.2018.01.026
35. Boulkedid R, Abdoul H, Loustau M, Sibony O, Alberti C. Using and reporting the Delphi method for selecting healthcare quality indicators: A systematic review. *PLoS One*. 2011;6(6):e20476. doi:10.1371/journal.pone.0020476
36. Darrudi A, Ketabchi Khoonsari MH, Tajvar M. Challenges to achieving universal health coverage throughout the world: A systematic review. *J Prev Med Public Health*. 2022;55(2):125–133. doi:10.3961/jpmph.21.542
37. Oliveira MD, Mataloto I, Kanavos P. Multi-criteria decision analysis for health technology assessment: Addressing methodological challenges to improve the state of the art. *Eur J Health Econ*. 2019;20(6):891–918. doi:10.1007/s10198-019-01052-3
38. Džakula A, Relić D, Michelutti P. Health workforce shortage: Doing the right things or doing things right? *Croat Med J*. 2022;63(2):107–109. doi:10.3325/cmj.2022.63.107
39. Michaeli DT, Michaeli T. The healthcare labour shortage: Practice, theory, evidence, and ways forward. *SSRN Electronic Journal*. 2022. <https://doi.org/10.2139/ssrn.4067462>.

Therapeutic efficiency and safety assessment of intradermal platelet-rich plasma combined with oral tranexamic acid in patients with facial melasma

Weeratian Tawanwongsri^{1,A,B,D–F}, Doungkamol Siri-Archawawat^{2,C,F}, Sasipaka Sindhusen^{3,C,D,F}, Chime Eden^{4,D–F}

¹ Division of Dermatology, Department of Internal Medicine, School of Medicine, Walailak University, Nakhon Si Thammarat, Thailand

² Division of Neurology, Department of Internal Medicine, School of Medicine, Walailak University, Nakhon Si Thammarat, Thailand

³ Bhumibol Adulyadej Hospital, Bangkok, Thailand

⁴ Jigme Dorji Wangchuck National Referral Hospital (JDWNRH), Thimphu, Bhutan

A – research concept and design; B – collection and/or assembly of data; C – data analysis and interpretation;

D – writing the article; E – critical revision of the article; F – final approval of the article

Advances in Clinical and Experimental Medicine, ISSN 1899–5276 (print), ISSN 2451–2680 (online)

Adv Clin Exp Med. 2025;34(4):529–537

Address for correspondence

Weeratian Tawanwongsri

E-mail: weeratian.ta@gmail.com

Funding sources

This study was funded by Walailak University, Thailand (grant No. WU-66236).

Conflict of interest

None declared

Received on October 2, 2023

Reviewed on November 20, 2023

Accepted on April 23, 2024

Published online on June 27, 2024

Cite as

Tawanwongsri W, Siri-Archawawat D, Sindhusen S, Eden C. Therapeutic efficiency and safety assessment of intradermal platelet-rich plasma combined with oral tranexamic acid in patients with facial melasma. *Adv Clin Exp Med*. 2025;34(4):529–537. doi:10.17219/acem/187874

DOI

10.17219/acem/187874

Copyright

Copyright by Author(s)

This is an article distributed under the terms of the Creative Commons Attribution 3.0 Unported (CC BY 3.0) (<https://creativecommons.org/licenses/by/3.0/>)

Abstract

Background. Melasma is a chronic, acquired hypermelanosis that primarily affects the face. Platelet-rich plasma (PRP) and tranexamic acid (TXA) are promising treatments for melasma. However, only a few randomized clinical trials have examined the efficacy and safety of combining these therapies for melasma.

Objectives. We aimed to compare the efficacy and safety of combining PRP and oral TXA with those of PRP alone in the treatment of facial melasma.

Materials and methods. A randomized controlled trial was conducted at Walailak University Hospital, Nakhon Si Thammarat, Thailand, between March and September 2023. Participants with mixed-type melasma were randomly allocated in a 1:1 ratio to either group A (PRP injection alone without placebo) or group B (PRP injection with oral TXA). Therapeutic efficacy and safety assessments were performed over a 12-week follow-up period.

Results. The study included 26 participants (mean age: 45.9 years, standard deviation (\pm SD): 5.0) who were predominantly female (84.6%). In group A, the modified Melasma Area and Severity Index (mMASI) scores significantly decreased from a median of 4.30 interquartile range (IQR): 4.10 to 3.60 (IQR: 3.10) between week 0 and week 12, respectively. In group B, the median mMASI decreased from 6.40 (IQR: 7.80) to 3.60 (IQR: 3.70) over the same period. The median change in mMASI scores in group B (2.90, IQR: 2.40) was significantly larger than in group A (0.90, IQR: 0.60) ($p < 0.001$, $U = 160.50$). However, there were no significant differences in the physicians' global assessment (PGA), melasma quality of life scale (MelasQoL) or patient satisfaction during follow-up. Four patients (15.4%) experienced transient erythema and swelling. In group B, 1 participant (7.7%) experienced transient mild gastrointestinal discomfort after receiving oral TXA.

Conclusions. The combination of intradermal PRP injection and oral TXA is effective for melasma, even in patients with poor prognostic treatment response factors. No serious adverse reactions were observed in either group.

Key words: efficiency, safety, platelet-rich plasma, tranexamic acid, melasma

Background

Melasma is a chronic, acquired hypermelanosis characterized by asymmetric, irregular, brown, reticulated macules and patches on photoexposed areas of the skin, especially the face. The most commonly affected facial sites are the zygomatic, labial superior and frontal areas,¹ with a prevalence ranging from 9% to 50% (higher in the Asian population).² Risk factors include genetic predisposition, sun exposure, skin tone, hormonal influences, and certain medications (e.g., antiepileptics and phototoxic drugs).^{1,3,4} Based on clinicopathologic findings, melasma is classified into 3 types: epidermal, dermal and mixed.⁵

Although melasma does not result in serious physical morbidities, approx. 80% of patients with melasma report psychiatric comorbidities, such as major depressive disorders, adjustment disorders and higher functional disabilities.⁶ To date, the treatment of melasma is challenging. The general recommendations include the avoidance of triggers, sun protection, avoiding the application of cosmetics containing excessive mercury and lead, sleeping well, and maintaining a good mood.⁷ According to the European Society of Laser Dermatology,⁸ lasers and intense pulsed light sources are recognized as viable treatment modalities for a variety of hyperpigmented lesions. This is primarily because melanosomes, which are the storage sites for melanin, are the principal target in most hyperpigmented disorders. Consequently, the majority of lasers employed for treating hyperpigmented lesions are Q-switched (QS). These lasers facilitate appropriate pulse durations based on the principle of selective photothermolysis.⁹ Notably, in the case of melasma, the combined use of Kligman's trio and a pulsed dye laser has been observed to significantly reduce the severity and recurrence of melasma.⁸ The therapeutic landscape has recently expanded to include an alternative treatment approach, particularly during a hydroquinone holiday. This novel method involves the combination of platelet-rich plasma (PRP) and oral tranexamic acid (TXA), which has been garnering increasing attention as an effective treatment option. Transforming growth factor- β 1 in PRP plays a crucial role in inhibiting melanin synthesis via extracellular signal-regulated kinases.¹⁰ Moreover, platelet-derived growth factor (PDGF) increases the skin volume with pigmentary improvement via the stimulation of blood vessel formation and synthesis of collagen and other components of the extracellular matrix (ECM).¹¹ Meanwhile, the anti-plasmin effect of TXA is regarded as the major hypopigmentary mechanism. Additionally, it competitively inhibits tyrosinase enzyme activity and decreases the intensity of keratinocyte–melanocyte interactions.^{12,13}

Both PRP and TXA have proven to be promising treatment options for melasma treatment.^{14,15} In Thailand, randomized clinical trials are limited in assessing the efficacy and safety of intradermal PRP combined with oral TXA for facial melasma. Sirithanabadeekul et al. conducted

a split-face, single-blinded trial comparing PRP to normal saline in treating this condition.¹⁶ The study noted a significant improvement in the PRP group with a mean modified Melasma Area and Severity Index (mMASI) score increase of 1.03 ± 0.44 from baseline to week 10. However, further research is needed to confirm the efficacy of this combination treatment of intradermal PRP combined with oral TXA for facial melasma.

Objectives

Our primary objective was to compare the effectiveness of combining PRP and oral TXA with PRP alone for treating facial melasma. The secondary objective was to assess the safety of these interventions.

Materials and methods

Participants

This prospective investigator-blinded randomized trial was conducted between March and September 2023 at the Walailak University Hospital, Nakhon Si Thammarat, Thailand. The inclusion criteria were as follows: 1) age between 18 and 55 years and 2) a clinical diagnosis of bilateral mixed-type melasma by a board-certified dermatologist. In patients with mixed-type melasma, assessments were conducted using a Wood's light. This type of melasma was identified by the simultaneous presence of both epidermal and dermal patterns. When examined under Wood's light, the epidermal type of melasma showed intensified pigmentation, characterized by uniform enhancement and a well-defined border. In contrast, the dermal type did not exhibit intensified pigmentation under Wood's light and was marked by an ill-defined border.^{17,18} The exclusion criteria included: 1) participants who refused to participate in the study; 2) having an allergic history to lidocaine, prilocaine, TXA, sodium citrate, chlorhexidine, or isopropyl alcohol; 3) any concurrent melasma treatments within 6 months; 4) pregnancy or lactation; 5) hematologic, neurologic or oncological diseases; 6) smoking or alcohol abuse; 7) taking hormonal therapy, retinoids, or antiarrhythmic medications, including amiodarone, bretylium, sotalol, dofetilide; and 8) severe hepatic or renal impairment. The participants were randomly allocated in a 1:1 ratio to either group A (PRP injection alone without placebo) or group B (PRP injection with oral TXA).

This clinical trial was registered with the Thai Clinical Trials Registry (No. TCTR20230317003). The ethics committee took into account and complied with Thailand's laws, including the Personal Data Protection Act. To ensure confidentiality, all data files and sensitive personal information were encrypted, password-protected, and saved on a secure computer that was accessible only by study coordinators.

The participants accessed their own data by directly contacting the study coordinators. No information linking individuals to the data was revealed. Twelve months after the completion of the study, all data were deleted.

This prospective study was approved by the Walailak Ethics Committee (approval No. WUEC-23-069-01). Written informed consent was obtained from all participants after a full explanation of the study. This study complied with the principles of the Declaration of Helsinki and the International Conference on the Harmonization of Good Clinical Practice.

Preparation of platelet-rich plasma

At each treatment session, whole blood (16 mL) was obtained by venipuncture and divided into 2 10-mL tubes containing acid citrate dextrose and gel (8 mL each; Bio-Medica, Gyeonggi-do, South Korea). A single centrifugation technique was used as the preparation method.¹⁹ Blood plasma was obtained by centrifugation of the whole blood at 3,200 rpm for 10 min, followed by collection of the final sample (0.8 mL) from the lower $\frac{1}{3}$ of the plasma. In accordance with the classification system for platelet concentrates established by Dohan Ehrenfest et al.,²⁰ which is based on 2 key parameters: the presence or absence of cellular content (such as leukocytes) and the characteristics of the fibrin architecture, we collected the blood component situated in the lower $\frac{1}{3}$ of the portion above the separation gel following centrifugation.¹⁹ This process resulted in our PRP being categorized as pure PRP (P-PRP). During the 1st treatment, additional blood (8 mL) was collected for PRP preparation and sent for platelet counting.

Procedure and evaluation

We adhered to the protocols recommended in previous studies.^{16,21} A local anesthetic cream containing 2.5% lidocaine and 2.5% prilocaine (EMLA; Recipharm Karlskoga AB, Karlskoga, Sweden) was applied to lesions and occluded with a film for 40 min before wiping, leaving the skin dry. After disinfecting the skin with 2% chlorhexidine in 70% isopropyl alcohol, PRP (0.1 mL/cm²) was injected intradermally into the bilateral affected areas. This procedure entailed multiple injections with a 30G needle into the dermis, spacing each injection about 1 cm apart. This treatment was administered 3 times at 4-week intervals. All participants were instructed to apply broad-spectrum sunscreen, avoid sun exposure, and not use any topical skin-whitening treatments on the lesions during the study. In group B, participants were given oral TXA at a dosage of 500 mg/day for 12 weeks, in addition to receiving PRP treatment. Assessments were conducted at baseline and 4, 8 and 12 weeks. The mMASI²² and Physician's Global Assessment (PGA)¹⁸ were evaluated by a blinded investigator (D.S.). The mMASI score ranged from 0 to 24, and the PGA scores ranged from 0 to 6. A score of 0 indicated

clear skin, except for possible residual discoloration, while a score of 6 indicated a worsening condition compared to week 0. Patient satisfaction and the Melasma Quality of Life Scale (MelasQoL) were collected for further analysis.²³ The instrument was constructed to evaluate the social life, recreation, leisure, and emotional wellbeing of patients. The MelasQoL score ranges from 7 to 70, with a higher score indicating worse melasma-related health-related quality of life (HRQoL). Their satisfaction levels were categorized as follows: very satisfied (>75% improvement), satisfied (51–75% improvement), average (25–50% improvement), or dissatisfied (<25% improvement).⁷

Statistical analyses

Our sample size calculation, determined by a preceding study,²⁴ was based on an alpha level of 0.01, a power of 90% and an effect size (Cohen's *d*) of 1.86. The total sample size initially included 22 adult participants. However, to accommodate a potential follow-up loss of 20%, we determined that approx. 26 participants would need to be recruited for the study, thereby ensuring the robustness of our findings.

Continuous data were reported as means and standard deviations (\pm SDs) or medians and interquartile ranges (IQRs). Categorical data were presented as frequencies and percentages. A paired *t*-test or Mann–Whitney–Wilcoxon test was used to compare variables, such as age, Fitzpatrick skin type, onset of melasma, mMASI, PGA, MelasQoL, and satisfaction scores. Spearman's rho was used to assess the correlation between ordinal or non-normally distributed variables. Due to the small sample size, Fisher's exact test was employed for analyzing associations among categorical data. The independent *t*-test was applied to compare means between 2 independent groups under the assumption of normal distribution. The Mann–Whitney *U* test, a non-parametric alternative, was used for comparing 2 independent groups when data did not follow a normal distribution. The statistical significance was determined using 2-tailed tests with a *p*-value of less than 0.05. Statistical analyses were performed using SPSS v. 18 software (SPSS Inc., Chicago, USA).

In addition, we employed a robust heteroscedastic repeated measures analysis of variance (ANOVA), complemented by post hoc tests, to evaluate within-group differences across repeated measurements and to conduct between-group comparisons of the mMASI and MelasQoL scores between groups A and B. This robust ANOVA approach allowed for the integration of both types of comparisons into a single model, thereby enhancing the coherence and statistical power of our analysis. The analyses were conducted using the WRS2 package in the R program (R Foundation for Statistical Computing, Vienna, Austria).²⁵ Supplementary Tables 3–8 display the detailed, robust ANOVA for mMASI, including main effects for the group and time, the interaction between group and time, and effect sizes for between-group and within-group comparisons at different

times. Supplementary Methods 1–4 detail the analysis methods and include the corresponding R scripts, ensuring the reproducibility of the statistical analyses.

Results

A total of 26 participants were enrolled in the study, and no patients were lost to follow-up. The participants had a mean age of 45.9 years with a SD of ± 5.0 , with the majority of participants being female (84.6% of the group). The majority ($n = 17$, 65.4%) of participants had no comorbidities. However, some participants had comorbidities, including dyslipidemia ($n = 7$, 26.9%), allergic rhinitis ($n = 3$, 11.5%), type 2 diabetes mellitus ($n = 1$, 3.8%), and essential hypertension ($n = 1$, 3.8%). Table 1 presents the characteristics of participants in both groups.

In group A, the median baseline mMASI score was 4.30 with an IQR of 4.10, while in group B, it was 6.40 with an IQR of 7.80. In group A, the mMASI scores demonstrated a notable decline from baseline. The scores were 3.70 (IQR: 3.80), 3.70 (IQR: 2.30) and 3.60 (IQR: 3.10) at weeks 4, 8 and 12, respectively. The mMASI scores showed a significant decrease from baseline at week 0 to week 12 ($p < 0.001$; test statistic = 0.922, 95% confidence interval (95% CI): 0.407–1.438), with a median change of 0.90 and an IQR of 0.60. In group B, the mMASI scores also demonstrated a notable decline from the baseline. The scores were 4.50 (IQR: 6.50), 4.00 (IQR: 4.60) and 3.60 (IQR: 3.70) at weeks 4, 8 and 12, respectively. From baseline to week 12, the mMASI scores showed a significant decrease ($p = 0.002$, test statistic = 3.344, 95% CI: 0.752–5.937), with a median change of 2.90 and an IQR of 2.40. The median change in mMASI from week 0 to week 12

Table 1. Participants' characteristics

Measured parameters		Group A ($n = 13$)	Group B ($n = 13$)	p-value
Gender, n (%)	female	10 (76.9)	12 (92.3)	0.593
	male	3 (23.1)	1 (7.7)	
Age [years], mean (\pm SD)		44.5 (± 3.5)	47.2 (± 6.0)	0.174
Fitzpatrick skin type, n (%)	type III	3 (23.1)	4 (30.8)	1.000
	type IV	10 (76.9)	9 (69.2)	
Onset [years], median (IQR)		5.0 (3.0)	5.0 (6.0)	0.545
mMASI, median (IQR)	week 0	4.30 (4.10)	6.40 (7.80)	0.208
	week 4	3.70 (3.80)	4.50 (6.50)	0.397
	week 8	3.70 (2.30)	4.00 (4.60)	0.523
	week 12	3.60 (3.10)	3.60 (3.70)	0.892
Changes of mMASI scores, median (IQR) (from week 0 to week 12)		0.90 (0.60)	2.90 (2.40)	0.006
MelasQoL, median (IQR)	week 0	26.00 (34.00)	45.00 (18.00)	0.810
	week 4	23.00 (16.00)	40.00 (24.00)	0.606
	week 8	20.00 (11.00)	40.00 (17.00)	0.223
	week 12	18.00 (12.00)	36.00 (27.00)	0.186
Changes of MelasQoL scores, mean (\pm SD) (from week 0 to week 12)		7.92 (± 12.33)	5.85 (± 11.55)	0.834
PGA week 12, n (%)	score 0	0 (0)	0 (0)	1.000
	score 1	0 (0)	0 (0)	
	score 2	3 (23.1)	4 (30.8)	
	score 3	7 (53.8)	7 (53.8)	
	score 4	3 (23.1)	2 (15.4)	
	score 5	0 (0)	0 (0)	
	score 6	0 (0)	0 (0)	
Patient satisfaction week 12, n (%)	score 1	0 (0)	0 (0)	0.215
	score 2	2 (15.4)	0 (0)	
	score 3	6 (46.2)	4 (30.8)	
	score 4	5 (38.5)	9 (69.2)	

Group A – PRP injection alone without placebo; Group B – PRP injection with oral tranexamic acid; IQR – interquartile range; MelasQoL – Melasma Quality of Life scale; mMASI – modified Melasma Area Severity Index; PGA – Physician's Global Assessment; PRP – platelet-rich plasma; SD – standard deviation. The names and values of the tests are presented in Supplementary File 1.

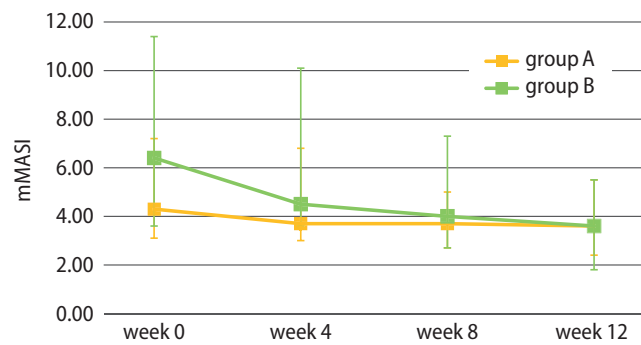


Fig. 1. The modified Melasma Area Severity Index (mMASI) scores recorded during follow-up visits

This line graph illustrates the mMASI. Group A, shown with a yellow line, consisted of participants who received platelet-rich plasma (PRP) injections without a placebo. Group B, indicated by a green line, included participants treated with PRP injections in conjunction with oral tranexamic acid. Squares represent the median mMASI scores for each group over a span of 12 weeks and error bars display the interquartile range (IQR).

was significantly greater in group B compared to group A ($p = 0.006$, test statistic = 3.610, 95% CI: -3.950 — 0.895 , $df = 9$). The comparative analysis between the 2 groups and the comparison of repeated data in groups A and B are provided in Supplementary File 1. The presentation of mMASI scores during the follow-up visit is depicted in Fig. 1. Photographs taken before (at week 0) and after (at week 12) the intervention, showcasing the comparison between groups A and B, are presented in Fig. 2,3. At week 12, melasma severity in group A was assessed using PGA scores, with 3 participants (23.1%) scoring 2, 7 participants (53.8%) scoring 3 and 3 participants (23.1%) scoring 4. In contrast, in group B, the melasma severity was rated by 4 participants (30.8%) with a score of 2, 7 participants (53.8%) with a score of 3 and 2 participants (15.4%) with a score of 4.

According to the MelasQoL scores, the median baseline scores were 26.00 (IQR: 34.00) in group A and 45.00 (IQR: 18.00) in group B. In group A, the score declined to 23.00 (IQR: 16.00), 20.00 (IQR: 11.00), and 18.00 (IQR: 12.00) at weeks 4, 8 and 12, respectively. From baseline to week 12, the MelasQoL scores exhibited a statistically

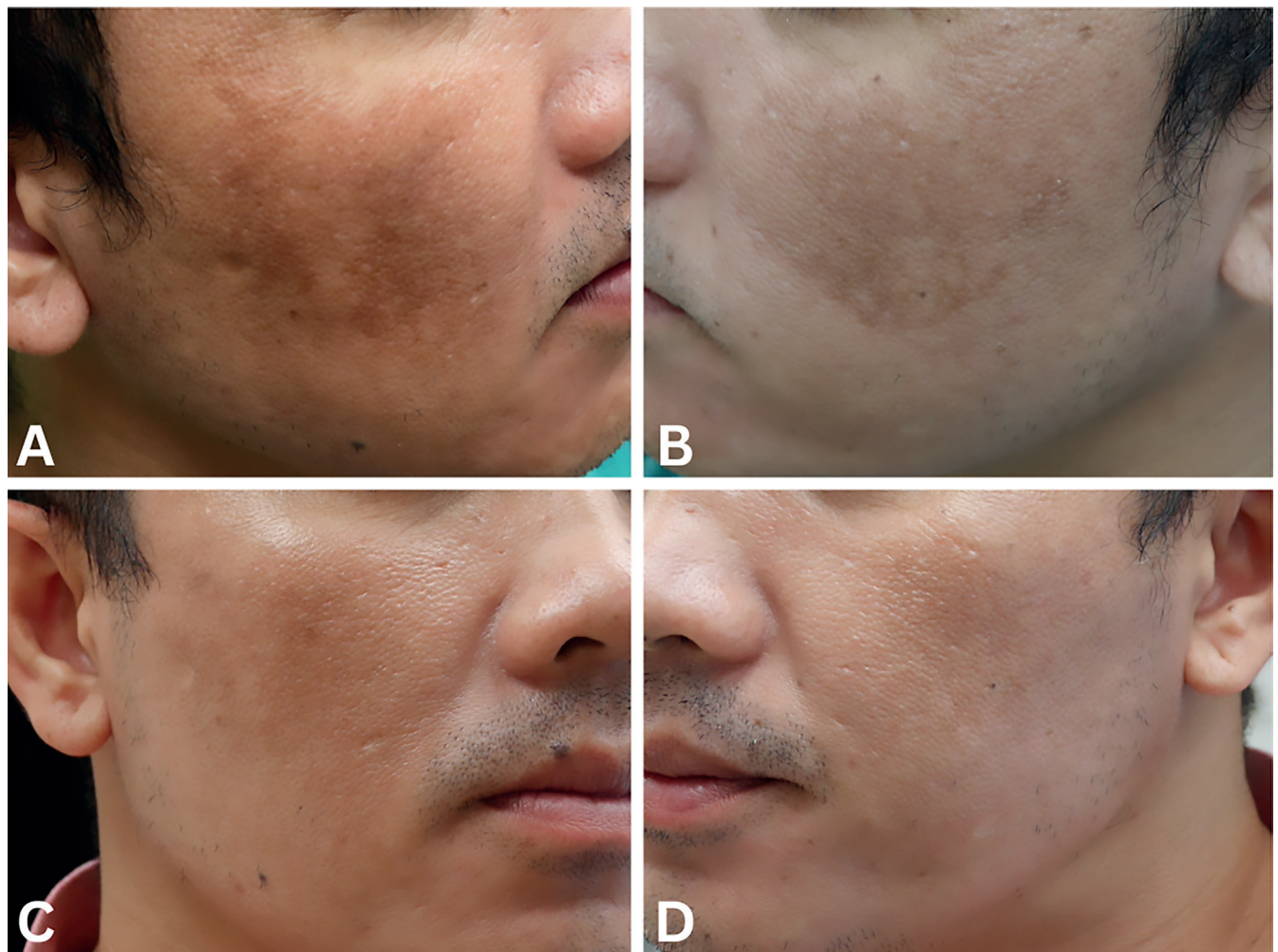


Fig. 2. Comparative photographs of group A, taken before the intervention (week 0) and after the intervention (week 12), illustrating the observed changes. The right side of the face (A) and the left side of the face (B) are shown at week 0, and the right side of the face (C) and the left side of the face (D) are shown at week 12

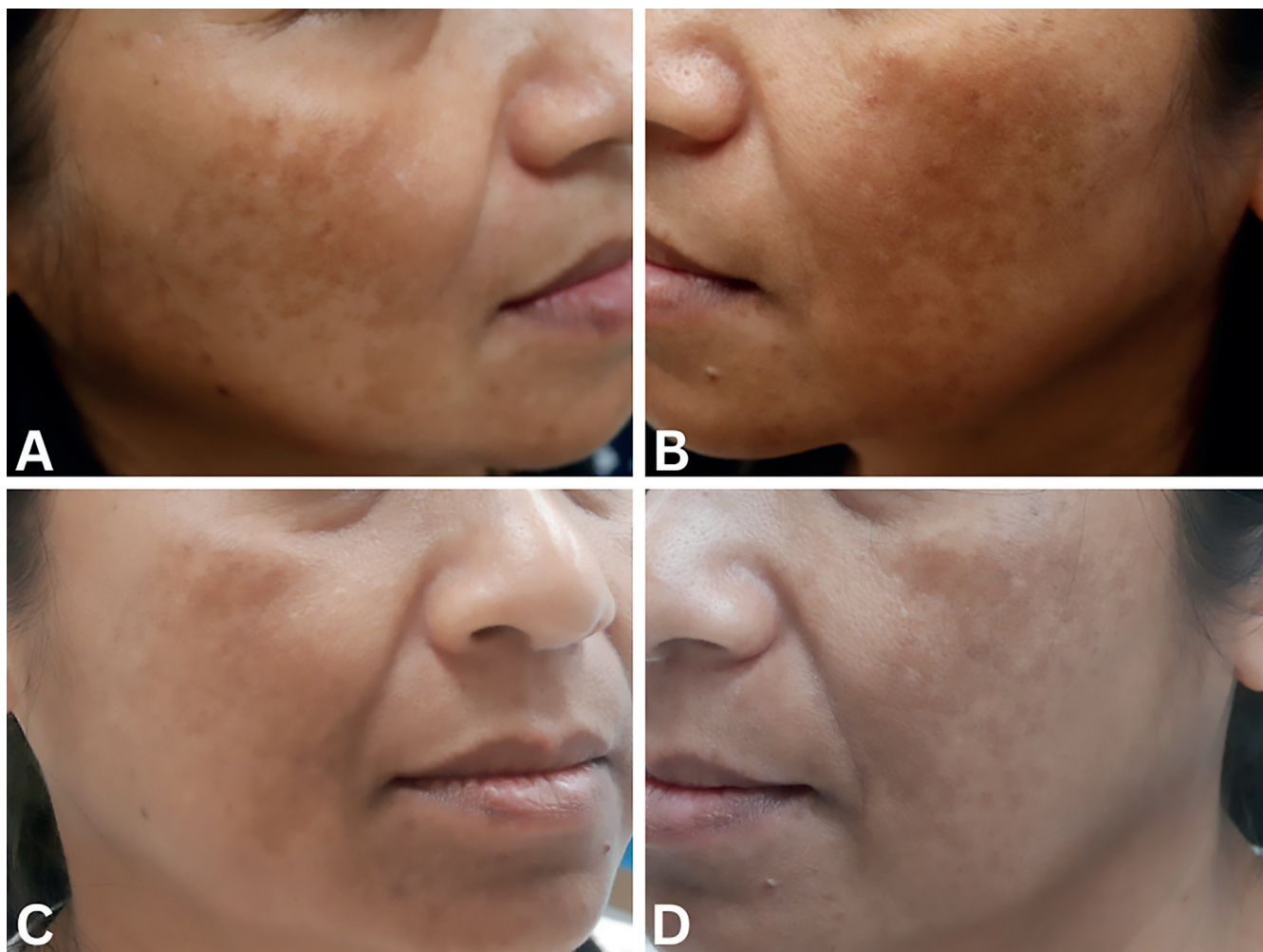


Fig. 3. Comparative photographs of group B taken before the intervention (week 0) and after the intervention (week 12), illustrating the observed changes. The right side of the face (A) and the left side of the face (B) are shown at week 0, and the right side of the face (C) and the left side of the face (D) are shown at week 12

significant decrease ($p = 0.047$, test statistic = 4.889, 95% CI: $-2.376-12.154$), with a mean change of 7.92 and an SD of 12.33. In group B, the score also declined to 40.00 (IQR: 24.00), 40.00 (IQR: 17.00) and 36.00 (IQR: 27.00) at weeks 4, 8 and 12, respectively. Between baseline and week 12, there was a nonsignificant reduction in MelasQoL scores ($p = 0.050$, test statistic = 9.444, 95% CI: $-4.841-23.730$), characterized by an average change of 5.85 with a SD of ± 11.55 . The mean change in MelasQoL from week 0 to week 12 did not differ significantly between both groups ($p = 0.834$, test statistic = 0.214, 95% CI: $-8.051-9.829$, $df = 13$). At week 12, in group A, patient satisfaction with treatment was rated as a score of 2 by 2 participants (15.4%), a score of 3 by 6 participants (46.2%) and a score of 4 by 5 participants (38.5%). In group B, 4 participants (30.8%) rated it with a score of 3, while 9 participants (69.2%) rated it with a score of 4. We utilized Spearman's correlations to analyze this ordinal or non-normally distributed data. There was no significant correlation between the mMASI and MelasQoL scores either at week 0 ($r = 0.34$, $p = 0.090$) or at week 12 ($r = 0.20$, $p = 0.321$). Additionally,

no correlation was observed between PGA and satisfaction levels at week 12 ($r = 0.15$, $p = 0.478$). However, a significant correlation was found between the improvement in mMASI scores and satisfaction levels at the conclusion of the study ($r = 0.52$, $p = 0.007$).

Four participants (15.4%) in our study experienced transient erythema and swelling, which mostly resolved within 4 h (IQR: 3.5). They also reported mild pain during the injection, with a mean of 3.4 (SD: ± 1.7). In group B, 1 participant (7.7%) experienced transient mild gastrointestinal discomfort within the 1st week of oral TXA administration, with no subsequent symptoms reported. The medication was not discontinued and was well tolerated for the entirety of the study period.

Discussion

Both PRP and TXA have proven to be efficacious treatments for melasma. However, there are still a limited number of controlled clinical trials to confirm the efficacy

of this combination.¹⁷ Our findings revealed a significantly larger decrease in melasma severity, as measured using mMASI, among participants treated with PRP injection combined with oral TXA compared to those treated with PRP injection alone. Additionally, no serious adverse reactions were noted in participants treated with oral TXA, except for mildly tolerable gastrointestinal symptoms.

Platelet-rich plasma consists of a mixture of growth factors and cytokines, which includes transforming growth factor beta 1 (TGF- β 1), PDGF and epidermal growth factor (EGF).²⁶ Transforming growth factor beta 1 inhibits melanogenesis by suppressing the signal transduction of microphthalmia-associated transcription factor, resulting in a decrease in tyrosinase and tyrosinase-related proteins.^{21,27} Furthermore, it promotes the expression of laminin, type IV collagen and tenascin, facilitating basement membrane repair and preventing the infiltration of melanocytes and melanin into the dermis.²⁸ Platelet-derived growth factor plays a pivotal role in angiogenesis and contributes to the synthesis of collagen and various components of the ECM, including hyaluronic acid, ultimately enhancing skin homogeneity and volume.²⁹ Epidermal growth factor curtails melanogenesis by suppressing prostaglandin E2 and tyrosinase activity.³⁰ The effectiveness of PRP in treating melasma resulted in a decrease in the mMASI score of 1.18 (95% CI: 0.89–1.47; $p = 0.02$).¹⁴

The main mechanism of action of TXA in the treatment of melasma is its anti-plasmin activity. Plasmin is involved in converting pro-opiomelanocortin (POMC) into melanocyte-stimulating hormone (MSH) and releasing basic fibroblast growth factor (bFGF), which promotes melanocyte proliferation.³¹ Tranexamic acid, due to its structural similarity to tyrosine, can competitively inhibit the tyrosinase enzyme's activity.¹³ Additionally, TXA decreases the quantity of blood vessels in the dermal layer and prevents neovascularization triggered by bFGF.³² The oral administration of TXA leads to a reduction in melasma severity, as measured using the MASI score, compared to its topical (–1.85, 95% CI: –2.56––1.14) and intradermal forms (–1.67, 95% CI: –1.99––1.36), with a greater reduction of –1.87 (95% CI: –2.46––1.28). Moreover, a meta-analysis revealed that oral TXA treatment exhibited less heterogeneity compared to that of topical TXA.³³

Gamea et al. demonstrated that individuals with melasma who received a combination of PRP and topical TXA experienced a significant improvement in the mMASI score compared with those treated solely with topical TXA. In the combination therapy group, the mMASI score decreased from 12.1 ± 2.9 to 3.6 ± 1.9 ($p < 0.001$).¹⁵ Our findings revealed that the improvement in the mMASI score within the combination therapy group was 2.90, with an IQR of 2.40. This change was more significant than that of PRP-alone or oral TXA-alone groups in previous studies.^{14,33} However, when compared to the findings of Gamea et al., the observed change appeared to be lower. The plausible explanation for this could be that

the participants in this study had poorer prognostic factors for melasma treatment, including a longer duration of disease (≥ 2 years) and mixed-type melasma.³⁴ Furthermore, the severity of melasma in our study was categorized as mild-to-moderate.³⁵ Therefore, it might not have been possible to observe a significant improvement.

In our study, we evaluated the efficacy of melasma treatments using 3 measures: The mMASI, PGA and patient satisfaction levels.⁷ The mMASI score has been established as a reliable, valid and responsive method for evaluating the severity of melasma.^{22,36,37} Additionally, PGA assessments have demonstrated moderate intra- and inter-rater agreement.³⁸ However, there is a notable gap in research regarding the correlation between these different evaluation methods. In a study by Tekam and Belgaumkar,³⁹ the efficacy of combining autologous platelet-rich plasma (PRP) with hydroquinone 4% was compared to that of hydroquinone alone. Their findings indicated that the combination therapy led to statistically significant improvements in mMASI, patient satisfaction and PGA scores. Conversely, Beyzaee et al.⁴⁰ discovered that a combination treatment involving Q-Switched Nd:YAG laser and topical methimazole 5% was significantly more effective in improving PGA scores than using methimazole 5% alone. Interestingly, there was no significant difference in mMASI scores between the 2 groups. Similarly, our results indicated significant changes in melasma severity when using mMASI scores but not when employing PGA assessments. We propose that although the PGA is a straightforward and easy-to-use scoring system, it may not capture detailed aspects such as the exact area affected and the depth of color. Therefore, the mMASI could be more sensitive in detecting minor improvements. Furthermore, considering that patient satisfaction levels were assessed by several evaluators, it is crucial to validate these assessments before the study and to re-evaluate the inter-rater reliability coefficient. Studies focusing on this correlation should be conducted to enhance our understanding of these measures in clinical settings. Moreover, a recent meta-analysis revealed that among 5 studies, a statistically significant correlation was observed between MASI and MELASQoL scores. However, 7 other studies reported no such statistical association.⁴¹ We concur that additional research, involving more substantial sample sizes, is necessary to validate the link between melasma and quality of life.

Following PRP injections, the common side effects included mild erythema, bruising, depigmentation, and hyperpigmentation.¹⁴ Similarly, only 4 participants in our study developed transient erythema and swelling, which mostly resolved within 4 h. They also reported mild pain during the injection. When considering the safety of TXA treatment, most studies reported no serious adverse drug reactions.³² They mainly noted mild gastrointestinal symptoms (2.5–5.4%), central nervous system effects (2.5%) and menstrual irregularities (0.7–8.1%). Only

1 study reported a single case of deep vein thrombosis that led to the discontinuation of TXA administration.¹² Similarly, in our study, 1 participant (7.7%) experienced transient, mild gastrointestinal discomfort within the 1st week of oral TXA administration. However, no symptoms were reported thereafter, despite continued use of the medication.

Limitations

Our study had several limitations. First, the study was conducted at a single center. Second, various techniques were used for PRP preparation in the studies, and specific bioactive concentrations were not evaluated.⁴² Therefore, this makes it challenging to directly compare the treatment outcomes between studies. Multicenter randomized controlled studies employing uniform PRP preparation methods and long-term follow-up are necessary to establish the efficacy and safety of these interventions. Third, no clinical data were collected or compared regarding sun exposure during the study period. Nevertheless, comprehensive guidance regarding sun protection and avoidance was provided to all the participants. Fourth, the majority of the participants in our study had mild-to-moderate melasma. To determine the efficacy in individuals with severe melasma, particularly those with poor prognostic treatment response factors, further studies should compare participants across a wider range of severity. Fifth, the use of anesthetics in PRP injections may reduce the effectiveness of PRP.⁴³ However, it is important to note that these in vitro studies mainly focused on tenocytes and did not include other cells or elements related to melasma. Therefore, this underscores the necessity for further verification through both in vitro and in vivo studies.

Conclusions

The combination of intradermal PRP and oral TXA is an effective treatment for melasma, even in patients with poor prognostic treatment response factors. The change in mMASI was significantly different in the combination group compared to the participants treated with intradermal PRP alone. No serious adverse reactions were observed in any group. Only mild, tolerable gastrointestinal symptoms have been reported in patients treated with oral TXA.

Supplementary data

The Supplementary materials are available at <https://doi.org/10.5281/zenodo.11297407>. The package includes the following files:

Supplementary Table 1. Normality assessment and two-group comparative analysis (n = 26).

Supplementary Table 2. Comparison of repeated data in groups A and B (n = 26).

Supplementary Table 3. Robust analysis of variance of mMASI scores by group and time using bootstrapped trimmed means.

Supplementary Table 4. The main effect for group on mMASI scores.

Supplementary Table 5. Main effect for time on mMASI scores.

Supplementary Table 6. Interaction Effect for Group × Time on mMASI scores.

Supplementary Table 7. Effect sizes from Yuen's test for trimmed means in between-group comparisons over time.

Supplementary Table 8. Effect sizes for within-group comparisons over time using Cliff's delta.

Supplementary Fig. 1. Correlation between the mMASI and MelasQoL scores at week 0 (n = 26).

Supplementary Fig. 2. Correlation between the mMASI and MelasQoL scores at week 12 (n = 26).

Supplementary Fig. 3. Correlation between PGA and satisfaction level at week 12 (n = 26).

Supplementary Fig. 4. Correlation between the improvement in mMASI scores from week 0 to week 12 and the satisfaction level at week 12 (n = 26).

Supplementary Method 1. Implementation of robust tests for two independent groups and analysis of median differences using the WRS2 package in R.

Supplementary Method 2. Implementation of robust ANOVA for repeated measures using the WRS2 package in R.

Supplementary Method 3. Computing a between-within subjects ANOVA on the trimmed means.

Supplementary Method 4. Computing effect sizes.

Data availability

The datasets generated and/or analyzed during the current study are available from the corresponding author on reasonable request.


Consent for publication


Not applicable.


ORCID IDs

Weeratani Tawanwongsri  <https://orcid.org/0000-0002-1949-7323>

Doungkamol Siri-Archawawat

 <https://orcid.org/0000-0002-5517-9023>

Sasipaka Sindhusen  <https://orcid.org/0009-0000-7498-9622>

Chime Eden  <https://orcid.org/0000-0002-6963-1092>

References

1. de Tamega A, Miot LDB, Bonfietti C, Gige TC, Marques MEA, Miot HA. Clinical patterns and epidemiological characteristics of facial melasma in Brazilian women. *Acad Dermatol Venereol.* 2013;27(2): 151–156. doi:10.1111/j.1468-3083.2011.04430.x

2. Majid I, Aleem S. Melasma: Update on epidemiology, clinical presentation, assessment, and scoring. *J Skin Stem Cell*. 2022;8(4):e120283. doi:10.5812/jssc.120283
3. Passeron T. Melasma pathogenesis and influencing factors: An overview of the latest research. *Acad Dermatol Venereol*. 2013;27(Suppl 1): 5–6. doi:10.1111/jdv.12049
4. Rostami Mogaddam M, Safavi Ardabili N, Iranparvar Alamdari M, Maleki N, Aghabalaee Danesh M. Evaluation of the serum zinc level in adult patients with melasma: Is there a relationship with serum zinc deficiency and melasma? *J Cosmet Dermatol*. 2018;17(3):417–422. doi:10.1111/jocd.12392
5. Rodrigues M, Pandya AG. Melasma: Clinical diagnosis and management options. *Aust J Dermatol*. 2015;56(3):151–163. doi:10.1111/ajd.12290
6. Deshpande S, Khatu S, Pardeshi G, Gokhale N. Cross-sectional study of psychiatric morbidity in patients with melasma. *Indian J Psychiatry*. 2018;60(3):324. doi:10.4103/psychiatry.IndianJPsychiatry_115_16
7. Gao TW, Gu H, He L, et al. Consensus on the Diagnosis and Treatment of Melasma in China (2021 Version). *Int J Dermatol Venereol*. 2021;4(3):133–139. doi:10.1097/JD9.0000000000000164
8. Passeron T, Genedy R, Salah L, et al. Laser treatment of hyperpigmented lesions: Position statement of the European Society of Laser in Dermatology. *Acad Dermatol Venereol*. 2019;33(6):987–1005. doi:10.1111/jdv.15497
9. Altshuler GB, Anderson RR, Manstein D, Zenzie HH, Smirnov MZ. Extended theory of selective photothermolysis. *Lasers Surg Med*. 2001;29(5):416–432. doi:10.1002/lsm.1136
10. Kim DS, Park SH, Park KC. Transforming growth factor- β 1 decreases melanin synthesis via delayed extracellular signal-regulated kinase activation. *Int J Biochem Cell Biol*. 2004;36(8):1482–1491. doi:10.1016/j.biocel.2003.10.023
11. Çayırılı M, Çalışkan E, Açıkgöz G, Erbil AH, Ertürk G. Regression of melasma with platelet-rich plasma treatment. *Ann Dermatol*. 2014; 26(3):401. doi:10.5021/ad.2014.26.3.401
12. Lee HC, Thng TGS, Goh CL. Oral tranexamic acid (TA) in the treatment of melasma: A retrospective analysis. *J Am Acad Dermatol*. 2016; 75(2):385–392. doi:10.1016/j.jaad.2016.03.001
13. Taraz M, Niknam S, Ehsani AH. Tranexamic acid in treatment of melasma: A comprehensive review of clinical studies. *Dermatol Ther*. 2017;30(3): e12465. doi:10.1111/dth.12465
14. Zhao L, Hu M, Xiao Q, et al. Efficacy and safety of platelet-rich plasma in melasma: A systematic review and meta-analysis. *Dermatol Ther (Heidelb)*. 2021;11(5):1587–1597. doi:10.1007/s13555-021-00575-z
15. Gamea MM, Kamal DA, Donia AA, Hegab DS. Comparative study between topical tranexamic acid alone versus its combination with autologous platelet rich plasma for treatment of melasma. *J Dermatolog Treat*. 2022;33(2):798–804. doi:10.1080/09546634.2020.1781755
16. Sirithanabadeekul P, Dannarongchai A, Suwanchinda A. Platelet-rich plasma treatment for melasma: A pilot study. *J Cosmet Dermatol*. 2020;19(6):1321–1327. doi:10.1111/jocd.13157
17. Mahajan VK, Patil A, Blicharz L, et al. Medical therapies for melasma. *J Cosmet Dermatol*. 2022;21(9):3707–3728. doi:10.1111/jocd.15242
18. Pandya A, Berneburg M, Ortonne JP, Picardo M. Guidelines for clinical trials in melasma. *Br J Dermatol*. 2006;156:21–28. doi:10.1111/j.1365-2133.2006.07590.x
19. Hamid MSA. Cost effectiveness of a platelet-rich plasma preparation technique for clinical use. *Wounds*. 2018;30(7):186–190. PMID: 30059343.
20. Dohan Ehrenfest DM, Rasmusson L, Albrektsson T. Classification of platelet concentrates: From pure platelet-rich plasma (P-PRP) to leucocyte- and platelet-rich fibrin (L-PRF). *Trends Biotechnol*. 2009;27(3): 158–167. doi:10.1016/j.tibtech.2008.11.009
21. Tuknayyat A, Bhalla M, Thami GP. Platelet-rich plasma is a promising therapy for melasma. *J Cosmet Dermatol*. 2021;20(8):2431–2436. doi:10.1111/jocd.14229
22. Pandya AG, Hynan LS, Bhore R, et al. Reliability assessment and validation of the Melasma Area and Severity Index (MASI) and a new modified MASI scoring method. *J Am Acad Dermatol*. 2011;64(1):78–83.e2. doi:10.1016/j.jaad.2009.10.051
23. Balkrishnan R, McMichael AJ, Camacho FT, et al. Development and validation of a health-related quality of life instrument for women with melasma. *Br J Dermatol*. 2003;149(3):572–577. doi:10.1046/j.1365-2133.2003.05419.x
24. Del Rosario E, Florez-Pollack S, Zapata L, et al. Randomized, placebo-controlled, double-blind study of oral tranexamic acid in the treatment of moderate-to-severe melasma. *J Am Acad Dermatol*. 2018; 78(2):363–369. doi:10.1016/j.jaad.2017.09.053
25. Mair P, Wilcox R. Robust statistical methods in R using the WRS2 package. *Behav Res*. 2020;52(2):464–488. doi:10.3758/s13428-019-01246-w
26. Pavlovic V, Ciric M, Jovanovic V, Stojanovic P. Platelet rich plasma: A short overview of certain bioactive components. *Open Med*. 2016; 11(1):242–247. doi:10.1515/med-2016-0048
27. Kim DH, Je YJ, Kim CD, et al. Can platelet-rich plasma be used for skin rejuvenation? Evaluation of effects of platelet-rich plasma on human dermal fibroblast. *Ann Dermatol*. 2011;23(4):424. doi:10.5021/ad.2011.23.4.424
28. Ding X, Liu SX. Progress in the use of platelet-rich plasma to treat vitiligo and melasma. *Int J Dermatol Venereol*. 2021;4(4):236–241. doi:10.1097/JD9.0000000000000171
29. Papakonstantinou E, Roth M, Karakiulakis G. Hyaluronic acid: A key molecule in skin aging. *Dermatoendocrinology*. 2012;4(3):253–258. doi:10.4161/derm.21923
30. Yun WJ, Bang SH, Min KH, Kim SW, Lee MW, Chang SE. Epidermal growth factor and epidermal growth factor signaling attenuate laser-induced melanogenesis. *Dermatol Surg*. 2013;39(12):1903–1911. doi:10.1111/dsu.12348
31. Maeda K. Mechanism of action of topical tranexamic acid in the treatment of melasma and sun-induced skin hyperpigmentation. *Cosmetics*. 2022;9(5):108. doi:10.3390/cosmetics9050108
32. Diehl C. Use of tranexamic acid in melasma. *Ukrainian J Dermatol Venerol Cosmetol*. 2019;3:104–112. doi:10.30978/UJDVK2019-3-104
33. Zhang L, Tan WQ, Fang QQ, et al. Tranexamic acid for adults with melasma: A systematic review and meta-analysis. *Biomed Res Int*. 2018;2018:1683414. doi:10.1155/2018/1683414
34. Doolan BJ, Gupta M. Melasma. *Aust J Gen Pract*. 2021;50(12):880–885. doi:10.31128/AJGP-05-21-6002
35. Rodrigues M, Ayala-Cortés AS, Rodríguez-Arámbula A, Hynan LS, Pandya AG. Interpretability of the Modified Melasma Area and Severity Index (mMASI). *JAMA Dermatol*. 2016;152(9):1051. doi:10.1001/jama-dermatol.2016.1006
36. Abou-Taleb DAE, Ibrahim AK, Youssef EMK, Moubasher AEA. Reliability, validity, and sensitivity to change overtime of the Modified Melasma Area and Severity Index Score. *Dermatol Surg*. 2017;43(2):210–217. doi:10.1097/DSS.0000000000000974
37. Heidemeyer K, Cazzaniga S, Feldmeyer L, et al. Skin hyperpigmentation index in melasma: A complementary method to classic scoring systems. *J Cosmet Dermatol*. 2023;22(12):3405–3412. doi:10.1111/jocd.15866
38. Bossart S, Cazzaniga S, Willenberg T, et al. Reliability assessment and validation of the Skin Hyperpigmentation Index compared to the Physician Global Assessment Score. *Dermatology*. 2022;238(4): 688–691. doi:10.1159/000520753
39. Tekam PS, Belgaumkar VA. Combination of autologous platelet rich plasma and hydroquinone 4% is more effective than hydroquinone alone in treatment of melasma: A split-face comparative study. *Dermatol Ther*. 2022;35(11):e15761. doi:10.1111/dth.15761
40. Beyzaee AM, Goldust M, Rokni GR, Patil A, Mostaghiman R, Golpour M. Comparative effectiveness and safety of topical methimazole 5% monotherapy versus combination of Q-Switched Nd:YAG Laser and topical methimazole 5% in patients with refractory melasma. *J Cosmet Dermatol*. 2023;22(6):1774–1779. doi:10.1111/jocd.15641
41. Zhu Y, Zeng X, Ying J, Cai Y, Qiu Y, Xiang W. Evaluating the quality of life among melasma patients using the MELASQoL scale: A systematic review and meta-analysis. *PLoS One*. 2022;17(1):e0262833. doi:10.1371/journal.pone.0262833
42. Hesseler MJ, Shyam N. Platelet-rich plasma and its utility in medical dermatology: A systematic review. *J Am Acad Dermatol*. 2019;81(3): 834–846. doi:10.1016/j.jaad.2019.04.037
43. Carofino B, Chowanec DM, McCarthy MB, et al. Corticosteroids and local anesthetics decrease positive effects of platelet-rich plasma: An in vitro study on human tendon cells. *Arthroscopy*. 2012;28(5): 711–719. doi:10.1016/j.arthro.2011.09.013

Comparison of median nerve area measurement between MRI and electromyography in patients diagnosed with carpal tunnel syndrome

Şule Göktürk^{1,A–F}, Yasin Göktürk^{1,A,B,D}, Ali Koç^{2,C,E}, Ahmet Payas^{3,E,F}

¹ Department of Neurosurgery, Kayseri City Hospital, University of Health Sciences, Turkey

² Department of Radiology, Kayseri City Hospital, University of Health Sciences, Turkey

³ Department of Anatomy, Faculty of Medicine, University of Amasya, Turkey

A – research concept and design; B – collection and/or assembly of data; C – data analysis and interpretation;

D – writing the article; E – critical revision of the article; F – final approval of the article

Advances in Clinical and Experimental Medicine, ISSN 1899–5276 (print), ISSN 2451–2680 (online)

Adv Clin Exp Med. 2025;34(4):539–547

Address for correspondence

Şule Göktürk

E-mail: suleGOKTURK@outlook.com

Funding sources

None declared

Conflict of interest

None declared

Received on February 1, 2024

Reviewed on April 1, 2024

Accepted on April 11, 2024

Published online on September 3, 2024

Abstract

Background. Carpal tunnel syndrome (CTS) is the most common entrapment neuropathy that occurs when the median nerve is compressed within the carpal tunnel. Electromyography (EMG) is accepted as the most frequently used and important diagnostic method for CTS. Recently, magnetic resonance imaging (MRI) has begun to be used in CTS patients to directly visualize the median nerve and examine the changes occurring in the nerve structure.

Objectives. In this study, the area of the median nerve was measured at various levels in the wrist in patients with CTS using MRI, examining its relationship with signal increase, and comparing this to results obtained with EMG.

Materials and methods. Overall, 35 patients diagnosed with CTS were included in the study. Patients with normal-mild and moderate-severe EMG tests were included in the study; wrist MRI was taken to investigate the area/mm² of the median nerve at various levels and whether there was an increase in signal. Thenar muscles included in the imaging were also evaluated.

Results. Of the 35 patients included in the study, 24 were women (68.6%) and 11 were men (31.4%). Measurements of the average median nerve area measured in mm² at the distal radioulnar junction (DRUJ) and the median nerve area measured in mm² at the hamate bone level were obtained, showing that DRUJ and hamate bone distance measurements were higher in patients with positive EMG. Electromyography findings were also significantly positive in patients with increased signal.

Conclusions. In some cases, the diagnosis of CTS can be easily made with history and physical examination or employing confirmatory tests such as EMG, which is considered the gold standard. Magnetic resonance imaging can be used as an alternative method for imaging the median nerve in patients with CTS. In our study, EMG findings were also significantly positive in patients with increased signal on MRI, making it a preferable method, especially in soft tissue-related pathological cases.

Key words: magnetic resonance imaging, median nerve, carpal tunnel syndrome, carpal tunnel measures

Cite as

Göktürk Ş, Göktürk Y, Koç A, Payas A. Comparison of median nerve area measurement between MRI and electromyography in patients diagnosed with carpal tunnel syndrome. *Adv Clin Exp Med.* 2025;34(4):539–547. doi:10.17219/acem/187054

DOI

10.17219/acem/187054

Copyright

Copyright by Author(s)

This is an article distributed under the terms of the Creative Commons Attribution 3.0 Unported (CC BY 3.0) (<https://creativecommons.org/licenses/by/3.0/>)

Background

Carpal tunnel syndrome (CTS) occurs as a result of compression of the median nerve in the carpal tunnel, resulting in entrapment neuropathy.¹ It often appears as idiopathic, but there are also some underlying causes, with many pathological conditions and some anatomical variations that can compress the nerve and cause CTS.² Symptoms of the disease range from numbness and paresthesia in mild cases of impingement to loss of dexterity and thenar muscle atrophy in moderate and severe cases. In 1956, Simpson demonstrated that median nerve distal motor conduction time was prolonged in patients with CTS.³ Thus, electromyography (EMG) began to be used in diagnosis.

Electromyography is accepted as the most frequently used and important diagnostic method.⁴ For the most part, electrodiagnostic tests performed with nerve conduction studies (NCS), especially when including needle EMG, have high sensitivity and specificity to confirm CTS and eliminate other diagnoses.^{4,5} Polyneuropathy, plexopathy and radiculopathy can also be considered in the differential diagnosis. Electromyography evaluates evidence of pathological changes in the muscles innervated by the median nerve. If a secondary axonal loss occurs, EMG can reveal either active denervation (e.g., spontaneous activity such as fibrillation potentials, positive sharp waves and fasciculation potentials) or chronic changes indicating denervation with subsequent reinnervation (e.g., changes in motor unit action potential amplitudes, durations and recruitment). These findings support the diagnosis of CTS in the context of normal findings both in muscles not innervated by the median nerve and in muscles innervated by the proximal median nerve.⁶

Electromyography and its components for the diagnosis of CTS

Electrodiagnostic evaluation of a patient with suspected CTS is performed to confirm the diagnosis, to exclude compression located more proximally to the median nerve (brachial plexus lesion, C6 or C7 radiculopathy) and to determine the severity of median nerve involvement. According to the symptoms and findings of clinically diagnosed patients, these tests are positive in approx. 95% of cases.⁷

The median nerve innervates 4 muscles in the hand, namely the abductor pollicis brevis, flexor pollicis brevis, opponens brevis in the thenar region, and the 1st and 2nd lumbrical muscles in the interosseous region. Two or more C6–C7 innervated muscles (pronator teres, triiceps brachii, extensordigitorum communis) are evaluated to look for evidence of cervical radiculopathy. If the abductor pollicis brevis is abnormal, additional muscles are typically evaluated.⁴ This includes median-innervated muscles proximal to the carpal tunnel (e.g., flexor carpi radialis, pronator teres, flexor pollicis longus) to exclude proximal median neuropathy. Non-median-innervated

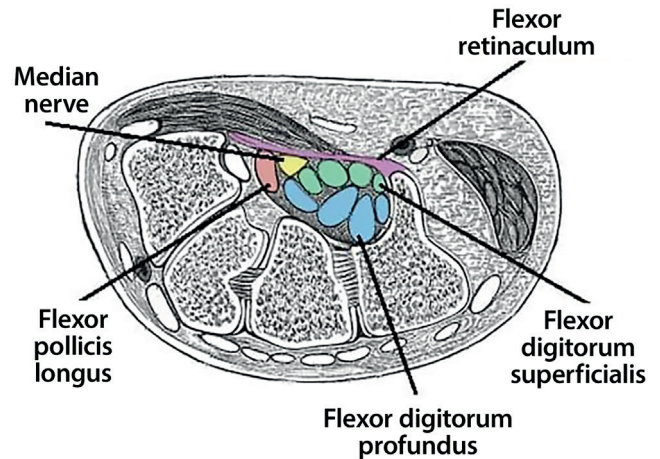


Fig. 1. Transverse section of the carpal tunnel

muscles are evaluated (e.g., the 1st dorsal interosseous and the extensor indicisproprius) to rule out brachial plexopathy, polyneuropathy and C8 to T1 radiculopathy.

In normal adults, median nerve distal motor conduction time varies between 2.0 μ s and 4.5 μ s and usually does not exceed 4.7 μ s.⁷ There may be a prolongation in CTS that exceeds this value. Meanwhile, in most cases, median nerve motor conduction velocity in the forearm is normal. Routine motor nerve conduction techniques are applied to the muscles innervated in the thenar region. In a patient with suspected CTS, the investigation begins with studies of the 1st finger sensory action potentials (SAP), 2nd finger SAP (median nerve) and 5th finger SAP (ulnar nerve), and it is monitored whether the signals received during EMG are different from normal. The lower limit of sensory nerve conduction in the hand is set at a conduction velocity of 42 m/s and amplitude of 10 μ V.

In recent years, the anatomical view of the carpal tunnel has been evaluated in detail with radiological imaging methods. Figure 1 shows the transverse section of the carpal tunnel anatomy. This has added a new dimension to CTS diagnosis and surgery. In magnetic resonance imaging (MRI), the median nerve in axial sections can be evaluated, which appears more rounded at the distal radioulnar junction (DRUJ) (Fig. 2A,B). The median nerve appears at the same intensity as skeletal muscles on T1-weighted images and minimally hyperintense on T2-weighted images.⁸ In patients with CTS, it was observed that the signal intensity of the median nerve increased at the level of the hamate bone (Fig. 3A).

Carpal tunnel syndrome most often occurs idiopathically, and can also be observed in pregnancy, diabetes, obesity, and hypothyroidism. The diagnosis of CTS is often made using history, clinical examination and electrodiagnostic tests. Recently, MRI has also been widely used in CTS to image the median nerve, evaluate nerve compression and detect additional pathologies.⁹

In our study, the area size/mm² of the median nerve at the hamate and DRUJ level, the signal increase

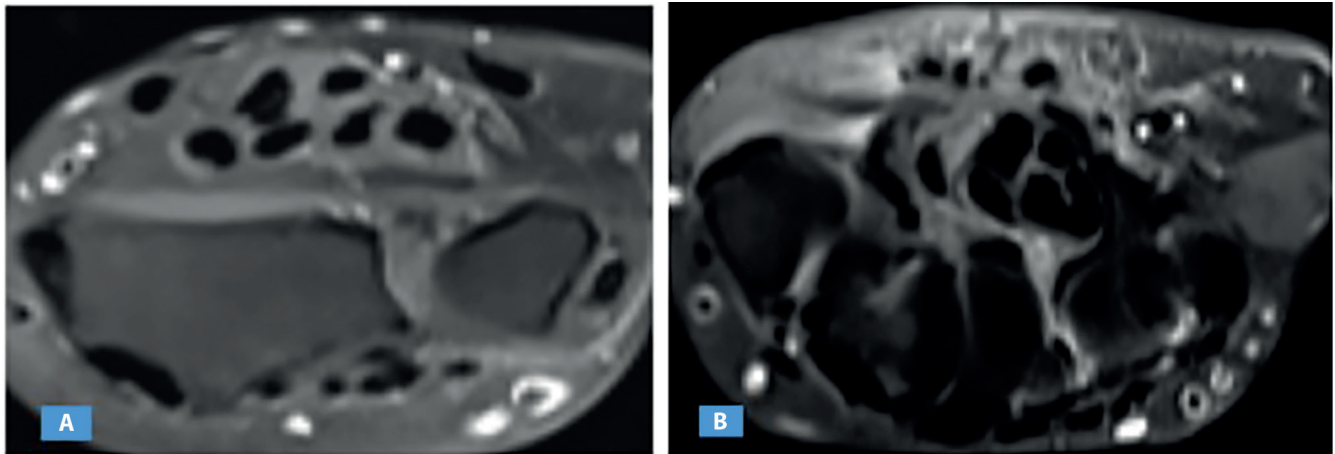


Fig. 2. A. Proton density-weighted fat-suppressed axial images show median nerve with a normal ovoid shape and signal intensity at the level of distal radioulnar joint; B. Elliptic shape at the level of the hamate bone

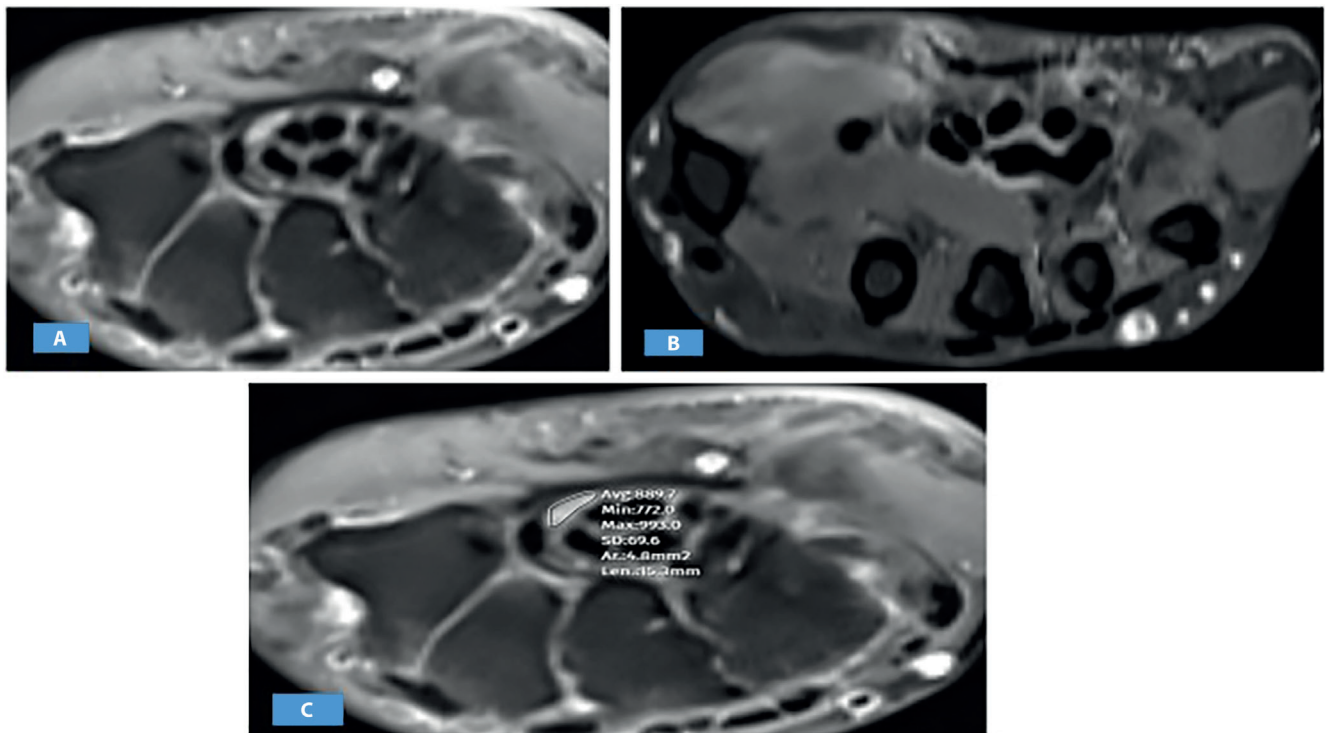


Fig. 3. A. Proton density-weighted fat-suppressed axial image shows the increased signal intensity of the median nerve at the level of the hamate bone in a patient with carpal tunnel syndrome (CTS); B. Proton density-weighted fat-suppressed axial image shows thenar muscle atrophy in a patient with CTS; C. Measurement of median nerve cross-sectional area with free region of interest (ROI) at the level of hamate bone on proton density-weighted fat-suppressed (PDW FS) axial image

of the nerve, and whether there was atrophy in the thenar muscles were investigated (Fig. 3B). Although they are more common in patients with CTS, these anatomical abnormalities seen on MRI are not specific. In its natural state, the median nerve is observed to be moderately flattened within the carpal tunnel. Studies have reported that the average flattening ratio at the level of the hook of the hamate bone is 2.9, and that the flattening ratio of a perfect circle is 1. In a study by Upadhyaya et al., the flattening ratio at the level of the distal radioulnar joint, pisiform and hamate was 1.7, 2.2, and 3.4, respectively. Patients with CTS usually demonstrate flattening ratio of more than 3 at this level.¹⁰

Carpal tunnel and median nerve anatomy

The carpal tunnel is a tunnel consisting of fibrous and osseous structures at the wrist and it is formed by 2 layers: a deep carpal arch and a superficial flexor retinaculum. The deep carpal arch forms a concave surface, which is converted into a tunnel by the overlying flexor retinaculum (transverse carpal ligament). The floor of the carpal tunnel is formed by the wrist bones, and the ceiling is formed by a thick ligament structure called the flexor retinaculum.¹¹ The flexor retinaculum is thickest distally and attaches to the hook of the hamate and

the tubercle of the trapezium. The median nerve divides into 2 branches at the exit of the carpal tunnel, the recurrent branch and the palmar digital nerves. The palmar digital nerves give sensory innervation to the palmar skin and dorsal nail beds of the lateral 3.5 digits. They also provide motor innervation to the lateral 2 lumbricals. The recurrent branch supplies the thenar muscle group.¹¹

Objectives

Electromyography is considered the most frequently used and important diagnostic method in the diagnosis of carpal tunnel syndrome. Recently, MRI has also started to be used for diagnostic purposes. This study aimed to demonstrate that MRI can be used to directly visualize median nerve morphological changes in CTS.

Hypothesis of the study

MRI can be used as an alternative diagnostic method. EMG findings and NCS results generally support the diagnosis of CTS, but specificity and sensitivity remain low in some cases. Magnetic resonance imaging allows to see the anatomical condition of the median nerve in detail before surgery, which is important for performing the surgery accordingly.

Materials and methods

A total of 35 patients with CTS symptoms who applied to Kayseri City Hospital Neurosurgery Clinic (Kayseri, Turkey) between July and October 2023 were included in the study. The EMG test was applied to all of them. Patients with normal EMG tests were also included in the study as a control group. Wrist MRIs were performed on all patients to monitor whether it was correlated with EMG. The study was approved by the Nuh Naci Yazgan University Ethics Committee (approval No. 2023/007-004 dated 20/07/2023).

Study design

The study was conducted in accordance with the Declaration of Helsinki, with the informed consent of the patients. The first choice in the diagnosis of CTS was an EMG test performed in all patients by a neurophysiologist. An MRI was taken to examine the wrist in those patients diagnosed with CTS as a result of EMG evaluation. The signal increase in the carpal tunnel of the median nerve, the area of the nerve/mm² and whether there was atrophy in the thenar muscles were evaluated by a radiologist (at the distal radioulnar junction and hamate bone levels) (Fig. 3C).

Diagnostic algorithm for patients with suspected CST

Clinical findings included numbness and paresthesia, the appearance of symptoms in the distribution of the median nerve, reduction of symptoms by changing hand position, provocation of symptoms by sleep, pain in the hand or arm, whether symptoms were provoked by the repetitive or sustained movement of the hand or arm, reduction of symptoms with hand-shaking, loss of sensation in the median nerve distribution, thenar muscle atrophy or weakness, and positive Tinel's or Phalen's tests. These were followed by EMG recordings, the data of which were then forwarded to our research group.

Electrophysiological methods

The diagnosis of CTS was made based on the patient's clinical findings and EMG studies.¹ Median nerve compression level in patients was measured using an EMG device with Keypoint.Net Software License® and serial No. 38375 (Natus Medical, Skovlunde, Denmark).

Electromyography measures the sum and activity of action potentials from muscle fibers under electrodes placed on the skin. The more muscles fibre, the greater the amount of action potential recorded and the higher the EMG value.¹²

Median nerve motor and sensory conduction velocities (SCVs), compound muscle action potential amplitudes, distal motor latencies (DMLs), and sensory nerve action potential amplitudes were analyzed. Patients with normal-to-mild median nerve compression were compared with patients with a moderate-to-high degree of compression. In the presence of CTS symptoms, the diagnosis was considered confirmed if at least 1 absolute and 1 comparative electrophysiological parameter or 2 comparative electrophysiological parameters were abnormal. The clinical severity of CTS was assessed using a validated 3-stage scale based on the clinical and electrophysiological severity scales for CTS that follows: mild, moderate and severe CTS (Table 1).¹³

Electroneurophysiological classification in patients with pre-diagnosis of CTS

Mild CTS is defined as orthodromic, antidromic or palmar median distal sensory conduction prolongation and an additional decrease in the amplitude of the distal action potential below normal.

Moderate CTS is the prolongation of median distal sensory conduction in an orthodromic, antidromic or palmar way is defined as a decrease in distal action potential amplitude below normal in addition to prolongation of median nerve DML.

Severe CTS is usually defined as the absence of distal action potential, a severe decrease in thenar motor response amplitude and a delay in distal latencies. It is defined

as the appearance of partial denervation findings on the thenar EMG.

The data obtained as a result of the evaluations made by the neurophysiologist were later reported for comparison with the MRI results. The clinical symptoms of the patients were added to the recorded EMG and MRI findings and analyzed.

Magnetic resonance imaging protocol

Images of all patients were acquired on a 3T scanner (Magnetom-Essen; Siemens AG, Munich, Germany). Patients were scanned in a prone position with their arms above their heads (Superman position). The wrist was located at the center of the scanner. The MRI protocol was created from a combination of 2-dimensional (2D) and 3-dimensional (3D) sequences in multiple planes. T1-weighted (T1W) and T2-weighted (T2W) spectral adiabatic inversion recovery (SPAIR) sequences were imaged in the axial plane. T1-weighted and proton density (PD) or fat-saturated (FS) sequences were generated in the coronal plane. The 3D PD SPAIR SPACE sequence was created in the sagittal plane. In the MRI image taken with the hand in the resting position, the area of the median nerve was measured, and the signal intensity was evaluated.

Statistical analyses

The data were curated and analyzed using IBM SPSS v. 22.0 software (IBM Corp., Armonk, USA). Frequency, percentage, mean value, standard deviation (\pm SD), and highest and lowest (min–max) values were used for descriptive statistics. For statistical analysis of categorical data, Fisher's exact test was applied for values below 5 in 4-well tables. Shapiro–Wilk test was used to check the suitability of the data for normal distribution. For

statistical analysis of quantitative data in independent groups, the Mann–Whitney U test was used for data that did not comply with normal distribution, and the Pearson's correlation coefficient was used to show the relationship between variables. A statistically significant difference was accepted as $p < 0.05$.

Results

Of the 35 patients included in the study, 24 were women (68.6%) and 11 were men (31.4%), with an average age of 48.11 ± 11.66 years (min–max = 20–69). While creating the qualitative values of EMG data, the “Severity of Carpal Tunnel Syndrome Scale” was defined for CTS and used as a basis in many studies (Table 1).¹³ The frequency of EMG results, increased MRI signal of the median nerve and atrophy in the thenar muscles according to patient's sex are presented in Table 2. Electromyography results did not differ between sexes, while signal measurements on MRI did not show a significant difference between men and women, and atrophy in the thenar muscles was seen in 56% of women and all men ($p = 0.015$).

The patient EMG results, including atrophy and median signal status in the thenar muscles, are shown in Table 3. Electromyography findings were normal in 64% of patients with atrophy ($p = 0.474$) and significantly positive in patients with increased signal.

The average median nerve area at the DRUJ level of the patients was 9.44 ± 3.27 mm² (min–max = 4.60–17.20 mm²), and the median nerve area at the hamate bone level was 8.78 ± 3.29 mm² (min–max = 4.00–19.20 mm²). According to the determined confidence level, area measurement of the median nerve at the DRUJ level ($p = 0.041$; Mann–Whitney U test) was significantly higher, and hamate ($p = 0.055$; Mann–Whitney U test) bone level was higher in EMG-positive patients.

Table 1. Clinical and electrophysiological severity scales for CTS

Electrophysiological severity of CTS	Severity of CTS sensory NCS motor NCS		APB needle EMG
Mild At least 3 of the following sensory and motor nerve conduction	1. 14-cm wrist stimulation, peak latency >3.7 ms 2. 14-cm wrist stimulation, peak latency: proximal 7 cm >distal 7 cm 3. Transcarpal 5 cm short-segmental latency: onset latency >1.3 ms, peak latency >1.5 ms 4. 14-cm 16–20 μ V amplitude 5. Conduction block greater than 50% in wrist palm stimulation if 14 cm stimulation amplitude ≥ 20 μ V	6. Distal latency >4.2 ms 7. CMAP amplitude 4. 1–4.5 mV	normal
Moderate Mild + at least 2 of the following	1. Wrist stimulation (14 cm) SNAP amplitude ≥ 6 –15 μ V 2. Conduction block greater than 50% in wrist palm stimulation if SNAP ≥ 10 μ V with 14 cm wrist stimulation	3. CMAP amplitude 2. 1–4 mV 4. 1–4 mV	4. Fibrillation (\pm) 5. Abnormal MUAP with intermediate interference pattern
Severe Moderate + 1 of the following	1. SNAP amplitude ≤ 5 μ V	2. CMAP amplitude ≤ 2 mV	3. Fibrillation (+) 4. Abnormal MUAP with discrete activity or single unit pattern

CTS – carpal tunnel syndrome; NCS – nerve conduction study; APB – abductor pollicis brevis; EMG – electromyography; CMAP – compound muscle action potential; SNAP – sensory nerve action potential; MUAP – motor unit action potential.

Table 2. Frequency of EMG results; increased magnetic resonance imaging (MRI) signal of the median nerve and atrophy in the thenar and hypotenar muscles according to the gender of the patients

Variables		All patients	Gender				p-value
			female		male		
		n	n	%	n	%	
EMG	normal	21	14	66.7	7	33.3	0.533
	moderate/severe	14	10	71.4	4	28.6	
Signal	normal	24	15	62.5	9	37.5	0.230
	increased	11	9	81.8	2	18.2	
Atrophy in thenar muscles	positive	25	14	56.0	11	44.0	0.015
	negative	10	10	100.0	0	0.0	

Percentage of rows used; Fisher's exact test. EMG – electromyography.

Table 3. Electromyography (EMG) results of the patients; atrophy in thenar and hypothenar muscles and median signal status

Variables		EMG				p-value
		normal		increased		
		n	%	n	%	
Signal	normal	18	75.0	6	25.0	0.011
	increased	3	27.3	8	72.7	
Atrophy in thenar muscles	positive	16	64.0	9	36.0	0.474
	negative	5	50.0	5	50.0	

Percentage of rows used; Fisher's exact test.

Table 4. The area of the median nerve at the hamate bone distance in patients with thenar-hypertrophic muscle atrophy; the relationship between the area measurements at the DRUJ distance and atrophy

Variables		Area of the median nerve [mm ²]					
		DRUJ			Hamate		
		mean ±SD	median	min–max	mean ±SD	median	min–max
EMG	normal	8.38 ±2.52	8.8	4.6–13.4	7.88 ±2.98	7.9	4–13.2
	moderate/severe	11.02 ±3.70	9.75	5.3–17.2	10.12 ±3.38	9.8	6.2–19.2
p/U		0.041/86.500			0.055/90.000		
Signal	normal	9.11 ±3.37	8.9	4.6–17.2	7.77 ±2.72	7.6	4.0–13.2
	increased	10.14 ±3.07	9.5	5.3–16.1	10.99 ±3.47	11.3	6.2–19.2
p/U		0.319/104.000			0.009/58.000		
Atrophy in thenar and hypothenar muscles	positive	8.91 ±3.10	8.8	4–16.1	8.01 ±2.59	7.9	4.3–13.2
	negative	10.75 ±3.48	9.5	5.9–17.2	10.71 ±4.15	11.3	4.0–19.2
p/U		0.100/80.000			0.48/71.000		

Mann–Whitney U test; EMG – electromyography; DRUJ – distal radioulnar junction; SD – standard deviation.

Based on the specified confidence level, area measurements of the median nerve at the DRUJ bone level were significantly higher in EMG-positive patients ($p = 0.041$; Mann–Whitney U test), but measurements at the hamate levels of EMG-positive patients were not statistically significant ($p = 0.055$; Mann–Whitney U test), although this value can be considered borderline significant.

In patients whose median nerve signal was increased on MRI, the area at the hamate bone level was found to be significantly higher ($p = 0.009$; Mann–Whitney U test), but no significant relationship was shown between the DRUJ

($p = 0.319$; Mann–Whitney U test) level measurements and the signal increase of the median nerve. While the area of the median nerve at the hamate bone level was found to be significantly lower ($p = 0.04$; Mann–Whitney U test) in patients with thenar muscle atrophy, no significant relationship was shown between area measurements at the DRUJ level and thenar muscle atrophy ($p = 0.100$; Mann–Whitney U test) (Table 4).

Finally, no correlation was found between the age of the patients and the area measurements of the median nerve at the hamate bone level and the area measurements

at the DRUJ level ($p > 0.05$) ($p > 0.05$ correlation coefficient 0.001 and 0.251, respectively). However, a positive correlation was detected between hamate and DRUJ levels ($p < 0.001$ correlation coefficient 0.639).

Discussion

Diagnosis of CTS is usually based on the patient's history, although clinical examination, electrophysiological tests or imaging methods support the diagnosis and guide the surgeon. Determining the level of compression of the median nerve in the carpal tunnel and the cause of CTS is also important for surgeons planning the operation, because failure to make an accurate and definitive diagnosis may result in failure of the surgical treatment. In this case, symptoms may not disappear or may reoccur. Recently, 2 different surgical techniques have been used, namely open surgery and endoscopic treatment. With surgery, symptoms are largely relieved, and the development of motor deficits can be prevented.¹⁴ Return to work time after endoscopic treatment, which is a minimally invasive technique, is shorter compared to conventional open surgery. However, it is also reported that minor complications occur more frequently after endoscopy.¹⁵

The most frequently used alternative type in the diagnosis of CTS is median nerve ultrasonography (USG). It is a low-cost procedure that is frequently used in clinical examination and is easily accessible. It allows visualization of the median nerve with a surface probe used over the carpal tunnel. It provides a subjective evaluation and the results depend on the physician performing the ultrasound.

In clinical practice, plain radiography is mostly used to check the bone morphology of wrist joints, but the role of plain radiography in the diagnosis of CTS is limited. Ultrasound and MRI are used more often to check soft tissue condition. Due to the inability to check the soft tissue condition, the role of plain radiography in the diagnosis of CTS is limited. Han et al. examined plain radiographs of patients with CTS compared to a control group, aiming to reveal radiographic predictive factors for the development of CTS by comparing the radiological parameters of simple wrist radiographs. Their results showed that excessive dorsiflexion or volar displacement of the lunate compared to the radial shaft is a risk factor for CTS development.¹⁶

Magnetic resonance imaging can be used as an alternative method to visualize the median nerve, and it also provides a detailed evaluation of the median nerve and surrounding anatomy. However, since it is an expensive procedure, it would be better to use it only in selected cases. In our study, signal intensity changes in the median nerve and atrophy in the thenar muscles can also be examined with MRI. Electrophysiological evaluation is the first choice in Turkey due to its practical value and low cost, and we found that EMG results did not differ between

genders. Notably, EMG findings were significantly positive in patients with increased signal on MRI in our study.

Goetz et al. measured and evaluated local deformations of the median nerve seen in MRI images of the carpal tunnel. Twelve patients with CTS and 12 matched normal controls underwent MRI scanning in 8 isometrically loaded hand positions. During hand movements, healthy study participants had a higher mean percentage of locally deformed nerve edges than CTS patients, despite having a more rounded median nerve shape.¹⁷

In this study, we found that area measurements at the DRUJ level were significantly higher, and hamate bone level measurements were higher in patients with median nerve compression detected on EMG. We observed that the area at the hamate bone level was significantly higher in patients with increased median nerve signal on MRI. This showed that the nerve trapped under the flexor retinaculum was thicker due to edema and was observed with increased signal on MRI. In 1972, Phalen studied 598 hands with CTS and 235 of them were treated with open surgery.¹⁸ The normal median nerve flattens to some extent as it passes beneath the transverse carpal ligament. Obvious compression of the nerve, characterized by excessive flattening and thinning and narrowing of the nerve, or by a transverse groove in the nerve at the level of the proximal edge of the ligament, was found in 145 wrists. Of these, 119 were classified as mild, 22 wrists as moderate and 4 wrists as severe. Overall, 215 hands were operated on, and 110 had thenar atrophy (to a greater or lesser degree).

Sasaki et al. examined all clinical and Nerve Conduction Study (NCS) data from 560 patients (1,120 hands; median age, 69.5 years; 264 male hands, 856 female hands) treated at the Department of Orthopedic Surgery at the Tokyo Medical and Dental University, Japan. Their large dataset revealed a strong negative correlation between SCVs and DMLs in their NCSs in patients with CTS.¹⁹

Magnetic resonance imaging sequences that display the median nerve in various ways (such as T2W SPAIR, T1W and T2W FS sequences) allow the signal intensity and size changes of the nerve to be monitored in more detail.^{20,21} Upadhyaya et al. patients who had previously received treatment and were diagnosed with CTS based on clinical findings. The authors evaluated the cause of nerve compression by evaluating the signal intensity, cross-sectional area and nerve flattening rate at certain levels. There were many female patients in this study, potentially complicating their results as women develop CTS more frequently than men, and the age of the patients ranged from 35 to 65.¹⁰ In our study, 24 (68.6%) of 35 patients were female and 11 (31.4%) were male. The average age of the patients was 48.11 ± 11.66 (min–max = 20–69) years.

In patients with CTS, it is observed that the most significant increase in nerve diameter due to edema in the median nerve occurs at the pisiform bone level.²²

In our study, we compared and analyzed the area measurements of the median nerve at the hamate bone and DRUJ levels. The average median nerve area at the DRUJ level was $9.44 \pm 3.27 \text{ mm}^2$ (min–max = $4.60\text{--}17.20 \text{ mm}^2$), and the median nerve area at the hamate bone level was $8.78 \pm 3.29 \text{ mm}^2$ (min–max = $4.00\text{--}19.20 \text{ mm}^2$). According to the determined confidence level, area measurements of the median nerve at the DRUJ ($p = 0.041$; Mann–Whitney U test) and hamate bone levels were higher in EMG-positive patients ($p = 0.055$; Mann–Whitney U test).

Nakamichi et al. measured the cross-sectional area of the median nerve at the proximal tunnel level in 414 hands of 275 patients and 408 normal individuals. They determined it to be $14.4 \pm 4.3 \text{ mm}^2$ in patients and $9.6 \pm 2.4 \text{ mm}^2$ in healthy individuals.²³ At the distal radial level, they reported it to be $4.9 \pm 1.0 \text{ mm}^2$ in CTS patients and $4.8 \pm 1.0 \text{ mm}^2$ in healthy controls. A statistically significant difference ($p < 0.0001$) was observed between the distal radial level and the proximal canal level in the nerve area measurements.

Monagle et al. showed that the cross-sectional area of the median nerve, which courses within the proximal carpal tunnel, is approx. 50% larger in patients with CTS than in normal individuals.²⁴ A study where researchers used high-resolution MRI showed that when the cadaveric median nerve was examined proximal of the carpal tunnel, it was shown that it had an elliptical shape and its area was 12.9 mm^2 (average diameter of 3.3 mm and 4.9 mm). Signal increase was also evident on T2W images.²⁵

It is not possible to identify a diagnostic test that will diagnose CTS with 100% accuracy.¹⁰ In this case, we need to take into account many parameters that can contribute to the diagnosis of CTS as much as possible. Nerve conduction studies, which are adequate according to the literature, should be considered a good candidate for this purpose with its high sensitivity and specificity. In some cases, CTS can be easily diagnosed employing history and physical examination, although confirmatory tests, such as EMG, may be required.²⁶ Electrodiagnostic studies, rather than other clinical methodologies, were determined to be the most sensitive and specific.²⁷ Currently, a detailed evaluation of the anatomy of the carpal tunnel with MRI has added a new dimension to CTS surgery. Notably, the increased signal on T2-A sections in the median nerve is compatible with edema or demyelination, excessive contrast is compatible with edema in the nerve, and absence of contrast is compatible with ischemia. In the event of fibrosis occurring in the nerve, a loss of signal is observed.²⁸

Limitations

This study contains several limitations. The study was conducted prospectively, but the data were obtained retrospectively from scanning magnetic resonance images. As a result of power analysis and literature studies,

the sample group of the study was determined to be 35 patients, 15 of whom were normal controls.^{17,28} Although the sample was small, it was comparable to similar studies. Conventional shape measurements (cross-sectional area) of the median nerve and locally deformed CTS patients within the tunnel with increased signal were compared between CTS patients and a matched control group. Patients with diabetes-related polyneuropathy were excluded from the study. This is a cross-sectional study and may not reflect the general population.

Conclusions

In many cases, the first choice for diagnosis may be EMG or MRI. If both are easily accessible, the first choice should be EMG, and NCS has diagnostic value as part of the routine management of CTS patients and should be performed before surgery on any patient with suspected CTS. In cases where diagnosis can not be established, both can be applied together. Magnetic resonance imaging may be preferred in soft tissue-related pathological cases. In some cases, the use of EMG or MRI alone may not be sufficient. In clinical practice, it can be seen that we operate with the same EMG findings and with the same surgical method, but the patients do not benefit sufficiently. Even if nerve conduction is impaired, anatomical disorders should be demonstrated with MRI to support the correctness of the surgical decision. This is how surgical failure incidence can be reduced in modern medicine.

Data availability

The datasets generated and/or analyzed during the current study are available from the corresponding author on reasonable request.

Consent for publication

Not applicable.

ORCID iDs

Şule Göktürk  <https://orcid.org/0000-0001-6590-4885>
Yasin Göktürk  <https://orcid.org/0000-0002-4779-9927>
Ali Koç  <https://orcid.org/0000-0003-0296-4914>
Ahmet Payas  <https://orcid.org/0000-0002-1629-9794>

References

1. Spagnolo F, Sestak I, Howell A, Forbes JF, Cuzick J. Anastrozole-induced carpal tunnel syndrome: Results from the International Breast Cancer Intervention Study II Prevention Trial. *J Clin Oncol*. 2016;34(2):139–143. doi:10.1200/JCO.2015.63.4972
2. Stevens JC, Beard CM, O'Fallon WM, Kurland LT. Conditions associated with carpal tunnel syndrome. *Mayo Clin Proc*. 1992;67(6):541–548. doi:10.1016/S0025-6196(12)60461-3
3. Simpson JA. Electrical signs in the diagnosis of carpal tunnel and related syndromes. *J Neurol Neurosurg Psychiatry*. 1956;19(4):275–280. doi:10.1136/jnnp.19.4.275

4. Jablecki CK, Andary MT, Floeter MK, et al. American Association of Electrodiagnostic Medicine; American Academy of Neurology; American Academy of Physical Medicine and Rehabilitation. Practice parameter: Electrodiagnostic studies in carpal tunnel syndrome: Report of the American Association of Electrodiagnostic Medicine, American Academy of Neurology, and the American Academy of Physical Medicine and Rehabilitation. *Neurology*. 2002;58(11):1589–1592. doi:10.1212/WNL.58.11.1589
5. American Association of Electrodiagnostic Medicine; American Academy of Neurology; American Academy of Physical Medicine and Rehabilitation. Practice parameter for electrodiagnostic studies in carpal tunnel syndrome: Summary statement. *Muscle Nerve*. 2002;25(6):918–922. doi:10.1002/mus.10185
6. Kothari MJ. Carpal tunnel syndrome: Clinical manifestations and diagnosis. Philadelphia, USA: Wolters Kluwer. 2023. <https://www.uptodate.com/contents/carpal-tunnel-syndrome-clinical-manifestations-and-diagnosis/print>. Accessed October 15, 2023.
7. Eroğlu S. Electrodiagnostic methods using for carpal tunnel syndrome and its diagnosis [in Turkish]. *Journal of Harran University Medical Faculty*. 2013;10(2):86. <https://dergipark.org.tr/en/download/article-file/838048>. Accessed October 15, 2023.
8. Kumari A, Singh S, Garg A, Prakash A, Sural S. Tingling hand: Magnetic resonance imaging of median nerve pathologies within the carpal tunnel. *Pol J Radiol*. 2019;84:484–490. doi:10.5114/pjr.2019.90354
9. Thawait SK, Chaudhry V, Thawait GK, et al. High-resolution MR neurography of diffuse peripheral nerve lesions. *AJNR Am J Neuroradiol*. 2011;32(8):1365–1372. doi:10.3174/ajnr.A2257
10. Upadhyaya V, Upadhyaya ND, Pandey SD. MRI of the median nerve in carpal tunnel syndrome. *J Peripher Nerve Surg*. 2020;4:15–21. <https://www.thieme.in/thieme-e-Journals/jpnspdf/Article-3.pdf>. Accessed October 15, 2023.
11. Mesgarzadeh M, Schneck CD, Bonakdarpour A, Mitra A, Conaway D. Carpal tunnel: MR imaging. Part II. Carpal tunnel syndrome. *Radiology*. 1989;171(3):749–754. doi:10.1148/radiology.171.3.2541464
12. Elamvazuthi I, Duy NHX, Ali Z, Su SW, Khan MKAA, Parasuraman S. Electromyography (EMG) based classification of neuromuscular disorders using multi-layer perceptron. *Proc Comp Sci*. 2015;76:223–228. doi:10.1016/j.procs.2015.12.346
13. Kang S, Kwon HK, Kim KH, Yun HS. Ultrasonography of median nerve and electrophysiologic severity in carpal tunnel syndrome. *Ann Rehabil Med*. 2012;36(1):72. doi:10.5535/arm.2012.36.1.72
14. Petrover D, Richette P. Treatment of carpal tunnel syndrome: From ultrasonography to ultrasound guided carpal tunnel release. *Joint Bone Spine*. 2018;85(5):545–552. doi:10.1016/j.jbspin.2017.11.003
15. Sayegh ET, Strauch RJ. Open versus endoscopic carpal tunnel release: A meta-analysis of randomized controlled trials. *Clin Orthop Relat Res*. 2015;473(3):1120–1132. doi:10.1007/s11999-014-3835-z
16. Han BS, Kim KH, Kim KJ. The radiographic risk factors predicting occurrence of idiopathic carpal tunnel syndrome in simple wrist X-ray. *J Clin Med*. 2022;11(14):4031. doi:10.3390/jcm11144031
17. Goetz JE, Kunze NM, Main EK, et al. MRI-apparent localized deformation of the median nerve within the carpal tunnel during functional hand loading. *Ann Biomed Eng*. 2013;41(10):2099–2108. doi:10.1007/s10439-013-0809-3
18. Phalen GS. The carpal-tunnel syndrome: Clinical evaluation of 598 hands. *Clin Orthop Relat Res*. 1972;83:29–40. doi:10.1097/00003086-197203000-00007
19. Sasaki T, Koyama T, Kuroiwa T, et al. Evaluation of the existing electrophysiological severity classifications in carpal tunnel syndrome. *J Clin Med*. 2022;11(6):1685. doi:10.3390/jcm11061685
20. Chalian M, Behzadi AH, Williams EH, Shores JT, Chhabra A. High-resolution magnetic resonance neurography in upper extremity neuropathy. *Neuroimaging Clin N Am*. 2014;24(1):109–125. doi:10.1016/j.nic.2013.03.025
21. Howe BM, Spinner RJ, Felmlee JP, Frick MA. MR imaging of the nerves of the upper extremity. *Magn Reson Imaging Clin N Am*. 2015;23(3):469–478. doi:10.1016/j.mric.2015.04.009
22. Beekman R, Visser LH. Sonography in the diagnosis of carpal tunnel syndrome: A critical review of the literature. *Muscle Nerve*. 2003;27(1):26–33. doi:10.1002/mus.10227
23. Nakamichi K, Tachibana S. Ultrasonographic measurement of median nerve cross-sectional area in idiopathic carpal tunnel syndrome: Diagnostic accuracy. *Muscle Nerve*. 2002;26(6):798–803. doi:10.1002/mus.10276
24. Monagle K, Dai G, Chu A, Burnham RS, Snyder RE. Quantitative MR imaging of carpal tunnel syndrome. *Am J Roentgenol*. 1999;172(6):1581–1586. doi:10.2214/ajr.172.6.10350293
25. Altınok MT, Ertem K, Fırat AK, Karakaş HM. Patent median artery in a case with carpal tunnel syndrome bifid median nerve [in Turkish]. *İnönü Üniversitesi Tıp Fakültesi Dergisi*. 2005;12(4):273–275. <https://dergipark.org.tr/tr/download/article-file/139603#158032>. Accessed October 15, 2023.
26. Sonoo M, Menkes DL, Bland JDP, Burke D. Nerve conduction studies and EMG in carpal tunnel syndrome: Do they add value? *Clin Neurophysiol Pract*. 2018;3:78–88. doi:10.1016/j.cnp.2018.02.005
27. Stoller DW, Stoller DW. The wrist and hand. In: *Magnetic Resonance Imaging in Orthopaedics and Sports Medicine*. 2nd ed. Philadelphia: Lippincott Williams & Wilkins; 1997:959–961. ISBN:978-1-85233-149-8.
28. Deniz FE, Öksüz E, Sarıkaya B, et al. Comparison of the diagnostic utility of electromyography, ultrasonography, computed tomography, and magnetic resonance imaging in idiopathic carpal tunnel syndrome determined by clinical findings. *Neurosurgery*. 2012;70(3):610–616. doi:10.1227/NEU.0b013e318233868f

Correlation analysis of patients with diabetic foot ulcers treated with tibial cortex transverse transport surgery and platelet-to-lymphocyte ratio and monocyte-to-neutrophil ratio

Sijie Yang^{1,2,A–D}, Kaixiang Pan^{2,B,C}, *Qikai Hua^{2,D–F}, Hongjie Su^{1,B,C}, Jun Hou^{1,B}, Kaibing Liu^{2,B,C}, *Jinmin Zhao^{1,2,E,F}

¹ Department of Bone and Joint Surgery, The First Affiliated Hospital of Guangxi Medical University, Nanning, China

² Collaborative Innovation Centre of Regenerative Medicine and Medical Bioresource Development and Application Co-constructed by the Province and Ministry, Guangxi Medical University, Nanning, China

A – research concept and design; B – collection and/or assembly of data; C – data analysis and interpretation;

D – writing the article; E – critical revision of the article; F – final approval of the article

Advances in Clinical and Experimental Medicine, ISSN 1899–5276 (print), ISSN 2451–2680 (online)

Adv Clin Exp Med. 2025;34(4):549–559

Address for correspondence

Jinmin Zhao

E-mail: Zhaojinmin202309@163.com

Funding sources

This study was supported by National Natural Science Foundation of China (grant No. 82260448), the Science and Technology Plan Project of Guangxi Province (grant No. 2021AB11027), Science and Technology Plan Project Contract of Qingxiu District, Nanning City, Guangxi Province (grant No. 2020053), and Clinical Research Climbing Plan Peak Project Contract of the First Affiliated Hospital of Guangxi Medical University (grant No. YYZS2020010).

Conflict of interest

None declared

* Jinmin Zhao and Qikai Hua contributed equally to this work.

Received on December 20, 2023

Reviewed on March 22, 2024

Accepted on April 19, 2024

Published online on June 27, 2024

Cite as

Yang S, Pan K, Hua Q, et al. Correlation analysis of patients with diabetic foot ulcers treated with tibial cortex transverse transport surgery and platelet-to-lymphocyte ratio and monocyte-to-neutrophil ratio. *Adv Clin Exp Med*. 2025;34(4):549–559. doi:10.17219/acem/187765

DOI

10.17219/acem/187765

Copyright

Copyright by Author(s)

This is an article distributed under the terms of the Creative Commons Attribution 3.0 Unported (CC BY 3.0) (<https://creativecommons.org/licenses/by/3.0/>)

Abstract

Background. Diabetic foot ulcers (DFUs) represent one of the most severe late-stage complications of diabetes. Tibial cortex transverse transport (TTT) surgery stands as the prevailing method for addressing DFUs. This surgical intervention holds the promise of expediting DFU wound healing and diminishing the rate of amputations, with the mitigation of inflammatory responses playing a pivotal role. In this study, we aim to explore the correlation between inflammation and TTT surgery, with the overarching goal of facilitating swift prognostic assessments in clinical practice.

Objectives. The correlation between the severity of DFUs and clinical test results remains ambiguous. A clinical prediction model was devised to explore the connection between DFU severity and the efficacy of TTT surgery, utilizing straightforward and efficient clinical indicators.

Materials and methods. Clinical data and examination results were gathered by tracking hospitalized DFU patients who underwent TTT surgery at the First Affiliated Hospital of Guangxi Medical University (Nanning, China). Indicators associated with DFU severity and wound healing time post-surgery were identified through logistic regression and least absolute shrinkage and selection operator (LASSO) regression analyses. Subsequently, a clinical prediction model was constructed. Finally, the intersection of these 2 sets of indicators revealed factors correlated with wound severity and post-operative healing duration.

Results. Our study was comprised of 202 patients who were categorized into 2 groups based on Wagner's grading classifications. Utilizing Student's t-tests, LASSO regression and logistic regression analyses, we identified 3 factors indicative of DFU severity: platelet-to-lymphocyte ratio (PLR), mixed lymphocyte reaction (MLR) and hemoglobin (HGB). Univariate COX regression analysis revealed 12 factors such as: white blood cells (WBC), neutrophils (NEUT), monocytes (MO), PLR, MLR, neutrophil-to-lymphocyte ratio (NLR), erythrocyte sedimentation rate (ESR), age, lymphocytes (LY), monocyte-to-neutrophil ratio (MNR), uric acid (UA), and albumin (ALB) associated with the postoperative healing duration. Ultimately, we identified 2 factors, PLR and MNR, at the intersection of these 2 datasets.

Conclusions. Platelet-to-lymphocyte ratio and MNR were identified as factors associated with both the severity of DFUs and the prognosis following TTT surgery.

Key words: platelet-to-lymphocyte ratio, diabetic foot ulcer, prognostic analysis, TTT surgery, monocyte-to-neutrophil ratio

Background

Diabetic foot ulcers (DFUs) are a severe late complication of diabetes and a public health problem.¹ Presently, the global morbidity of DFUs is about 6.3%.² Moreover, patients with DFU have a higher amputation rate and mortality. Around 1/4 of diabetic patients develop a DFU in their lifetime.³ Many factors contribute to the occurrence and development of a DFU. Improper management of blood glucose levels, longer duration of diabetes, insulin use, foot ischemia, and ulcers have been proven to be important risk factors leading to foot ulcers,⁴ and among these factors, infection plays an extremely important role.

The pathologic mechanism of DFUs is not completely understood. However, the role of the inflammatory response cannot be ignored in DFUs. The inflammatory stage is an important process in wound healing, which can directly affect the normal healing of the wound. However, a prolonged presence of inflammation is often cited as the primary reason for the failure of diabetic foot wounds to heal. Some studies have shown that chronic inflammation is associated with the pathogenesis of diabetes and the development of its complications.⁵ In the past, clinical doctors have used simple laboratory tests to determine inflammation within the patient's body, such as white blood cell (WBC) count, erythrocyte sedimentation rate (ESR) and C-reactive protein (CRP). However, these test results cannot be analyzed separately and must be combined with others. Recent studies have demonstrated that alterations in the composition of circulating leukocytes serve as a more effective indicator of inflammation, enabling a swift and accurate determination of the inflammatory status in patients.^{6,7}

The platelet-to-lymphocyte ratio (PLR) and monocyte-to-neutrophil ratio (MNR) are novel systemic inflammatory response markers that reflect the inflammatory status. Several studies have investigated these markers because they are easily determined from the peripheral blood.

The tibial cortex transverse transport (TTT) surgery is a novel and significantly effective surgery to treat DFUs.⁸ It was developed based on Ilizarov technology. Qu et al. first reported the successful treatment of thromboangiitis obliterans (TAO) using TTT surgery.⁹ Chen et al. first used TTT surgery to treat DFUs, achieving a good wound healing rate and limb salvage rate.⁸ Yang et al. pointed out that TTT surgery can not only promote wound healing by enhancing vascular regeneration but also enhance wound immunity.¹⁰ The immune system of the affected person determines the inflammatory state of the body. However, the correlation between DFUs after TTT surgery and PLR and MNR was not reported.

Objectives

To our knowledge, no research on predicting the prognosis of patients undergoing TTT surgery has been published. This study aimed to assess the correlation between PLR

and MNR levels and the severity of DFUs. Additionally, we investigated the association between PLR, MNR and the prognosis of DFUs following TTT surgery.

Materials and methods

TTT surgery

The surgical procedure was conducted following the methodology outlined in a previous study,⁸ and detailed research procedures are provided in Fig. 1.

The patients included in the study were diagnosed with diabetes based on the American Diabetes Association (ADA) criteria.¹¹ They were at least 18 years old and had 1 or more non-healing ulcers below the ankle for 6 months or more. All patients had previously undergone TTT surgery. They were excluded if they suffered from severe pulmonary, urinary tract, a systemic infection, or from severe dysfunction of the heart, lung, kidney, brain, or other organs. The participants were also excluded if they had used anticoagulation, antiplatelet, antibiotics, or other drugs known to affect the examination results in the previous months. In addition, patients were excluded if their clinical data were incomplete or if they had undergone amputation surgery or a repeat TTT surgery.

The research process is clearly shown in Fig. 1, including 2 main aspects of the research. First, based on the Wagner's grading of the selected patients, they were divided into 2 groups (Wagner's 2–3 and Wagner's 4). By comparing the differences in baseline data between the 2 groups, differential factors were obtained (Table 1). In order to identify differential factors related to the severity of DFU patients, least absolute shrinkage and selection operator (LASSO) and logistic regression analysis were employed. These factors are referred to as severity factors (SFs). Second, Cox regression analysis was used to analyze patients after TTT surgery and identify factors related to wound healing. We refer to these factors as TTT-prognosis-related factors (TTT-PFs). By intersecting these 2 datasets, factors that are both related to wound severity and can predict the prognosis after TTT surgery were obtained (TTT-SFs and PFs).

After the above screening, 202 DFU patients were included in the study from July 2016 to July 2021. These patients were divided into 2 groups based on the Wagner's grading stages. Their clinical data, such as age, sex and inspection results, are presented in Table 1. All the patients were followed up for at least 1 year.

Statistical analyses

Student's t-test was used to compare the means of the continuous variables between 2 groups and a one-way analysis of variance (ANOVA) test compared 3 or more groups. Logistic regression analysis screened for correlations between the variables. The Box–Tidwell test, variance influence factor (VIF) and Cook's distances were used to test the accuracy

Table 1. Baseline of patients based on Wagner's grade 2/3 (n = 135) and 4 (n = 67). The χ^2 test was used to test for gender differences. Student's t-test was used to compare the means of the continuous variables between 2 groups

Factors		Wagner's 2/3 (n = 135) (n/M \pm SD)	Wagner's 4 (n = 67) (n/M \pm SD)	Overall (n = 202) (n/M \pm SD)	t/ χ^2	p-value
Sex	female	34	11	45	1.988	0.159
	male	101	56	157	–	–
Age		62.40 \pm 9.68	61.12 \pm 9.07	61.98 \pm 9.48	0.904	0.367
BMI		24.03 \pm 3.15	24.80 \pm 2.99	24.28 \pm 3.11	1.658	0.099
WBC		9.42 \pm 3.34	15.20 \pm 7.10	11.33 \pm 5.61	6.322	<0.001*
PLT		390.55 \pm 150.47	380.64 \pm 123.24	387.26 \pm 141.79	0.499	0.618
NEUT		6.43 \pm 3.01	12.66 \pm 6.77	8.49 \pm 5.46	7.184	<0.001*
LY		1.91 \pm 0.64	1.34 \pm 0.53	1.72 \pm 0.69	6.730	<0.001*
MO		0.75 \pm 0.29	1.00 \pm 0.50	0.83 \pm 0.39	3.850	<0.001*
PLR		229.86 \pm 125.96	318.94 \pm 132.08	259.41 \pm 134.44	4.582	<0.001*
MLR		0.43 \pm 0.21	0.84 \pm 0.44	0.56 \pm 0.36	7.278	<0.001*
MNR		0.13 \pm 0.06	0.08 \pm 0.03	0.12 \pm 0.06	7.438	<0.001*
NLR		3.74 \pm 2.27	11.13 \pm 7.09	6.19 \pm 5.67	8.320	<0.001*
HGB		104.8 \pm 20.51	94.93 \pm 25.95	101.04 \pm 22.81	2.726	0.007*
CR		100.84 \pm 101.73	181.62 \pm 247.46	127.63 \pm 168.70	2.567	0.012*
UA		327.27 \pm 109.08	311.44 \pm 157.08	322.02 \pm 126.84	0.741	0.461
CCR		70.77 \pm 27.92	63.93 \pm 31.12	68.50 \pm 30.20	1.422	0.158
ALB		33.81 \pm 5.83	30.53 \pm 6.21	32.72 \pm 6.16	3.686	<0.001*
ESR		70.2 \pm 30.38	89.63 \pm 34.16	76.52 \pm 32.92	4.142	<0.001*
TC		4.27 \pm 1.33	4.50 \pm 2.27	4.34 \pm 1.70	0.756	0.452
TG		1.53 \pm 0.93	1.68 \pm 1.03	1.58 \pm 0.97	1.060	0.291
HDL		0.90 \pm 0.31	0.89 \pm 0.46	0.90 \pm 0.36	0.214	0.831
LDL		2.62 \pm 1.04	2.75 \pm 1.60	2.66 \pm 1.25	0.582	0.562

Shapiro–Wilk test was used to test the normality of data; F-test was used to test the variance of 2 sets of data; *p \leq 0.05; BMI – body mass index; SD – standard deviation; WBC – white blood cells; PLT – platelets; NEUT – neutrophils; LY – lymphocytes; MO – monocytes; PLR – platelet-to-lymphocyte ratio; MLR – mixed lymphocyte reaction; MNR – monocyte-to-neutrophil ratio; NLR – neutrophil-to-lymphocyte ratio; HGB – hemoglobin; CR – creatinine; UA – uric acid; CCR – creatinine reduction ratio; ALB – albumin; ESR – erythrocyte sedimentation rate; TC – total cholesterol; TG – thyroglobulin; HDL – high-density lipoprotein, LDL – low-density lipoprotein.

of the logistic regression model. Nagelkerke's R^2 was used to evaluate the goodness of fit in logistic regression analysis and to evaluate the interpretability of classification models. The “Lars” package of the R software (R Foundation for Statistical Computing, Vienna, Austria) was employed for the LASSO regression analysis and visualization. The “pROC” package computed the receiver operating characteristic (ROC) curves to assess the accuracy of the factors and nomogram.¹² A univariate Cox regression analysis was conducted to identify prognostic factors. The proportional risk hypothesis, logarithmic risk function and linear relationships between predictive factors were identified using Schoenfeld residuals. The goodness of fit of the Cox regression model was evaluated using the concordance index (C-Index). The survival package was used to perform a predictive analysis. In the absence of further specification, statistical significance was defined as a 2-sided probability value less than 0.05. The IBM SPSS v. 26 (IBM Corp., Armonk, USA) and R. 4.1.0 were employed in separate instances.

Results

PLR, MNR and HGB are associated with the severity of DFUs

Significant difference analyses were identified for 12 factors between the 2 groups (Table 1). The ROC curves indicated good accuracy of every factor (Fig. 2A,B). After the LASSO and logistic regression analysis, which identified 7 factors (LY, PLR, MLR, MNR, NLR, HGB, and CR) and 3 factors (PLR, MNR and HGB), respectively, by taking the intersection of the 2 sets, 3 factors (PLR, MNR and HGB) were identified as SFs (Table 2, Fig. 2C–F). Additionally, a nomogram was established based on these factors to describe DFU severity (Fig. 3A–C). Moreover, the ROC curve was determined to be accurate (Fig. 3B).

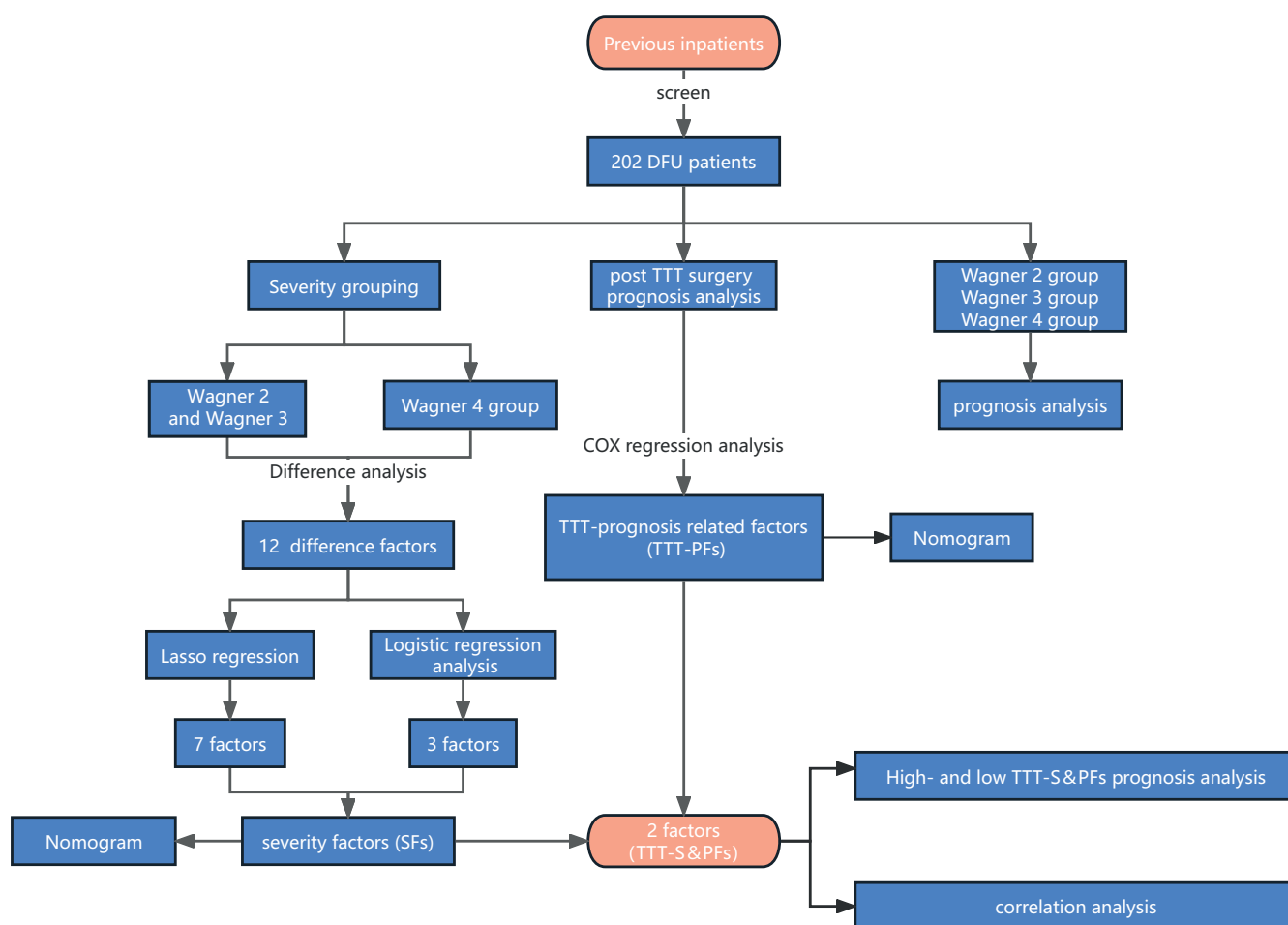


Fig. 1. Research process of this study. This study is mainly divided into 3 parts, all based on 202 diabetic foot ulcer (DFU) patients who underwent tibial cortex transverse transport (TTT) surgery. Through differential analysis and correlation analysis of the patients, TTT-S and PFs were identified, and a survival analysis of wound healing in patients was conducted

TTT-S and PFs – TTT-severity and prognosis related factors.

Table 2. Binary logistic regression analysis based on 11 factors

Factors	Wald	p-value	OR	95% CI low	95% CI up
WBC	0.907	0.341	0.528	0.142	1.963
NEUT	0.592	0.442	1.752	0.420	7.313
MO	0.204	0.652	4.300	0.008	2,423.260
PLR	7.254	0.007*	0.856	0.745	0.928
MLR	1.753	0.185	107.882	0.106	110,233.896
MNR	4.581	0.032*	0.032	0.015	0.079
NLR	0.251	0.616	1.147	0.671	1.959
HGB	6.455	0.011*	0.903	0.824	0.997
CR	0.265	0.607	1.008	0.971	1.128
ALB	0.007	0.932	0.987	0.905	1.174
ESR	0.097	0.756	0.995	0.953	1.083

*p < 0.05. WBC – white blood cells; PLT – platelets; NEUT – neutrophils; LY – lymphocytes; MO – monocytes; PLR – platelet-to-lymphocyte ratio; MLR – mixed lymphocyte reaction; MNR – monocyte-to-neutrophil ratio; NLR – neutrophil-to-lymphocyte ratio; HGB – hemoglobin; CR – creatinine; UA – uric acid; CCR – creatinine reduction ratio; ALB – albumin; ESR – erythrocyte sedimentation rate; TC – total cholesterol; TG – thyroglobulin; HDL – high-density lipoprotein; LDL – low-density lipoprotein; 95% CI – 95% confidence interval; OR – odds ratio.

Nomogram for prognosis-related factors for DFU patients

Univariate Cox regression analysis identified 12 TTT-PFs related to wound healing in DFU patients after TTT surgery (Fig. 4A). Among them, 7 factors (WBC, NEUT, MO, PLR, MLR, NLR, and ESR) negatively affected the recovery of DFUs. Conversely, 5 factors (age, LY, MNR, UA, and ALB) predicted a better prognosis for DFUs (Fig. 4A). The prediction nomogram was established from these 12 factors (Fig. 4B)

By taking the intersection of SFs and TTT-PFs, 2 factors (PLR and MNR) were considered to be TTT-S and PFs (Fig. 4C) and the nomogram was accurately predicted (Fig. 4D).

Prognostic analysis

Patients were separated into 3 groups based on the Wagner's grading (Fig. 5A). The prognosis analysis results showed that patients with a Wagner's grade 4 ulcer had a lower healing rate and took a longer time to heal. In contrast, patients

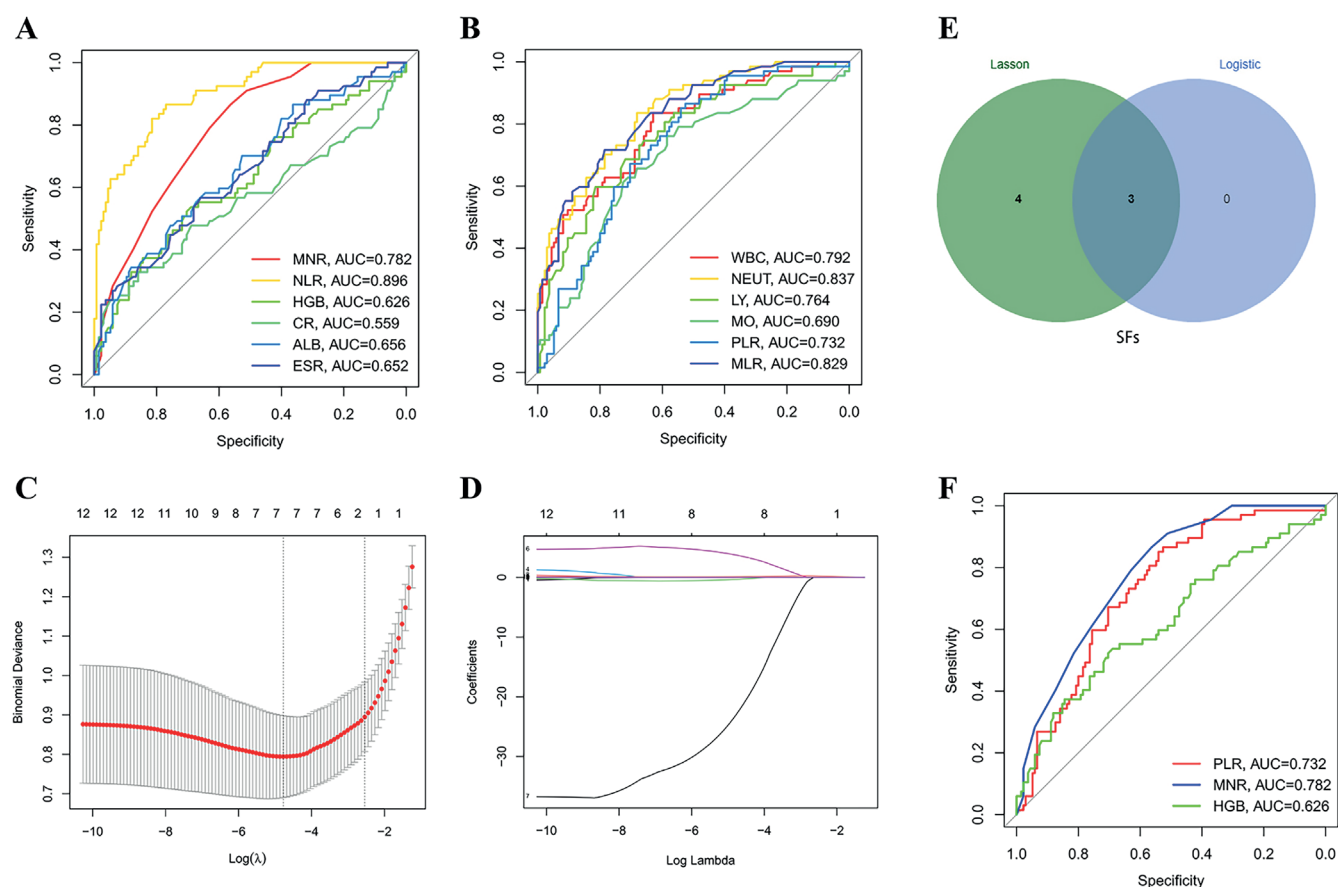


Fig. 2. Identification of SFs. A,B. ROC curves of the 12 differential factors; C. Least absolute shrinkage and selection operator (LASSO) coefficient profiles of the 7 characteristics; D. 1000-fold cross-validation was used to generate the optimal penalty parameter lambda; E. Identification of SF Venn diagrams. After LASSO and logistic regression analysis of the 12 differential factors, 3 SFs were discerned, identifying the point of intersection; F. ROC curves for the 3 SFs

SFs – severity factors; ROC curve – receiver operating characteristic curve; AUC – area under the ROC curve; WBC – white blood cells; PLT – platelets; NEUT – neutrophils; LY – lymphocytes; MO – monocytes; PLR – platelet-to-lymphocyte ratio; MLR – mixed lymphocyte reaction; MNR – monocyte-to-neutrophil ratio; NLR – neutrophil-to-lymphocyte ratio; HGB – hemoglobin; CR – creatinine; UA – uric acid; CCR – creatinine reduction ratio; ALB – albumin; ESR – erythrocyte sedimentation rate.

with Wagner's grades 2 and 3 exhibited a higher healing rate and a shorter healing time (Fig. 5A). When we divided patients into high- and low-groups based on the optimal cutoff values for PLR and MNR values, their survival analysis results showed different outcomes. The high-MNR group had a higher healing rate and shorter healing time (Fig. 5B). In contrast, the PLR group exhibited the opposite trend (Fig. 5C). When analyzing the PLR and MNR values of patients with different Wagner's grades, we found that as the Wagner's grade increased, the MNR values tended to decrease (Fig. 6A). However, the PLR values exhibited the opposite trend (Fig. 6B). In other words, the PLR increased, and the MNR decreased as the Wagner's grade increased. Correlation analysis also showed that PLR was negatively related to MNR ($R = -0.44$; $p = 3.5e-11$) (Fig. 6C,D).

Discussion

Diabetes is a major chronic disease, with the number of affected individuals continuously growing. In 2015,

it reached 450 million.^{13,14} Diabetic foot ulcers are a significant complication of diabetes, affecting about 25% of people with diabetes.^{2,15} Diabetic foot ulcers are mainly associated with peripheral neuropathy and lower extremity arterial disease.¹⁶ However, despite extensive research, the precise mechanism of DFUs remains unclear. Diabetes causes systemic effects on the patient's immune function and alters the state of inflammation. Diabetic foot ulcers are prone to co-infection, which can lead to complications such as gangrene, osteomyelitis and the progression to severe DFUs. Patients with DFUs have a higher mortality and amputation rate than the general diabetic population.

Treatment of DFUs, especially severe DFUs, is a worldwide challenge. Conventional surgical treatment includes debridement and revascularization. These treatments help avoid amputations in some patients and heal the ulcer. However, the rate of recurrence remains high.¹⁵ Tibial cortex transverse transport surgery is effective for treating severe and recalcitrant DFUs. Tibial cortex transverse transport surgery has been shown to result in a higher rate of wound healing and limb salvage, as well as a lower recurrence rate.

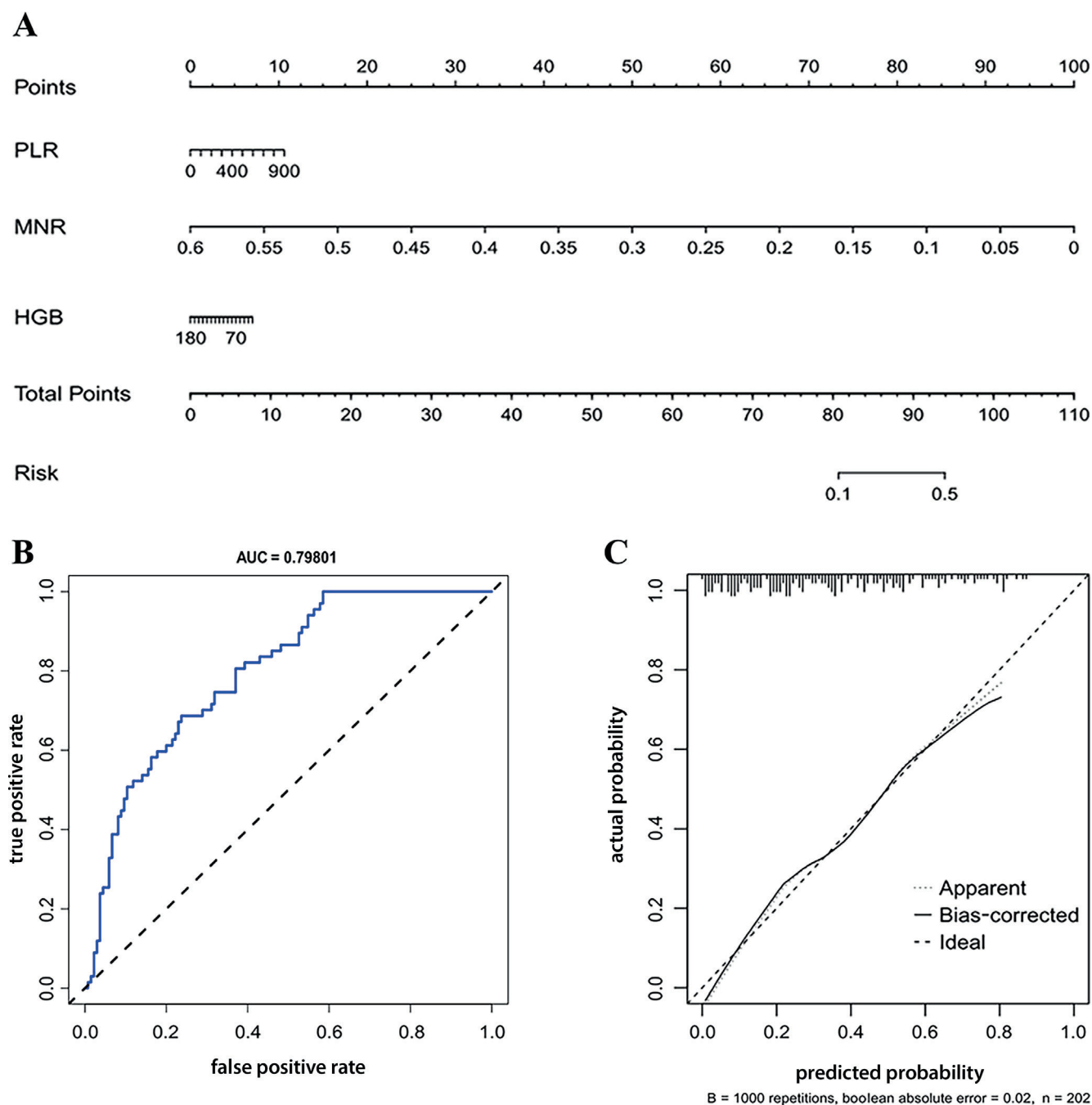


Fig. 3. Establishing a nomogram based on SFs. A. The nomogram is used to identify the severity of DFUs; B. ROC curve of the nomogram; C. Calibration curves for predicting DFU severity

SFs – severity factors; ROC curve – receiver operating characteristic curve; DFU – diabetic foot ulcer; AUC – area under the ROC curve; PLR – platelet-to-lymphocyte ratio; HGB – hemoglobin.

This surgical approach has also been shown to enhance angiogenesis and immunomodulation in patients.¹⁷

In this study, we proposed the concept of TTT-S and PFs for the first time, which had not been explored in previous research. Our study identified 2 TTT-S and PFs, PLR and MNR, which were correlated with the Wagner's grading of DFUs. Additionally, these factors predicted the prognosis of DFU patients treated with TTT surgery. Platelet-to-lymphocyte ratio is an inflammatory index that has been

linked to both the diagnosis and prognosis of diabetes.^{17–20}

In the present study, PLR showed a positive correlation with the severity of the DFU, as indicated by the Wagner's DFU grading system. These findings are consistent with previous research, indicating the reliability of our results. At the same time, PLR was associated with the prognosis of wound healing in DFU patients treated with TTT surgery. A higher PLR predicted a longer time to heal after TTT surgery. This correlation has not been reported

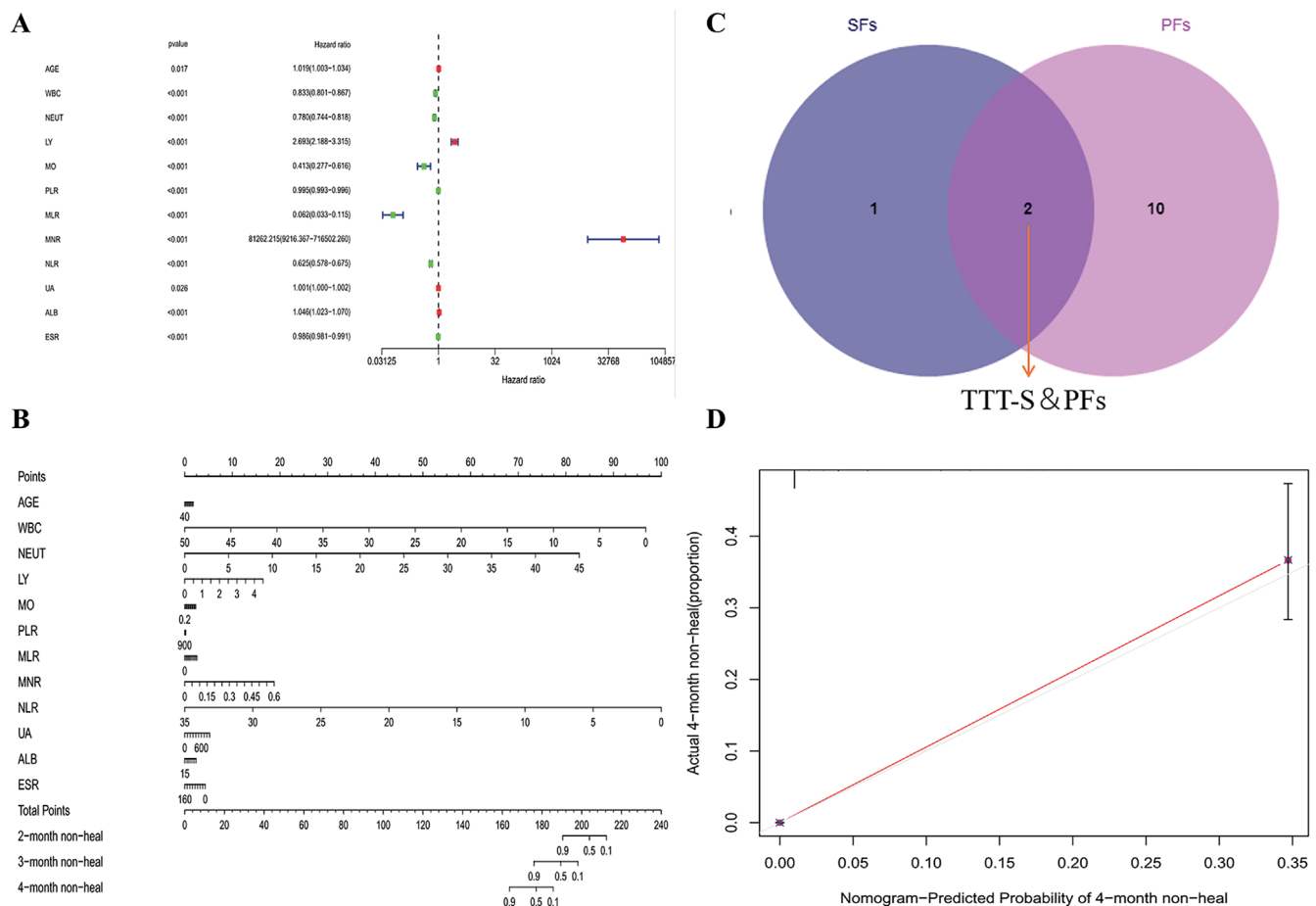


Fig. 4. Identification of TTT-S and PFs and establishment of a nomogram related to wound healing after tibial cortex transverse transport (TTT) surgery. A. Univariate Cox regression analysis identified TTT-PFs; B. Nomogram established based on TTT-PFs; C. Venn diagram shows the intersection of severity factors (SFs) and TTT-PFs to derive TTT-S and PFs; D. Calibration curves for predicting the possibility of 4-month non-healing after TTT surgery based on the nomogram

TTT-PFs – wound prognosis relative factors post TTT surgery; AGE – advanced glycation end products; WBC – white blood cells; PLT – platelets; NEUT – neutrophils; LY – lymphocytes; MO – monocytes; PLR – platelet-to-lymphocyte ratio; MLR – mixed lymphocyte reaction; MNR – monocyte-to-neutrophil ratio; NLR – neutrophil-to-lymphocyte ratio; HGB – hemoglobin; CR – creatinine; UA – uric acid; CCR – creatinine reduction ratio; ALB – albumin; ESR – erythrocyte sedimentation rate.

earlier. Therefore, PLR can serve as a simple clinical index for predicting the time required for wound healing after TTT surgery.

Diabetes creates a chronic inflammatory state in patients. Therefore, detecting inflammation indicators can provide insights into the severity of diabetes and the associated risk of complications.^{21–23} One of the main causes of a DFU is linked to peripheral arterial disease (PAD).^{24,25} Patients with DFUs and PAD are at higher risk of experiencing unhealed wounds, requiring amputations and facing increased mortality rates.^{26,27} Additionally, PAD serves as a predictive factor for the risk of amputation in DFU patients.²⁸ Previous studies have reported the association between increased PLR and critical limb ischemia (CLI) and PAD.²⁹ Chronic inflammation over a long period impairs immune function and reduces the number of lymphocytes. Chronic inflammation over a long period leads to an elevation in platelets and inflammatory factors. This process damages the vascular endothelium and

contributes to the development of atherosclerosis, which is the pathological basis for the further PAD formation.³⁰

The MNR is a ratio of peripheral blood cells and serves as a novel indicator reflecting the level of inflammation. Related studies have demonstrated that MNR represents a combination of thrombosis and inflammation.³¹ The current study revealed that monocytes and neutrophils negatively impact healing in DFU patients treated with TTT surgery, whereas MNR exhibits the opposite effect. However, these findings are not contradictory. Monocytes are the primary cells of innate immunity and play a central role in initiating and resolving inflammatory responses to pathogens. Several studies have shown that monocytes are functionally impaired in diabetic patients, with reduced anti-inflammatory capacity and immune differentiation.^{32,33} Monocytes maintain a balance between pro-inflammatory and anti-inflammatory responses. Inflammatory development is stronger in the early stages of wound healing when the M1 phenotype dominates

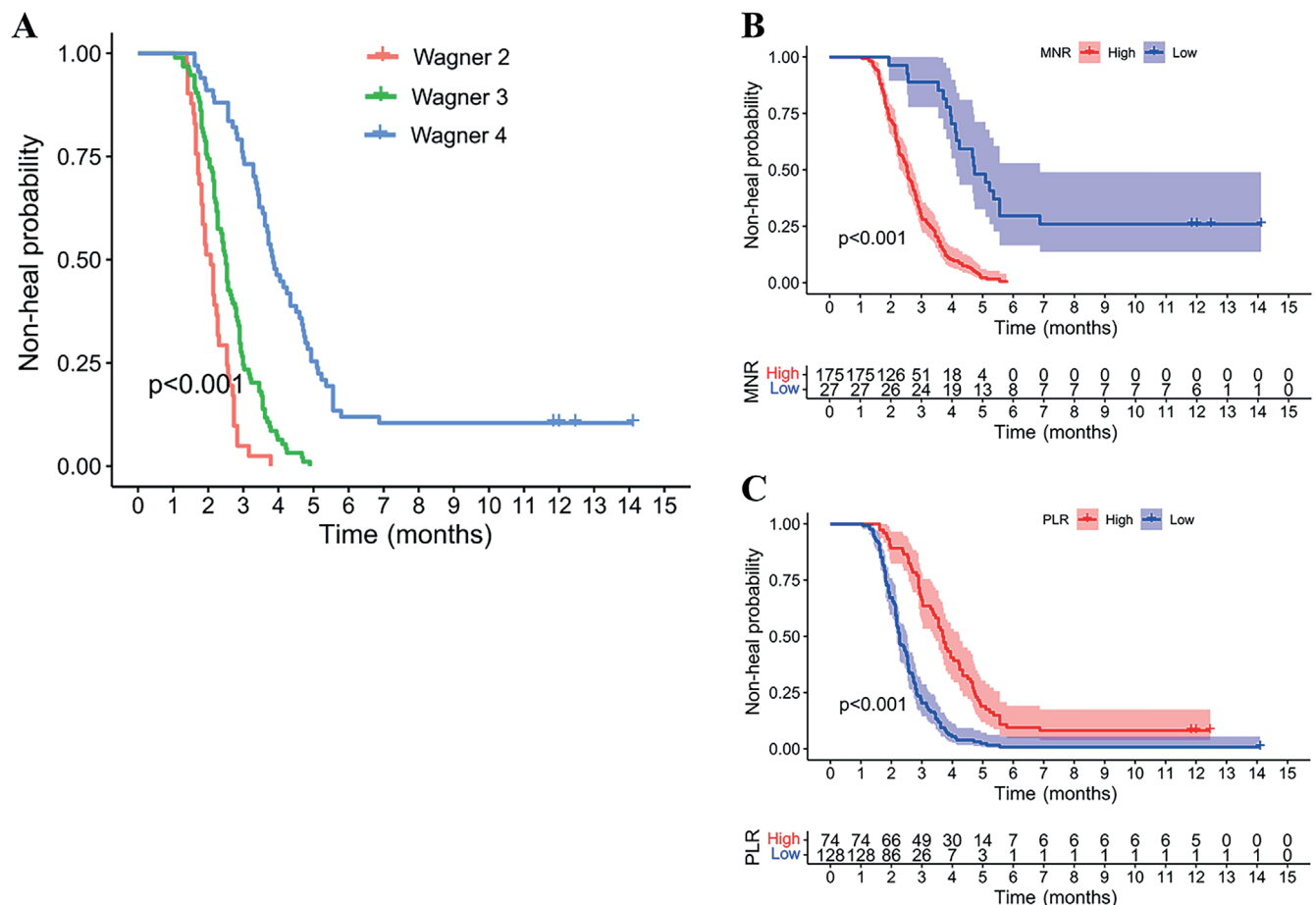


Fig. 5. Kaplan–Meier curve analysis for wound prognosis. A. Prognostic analysis of wound healing in diabetic foot ulcer (DFU) patients with the Wagner’s grades 2/3 group and Wagner’s 4 group after tibial cortex transverse transport (TTT) surgery ($\chi^2 = 96.207$); B. Prognostic analysis of wound healing in DFU patients with high- and low-monocyte-to-neutrophil ratios (MNRs) after TTT surgery ($\chi^2 = 74.918$); C. Prognostic analysis of wound healing in DFU patients with high- and low-platelet-to-lymphocyte ratios (PLRs) after TTT surgery ($\chi^2 = 65.214$)

monocytes. In the later stages of wound healing, the state of inflammation decreases, and the M2 phenotype predominates. Diabetic foot ulcers are persistent non-healing wounds in a state of chronic inflammation, with a predominant M1 phenotype for the mononuclear cells. These wounds have been in the early stages of healing for a long time, with an increased number of mononuclear cells and delayed healing. Elevated WBC counts in patients with impaired glucose tolerance increase the neutrophils.^{34,35} The neutrophil elevation is more pronounced in DFU patients with co-infection, suggesting a significant inflammatory response. The MNR increases as inflammation decreases during wound healing. The observation is consistent with the present finding. This study also observed reduced MNR in patients with high Wagner’s grades. The possible reason could be a greater severity of wound infections and higher levels of inflammation in these patients. Therefore, the detection of these inflammatory indicators can provide us with some strategies for the early prediction of wound healing after TTT surgery.

It is evident that certain baseline data (such as gender, age and body mass index (BMI)) in this study do not show significant differences across different Wagner’s grades.

While some studies indicate an association between baseline data and the severity of DFUs, others present conflicting findings.^{36,37} Thus, there remains controversy regarding the relationship between gender, age, BMI, and the severity of DFUs, necessitating further research for deeper exploration. Additionally, in the context of blood tests, the focus primarily lies on immune-related cells correlating with the Wagner’s classification of DFUs, aligning precisely with the pathophysiological processes of DFUs. Furthermore, certain inflammatory markers, such as ESR, also correlate with DFUs. It is evident that the healing of DFUs is a highly complex process.³⁸ Hence, the mere elevation or reduction of a single indicator cannot entirely predict the healing of DFUs. Therefore, a comprehensive analysis of various indicators is crucial for predicting the healing of DFUs. Our research findings precisely support this viewpoint, highlighting the urgency of further refining comprehensive indicators for predicting DFU healing.

Limitations

This study has several limitations that should be acknowledged. First, there may be some information bias

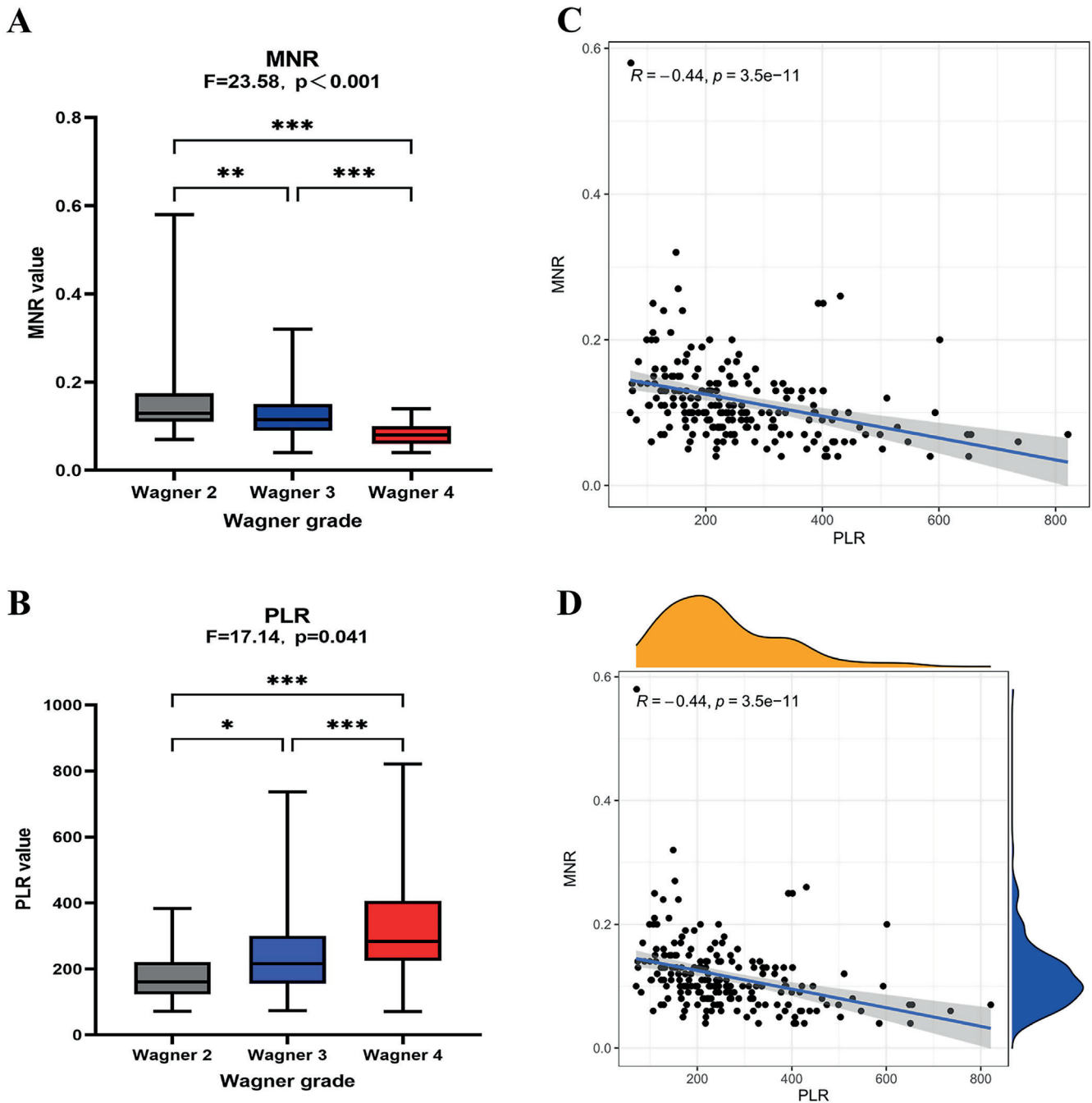


Fig. 6. Correlation analysis between platelet-to-lymphocyte ratio (PLR) and monocyte-to-neutrophil ratio (MNR). A. Comparison of MNR values in patients with different Wagner's grades. The MNR value decreased as the Wagner's level increased; B. Comparison of PLR values in patients with different Wagner's grades. The PLR value increased as the Wagner's level increased; C,D. Correlation analysis of the PLR and MNR (Spearman's analysis)

because it is a retrospective study. Additionally, the study only analyzed a limited number of influencing factors. It did not examine all indicators associated with DFU severity and healing after receiving TTT surgery for DFUs. Furthermore, although the ROC curve showed good accuracy, the developed nomogram model was not sufficient for use in clinical practice. Follow-up studies are needed to refine the diagnostic model. Therefore, a multicenter and more extensive cohort study is required. In the future, the model can be updated for better accuracy and improved prediction to help guide the treatment of DFUs.

Conclusions

The present study provides a comprehensive summary of the risk factors associated with the severity of DFUs and their prognosis. Platelet-to-lymphocyte ratio and MNR are critical predictors of DFU severity and prognosis after TTT surgery. The results of this study can guide risk stratification and inform preoperative prevention strategies for DFU patients. Additionally, they can contribute to a better prognosis for patients undergoing TTT surgery.

Supplementary data

The supplementary materials are available at <https://doi.org/10.5281/zenodo.10952319>. The package includes the following files:

Supplementary Fig. 1. A scatter plot illustrating the Cook's distance based on a binary logistic regression analysis established from 202 samples. Each point represents the Cook's distance for a sample. When the Cook's distance is greater than 1, it indicates an extreme outlier, which should be excluded from the model.

Supplementary Fig. 2. The Schoenfeld residuals of 12 models in a univariate Cox regression analysis. It is evident that the residuals of all models show no trend over time, indicating that the professional hazards assessment of the Cox regression is valid.

Supplementary Table 1. Box–Sidewell test for validation linear relationship between predictors and the logit of the response variable.

Supplementary Table 2. VIF and tolerance are used to analyze the collinearity of logistic regression analysis models. Setting tolerance greater than 0.1 and VIF less than 5 is considered a perfect result.

Data availability

The datasets generated and/or analyzed during the current study are available from the corresponding author on reasonable request.

Consent for publication

Not applicable.

ORCID iDs

Sijie Yang  <https://orcid.org/0000-0002-4856-8717>

Hongjie Su  <https://orcid.org/0000-0001-7685-6970>

Jun Hou  <https://orcid.org/0009-0001-4437-9580>

References

- Apelqvist J. Diagnostics and treatment of the diabetic foot. *Endocrine*. 2012;41(3):384–397. doi:10.1007/s12020-012-9619-x
- Zhang P, Lu J, Jing Y, Tang S, Zhu D, Bi Y. Global epidemiology of diabetic foot ulceration: A systematic review and meta-analysis. *Ann Med*. 2017;49(2):106–116. doi:10.1080/07853890.2016.1231932
- Ibrahim A. IDF Clinical Practice Recommendation on the Diabetic Foot: A guide for healthcare professionals. *Diabetes Res Clin Pract*. 2017;127:285–287. doi:10.1016/j.diabres.2017.04.013
- Hu Y, Bakhotmah BA, Alzahrani OH, Wang D, Hu FB, Alzahrani HA. Predictors of diabetes foot complications among patients with diabetes in Saudi Arabia. *Diabetes Res Clin Pract*. 2014;106(2):286–294. doi:10.1016/j.diabres.2014.07.016
- Verdoia M, Schaffer A, Barbieri L, et al. Impact of diabetes on neutrophil-to-lymphocyte ratio and its relationship to coronary artery disease. *Diabetes Metab*. 2015;41(4):304–311. doi:10.1016/j.diabet.2015.01.001
- Medzhitov R. Origin and physiological roles of inflammation. *Nature*. 2008;454(7203):428–435. doi:10.1038/nature07201
- Sen V, Bozkurt IH, Aydogdu O, et al. Significance of preoperative neutrophil–lymphocyte count ratio on predicting postoperative sepsis after percutaneous nephrolithotomy. *Kaohsiung J Med Sci*. 2016;32(10):507–513. doi:10.1016/j.kjms.2016.08.008
- Chen Y, Kuang X, Zhou J, et al. Proximal tibial cortex transverse distraction facilitating healing and limb salvage in severe and recalcitrant diabetic foot ulcers. *Clin Orthop Relat Res*. 2020;478(4):836–851. doi:10.1097/CORR.0000000000001075
- Qu L, Wang A, Tang F. The therapy of transverse tibial bone transport and vessel regeneration operation on thromboangitis obliterans [in Chinese]. 2001;81(10):622–624. <https://rs.yiigle.com/cmaid/839246>. Accessed December 6, 2023.
- Yang Y, Li Y, Pan Q, et al. Tibial cortex transverse transport accelerates wound healing via enhanced angiogenesis and immunomodulation. *Bone Joint Res*. 2022;11(4):189–199. doi:10.1302/2046-3758.114.BJR-2021-0364.R1
- American Diabetes Association. Executive summary: Standards of medical care in diabetes 2014. *Diabetes Care*. 2014;37(Suppl 1):S5–S13. doi:10.2337/dc14-S005
- Robin X, Turck N, Hainard A, et al. pROC: An open-source package for R and S+ to analyze and compare ROC curves. *BMC Bioinformatics*. 2011;12(1):77. doi:10.1186/1471-2105-12-77
- Shaw JE, Sicree RA, Zimmet PZ. Global estimates of the prevalence of diabetes for 2010 and 2030. *Diabetes Res Clin Pract*. 2010;87(1):4–14. doi:10.1016/j.diabres.2009.10.007
- Zheng Y, Ley SH, Hu FB. Global aetiology and epidemiology of type 2 diabetes mellitus and its complications. *Nat Rev Endocrinol*. 2018;14(2):88–98. doi:10.1038/nrendo.2017.151
- Armstrong DG, Boulton AJM, Bus SA. Diabetic foot ulcers and their recurrence. *N Engl J Med*. 2017;376(24):2367–2375. doi:10.1056/NEJMr1615439
- Amin N, Doupis J. Diabetic foot disease: From the evaluation of the “foot at risk” to the novel diabetic ulcer treatment modalities. *World J Diabetes*. 2016;7(7):153. doi:10.4239/wjd.v7.i7.153
- Ulu SM, Dogan M, Ahsen A, et al. Neutrophil-to-lymphocyte ratio as a quick and reliable predictive marker to diagnose the severity of diabetic retinopathy. *Diabetes Technol Ther*. 2013;15(11):942–947. doi:10.1089/dia.2013.0097
- Liu N, Sheng J, Pan T, Wang Y. Neutrophil to lymphocyte ratio and platelet to lymphocyte ratio are associated with lower extremity vascular lesions in Chinese patients with type 2 diabetes. *Clin Lab*. 2019;65(3):180804. doi:10.7754/Clin.Lab.2018.180804
- Liu J, Liu X, Li Y, et al. The association of neutrophil to lymphocyte ratio, mean platelet volume, and platelet distribution width with diabetic retinopathy and nephropathy: A meta-analysis. *Biosci Rep*. 2018;38(3):BSR20180172. doi:10.1042/BSR20180172
- Mertoglu C, Gunay M. Neutrophil–lymphocyte ratio and platelet–lymphocyte ratio as useful predictive markers of prediabetes and diabetes mellitus. *Diabetes Metab Syndr*. 2017;11(Suppl 1):S127–S131. doi:10.1016/j.dsx.2016.12.021
- Demirtas L, Degirmenci H, Akbas EM, et al. Association of hematological indices with diabetes, impaired glucose regulation and microvascular complications of diabetes. *Int J Clin Exp Med*. 2015;8(7):11420–11427. PMID:26379958. PMID:PMC4565341.
- Pitsavos C, Tampourlou M, Panagiotakos DB, et al. Association between low-grade systemic inflammation and type 2 diabetes mellitus among men and women from the ATTICA study. *Rev Diabet Stud*. 2007;4(2):98–104. doi:10.1900/RDS.2007.4.98
- Imtiaz F, Shafique K, Mirza S, Ayooob Z, Vart P, Rao S. Neutrophil–lymphocyte ratio as a measure of systemic inflammation in prevalent chronic diseases in Asian population. *Int Arch Med*. 2012;5(1):2. doi:10.1186/1755-7682-5-2
- Schaper NC, Van Netten JJ, Apelqvist J, et al. Practical Guidelines on the Prevention and Management of Diabetic Foot Disease (IWGDF 2019 update). *Diabetes Metab Res Rev*. 2020;36(Suppl 1):e3266. doi:10.1002/dmrr.3266
- Soyoye DO, Abiodun OO, Ikem RT, Kolawole BA, Akintomide AO. Diabetes and peripheral artery disease: A review. *World J Diabetes*. 2021;12(6):827–838. doi:10.4239/wjd.v12.i6.827
- Yazdanpanah L, Shahbazian H, Nazari I, et al. Risk factors associated with diabetic foot ulcer-free survival in patients with diabetes. *Diabetes Metab Syndr*. 2018;12(6):1039–1043. doi:10.1016/j.dsx.2018.06.020
- Wang N, Yang B, Wang G, et al. A meta-analysis of the relationship between foot local characteristics and major lower extremity amputation in diabetic foot patients. *J Cell Biol*. 2019;120(6):9091–9096. doi:10.1002/jcb.28183

28. Peng B, Min R, Liao Y, Yu A. Development of predictive nomograms for clinical use to quantify the risk of amputation in patients with diabetic foot ulcer. *J Diabetes Res.* 2021;2021:6621035. doi:10.1155/2021/6621035
29. Gary T, Pichler M, Belaj K, et al. Platelet-to-lymphocyte ratio: A novel marker for critical limb ischemia in peripheral arterial occlusive disease patients. *PLoS One.* 2013;8(7):e67688. doi:10.1371/journal.pone.0067688
30. Fujita T, Hemmi S, Kajiwaru M, et al. Complement-mediated chronic inflammation is associated with diabetic microvascular complication. *Diabetes Metab Res Rev.* 2013;29(3):220–226. doi:10.1002/dmrr.2380
31. Gao B, Pan W, Hu X, et al. Neutrophil-related ratios predict the 90-day outcome in acute ischemic stroke patients after intravenous thrombolysis. *Front Physiol.* 2021;12:670323. doi:10.3389/fphys.2021.670323
32. Kumar NP, Moideen K, Dhakshinraj SD, et al. Profiling leucocyte subsets in tuberculosis–diabetes co-morbidity. *Immunology.* 2015;146(2):243–250. doi:10.1111/imm.12496
33. Valtierra-Alvarado MA, Castañeda Delgado JE, Ramírez-Talavera SI, et al. Type 2 diabetes mellitus metabolic control correlates with the phenotype of human monocytes and monocyte-derived macrophages. *J Diabetes Complications.* 2020;34(11):107708. doi:10.1016/j.jdiacomp.2020.107708
34. Ohshita K, Yamane K, Hanafusa M, et al. Elevated white blood cell count in subjects with impaired glucose tolerance. *Diabetes Care.* 2004;27(2):491–496. doi:10.2337/diacare.27.2.491
35. Duman TT, Aktas G, Atak BM, Kocak MZ, Erkus E, Savli H. Neutrophil to lymphocyte ratio as an indicative of diabetic control level in type 2 diabetes mellitus. *Afr Health Sci.* 2019;19(1):1602. doi:10.4314/ahs.v19i1.35
36. Sutkowska E, Sutkowski K, Sokołowski M, Franek E, Dragan S. Distribution of the highest plantar pressure regions in patients with diabetes and its association with peripheral neuropathy, gender, age, and BMI: One centre study. *J Diabetes Res.* 2019;2019:7395769. doi:10.1155/2019/7395769
37. Khan MS, Azam M, Khan MN, et al. Identification of contributing factors, microorganisms and antimicrobial resistance involved in the complication of diabetic foot ulcer treatment. *Microb Pathog.* 2023;184:106363. doi:10.1016/j.micpath.2023.106363
38. Falanga V, Isseroff RR, Soulika AM, et al. Chronic wounds. *Nat Rev Dis Primers.* 2022;8(1):50. doi:10.1038/s41572-022-00377-3

Association of oxygen saturation and mortality in patients with acute respiratory failure

Li Ai^{A,D–F}, Ran Li^{B,C,F}, Xixian Teng^{B,C,F}, Jing Li^{B,C,F}, Bing Hai^{A,F}

Department of Respiratory and Critical Care Medicine, The Second Affiliated Hospital of Kunming Medical University, China

A – research concept and design; B – collection and/or assembly of data; C – data analysis and interpretation;

D – writing the article; E – critical revision of the article; F – final approval of the article

Advances in Clinical and Experimental Medicine, ISSN 1899–5276 (print), ISSN 2451–2680 (online)

Adv Clin Exp Med. 2025;34(4):561–571

Address for correspondence

Bing Hai

E-mail: haibingkmmu@outlook.com

Funding sources

The program of “Study on the relationship between the characteristics of social support network and smoking behavior of smoking cessation outpatients in Grade A Hospital of Kunming city” (grant No. 2020ynlc003).

Conflict of interest

None declared

Received on June 25, 2023

Reviewed on November 17, 2023

Accepted on June 10, 2024

Published online on December 6, 2024

Abstract

Background. The variability and disparities in the recommended targets across different international guidelines suggest the optimal oxygen saturation (SpO₂) target for acute respiratory failure (ARF) patients be further explored.

Objectives. To explore the association between SpO₂ and in-hospital mortality of ARF patients, as well as to determine the optimum SpO₂ for ARF patients.

Materials and methods. In this cohort study, 3,225 ARF patients were included at the end of the follow-up; among them, and 1,249 patients survived and 1,976 died. The restricted cubic spline (RCS) was drawn to show the nonlinear association between the median SpO₂ and the risk of in-hospital mortality of ARF patients and to identify the optimal range of SpO₂. Cox regression was applied to identify the association between the median SpO₂ and the risk of in-hospital mortality in ARF patients. Kaplan–Meier curves were plotted to identify the in-hospital mortality of ARF patients.

Results. The in-hospital mortality rate was 61.2% in all ARF patients at the end of the follow-up. The median SpO₂ was associated with decreased risk of in-hospital mortality of ARF patients after adjusting for confounders (hazard ratio (HR) = 0.95, 95% confidence interval (95% CI): 0.93–0.97). The median SpO₂ was non-linearly correlated with the in-hospital mortality of ARF patients. The overall survival (OS) was higher in the 96–98% group. A median SpO₂ ≤ 96% was associated with an increased risk of in-hospital mortality in ARF patients accompanied by malignant cancer (HR = 1.55, 95% CI: 1.24–1.94), renal failure (HR = 1.45, 95% CI: 1.24–1.70), chronic obstructive pulmonary disease (COPD; HR = 1.70, 95% CI: 1.27–2.28) and atrial fibrillation (AF; HR = 1.25, 95% CI: 1.02–1.53). The median SpO₂ > 98% was associated with an elevated risk of in-hospital mortality in ARF patients accompanied by AF (HR = 1.22, 95% CI: 1.04–1.44).

Conclusions. The median SpO₂ was linked to a decreased risk of in-hospital mortality in ARF patients.

Key words: in-hospital mortality, acute respiratory failure, oxygen saturation, non-linear correlation

Cite as

Ai L, Li R, Teng X, Li J, Hai B. Association of oxygen saturation and mortality in patients with acute respiratory failure.

Adv Clin Exp Med. 2025;34(4):561–571.

doi:10.17219/acem/189879

DOI

10.17219/acem/189879

Copyright

Copyright by Author(s)

This is an article distributed under the terms of the Creative Commons Attribution 3.0 Unported (CC BY 3.0) (<https://creativecommons.org/licenses/by/3.0/>)

Background

As a common disease in critically ill patients in intensive care units (ICUs), acute respiratory failure (ARF) is a heavy healthcare burden.¹ The reasons causing ARF are usually acute pathogenic factors, including severe shock, electric shock, trauma, lung diseases, and acute airway obstruction, resulting in a precipitous deterioration of pulmonary function.^{2,3} Acute respiratory failure was reported to result in about 2.5 million ICU admissions^{4,5} and causing a mortality rate of over 30% every year.⁶ In patients with ARF, the body's compensation does not occur within the short timeframe in which rescue needs to be performed.⁷ Mechanical ventilation (MV) is one of the most vital life-supporting interventions for ARF patients.⁸ Supplemental oxygen is important for ARF patients receiving MV in ICUs.⁹ When oxygen is provided to patients in ICUs requiring MV, the absence of appropriate oxygen management might lead to potential iatrogenic harm to patients.¹⁰ Improving the oxygen management for ARF patients requiring MV is essential.

The maintenance of arterial oxygen saturation, evaluated using oxygen saturation (SpO₂), is crucial in clinical care. The need for oxygen supplementation in patients is dependent upon peripheral SpO₂ thresholds. Setting SpO₂ targets towards the higher end of the range provides a safety margin against hypoxemia but may increase the risk of hyperoxemia and tissue hyperoxia, leading to oxidative damage and inflammation.^{11,12} Evidence published in 2018 and 2019 suggested that ARF patients receiving MV with high fractions of inspired oxygen were associated with excess morbidity and mortality.^{13,14} Also, patients with ARF experienced hypoxic damage when the delivery of oxygen to tissues failed to meet their oxygenation demands, potentially resulting in organ failure and mortality.¹⁵ The study conducted by Siemieniuk et al. in 2018 demonstrated that a SpO₂ > 96% might increase the mortality of patients compared to a SpO₂ < 96%.¹⁶ Another study by Barrot et al. in 2020 revealed that conservative oxygen therapy was harmful for acute respiratory distress syndrome (ARDS) patients.¹⁷ Some recent guidelines recommend a SpO₂ < 96% in patients receiving MV; however, the acceptable lower limit was unclear.^{16,18} The variability in current clinical practice¹⁹ and disparities in the recommended targets across different international guidelines^{16,18} suggested the need for further exploration of the optimal SpO₂ target for ARF patients.

Objectives

This study aimed to explore the correlation between SpO₂ levels and in-hospital mortality among patients with ARF. The optimum SpO₂ range was also determined. Subgroup analysis explored the association between SpO₂ and in-hospital mortality among patients with ARF in patients with different types of complications.

Material and methods

Study design and population

This was a cohort study involving 5,461 ARF patients admitted to ICUs from the Medical Information Mart for Intensive Care-III (MIMIC)-III (v. 1.4) and MIMIC-IV (v. 1.0). Medical Information Mart for Intensive Care is a free critical care database from a single center, containing data on 46,520 patients admitted to the ICU of the Beth Israel Deaconess Medical Center (BIDMC; Boston, USA) between 2001 and 2012.²⁰ This study encompassed demographics, fluid balance, laboratory tests, and vital status and signs. International Classification of Diseases and 9th Revision (ICD-9) codes, hourly physiologic data from bedside monitors validated by nurses in the ICU, and written estimates of radiologic films from specialists covering respective time periods for each patient were recorded.²¹ Medical Information Mart for Intensive Care-IV is an updated version of MIMIC-III, including data of patients from 2008 to 2019.²² In our study, patients with a MV duration <48 h and those without data on SpO₂ were excluded, and finally, the data of 3,225 patients were followed up. After the conclusion of the follow-up period, 1,249 patients survived, while 1,976 patients succumbed to their illnesses. The project received approval from the Institutional Review Boards of Beth Israel Deaconess Medical Center and the Massachusetts Institute of Technology (MIT; Cambridge, USA). The requirement for individual patient consent was waived due to the project's lack of impact on clinical care and the de-identification of all protected health information.

Data collection

The collected data included, age (years), heart rate (breaths/min), diastolic blood pressure (DBP, mm Hg), systolic blood pressure (SBP, mm Hg), mean arterial pressure (MAP, mm Hg), history of diseases including chronic obstructive pulmonary disease (COPD), atrial fibrillation (AF), lung cancer, liver cirrhosis, congestive heart failure, heart disease, diabetes mellitus, hyperlipidemia, renal failure, malignant cancer, and respiratory-related parameters including fraction of inspired oxygen (FiO₂), SpO₂ (%), partial pressure of arterial carbon dioxide (PaCO₂, mm Hg), Glasgow Coma Score (GCS), the Sequential Organ Failure Assessment (SOFA) score, Simplified Acute Physiology Score II (SAPSII), MV duration, and MV fraction. All data were collected using the first measurements during ICU admission.

Outcome variables

The outcome was assessed by evaluating in-hospital mortality among ARF patients. The follow-up was started 48 h after ICU admission with an endpoint of follow-up when the patients died in the hospital or were discharged. The median duration of follow-up was 15 (10–23) days.

Statistical analyses

The Levene's test was used to test the homogeneity of variance. The results of the Levene's test of variables are shown in Supplementary Table 1. The central limit theorem (CLT) assumes that the distribution of variables differs statistically insignificantly from the normal distribution, and measurement data were described as mean and standard deviation (mean (\pm SD)). A t-test was used for comparison among groups with homogeneous variances, and a t-test was used for heterogeneity of variance. The enumeration data were described in terms of numbers and percentages of cases (n (%)). If the assumption of expected abundance ($n < 5 \leq 20\%$ of cells) for the χ^2 test was achieved, Pearson's nonparametric χ^2 test of independence without Yates's continuity was used. A univariable Cox proportional hazards model was established to identify potential confounding factors. The Cox proportional hazards assumption was tested. As shown in Supplementary Fig. 1, there was no linear relationship between covariates and logarithmic hazards. Likelihood ratio (LR) test and Wald's test were used to judge whether the fitting of the model was significant. The former uses the logarithmic likelihood values of the 2 models to test the difference. The latter is a hypothesis that tests whether the value of a set of parameters is equal to 0. If the variable remained significant under both tests, it was regarded as a statistical difference and adjusted as covariates in the multivariable proportional Cox hazards model. The assumption of collinearity among predictors was tested for proportional Cox hazard regression. The non-collinearity of predictors assumption was evaluated with a multicollinearity, variance inflation factor (VIF) < 10 , which was then regarded as no multicollinearity among the variables. Whether the standardized Schoenfeld residuals were related to time was used to assess whether the model met the proportional hazards assumption. If a $p > 0.05$ in both the single variable and global variable was found, it was considered that the Schoenfeld residuals were independent of time. More detailed information on Schoenfeld residues is shown in Supplementary Table 2. A standardized Schoenfeld residual relative to time correlation of each covariate is shown in Supplementary Fig. 2. Comprised of the magnitude of the maximum df-beta value with the regression coefficients, all observations are not very different from those in each row and are uniformly distributed on both sides of the $y = 0$ reference line, with relative symmetry. The restricted cubic spline (RCS) was drawn to show the nonlinear association between median SpO₂ and the risk of in-hospital mortality of ARF patients and identify the optimal range of SpO₂ using ggplot2, rms, ggthemes, ggsci, and cowplot packages in R (R Foundation for Statistical Computing, Vienna, Austria). The function name and basic code are shown in the Supplementary File 1. To further illustrate the different median SpO₂ groups with the risk of in-hospital

mortality of ARF patients, a subgroup analysis was performed. R was applied for data analysis with a $p < 0.05$ set as statistical difference.

Results

The baseline data of the participants

In total, 5,461 ARF patients were involved in this study. Among them, patients with a MV duration < 48 h ($n = 2,027$) and patients without the data on SpO₂ ($n = 209$) were excluded. Finally, 3,225 patients were included. The screening process is shown in Fig. 1. At the end of follow-up, those who survived were classified into the survival group ($n = 1,249$), and those who died were allocated into the death group ($n = 1,976$).

As for the characteristics of participants in the survival and death groups, the mean SBP (125.7 mm Hg vs 123.2 mm Hg), DBP (67.9 mm Hg vs 64.2 mm Hg), MAP (89.3 mm Hg vs 81.3 mm Hg), FiO₂ (50.0% vs 1.0%), and SpO₂ (97.6% vs 97.4%) were higher in the survival group.

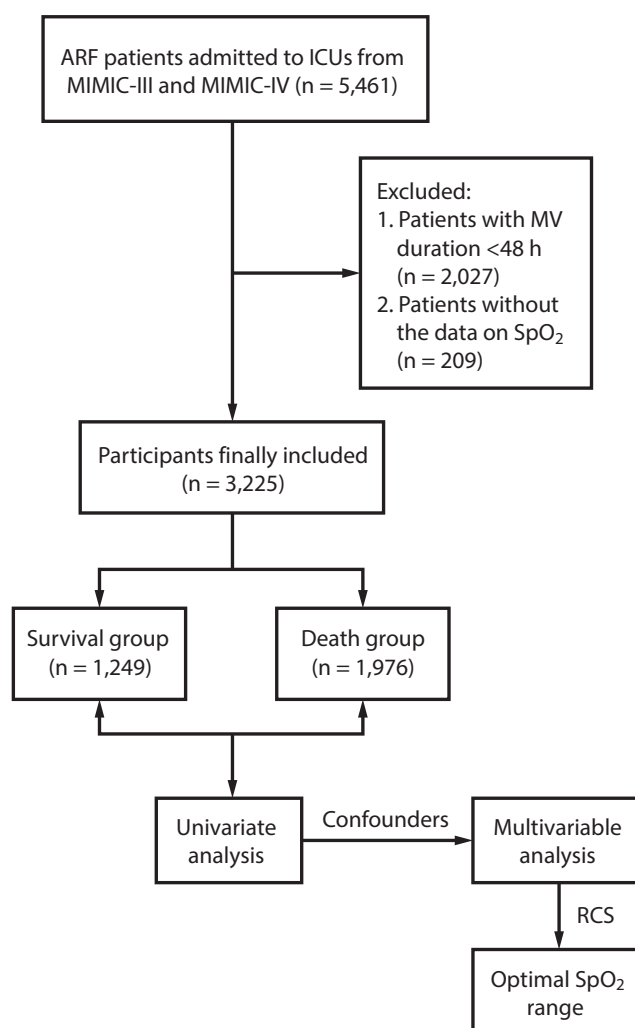


Fig. 1. The screening process for the participants

The percentages of ARF patients complicated with COPD (17.6% vs 10.3%), lung cancer (3.4% vs 1.0%), liver cirrhosis (12.5% vs 6.4%), congestive heart failure (44.2% vs 29.2%), heart disease (12.9% vs 9.7%), renal failure (55.9% vs

44.0%), and malignant cancer (26.7% vs 12.3%) was higher in the death group compared to the survival group. The detailed characteristics of patients in the survival and death groups are presented in Table 1.

Table 1. The baseline characteristics of participants

Variables		Total (n = 3225)	Survival (n = 1249)	Death (n = 1976)	Statistics	p-value
Gender; n (%)	female	1429 (44.3)	543 (43.5)	886 (44.8)	$\chi^2 = 0.52$	0.470
	male	1796 (55.7)	706 (56.5)	1090 (55.2)		
Age [years], mean \pm SD		72.9 \pm 50.0	60.9 \pm 33.8	80.5 \pm 56.6	t' = -12.35	<0.001
SBP [mm Hg], mean \pm SD		124.2 \pm 27.9	125.7 \pm 26.5	123.2 \pm 28.7	t' = 2.51	0.012
DBP [mm Hg], mean \pm SD		65.6 \pm 19.3	67.9 \pm 18.8	64.2 \pm 19.5	t = 5.35	<0.001
Heart rate [bpm], mean \pm SD		94.9 \pm 22.0	95.5 \pm 22.3	94.5 \pm 21.7	t = 1.33	0.183
MAP [mm Hg], mean \pm SD		84.4 \pm 112.2	89.3 \pm 178.4	81.3 \pm 20.4	t = 1.98	0.048
History of disease						
COPD, n (%)	no	2748 (85.2)	1120 (89.7)	1628 (82.4)	$\chi^2 = 31.63$	<0.001
	yes	477 (14.8)	129 (10.3)	348 (17.6)		
Lung cancer; n (%)	no	3146 (97.6)	1237 (99.0)	1909 (96.6)	$\chi^2 = 17.91$	<0.001
	yes	79 (2.4)	12 (1.0)	67 (3.4)		
AF, n (%)	no	2157 (66.9)	953 (76.3)	1204 (60.9)	$\chi^2 = 80.93$	<0.001
	yes	1068 (33.1)	296 (23.7)	772 (39.1)		
Liver cirrhosis, n (%)	no	2898 (89.9)	1169 (93.6)	1729 (87.5)	$\chi^2 = 30.54$	<0.001
	yes	327 (10.1)	80 (6.4)	247 (12.5)		
Congestive heart failure, n (%)	no	1987 (61.6)	884 (70.8)	1103 (55.8)	$\chi^2 = 71.75$	<0.001
	yes	1238 (38.4)	365 (29.2)	873 (44.2)		
Heart disease, n (%)	no	2849 (88.3)	1128 (90.3)	1721 (87.1)	$\chi^2 = 7.38$	0.007
	yes	376 (11.7)	121 (9.7)	255 (12.9)		
Diabetes mellitus, n (%)	no	2394 (74.2)	927 (74.2)	1467 (74.2)	$\chi^2 = 0.00$	0.989
	yes	831 (25.8)	322 (25.8)	509 (25.8)		
Hyperlipidemia, n (%)	no	2369 (73.5)	866 (69.3)	1503 (76.1)	$\chi^2 = 17.42$	<0.001
	yes	856 (26.5)	383 (30.7)	473 (23.9)		
Renal failure; n (%)	no	1572 (48.7)	700 (56.0)	872 (44.1)	$\chi^2 = 43.01$	<0.001
	yes	1653 (51.3)	549 (44.0)	1104 (55.9)		
Malignant cancer, n (%)	no	2544 (78.9)	1095 (87.7)	1449 (73.3)	$\chi^2 = 93.62$	<0.001
	yes	681 (21.1)	154 (12.3)	527 (26.7)		
Respiratory related parameters						
FiO ₂ , mean \pm SD		38.9 \pm 42.1	46.5 \pm 41.6	34.0 \pm 41.8	t = 8.32	<0.001
SpO ₂ , mean \pm SD		96.6 \pm 5.8	96.8 \pm 5.6	96.5 \pm 6.0	t = 1.73	0.084
GCS, mean \pm SD		9.2 \pm 4.4	9.0 \pm 4.5	9.3 \pm 4.3	t' = -1.34	0.182
PaCO ₂ , mean \pm SD		43.8 \pm 13.8	43.2 \pm 12.7	44.0 \pm 14.2	t' = -1.18	0.240
Mean SpO ₂ , mean \pm SD		97.5 \pm 1.8	97.6 \pm 1.5	97.4 \pm 2.0	t' = 3.66	<0.001
Median SPO ₂ , mean \pm SD		97.8 \pm 1.9	97.9 \pm 1.6	97.8 \pm 2.1	t' = 1.89	0.058
SAPSII, mean \pm SD		45.3 \pm 14.9	40.3 \pm 14.1	48.5 \pm 14.6	t = -15.78	<0.001
SOFA score, mean \pm SD		7.9 \pm 3.5	7.6 \pm 3.4	8.10 \pm 3.6	t' = -3.84	<0.001
MV duration, mean \pm SD		215.9 \pm 182.8	215.4 \pm 171.7	216.2 \pm 189.5	t' = -0.13	0.897
MV fraction, mean \pm SD		2.0 \pm 2.0	2.0 \pm 1.8	1.9 \pm 2.1	t = 0.37	0.714

t' – the Welch test for independent variance estimation; t – the value of the test statistic for the Student's t -test; SD – standard deviation; SBP – systolic blood pressure; DBP – diastolic blood pressure; MAP – mean arterial pressure; COPD – chronic obstructive pulmonary disease; AF – atrial fibrillation; FiO₂ – fraction of inspiration oxygen; GCS – Glasgow Coma Score; PaCO₂ – partial arterial pressure of CO₂; SOFA – the Sequential Organ Failure Assessment; SAPSII – Simplified Acute Physiology Score II; MV – mechanical ventilation; SpO₂ – oxygen saturation. Multivariate model adjusting for confounding factors including DBP, MAP, age, SBP, and FiO₂, COPD, lung cancer, liver cirrhosis, congestive heart failure, AF, myocardial infarction, hyperlipidemia, malignant cancer, and SOFA score.

Potential confounding factors associated with in-hospital mortality of ARF patients

To identify the association between SpO₂ and in-hospital mortality of ARF patients, univariate Cox regression analysis was conducted to identify potential confounding factors associated with the in-hospital mortality of ARF patients. According to the data in Table 2, age (hazard ratio (HR) = 1.02, 95% confidence interval (95% CI): 1.02–1.02), SBP (HR = 1.00, 95% CI: 1.00–1.00), DBP (HR = 1.00, 95% CI: 1.00–1.00), MAP (HR = 1.00, 95% CI: 1.00–1.00), FiO₂ (HR = 1.00, 95% CI: 1.00–1.00), complicated with COPD (HR = 1.20, 95% CI: 1.07–1.35), lung cancer (HR = 2.53, 95% CI: 1.98–3.23), AF (HR = 1.18, 95% CI: 1.08–1.29), liver cirrhosis (HR = 1.39, 95% CI: 1.22–1.59), congestive heart failure (HR = 1.25, 95% CI: 1.15–1.37), hyperlipidemia (HR = 0.89, 95% CI: 0.80–0.99), and malignant cancer (HR = 1.54, 95% CI: 1.40–1.71), and a SOFA score (HR = 1.02, 95% CI: 1.01–1.03) were potential confounders associated with the in-hospital mortality of ARF patients. The results of the non-collinearity of the predictors' assumptions showed there was no multicollinearity among the variables (VIF < 10, Table 3) and all the variables were not related to time (Fig. 2).

Table 3. The VIF of variables associated with mortality of ARF patients

Variables	VIF
Age	1.115
SBP	1.804
DBP	1.896
MAP	1.261
FiO ₂	1.187
Median SpO ₂	1.033
COPD	1.057
Lung cancer	1.174
AF	1.144
Liver cirrhosis	1.137
Heart failure congestive	1.175
Heart disease	1.075
Hyperlipidemia	1.084
Malignant cancer	1.170
SOFA score	1.210

VIF – variance inflation factor; SBP – systolic blood pressure; DBP – diastolic blood pressure; MAP – mean arterial pressure; COPD – chronic obstructive pulmonary disease; ARF – acute respiratory failure; AF – atrial fibrillation; FiO₂ – fraction of inspiration oxygen; SOFA – the Sequential Organ Failure Assessment; SpO₂ – oxygen saturation.

Table 2. Univariate Cox regression of the association between SpO₂ and in-hospital mortality of ARF patients

Variables	HR (95% CI)	p-value (Wald's test)	p-value (LR-test)
Gender (male vs female)	0.93 (0.85–1.01)	0.101	0.102
Age	1.02 (1.02–1.02)	<0.001	<0.001
Heart rate	1.00 (1.00–1.00)	0.123	0.122
SBP	1.00 (1.00–1.00)	0.005	0.005
DBP	1.00 (1.00–1.00)	0.002	0.001
MAP	1.00 (1.00–1.00)	0.008	0.003
FiO ₂	1.00 (1.00–1.00)	<0.001	<0.001
SpO ₂	1.00 (1.00–1.00)	0.906	0.906
Median SpO ₂	0.97 (0.94–0.99)	0.012	0.013
GCS	1.00 (1.00–1.00)	0.801	0.801
PaCO ₂	1.00 (1.00–1.00)	0.597	0.598
COPD (yes vs no)	1.20 (1.07–1.35)	0.002	0.003
Lung cancer (yes vs no)	2.53 (1.98–3.23)	<0.001	<0.001
AF (yes vs no)	1.18 (1.08–1.29)	<0.001	<0.001
Liver cirrhosis (yes vs no)	1.39 (1.22–1.59)	<0.001	<0.001
Congestive heart failure (yes vs no)	1.25 (1.15–1.37)	<0.001	<0.001
Heart disease (yes vs no)	1.15 (1.01–1.31)	0.035	0.038
Hyperlipidemia (yes vs no)	0.89 (0.80–0.99)	0.028	0.027
Malignant cancer (yes vs no)	1.54 (1.40–1.71)	<0.001	<0.001
SOFA score	1.02 (1.01–1.03)	<0.001	<0.001

HR – hazard ratio; 95% CI – 95% confidence interval; SBP – systolic blood pressure; DBP – diastolic blood pressure; MAP – mean arterial pressure; COPD – chronic obstructive pulmonary disease; ARF – acute respiratory failure; AF – atrial fibrillation; FiO₂ – fraction of inspiration oxygen; GCS – Glasgow Coma Score; SOFA – the Sequential Organ Failure Assessment; SpO₂ – oxygen saturation; HR – hazards ratio.

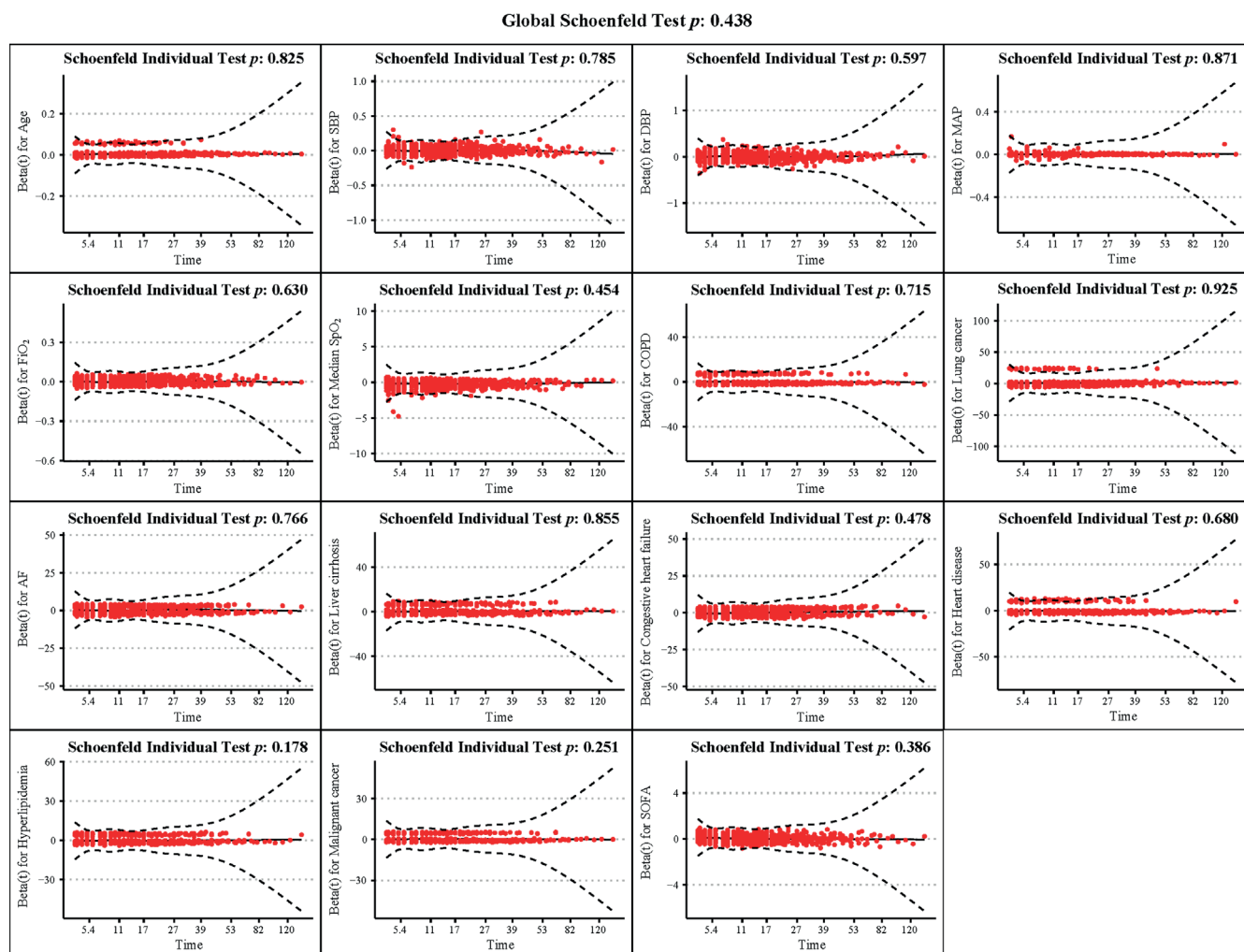


Fig. 2. The global Schoenfeld test for all variables

The association between SpO₂ and in-hospital mortality of acute respiratory failure (ARF) patients

In the unadjusted model, the median SpO₂ level might be related to a decreased in-hospital mortality risk of ARF patients (HR = 0.97, 95% CI: 0.94–0.99). Multivariable Cox regression depicted that the median SpO₂ was related to a decrease in the in-hospital mortality risk of ARF patients (HR = 0.95, 95% CI: 0.93–0.97) after adjusting for confounders including DBP, SBP, age, FiO₂, lung cancer, liver cirrhosis, AF, hyperlipidemia, malignant cancer, and SOFA score (Table 4).

The non-linear association between median SpO₂ and in-hospital mortality of ARF patients

Furthermore, we wanted to identify the optimum SpO₂ range for ARF patients. The data of RCS delineated that there was a nonlinear correlation between the median SpO₂ and in-hospital mortality of ARF patients (Fig. 3). There were 2 nodes of median SpO₂ in this RSC, which were at 96.8% and 98.3%. When the median SpO₂ was between 96% and 98%, the HR for in-hospital mortality of ARF patients was <1, suggesting the risk of in-hospital mortality of ARF patients was decreased. The survival curves showed

Table 4. The association between median SpO₂ and mortality of ARF patients

Variables	Univariate model		Multivariate model	
	OR (95% CI)	p-value	OR (95% CI)	p-value
Median SpO ₂	0.97 (0.94–0.99)	0.012	0.95 (0.93–0.97)	<0.001

SpO₂ – oxygen saturation; OR – odds ratio; 95% CI – 95% confidence interval.

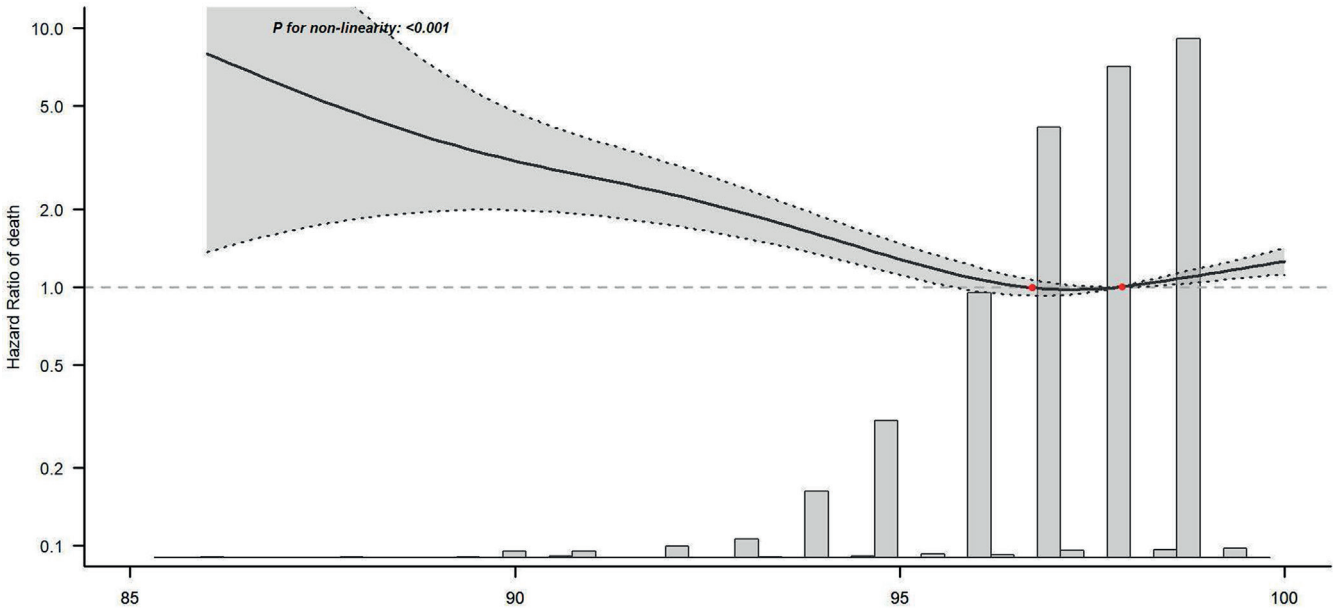


Fig. 3. The restricted cubic spline (RCS) revealed a non-linear association between median SpO₂ (oxygen saturation) levels and in-hospital mortality in acute respiratory failure (ARF) patients

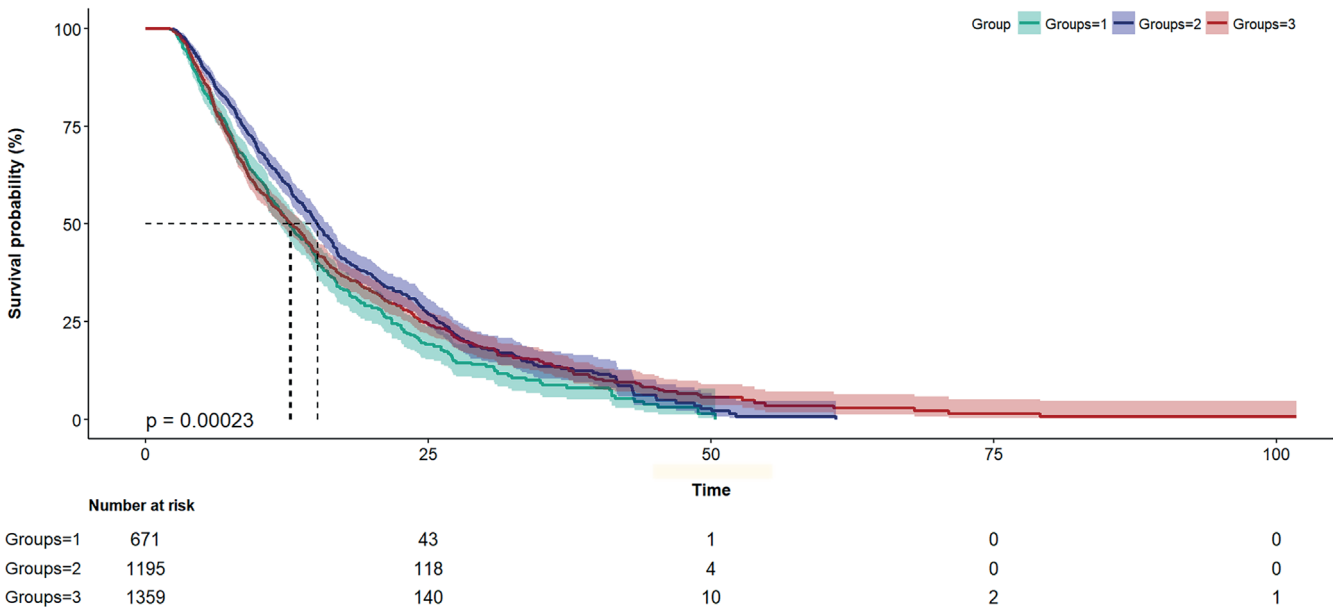


Fig. 4. The Kaplan–Meier curves show the in-hospital mortality of acute respiratory failure (ARF) patients in different groups. Group 1 had a median oxygen saturation (SpO₂) ≤96%, Group 2 had a median SpO₂ > 96% but ≤98%, and Group 3 had a median SpO₂ > 98%

that overall survival (OS) was higher in the median SpO₂ between 96% and 98% group than both the SpO₂ ≤ 96% group and SpO₂ > 98% group (Fig. 4).

The correlation between median SpO₂ and in-hospital mortality of ARF patients with different complications

Subgroup analysis was conducted in ARF patients with different comorbidities. The median SpO₂ level was correlated with a reduced risk of in-hospital mortality among patients diagnosed with malignant cancer (HR = 0.92, 95% CI: 0.87–0.96), renal failure (HR = 0.93, 95% CI:

0.90–0.96), lung cancer (HR = 0.86, 95% CI: 0.74–0.99), and COPD (HR = 0.92, 95% CI: 0.87–0.97) after adjusting for age, SBP, DBP, FiO₂, lung cancer, liver cirrhosis, AF, hyperlipidemia, malignant cancer, and SOFA score (Table 5). In addition, we observed that ARF patients with malignant cancer (HR = 1.55, 95% CI: 1.24–1.94), renal failure (HR = 1.45, 95% CI: 1.24–1.70), COPD (HR = 1.70, 95% CI: 1.27–2.28) or AF (HR = 1.25, 95% CI: 1.02–1.53) who had a median SpO₂ ≤ 96% were at an increased in-hospital mortality risk. The presence of a median SpO₂ > 98% was related to an elevated risk of in-hospital mortality among ARF patients with AF (HR = 1.22, 95% CI: 1.04–1.44, Table 6).

Table 5. The association between median SpO₂ and the mortality of ARF patients with different complications

Subgroup	n (%)	HR (95% CI)	p-value
Diabetes mellitus	509 (61.3)	0.98 (0.93–1.04)	0.539
Malignant cancer	527 (77.4)	0.92 (0.87–0.96)	<0.001
Liver cirrhosis	247 (75.5)	0.95 (0.88–1.02)	0.159
Hyperlipidemia	473 (55.3)	0.98 (0.93–1.04)	0.546
Renal failure	1104 (66.8)	0.93 (0.90–0.96)	<0.001
Lung cancer	67 (84.8)	0.86 (0.74–0.99)	0.041
COPD	348 (73.0)	0.92 (0.87–0.97)	0.002
AF	772 (72.3)	0.99 (0.94–1.04)	0.625

HR – hazard ratio; p – significance level; COPD – chronic obstructive pulmonary disease; AF – atrial fibrillation; SpO₂ – oxygen saturation; ARF – acute respiratory failure; HR – hazards ratio; 95% CI – 95% confidence interval; SBP – systolic blood pressure; DBP – diastolic blood pressure; MAP – mean arterial pressure; COPD – chronic obstructive pulmonary disease; AF – atrial fibrillation; FiO₂ – fraction of inspiration oxygen; GCS – Glasgow Coma Score; PaCO₂ – partial arterial pressure of CO₂; SOFA – the Sequential Organ Failure Assessment. Multivariate model adjusting for confounding factors including DBP, MAP, age, SBP, and FiO₂, COPD, lung cancer, liver cirrhosis, congestive heart failure, AF, myocardial infarction, hyperlipidemia, malignant cancer, and SOFA score.

Table 6. The association between different median SpO₂ groups and the mortality of ARF patients with different complications

Subgroup	Variables	Total	n (%)	HR (95%CI)	p-value
Diabetes mellitus	96% < median SpO ₂ ≤ 98%	298	174 (58.4)	Ref	–
	median SpO ₂ ≤ 96%	173	96 (55.5)	1.10 (0.85–1.42)	0.462
	median SpO ₂ > 98%	360	239 (66.4)	1.06 (0.87–1.30)	0.560
Malignant cancer	96% < median SpO ₂ ≤ 98%	250	188 (75.2)	Ref	–
	median SpO ₂ ≤ 96%	155	133 (85.8)	1.55 (1.24–1.94)	<0.001
	median SpO ₂ > 98%	276	206 (74.6)	1.15 (0.94–1.40)	0.183
Liver cirrhosis	96% < median SpO ₂ ≤ 98%	115	86 (74.8)	Ref	–
	median SpO ₂ ≤ 96%	98	80 (81.6)	1.35 (0.98–1.86)	0.067
	median SpO ₂ > 98%	114	81 (71.1)	1.06 (0.78–1.45)	0.692
Hyperlipidemia	96% < median SpO ₂ ≤ 98%	311	166 (53.4)	Ref	–
	median SpO ₂ ≤ 96%	174	92 (52.9)	1.05 (0.81–1.37)	0.691
	median SpO ₂ > 98%	371	215 (58.0)	1.16 (0.95–1.43)	0.155
Renal failure	96% < median SpO ₂ ≤ 98%	615	375 (61.0)	Ref	–
	median SpO ₂ ≤ 96%	369	268 (72.6)	1.45 (1.24–1.70)	<0.001
	median SpO ₂ > 98%	669	461 (68.9)	1.09 (0.95–1.25)	0.218
Lung cancer	96% < median SpO ₂ ≤ 98%	28	21 (75.0)	Ref	–
	median SpO ₂ ≤ 96%	25	24 (96.0)	1.86 (0.91–3.81)	0.088
	median SpO ₂ > 98%	26	22 (84.6)	0.95 (0.47–1.91)	0.887
COPD	96% < median SpO ₂ ≤ 98%	179	126 (70.4)	Ref	–
	median SpO ₂ ≤ 96%	120	87 (72.5)	1.70 (1.27–2.28)	<0.001
	median SpO ₂ > 98%	178	135 (75.8)	1.28 (1.00–1.64)	0.053
AF	96% < median SpO ₂ ≤ 98%	387	259 (66.9)	Ref	–
	median SpO ₂ ≤ 96%	196	144 (73.5)	1.25 (1.02–1.53)	0.035
	median SpO ₂ > 98%	485	369 (76.1)	1.22 (1.04–1.44)	0.015

HR – hazard ratio; 95% CI – 95% confidence interval; COPD – chronic obstructive pulmonary disease; AF – atrial fibrillation; SpO₂ – oxygen saturation; ARF – acute respiratory failure; HR – hazards ratio; SBP – systolic blood pressure; DBP – diastolic blood pressure; MAP – mean arterial pressure; COPD – chronic obstructive pulmonary disease; AF – atrial fibrillation; FiO₂ – fraction of inspiration oxygen; GCS – Glasgow Coma Score; PaCO₂ – partial arterial pressure of CO₂; SOFA – the Sequential Organ Failure Assessment. Multivariate model, if not stratified, adjusting for confounding factors including DBP, MAP, age, SBP, FiO₂, COPD, lung cancer, liver cirrhosis, congestive heart failure, AF, myocardial infarction, hyperlipidemia, malignant cancer, and SOFA score.

Discussion

In the current study, the relationship between SpO₂ and in-hospital mortality of ARF patients, as well as the optimum SpO₂ target for ARF patients, was explored. The results indicated that the median SpO₂ correlated with a decrease in the in-hospital mortality risk of ARF patients, and there was a nonlinear association between median SpO₂ and in-hospital mortality of ARF patients. The optimum SpO₂ range for ARF patients may be 96–98%. Subgroup analysis depicted that a median SpO₂ ≤ 96% was associated with an increased risk of in-hospital mortality among ARF patients with malignant cancer, renal failure or COPD. In ARF patients accompanied by AF, both a median SpO₂ ≤ 96% and a median SpO₂ > 98% were correlated with an elevated in-hospital mortality risk. These findings might offer insight for clinicians in choosing the optimum SpO₂ in ARF patients and help improve the prognosis in ARF patients.

In our study, we found that there was a nonlinear correlation between median SpO₂ and in-hospital mortality. A former study similarly demonstrated a U-shaped correlation between time-weighted partial pressure of arterial oxygen (PaO₂) values and death of mechanically ventilated intensive care unit (ICU) patients, with both lower and higher levels of PaO₂ being linked to an increased mortality risk.²³ In several previous studies, the SpO₂ target for improving outcomes of ICU patients was explored. Girardis et al. found that conservative oxygen therapy with a SpO₂ between 94% and 98% correlated with reduced ICU mortality compared to conventional oxygen therapy between 97% and 100% in critically ill patients admitted to the ICU for ≥72 h.²⁴ Another study revealed that the 28-day mortality in the conservative-oxygen group using a SpO₂ from 88% to 92% was 34.3%, and in the liberal-oxygen group with a SpO₂ ≥ 96% was 6.5% in ARDS patients.¹⁷ Asfar et al. delineated that hyperoxia was correlated to increased weakness, atelectasis and mortality in patients.²⁵ Another study based on the eICU Collaborative Research Database and the MIMIC Database indicated that the optimal range of SpO₂ in critically ill patients was 94–98%.^{26,27} The British Thoracic Society recommended a SpO₂ target of 94–98% for most acutely ill patients. These findings implied that the SpO₂ target should be <98%.

Herein, the optimal target of SpO₂ for ARF patients might be 96–98%. The in-hospital mortality risk of ARF patients was decreased in those with SpO₂ between the 96% and 98%. This was because a SpO₂ ≤ 96% might cause hypoxemia. Hypoxemia might lead to damage to multiple organs causing a lack of oxygen to the brain, which can cause drowsiness or coma or affect the blood supply to the myocardium, resulting in myocardial injury.²⁸ On the other hand, a SpO₂ > 98% might lead to hyperoxemia in ARF patients. Several studies uncovered that hyperoxemia may be associated with a variety of sequelae in patients receiving MV through lung tissue damage or reactive oxygen species (ROS) formation.²⁹ Hyperoxia

might also affect the innate immune system, such as attenuating cytokine production by human leukocytes, inducing structural changes within alveolar macrophages, and increasing in production of serum interleukin (IL)-10, IL-6 and ROS.³⁰ For patients with ARF, clinicians should be careful with the SpO₂ level, and the target SpO₂ should be controlled at 96–98%.

Herein, subgroup analysis found that for ARF patients with malignant cancer, renal failure, lung cancer, or COPD, the accepted lower limit of SpO₂ might be 96%. Some clinicians suggested adjusting the oxygenation target based on the severity of pulmonary disease.³¹ In ARF patients with lung cancer or COPD, ARF may be a result of the disease itself, complications in treatment or comorbidities.³² The co-occurrence of these diseases might increase mortality by 20% relative to those without comorbidities.³³ In ARF patients complicated with other diseases, lung diseases may be more serious, and a higher target for SpO₂ might be required. Previously, Adda et al. found that the PaO₂/FiO₂ ratio was lower (175 vs 248) in ARF patients with hematologic malignancies who failed noninvasive ventilation and required endotracheal intubation compared with those not requiring MV,³⁴ indicating that ARF patients with malignancies, a sufficient SpO₂ is needed.

This study identified a nonlinear association between SpO₂ and in-hospital mortality of ARF patients, indicating the importance of selecting an optimal SpO₂ target for ARF patients. Further, the optimum SpO₂ target for ARF patients was identified. The levels of SpO₂ were non-normally distributed, which could better reflect the status of patients at the beginning and end of treatments than the mean value. Some previous studies explored PaO₂ rather than SpO₂ to determine the status of oxygenation.^{10,35} Arterial blood oxygen pressure cannot be measured continuously, and frequently arterial blood draws for blood gas analysis are required for measuring it.³⁶ The acquisition of PaO₂ is invasive, requiring special equipment, which cannot be used for real-time monitoring. On the other hand, oxygen saturation, measured with pulse oximetry, is simple and noninvasive and can be used for the real-time monitoring of patients.¹⁷ Oxygen saturation can be continuously monitored, enabling earlier detection of potential ARDS patients, which is of great significance as early interventions can improve the outcomes of patients. We also analyzed the SpO₂ target in patients complicated with different diseases, which might provide specific suggestions to those with different underlying diseases. These findings might offer a guide for informing future trials of oxygen therapy to help clinicians in the management of MV in ARF patients. Future clinicians may also place a greater emphasis on the continuous monitoring of SpO₂ and titration of oxygen supplementation for ARF patients in the ICU, exercising caution when conducting detailed evaluations of adherence to oxygen targets, exposure to supplemental oxygen, and the incidence and duration of hypoxemia in patients with ARF.

Limitations

There were several limitations to this study. First, the detailed information on MV treatment was not analyzed. Second, the data of SpO₂ was measured once an hour, and the measurement of SpO₂ could be more frequent and flexible depending on the clinical practice. Third, all the data were identified in the MIMIC database, resulting in some recall bias. The findings in this study still require validation in future studies.

Conclusions

The relationship between SpO₂ and in-hospital mortality in ARF patients and the optimal SpO₂ range for ARF patients were investigated. The results identified that the median SpO₂ was linked to a decreased risk of in-hospital mortality of ARF patients, and there was a nonlinear correlation between median SpO₂ and in-hospital mortality of ARF patients. For ARF patients, continuous monitoring of SpO₂ is necessary, and the optimal SpO₂ range might be 96–98%.

Supplementary data

The Supplementary files are available at <https://doi.org/10.5281/zenodo.11463445>. The package includes the following files:

Supplementary Table 1 The results of the Levene's test of variables.

Supplementary Table 2 The information of Schoenfeld residues of variables.

Supplementary Fig. 1. The RSC shows a nonlinear relationship between covariates and logarithmic hazards.

Supplementary Fig. 2. A standardized Schoenfeld residual relative to the time correlation of each covariate.

Supplementary File 1. The function name and basic code of statistical analysis.

Data availability


The datasets generated and/or analyzed during the current study are available from the corresponding author on reasonable request.

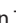
Consent for publication

Not applicable.


ORCID

Li Ai  <https://orcid.org/0000-0003-3545-0311>

Ran Li  <https://orcid.org/0009-0006-1306-091X>

Xixian Teng  <https://orcid.org/0009-0002-2089-0672>

Jing Li  <https://orcid.org/0009-0003-8746-3832>

Bing Hai  <https://orcid.org/0000-0003-2632-1075>

References

1. Abe T, Takagi T, Fujii T. Update on the management of acute respiratory failure using non-invasive ventilation and pulse oximetry. *Crit Care*. 2023;27(1):92. doi:10.1186/s13054-023-04370-4
2. Shi T, Feng L. Blood biomarkers associated with acute type II respiratory failure in COPD: A meta-analysis. *Clin Respir J*. 2022;16(2):75–83. doi:10.1111/crj.13464
3. Czerwińska-Jelonkiewicz K, Grand J, Tavazzi G, et al. Acute respiratory failure and inflammatory response after out-of-hospital cardiac arrest: Results of the Post-Cardiac Arrest Syndrome (PCAS) pilot study. *Eur Heart J Acute Cardiovasc Care*. 2020;9(4 Suppl):S110–S121. doi:10.1177/2048872619895126
4. Nadig NR, Sterba KR, Simpson AN, et al. Psychological outcomes in family members of patients with acute respiratory failure. *Chest*. 2021;160(3):890–898. doi:10.1016/j.chest.2021.03.025
5. Bellani G, Laffey JG, Pham T, et al. Epidemiology, patterns of care, and mortality for patients with acute respiratory distress syndrome in intensive care units in 50 countries. *JAMA*. 2016;315(8):788. doi:10.1001/jama.2016.0291
6. Kruser JM, Sharma K, Holl JL, Nohadani O. Identifying patterns of medical intervention in acute respiratory failure: A retrospective observational study. *Crit Care Explor*. 2023;5(10):e0984. doi:10.1097/CCE.0000000000000984
7. Scala R, Heunks L. Highlights in acute respiratory failure. *Eur Respir Rev*. 2018;27(147):180008. doi:10.1183/16000617.0008-2018
8. Chen C, Cheng A, Chou W, Selvam P, Cheng CM. Outcome of improved care bundle in acute respiratory failure patients. *Nurs Crit Care*. 2021;26(5):380–385. doi:10.1111/nicc.12530
9. Curtis BR, Rak KJ, Richardson A, Linstrum K, Kahn JM, Girard TD. Perceptions of hyperoxemia and conservative oxygen therapy in the management of acute respiratory failure. *Ann Am Thorac Soc*. 2021;18(8):1369–1379. doi:10.1513/AnnalsATS.202007-802OC
10. Yang W, Zhang L. Observation of the curative effect of conservative oxygen therapy in mechanical ventilation of patients with severe pneumonia [in Chinese]. *Zhonghua Wei Zhong Bing Ji Jiu Yi Xue*. 2021;33(9):1069–1073. doi:10.3760/cma.j.cn121430-20210617-00902
11. Fridovich I. Oxygen toxicity: A radical explanation. *J Exp Biol*. 1998;201(8):1203–1209. doi:10.1242/jeb.201.8.1203
12. Griffith DE, Garcia JGN, James HL, Callahan KS, Iriana S, Holiday D. Hyperoxic exposure in humans. *Chest*. 1992;101(2):392–397. doi:10.1378/chest.101.2.392
13. Palmer E, Post B, Klapaukh R, et al. The association between supra-physiologic arterial oxygen levels and mortality in critically ill patients: A multicenter observational cohort study. *Am J Respir Crit Care Med*. 2019;200(11):1373–1380. doi:10.1164/rccm.201904-0849OC
14. Chu DK, Kim LHY, Young PJ, et al. Mortality and morbidity in acutely ill adults treated with liberal versus conservative oxygen therapy (IOTA): A systematic review and meta-analysis. *Lancet*. 2018;391(10131):1693–1705. doi:10.1016/S0140-6736(18)30479-3
15. Louman S, Van Stralen KJ, Pijnenburg MWH, Koppelman GH, Boehmer ALM. Oxygen saturation targets for children with respiratory distress: A systematic review. *ERJ Open Res*. 2023;9(5):00256–02023. doi:10.1183/23120541.00256-2023
16. Siemieniuk RAC, Chu DK, Kim LHY, et al. Oxygen therapy for acutely ill medical patients: A clinical practice guideline. *BMJ*. October 2018; k4169. doi:10.1136/bmj.k4169
17. Barrot L, Asfar P, Mauny F, et al. Liberal or conservative oxygen therapy for acute respiratory distress syndrome. *N Engl J Med*. 2020;382(11):999–1008. doi:10.1056/NEJMoa1916431
18. O'Driscoll BR, Howard LS, Earis J, Mak V. BTS guideline for oxygen use in adults in healthcare and emergency settings. *Thorax*. 2017;72(Suppl 1):ii1–ii90. doi:10.1136/thoraxjnl-2016-209729
19. Helmerhorst HJ, Schultz MJ, Van Der Voort PH, et al. Self-reported attitudes versus actual practice of oxygen therapy by ICU physicians and nurses. *Ann Intensive Care*. 2014;4(1):23. doi:10.1186/s13613-014-0023-y
20. Li F, Xin H, Zhang J, Fu M, Zhou J, Lian Z. Prediction model of in-hospital mortality in intensive care unit patients with heart failure: Machine learning-based, retrospective analysis of the MIMIC-III database. *BMJ Open*. 2021;11(7):e044779. doi:10.1136/bmjopen-2020-044779
21. Johnson AEW, Pollard TJ, Shen L, et al. MIMIC-III, a freely accessible critical care database. *Sci Data*. 2016;3(1):160035. doi:10.1038/sdata.2016.35

22. Zhou S, Zeng Z, Wei H, Sha T, An S. Early combination of albumin with crystalloids administration might be beneficial for the survival of septic patients: A retrospective analysis from MIMIC-IV database. *Ann Intensive Care*. 2021;11(1):42. doi:10.1186/s13613-021-00830-8
23. De Jonge E, Peelen L, Keijzers PJ, et al. Association between administered oxygen, arterial partial oxygen pressure and mortality in mechanically ventilated intensive care unit patients. *Crit Care*. 2008; 12(6):R156. doi:10.1186/cc7150
24. Girardis M, Busani S, Damiani E, et al. Effect of conservative vs conventional oxygen therapy on mortality among patients in an intensive care unit: The Oxygen-ICU Randomized Clinical Trial. *JAMA*. 2016; 316(15):1583. doi:10.1001/jama.2016.11993
25. Asfar P, Schortgen F, Boissramé-Helms J, et al. Hyperoxia and hypertonic saline in patients with septic shock (HYPER52S): A two-by-two factorial, multicentre, randomised, clinical trial. *Lancet Respir Med*. 2017;5(3):180–190. doi:10.1016/S2213-2600(17)30046-2
26. Van Den Boom W, Hoy M, Sankaran J, et al. The search for optimal oxygen saturation targets in critically ill patients. *Chest*. 2020;157(3): 566–573. doi:10.1016/j.chest.2019.09.015
27. Choudhury A, Young G, Reyad B, Shah N, Rahman R. Can we improve the prescribing and delivery of oxygen on a respiratory ward in accordance with new British Thoracic Society oxygen guidelines? *BMJ Open Qual*. 2018;7(4):e000371. doi:10.1136/bmjoq-2018-000371
28. Breville G, Accorroni A, Allali G, Adler D. Pathophysiology of COVID-19 related happy hypoxemia [in French]. *Rev Med Suisse*. 2021;17(736): 831–834. PMID:33908720.
29. Helmerhorst HJF, Schultz MJ, Van Der Voort PHJ, De Jonge E, Van Westerloo DJ. Bench-to-bedside review: The effects of hyperoxia during critical illness. *Crit Care*. 2015;19(1):284. doi:10.1186/s13054-015-0996-4
30. Amarelle L, Quintela L, Hurtado J, Malacrida L. Hyperoxia and unlgS: What we have learned from animal models. *Front Med (Lausanne)*. 2021;8:606678. doi:10.3389/fmed.2021.606678
31. Bein T, Grasso S, Moerer O, et al. The standard of care of patients with ARDS: Ventilatory settings and rescue therapies for refractory hypoxemia. *Intensive Care Med*. 2016;42(5):699–711. doi:10.1007/s00134-016-4325-4
32. Kızılgöz D, Akin Kabalak P, Kavurgacı S, İnal Cengiz T, Yılmaz Ü. The success of non-invasive mechanical ventilation in lung cancer patients with respiratory failure. *Int J Clin Pract*. 2021;75(10):e14712. doi:10.1111/ijcp.14712
33. Chen WC, Su VYF, Yu WK, Chen YW, Yang KY. Prognostic factors of noninvasive mechanical ventilation in lung cancer patients with acute respiratory failure. *PLoS One*. 2018;13(1):e0191204. doi:10.1371/journal.pone.0191204
34. Adda M, Coquet I, Darmon M, Thiery G, Schlemmer B, Azoulay É. Predictors of noninvasive ventilation failure in patients with hematologic malignancy and acute respiratory failure. *Crit Care Med*. 2008;36(10):2766–2772. doi:10.1097/CCM.0b013e31818699f6
35. Schjørring OL, Klitgaard TL, Perner A, et al. Lower or higher oxygenation targets for acute hypoxemic respiratory failure. *N Engl J Med*. 2021;384(14):1301–1311. doi:10.1056/NEJMoa2032510
36. Xu W, Li C, Chen Y, et al. Comparison of pulse oxygen saturation/fraction of inhaled oxygen and arterial partial pressure of oxygen/fraction of inhaled oxygen in the assessment of oxygenation in acute respiratory distress syndrome patients at different high altitudes in Yunnan Province [in Chinese]. *Zhonghua Wei Zhong Bing Ji Jiu Yi Xue*. 2021;33(7):826–831. doi:10.3760/cma.j.cn121430-20210301-00303

Association between preoperative advanced lung cancer inflammation index and recurrence of hepatocellular carcinoma after curative resection

Weidong Yuan^{A,D–F}, Hewei Zhao^{B,C,F}, Shaochuang Wang^{B,C}

Department of Hepatobiliary Surgery, The Affiliated Huai'an No. 1 People's Hospital of Nanjing Medical University, China

A – research concept and design; B – collection and/or assembly of data; C – data analysis and interpretation;

D – writing the article; E – critical revision of the article; F – final approval of the article

Advances in Clinical and Experimental Medicine, ISSN 1899–5276 (print), ISSN 2451–2680 (online)

Adv Clin Exp Med. 2025;34(4):573–583

Address for correspondence

Weidong Yuan

E-mail: ywdhayy@outlook.com

Funding sources

None declared

Conflict of interest

None declared

Received on September 12, 2023

Reviewed on February 3, 2024

Accepted on May 8, 2024

Published online on October 16, 2024

Abstract

Background. The association between the advanced lung cancer inflammation index (ALI) and the recurrence of hepatocellular carcinoma (HCC) in patients treated with curative resection and its predictive value remains unclear.

Objectives. To assess the association between preoperative ALI and the recurrence of HCC in patients treated with surgical resection.

Materials and methods. This retrospective study analyzed patients with HCC treated with surgical resection at The Affiliated Huai'an No. 1 People's Hospital of Nanjing Medical University (Huai'an, China) from 2019 to 2021. The advanced lung cancer inflammation index was calculated as $(\text{BMI} \times \text{ALB}/\text{NLR})$, where BMI = body mass index, ALB = serum albumin and NLR = neutrophil-lymphocyte ratio. Univariate and multivariable Cox proportional risk models were performed to evaluate the association between the ALI and recurrence of HCC patients treated with surgical resection. Subgroup analyses were conducted based on age, sex, performance status (PS), cirrhosis, pathological staging, tumor grading, tumor size, and number of tumors.

Results. Among the 295 HCC patients treated with surgical resection, 180 patients (61.02%) had recurrences, with the mean follow-up being 462 (187, 730) days. Patients with higher ALI scores were significantly less likely to have a recurrence of HCC after surgical resection (hazard ratio (HR): 0.59, 95% confidence interval (95% CI): 0.42–0.83, $p = 0.003$). Based on subgroup analyses, HCC patients undergoing surgical resection with higher ALI scores were associated with recurrence in those ≥ 60 years of age, with tumors ≥ 5 cm, and in patients with single tumors and ≥ 2 tumors.

Conclusions. This study confirms the association between ALI and the reduced risk of recurrence in HCC patients treated with surgical resection.

Key words: recurrence, hepatocellular carcinoma, surgical resection, advanced lung cancer inflammation index

Cite as

Yuan W, Zhao H, Shaochuang W. Association between preoperative advanced lung cancer inflammation index and recurrence of hepatocellular carcinoma after curative resection. *Adv Clin Exp Med.* 2025;34(4):573–583. doi:10.17219/acem/188424

DOI

10.17219/acem/188424

Copyright

Copyright by Author(s)

This is an article distributed under the terms of the Creative Commons Attribution 3.0 Unported (CC BY 3.0) (<https://creativecommons.org/licenses/by/3.0/>)

Background

Primary liver cancer is the 6th most common malignant tumor worldwide and the 3rd leading cause of cancer-related deaths.¹ Hepatocellular carcinoma (HCC) is the most common type of primary liver cancer and accounts for approx. 80–90% of all cases of primary liver cancer.^{2,3} The incidence of HCC has been increasing over the past decades, and by 2025, more than 1 million people will be affected each year.⁴ Hepatocellular carcinoma is an aggressive disease with a poor clinical outcome.⁵ Currently, surgery is still the main treatment for patients with early-stage HCC.⁶ According to statistics, the 5-year survival rates for patients in the early stages of HCC reached 40–70% following radical surgery.^{7,8} Unfortunately, even with radical surgical resection, the 5-year recurrence rate after surgery is as high as 70–80%, severely limiting the long-term survival of HCC patients.^{9–11} Therefore, it is crucial to identify the factors associated with recurrence after surgery for HCC and patients with a high risk of recurrence after surgery to implement reasonable risk stratification management options and improve the patient's prognosis.

Inflammation is closely associated with tumor development and progress.¹² A prolonged state of inflammation may lead to dysfunction of the immune system, undermining its ability to recognize and clear tumor cells, and may also provide a microenvironment for further tumor cell growth.¹³ Nutritional indicators are also associated with the prognosis of various malignancies.^{14,15} Inflammatory and nutritional markers have been shown to be independent predictors of recurrence after HCC surgery, including the neutrophil-to-lymphocyte ratio (NLR), monocyte-to-lymphocyte ratio (MLR) and prognostic nutritional index (PNI).^{16–18} Body mass index (BMI) is an anthropometric indicator that can reflect the nutritional status of patients with cancer and is independently associated with patient prognosis.¹⁹ A recent study showed that the combination of PNI and BMI had a higher predictive value for postoperative survival in HCC patients undergoing hepatectomy.²⁰ The advanced lung cancer inflammation index (ALI), a novel inflammation and nutrition-based index defined by combining BMI, preoperative serum albumin (ALB) levels and the NLR, has been proposed as a prognostic biomarker for various malignant tumors, including lung, oral, colon, and gastrointestinal cancers.^{21–24} A recent study found that ALI was independently associated with overall survival (OS) in advanced HCC patients receiving immunotherapy.²⁵ However, the association between ALI and the recurrence of HCC patients treated with curative resection and its predictive value remains unclear.

Objectives

The present study aimed to assess the association between ALI and the recurrence of HCC in patients treated with surgical resection and to determine

the prognostic potential of ALI in HCC patients after surgical resection.

Materials and methods

Study design and patients

In this retrospective cohort study, patients with HCC who underwent surgical resection at The Affiliated Huai'an No. 1 People's Hospital of Nanjing Medical University (China) between August 9, 2019, and August 9, 2021, were identified and retrospectively analyzed. The inclusion criteria were as follows: 1) age ≥ 30 years; 2) patients with pathologically confirmed primary HCC; 3) patients who underwent initial surgical resection for radical treatment and had negative margins; and 4) those with complete preservation of clinical, pathological and follow-up data. The exclusion criteria included: 1) patients undergoing surgery for ruptured tumors; 2) those undergoing palliative tumor resection; 3) those suffering from autoimmune diseases, bone marrow or hematological disorders and coagulation disorders; 4) pregnant or lactating women; 5) those who have received preoperative anti-cancer treatments such as portal vein cannulation chemotherapy, hepatic artery chemoembolization or radiotherapy; 6) those with other malignant tumors; and 7) those with extrahepatic metastasis or invasion of the hepatic vein, inferior vena cava, portal vein, artery, or biliary system. A total of 295 patients were included in this study. The flow diagram of patient selection is shown in Fig. 1. The study was approved by the Ethics Committee of Huai'an's First People's Hospital (approval No. KY-2022-013-01). Because of the retrospective nature of the article, informed patient consent was not required.

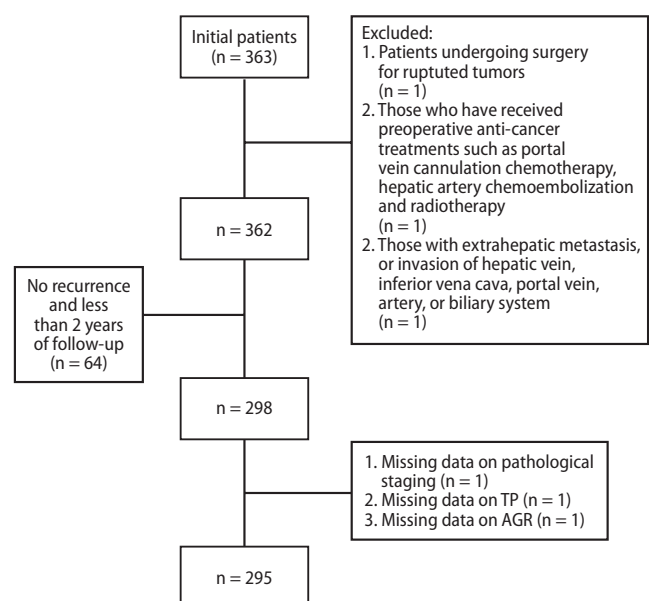


Fig. 1. The flow diagram of patient selection

TP – total protein; AGR – albumin/globulin ratio.

Data collection and measurement

Data were collected using a case report form and included: 1) demographic data: age (years), sex (male/female) and BMI (kg/m^2); 2) family medical history: family history of liver cancer (yes or no) and family history of hepatitis B (yes or no); 3) past medical history and history of present illness such as smoking (yes or no), chronic hepatitis B (yes or no), hepatitis C (yes or no), hypertension (yes or no), diabetes mellitus (yes or no), and comorbidities (yes or no); 4) blood routine examination of hemoglobin (g/L), erythrocytes ($\times 10^{12}/\text{L}$), leukocytes ($\times 10^9/\text{L}$), platelets ($\times 10^9/\text{L}$), neutrophils (%), lymphocytes (%), monocytes (%), eosinophils (%), and basophils (%); 5) liver function tests including alanine aminotransferase (ALT, U/L), aspartate aminotransferase (AST, U/L), gamma-glutamyl transferase (GGT, U/L), alkaline phosphatase (ALP, U/L), total bilirubin (TBIL, $\mu\text{mol}/\text{L}$), direct bilirubin (DBIL, $\mu\text{mol}/\text{L}$), indirect bilirubin (IBIL, $\mu\text{mol}/\text{L}$), total protein (TP, g/L), ALB (g/L), globulin (GLB, g/L), and albumin/globulin ratio (AGR, ratio); 6) coagulation function assessed with prothrombin time (PT, s), activated partial thromboplastin time (APTT, s), thrombin time (TT, s), and fibrinogen (FIB, g/kg); 7) tumor markers such as alpha-fetoprotein (AFP, $\mu\text{g}/\text{L}$) and carcinoembryonic antigen (CAE, $\mu\text{g}/\text{L}$); 8) infectious disease screening for human immunodeficiency virus antibody (HIV-Ab, yes or no); 9) tumor features including comorbidity with cirrhosis (yes or no), Child–Pugh classification (class A and class B), Eastern Cooperative Oncology Group Performance Status (ECOG PS) score (0 or 1), pathological staging (IB, IA and II), tumor grading (poorly differentiated, moderately differentiated and well-differentiated), maximum diameter of the tumor (cm), number of tumors, vascular invasion (microvascular invasion or no vascular invasion), satellite nodules (yes or no), envelope status (yes or no), other adjuvant therapy (none, transcatheter arterial chemoembolization (TACE) and radiotherapy); and 10) inflammation indices including the NLR, MLR, PNI, systemic immune-inflammation index (SII), and ALI. All data were measured prior to surgery.

The ALI score was calculated using the following formula: $\text{ALI score} = \text{BMI} \times \text{ALB}/\text{NLR}$, where $\text{BMI} = \text{body weight (kg)}/[\text{height squared (m}^2\text{)}]$, $\text{NLR} = \text{neutrophil count}/\text{absolute lymphocyte count}$, $\text{SII} = \text{absolute neutrophil counts} \times \text{absolute platelet counts}/\text{absolute lymphocyte counts}$, $\text{MLR} = \text{absolute monocyte count}/\text{absolute lymphocyte count}$, and $\text{PNI} = \text{serum ALB level (g/L)} + 5 \times \text{absolute lymphocyte count}$. Child–Pugh scores were calculated and defined as follows: grade A – 5–6 points (mild); grade B – 7–9 points (moderate); and grade C – ≥ 10 points (severe impairment). Eastern Cooperative Oncology Group Performance Status scores assessed the level of functioning based on activity, ambulatory status and need for care ranging from grade 0 (normal activity) to grade 4 (completely bedridden).

Outcome and follow-up

The outcome of the study was recurrence. Recurrence was defined as recurrent lesions detected with imaging, such as ultrasound, computed tomography (CT), magnetic resonance imaging (MRI), etc., after surgical resection in patients with HCC, and if there was insufficient imaging evidence, further puncture or surgery for pathological examinations were performed. Follow-up methods included face-to-face visits with the study population, telephone callbacks, home visits, self-administered questionnaires, regular medical check-ups, and outpatient reviews. Information regarding death was obtained from hospital records, death certificates or telephone contact with the patient's relatives or physicians. All patients were regularly followed up after discharge from the hospital. Patients were reviewed once a month during the first 6 months after surgery and once every 3–6 months thereafter. Routine blood tests, tumor markers and abdominal ultrasounds were performed in outpatient clinics, and CT or MRI examinations were performed every 3–6 months to observe and record the prognosis of patients, such as recurrence and mortality. Patients were followed for 2 years. The median follow-up time with interquartile range (IQR) was 462 (187, 730) days.

Statistical analyses

The Shapiro–Wilk test was used for testing the normality of the dataset, and the Levene's test was employed to assess the homogeneity of variances across 2 or more groups (Supplementary Table 1). The measurement data conforming to a normal distribution were described as means \pm standard deviations ($\pm\text{SD}$), and t-tests were used for comparisons between the 2 groups. Medians and quartiles (Me (Q_1 , Q_3)) were used to describe the distribution of measurement data that did not follow normal distribution, and the Wilcoxon rank sum test was used to compare the differences between the 2 groups. The categorical data were described by the number of cases and the constituent ratio (n (%)), and a χ^2 test was used for comparison between groups. Data were preliminarily examined for missing values, and cases with missing data were excluded.

Advanced lung cancer inflammation index, NLR, MLR, PNI, and SII were categorized according to their respective medians. Advanced lung cancer inflammation index was grouped as $\leq 4,436.12$ and $> 4,436.12$. The survival analysis was performed according to the Kaplan–Meier (KM) method. The log-rank test was used to compare differences in KM curves. The proportional hazards assumption for all models was tested using the residual method. The common residuals for the Cox model included: 1) Schoenfeld residuals to test the proportional hazards assumption (Supplementary Fig. 1–5 and Supplementary Table 2); 2) Martingale residuals to assess nonlinearity (Supplementary Table 3); and 3) deviance

residuals to examine influential observations (Supplementary Fig. 6–10). To check the linearity between the log-hazard function and the predictive variables, Martingale residuals were plotted (Supplementary Fig. 11–15). A Cox proportional hazards model was used to calculate hazard ratios (HRs) and 95% confidence intervals (95% CIs). The univariate Cox proportional risk model was applied to screen potential covariates. Covariates included ALB, lymphocytes, neutrophils, ALT, AST, GGT, IBIL, AGR, PT, TT, AFP, CAE, the presence or absence of comorbidity with cirrhosis, PS scores, pathological staging, maximum diameter of the tumor, number of tumors, vascular invasion, satellite nodules, and other adjuvant therapy. Statistical significance ($p < 0.05$) was reached for inclusion in the Cox proportional risk regression multivariable analyses. The multivariable Cox proportional risk models were performed to evaluate the association between ALI, NLR, PNI, MLR, and SII and the recurrence of HCC in patients treated with surgical resection. We conducted Kolmogorov–Smirnov (KS) goodness-of-fit (GOF) tests for each of the 5 models in our study. The consistency across all models was notable, with the KS GOF tests yielding a p -value of less than 0.001 for each. Subgroup analyses were conducted on age (<60 years and ≥ 60 years), sex (male and female), PS (0 and 1), cirrhosis (yes or no), pathological staging (I and II), tumor grading (poorly–moderately differentiated and well-differentiated), tumor size, and the number of tumors. The concordance index (C-index) was calculated to assess the predictive ability of inflammation indices, which estimates the probability of agreement between predicted and observed responses. Results were considered significant at an $\alpha = 0.05$. Data were cleaned using SAS v. 9.4 (SAS Institute, Cary, USA) and analyzed using R v. 4.2.1 (2022-06-23 ucrt) (R Foundation for Statistical Computing, Vienna, Austria).

Results

Baseline characteristics of patients

Among the 295 HCC patients treated with surgical resection, 180 patients (61.02%) had recurrences during follow-up. The mean follow-up was 462 (187, 730) days. The mean age of the included patients was 57.63 ± 9.92 years, and the mean BMI of the patients was 23.39 ± 3.90 kg/m². The majority of patients included (79.32%) were men. Among 295 HCC patients treated with surgical resection, 292 patients (98.98%) were without a family history of liver cancer; however, 177 patients (60%) had chronic hepatitis B. There were significant differences between sex ($p = 0.015$; $\chi^2 = 5.871$), neutrophils ($p = 0.017$; $t = -2.40$), lymphocytes ($p = 0.009$; $Z = 2.631$), ALT ($p = 0.007$; $Z = -2.688$), AST ($p < 0.001$; $Z = -3.681$), GGT ($p < 0.001$; $Z = -3.756$), ALP ($p = 0.043$; $Z = -2.028$), TBIL ($p = 0.028$; $Z = 2.197$), TP ($p = 0.004$; $Z = 2.877$),

GLB ($p = 0.047$; $t = 1.99$), PT ($p = 0.011$; $t = 2.56$), TT ($p = 0.039$; $t = -2.07$), AFP ($p = 0.007$; $Z = -2.688$), CAE ($p < 0.001$; $Z = -3.756$), presence or absence of cirrhosis ($p = 0.007$; $\chi^2 = 7.172$), PS score ($\chi^2 = 5.790$; $p = 0.016$), pathological staging ($\chi^2 = 34.654$; $p < 0.001$), tumor grading ($\chi^2 = 6.707$; $p = 0.035$), maximum diameter of the tumor ($Z = -5.844$; $p < 0.001$), number of tumors ($Z = -2.358$; $p = 0.018$), vascular invasion ($\chi^2 = 7.754$; $p = 0.005$), satellite nodules ($\chi^2 = 5.896$; $p = 0.015$), other adjuvant therapies ($\chi^2 = 36.060$; $p < 0.001$), NLR ($Z = -2.476$; $p = 0.013$), MLR ($Z = -2.699$; $p = 0.007$), PNI ($Z = 2.223$; $p = 0.026$), ALI ($Z = 3.152$; $p = 0.002$), and follow-up time ($Z = 14.862$; $p < 0.001$) between patients with and without recurrences. The baseline demographic and clinicopathological characteristics of the study cohort are presented in Table 1.

Associations of ALI, NLR, MLR, PNI, and SII with recurrence in HCC patients treated with surgical resection

The result demonstrated that a higher ALI was associated with a decreased risk of recurrence in HCC patients treated with surgical resection (HR: 0.59, 95% CI: 0.42–0.83, $p = 0.003$). A lower risk of recurrence in HCC patients treated with surgical resection was also observed in patients with a higher PNI (HR: 0.62, 95% CI: 0.45–0.87, $p = 0.006$). However, there were no statistical associations between NLR, MLR and SII and the recurrence of HCC in patients treated with surgical resection. Associations of ALI, NLR, MLR, PNI, and SII with recurrence in HCC patients treated with surgical resection are presented in Table 2. The C-index value of ALI (C-index: 0.579, 95% CI: 0.543–0.616) was higher than the C-index value of PNI (C-index: 0.551, 95% CI: 0.514–0.588, Table 3). The KM curve showed that patients with a lower ALI had a bad survival probability (Fig. 2).

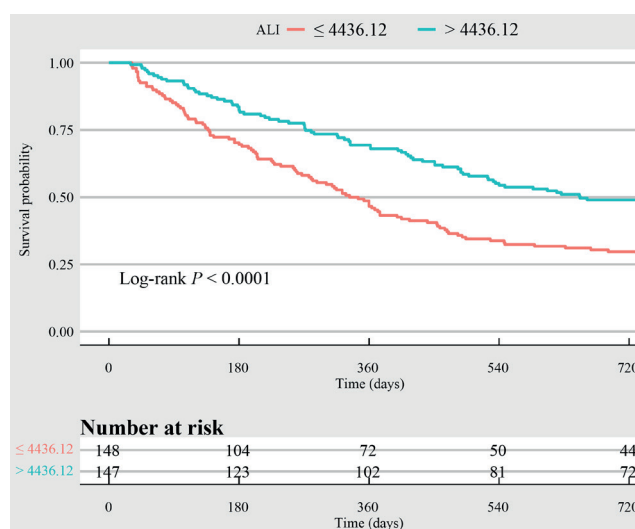


Fig. 2. The survival probability of hepatocellular carcinoma (HCC) patients with a low and a high advanced lung cancer inflammation index (ALI) score

Table 1. Baseline characteristics of included patients

Variables		Total (n = 295)	Recurrences		Statistics	p-value
			no (n = 115)	yes (n = 180)		
Age [years], Me (Q ₁ , Q ₃)		57 (50.00, 65.00)	57 (50.50, 64.00)	56 (50.00, 66.00)	Z = -0.223	0.823
Sex, n (%)	male	234 (79.32)	83 (72.17)	151 (83.89)	$\chi^2 = 5.871$	0.015
	female	61 (20.68)	32 (27.83)	29 (16.11)		
BMI [kg/m ²], Me (Q ₁ , Q ₃)		23.88 (22.05, 24.77)	23.88 (22.15, 24.77)	23.77 (22.03, 24.66)	Z = 0.294	0.769
Family history of liver cancer, n (%)	no	292 (98.98)	113 (98.26)	179 (99.44)	–	0.563
	yes	3 (1.02)	2 (1.74)	1 (0.56)		
Family history of hepatitis B, n (%)	no	288 (97.63)	112 (97.39)	176 (97.78)	–	1.000
	yes	7 (2.37)	3 (2.61)	4 (2.22)		
Smoking, n (%)	no	288 (97.63)	114 (99.13)	174 (96.67)	–	0.253
	yes	7 (2.37)	1 (0.87)	6 (3.33)		
Chronic hepatitis B, n (%)	no	118 (40.00)	45 (39.13)	73 (40.56)	$\chi^2 = 0.059$	0.807
	yes	177 (60.00)	70 (60.87)	107 (59.44)		
Hepatitis C, n (%)	no	292 (98.98)	115 (100.00)	177 (98.33)	–	0.284
	yes	3 (1.02)	0 (0.00)	3 (1.67)		
Hypertension, n (%)	no	231 (78.31)	85 (73.91)	146 (81.11)	$\chi^2 = 2.140$	0.143
	yes	64 (21.69)	30 (26.09)	34 (18.89)		
Diabetes mellitus, n (%)	no	252 (85.42)	99 (86.09)	153 (85.00)	$\chi^2 = 0.067$	0.796
	yes	43 (14.58)	16 (13.91)	27 (15.00)		
Comorbidities, n (%)	no	292 (98.98)	113 (98.26)	179 (99.44)	–	0.563
	yes	3 (1.02)	2 (1.74)	1 (0.56)		
Hemoglobin [g/L], Me (Q ₁ , Q ₃)		141 (128.50, 152.00)	141 (126.00, 152.50)	140.50 (130.00, 152.00)	Z = -0.281	0.778
Erythrocytes [$\times 10^{12}$ /L], mean \pm SD		4.57 \pm 0.55	4.55 \pm 0.58	4.59 \pm 0.53	t = -0.510	0.607
Leukocytes [$\times 10^9$ /L], Me (Q ₁ , Q ₃)		4.86 (3.85, 5.98)	4.60 (3.49, 5.97)	4.92 (4.04, 6.00)	Z = -1.520	0.129
Platelets [$\times 10^9$ /L], Me (Q ₁ , Q ₃)		146.00 (104.00, 188.00)	149.00 (102.00, 185.00)	142.00 (107.50, 190.00)	Z = -0.090	0.928
Neutrophils [%], mean \pm SD		60.89 \pm 10.87	59.00 \pm 10.58	62.09 \pm 10.92	t = -2.400	0.017
Lymphocytes [%], mean \pm SD		29.03 \pm 9.7	30.82 \pm 9.29	27.89 \pm 9.81	t = 2.55	0.011
Monocytes [%], Me (Q ₁ , Q ₃)		7 (5.90, 8.40)	7 (5.95, 8.50)	6.95 (5.88, 8.33)	Z = 0.067	0.946
Eosinophils [%], Me (Q ₁ , Q ₃)		1.80 (1.10, 2.90)	2.00 (1.20, 3.00)	1.80 (0.90, 2.90)	Z = 0.808	0.419
Basophils [%], Me (Q ₁ , Q ₃)		0.40 (0.20, 0.60)	0.40 (0.30, 0.60)	0.40 (0.20, 0.60)	Z = 0.298	0.765
ALT [U/L], Me (Q ₁ , Q ₃)		26.00 (18.00, 42.00)	23.00 (16.00, 39.90)	28.80 (19.00, 44.70)	Z = -2.688	0.007
AST [U/L], Me (Q ₁ , Q ₃)		30.00 (22.00, 45.00)	27.00 (20.00, 36.00)	32.00 (23.30, 48.85)	Z = -3.681	<0.001
GGT [U/L], Me (Q ₁ , Q ₃)		49.00 (29.00, 92.00)	40.00 (21.00, 73.00)	57.50 (32.50, 116.00)	Z = -3.756	<0.001
ALP [U/L], Me (Q ₁ , Q ₃)		92.00 (73.00, 115.00)	86.00 (71.00, 109.00)	96.50 (74.00, 123.50)	Z = -2.028	0.042
TBIL [μ mol/L], Me (Q ₁ , Q ₃)		15.50 (11.60, 21.70)	16.30 (12.70, 22.80)	14.85 (10.85, 21.55)	Z = 2.197	0.028
DBIL [μ mol/L], Me (Q ₁ , Q ₃)		5.80 (4.50, 8.20)	5.60 (4.70, 8.00)	5.85 (4.35, 8.20)	Z = 0.273	0.785
IBIL [μ mol/L], Me (Q ₁ , Q ₃)		9.60 (6.70, 14.00)	10.60 (7.60, 15.20)	9.15 (6.50, 13.20)	Z = 2.877	0.004
TP [g/L], Me (Q ₁ , Q ₃)		68.20 (64.10, 72.10)	68.20 (64.70, 71.60)	68.20 (63.40, 72.20)	Z = -0.108	0.914
ALB [g/L], mean \pm SD		42.06 \pm 4.25	42.68 \pm 4.12	41.67 \pm 4.30	t = 1.99	0.047
GLB [g/L], Me (Q ₁ , Q ₃)		25.70 (22.90, 28.75)	25.50 (22.55, 28.10)	26.30 (23.17, 29.20)	Z = -1.68	0.093
AGR ratio, mean \pm SD		1.66 \pm 0.34	1.73 \pm 0.35	1.62 \pm 0.32	t = 2.74	0.007
PT [s], Me (Q ₁ , Q ₃)		13.20 (12.60, 13.80)	13.30 (12.80, 14.00)	13.10 (12.30, 13.70)	Z = 2.49	0.013
APTT [s], Me (Q ₁ , Q ₃)		35.60 (31.70, 38.65)	35.90 (32.55, 39.15)	35.30 (30.58, 38.32)	Z = 1.54	0.124
TT [s], Me (Q ₁ , Q ₃)		17.50 (16.70, 18.50)	17.40 (16.50, 18.25)	17.50 (16.78, 18.70)	Z = -1.59	0.113
FIB [g/L], Me (Q ₁ , Q ₃)		2.84 (2.33, 3.44)	2.79 (2.3, 3.36)	2.86 (2.37, 3.6)	Z = -1.00	0.317
AFP [μ g/L], Me (Q ₁ , Q ₃)		26.00 (18.00, 42.00)	23.00 (16.00, 39.90)	28.80 (19.00, 44.70)	Z = -2.688	0.007
CAE [μ g/L], Me (Q ₁ , Q ₃)		49.00 (29.00, 92.00)	40.00 (21.00, 73.00)	57.50 (32.50, 116.00)	Z = -3.756	<0.001

Table 1. Baseline characteristics of included patients – cont.

Variables		Total (n = 295)	Recurrences		Statistics	p-value
			no (n = 115)	yes (n = 180)		
HIV-Ab, n (%)	no	1 (0.34)	1 (0.88)	0 (0.00)	–	0.389
	yes	292 (99.66)	113 (99.12)	179 (100.00)		
Comorbidity with cirrhosis, n (%)	no	99 (33.56)	28 (24.35)	71 (39.44)	$\chi^2 = 7.172$	0.007
	yes	196 (66.44)	87 (75.65)	109 (60.56)		
Child–Pugh score, n (%)	A	288 (97.63)	113 (98.26)	175 (97.22)	–	0.709
	B	7 (2.37)	2 (1.74)	5 (2.78)		
ECOG PS, n (%)	0	180 (61.02)	80 (69.57)	100 (55.56)	$\chi^2 = 5.790$	0.016
	1	115 (38.98)	35 (30.43)	80 (44.44)		
Pathological staging, n (%)	IB	124 (42.03)	29 (25.22)	95 (52.78)	$\chi^2 = 34.654$	<0.001
	IA	137 (46.44)	78 (67.83)	59 (32.78)		
	II	34 (11.53)	8 (6.96)	26 (14.44)		
Tumor grading, n (%)	poorly differentiated	13 (4.41)	4 (3.48)	9 (5.00)	$\chi^2 = 6.707$	0.035
	well-differentiated	51 (17.29)	28 (24.35)	23 (12.78)		
	moderately differentiated	231 (78.31)	83 (72.17)	148 (82.22)		
Maximum diameter of the tumor [cm], Me (Q ₁ , Q ₃)		5.00 (3.00, 7.50)	4.00 (2.50, 5.50)	6.00 (3.50, 9.00)	Z = –5.844	<0.001
Number of tumors, Me (Q ₁ , Q ₃)		1.00 (1.00, 1.00)	1.00 (1.00, 1.00)	1.00 (1.00, 1.00)	Z = –2.358	0.018
Vascular invasion, n (%)	microvascular invasion	63 (21.36)	15 (13.04)	48 (26.67)	$\chi^2 = 7.754$	0.005
	no	232 (78.64)	100 (86.96)	132 (73.33)		
Satellite nodules, n (%)	no	257 (87.12)	107 (93.04)	150 (83.33)	$\chi^2 = 5.896$	0.015
	yes	38 (12.88)	8 (6.96)	30 (16.67)		
Envelope status, n (%)	no	2 (0.68)	0 (0.00)	2 (1.11)	–	0.523
	yes	293 (99.32)	115 (100.00)	178 (98.89)		
Other adjuvant therapy, n (%)	no	63 (21.36)	44 (38.26)	19 (10.56)	$\chi^2 = 36.060$	<0.001
	TACE	226 (76.61)	71 (61.74)	155 (86.11)		
	radiotherapy	6 (2.03)	0 (0.00)	6 (3.33)		
NLR, Me (Q ₁ , Q ₃)		2.17 (1.57, 3.12)	1.94 (1.35, 2.74)	2.33 (1.61, 3.37)	Z = –2.476	0.013
MLR, Me (Q ₁ , Q ₃)		0.25 (0.19, 0.33)	0.22 (0.19, 0.29)	0.26 (0.20, 0.35)	Z = –2.699	0.007
PNI, mean \pm SD		49.20 \pm 5.33	50.02 \pm 5.01	48.67 \pm 5.47	t = 2.12	0.035
SII, Me (Q ₁ , Q ₃)		314.34 (170.15, 487.00)	280.07 (163.84, 449.29)	324.16 (178.22, 567.60)	Z = –1.725	0.085
ALI, Me (Q ₁ , Q ₃)		4,462.74 (3100.91, 6,601.70)	5237.89 (3,732.88, 74,11.59)	40,56.92 (2881.25, 5942.01)	Z = 3.152	0.002
Follow-up time [days], Me (Q ₁ , Q ₃)		462.00 (187.00, 730.00)	730.00 (730.00, 730.00)	252.00 (114.00, 408.00)	Z = 14.862	<0.001

BMI – body mass index; ALT – alanine aminotransferase; AST – aspartate aminotransferase; GGT – gamma glutamyltransferase; ALP – alkaline phosphatase; TBIL – total bilirubin; DBIL – direct bilirubin; IBIL – indirect bilirubin; TP – total protein; ALB – albumin; GLB – globulin; AGR – albumin/globulin ratio; PT – prothrombin time; APTT – activated partial thromboplastin time; TT – thrombin time; FIB – fibrinogen; AFP – alpha-fetoprotein; CAE – carcinoembryonic antigen; HIV-Ab – human immunodeficiency virus antibody; ECOG PS – Eastern Cooperative Oncology Group Performance Status; NLR – neutrophil-to-lymphocyte ratio; MLR – monocyte-to-lymphocyte ratio; PNI – prognostic nutritional index; ALI – advanced lung cancer inflammation index; SII – systemic immune-inflammation index; t – t-test; Z – Wilcoxon rank sum test; SD – standard deviation; Me (Q₁, Q₃) – median and 1st and 3rd quartile.

Subgroup analyses of the associations of ALI and PNI with recurrence of HCC in patients treated with surgical resection

In patients younger than 60 years, a higher ALI was associated with a lower risk of recurrence in patients with surgically resected HCC (HR: 0.45, 95% CI: 0.28–0.73, $p = 0.001$). However, in patients aged ≥ 60 years, no association between ALI and recurrence of HCC in patients

treated with surgical resection was observed (HR: 0.73, 95% CI: 0.41–1.27, $p = 0.265$). Among male HCC patients treated with surgical resection, a higher ALI (HR: 0.57, 95% CI: 0.39–0.84, $p = 0.005$) and PNI (HR: 0.60, 95% CI: 0.41–0.87, $p = 0.007$) were correlated with a decreased risk of recurrence. In HCC patients undergoing surgical resection, a higher ALI correlated with a lower risk of recurrence in those with (HR: 0.61, 95% CI: 0.40–0.94, $p = 0.026$) or without cirrhosis (HR: 0.52, 95% CI: 0.29–0.93,

Table 2. Associations of ALI, NLR, MLR, PNI, and SII with recurrence in HCC patients treated with surgical resection

Variables	Model 1		Model 2	
	HR (95% CI)	p-value	HR (95% CI)	p-value
ALI				
≤4,436.12	Ref.		Ref.	
>4,436.12	0.55 (0.41–0.74)	<0.001	0.59 (0.42–0.83)	0.003
NLR				
≤2.17	Ref.		Ref.	
>2.17	1.45 (1.08–1.94)	0.013	1.38 (0.98–1.95)	0.064
MLR				
≤0.25	Ref.		Ref.	
>0.25	1.65 (1.23–2.21)	<0.001	1.19 (0.85–1.68)	0.309
PNI				
≤49.3	Ref.		Ref.	
>49.3	0.70 (0.52–0.93)	0.016	0.62 (0.45–0.87)	0.006
SII				
≤314.58	Ref.		Ref.	
>314.58	1.18 (0.88–1.58)	0.275	0.93 (0.66–1.32)	0.683

Model 1 was an unadjusted model. Model 2 was adjusted for ALB, lymphocytes, neutrophils, ALT, AST, GGT, IBIL, AGR, PT, TT, AFP, CAE, presence or absence of comorbidity with cirrhosis, PS score, pathological staging, maximum diameter of tumor, number of tumors, vascular invasion, satellite nodules, and other adjuvant therapy, of which Model 2 of ALI was not adjusted for ALB, lymphocytes and neutrophils. Model 2 of NLR was not adjusted for lymphocytes and neutrophils. Model 2 of MLR was not adjusted for lymphocytes. Model 2 of PNI was not adjusted for ALB and lymphocytes. Model 2 of SII was not adjusted for lymphocytes and neutrophils.

ALT – alanine aminotransferase; AST – aspartate aminotransferase; GGT – gamma glutamyltransferase; ALP – alkaline phosphatase; IBIL – indirect bilirubin; AGR – albumin globulin ratio; PT – prothrombin time; APTT – activated partial thromboplastin time; TT – thrombin time; AFP – alpha-fetoprotein; CAE – carcinoembryonic antigen; NLR – neutrophil-to-lymphocyte ratio; MLR – monocyte-to-lymphocyte ratio; PNI – prognostic nutritional index; ALI – advanced lung cancer inflammation index; SII – systemic immune-inflammation index; HCC – hepatocellular carcinoma; HR – hazard ratio; 95% CI – 95% confidence interval; Ref. – reference.

Table 3. The predictive performances of ALI, NLR, MLR, PNI, and SII in predicting recurrence in HCC patients treated with surgical resection

Variables	C-index (95% CI)
ALI	0.579 (0.543–0.616)
NLR	0.550 (0.512–0.587)
MLR	0.570 (0.534–0.607)
PNI	0.551 (0.514–0.588)
SII	0.526 (0.488–0.563)

NLR – neutrophil-to-lymphocyte ratio; MLR – monocyte-to-lymphocyte ratio; PNI – prognostic nutritional index; ALI – advanced lung cancer inflammation index; SII – systemic immune-inflammation index; HCC – hepatocellular carcinoma; C-index – concordance index; 95% CI – 95% confidence interval.

$p = 0.028$). Nevertheless, in HCC patients undergoing surgical resection, a higher PNI was only associated with a lower risk of recurrence in those without cirrhosis (HR: 0.47, 95% CI: 0.26–0.85, $p = 0.012$). In HCC patients treated with surgical resection, a higher ALI (HR: 0.48, 95% CI: 0.30–0.76, $p = 0.002$) and PNI (HR: 0.57, 95% CI: 0.35–0.93, $p = 0.023$) were correlated with a lower risk of recurrence in those with a PS = 0. In HCC patients undergoing surgical resection, a higher ALI was linked to a decreased risk of recurrence in those with stage I (HR: 0.61, 95% CI:

0.42–0.89, $p = 0.009$); however, a higher PNI was linked to a decreased risk of recurrence in those with stage II (HR: 0.18, 95% CI: 0.04–0.76, $p = 0.020$). Both a high ALI (HR: 0.54, 95% CI: 0.37–0.78, $p = 0.001$) and PNI (HR: 0.64, 95% CI: 0.45–0.92, $p = 0.016$) were associated with a low risk of recurrence in poorly–moderately differentiated HCC patients undergoing surgical resection. Among HCC patients undergoing surgical resection, a higher ALI was associated with a decreased risk of recurrence in those with a tumor size ≤2 cm (HR: 0.26, 95% CI: 0.08–0.79, $p = 0.018$). Additionally, in HCC patients undergoing surgical resection, a higher ALI (HR: 0.40, 95% CI: 0.25–0.66, $p < 0.001$) and PNI (HR: 0.57, 95% CI: 0.35–0.91, $p = 0.019$) were associated with a decreased risk of recurrence in those with a tumor size >5 cm. Among HCC patients undergoing surgical resection, a higher ALI was associated with a decreased risk of recurrence in those with a single tumor (HR: 0.62, 95% CI: 0.43–0.91, $p = 0.014$) and in those with ≥2 tumors (HR: 0.18, 95% CI: 0.04–0.78, $p = 0.022$). However, in HCC patients undergoing surgical resection, a higher PNI was only associated with a decreased risk of recurrence in those with a single tumor (HR: 0.66, 95% CI: 0.45–0.95, $p = 0.026$). Subgroup analyses of the associations between ALI and PNI and the recurrence of HCC in patients treated with surgical resection are presented in Table 4.

Table 4. Subgroup analyses of the associations of ALI and PNI with recurrence in HCC patients treated with surgical resection

Subgroup analyses	ALI (Ref.: ≤ 4436.12)		PNI (Ref.: ≤ 49.3)	
	HR (95% CI)	p-value	HR (95% CI)	p-value
Age <60 years	0.45 (0.28–0.73)	0.001	0.68 (0.44–1.07)	0.094
Age ≥ 60 years	0.73 (0.41–1.27)	0.265	0.63 (0.35–1.13)	0.120
Male	0.57 (0.39–0.84)	0.005	0.60 (0.41–0.87)	0.007
Female	0.86 (0.29–2.60)	0.791	0.48 (0.16–1.43)	0.188
Non-cirrhosis	0.52 (0.29–0.93)	0.028	0.47 (0.26–0.85)	0.012
Comorbidity with cirrhosis	0.61 (0.40–0.94)	0.026	0.87 (0.55–1.37)	0.534
PS = 0	0.48 (0.30–0.76)	0.002	0.57 (0.35–0.93)	0.023
PS = 1	0.69 (0.41–1.14)	0.145	0.75 (0.43–1.31)	0.307
Stage: I	0.61 (0.42–0.89)	0.009	0.70 (0.49–1.01)	0.058
Stage: II	0.27 (0.05–1.49)	0.133	0.18 (0.04–0.76)	0.020
Grade: poorly-moderately differentiated	0.54 (0.37–0.78)	0.001	0.64 (0.45–0.92)	0.016
Grade: well-differentiated	1.09 (0.31–3.87)	0.889	0.93 (0.27–3.18)	0.903
Tumor size: ≤ 2 cm	0.26 (0.08–0.79)	0.018	0.42 (0.13–1.37)	0.149
Tumor size: 2–5 cm	0.78 (0.43–1.40)	0.404	1.06 (0.59–1.88)	0.847
Tumor size: > 5 cm	0.40 (0.25–0.66)	< 0.001	0.57 (0.35–0.91)	0.019
Number of tumors: 1	0.62 (0.43–0.91)	0.014	0.66 (0.45–0.95)	0.026
Number of tumors: ≥ 2	0.18 (0.04–0.78)	0.022	0.50 (0.21–1.18)	0.114

Model of ALI was adjusted for ALT, AST, GGT, IBIL, AGR, PT, TT, AFP, CAE, presence or absence of comorbidity with cirrhosis, PS score, pathological staging, maximum diameter of tumor, number of tumors, vascular invasion, satellite nodules, and other adjuvant therapy.

Model of PNI was adjusted for neutrophils, ALT, AST, GGT, IBIL, AGR, PT, TT, AFP, CAE, presence or absence of comorbidity with cirrhosis, PS score, pathological staging, maximum diameter of tumor, number of tumors, vascular invasion, satellite nodules, and other adjuvant therapy.

95% CI – 95% confidence interval; PNI – prognostic nutritional index; ALI – advanced lung cancer inflammation index; HR – hazard ratio; Ref. – reference; PS – performance status; HCC – hepatocellular carcinoma; ALT – alanine aminotransferase; AST – aspartate aminotransferase; GGT – gamma glutamyltransferase; ALP – alkaline phosphatase; IBIL – indirect bilirubin; AGR – albumin globulin ratio; PT – prothrombin time; APTT – activated partial thromboplastin time; TT – thrombin time; AFP – alpha-fetoprotein; CAE – carcinoembryonic antigen.

Discussion

We examined the association between ALI and the recurrence of HCC by analyzing retrospective clinical data from patients treated with surgical resection. The findings revealed that among HCC patients treated with surgical resection, patients with a higher ALI had a reduced risk of recurrence. The predictive ability of ALI for the risk of recurrence in HCC patients undergoing surgical resection was higher than that of PNI. Based on the subgroup analyses, in HCC patients undergoing surgical resection, a higher ALI was associated with recurrence in those <60 years of age, male sex, with and without cirrhosis, with a PS = 0, with stage I cancer, with poorly–moderately differentiated tumors, with a tumor size ≤ 2 cm and a tumor size > 5 cm, and with a single tumor and ≥ 2 tumors. Compared with PNI, ALI had a greater association with recurrence in different subgroups of HCC patients treated with surgical resection.

Cancer and inflammation are closely intertwined, and inflammation is not only associated with an increased incidence of cancer but also with a bad prognosis for individuals with tumors, according to previous research.²⁶ Notably, the NLR has been found to be a poor prognostic

factor for several tumors.^{27,28} However, as cachexia due to chronic systemic inflammation may affect patient prognosis through BMI and serum ALB levels,^{27,29} an ALI indicator that includes both these factors could theoretically better reflect a patient's nutritional status and systemic inflammation.³⁰ In 2013, a retrospective review by Jafri et al. found that a low ALI was significantly and independently associated with worse outcomes in advanced non-small cell lung cancer (NSCLC).³¹ The pretreatment ALI was found to be a significant independent predictor of early progression in patients with advanced NSCLC receiving nivolumab.³⁰ A previous study also demonstrated that the ALI score was a powerful prognostic and predictive marker for advanced NSCLC lung cancer patients treated with PD-L1 inhibitors alone.³² In a retrospective cohort study by Li et al., the ALI score was an independent prognostic factor of OS in patients with advanced HCC who had been treated with immunotherapy.²⁵ Similarly, in a recent study, a high ALI was an independent prognostic factor for OS in HCC patients receiving immunotherapy.³³ In the present study, we found that the ALI index was associated with a reduced risk of recurrence in patients with HCC who had been treated with surgical resection. Furthermore, ALI had a better ability for recurrence

assessment than PNI in patients with HCC who had been treated with surgical resection. Prognostic nutritional index has been found to be an important prognostic parameter for HCC patients who underwent hepatectomy.¹⁸ In a study, the author compared and explored the prognostic value of ALI, PNI and SII in newly diagnosed diffuse large B-cell lymphoma and found that ALI had the highest area under the curve (AUC).³⁴ A prospective multicenter study suggested that ALI was better than NLR, PNI, SII, and PLR in patients with cancer sarcopenia.³⁵ Whether the ALI index has an improved prognostic, predictive ability relative to recurrence in patients with HCC who had been treated with surgical resection needs further elucidation. All in all, the study provides a complete view of recurrence in patients with HCC treated with surgical resection regarding inflammation indexes.

In the subgroup analyses, a higher ALI was associated with a lower risk of recurrence after curative resection of HCC in patients younger than 60 years and in male patients. A study assessing the clinical significance of ALI in colorectal cancer patients after curative resection revealed that a low ALI was an independent predictor of poor survival, especially in older patients.³⁶ In a study evaluating the prognostic significance of ALI in non-metastatic gastric cancer patients who underwent radical surgical resection, a low preoperative ALI was significantly correlated with older age.³⁷ After stratification by sex, a low ALI was an independent risk factor for survival in male patients but not in female patients.³⁸ A meta-analysis showed that a decreased ALI correlated with the depth of tumor invasion and presence of distant metastasis and tended to be associated with the male sex.²⁴ These findings may also be due to the factors associated with HCC recurrence, including age and sex,^{39,40} that affect the association between ALI and recurrence of HCC in patients treated after surgical resection.

Performance status may be a good prognostic indicator in HCC patients treated with proton beam therapy.⁴¹ Stage I tumors were also a relatively good prognostic factor for HCC.⁴² From our results, a higher ALI was associated with recurrence in those with a PS = 0 and stage I disease, indicating the importance of malnutrition and the inflammatory status concerning recurrence after curative resection of HCC in early-stage cases. However, we also found an association between ALI and recurrence in HCC patients treated with surgical resection of poorly–moderately differentiated tumors. We speculate that the reason for these results may be that the degree of inflammation can differ in different cancer stages.³³ We observed that the association between ALI and recurrence in HCC patients treated after surgical resection with a tumor size ≤ 2 cm, a tumor size > 5 cm, and in patients with and without liver cirrhosis, suggests that the association between ALI and recurrence after surgical resection of HCC applies to a more extensive population of HCC. We concluded that ALI showed more associations with recurrence than PNI in different population subgroups

of HCC patients undergoing surgical resection. A multicenter study evaluating the prognostic value of ALI in HPV-negative head and neck squamous cell carcinoma indicated that ALI was a more reliable prognostic index, with stronger associations with survival compared to PNI.⁴³ This may be due to the more complete representation and synthesis of the inflammatory and nutritional status of the patient. Our results support the use of pretreatment ALI, an easily measurable inflammatory/nutritional index, in routine clinical practice to improve the prognostic stratification of HCC patients undergoing surgical resection.

Limitations

By monitoring inexpensive and easily available blood indicators, our study can help clinicians identify patients at high risk of postoperative recurrence at an early stage and assist in therapeutic decision-making to improve the prognosis and quality of life and reduce the burden of disease in HCC patients. To our knowledge, this is the first study to investigate the prognostic importance of ALI in patients with HCC treated with surgical resection. However, there are limitations to our study that must be acknowledged. First, the single-center, retrospective design may have biased the results. Second, it is possible that our findings may be affected by potential confounding factors, such as treatment received at other hospitals during follow-up. Further prospective, multicenter studies are needed to verify the prognostic value of ALI.

Conclusions

The findings suggest an association between ALI and a reduced risk of recurrence in HCC patients undergoing surgical resection. The advanced lung cancer inflammation index may be an easily calculated tool to assess the prognosis of HCC patients undergoing surgical resection.

Supplementary data

The Supplementary materials are available at <https://zenodo.org/records/11124384>. The package includes the following files:

Supplementary Table 1. Analysis of normality and homogeneity.

Supplementary Table 2. Assessment of proportional hazards assumption in preoperative biomarker analysis using Cox models.

Supplementary Table 3. Collinearity test using Martingale residual.

Supplementary Fig. 1. The plot of Schoenfeld residual of ALI model.

Supplementary Fig. 2. The plot of Schoenfeld residual of NLR model.

Supplementary Fig. 3. The plot of Schoenfeld residual of MLR model.

Supplementary Fig. 4. The plot of Schoenfeld residual of PNI model.

Supplementary Fig. 5. The plot of Schoenfeld residual of SII model.

Supplementary Fig. 6. Testing influential observation in ALI model.

Supplementary Fig. 7. Testing influential observation in NLR model.

Supplementary Fig. 8. Testing influential observation in MLR model.

Supplementary Fig. 9. Testing influential observation in PNI model.

Supplementary Fig. 10. Testing influential observation in SII model.

Supplementary Fig. 11. The relationship between the log-hazard function and the predictive variables in ALI model.

Supplementary Fig. 12. The relationship between the log-hazard function and the predictive variables in NLR model.

Supplementary Fig. 13. The relationship between the log-hazard function and the predictive variables in MLR model.

Supplementary Fig. 14. The relationship between the log-hazard function and the predictive variables in PNI model.

Supplementary Fig. 15. The relationship between the log-hazard function and the predictive variables in SII model.

Data availability

The datasets generated and/or analyzed during the current study are available from the corresponding author on reasonable request.

Consent for publication

Not applicable.

ORCID iDs

Weidong Yuan  <https://orcid.org/g/0009-0007-7877-2050>

Hewei Zhao  <https://orcid.org/0009-0000-2154-4013>

Shaochuang Wang  <https://orcid.org/0000-0001-9328-1662>

References

- Sung H, Ferlay J, Siegel RL, et al. Global cancer statistics 2020: GLOBOCAN estimates of incidence and mortality worldwide for 36 cancers in 185 countries. *CA Cancer J Clin*. 2021;71(3):209–249. doi:10.3322/caac.21660
- Chidambaranathan-Reghupaty S, Fisher PB, Sarkar D. Hepatocellular carcinoma (HCC): Epidemiology, etiology and molecular classification. *Adv Cancer Res*. 2021;149:1–61. doi:10.1016/bs.acr.2020.10.001
- Galle PR, Forner A, Llovet JM, et al. EASL Clinical Practice Guidelines: Management of hepatocellular carcinoma. *J Hepatol*. 2018;69(1):182–236. doi:10.1016/j.jhep.2018.03.019
- Renne SL, Sarcognato S, Sacchi D, et al. Hepatocellular carcinoma: A clinical and pathological overview. *Pathologica*. 2021;113(3):203–217. doi:10.32074/1591-951X-295
- Lee TKW, Guan XY, Ma S. Cancer stem cells in hepatocellular carcinoma: From origin to clinical implications. *Nat Rev Gastroenterol Hepatol*. 2022;19(1):26–44. doi:10.1038/s41575-021-00508-3
- Sugawara Y, Hibi T. Surgical treatment of hepatocellular carcinoma. *Biosci Trends*. 2021;15(3):138–141. doi:10.5582/bst.2021.01094
- Bruix J, Reig M, Sherman M. Evidence-based diagnosis, staging, and treatment of patients with hepatocellular carcinoma. *Gastroenterology*. 2016;150(4):835–853. doi:10.1053/j.gastro.2015.12.041
- Omata M, Cheng AL, Kokudo N, et al. Asia-Pacific clinical practice guidelines on the management of hepatocellular carcinoma: A 2017 update. *Hepatol Int*. 2017;11(4):317–370. doi:10.1007/s12072-017-9799-9
- Zeng J, Zeng J, Lin K, et al. Development of a machine learning model to predict early recurrence for hepatocellular carcinoma after curative resection. *Hepatobiliary Surg Nutr*. 2022;11(2):176–187. doi:10.21037/hbsn-20-466
- Chan AWH, Zhong J, Berhane S, et al. Development of pre and post-operative models to predict early recurrence of hepatocellular carcinoma after surgical resection. *J Hepatol*. 2018;69(6):1284–1293. doi:10.1016/j.jhep.2018.08.027
- Wang D, Xiao M, Wan ZM, Lin X, Li QY, Zheng SS. Surgical treatment for recurrent hepatocellular carcinoma: Current status and challenges. *World J Gastrointest Surg*. 2023;15(4):544–552. doi:10.4240/wjgs.v15.i4.544
- Zhao H, Wu L, Yan G, et al. Inflammation and tumor progression: Signaling pathways and targeted intervention. *Sig Transduct Target Ther*. 2021;6(1):263. doi:10.1038/s41392-021-00658-5
- Hanahan D, Weinberg RA. Hallmarks of cancer: The next generation. *Cell*. 2011;144(5):646–674. doi:10.1016/j.cell.2011.02.013
- Cao X, Cui J, Yu T, Li Z, Zhao G. Fibrinogen/albumin ratio index is an independent prognosis predictor of recurrence-free survival in patients after surgical resection of gastrointestinal stromal tumors. *Front Oncol*. 2020;10:1459. doi:10.3389/fonc.2020.01459
- Li H, Cheng ZJ, Liang Z, et al. Novel nutritional indicator as predictors among subtypes of lung cancer in diagnosis. *Front Nutr*. 2023;10:1042047. doi:10.3389/fnut.2023.1042047
- Wu Y, Tu C, Shao C. Inflammatory indexes in preoperative blood routine to predict early recurrence of hepatocellular carcinoma after curative hepatectomy. *BMC Surg*. 2021;21(1):178. doi:10.1186/s12893-021-01180-9
- Ren Y, Fan X, Chen G, Zhou D, Lin H, Cai X. Preoperative C-reactive protein/albumin ratio to predict mortality and recurrence of patients with hepatocellular carcinoma after curative resection. *Med Clin (Barc)*. 2019;153(5):183–190. doi:10.1016/j.medcli.2018.11.010
- Wang D, Hu X, Xiao L, et al. Prognostic nutritional index and systemic immune-inflammation index predict the prognosis of patients with HCC. *J Gastrointest Surg*. 2021;25(2):421–427. doi:10.1007/s11605-019-04492-7
- Shepshelovich D, Xu W, Lu L, et al. Body mass index (BMI), BMI change, and overall survival in patients with SCLC and NSCLC: A pooled analysis of the International Lung Cancer Consortium. *J Thorac Oncol*. 2019;14(9):1594–1607. doi:10.1016/j.jtho.2019.05.031
- Ji F, Liang Y, Fu S, et al. Prognostic value of combined preoperative prognostic nutritional index and body mass index in HCC after hepatectomy. *HPB (Oxford)*. 2017;19(8):695–705. doi:10.1016/j.hpb.2017.04.008
- Mandaliya H, Jones M, Oldmeadow C, Nordman IIC. Prognostic biomarkers in stage IV non-small cell lung cancer (NSCLC): Neutrophil to lymphocyte ratio (NLR), lymphocyte to monocyte ratio (LMR), platelet to lymphocyte ratio (PLR) and advanced lung cancer inflammation index (ALI). *Transl Lung Cancer Res*. 2019;8(6):886–894. doi:10.21037/tlcr.2019.11.16
- Tsai YT, Hsu CM, Chang GH, et al. Advanced lung cancer inflammation index predicts survival outcomes of patients with oral cavity cancer following curative surgery. *Front Oncol*. 2021;11:609314. doi:10.3389/fonc.2021.609314
- Deng Y, Sun Y, Lin Y, Huang Y, Chi P. Clinical implication of the advanced lung cancer inflammation index in patients with right-sided colon cancer after complete mesocolic excision: A propensity score-matched analysis. *World J Surg Oncol*. 2022;20(1):246. doi:10.1186/s12957-022-02712-0
- Xie WJ, Li X, Li YH, et al. Prognostic significance of advanced lung cancer inflammation index, a nutritional and inflammation index, in patients with gastrointestinal cancers: A meta-analysis. *Nutr Cancer*. 2023;75(4):1233–1242. doi:10.1080/01635581.2023.2186267

25. Li Q, Ma F, Tsilimigras DI, Åberg F, Wang JF. The value of the advanced lung cancer inflammation index (ALI) in assessing the prognosis of patients with hepatocellular carcinoma treated with camrelizumab: A retrospective cohort study. *Ann Transl Med.* 2022;10(22):1233–1233. doi:10.21037/atm-22-5099
26. Todoric J, Antonucci L, Karin M. Targeting inflammation in cancer prevention and therapy. *Cancer Prev Res.* 2016;9(12):895–905. doi:10.1158/1940-6207.CAPR-16-0209
27. Kim EY, Kim N, Kim YS, et al. Prognostic significance of modified Advanced Lung Cancer Inflammation Index (ALI) in patients with small cell lung cancer: Comparison with original ALI. *PLoS One.* 2016;11(10):e0164056. doi:10.1371/journal.pone.0164056
28. Lai C, Zhang C, Lv H, et al. A novel prognostic model predicts overall survival in patients with nasopharyngeal carcinoma based on clinical features and blood biomarkers. *Cancer Med.* 2021;10(11):3511–3523. doi:10.1002/cam4.3839
29. Levogler S, Van Vugt JLA, De Bruin RWF, IJzermans JNM. Systematic review of sarcopenia in patients operated on for gastrointestinal and hepatopancreatobiliary malignancies. *Br J Surg.* 2015;102(12):1448–1458. doi:10.1002/bjs.9893
30. Shiroyama T, Suzuki H, Tamiya M, et al. Pretreatment advanced lung cancer inflammation index (ALI) for predicting early progression in nivolumab-treated patients with advanced non-small cell lung cancer. *Cancer Med.* 2018;7(1):13–20. doi:10.1002/cam4.1234
31. Jafri SH, Shi R, Mills G. Advance lung cancer inflammation index (ALI) at diagnosis is a prognostic marker in patients with metastatic non-small cell lung cancer (NSCLC): A retrospective review. *BMC Cancer.* 2013;13(1):158. doi:10.1186/1471-2407-13-158
32. Kazandjian D, Gong Y, Keegan P, Pazdur R, Blumenthal GM. Prognostic value of the lung immune prognostic index for patients treated for metastatic non-small cell lung cancer. *JAMA Oncol.* 2019;5(10):1481. doi:10.1001/jamaoncol.2019.1747
33. Li Q, Ma F, Wang JF. Advanced lung cancer inflammation index predicts survival outcomes of hepatocellular carcinoma patients receiving immunotherapy. *Front Oncol.* 2023;13:997314. doi:10.3389/fonc.2023.997314
34. Liu T, Ye F, Li Y, Liu A. Comparison and exploration of the prognostic value of the advanced lung cancer inflammation index, prognostic nutritional index, and systemic immune-inflammation index in newly diagnosed diffuse large B-cell lymphoma. *Ann Palliat Med.* 2021;10(9):9650–9659. doi:10.21037/apm-21-2067
35. Ruan GT, Ge YZ, Xie HL, et al. Association between systemic inflammation and malnutrition with survival in patients with cancer sarcopenia: A prospective multicenter study. *Front Nutr.* 2022;8:811288. doi:10.3389/fnut.2021.811288
36. Horino T, Tokunaga R, Miyamoto Y, et al. The advanced lung cancer inflammation index is a novel independent prognosticator in colorectal cancer patients after curative resection. *Ann Gastroenterol Surg.* 2022;6(1):83–91. doi:10.1002/ags3.12499
37. Chen H, Zhang F, Luo D, et al. Advanced lung cancer inflammation index predicts the outcomes of patients with non-metastatic gastric cancer after radical surgical resection. *J Gastrointest Oncol.* 2023;14(1):85–96. doi:10.21037/jgo-22-657
38. Zhang X, Wang D, Sun T, Li W, Dang C. Advanced lung cancer inflammation index (ALI) predicts prognosis of patients with gastric cancer after surgical resection. *BMC Cancer.* 2022;22(1):684. doi:10.1186/s12885-022-09774-z
39. Wang Q, Qiao W, Zhang H, et al. Nomogram established on account of Lasso–Cox regression for predicting recurrence in patients with early-stage hepatocellular carcinoma. *Front Immunol.* 2022;13:1019638. doi:10.3389/fimmu.2022.1019638
40. Liang T, He Y, Mo S, et al. Gender disparity in hepatocellular carcinoma recurrence after curative hepatectomy. *Ann Hepatol.* 2022;27(3):100695. doi:10.1016/j.aohep.2022.100695
41. Fukuda K, Okumura T, Abei M, et al. Long-term outcomes of proton beam therapy in patients with previously untreated hepatocellular carcinoma. *Cancer Sci.* 2017;108(3):497–503. doi:10.1111/cas.13145
42. Gao X, Zhao C, Zhang N, et al. Genetic expression and mutational profile analysis in different pathologic stages of hepatocellular carcinoma patients. *BMC Cancer.* 2021;21(1):786. doi:10.1186/s12885-021-08442-y
43. Gaudioso P, Borsetto D, Tirelli G, et al. Advanced lung cancer inflammation index and its prognostic value in HPV-negative head and neck squamous cell carcinoma: A multicenter study. *Support Care Cancer.* 2021;29(8):4683–4691. doi:10.1007/s00520-020-05979-9

Identification of a pyroptosis-related long noncoding RNA signature for determining the prognosis and immune status of hepatocellular carcinoma patients

Shaohua Xu^{1,A–D}, Guoxu Fang^{2,3,B,C,E,F}

¹ Department of Hepatobiliary and Pancreatic Surgery, Clinical Oncology School of Fujian Medical University, Fujian Cancer Hospital, Fuzhou, China

² Department of Hepatopancreatobiliary Surgery, Mengchao Hepatobiliary Hospital of Fujian Medical University, Fuzhou, China

³ The Big Data Institute of Southeast Hepatobiliary Health Information, Mengchao Hepatobiliary Hospital of Fujian Medical University, Fuzhou, China

A – research concept and design; B – collection and/or assembly of data; C – data analysis and interpretation;

D – writing the article; E – critical revision of the article; F – final approval of the article

Advances in Clinical and Experimental Medicine, ISSN 1899–5276 (print), ISSN 2451–2680 (online)

Adv Clin Exp Med. 2025;34(4):585–596

Address for correspondence

Guoxu Fang

E-mail: guoxufang2020@163.com

Funding sources

The study was funded by the Science and Technology Innovation Platform Project of Fuzhou Science and Technology Bureau (grant No. 2021-P-055), Startup Fund for scientific research, Fujian Medical University (grant No. 2019QH1197) and Natural Science Foundation of Fujian Province (grant No. 2021J011283).

Conflict of interest

None declared

Received on April 11, 2023

Reviewed on January 16, 2024

Accepted on June 18, 2024

Published online on October 21, 2024

Cite as

Xu S, Fang G. Identification of a pyroptosis-related long noncoding RNA signature for determining the prognosis and immune status of hepatocellular carcinoma patients. *Adv Clin Exp Med.* 2025;34(4):585–596. doi:10.17219/acem/190201

DOI

10.17219/acem/190201

Copyright

Copyright by Author(s)

This is an article distributed under the terms of the Creative Commons Attribution 3.0 Unported (CC BY 3.0) (<https://creativecommons.org/licenses/by/3.0/>)

Abstract

Background. Despite improvements in cancer screening and diagnosis, hepatocellular carcinoma (HCC) is still diagnosed at an advanced stage, and the prognosis is worse than that of early HCC patients. Therefore, better molecular markers and therapeutic targets in HCC are required.

Objectives. We investigated the predictive value of pyroptosis-related long noncoding RNAs (lncRNAs) in HCC and the effects of these lncRNAs on the immune microenvironment of HCC.

Materials and methods. RNA sequencing data of HCC patients were extracted from The Cancer Genome Atlas (TCGA) database to identify differentially expressed pyroptosis-related lncRNAs related to overall survival (OS). A model was established to verify the character of pyroptosis-associated lncRNAs in the tumor microenvironment, and their prognostic value was evaluated.

Results. A total of 721 PR lncRNAs were identified based on the analysis of the TCGA database. Univariate Cox analysis revealed 37 survival-related PRlncRNAs with prognostic values. As a result of least absolute shrinkage and selection operator (LASSO) regression analysis, 'ELFN-AS1', AC099850.3, AC073389.3, 'HPN-AS1', AC009283.1, and AL139289.1 showed prognostic value. Kaplan–Meier analysis indicated that the OS of the high-risk set was worse than those of the low-risk set in both the training and testing cohorts. Univariate and multivariate analyses revealed that the risk score was a better independent prognostic factor than the stage. The precision of the lncRNA signature was confirmed using receiver operating characteristic curve (ROC) analysis. Immune- and metabolism-related pathways were enriched in both the low- and high-risk groups. Gene set enrichment analysis suggested that the identified lncRNAs regulate HCC tumorigenesis and prognosis by modulating metabolism. Various algorithms were used to confirm the significant differences in immune cells between these 2 groups.

Conclusions. These findings could contribute to the development and validation of favorable biomarkers, improve the prognosis and survival of HCC, and help in developed individualized treatment plans for HCC.

Key words: prognosis, hepatocellular carcinoma, lncRNAs, pyroptosis

Background

Hepatocellular carcinoma (HCC) is the most commonly diagnosed primary liver cancer and the 3rd leading cause of cancer-related mortality worldwide.¹ Surgical resection is still the preferred clinical treatment for early-stage HCC.² Although recent technological advances have improved cancer screening and diagnosis, HCC, a destructive malignant tumor, is still generally diagnosed at an advanced stage with a 5-year overall survival (OS) of less than 18%.³ Immunotherapy with anti-PD-1, anti-PD-L1 and anti-CTLA-4 antibodies is the most popular systematic treatment for advanced HCC.⁴ KEYNOTE-224, a phase II trial, revealed a satisfactory curative effect of pembrolizumab against HCC after sorafenib failure. The overall response rate reached 17% with 1 complete response (CR), while the disease control rate was 61%.⁵ Moreover, the anti-CTLA-4 monoclonal antibody tremelimumab demonstrated a partial response and stable disease rates of 17.6% and 58.8%, respectively, in a small phase II pilot trial (NCT01008358) in advanced HCC patients.⁶

The major node in the gene regulatory networks was believed to be protein-coding genes. However, noncoding RNAs, with a length of >200 nts, have been reported to play an essential role in tumorigenesis and cancer development.⁷ Long noncoding RNAs (lncRNAs) mediate and regulate signaling transduction pathways in immune and tumor cells.⁸ Aberrant expression of lncRNAs can indicate the spectrum of disease progression, and some of these lncRNAs have diagnostic and prognostic value.^{9,10} Expression levels of lncRNAs highly correlate with the tumor microenvironment and immune response. The sensitivity of low-risk groups to immunotherapy is high owing to the differences in lncRNA expression levels that lead to differential expression patterns of immune checkpoint genes.¹¹ A detailed understanding of the pathogenesis and molecular mechanisms of HCC is essential to identify novel targets and explore immunotherapy efficacy.

Pyroptosis, a newly discovered process of adjusted cell death, is mediated by various inflammasomes. Pyroptosis initiates the inflammatory process and is involved in the pathogenesis of multiple inflammatory and immune-mediated diseases, such as systemic lupus erythematosus, myositis, acute myeloid leukemia, cervical cancer, and HCC.^{12–15} Additionally, pyroptosis is mediated by activation of inflammatory caspases (caspase-1, 4, 5, and 11).^{16,17} Several mechanisms regulate the pyroptosis of tumor cells,^{18–20} but the principal mechanism is related to several signal transduction pathways and pathologic molecular changes. However, currently, studies on the effects of pyroptosis-associated lncRNAs (PRlncRNAs) in the tumor microenvironment, especially the microenvironment of HCC cells, are limited. In this study, the functions of lncRNAs in pyroptosis were investigated, and their potential mechanisms of action in HCC were elucidated.

Objectives

Hepatocellular carcinoma has a high malignancy rate and poor prognosis, and the knowledge related to etio-pathological mechanisms is limited. Our objective was to build a lncRNA model to verify the role of pyroptosis-related RNA in HCC, aiming to clarify immunotherapy responses, guide the treatment of HCC patients and predict the curative effect.

Materials and methods

Identification of PRlncRNAs using RNA sequencing data

The clinical and RNA sequencing (RNA-seq; fragments per kilobase million) data (comprising 374 cancerous and 50 noncancerous samples) of HCC cases were obtained from The Cancer Genome Atlas (TCGA) website (<https://tcga-data.nci.nih.gov/tcga/>). To identify PRlncRNAs, the correlation between lncRNAs and pyroptosis-related genes (PRGs) was examined employing Pearson's correlation analysis. Pyroptosis-associated lncRNAs were identified based on the following criteria: $p < 0.001$ and correlation coefficient $|R^2| > 0.4$.

Unsupervised clustering of PRlncRNAs

To identify different PRlncRNAs, patients were classified for further analysis, including unsupervised cluster analysis. The consistency of the clustering algorithm determines the number and stability of clustering. To this end, we used the ConsensusClusterPlus R package. To ensure the stability of the classification, 1,000 repeats were performed.

Construction and validation of the prognostic PRlncRNA signature

Data of the HCC cases from the TCGA database were categorized into training and testing cohorts using the caret R package (6.0–93). PRlncRNA prognostic significance was evaluated using univariate Cox regression analyses. Significant lncRNAs (as per the least absolute shrinkage and selection operator (LASSO) regression analyses) were selected as candidate characteristic lncRNAs. Furthermore, hub lncRNAs were identified using a multivariate-penalized Cox regression analysis to generate a lncRNA risk signature. The risk score of the prognostic signature was calculated as follows (Equation 1):

$$\text{risk score} = \sum_{i=1}^n a_i \times x_i, \quad (1)$$

where a_i and x_i are the expression and regression coefficient values of each PRlncRNA, respectively.

The risk score was calculated for each patient. Based on the median risk score, patients with HCC were divided into low-risk and high-risk groups. The accuracy of the prognostic signatures was predicted using receiving operating characteristic (ROC) curves. Thereafter, the effect of the PRlncRNA signature on the prognosis of patients was evaluated using Kaplan–Meier analysis. The validity of the model was subsequently verified using a calibration curve and consistency index (C-index). A hybrid nomogram comprised of the PRlncRNA signature and clinicopathological attributes was constructed using the rms R package (6.5–0) to predict the OS of HCC patients.

Gene set enrichment analysis

Gene Set Enrichment Analysis (GSEA; <https://www.gseamsigdb.org/gsea/index.jsp>) aims to explore the possible biological functions of lncRNA. The contribution of target genes to a phenotype was evaluated using GSEA by investigating their distribution tendency between the 2 groups according to phenotype relevance. To this end, we utilized the ggplot2 R package (3.3.6) and pRRophetic R package; statistical significances were defined as a nominal $p < 0.05$ and a false discovery rate < 0.25 .

Immune response in the 2 risk groups

The heatmap of immune responses was generated using the XCELL, TIMER, QUANTISEG, MCPOUNTER, EPIC, CIBERSORT-ABS, and CIBERSORT algorithms. The correlation between the risk score values and tumor-infiltrating immune cells (TIICs) was determined using Spearman's correlation analysis. A heatmap was drawn to depict the distribution differences in immune cells between the low- and high-risk groups and the risk score values.

Statistical analyses

Data analyses were conducted using R v. 4.2.0 (R Foundation for Statistical Computing, Vienna, Austria). The differences between normal and HCC tissues were analyzed using a Student's t-test or Wilcoxon's rank-sum test. The LASSO Cox and Cox regression analyses were used to construct a PRlncRNA prognostic model. We tested the proportional hazards assumption for the Cox model and generated plots of the proportional Schoenfeld residuals relative to the transformed time of the residuals for each covariate. Kaplan–Meier and ROC curve analyses aided in verifying the prognostic and predictive power of the risk model. The test comparing Kaplan–Meier curves in this study was the log-rank test. Spearman's correlation analysis was used to further analyze the association between the TIIC ratio and risk scores. Using the “pRRophetic” package and the expression matrix of liver cancer patients, the minimum

inhibitory concentration (IC50) of drugs in high- and low-risk groups of liver cancer patients was predicted, and the drugs with statistically different IC50 values were obtained, which may become candidates for the treatment of liver cancer. The Wilcoxon signed-rank test was applied to compare IC50 between the high- and low-risk patients. All statistical analyses involved a 2-tailed test. A $p < 0.05$ determined a statistically significant difference.

Results

Unsupervised cluster analysis

The workflow of the study is illustrated in Fig. 1. The expression data of 52 PRGs from 50 noncancerous and 374 HCC tissues comprising the HCC cohort were retrieved from the TCGA. In total, 721 PRlncRNAs were identified based on the analysis of these 52 PRGs. Supplementary Table 1 shows the corresponding clinicopathological characteristics of 377 HCC patients. These patients were classified using the ConsensusClusterPlus R package based on the expression of 721 PRlncRNAs. The following 3 clusters were identified using the unsupervised clustering method: clusters 1, 2 and 3 with 145, 105 and 120 cases, respectively. Kaplan–Meier analysis revealed that the cases in cluster 2 were associated with adverse survival outcomes (Supplementary Fig. 1A). The heatmap of the top 231 lncRNAs relevant to favorable and poor prognosis and clinicopathological features is shown in Supplementary Fig. 1B, and the expression of lncRNA in cluster 2 was heterogeneous.

Construction and validation of the prognostic PRlncRNA signature

PRlncRNAs associated with the prognosis of HCC were screened using univariate Cox analysis, which revealed 37 survival-related PRlncRNAs with prognostic values (Fig. 2A). The number of lncRNAs was narrowed down to 13 using the LASSO Cox regression analysis (Fig. 2B,C). Multivariate Cox analysis identified the following 6 lncRNAs and their correlation coefficients, which were used for subsequent model construction: ‘*ELFN-AS1*’, *AC099850.3*, *AC073389.3*, ‘*HPN-AS1*’, *AC009283.1*, and *AL139289.1* (Fig. 2D). The results of our proportional hazards hypothesis test using the Cox proportional hazards model and the Schoenfeld residuals plot both indicated that the proportional hazards assumption was valid. Additionally, we conducted a linearity test for continuous variables within the Cox proportional hazards model using the easystats package, and the results confirm that the linearity assumption was valid. Consequently, we employed LASSO Cox and Cox regression analysis to construct the PRlncRNA prognostic model.

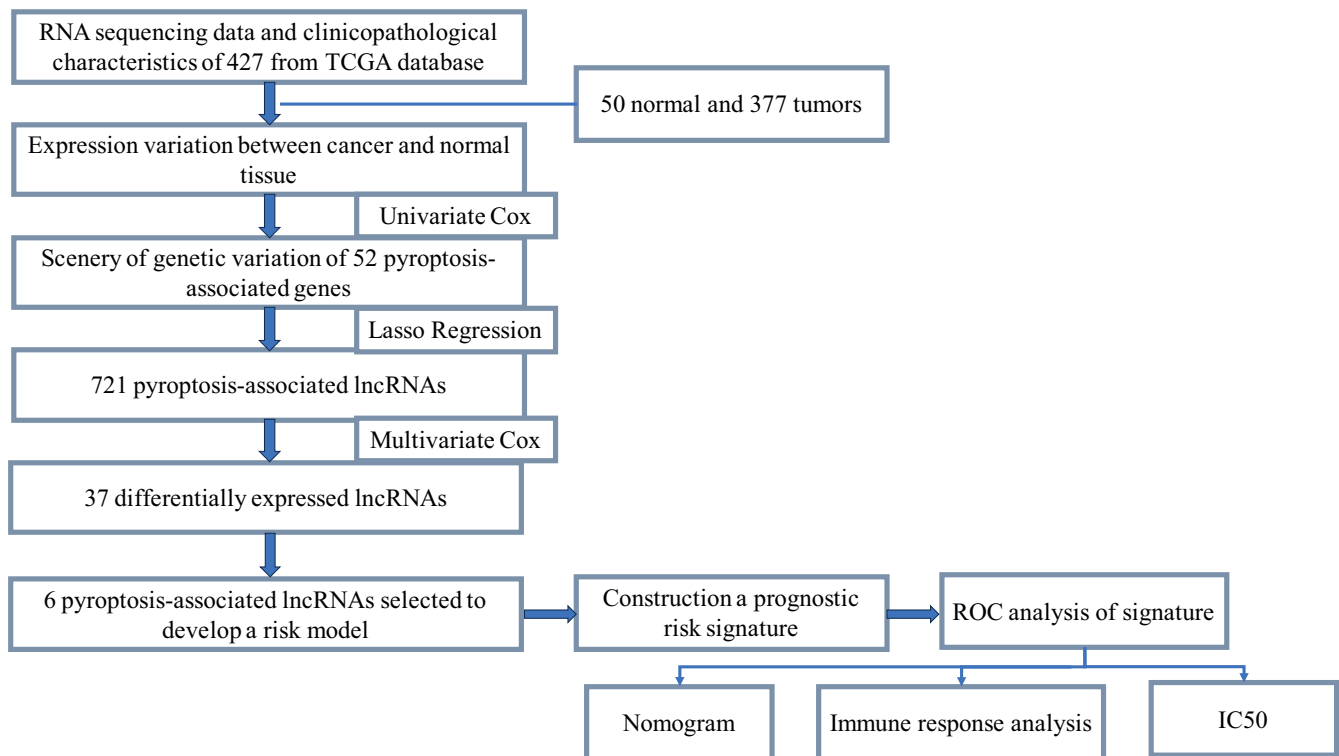


Fig. 1. Study workflow

Prognostic value of PRlncRNAs in HCC

The study cohort was separated into training (256 cases) and testing (109 cases) cohorts in a ratio of 7:3. The risk score was calculated as follows:

$$\text{Risk score} = [\textit{ELFN-AS1} \times 0.05564] + [\textit{AC099850.3} \times 0.1184] + [\textit{AC073389.3} \times 1.041] + [\textit{HPN-AS1} \times (-0.4541)] + [\textit{AC009283.1} \times (-0.1988)] + [\textit{AL139289.1} \times 0.6448]$$

Based on the risk score model, the prognostic risk of HCC patients could be measured, and the median risk score obtained through statistical analysis could be used as the cutoff value between high- and low-risk groups to guide subsequent analyses. Kaplan–Meier survival curve analysis of the 2 cohorts revealed that the PRlncRNA signature was associated with the prognosis of HCC patients, which could also be effectively predicted. In the training and testing cohorts, the prognosis of the high-risk group was significantly poorer compared to the low-risk group (Fig. 3A,B). Additionally, the potential expression patterns of survival-related lncRNAs served as early predictors of HCC and were determined using ROC curves. The area under the ROC curve (AUC) at years 1, 2 and 3 was 0.807 (95% confidence interval (95% CI): 0.711–0.904), 0.799 (95% CI: 0.710–0.888) and 0.789 (95% CI: 0.693–0.884) in the training cohort, respectively, which had greater accuracy than that in the testing cohort (AUC at years 1, 2 and 3 was 0.708 (95% CI: 0.535–0.882), 0.724 (95% CI: 0.559–0.889) and 0.719 (95% CI: 0.562–0.876), respectively;

Fig. 3C,D). The C-index of the risk score model was 0.724 (95% CI: 0.661–0.779).

Supplementary Fig. 2A,C show the survival outcome and risk status of patients in the training cohort. The probability of mortality was higher among patients in the high-risk group than among patients in the low-risk group. Comparable results were achieved in the testing group (Supplementary Fig. 2B,D). The lncRNA expression levels in each group are shown in Supplementary Fig. 2E,F.

The correlation between clinicopathological factors, including clinical stage, risk score and prognosis of HCC patients, was examined using Cox regression analyses. The result revealed that the clinical stage, T stage, M stage, and risk score were independent prognostic factors during univariate Cox regression analysis (Fig. 4A), whereas only T stage and risk score remained significant associations during multivariate Cox regression analysis (Fig. 4B). The sensitivity and specificity of the lncRNA signature were evaluated using ROC curve analysis. The AUC values of the PRlncRNA signature in the training and testing cohorts were 0.789 (95% CI: 0.693–0.884) and 0.719 (95% CI: 0.562–0.876), respectively, which were more than those of other clinical indices, suggesting the robustness and validity of the lncRNA signature in determining HCC prognosis (Fig. 4C,D).

A nomogram was constructed to determine the prognosis of HCC patients based on clinical characteristics and risk scores (Fig. 5A). Calibration curves and a C-index were applied to evaluate the predictive capacity of the signature (Fig. 5B). The heatmap of clinical features and risk subgroups revealed that the signature was markedly associated with the T stage and risk score (Fig. 5C).

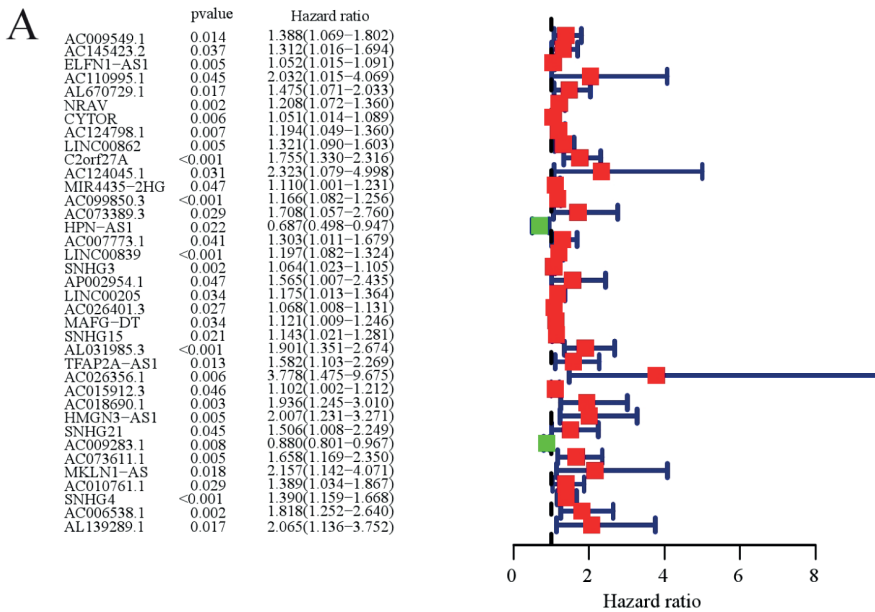
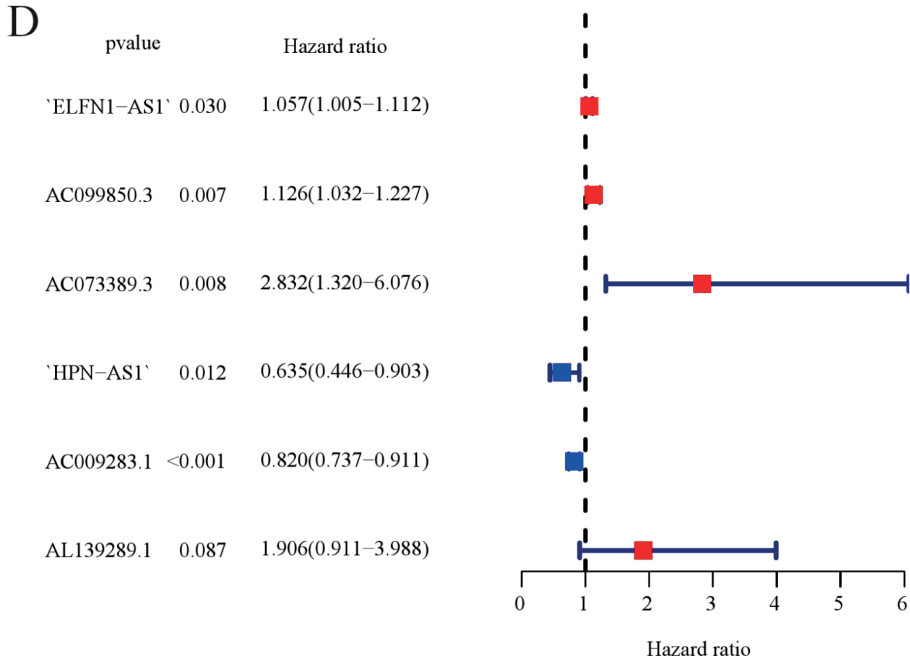
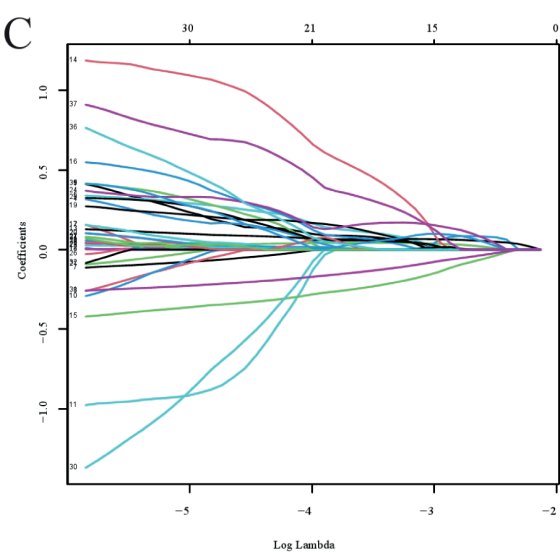
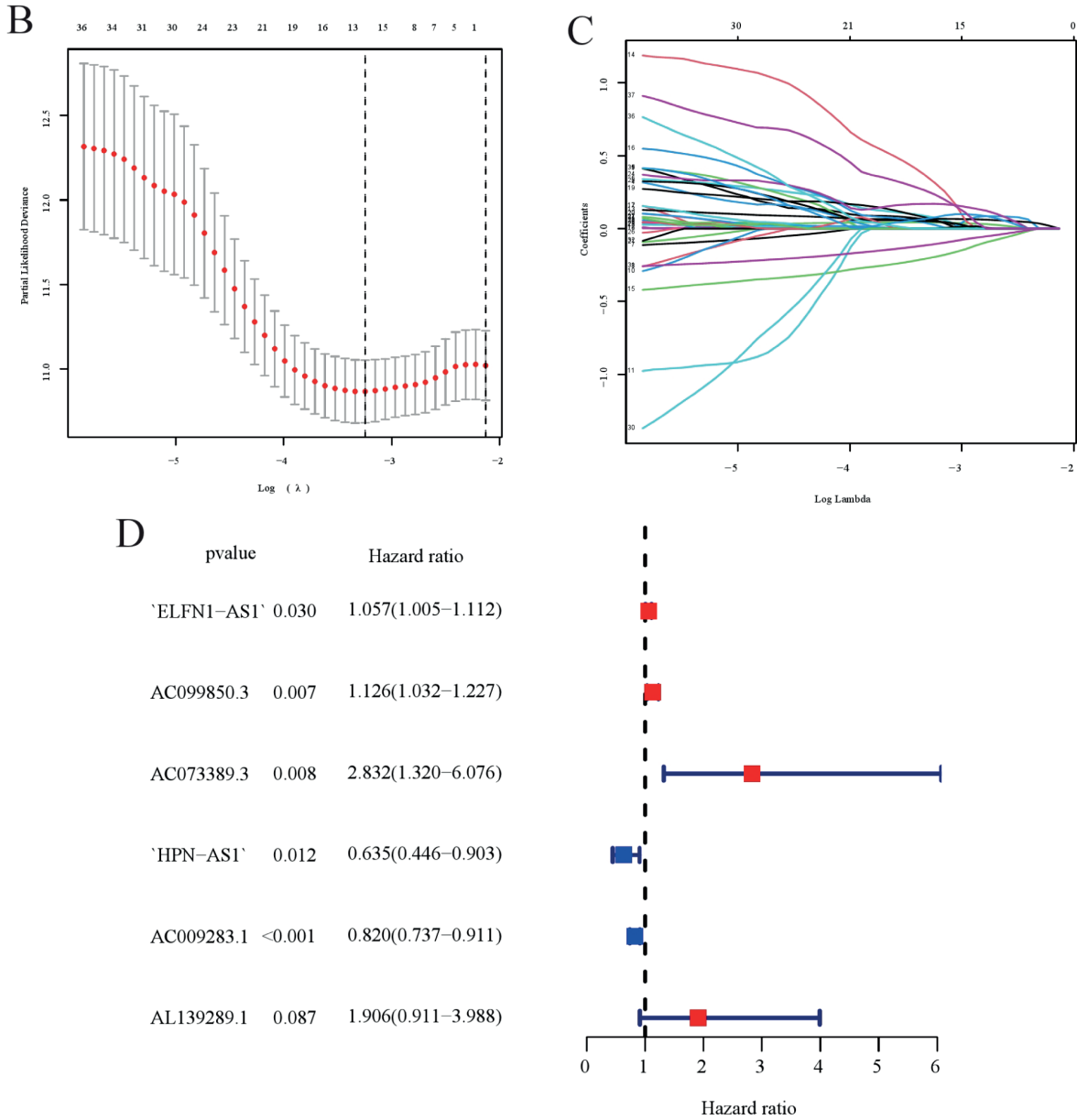


Fig. 2. Construction of a prognostic model for hepatocellular carcinoma (HCC) patients. A. Forest plots showing the results of univariate Cox regression analysis of 37 pyroptosis-related long noncoding RNAs (lncRNAs); B. Thirteen pyroptosis-related lncRNAs were selected using least absolute shrinkage and selection operator (LASSO) regression analysis; C. The coefficient of pyroptosis-related lncRNAs was calculated using LASSO regression analysis; D. Identification of the lncRNA signature



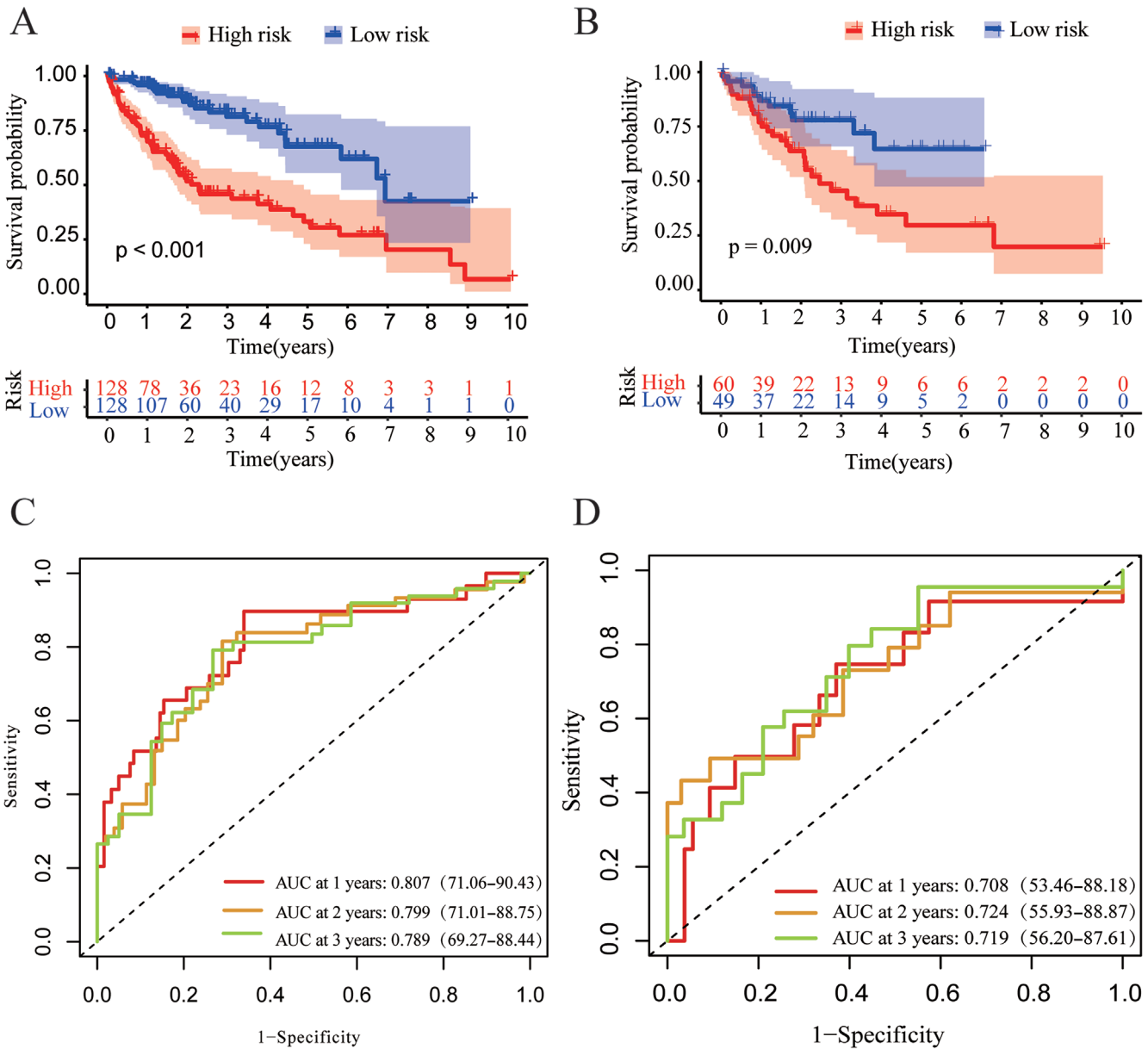


Fig. 3. Characteristics of the pyroptosis-related long noncoding RNA signature in the training and testing cohorts. Kaplan–Meier survival analysis of the training (A) and testing (B) cohorts; C. Receiving operating characteristic (ROC) curves indicate the accuracy of the prognostic model in the training cohort. The area under the ROC curve (AUC) at years 1, 2 and 3 was 0.807 (95% confidence interval (95% CI): 0.711–0.904), 0.799 (95% CI: 0.710–0.888) and 0.789 (95% CI: 0.693–0.884) in the training cohort; D. The area under the time-dependent ROC curves indicates the prognostic accuracy of the risk scores in the testing cohort. The area under the ROC curve (AUC) at years 1, 2, and 3 was 0.708 (95% CI: 0.535–0.882), 0.724 (95% CI: 0.559–0.889), and 0.719 (95% CI: 0.562–0.876) in the testing cohort

Thus, the nomogram constructed based on clinical features and risk scores accurately indicated the prognosis of the patients.

GSEA

To identify potential enrichment pathways for PRlncRNA in the risk groups, we used GSEA for biological function analysis. The results showed that phenotypic enrichment of PRlncRNAs in both the high- and low-risk groups was mainly reflected in tumor and metabolism-related pathways, such as apoptosis and the mTOR/NOTCH signaling

pathway. By contrast, phenotypic enrichment, although low, was mainly manifested in metabolism-related pathways, such as linoleic acid, drug metabolism and retinol metabolism (Supplementary Fig. 3A). This finding suggests that the prognostic features are related to tumor immunity and metabolism, which helps analyze the principles and mechanisms of the lncRNA signature affecting the metabolism of HCC cells. In addition, testing risk scores can improve the ability to predict chemotherapy efficacy. Among them, the score of the low-risk group was related to the half-maximal IC₅₀ value of aminoimidazole carboxamide ribonucleotide and BI ($p < 0.001$). In addition, the high-risk

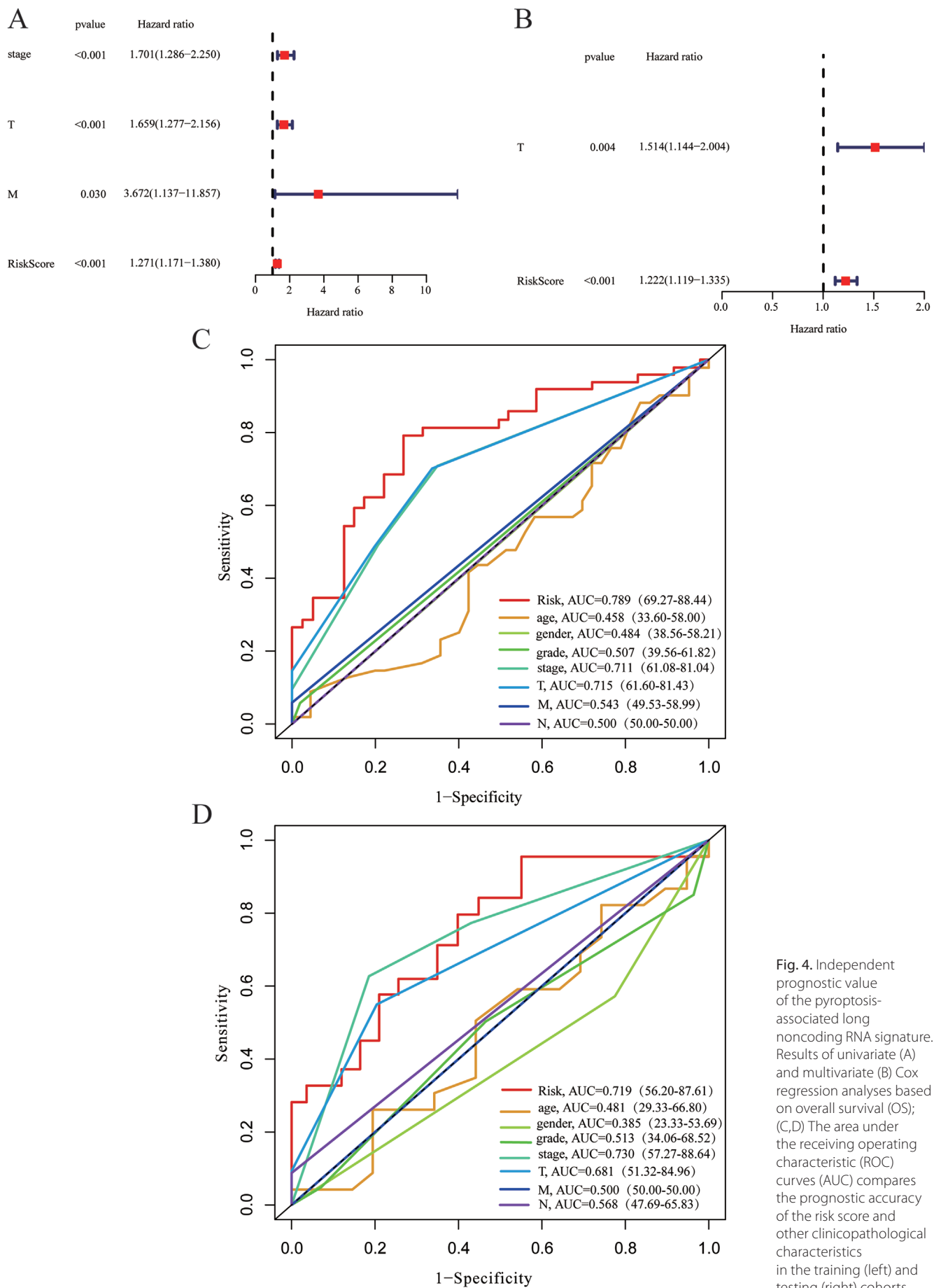


Fig. 4. Independent prognostic value of the pyroptosis-associated long noncoding RNA signature. Results of univariate (A) and multivariate (B) Cox regression analyses based on overall survival (OS); (C,D) The area under the receiving operating characteristic (ROC) curves (AUC) compares the prognostic accuracy of the risk score and other clinicopathological characteristics in the training (left) and testing (right) cohorts

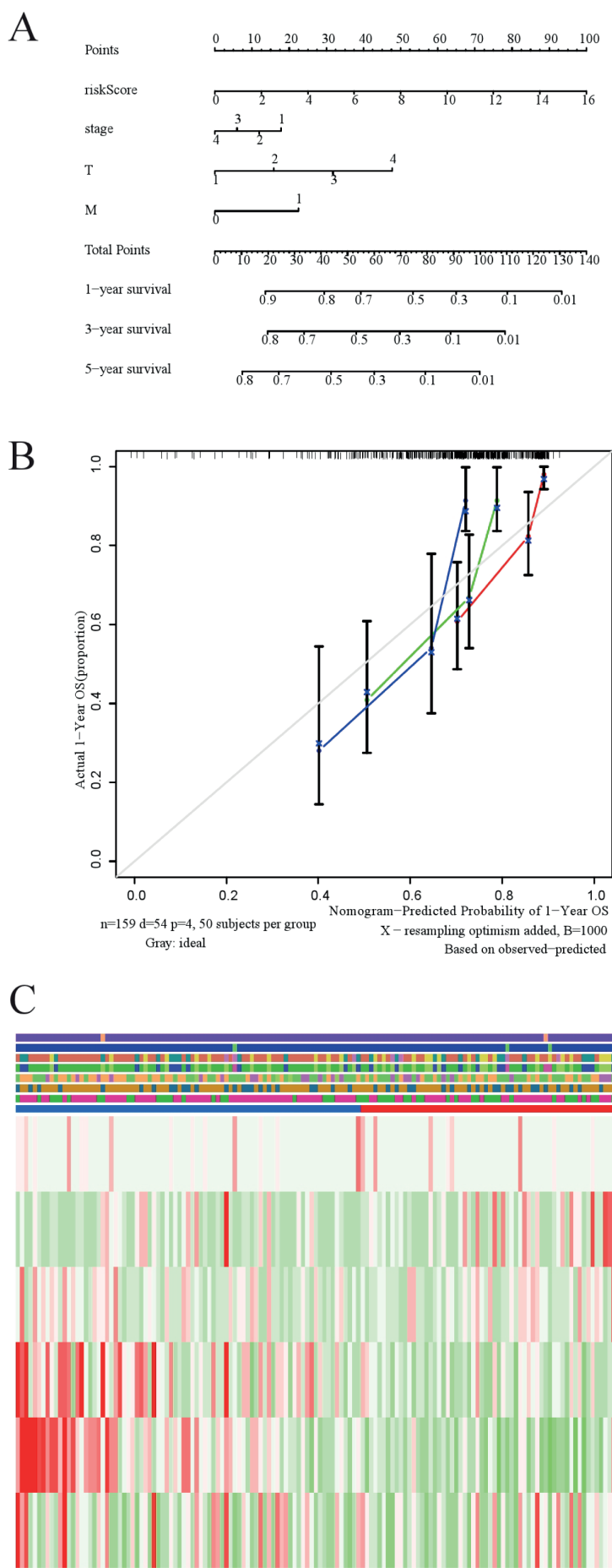


Fig. 5. Construction and validation of a nomogram to predict the overall survival (OS) of patients in the whole cohort. A. Nomogram was constructed based on the risk and clinical stage in the whole cohort; B. Calibration curve of the nomogram; C. Heatmap of clinicopathological features and expression of hub-long noncoding RNAs in the 2 risk subgroups

group scores were correlated with the IC₅₀ values of bortezomib, LFM-A13 and AKT inhibitors ($p < 0.001$). These results established that the lncRNA signal can predict the sensitivity to drugs in HCC (Supplementary Fig. 3B–I).

The differential immune cell composition and risk score values between the high- and low-risk groups were examined. Spearman's correlation analysis was performed using different algorithms. As shown in Fig. 6A, a lollipop-shape curve was obtained. Thus, we concluded that most immune cells were significantly and positively correlated with risk scores. Unanimously, compared with that in the low-risk group, the lncRNA signature in the high-risk group was mostly enhanced in immune-associated pathways. Thus, the prognostic PRlncRNA signature plays a critical role in predicting the tumor immune microenvironment, tumorigenesis and progression of HCC.

Additionally, we used distinctive algorithms in constructing the heatmap of immune responses, which is shown in Fig. 6B. The proportion of most immune cells (CD4⁺ T cells, type 2 helper cells, monocytes, resting mast cells, myeloid dendritic cells, and macrophages) in the high-risk group was higher than that in the low-risk group. Compared with those in the low-risk group, the expression levels of immune checkpoint molecules, including CD200, TNFSF9, CD200R1, and TNFRSF4, were upregulated in the high-risk group (Supplementary Fig. 4), indicating that the signature could predict the immunotherapy response in HCC patients. Thus, the PRlncRNA signature may indicate the pyroptosis status of HCC patients and reveal potential biomarkers for clinical therapeutic intervention.

Discussion

The etiology of various tumors, including HCC, is complex. However, hepatitis is a major etiological factor for HCC. Chronic inflammation can lead to dysplasia of liver cells, resulting in HCC. Pyroptosis-mediated inflammatory necrosis may be the key factor regulating tumor cell necrosis.²¹ To explore the role of pyroptosis in the development of HCC, this study examined the characteristics of PRlncRNAs and PRGs and the clinical prognosis of HCC and elucidated the factors related to immune cell dysfunction in HCC patients.

In this study, 6 lncRNAs (*'ELFN-AS1'*, *AC099850.3*, *AC073389.3*, *'HPN-AS1'*, *AC009283.1*, and *AL139289.1*) were selected and used to generate a risk signature. Additionally, a nomogram comprising the clinical stage and signature was constructed to predict the OS. Collectively, based on these findings, we concluded that this risk signature could be used to determine the prognosis of HCC patients and can be used to develop a staging system. The GSEA was performed to analyze the coordinated expression changes at the pathway levels. The PRlncRNA prognostic signature was correlated with tumor immunity and metabolism. The heatmap of immune cells generated using different algorithms and the expression status of ubiquitous immune

checkpoint molecules predicted the immunotherapy response of HCC. Thus, this study demonstrated a strong correlation between gene expression levels and OS. Six differentially expressed lncRNAs were identified as independent prognostic factors for HCC. Among these 6 lncRNAs, some were involved in tumor pathogenesis.

ELFN-AS1, an autophagy-related and immune-related lncRNA, can determine the HCC prognosis.^{22,23} *AC099850.3* knockdown can promote cell apoptosis by inhibiting the proliferation and metastasis potential of HCC cells. *AC099850.3*, which mediates its effects through the PI3K/AKT pathway, was positively correlated with key immune checkpoint molecules (PD-1, PD-L1, PD-L2, and CTLA4). Thus, *AC099850.3* is a potential immunotherapeutic target for HCC.²⁴ *HPN-AS1* can serve as a biomarker for hormone-related cancers, such as prostate, breast and renal clear cell cancers, as its expression level is significantly correlated with OS.²⁵ Additionally, *HPN-AS1* functions as a competitive endogenous RNA in HCC patients, and its expression is highly correlated with the tumor mutational burden. The role of *AC009283.1* in HCC has not yet been reported. However, *AC009283.1* is upregulated in the HER2-enriched cancer subtype. *AC009283.1* knockdown modulated the expression of 158 genes, which were enriched in various pathways, including those associated with proliferation, the cell cycle and apoptosis, such as *NOTCH3*, *TNFA*, and *FOSB*, which are reported to regulate proliferation and the cell cycle in cancer.²⁶ *AC009283.1* is also considered a ferroptosis-related lncRNA that demonstrates a regulatory role in the tumor microenvironment and immune cell infiltration in colon cancer. Thus, *AC009283.1* may aid in determining the prognosis and devising a personalized treatment for colon cancer patients.²⁷ However, the exact mechanisms of *AC009283.1* have not been elucidated. Additionally, the oncogenic roles of *AC073389.3* and *AL139289.1* have not been reported.

From the existing data, it appears that the underlying mechanism by which lncRNAs mediate the pathogenesis of multiple tumors is through the regulation of microRNAs that modulate proteins related to the pyroptosis signaling pathway. Furthermore, the indirect role of lncRNAs in the regulation of pyroptosis can also contribute to the development of tumors. Knockdown of *RP1-85F18.6*, a newly identified lncRNA with upregulated expression in colorectal cancer tissues, can promote the pyroptosis of colorectal cancer cells by cleaving GSDMD.²⁸ By contrast, *XLOC_000647* (an intergenic lncRNA located on chromosome 1) overexpression suppressed the proliferation, invasion and endothelial–mesenchymal transition in pancreatic cancer cells by downregulating *NRLP3*.²⁹ These findings indicate that lncRNAs have contrasting roles in pyroptosis in different cancers. Nonetheless, within the scope of HCC, Li et al.³⁰ developed a pyroptosis score using principal component analysis to uncover the association between pyroptosis and tumor immunity in individuals with hepatitis B virus-associated HCC. Their research demonstrated that patients

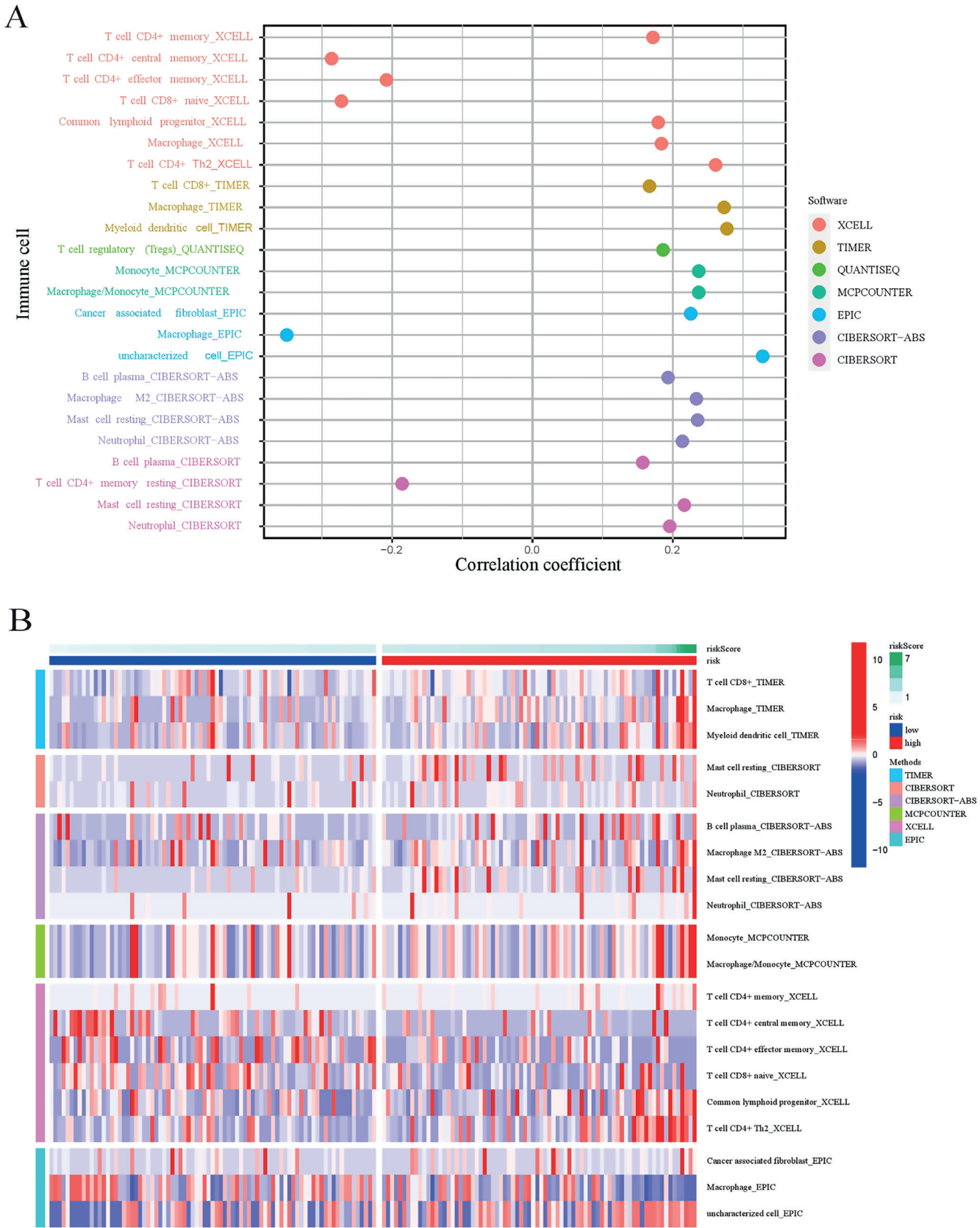


Fig. 6. A. Detailed Spearman's correlation analysis was performed using different algorithms; B. The heatmap of immune responses, generated using different algorithms, among the high- and low-risk groups

with higher pyroptosis scores had a worse prognosis but were more responsive to anti-PD-L1 treatment.

Our study has revealed significant correlations between the signature and numerous immune-associated signaling pathways. Patients with higher risk scores exhibit elevated expression levels of various immune checkpoints, such as CD200, TNFSF9, CD200R1, and TNFRSF4. CD200 and its receptor, CD200R, play a crucial role in the immune system,³¹ where the CD200R pathway can lead to immune tolerance and inhibit immune function in patients with HCC.³² Huang et al. conducted a study to investigate the impact of the CD200/CD200R pathway on CD4⁺ T cell subsets in patients with HCC and evaluated the effect of thermal ablation on HCC in rats.³³ Furthermore, TNFSF9 represents a potential novel tumor suppressor and therapeutic target for HCC. Activating TNFSF9 signaling could not only serve as a promising adjuvant strategy for immunomodulation therapy but also have a direct inhibitory effect on HCC.³⁴ And based on their findings, TNFRSF4 indeed has a simultaneous impact on both immune cell infiltration and the frequency of gene mutations in HCC.³⁵ Thus, further studies are needed to examine the roles of pyroptosis and lncRNAs in HCC.

Pyroptosis, a newly discovered method of cell death, has dual consequences on tumors. On one hand, key inflammatory bodies in pyroptosis can promote tumor cell death and inhibit the proliferation and metastasis of tumor cells. On the other hand, the accumulation of inflammasomes can create a microenvironment that is conducive to tumor cell growth, proliferation and metastasis. This study aimed to integrate several lncRNA biomarkers to determine their impact on patient outcomes, which could aid in the identification of novel biomarkers and precise therapeutic targets in HCC. Furthermore, the study has the potential to assist in the prognostic prediction, diagnosis and management strategies for HCC patients. However, it is crucial to conduct further independent studies to confirm the results of lncRNAs associated with predictive apoptosis. Although the study explored the potential of developing a prognostic model, further improvement is necessary.

Limitations

This study has some limitations. Currently, lncRNAs have not been utilized as therapeutic targets.³⁶ Our study is established principally on bioinformatics, based on a small number of HCC cases from the TCGA database and limited clinical data; therefore, the results may be biased to a certain extent. The role of pyroptosis RNA in HCC needs to be further validated in clinical practice.

Conclusions

The findings of this study further elucidate the role of PRGs in HCC progression. The establishment of a prognostic model and elucidation of the role of the PRlncRNA

signature in immunotherapy response will aid future studies on HCC molecular pathology. Detailed studies will help elucidate the regulatory mechanisms of PRlncRNAs in the pyroptosis pathway of HCC cells. In vivo, modification of lncRNAs using novel therapies is a potential strategy for determining the diagnosis, treatment and prognosis in HCC patients.

Supplementary data

The Supplementary materials are available at <https://doi.org/10.5281/zenodo.11638461>. The package includes the following files:

Supplementary Table 1. Clinicopathological characteristics of 377 HCC patients.

Supplementary Fig. 1. Identification of the clusters based on expression levels of 721 differentially expressed pyroptosis-related lncRNAs. A. Three clusters were identified using the unsupervised clustering method. B. The heatmap of the top 231 lncRNAs.

Supplementary Fig. 2. Risk survival status chart of TCGA-HCC cohort. The risk survival status plot of patients in the training (A) and testing cohorts (B). Survival outcomes of the patients in the training (C) and testing cohorts (D). Heatmap of the expression of 6 pyroptosis-related lncRNAs in the training (E) and testing (F) cohorts.

Supplementary Fig. 3. GSEA and IC50 values of chemotherapeutic drugs between the high- and low-risk groups based on the pyroptosis-related lncRNA signature in TCGA-HCC cohort. A. GSEA results suggested that the differentially expressed lncRNAs in 2 risk groups were mainly enriched in the tumor-related, immune-related and metabolism-related pathways. B–I Comparative analysis of the IC50 values of chemotherapeutics between the high- and low-risk groups.

Supplementary Fig. 4. Expression levels of immune checkpoints between high- and low-risk groups in patients with HCC.

Data availability


The datasets generated and/or analyzed during the current study are available from the corresponding author on reasonable request.

Consent for publication

Not applicable.

ORCID iDs

Shaohua Xu  <https://orcid.org/0000-0003-4050-5532>

Guoxu Fang  <https://orcid.org/0000-0002-4832-7462>

References

1. Sung H, Ferlay J, Siegel RL, et al. Global Cancer Statistics 2020: GLOBOCAN estimates of incidence and mortality worldwide for 36 cancers in 185 countries. *CA Cancer J Clin.* 2021;71(3):209–249. doi:10.3322/caac.21660

2. Demir T, Lee SS, Kaseb AO. Systemic therapy of liver cancer. *Adv Cancer Res.* 2021;149:257–294. doi:10.1016/bs.acr.2020.12.001
3. Villanueva A. Hepatocellular carcinoma. *N Engl J Med.* 2019;380(15):1450–1462. doi:10.1056/NEJMra1713263
4. Zongyi Y, Xiaowu L. Immunotherapy for hepatocellular carcinoma. *Cancer Lett.* 2020;470:8–17. doi:10.1016/j.canlet.2019.12.002
5. Yau T, Park JW, Finn RS, et al. CheckMate 459: A randomized, multi-center phase III study of nivolumab (NIVO) vs sorafenib (SOR) as first-line (1L) treatment in patients (pts) with advanced hepatocellular carcinoma (aHCC). *Ann Oncol.* 2019;30:v874–v875. doi:10.1093/annonc/mdz394.029
6. Kelley RK, Sangro B, Harris W, et al. Safety, efficacy, and pharmacodynamics of tremelimumab plus durvalumab for patients with unresectable hepatocellular carcinoma: Randomized expansion of a phase I/II study. *J Clin Oncol.* 2021;39(27):2991–3001. doi:10.1200/JCO.20.03555
7. Statello L, Guo CJ, Chen LL, Huarte M. Gene regulation by long non-coding RNAs and its biological functions. *Nat Rev Mol Cell Biol.* 2021;22(2):96–118. doi:10.1038/s41580-020-00315-9
8. Bhan A, Soleimani M, Mandal SS. Long noncoding RNA and cancer: A new paradigm. *Cancer Res.* 2017;77(15):3965–3981. doi:10.1158/0008-5472.CAN-16-2634
9. Cai J, Yang F, Chen X, Huang H, Miao B. Signature panel of 11 methylated mRNAs and 3 methylated lncRNAs for prediction of recurrence-free survival in prostate cancer patients. *Pharmgenomics Pers Med.* 2021;14:797–811. doi:10.2147/PGPM.S312024
10. Yang C, Shen C, Feng T, Li H. Noncoding RNA in NK cells. *J Leukoc Biol.* 2018;105(1):63–71. doi:10.1002/JLB.1RU0518-197RR
11. Nie Y, Li J, Wu W, et al. A novel nine-lncRNA risk signature correlates with immunotherapy in hepatocellular carcinoma. *Front Oncol.* 2021;11:706915. doi:10.3389/fonc.2021.706915
12. Magna M, Pisetsky DS. The role of HMGB1 in the pathogenesis of inflammatory and autoimmune diseases. *Mol Med.* 2014;20(1):138–146. doi:10.2119/molmed.2013.00164
13. Johnson DC, Taabazuing CY, Okondo MC, et al. DPP8/DPP9 inhibitor-induced pyroptosis for treatment of acute myeloid leukemia. *Nat Med.* 2018;24(8):1151–1156. doi:10.1038/s41591-018-0082-y
14. So D, Shin HW, Kim J, et al. Cervical cancer is addicted to SIRT1 disarming the AIM2 antiviral defense. *Oncogene.* 2018;37(38):5191–5204. doi:10.1038/s41388-018-0339-4
15. Wei Q, Zhu R, Zhu J, Zhao R, Li M. E2-induced activation of the NLRP3 inflammasome triggers pyroptosis and inhibits autophagy in HCC cells. *Oncol Res.* 2019;27(7):827–834. doi:10.3727/096504018X15462920753012
16. Aachoui Y, Sagulenko V, Miao EA, Stacey KJ. Inflammasome-mediated pyroptotic and apoptotic cell death, and defense against infection. *Curr Opin Microbiol.* 2013;16(3):319–326. doi:10.1016/j.mib.2013.04.004
17. Wang Y, Gao W, Shi X, et al. Chemotherapy drugs induce pyroptosis through caspase-3 cleavage of a gasdermin. *Nature.* 2017;547(7661):99–103. doi:10.1038/nature22393
18. He D, Zheng J, Hu J, Chen J, Wei X. Long non-coding RNAs and pyroptosis. *Clin Chim Acta.* 2020;504:201–208. doi:10.1016/j.cca.2019.11.035
19. Li L, Jiang M, Qi L, et al. Pyroptosis, a new bridge to tumor immunity. *Cancer Sci.* 2021;112(10):3979–3994. doi:10.1111/cas.15059
20. Tsuchiya K. Switching from apoptosis to pyroptosis: Gasdermin-elicited inflammation and antitumor immunity. *Int J Mol Sci.* 2021;22(1):426. doi:10.3390/ijms22010426
21. Xia X, Wang X, Cheng Z, et al. The role of pyroptosis in cancer: Pro-cancer or pro-“host”? *Cell Death Dis.* 2019;10(9):650. doi:10.1038/s41419-019-1883-8
22. Jia Y, Chen Y, Liu J. Prognosis-predictive signature and nomogram based on autophagy-related long non-coding RNAs for hepatocellular carcinoma. *Front Genet.* 2020;11:608668. doi:10.3389/fgene.2020.608668
23. Polev DE, Karnaukhova IK, Krukovskaya LL, Kozlov AP. *ELFN1-AS1*: A novel primate gene with possible microRNA function expressed predominantly in human tumors. *Biomed Res Int.* 2014;2014:398097. doi:10.1155/2014/398097
24. Zhong F, Liu S, Hu D, Chen L. lncRNA AC099850.3 promotes hepatocellular carcinoma proliferation and invasion through PRR11/PI3K/AKT axis and is associated with patients prognosis. *J Cancer.* 2022;13(3):1048–1060. doi:10.7150/jca.66092
25. Wang D, Li M, Li J, et al. Comprehensive characterization of androgen-responsive lncRNAs mediated regulatory network in hormone-related cancers. *Dis Markers.* 2020;2020:8884450. doi:10.1155/2020/8884450
26. Cedro-Tanda A, Ríos-Romero M, Romero-Córdoba S, et al. A lncRNA landscape in breast cancer reveals a potential role for AC009283.1 in proliferation and apoptosis in HER2-enriched subtype. *Sci Rep.* 2020;10(1):13146. doi:10.1038/s41598-020-69905-z
27. Chen W, Chen Y, Liu L, et al. Comprehensive analysis of immune infiltrates of ferroptosis-related long noncoding RNA and prediction of colon cancer patient prognoses. *J Immunol Res.* 2022;2022:9480628. doi:10.1155/2022/9480628
28. Ma Y, Chen Y, Lin C, Hu G. Biological functions and clinical significance of the newly identified long non-coding RNA RP1-85F18.6 in colorectal cancer. *Oncol Rep.* 2018;40(5):2648–2665. doi:10.3892/or.2018.6694
29. Hu H, Wang Y, Ding X, et al. Long non-coding RNA XLOC_000647 suppresses progression of pancreatic cancer and decreases epithelial-mesenchymal transition-induced cell invasion by down-regulating NLRP3. *Mol Cancer.* 2018;17(1):18. doi:10.1186/s12943-018-0761-9
30. Li J, Yu J, Zhang T, Pu X, Li Y, Wu Z. Genomic analysis quantifies pyroptosis in the immune microenvironment of HBV-related hepatocellular carcinoma. *Front Immunol.* 2022;13:932303. doi:10.3389/fimmu.2022.932303
31. Wang L, Yan C, Zhao Y, Chu J, Yu X. Reduced CD 200 and CD 200R1 expression in human chorionic villi contributes to early spontaneous abortion. *Acta Obstet Gynecol Scand.* 2014;93(12):1248–1254. doi:10.1111/aogs.12476
32. Clark DA. Fgl2 prothrombinase expression in mouse trophoblast and decidua triggers abortion but may be countered by OX-2. *Mol Hum Reprod.* 2001;7(2):185–194. doi:10.1093/molehr/7.2.185
33. Huang S, Pan Y, Zhang Q, Sun W. Role of CD200/CD200R signaling pathway in regulation of CD4⁺ T cell subsets during thermal ablation of hepatocellular carcinoma. *Med Sci Monit.* 2019;25:1718–1728. doi:10.12659/MSM.913094
34. Shen YL, Gan Y, Gao HF, et al. TNFSF9 exerts an inhibitory effect on hepatocellular carcinoma. *J Digest Dis.* 2017;18(7):395–403. doi:10.1111/1751-2980.12489
35. Wang D, Hu H, Ding H, Zhao H, Tian F, Chi Q. Elevated expression of TNFRSF4 impacts immune cell infiltration and gene mutation in hepatocellular carcinoma. *Cancer Biomark.* 2023;36(2):147–159. doi:10.3233/CBM-210538
36. Yu SY, Tang L, Zhou SH. Long noncoding RNAs: New players in ischaemia-reperfusion injury. *Heart Lung Circ.* 2018;27(3):322–332. doi:10.1016/j.hlc.2017.09.011

Endocardial lead insulation wear in a scanning and optical microscope

Mateusz Ulman^{1,A–D}, Krzysztof Boczar^{1,A–C,E}, Katarzyna Holcman^{2,3,B},
Magdalena Ziąbka^{4,B,C}, Maciej Dębski^{5,B–D}, Jacek Lelakowski^{1,3,F}, Andrzej Ząbek^{1,3,A,C,E,F}

¹ Department of Electrophysiology, The John Paul II Hospital, Cracow, Poland

² Department of Cardiac and Vascular Diseases, The John Paul II Hospital, Cracow, Poland

³ Institute of Cardiology, Jagiellonian University Medical College, Cracow, Poland

⁴ Department of Ceramics and Refractories, Faculty of Materials Science and Ceramics, AGH University, Cracow, Poland

⁵ Norwich Medical School, University of East Anglia, UK

A – research concept and design; B – collection and/or assembly of data; C – data analysis and interpretation;

D – writing the article; E – critical revision of the article; F – final approval of the article

Advances in Clinical and Experimental Medicine, ISSN 1899–5276 (print), ISSN 2451–2680 (online)

Adv Clin Exp Med. 2025;34(4):597–604

Address for correspondence

Krzysztof Boczar

E-mail: krzysiek.boczar@gmail.com

Funding sources

This article was supported by the science fund of the St. John Paul II Hospital, Cracow, Poland (grant No. FN/04/2024 to Mateusz Ulman).

Conflict of interest

None declared

Received on January 13, 2024

Reviewed on March 4, 2024

Accepted on April 5, 2024

Published online on June 27, 2024

Abstract

Background. The path and interaction of leads within the cardiovascular system are influenced by various factors, including the implantation technique. Furthermore, the multifaceted composition of these leads, often comprising multiple materials, can contribute to their potential degradation and wear over time.

Objectives. Our aim was to investigate the wear of lead insulation following the removal of transvenous leads and pinpoint the regions of the lead most vulnerable to damage.

Materials and methods. We undertook a prospective analysis of patients from a single tertiary center who underwent transvenous lead explantation (TLE) between October 1, 2013, and July 31, 2015. Specifically, our examination focused on endocardial leads removed using simple screw-out and gentle traction techniques. Subsequent lead evaluations were conducted utilizing scanning electron and optical microscopes.

Results. Among the 86 patients who underwent the TLE procedure, 26 patients (30%) required the removal of 39 leads through simple traction. Inspection using scanning electron microscopy consistently indicated insulation damage across all leads. A total of 347 damaged sites were identified: 261 without lead unsealing and 86 exhibiting unsealing. Notably, the sections of the leads located within the intra-pocket area demonstrated the highest vulnerability to damage (odds ratio (OR): = 9.112, 95% confidence interval (95% CI): 3.326–24.960), whereas the intravenous regions displayed the lowest susceptibility (OR: 0.323, 95% CI: 0.151–0.694).

Conclusions. Our study reveals that all evaluated leads exhibited insulation damage, with the intra-pocket segments manifesting a notably higher prevalence of damage than the intravenous segments.

Key words: endocardial leads insulation, microscope analysis, simple traction, transvenous lead explantation, fatigue wear of endocardial leads

Cite as

Ulman M, Boczar K, Holcman K, et al. Endocardial lead insulation wear in a scanning and optical microscope.

Adv Clin Exp Med. 2025;34(4):597–604.

doi:10.17219/acem/186864

DOI

10.17219/acem/186864

Copyright

Copyright by Author(s)

This is an article distributed under the terms of the Creative Commons Attribution 3.0 Unported (CC BY 3.0) (<https://creativecommons.org/licenses/by/3.0/>)

Background

Endocardial leads are comprised of multiple components: an electrode, conductor, insulation, and connector pin. Functionally, these leads are classified into pacing (permanent pacemaker (PPM)) and defibrillating (implantable cardioverter-defibrillator (ICD)) categories.

The conductor, found universally in these leads, consists of 1 or more wires that can be coiled into helices or woven into cables. In current clinical lead models, the coil's filament count for a single electrode ranges from 1 to 8. Typically, these conductor coils and cables are made of a MP35N alloy (Fort Wayne Metals, Fort Wayne, USA), valued for its mechanical strength and resistance to chemical corrosion.¹

These conductor elements are encased in a polymer insulation layer that serves a dual role: It provides both physical and electrical isolation for the lead components. While the outer insulation shield protects against external tissue interactions, the internal insulation ensures inter-component isolation.^{2,3}

Additionally, the insulation layers play a crucial role in maintaining the lead's structural integrity. They also aid in transmitting torque and tension during lead implantation and subsequent explantation. Commonly used insulation materials include silicone (polydimethylsiloxane), polyurethane (often types 55D and 80A), fluoropolymers (typically ETFE), and silicone-polyurethane copolymers.^{4,5}

Medtronic (Medtronic, Dublin, Ireland) leads, like the CapSureFix Novus and Attain Ability+, demonstrate a layered insulation structure. They are comprised of an external layer of 55D polyurethane for tissue contact and an internal silicone layer for conductor isolation. In contrast, Medtronic DF leads, such as the Sprint Quattro, possess a more complex insulation system with multiple layers of ETFE and PTFE.⁶ Vitatron (Vitatron, Maastricht, the Netherlands) electrodes (Crystalline ICF 09B) are characterized by a single silicone insulation layer,⁷ while Biotronik (Biotronik, Berlin, Germany) offers dual-layer (Siello S, Solia S) or single-layer (Setrox S) insulation options.⁸

Previous studies have reported that around 25% of removed endocardial leads exhibit insulation damage.^{9,10} Additionally, isolated cases of insulation damage have been noted even in single-lead pacing systems without inter-lead interactions.¹¹

Material fatigue processes have been more widely researched since the 1960s.¹² While existing literature touches upon the wear of leads,^{3,9–11,13–18} there is a gap in understanding the specific types of damage to the outer insulation near the generator pocket. This study seeks to explore the role of fatigue mechanisms in shaping wear patterns on intracardiac electrodes.

Objectives

This study aims to conduct a comprehensive qualitative and quantitative assessment of fatigue wear on lead

insulation, focusing specifically on the 4 distinct anatomical regions of leads explanted via simple traction.

Materials and methods

Study design and setting

This study adopted a prospective approach, focusing on patients who underwent transvenous lead extraction (TLE) at a tertiary cardiac center (Department of Electrophysiology at St. John Paul II Hospital, Cracow, Poland) between October 1, 2013, and July 31, 2015. The study specifically targeted patients whose leads were removed using only simple screw-out methods and gentle traction to ensure no inadvertent damage to the lead.

Participants

Ethical clearance was secured from the Research and Ethics Committee of the Jagiellonian University, Cracow, Poland (decision No. KBET/259/B/2011). Every participant provided written informed consent for the use of their anonymized data in this study. The research strictly adhered to the 1975 Declaration of Helsinki and World Health Organization (WHO) Good Clinical Practice guidelines.

Data collection

The dataset incorporated:

- Patient's baseline information: birth date and gender.
- Clinical profile: information on diabetes mellitus, height, weight, and age during the TLE.
- Lead specifications: dwell-time, lead model, manufacturer (Medtronic, Vitatron and Biotronik), and specific model details.
- Lead performance parameters: threshold, sensing and impedance.

The study contrasted the patterns of insulation damage among 4 indications for TLE: lead dysfunction, dislocation, lead-dependent infective endocarditis (LDIE), and pocket infections.

Evaluation techniques

Electrode positioning was determined pre-extraction using chest X-rays (CXR). Lead lengths across the intracardiac, intravenous, subclavian, and intra-pocket regions were derived from these X-rays. Post-extraction, leads underwent detailed microscopic analysis. Lead segments were sectioned into 2-cm intervals and examined under an optical microscope (Nikon Corp., Tokyo, Japan). Further evaluations utilized a scanning electron microscope (SEM; Nova Nano SEM 200; FEI Europe B.V., Eindhoven, the Netherlands) combined with an energy dispersive X-ray (EDX) detector for microstructural and chemical assessments

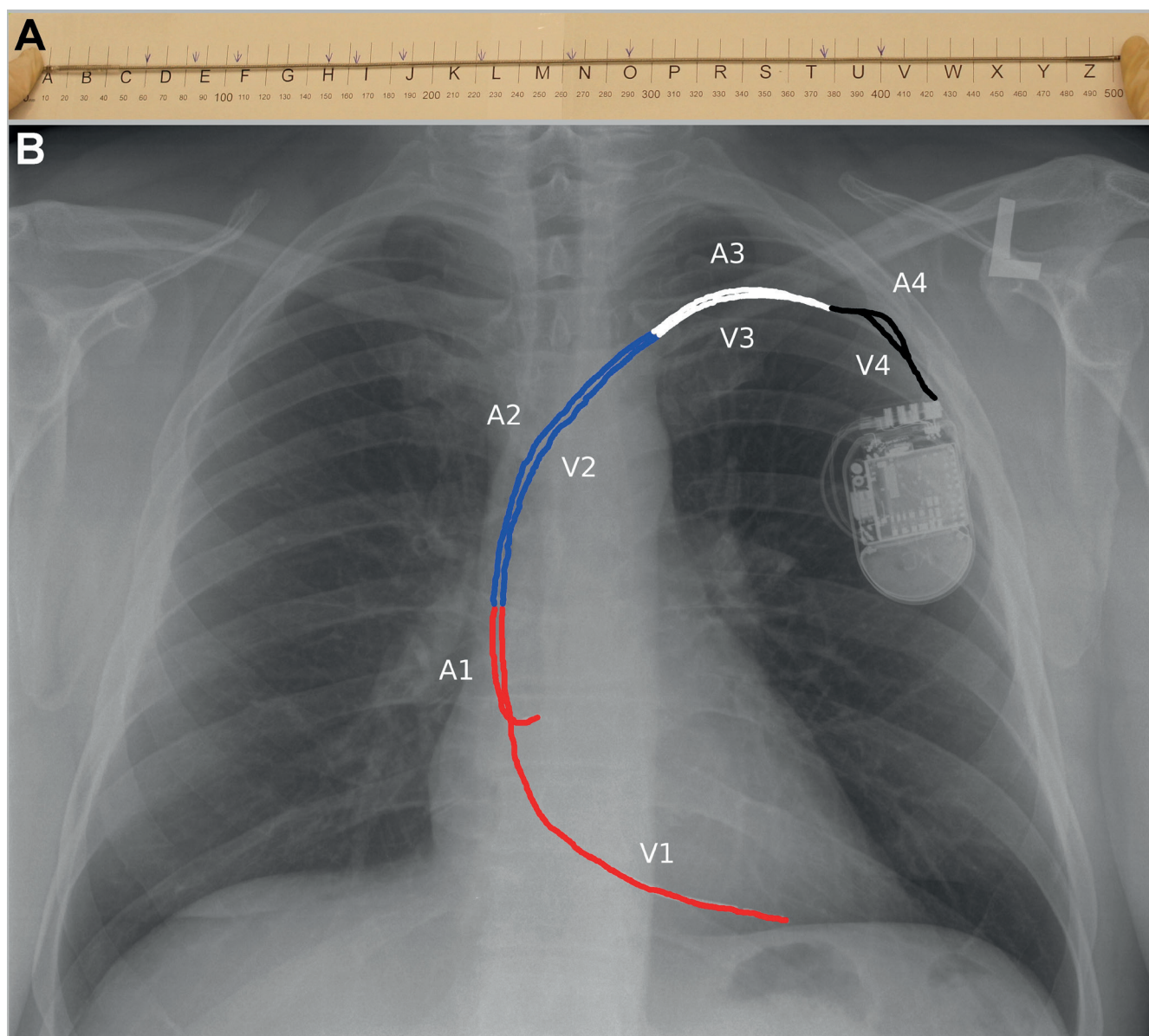


Fig. 1. Measuring the location of the lesion. A. The analyzed leads were divided into 2-cm sections. The small arrows at the top of the ruler indicate the locations of destruction; B. Chest X-ray – posteroanterior projection; A – atrial lead; V – ventricular lead; 1 – the intracardiac region, 2 – the intravenous region, 3 – the subclavian region, 4 – the intra-pocket region; the section length measurement was made using the Digital Imaging and Communications in Medicine (DICOM) system; the invisible part of the electrode belongs to the intra-pocket region

(Fig. 1). A comparative analysis was also conducted using brand-new lead models.

The study methodically assessed outer lead insulation wear across these anatomical regions, categorizing damage types based on lead unsealing. Additionally, correlations between damage pattern variables like lead make, manufacturer and insulation material were explored.

Statistical analyses

Data were analyzed using IBM SPSS Statistics v. 24.0 (IBM Corp., Armonk, USA). Descriptive statistics depicted data distributions, while appropriate tests determined comparisons between continuous and categorical variables. Continuous variables were tested for normal

distribution with the use of the Kolmogorov–Smirnov test and compared using Student’s t-test or the Mann–Whitney U test, depending on the data distribution. Spearman’s rank correlations assessed relationships, and uni- and multivariable logistic regression models unveiled predictors of lead damage, represented as odds ratios (ORs) with a 95% confidence interval (95% CI). A p-value <0.05 was deemed significant for all analyses.

Results

A total of 86 consecutive patients underwent the TLE procedure. Among these, 26 patients (30%) had 39 leads extracted using simple traction, with 11 (42%) being female.

Table 1. Types of the leads

Manufacturer	Model	Localization	Outer insulation material	Number of leads
Medtronic	CapSureFix Novus 52 cm	atrial	polyurethane 55D	11
Medtronic	CapSureFix Novus 58 cm	ventricular	polyurethane 55D	6
Medtronic	Sprint Quattro 65 cm	ventricular, ICD	polyurethane 55D, 80A	2
Medtronic	Attain Ability+ 88 cm	coronary sinus	polyurethane 55D	2
Biotronik	Selox JT	atrial	silicone	2
Biotronik	Selox ST	ventricular	silicone	1
Biotronik	Setrox S53	atrial	silicone	1
Biotronik	Setrox S60	ventricular	silicone	5
Biotronik	Siello S53	atrial	polyurethane	1
Biotronik	Siello S60	ventricular	polyurethane	1
Biotronik	Solia S53	atrial	polyurethane	1
Biotronik	Solia S60	ventricular	polyurethane	1
Vitatron	Crystalline 52 cm	atrial	silicone MED 4719	3
Vitatron	Crystalline 58 cm	ventricular	silicone MED 4719	2

ICD – implantable cardioverter-defibrillator.

On average (\pm standard deviation (\pm SD)) the examined patients had 2.15 (0.6) electrodes implanted prior to the TLE procedure. Distribution among lead manufacturers was as follows: Medtronic 54%, Biotronik 33% and Vitatron 13%.

The average (\pm SD) age at initial cardiac implantable electronic device (CIED) implantation was 68.2 (\pm 10.4) years, with a median of 70.6 and an interquartile range (IQR) of 17.0. By the time of the TLE procedure, the patient's mean (\pm SD) age was 71.2 (\pm 10.0) years, with a median of 75.3 and an IQR of 19.3. The lead's mean age was 35.8 (\pm 21.4) months, with a median of 27.8 and an IQR of 37.1. The range for lead dwell-time spanned from 18 days to 76.9 months. The mean body mass index (BMI) recorded was 29.8 (\pm 4.4), with a median identical to the mean and an IQR of 7.6. Diabetes mellitus was present in 12 patients (46.2%).

Among the leads extracted, 18 (46.2%) were for malfunctioning, 7 (17.9%) were dislocated, 4 (10.3%) were due to LDIE, and 10 (25.6%) were due to local infections. A detailed division is provided in Table 1. All analyzed leads were bipolar, categorized as 19 (48.7%) atrial leads, 16 (41%) right ventricular pacing leads, 2 (5.1%) implantable cardioverter defibrillator leads, and 2 (5.1%) left ventricular leads.

Scanning electron microscopy examinations identified lead insulation damage across all samples (Fig. 2,3). A total of 347 instances of lead damage were recorded: 261 (75.2%) without unsealing and 86 (24.8%) with unsealing. Damage was predominantly observed at the intra-pocket (56.2%) and subclavian (18.2%) regions, while the intracardiac (17.0%) and intravenous (8.6%) regions showed lesser damage. A detailed division of electrode defects is outlined in Table 2.

Table 3 presents the correlation between selected variables and lead damage, with or without unsealing. The univariable analysis incorporated factors such as lead region, type, age of the patient and electrode, gender, diabetes

Table 2. Localization and types of damage of endocardial leads

Localization of damage	Damage of lead insulation with the absence of unsealing	Damage of lead insulation with the presence of unsealing
Number of damage over the entire length of all electrodes*, n (%)	261 (75.2)	86 (24.8)
Intracardiac region, n (number of damage/cm)	49 (0.0864)	10 (0.0176)
Intravenous region, n (number of damage/cm)	27 (0.0372)	3 (0.0041)
Subclavian region, n (number of damage/cm)	46 (0.1474)	17 (0.0545)
Intra-pocket region, n (number of damage/cm)	139 (0.1463)	56 (0.0589)

*excluding anchoring sleeve location.

status, BMI, insulation material, TLE indications, and manufacturer. Significantly, the intra-pocket region of the lead (OR: 9.112, 95% CI: 3.326–24.960), use of Vitatron leads (OR: 2.913, 95% CI: 1.002–8.463) and an extended dwell-time (OR: 1.018 per 1-month, 95% CI: 1.002–1.034) were notable predictors for lead damage without unsealing.

During multivariable analysis, these predictors remained significant. The intra-pocket lead region (OR: 9.740, 95% CI: 2.856–33.219), Vitatron leads (OR 3.438, 95% CI: 1.111–10.641) and older electrode age (OR: 1.031 per 1-month, 95% CI: 1.010–1.054) were especially noteworthy. The amount of lead damage over time is presented in Fig. 4.

While the intravenous region showed minimal damage during the univariable analysis (OR: 0.323, 95% CI: 0.151–0.694), its significance waned during the multivariable assessment.

For leads exhibiting unsealing, only the intra-pocket region (OR: 4.844, 95% CI: 1.595–14.708) and lead dysfunction (OR: 6.096, 95% CI: 1.386–26.819) retained significance during multivariable analysis. Vitatron's influence approached significance (OR: 2.454, 95% CI: 0.937–6.427). Notably, the intravenous region emerged with the least amount of damage in the context of unsealing (OR: 0.186, 95% CI: 0.044–0.771). Further details are available in Table 3.

Discussion

One of the principal observations of our investigation is the pronounced onset of fatigue wear in endocardial leads. This wear manifests remarkably early, emerging within the initial weeks following the implantation of CIEDs, and is consistently evident across all evaluated leads. The initiation and propagation of lead cracks are not confined to specific locations but extend throughout the entire length of the endocardial lead wherever it interfaces with the valve apparatus, veins, connective tissue, or the device itself. The wear progression initiates with fatigue wear, primarily targeting the lead's insulation. A critical consideration is the insulation's thickness; inadequately robust or excessively thin insulations can precipitate lead unsealing due to cyclic stress. This fatigue wear is instigated by the repeated bending of the pacing lead external insulation layer by the surrounding tissues.^{19–21} Notably, the genesis of initial electrode impairment is localized at the Bielayev's point, a region subjected to maximal stresses. This phenomenon is further accentuated when the lead's surface remains unblemished. Over time, these microscopic fissures have the propensity to amalgamate, culminating in the emergence of a “macro crack”, which can subsequently propagate, resulting in the stratification and disintegration of the polymer insulation.²¹

In our investigation, a statistically significant predominance of damage was discerned within the intra-pocket region, juxtaposed with diminished damage

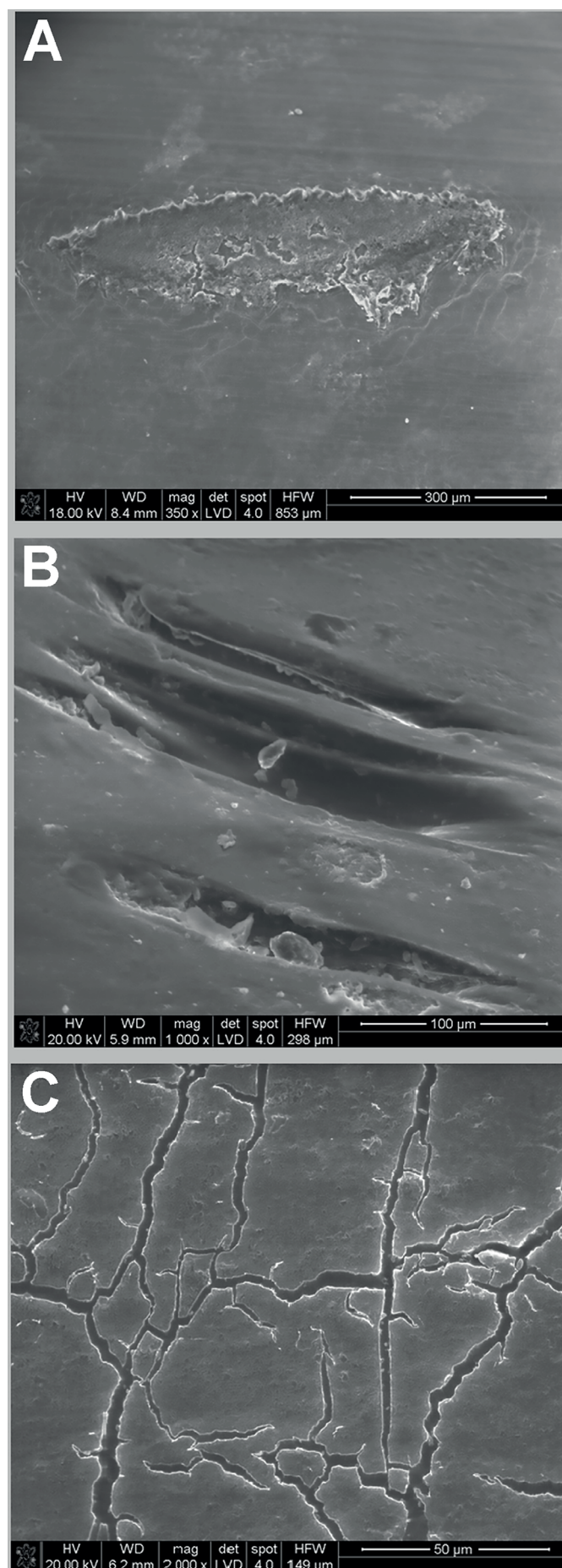


Fig. 2. Scanning electron microscopy (SEM) images. Examples of damage to the lead insulation with the absence of unsealing. Visible polishing of the insulation surface resulting from friction contact. A. Bipolar active-fixation atrial Medtronic CapSureFix Novus lead (lead insulation composed of 2 layers: outer – polyurethane 55D, contacting the surrounding tissues, and inner – silicone, adhering to the metal wire) with a 1-year dwell time in the defibrillator with cardiac resynchronization therapy (CRT-D) device. Indication for removal: dislocation of lead. Destruction at the right atrium level near the entrance to the tricuspid valve; B. Bipolar active-fixation ventricular Biotronik Setrox lead (insulation: only silicone) with a 5-year dwell time in the dual-chamber atrioventricular pacing (DDD) pacemaker device. Indication for removal: lead damage. Destruction at the level of the subclavian region; C. Bipolar active-fixation atrial Biotronik Setrox lead with a 2-year dwell time in the DDD pacemaker device. Indication for removal: pocket infection. Destruction at the level of the intra-pocket region

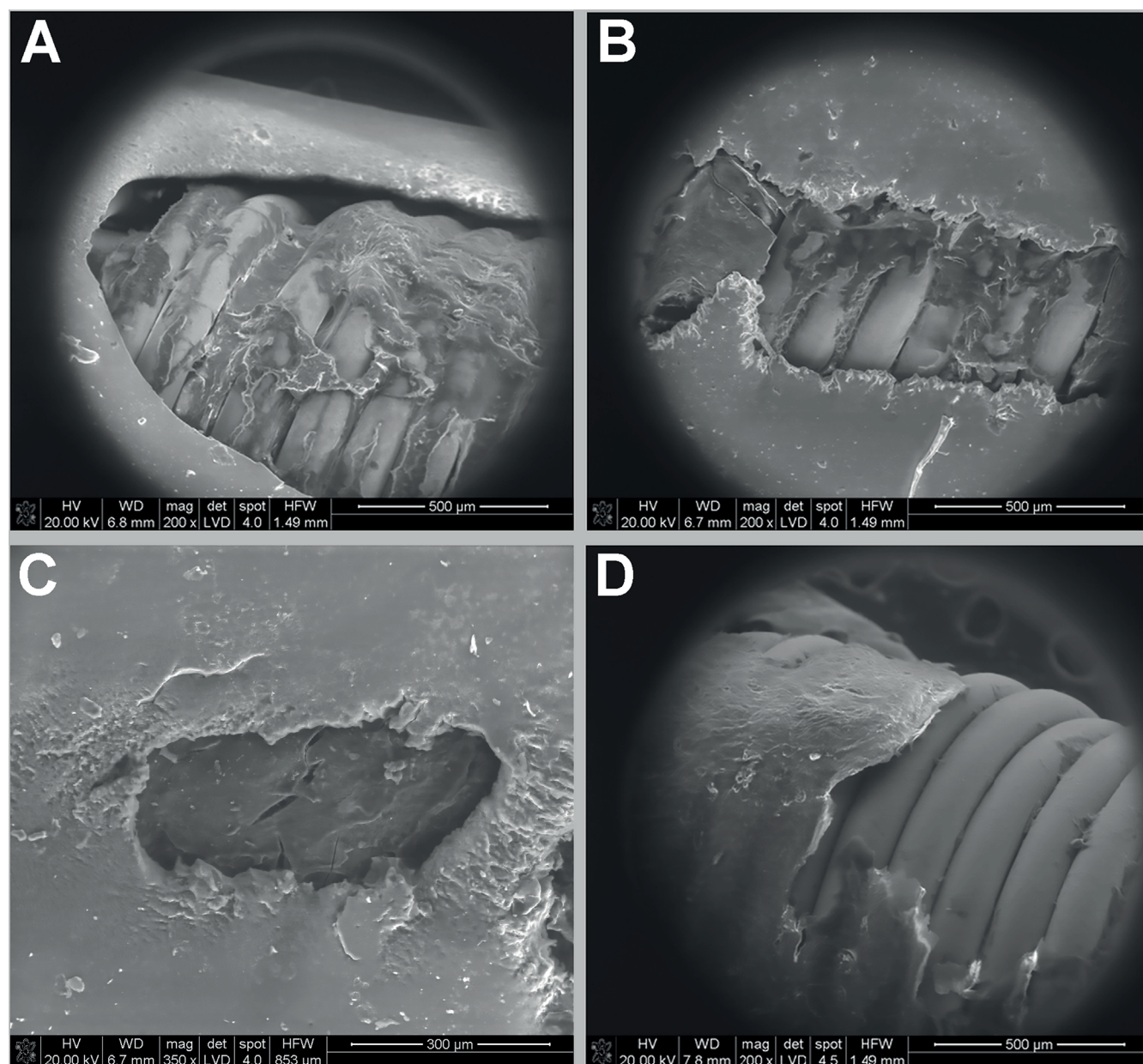


Fig. 3. Scanning electron microscopy (SEM) images. Examples of damage to lead insulation with the presence of unsealing. View of the worn-out lead insulation and silicone shift on the metal wire visible in the abraded opening. A, B. Bipolar active-fixation ventricular Medtronic CapSureFix Novus lead (lead insulation composed of 2 layers: outer – polyurethane 55D, contacting the surrounding tissues, and inner – silicone, adhering to the metal wire) with 4-year dwell time in the dual-chamber atrioventricular pacing (DDD) pacemaker device. Indication for removal: lead-dependent infective endocarditis. Destruction at the level of intra-pocket region (A) and subclavian region (B); C, D. Bipolar active-fixation atrial Biotronik Setrox lead (insulation: only silicone) with 5-year dwell time in the DDD pacemaker device. Indication for removal: lead damage. Destruction at the level of the intra-pocket region

in the intravenous region, irrespective of the presence or absence of lead unsealing. This observation diverges from the findings of Małecka et al., who, in their study of 22 leads spanning an age range of 3–25 years with a mean duration of 8.3 years, reported a proclivity towards increased damage in the intra-cardiac region.³ Similarly, Kolodzinska et al., in their assessment of 212 leads with an age range of 6–276 months and a mean age of 83.6 months, presented contrasting outcomes.¹⁵ The observed disparities might emanate from

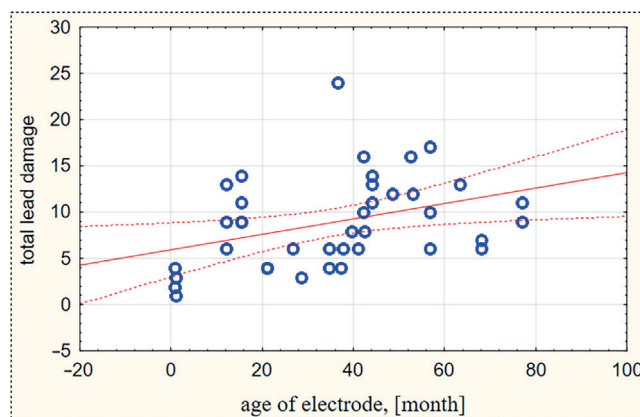


Fig. 4. The amount of lead damage over time; Spearman's R-value 0.3669

Table 3. Predictors of all-cause lead damage

Variable	Univariable				Multivariable			
	OR	95% CI		p-value	OR	95% CI		p-value
Lead damage with the absence of unsealing								
Intracardiac region vs other	0.662	0.319	1.371	0.2673	–	–	–	–
Intravenous region vs other	0.323	0.151	0.694	0.0037	0.465	0.171	1.269	0.1352
Subclavian region vs other	0.760	0.367	1.570	0.4588	–	–	–	–
Intra-pocket region vs other	9.112	3.326	24.960	<0.001	9.740	2.856	33.219	0.0002
ICD/PM leads	1.456	0.336	6.314	0.6160	–	–	–	–
Manufacturer (Biotronik vs other)	0.891	0.457	1.735	0.7334	–	–	–	–
Manufacturer (Medtronic vs other)	0.714	0.378	1.347	0.2985	–	–	–	–
Manufacturer (Vitatron vs other)	2.913	1.002	8.463	0.0494	3.438	1.111	10.641	0.0321
Silicone leads vs other	1.093	0.517	2.312	0.8145	–	–	–	–
Age of electrode (1 month decrease)	1.018	1.002	1.034	0.0236	1.031	1.010	1.054	0.0050
Female sex	1.231	0.637	2.378	0.5367	–	–	–	–
Diabetes mellitus	0.980	1.008	0.537	1.8920	–	–	–	–
BMI (1 kg/m² decrease)	0.999	0.930	1.073	0.9706	–	–	–	–
Age of patient during TLE (1 year decrease)	1.003	0.971	1.035	0.8678	–	–	–	–
Lead dysfunction	1.462	0.767	2.785	0.2471	–	–	–	–
Lead dislocation	0.665	0.259	1.709	0.3961	–	–	–	–
LDIE	0.842	0.299	2.370	0.7449	–	–	–	–
Pocket infection	0.813	0.396	1.669	0.5718	–	–	–	–
Lead damage with the presence of unsealing								
Intracardiac region vs other	0.492	0.198	1.219	0.1256	–	–	–	–
Intravenous region vs other	0.160	0.046	0.553	0.0038	0.186	0.044	0.771	0.0204
Subclavian region vs other	1.043	0.465	2.339	0.9176	–	–	–	–
Intra-pocket region vs other	5.915	2.685	13.030	<0.001	4.844	1.595	14.708	0.0050
ICD/PM leads	1.620	0.370	7.093	0.5219	–	–	–	–
Manufacturer (Biotronik vs other)	0.706	0.327	1.526	0.3763	–	–	–	–
Manufacturer (Medtronic vs other)	0.861	0.426	1.741	0.6784	–	–	–	–
Manufacturer (Vitatron vs other)	2.454	0.937	6.427	0.0675	2.088	0.671	6.500	0.2040
Silicone leads vs other	0.843	0.359	1.977	0.6948	–	–	–	–
Age of electrode (1 month decrease)	1.019	1.002	1.037	0.0290	1.027	0.987	1.068	0.1895
Female sex	0.941	0.451	1.962	0.8707	–	–	–	–
Diabetes mellitus	1.145	0.567	2.311	0.7064	–	–	–	–
BMI (1 kg/m² decrease)	0.949	0.877	1.028	0.2015	–	–	–	–
Age of patient during TLE (1 year decrease)	0.998	0.964	1.035	0.9329	–	–	–	–
Lead dysfunction	2.305	1.128	4.711	0.0220	6.096	1.386	26.819	0.0170
Lead dislocation	0.665	0.259	1.709	0.9972	–	–	–	–
LDIE	0.577	0.156	2.134	0.4098	–	–	–	–
Pocket infection	1.380	0.632	3.015	0.4189	–	–	–	–

95% CI – 95% confidence interval; ICD – implantable cardioverter-defibrillator; OR – odds ratio; PM – pacemaker; TLE – transvenous lead extraction; LDIE – lead-dependent infective endocarditis; BMI – body mass index.

the inclusion of leads extracted using mechanical methodologies, variances in electrode regional categorization, or extended lead dwell times.

Furthermore, a salient observation from our investigation underscores the statistically significant correlation

between prolonged dwell times of endocardial leads and associated damage, regardless of the presence of lead unsealing. This finding aligns harmoniously with extant literature emphasizing the implications of extended lead duration on their overall performance.²²

Limitations

While our investigation provides critical insights into the fatigue wear of endocardial leads, several limitations warrant acknowledgment. Primarily, the modest sample size may restrict the broader applicability of our results. Additionally, our study's focus on leads extracted using gentle traction and screw-out techniques potentially excluded cases with iatrogenic lead damage, limiting the comprehensiveness of our findings. Furthermore, the predominant inclusion of dual-chamber systems in our cohort diminishes our ability to definitively assess the impact of lead number variations on damage outcomes. A more diverse representation, particularly of single-chamber pacemakers and defibrillator with cardiac resynchronization therapy (CRT-D) systems, would have provided a more comprehensive perspective on this subject.

Conclusions

The endocardial leads exhibited greater susceptibility to insulation damage in the intra-pocket region than in the intravenous segment, irrespective of lead unsealing. Extended lead dwell time and the utilization of Vitatron leads were identified as key predictors of damage, regardless of lead seal status. There is a critical need for ongoing monitoring and re-evaluation of lead designs and materials to bolster their durability and safety in clinical applications.

Data availability

The datasets generated and/or analyzed during the current study are available from the corresponding author on reasonable request.

Consent for publication

Not applicable.

ORCID iDs

Mateusz Ulman  <https://orcid.org/0009-0007-2709-9302>
 Krzysztof Boczar  <https://orcid.org/0000-0002-1833-2404>
 Katarzyna Holcman  <https://orcid.org/0000-0002-6895-4076>
 Magdalena Ziabka  <https://orcid.org/0000-0003-0702-7137>
 Maciej Dębski  <https://orcid.org/0000-0002-3669-3916>
 Jacek Lelakowski  <https://orcid.org/0000-0003-0301-8946>
 Andrzej Ząbek  <https://orcid.org/0000-0001-8331-3210>

References

- Ellenbogen KA, Wilkoff BL, Kay NG, Lau CP. *Clinical Cardiac Pacing, Defibrillation, and Resynchronization Therapy*. 4th ed. Philadelphia, USA: Elsevier/Saunders; 2011. ISBN:978-1-4377-1616-0.
- Grant IS, Phillips WR. *Electromagnetism*. 2nd ed. New York, USA: Wiley & Sons; 1990. ISBN: 978-0-471-92711-2, 978-0-471-92712-9.
- Małecka B, Ząbek A, Ciał A, et al. Endocardial silicone lead wear: Description of tribological phenomena on the basis of microscopic examination of removed leads. Preliminary report. *Kardiol Pol*. 2014; 72(10):960–968. doi:10.5603/KP.a2014.0108
- Simmons A, Hyvarinen J, Odell RA, et al. Long-term in vivo biostability of poly(dimethylsiloxane)/poly(hexamethylene oxide) mixed macrodiol-based polyurethane elastomers. *Biomaterials*. 2004;25(20): 4887–4900. doi:10.1016/j.biomaterials.2004.01.004
- Chaffin KA, Wilson CL, Himes AK, et al. Abrasion and fatigue resistance of PDMS containing multiblock polyurethanes after accelerated water exposure at elevated temperature. *Biomaterials*. 2013; 34(33):8030–8041. doi:10.1016/j.biomaterials.2013.06.049
- Medtronic manuals. Sprint Quattro. Implantable Cardioverter Defibrillator (ICD) Leads. Dublin, Ireland: Medtronic; 2017. <https://www.medtronic.com/ca-en/healthcare-professionals/products/cardiac-rhythm/implantable-cardiac-defibrillators/sprint-quattro.html>. Accessed January 5, 2024.
- Vitatron manuals. Leads – ICF 09B, ICQ 09B. Maastricht, the Netherlands: Vitatron. <http://www.vitatron.com/inserts/lead-1.html>. Accessed January 5, 2024.
- Biotronik manuals. Setrox S ProMRI®. Bipolar, steroid-eluting endocardial lead with extendable and retractable screw. Berlin, Germany: Biotronik; 2005. https://manuals.biotronik.com/emanuals-professionals-rest/manual/PacemLeads/Setrox/Setrox_S/IE/en/G?type=manual. Accessed January 5, 2024.
- Kutarski A, Małecka B. Przetarcie silikonowych izolacji elektrod wewnątrzsercowych – nowo odkryte zjawisko w elektroterapii: obserwacje własne. *FoL Cardiol*. 2009;4:126–131. https://journals.via-medica.pl/fofia_cardiologica/article/view/23761/18947. Accessed January 5, 2024.
- Kutarski A, Małecka B, Kołodzinska A, Grabowski M. Mutual abrasion of endocardial leads: Analysis of explanted leads. *Pacing Clin Electrophysiol*. 2013;36(12):1503–1511. doi:10.1111/pace.12216
- Małecka B, Rydlewska A, Ząbek A, Sadowski J, Lelakowski J. Intracardiac damage of silicone insulation of a single lead and infective endocarditis. *Kardiol Pol*. 2013;71(10):1095–1095. doi:10.5603/KP.2013.0272
- Jost P. *Lubrication (Tribology) Education and Research: A Report of the Present Position and Industry's Needs*. London, UK: Department of Education and Science, The Majesty's Station Office; 1966. OCLC Number 258437307.
- Helguera ME, Maloney JD, Pinski SL, Woscoboinik JR, Wilkoe BL, Castle LW. Long-term performance of endocardial pacing leads. *Pacing Clin Electrophysiol*. 1994;17(1):56–64. doi:10.1111/j.1540-8159.1994.tb01351.x
- Boczar K, Małecka B, Ząbek A, Haberka K, Lelakowski J. Late complication of heart stimulation: Lead abrasion in pacemaker pocket. *Kardiol Pol*. 2014;72(6):555–555. doi:10.5603/KP.2014.0123
- Kołodzinska A, Kutarski A, Grabowski M, Jarzyna I, Małecka B, Opol-ski G. Abrasions of the outer silicone insulation of endocardial leads in their intracardiac part: A new mechanism of lead-dependent endocarditis. *Europace*. 2012;14(6):903–910. doi:10.1093/europace/eus003
- Ząbek A, Małecka B, Kołodzinska A, Maziarz A, Lelakowski J, Kutarski A. Early abrasion of outer silicone insulation after intracardiac lead friction in a patient with cardiac device-related infective endocarditis. *Pacing Clin Electrophysiol*. 2012;35(6):e165–e168. doi:10.1111/j.1540-8159.2010.02954.x
- Ząbek A, Boczar K, Dębski M, et al. Analysis of electrical lead failures in patients referred for transvenous lead extraction procedures. *Pacing Clin Electrophysiol*. 2018;41(9):1217–1223. doi:10.1111/pace.13463
- Ząbek A, Małecka B, Haberka K, et al. The analysis of indications and early results of transvenous lead extraction in patients with a pacemaker, ICD and CRT: Single-centre experience. *Acta Cardiol*. 2015;70(6):685–691. doi:10.1080/AC.70.6.3120181
- Rymuza Z. Tribology of polymers. *Arch Civil Mech Eng*. 2007;7(4):177–184. doi:10.1016/S1644-9665(12)60235-0
- Zhang SW. State-of-the-art of polymer tribology. *Tribol Int*. 1998;31(1–3): 49–60. doi:10.1016/S0301-679X(98)00007-3
- Zhang SW. State-of-the-art of rubber tribology: Polymer tribology. In: Sinha SK, Briscoe BJ, eds. *Polymer Tribology*. Singapore: Imperial College Press; 2009:312–343. ISBN:978-1-84816-202-0.
- Dębski M, Ulman M, Ząbek A, et al. Lead-related complications after DDD pacemaker implantation. *Kardiol Pol*. 2018;76(8):1224–1231. doi:10.5603/KP.a2018.0089

Plasma N-terminal pro-brain natriuretic peptide concentrations may help to identify patients with very low-risk acute pulmonary embolism: A preliminary study

Bartosz Karolak^{1,A–D}, Marta Skowrońska^{1,B,C,E}, Michał Machowski^{1,B,E}, Olga Dzikowska-Diduch^{1,B,E}, Piotr Bienias^{1,B,E}, Martyna Kuryła^{1,B}, Małgorzata Wiśniewska^{2,B}, Marek Gołębiowski^{2,B}, Piotr Pruszczyk^{1,E,F}, Michał Ciurzyński^{1,A,E,F}

¹ Department of Internal Medicine and Cardiology, Infant Jesus Clinical Hospital, University Clinical Center, Medical University of Warsaw, Poland

² Department of Clinical Radiology, Medical University of Warsaw, Poland

A – research concept and design; B – collection and/or assembly of data; C – data analysis and interpretation; D – writing the article; E – critical revision of the article; F – final approval of the article

Advances in Clinical and Experimental Medicine, ISSN 1899–5276 (print), ISSN 2451–2680 (online)

Adv Clin Exp Med. 2025;34(4):605–611

Address for correspondence

Bartosz Karolak
E-mail: b.karolak92@gmail.com

Funding sources

None declared

Conflict of interest

None declared

Received on December 30, 2023

Reviewed on April 2, 2024

Accepted on April 15, 2024

Published online on September 3, 2024

Abstract

Background. Patients with an acute pulmonary embolism (APE) are a heterogeneous group, and some of them may benefit from early discharge and an ambulatory care referral. We aimed to evaluate the use of N-terminal pro-brain natriuretic peptide (NT-proBNP) plasma level assessment in patients with low-risk APE based on clinical findings (0 points on the simplified Pulmonary Embolism Severity Index (sPESI)).

Materials and methods. Preliminary analysis of an ongoing prospective study including 1,151 normotensive patients with at least a segmental APE. In the final analysis, 348 patients with a 0-point sPESI were included. Blood samples were collected within the first 24 h of admission. The clinical endpoint (CE) included APE-related mortality and/or rescue thrombolysis in patients with clinical deterioration.

Results. Clinical endpoints occurred in 3 patients who had higher plasma NT-proBNP levels than study participants with a favorable clinical course (164 [64–650] pg/mL compared to 2,930 [2,285.5–13,965] pg/mL; $p = 0.01$). Receiver operating characteristic (ROC) analysis showed that the area under the curve (AUC) for NT-proBNP for the prediction of the CEs was 0.918 (95% confidence interval [95% CI]: 0.831–1.00; $p = 0.013$). We defined the cutoff value of NT-proBNP at $\geq 1,641$ pg/mL.

Conclusions. Among subjects with 0 points on the sPESI, those with concentrations of NT-proBNP exceeding 1,641 pg/mL might require closer attention; remaining patients could be considered candidates for outpatient treatment. However, these findings warrant further investigation in a large, prospective group of patients.

Key words: N-terminal pro-brain natriuretic peptide, pulmonary embolism, outcome prediction

Cite as

Karolak B, Skowrońska M, Machowski M, et al.
Plasma N-terminal pro-brain natriuretic peptide concentrations may help to identify patients with very low-risk acute pulmonary embolism: A preliminary study.
Adv Clin Exp Med. 2025;34(4):605–611.
doi:10.17219/acem/187187

DOI

10.17219/acem/187187

Copyright

Copyright by Author(s)

This is an article distributed under the terms of the Creative Commons Attribution 3.0 Unported (CC BY 3.0) (<https://creativecommons.org/licenses/by/3.0/>)

Background

Acute pulmonary embolism (APE) occurs frequently, with an estimated incidence rate reaching up to 200 cases a year per 100,000 people worldwide.^{1,2} The prevalence of APE increases with age; therefore, in aging populations, such as in Europe, this number is likely to rise. Furthermore, among cardiovascular diseases, APE is the 3rd most common cause of death, behind myocardial and cerebral infarctions.^{1,3} Taking these data into consideration, in the foreseeable future, APE management is going to remain an important challenge for healthcare professionals. Multiple risk factors increasing chances of developing APE have been described, such as trauma, postoperative state, malignancy, inflammatory diseases, COVID-19, congenital coagulation disorders, and many others.

The course of the disease depends on the thromboembolic material burden as well as individual features such as age, comorbidities, etc. Small thrombi may dissolve spontaneously and remain clinically irrelevant. Conversely, rapid occlusion of the pulmonary arteries can lead to substantial increase in pulmonary vessel resistance. As a result, high heart rate and increased right ventricular contractility are required to provide flow through the pulmonary circulatory system. In this case, RV oxygen demand significantly rises, and its insufficient supply may cause myocardial injury. Acute RV volume overload leads to N-terminal pro-brain natriuretic peptide (NT-proBNP) release and may be visualized in imaging studies (e.g., echocardiography and computed tomography (CT)), while plasma cardiac troponin concentration assessments are used to detect myocardial damage.^{3,4}

The clinical spectrum of APE is wide, ranging from asymptomatic to cardiogenic shock. In patients with no signs of RV overload or myocardial damage, the mortality during the acute phase does not exceed 1%, while in cases associated with hemodynamic instability, it can reach up to 60%.⁵ Even though the majority of APE patients do not present with shock or sustained hypotension on admission, some of them are at substantial risk of clinical deterioration; therefore, each individual may require a different approach. Thus, proper initial risk stratification is crucial, as it indicates further optimal management strategies. Recent guidelines issued by the European Society of Cardiology (ESC) suggest that each patient should be categorized into low, low-intermediate, high-intermediate, or high-risk group, based on clinical findings, biomarker assessment and imaging studies.³

Objectives

In the past, when vitamin K antagonists (VKA) were the standard of care, treatment initiation was difficult due to the need for individual dose adjustments. Currently, new oral anticoagulants (NOACs) are available,

and the treatment in a simple dosing scheme can be implemented immediately after diagnosis. Selected individuals may benefit from early discharge and ambulatory treatment; however, identifying them among patients not presenting with hemodynamic instability on admission can be challenging, especially if a properly trained echocardiographer is not immediately available.⁶ Therefore, this study aimed to evaluate the use of NT-proBNP level assessments, which are usually available in any emergency department, in patients with 0 points on the simplified Pulmonary Embolism Severity Index (sPESI).

Materials and methods

Study population

We performed an analysis of an ongoing prospective observational study, “PE-Aware”, registered at ClinicalTrials.gov (unique identifier NCT03916302). The study population consisted of 1,151 adult patients (517 men, 634 women, median age = 67 years [51; 79]), hospitalized in a single referral center for APE between January 2006 and December 2019. None of the participants presented with hemodynamic instability, defined as a systolic blood pressure (SBP) below 90 mm Hg and signs of peripheral hypoperfusion. Diagnostic criteria for APE included the presence of thromboembolic material, visualized on computed tomography pulmonary angiography (CTPA), in at least 1 segmental pulmonary artery with a duration of symptoms not exceeding 14 days before diagnosis. Each individual was managed in accordance with the current guidelines by a physician having unlimited access to the medical records.

Risk stratification was performed as described in the current ESC guidelines. Among subjects with neither signs of RV distress nor cardiac troponin elevation, those with 0 points on the sPESI formed low risk group, while those with sPESI ≥ 1 were classified to intermediate-low risk category. Patients with both signs of RV distress on imaging (echocardiography or CTPA) and elevated myocardial injury markers were included to the intermediate-high risk category, while those meeting only 1 of the 2 criteria mentioned above were classified into the intermediate-low-risk category.³ Patients diagnosed with chronic thromboembolic pulmonary hypertension and participants in therapeutic clinical trials were not included in this study.

An echocardiographic examination was performed within the first 24 h of admission, and the results were digitally recorded. Patients were examined in the left lateral position. The dimensions of the right and left ventricles were measured using the 4-chamber RV-focused view at the level of the mitral and tricuspid valve tips in late diastole, as defined by the R wave of continuous electrocardiographic (ECG) tracing. After recording the tricuspid valve peak systolic velocity with continuous-wave Doppler echocardiography, the tricuspid regurgitation peak

gradient (TRPG) was calculated using the simplified Bernoulli equation. Right ventricular dysfunction was defined as a RV/left ventricle (RV/LV) ratio in the apical 4-chamber view ≥ 1.0 and/or a TRPG ≥ 31 mm Hg.

Biochemical analysis

Blood samples were collected from patients within the first 24 h of admission. The NT-proBNP plasma concentrations were measured quantitatively using an automated sandwich electrochemiluminescence immunoassay (Roche Diagnostics GmbH, Mannheim, Germany). Based on current guidelines and other available scientific data, results above 600 pg/mL were considered elevated.^{3,7,8} Serum cardiac troponin I (cTnI) and high-sensitivity cardiac troponin T (cTnT-hs) levels were measured quantitatively using an automated sandwich electrochemiluminescence (ECL) immunoassay (Roche Diagnostics GmbH). Levels above 0.014 ng/mL for cTnT-hs and 0.1 ng/mL for cTnI were considered elevated.

The clinical endpoint of the study

The clinical endpoint (CE) of the study was designed to reflect fatal and possibly fatal complications if advanced medical care procedures had not been implemented immediately. They were defined as 1) in-hospital, APE-related death and/or 2) rescue thrombolysis performed due to hemodynamic collapse, which was defined as the occurrence of at least 1 of the following: 1) need for advanced life support; 2) SBP below 90 mm Hg for at least 15 min with signs of end-organ hypoperfusion; or 3) need for intravenous catecholamines in vasopressor doses. The CEs analysis concerned the patient's hospital stay.

Statistical analyses

The Shapiro–Wilk test was used to verify the statistical distribution of the analyzed parameters. Parameters characterized by a non-normal distribution were expressed as median followed by interquartile range (IQR). The Mann–Whitney U test was used to compare parameters between the study groups. Categorical variables were compared using Fisher's exact t-test. Youden's index from a receiver-operating curve (ROC) was calculated to identify the optimal cutoff value for NT-proBNP concentration for the prediction of the CEs. Diagnostic performance markers (sensitivity and specificity) were calculated for the chosen cutoff value.

Results

Overall, 410 study participants were classified into the sPESI 0-point group. Subsequently, 62 patients were excluded: 61 due to unknown NT-proBNP concentrations

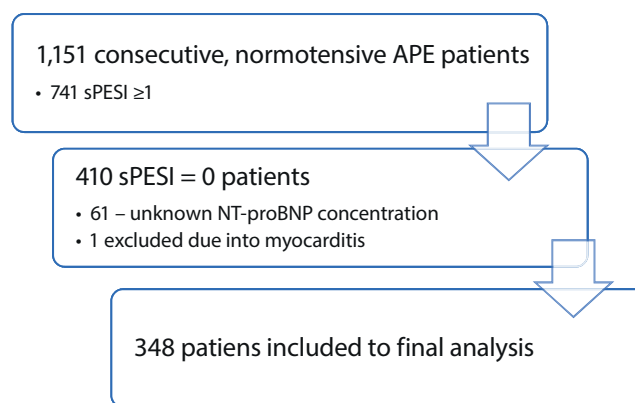


Fig. 1. The flow of patients

APE – acute pulmonary embolism; sPESI – simplified Pulmonary Embolism Severity Index.

and 1 due to myocarditis (diagnosed with the use of cardiac magnetic resonance imaging), as this comorbidity most probably would significantly impact the biochemical test results. In each patient, treatment was initiated with rivaroxaban (15 mg twice/day), apixaban (10 mg twice/day), low molecular weight heparin (LMWH), or unfractionated heparin (UFH). Low molecular weight heparin was administered subcutaneously, in doses adjusted for body weights and glomerular filtration rates (GFRs), and UFH was administered intravenously in doses modified based on the activated partial thromboplastin time. The flow of patients is presented in Fig. 1.

The final analysis included 348 (179 M, 169 F, age median = 52 (39; 66)) sPESI 0-point patients. In this group, rescue thrombolysis was performed due to hemodynamic collapse in 3 (0.86%) patients, and 2 of them survived. The in-hospital APE-related mortality was 0.29% (1 patient). The CEs, which included APE-related death (1 study participant, 0.29%) and/or thrombolysis (3 study participants, 0.86%), occurred in 3 (0.86%) patients.

Patients with a complicated course of the disease had significantly higher plasma NT-proBNP concentrations than those who did not experience the CE. No significant differences between the studied groups for creatinine and D-dimer concentrations were noted. The clinical characteristics of acute pulmonary embolism (APE) study participants are provided in Table 1.

We carefully analyzed the data of patients who experienced the CE and presented them in Table 2. The first patient to reach the CE was a 76-year-old man with a history of stage G4 chronic kidney disease and type 2 diabetes. After several hours, a significant blood pressure drop was observed, which required thrombolytic treatment. Immediate echocardiography revealed RV overload and no signs of LV dysfunction. Similarly, the 2nd patient was a 30-year-old man with a history of ulcerative colitis, who received thrombolytic treatment due to hypotension on the 2nd day of hospitalization. The 3rd patient was a 79-year-old woman

Table 1. Clinical characteristics of APE patients. Data are presented as median followed by interquartile range (IQR) or range in the CE column

Parameter	Non-CE patients (n = 345)	CE patients (n = 3)	All sPESI = 0 patients (n = 348)	p-value
Female/male	168/177	1/2	169/179	–
Age [years]	52 (39–66)	76 (30–79)	52 (39–66)	0.27
HR [bpm]	80 (70–90)	105 (80–105)	80 (70–90)	0.06
SBP [mm Hg]	130 (120–140)	140 (110–160)	130 (120–140)	0.9
NT-proBNP [pg/mL]	164 (64–650)*	2,930 (1,641–25,001)	166 (64–660)	0.01
Elevated NT-proBNP, n (%)	89/345 (26)	3/3 (100)	92/348 (26.4)	0.02
Creatinine [mg/dL]	0.87 (0.73–1.02)	1 (0.8–2.3)	0.88 (0.73–1.02)	0.25
D-dimer [ng/mL]	4,157 (1,784–6,577)	20,680 (4,480–36,880)	4,174 (1,795–6,069)	0.19
ESC risk group, low/intermediate-low/ intermediate-high	166/103/76	0/0/3	166/103/79	–

CE – clinical endpoint; HR – heart rate; SBP – systolic blood pressure; ESC – European Society of Cardiology; sPESI – simplified Pulmonary Embolism Severity Index; NT-proBNP – N-terminal pro-brain natriuretic peptide; p-values were calculated using the Mann–Whitney U test or Fisher's exact test comparing CE (+) to CE (–) patients.

Table 2. The clinical characteristics of patients reaching CEs

Patient No.	Age [years]	Sex	HR [bpm]	SBP [mm Hg]	NT-proBNP [pg/mL]	Creatinine [mg/dL]	D-dimer [ng/mL]	Comorbidities
Patient 1	76	male	80	160	25,001	2.3	36,880	type 2 diabetes, chronic kidney disease
Patient 2	30	male	105	110	2,930	0.8	4,480	ulcerative colitis
Patient 3	79	female	105	130	1,641	1	unknown	rheumatoid arthritis, pneumonia on admission

NT-proBNP – N-terminal pro-brain natriuretic peptide; HR – heart rate; SBP – systolic blood pressure.

Table 3. ROC analysis of NT-proBNP in predicting a complicated clinical course

Parameter	AUC	95% CI	p-value
NT proBNP	0.918	0.831–1.0	<0.013

AUC – area under the ROC curve; 95% CI – 95% confidence interval.

with a history of rheumatoid arthritis and co-existing pneumonia. On the 10th day of the hospital stay, a sudden cardiac arrest occurred, which resulted in death. During CPR, an echocardiographic study was performed, which revealed a widely enlarged right ventricle. It should be noted that each patient with a CE was classified as intermediate-to-high risk after echocardiography.

The Receiver operating characteristic (ROC) analysis showed that the area under the curve (AUC) for NT-proBNP in the prediction of CE was 0.918 (95% CI: 0.831–1.00; $p = 0.013$, Table 3). With reference to Youden's index, an optimal cutoff was determined to be $\geq 1,641$ pg/mL with 100% sensitivity and 85% specificity (Fig. 2). Therefore, all patients who experienced CEs had NT-proBNP concentrations exceeding this value, and all 292 patients with NT-proBNP concentrations below this level had a favorable clinical course. A comparison between the thresholds of $\geq 1,641$ and ≥ 600 pg/mL (which is recommended in the current ESC guidelines) is presented in Table 4.

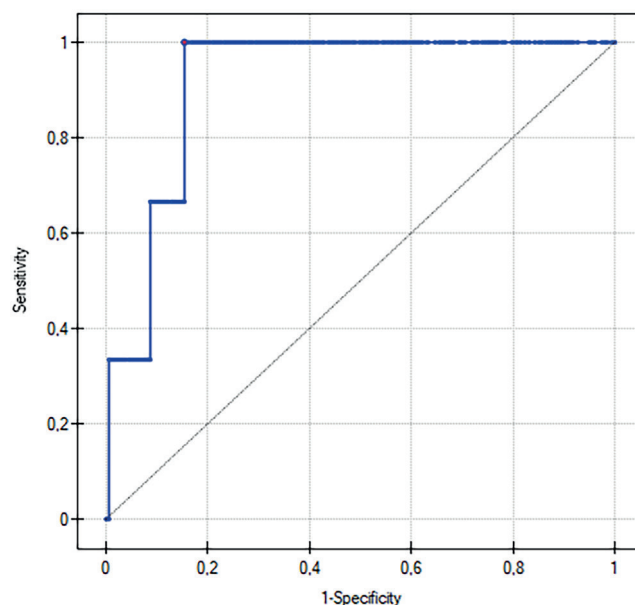


Fig. 2. Receiver operating characteristic (ROC) curve for NT-proBNP in the prediction of a complicated clinical course. The proposed cutoff is marked with a red dot

Discussion

First of all, our study revealed that a risk stratification model based exclusively on clinical findings is not sufficient

Table 4. NT-proBNP cutoff values

Cutoff value [pg/mL]	PPV	NPV	Sensitivity	Specificity
≥600	3.3	100	100%	74%
≥1,641	5.4	100	100%	85%

PPV – positive predictive value; NPV – negative predictive value.

to select candidates for outpatient treatment, as 0.86% of initially sPESI 0-point patients experienced clinical deterioration and required intensive medical care. Moreover, plasma NT-proBNP concentrations $\geq 1,641$ pg/mL seemed to identify those with an elevated risk of severe adverse events and requiring closer attention. Conversely, the remaining patients could be classified as the “very low-risk” group and might be considered for treatment in ambulatory care. These findings may be useful as a part of a quick decision-making algorithm that could be utilized to predict outcomes, especially when the echocardiographic study required to perform the risk stratification model suggested by ESC is not immediately available.

Several scales used to describe the APE patient’s clinical status are available (e.g., PESI, sPESI, Hestia); however, the main advantage of sPESI is its simplicity, which makes it preferable to use in everyday clinical practice. Furthermore, its value in predicting outcomes was confirmed in numerous studies. In a meta-analysis by Elias et al., the overall 30-day mortality rate was 1.5% (0.9–2.5%) in the low-risk group and 10.7% (8.8–12.9%) in the high-risk group for sPESI (11 studies).⁹ In the HOME-PE randomized trial, decision-making regarding ambulatory treatment based on Hestia and sPESI had comparable safety and effectiveness, no deaths or recurrent pulmonary embolism (PE) were observed in patients selected for home treatment with the use of both discussed scales.¹⁰ Nevertheless, final decisions regarding outpatient treatment in each case were made by the physician in charge. Combining clinical findings with a biomarker assessment (such as NT-proBNP or cardiac troponin) would supposedly provide objective criteria for safe early discharge.¹⁰ According to scientific knowledge, the sPESI scale alone is not sufficient to identify candidates for safe home treatment and it should be accompanied by biomarkers and/or RV assessment on imaging studies.³

Although a number of studies revealed the usefulness of NT-proBNP as an indicator of RV dysfunction, data on the prognostic significance of NT-proBNP in low-risk APE patients comes mainly from recent years.^{4,7,11} In 2019, Barco et al. published a meta-analysis including 22 cohort studies with 3,295 low-risk APE patients according to PESI or sPESI. Early all-cause or APE-related mortality rates were significantly higher in study participants with RV dysfunction on imaging studies or elevated plasma troponin or natriuretic peptide levels.¹² Becattini et al. published a meta-analysis, incorporating data from 5,010 low-risk APE patients from 18 studies, which

revealed similar results.¹³ Both meta-analyses identified NT-proBNP as an independent predictor of severe adverse events in low-risk APE patients. However, the cutoff value for NT-proBNP for each incorporated study was different, ranging from 90 pg/mL to 1,136 pg/mL. Our study revealed that using a combination of sPESI and a NT-proBNP assessment with a cutoff value of 600 pg/mL identified patients with a favorable outcome. Furthermore, it appears to be safe to raise the threshold to 1,641 pg/mL, which increases the positive predictive value of the test. Applying our findings in clinical practice would allow early discharge of 292 out of the 348 (84%) patients in the studied population. Thus, it is worth considering a higher cutoff value for NT-proBNP than suggested in the current guidelines for predicting adverse events in low-risk APE patients. Nevertheless, due to a very low number of endpoints in our study, those findings require further validation.

Another biomarker used in outcome prediction in APE is cardiac troponin.³ Its clinical value was confirmed in multiple studies, including those incorporating sPESI 0-point patients. A meta-analysis by Barco et al. identified troponin as an independent predictor of all-cause mortality in low-risk APE patients.¹² Similarly, in a meta-analysis by Becattini et al., elevated plasma troponin levels were linked to greater short-term mortality and death within 3 months.¹³ We previously analyzed data from 409 sPESI 0-point APE patients. The study participants with troponin levels not exceeding 1.7 times the upper limit of normal could be classified to the group of “very low-risk” with an excellent prognosis.⁶ Taking available scientific data into consideration, we recommend assessing plasma cardiac troponin levels as well as NT-proBNP in all sPESI 0-point patients before making a decision regarding outpatient treatment. This procedure is likely to increase patient safety and may be easily performed in most medical facilities.

Apart from biomarkers, imaging studies are another way of detecting RV dysfunction secondary to an APE. The role of echocardiography in the risk stratification process is well established.^{3,12–15} Nevertheless, performing this study requires an experienced physician, who is not always immediately reachable, whereas biochemical tests (such as NT-proBNP level assessment) are usually easily accessible and enable quick and efficient decision-making. The use of CTPA for RV dysfunction detection is an interesting idea as this study is usually necessary to confirm the diagnosis of APE; however, results from available scientific studies are equivocal. A study by Singanayagam et al. identified RV dilatation as an independent predictor of 30-day mortality in APE.¹⁶ Similarly, a meta-analysis by Trujillo-Santos et al. revealed a connection between APE-related adverse events and right ventricular dysfunction (RVD) on CT.¹⁷ Conversely, a study by Cote et al. showed no association between RV dilatation on CT, defined as a RV/LV ≥ 0.9

or ≥ 1.0 , and a complicated course of the disease. However, a link was observed after increasing the cutoff value to ≥ 1.1 .¹⁸ In the PROTECT study, RVD on CT did not affect the prognosis in the cohort of normotensive patients with a cutoff value (RV/LV) ≥ 0.9 .¹⁹ Recently, O'Hare et al. analyzed data of 817 APE patients of which 331 (40.5%) were low-risk using the PESI score. Low-risk patients had similar short-term outcomes regardless of CT scan results.²⁰ Although available scientific data gives the impression that CT might play a significant role in the risk stratification process, optimal criteria for RV overload recognition have yet to be determined.

Limitations

It is commonly known that the risk of APE-related severe adverse events in sPESI 0-point patients is below 1%; therefore, only a few patients from the studied population reached the CE. Furthermore, CEs were limited to in-hospital severe adverse events and data regarding possible complications that study participants might have experienced after discharge were not available. In addition, this was a single-center study. Taking those facts into consideration, our results, especially the cutoff value of 1,641 pg/mL for NT-proBNP assessment, should be interpreted with caution and require external validation.

Conclusions

Risk assessment in APE based exclusively on clinical examination is insufficient and each patient with 0 points on the sPESI requires further risk stratification, in which the assessment of NT-proBNP levels might play an important role. Study participants with a concentration of this biomarker exceeding 1,641 pg/mL belong to the group with an elevated risk of clinical deterioration and might require close attention, while those who do not meet this criterion could be considered as candidates for outpatient treatment. Nevertheless, taking into consideration the limitations of this study, these findings, with special emphasis on the cutoff point of 1,641 pg/mL, require further analyses in a large, prospective group of patients to be introduced in clinical practice.








Data availability

The datasets generated and/or analyzed during the current study are available from the corresponding author on reasonable request.

Consent for publication

Not applicable.

ORCID iDs

Bartosz Karolak  <https://orcid.org/0000-0003-2520-4811>
 Marta Skowrońska  <https://orcid.org/0000-0002-0826-7821>
 Michał Machowski  <https://orcid.org/0000-0001-6833-1066>
 Olga Dzikowska-Diduch  <https://orcid.org/0000-0002-8132-1660>
 Piotr Bienias  <https://orcid.org/0000-0003-3567-338X>
 Piotr Pruszczyk  <https://orcid.org/0000-0002-9768-0000>
 Michał Ciurzyński  <https://orcid.org/0000-0001-8393-5415>

References

- Giordano NJ, Jansson PS, Young MN, Hagan KA, Kabrheh C. Epidemiology, pathophysiology, stratification, and natural history of pulmonary embolism. *Tech Vasc Interv Radiol*. 2017;20(3):135–140. doi:10.1053/j.tvir.2017.07.002
- Wendelboe AM, Raskob GE. Global burden of thrombosis: Epidemiologic aspects. *Circ Res*. 2016;118(9):1340–1347. doi:10.1161/CIRCRESAHA.115.306841
- Konstantinides SV, Meyer G. The 2019 ESC Guidelines on the Diagnosis and Management of Acute Pulmonary Embolism. *Eur Heart J*. 2019;40(42):3453–3455. doi:10.1093/eurheartj/ehz726
- Pruszczyk P. N-terminal pro-brain natriuretic peptide as an indicator of right ventricular dysfunction. *J Cardiac Fail*. 2005;11(Suppl 5):S65–S69. doi:10.1016/j.cardfail.2005.04.016
- Becattini C, Agnelli G. Predictors of mortality from pulmonary embolism and their influence on clinical management. *Thromb Haemost*. 2008;100(5):747–751. PMID:18989514.
- Karolak B, Ciurzyński M, Skowrońska M, et al. Plasma troponins identify patients with very low-risk acute pulmonary embolism. *J Clin Med*. 2023;12(4):1276. doi:10.3390/jcm12041276
- Kostrubiec M, Pruszczyk P, Bochowicz A, et al. Biomarker-based risk assessment model in acute pulmonary embolism. *Eur Heart J*. 2005;26(20):2166–2172. doi:10.1093/eurheartj/ehi336
- Lankeit M, Jimenez D, Kostrubiec M, et al. Validation of N-terminal pro-brain natriuretic peptide cut-off values for risk stratification of pulmonary embolism. *Eur Respir J*. 2014;43(6):1669–1677. doi:10.1183/09031936.00211613
- Elias A, Mallett S, Daoud-Elias M, Poggi JN, Clarke M. Prognostic models in acute pulmonary embolism: A systematic review and meta-analysis. *BMJ Open*. 2016;6(4):e010324. doi:10.1136/bmjopen-2015-010324
- Roy PM, Penaloza A, Hugli O, et al. Triaging acute pulmonary embolism for home treatment by Hestia or simplified PESI criteria: The HOME-PE randomized trial. *Eur Heart J*. 2021;42(33):3146–3157. doi:10.1093/eurheartj/ehab373
- Kostrubiec M, Pruszczyk P, Kaczynska A, Kucher N. Persistent NT-proBNP elevation in acute pulmonary embolism predicts early death. *Clin Chim Acta*. 2007;382(1–2):124–128. doi:10.1016/j.cca.2007.04.010
- Barco S, Mahmoudpour SH, Planquette B, Sanchez O, Konstantinides SV, Meyer G. Prognostic value of right ventricular dysfunction or elevated cardiac biomarkers in patients with low-risk pulmonary embolism: A systematic review and meta-analysis. *Eur Heart J*. 2019;40(11):902–910. doi:10.1093/eurheartj/ehy873
- Becattini C, Maraziti G, Vinson DR, et al. Right ventricle assessment in patients with pulmonary embolism at low risk for death based on clinical models: An individual patient data meta-analysis. *Eur Heart J*. 2021;42(33):3190–3199. doi:10.1093/eurheartj/ehab329
- Pruszczyk P, Goliszek S, Lichodziejewska B, et al. Prognostic value of echocardiography in normotensive patients with acute pulmonary embolism. *JACC Cardiovasc Imaging*. 2014;7(6):553–560. doi:10.1016/j.jcmg.2013.11.004
- Ciurzyński M, Kurnicka K, Lichodziejewska B, et al. Tricuspid regurgitation peak gradient (TRPG)/tricuspid annulus plane systolic excursion (TAPSE): A novel parameter for stepwise echocardiographic risk stratification in normotensive patients with acute pulmonary embolism. *Circ J*. 2018;82(4):1179–1185. doi:10.1253/circj.CJ-17-0940
- Singanayagam A, Chalmers JD, Scally C, et al. Right ventricular dilation on CT pulmonary angiogram independently predicts mortality in pulmonary embolism. *Respir Med*. 2010;104(7):1057–1062. doi:10.1016/j.rmed.2010.02.004

17. Trujillo-Santos J, Den Exter PL, Gómez V, et al. Computed tomography-assessed right ventricular dysfunction and risk stratification of patients with acute non-massive pulmonary embolism: Systematic review and meta-analysis. *J Thromb Haemost.* 2013;11(10): 1823–1832. doi:10.1111/jth.12393
18. Côté B, Jiménez D, Planquette B, et al. Prognostic value of right ventricular dilatation in patients with low-risk pulmonary embolism. *Eur Respir J.* 2017;50(6):1701611. doi:10.1183/13993003.01611-2017
19. Jiménez D, Lobo JL, Monreal M, et al. Prognostic significance of multidetector CT in normotensive patients with pulmonary embolism: Results of the protect study. *Thorax.* 2014;69(2):109–115. doi:10.1136/thoraxjnl-2012-202900
20. O'Hare C, Grace KA, Schaeffer WJ, et al. Adverse clinical outcomes among patients with acute low-risk pulmonary embolism and concerning computed tomography imaging findings. *JAMA Netw Open.* 2023;6(5):e2311455. doi:10.1001/jamanetworkopen.2023.11455

Determination of the best point of entry of percutaneous insertion of sacroiliac screws depending on patient positioning for surgery: A cadaveric study

Michał Kułakowski^{1,A–F}, Karol Elster^{1,B,C,E,F}, Wojciech Piotrowski^{1,B,C,E,F}, Paweł Ślęczka^{2,B,C,E,F}, Aleksandra Królikowska^{3,C,D,F}, Jarosław Witkowski^{4,C,E,F}, Łukasz Oleksy^{4,5,C,D,F}, Dariusz Janczak^{6,C–F}, Paweł Reichert^{4,A,D–F}

¹ Independent Public Healthcare Center in Rypin, Poland

² Independent Public Healthcare Center in Myślenice, Poland

³ Ergonomics and Biomedical Monitoring Laboratory, Department of Physiotherapy, Faculty of Health Sciences, Wrocław Medical University, Poland

⁴ Department of Orthopedics, Traumatology and Hand Surgery, Faculty of Medicine, Wrocław Medical University, Poland

⁵ Department of Physiotherapy, Faculty of Health Sciences, Jagiellonian University Medical College, Cracow, Poland

⁶ Department of Vascular, General, and Transplantation Surgery, Faculty of Medicine, Wrocław Medical University, Poland

A – research concept and design; B – collection and/or assembly of data; C – data analysis and interpretation;

D – writing the article; E – critical revision of the article; F – final approval of the article

Advances in Clinical and Experimental Medicine, ISSN 1899–5276 (print), ISSN 2451–2680 (online)

Adv Clin Exp Med. 2025;34(4):613–621

Address for correspondence

Aleksandra Królikowska

E-mail: aleksandra.krolikowska@umw.edu.pl

Funding sources

None declared

Conflict of interest

None declared

Received on September 23, 2023

Reviewed on January 28, 2024

Accepted on May 15, 2024

Published online on August 1, 2024

Cite as

Kułakowski M, Elster K, Piotrowski W, et al. Determination of the best point of entry of percutaneous insertion of sacroiliac screws depending on patient positioning for surgery: A cadaveric study. *Adv Clin Exp Med.* 2025;34(4):613–621. doi:10.17219/acem/188780

DOI

10.17219/acem/188780

Copyright

Copyright by Author(s)

This is an article distributed under the terms of the Creative Commons Attribution 3.0 Unported (CC BY 3.0) (<https://creativecommons.org/licenses/by/3.0/>)

Abstract

Background. The standard starting point for percutaneous sacroiliac screw insertion was initially determined at the intersection of the line posterior to the anterior superior iliac spine and the line continuing the anatomical axis of the femur. The technique was pioneered in patients lying prone in surgery, although it has been used with patients in the supine position. The optimal starting point for patients in both prone and supine positions remains uncertain.

Objectives. This cadaveric study aimed to determine the best entry point for the percutaneous insertion of sacroiliac screws depending on the patient's positioning for surgery.

Materials and methods. Kirschner wires (K-wires) were percutaneously inserted into the sacral body of 8th human cadavers. In addition to the so-called standard sacroiliac screw entry point (point A), points located consecutively 1 cm (point B) and 2 cm (point C) cranially from the point along the line, prolonging the femoral axis were also studied. The K-wires were inserted into the studied entry points on the right side in a supine position and on the left side of the same cadaver in a prone position. The placement of the K-wires was assessed using radiographic imaging and cadaver dissection.

Results. An analysis of the K-wire placement in the supine position revealed incorrect positioning of 100% of the K-wires inserted at entry point A and 87% at entry point B. All the K-wires inserted in the supine position at entry point C were correctly placed. All K-wires inserted in the prone position were correctly positioned.

Conclusions. All 3 studied entry points enabled the correct placement of orthopedic implants for prone position surgery. The best entry point for surgery performed in the supine position was located 2 cm cranially from the standard entry point, along the line prolonging the femoral axis.

Key words: fracture fixation, pelvis, traumatology

Background

Pelvic fractures, one of the most severe and life-threatening traumatic injuries, constitute approx. 1.5–3% of all skeletal fractures.^{1,2} Of these, around 40% are unstable because of posterior pelvic ring disruption,³ which may or may not be associated with severe trauma.^{4,5} While not considered frequent, sacroiliac joint injuries are associated with significant morbidity and mortality.^{6–12}

The advantages of surgical treatment for unstable pelvic fractures over nonsurgical treatment have been well-known for the last 30 years, including increased effectiveness in fracture reduction, earlier weight-bearing and mobilization, lower mortalities, shorter hospital stays, and generally better functional outcomes.^{11,13–16} The standard technique for surgical fixation of the sacroiliac joint used to be an open reduction and internal fixation (ORIF) using sacral bars or posterior plating. Yet, a minimally invasive approach that reduces the risk of wound infection and blood loss and provides relatively good fracture fixation strength using percutaneously inserted sacroiliac screws was introduced by Matta and Saucedo and is now a commonly used treatment for pelvic ring injuries, replacing open procedures.^{17–20}

However, incorrect placement of the sacroiliac screws may cause severe complications, including iatrogenic injuries of large vessels and nerves and loss of fixation.^{16,21} Therefore, intraoperative visualization with conventional fluoroscopy remains the current standard in most hospitals. In addition, computed tomography, fluoroscopic computed tomography and computer-assisted techniques have also been utilized.^{22–25} Some authors propose digital 3-dimensional navigation printing to minimize complications arising from sacroiliac screw misplacement.²⁶

The starting point for the percutaneous sacroiliac screw insertion initially defined by Matta and Saucedo is located 15 mm anterior to the gluteal crest at a point 50% of the distance between the greater sciatic notch and the iliac crest, which corresponds to the intersection of the line posterior to the anterior superior iliac spine and the line that is a continuation of the anatomic axis of the femur.¹⁸ The technique was pioneered in patients in the prone position but has been modified and used with patients in the supine position.¹⁹ Whether the starting point for percutaneous sacroiliac screw insertion determined by Matta and Saucedo is an appropriate entry point for patients in prone and supine surgical positions remains unknown.

Unfortunately, the literature is also sparse regarding research on the development of new methods, including new entry points of percutaneous sacroiliac screw insertion, which could be more effective in terms of safety and time of the surgery. In their 2018 cadaveric study, Javidmehr et al.²⁷ demonstrated a new iliosacral screw insertion method that was found to be safer and faster to implement than its conventional counterpart. Both modified and conventional methods were similar regarding the safety index for distance

from the anterior cortex and 1st sacral vertebra (S1) foramen. However, the new modified method was also found to be safer in terms of the distance from the sacral canal. Additionally, the method introduced by Javidmehr et al. was easier and faster to implement than the conventional method. Neither method penetrated the sacral canal, anterior cortex and S1 foramen during guidewire insertion,²⁷ although the study was carried out only for 1 surgical positioning.

Objectives

The present cadaveric study aimed to determine the best entry point for the percutaneous insertion of sacroiliac screws depending on the patient's positioning for surgery.

In the context of a cadaveric study, it was hypothesized that the choice of the best point of entry for percutaneous sacroiliac screw insertion is influenced by the positioning of the cadaver during the procedure. It was postulated that variations in cadaveric positioning would impact the accuracy of screw placement, with specific positions demonstrating superior precision and reduced variability. Through examination of different entry points for 2 surgical positions, it was anticipated to identify a preferred point of entry that maximizes the correctness of sacroiliac screw fixation, thus providing valuable insights for optimizing surgical outcomes in clinical practice.

Materials and methods

The study was conducted in the laboratory of a medical institute. The pelvic preparations were brought to the institute in a lawful manner and with the knowledge of the Polish Ministry of Health. In the present study, informed consent was obtained prior to the donors' deaths through a body donation program, where individuals voluntarily agreed to donate their bodies for scientific research and education. The authors of the paper obtained written consent from the institute for using unfixed human pelvic preparations for research and scientific purposes of the current project. In addition, the authors obtained written permission to publish the photographs in the present article. The study was carried out according to the Declaration of Helsinki as the ethical standard for research involving human biological material and approved by the Kuyavian-Pomeranian Local Medical Chamber (approval No. 21/KB/2022).

The studied material consisted of 8 adult, fresh-frozen, full-body cadavers of 3 men and 5 women with a mean age at death of 68.00 ± 2.00 years. None of the cadavers demonstrated subjective osteopenia. Additionally, none of the cadavers was identified as having sacral dysmorphism, and none had undergone pelvic surgery during their lifetime or had fractures in the pelvic area. Each cadaver was thawed at room temperature overnight before being used for study purposes.

Percutaneous Kirschner wire insertion

Initially, 3 Kirschner wire (K-wire) entry points were marked bilaterally. The 1st was a standard starting point for the sacroiliac screw, initially defined by Matta and Saucedo, located at the intersection of the line posterior to the anterior superior iliac spine and the line that is a continuation of the anatomic axis of the femur.¹⁸ For this study it was named point A. Entry point B was placed 1 cm cranially from entry point A along the line, prolonging the anatomical femoral axis. Entry point C was situated 1 cm cranially from entry point B and 2 cm cranially from entry point A along the line, prolonging the anatomical femoral axis. The 3 K-wires were percutaneously inserted into the sacral body at the 3 consecutive entry points on the right side of a cadaver in a supine position (Fig. 1).

Next, the 3 K-wires were inserted into consecutive entry points on the left side of the same cadaver, set in a prone position. The wires were inserted under conventional C-arm fluoroscopy (C-arm Cios Flow; Siemens AG, Munich, Germany). The insertion procedure for all cadavers was performed by the same specialist in orthopedics and traumatology, who has many years of experience in pelvic surgery.

Radiographic imaging and cadaver dissection

The placement of the inserted K-wires in the sacral bone was assessed using radiographic imaging and cadaver dissection. A radiograph was performed supine to visualize

the pelvis in the inlet view using C-arm, the inserted K-wires in the supine position on the right side and those inserted in the prone position on the left side. The inserted distance of the K-wires from the medial axis of the sacrum was assessed in the inlet view and expressed in millimeters. A negative value meant that the inserted K-wire was posterior to the medial axis, while 0 indicated insertion along the medial axis. A positive value indicated that the inserted K-wire was placed anterior to the midline of the sacrum. All radiographs were analyzed by a single specialist in orthopedics and traumatology, who has extensive experience in pelvic surgery. Subsequently, cadaver dissection was performed. In cases where the K-wire was not seen to penetrate the pelvis, the penetration distance was indicated as 0 mm, meaning that the inserted K-wire was entirely within the bone. In other cases, the distance between the K-wire and the margin of the cortex of the sacrum was measured with a ruler and expressed in mm (Fig. 2). The same highly experienced specialist performed all cadaver dissections.

Statistical analyses

The statistical analysis was performed using IBM SPSS Statistics Premium v. 28 (IBM Corp. Armonk, USA), and Microsoft Office Excel 365 (Microsoft Corp., Redmond, USA). As the study included fewer than 10 samples, non-parametric tests were used.

The median (Me), 1st quartile (Q1) and 3rd quartile (Q3) were calculated for the measured distances between the K-wire and the transverse axis of the sacrum in radiographic

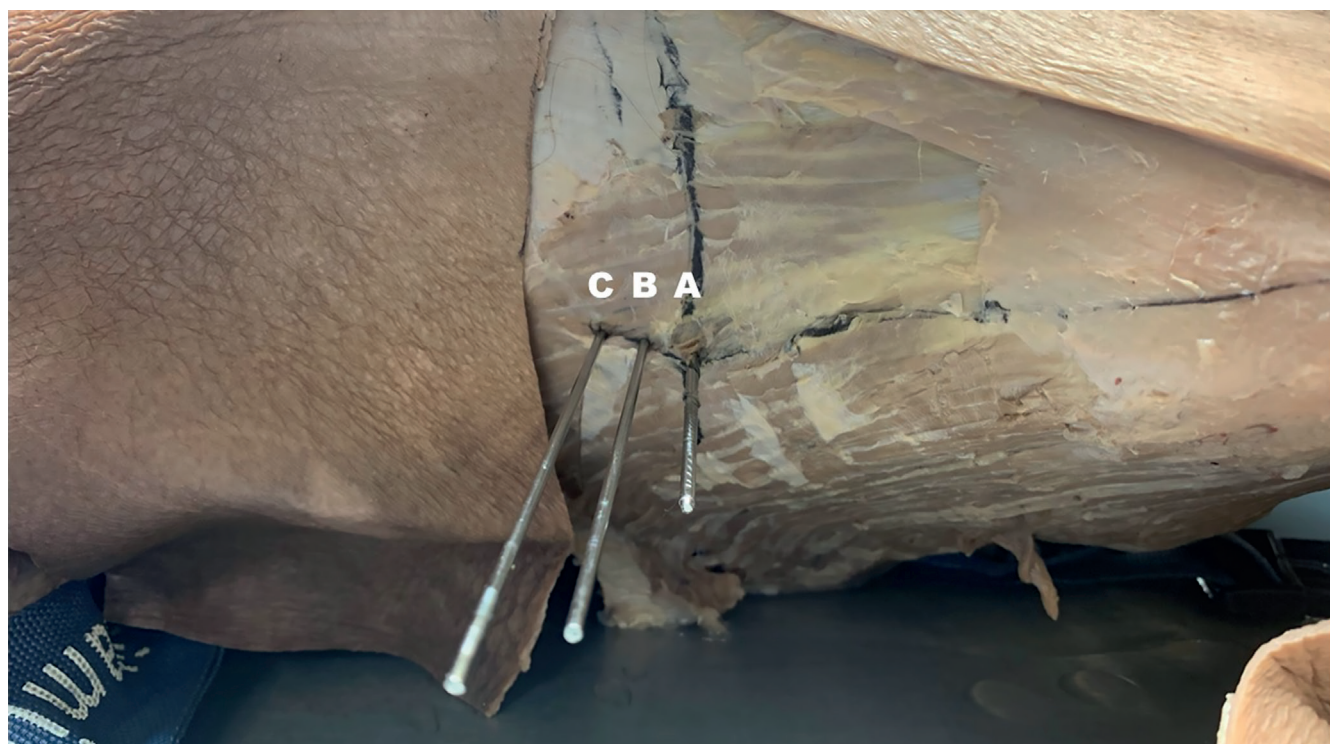


Fig. 1. Percutaneously inserted Kirschner wires on the right side of the cadaver in a supine surgical position at the 3 consecutive entry points, namely, point A, point B and point C



Fig. 2. Picture of the dissection of 1 of the studied cadavers

inlet view images and between the K-wire and the sacral bone anterior cortex in cadaver dissection. The Friedman's test was used to compare distances between K-wires inserted in the 3 consecutive entry points.

If the Friedman's test yielded a significant result, indicating differences among the dependent groups, Wilcoxon signed-rank post hoc tests were conducted to identify which specific pairs of groups differ significantly. To correct for multiple comparisons, the desired significance level, precisely 0.05, was divided by the number of comparisons being made, precisely 3, resulting in a corrected significance level of approx. 0.017.

Correct placement of the K-wire inserted using a particular entry point for the supine and prone surgical positions was defined when the wire was located entirely within the sacral cortical boundaries. When the K-wire was not entirely within the sacral bone, its placement was determined as incorrect. The Cochran's Q test and, consecutively, McNemar's test were used for the comparison of the number of cadavers with correctly inserted K-wires at the particular entry points separately for supine and prone positions. Bonferroni correction for multiple corrections was applied. Statistical significance was set at $p < 0.050$.

Results

Kirschner wires inserted in the supine surgical position

Detailed analysis of the distances between the K-wires inserted in the supine position and the midline (inlet view) or margin of the cortex (cadaver dissection) of the sacral bone was presented in Table 1.

The performed Friedman's test revealed statistically significant differences ($\chi^2(2) = 15.548$, $p < 0.001$) between K-wires inserted in the 3 consecutive entry points in the supine position in terms of measured distances between the K-wires and the transverse axis of the sacrum in radiographic inlet view images. Moreover, in terms of distances measured during cadaver dissection between the K-wires and the margin of the sacral bone, the Friedman's test revealed statistically significant differences between the 3 studied entry points ($\chi^2(2) = 15.200$, $p < 0.001$).

Consecutively performed Wilcoxon signed-rank tests revealed that for the K-wires inserted percutaneously in the supine position in entry point C, the median distance between the wires and the midline of the sacral bone in the inlet view was significantly smaller than those inserted in entry point A ($Z = -2.527$, $p = 0.012$) and entry point B ($Z = -2.539$, $p = 0.011$) (Table 2).

The results of the Wilcoxon signed-rank test also revealed that the distance between the K-wires inserted

Table 1. Comparison between the 3 studied entry points in terms of distance between the Kirschner wires inserted in the supine position and the midline (inlet view) or margin of the cortex (cadaver dissection) of the sacral bone (Friedman's test results)

Insertion entry point		Inlet view			Cadaver dissection		
		Me	Q1	Q3	Me	Q1	Q3
Entry point A		11.50	10.25	12.75	6.50	5.25	7.75
Entry point B		7.00	6.00	8.00	1.00	0.25	2.00
Entry point C		1.00	0.00	1.75	0.00	0.00	0.00
Friedman's test results	χ^2	15.548			15.200		
	df	2			2		
	p-value	<0.001			<0.001		

Values are expressed as the median (Me), the 1st quartile (Q1) and the 3rd quartile (Q3); df – degrees of freedom. Statistically significant p-values are in bold.

in the supine position and the margin of the sacral bone was significantly larger ($Z = -2.530$, $p = 0.011$) than for the wires inserted in entry point A than in entry point B (Table 2). Because no K-wires inserted in entry point C were outside the bone during the cadaver dissections, the Wilcoxon signed-rank test revealed significantly larger distances between the K-wires inserted in the supine position in entry point A ($Z = -2.527$, $p = 0.012$) and the margin of the sacral bone.

Kirschner wires inserted in the prone surgical position

The radiographic analysis of the inlet view revealed the most profound penetration for the K-wires inserted in entry point A (Table 3). The negative median values obtained on inlet views for K-wires inserted in entry points B and C indicate that the wires were entirely within the bone and posterior to the midline of the sacrum.

The Friedman's test revealed statistically significant differences ($\chi^2(2) = 16.000$, $p < 0.001$) between K-wires inserted in the 3 consecutive entry points in the prone position in terms of distances measured between the K-wires and the transverse axis of the sacrum in radiographic inlet view images. The Wilcoxon signed-rank test revealed that the penetration for the K-wires inserted in entry point A was significantly larger than for the K-wires inserted in entry point B ($Z = -2.640$, $p = 0.008$) and entry point C ($Z = -2.588$, $p = 0.010$) (Table 4).

During the cadaver dissections, no K-wires inserted in entry points A, B or C were outside the bone.

Percentage of cadavers with correctly placed Kirschner wires

In all of the studied cadavers, the radiographic analysis of the inlet view revealed the incorrect placement of K-wires inserted in the supine position at entry point A

Table 2. Comparison between the 3 studied entry points in terms of distance between the Kirschner wires inserted in the supine position and the midline (inlet view) or margin of the cortex (cadaver dissection) of the sacral bone (Wilcoxon signed-rank test results)

Compared entry points	Wilcoxon signed-rank test's results			
	inlet view		cadaver dissection	
	Z	p-value	Z	p-value
Entry points A vs B	-2.388	0.017	-2.530	0.011
Entry points A vs C	-2.527	0.012	-2.527	0.012
Entry points B vs C	-2.539	0.011	-2.232	0.026

Statistically significant p-values are in bold.

Table 3. Comparison between the 3 studied entry points in terms of distance between the Kirschner wires inserted in the prone position and the midline (inlet view) or margin of the cortex (cadaver dissection) of the sacral bone (Friedman test results)

Insertion entry point		Inlet view			Cadaver dissection		
		Me	Q1	Q3	Me	Q1	Q3
Entry point A		1.00	0.00	2.00	0.00	0.00	0.00
Entry point B		-1.50	-2.00	0.00	0.00	0.00	0.00
Entry point C		-4.00	-4.75	-3.25	0.00	0.00	0.00
Friedman's test results	χ^2	16.000			N/A		
	df	2			N/A		
	p-value	<0.001			N/A		

Values are expressed as the median (Me), the 1st quartile (Q1), and the 3rd quartile (Q3); df – degrees of freedom; N/A – not applicable. Statistically significant p-values are in bold.

Table 4. Comparison between the 3 studied entry points in terms of distance between the Kirschner wires inserted in the prone position and the midline (inlet view) or margin of the cortex (cadaver dissection) of the sacral bone (Wilcoxon signed-rank test results)

Compared entry points	Wilcoxon signed-rank test's results			
	inlet view		cadaver dissection	
	Z	p-value	Z	p-value
Entry points A vs B	-2.640	0.008	N/A	N/A
Entry points A vs C	-2.588	0.010	N/A	N/A
Entry points B vs C	-2.588	0.010	N/A	N/A

N/A – not applicable. Statistically significant p-values are in bold.

and entry point B (Fig. 3). In contrast, the correct placement of K-wires inserted in the supine position at entry point C was observed in 38% of the cadavers. Using the Q Cochran test, our results demonstrated significant differences ($Q(2) = 6.00$, $p = 0.050$) between the number of correctly placed K-wires determined on the radiographic analysis of the inlet view inserted in the 3 entry points (Table 5).

Consecutive comparisons are presented in Table 6. The final analysis of the placement of K-wires during

cadaver dissection revealed no correct positioning of any of the K-wires inserted at entry point A in the supine position (Fig. 4). In 13% of cadavers, we noted the correct placement of K-wires inserted in the supine position at entry point B. All K-wires inserted in the supine position at entry point C were correctly placed.

The radiographic analysis of the inlet view determined that the percentage of cadavers with correctly placed K-wires inserted in the prone position at entry points

Table 5. Comparison between the three studied entry points in terms of distance of the correctness of placement of the inserted Kirschner wires in the sacral bone (the results of Cochran's Q test).

Surgical positioning		Insertion in supine position		Insertion in prone position	
compared entry points		inlet view	cadaver dissection	inlet view	cadaver dissection
Entry point A		0/8	0/8	3/5	8/0
Entry point B		0/8	2/6	7/1	8/0
Entry point C		3/5	8/0	8/0	8/0
Cochran's test results	Q	6.00	13.00	8.40	N/A
	df	2	2	2	N/A
	p-value	0.050	0.002	0.015	N/A

Values are expressed as a number of cadavers with correct/incorrect placement; N/A – not applicable. Statistically significant p-values are in bold.

Table 6. Comparison between the 3 studied entry points in terms of distance of the correctness of placement of the inserted Kirschner wires in the sacral bone (the results of McNemar's test)

Surgical positioning		Insertion in supine position		Insertion in prone position	
compared entry points		inlet view	cadaver dissection	inlet view	cadaver dissection
Entry points A vs B		N/A	$p = 0.386$ $p = 1.000^*$	$p = 0.028$ $p = 0.085^*$	N/A
Entry points A vs C		$p = 0.034$ $p = 0.102^*$	$p < 0.001$ $p = 0.002^*$	$p = 0.006$ $p = 0.019^*$	N/A
Entry points B vs C		$p = 0.034$ $p = 0.102^*$	$p = 0.009$ $p = 0.028^*$	$p = 0.584$ $p = 1.000^*$	N/A

Values expressed as McNemar's test results. N/A – not applicable. *Bonferroni correction for multiple corrections. Statistically significant p-values after providing Bonferroni correction are in bold.

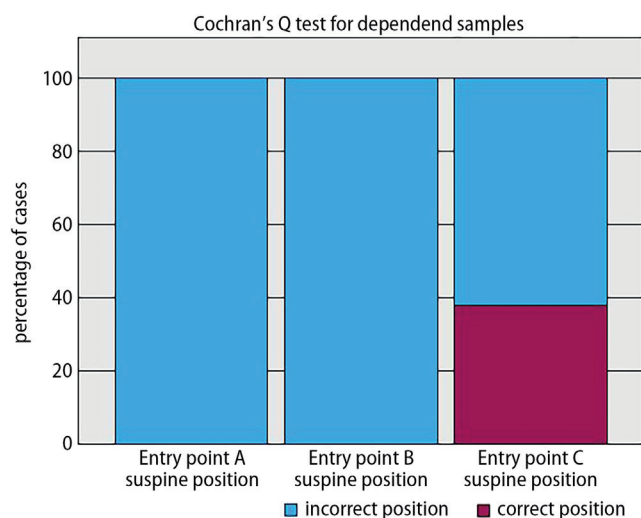


Fig. 3. Analysis of the percentage of cadavers in which correct and incorrect Kirschner wire placement was observed on radiographic imaging in the inlet view at particular entry points in the supine surgical position

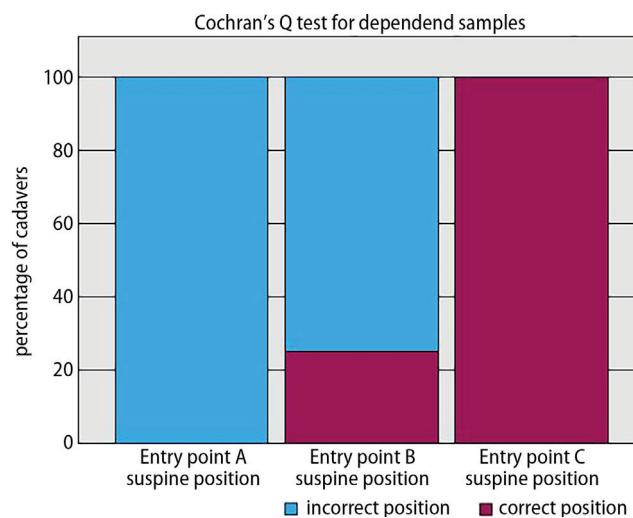


Fig. 4. Analysis of the percentage of cadavers in which correct and incorrect Kirschner wire placement was observed during cadaver dissection at particular entry points in the supine surgical position

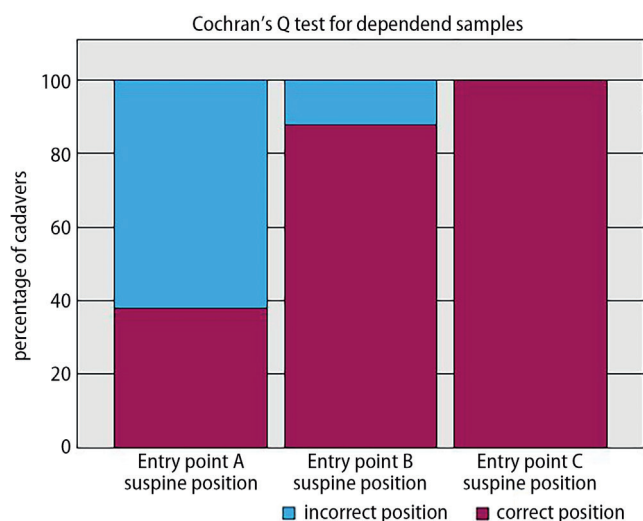


Fig. 5. Analysis of the percentage of cadavers in which correct and incorrect Kirschner wire placement was observed on radiographic imaging in the inlet view at particular entry points in the prone surgical position

A, B, and C exceeded 38%, 88% and 100%, respectively (Fig. 5), and Tables 5,6 present detailed comparisons. The cadaver dissection revealed that all the K-wires inserted in the prone position were in the correct position regardless of the insertion entry point.

Discussion

This cadaver study demonstrated that the best entry points for percutaneous insertion of sacroiliac screws are different for surgeries performed in the prone and supine positions. The standard entry point, initially defined by Matta and Saucedo, and points located 1 cm and 2 cm cranially from the mentioned standard point along the line prolonging the femoral axis enabled the correct placement of orthopedic implants for surgery performed in the prone position. Moreover, the best entry point for surgery performed in the supine position was located 2 cm cranially from the mentioned standard entry point along the line extending the femoral axis.

Percutaneous sacroiliac-screw fixation is considered the gold standard when it comes to the treatment of posterior pelvic ring fractures. It was developed as an alternative to the previous ORIF technique. Unfortunately, it had a high risk of extensive dissections, prominent implants, iatrogenic injuries, infection, and blood loss in already traumatized patients.^{11,16,28–30} Sacroiliac screws are multipurpose and can be used to treat a variety of sacral fractures or sacroiliac joint dislocations.¹⁶ They are utilized to stabilize pelvic ring injuries using a corridor of bone through the ilium, sacroiliac joint, sacral ala, and sacral promontory.³¹

The sacroiliac screws can be inserted in a supine, prone or lateral position.¹⁶ Initially, the starting point for the percutaneous sacroiliac screw insertion, as defined by Matta and Saucedo, is located 15 mm anterior to the gluteal crist

at 50% of the distance between the greater sciatic notch and the iliac crest.¹⁸ It corresponds to the intersection of the line posterior to the anterior superior iliac spine and the line that continues the anatomic axis of the femur.¹⁸ Ebraheim et al. determined the starting point for the sacroiliac screw on the outer table of the ilium 3 cm anterior to the posterior superior iliac spine and 4 cm cephalad to the greater sciatic notch.³² While Matta and Saucedo determined the best entry point for percutaneous sacroiliac screw fixation in patients operated in the prone position,¹⁸ Routt et al. subsequently used the same entry point for surgeries performed on patients in the supine position.¹⁹ However, no studies have examined the adequacy of the same entry point for patients in prone and supine surgical positions. The present cadaver study indicated that the best entry points for percutaneous insertion of sacroiliac screws are different for surgeries in the prone and supine positions. While the standard entry point, as defined by Matta and Saucedo, was adequate for correctly placing sacroiliac screws into cadavers in the prone position, it was ineffective for surgeries performed in the supine position.

The most effective entry point for the correct placement of sacroiliac screws in cadavers in the prone position was determined to be located 2 cm cranially from Matta and Saucedo's entry point along the line extending the femoral anatomic axis. This finding is crucial for clinical practice, as placing a patient in a supine position is required for anterior pelvic ring stabilization. Hence, using the best entry point for surgeries performed in the supine position eliminates the need to change the patient's position intraoperatively from supine to prone.

Despite its many advantages, percutaneous sacroiliac screw fixation presents a considerable risk of iatrogenic injuries.¹⁶ Sacroiliac screw placement also carries a risk of neurovascular structure injuries, including to the L5 and S1 nerve roots. However, the superior gluteal neurovascular bundle may also be injured by percutaneously inserted sacroiliac screws.^{33,34} Furthermore, the superior gluteal artery and iliac vessels are at risk of injury,¹⁶ and screw malposition rates can be up to 25%.³⁵ Therefore, various imaging modalities are used to support the insertion. Preoperative planning and understanding of sacroiliac screw placement are crucial to minimizing the occurrence of complications.

Limitations

This study has several limitations. First, it should be highlighted that none of the studied cadavers had sacral dysmorphism. In other words, the best entry points were determined for normal sacral anatomy. Variations in the normal sacral anatomy, including angulated upsloping ala and incomplete upper sacral segment disc space defined as sacral dysmorphism, occur at a relatively high incidence of 20–40%.^{23,24} Because patients may have different anatomies, preoperative and intraoperative imaging is crucial

to maintain their safety.²³ In combination with anteroposterior, inlet and outlet views, lateral sacral images are required for intraoperative visualization. Second, the sample size was small, and a larger sample may allow a more decisive conclusion. A 3rd limitation of the present study is its design, with clinical studies being needed to investigate whether the best entry points that theoretically improve surgical accuracy translate into better clinical outcomes.






Conclusions

The cadaver study showed that the best entry points for percutaneous insertion of sacroiliac screws are different for surgeries in the prone and supine positions. The standard entry point, initially defined by Matta and Saucedo, and points located 1 cm and 2 cm cranially from the mentioned standard point along the line extending the femoral axis enabled the correct placement of orthopedic hardware for surgery performed in the prone position. However, the best entry point for surgery performed in the supine position was located 2 cm cranially from the mentioned standard entry point, along the line prolonging the femoral axis.

Data availability statement

All data generated and analyzed during this study are included and available to the readers as they were deposited in an online repository (<https://doi.org/10.5281/zenodo.8357116>).

ORCID IDs

Michał Kułakowski  <https://orcid.org/0000-0003-1979-849X>
 Karol Elster  <https://orcid.org/0000-0002-1894-2835>
 Wojciech Piotrowski  <https://orcid.org/0000-0002-3267-0709>
 Paweł Ślęczka  <https://orcid.org/0000-0002-0440-688X>
 Aleksandra Królikowska  <https://orcid.org/0000-0002-6283-5500>
 Jarosław Witkowski  <https://orcid.org/0000-0002-2754-1339>
 Łukasz Oleksy  <https://orcid.org/0000-0002-0589-0554>
 Dariusz Janczak  <https://orcid.org/0000-0003-4671-9128>
 Paweł Reichert  <https://orcid.org/0000-0002-0271-4950>

References

- Arvieux C, Thony F, Broux C, et al. Current management of severe pelvic and perineal trauma. *J Visc Surg*. 2012;149(4):e227–e238. doi:10.1016/j.jvisurg.2012.06.004
- Faillinger MS, McGanity PL. Unstable fractures of the pelvic ring. *J Bone Joint Surg Am*. 1992;74(5):781–791.
- Nelson DW, Duwelius PJ. CT-guided fixation of sacral fractures and sacroiliac joint disruptions. *Radiology*. 1991;180(2):527–532. doi:10.1148/radiology.180.2.2068323
- Pizanis A, Pohlmann T, Burkhardt M, Aghayev E, Holstein JH. Emergency stabilization of the pelvic ring: Clinical comparison between three different techniques. *Injury*. 2013;44(12):1760–1764. doi:10.1016/j.injury.2013.07.009
- Yang NP, Chan CL, Chu D, et al. Epidemiology of hospitalized traumatic pelvic fractures and their combined injuries in Taiwan: 2000–2011 National Health Insurance Data Surveillance. *Biomed Res Int*. 2014;2014:878601. doi:10.1155/2014/878601
- Mostafavi HR, Tornetta P. Radiologic evaluation of the pelvis. *Clin Orthop Relat Res*. 1996;329:6–14. doi:10.1097/00003086-199608000-00003
- Rinne PP, Laitinen MK, Kannus P, Mattila VM. The incidence of pelvic fractures and related surgery in the Finnish adult population: A nationwide study of 33,469 patients between 1997 and 2014. *Acta Orthop*. 2020;91(5):587–592. doi:10.1080/17453674.2020.1771827
- Cole JD, Blum DA, Ansel LJ. Outcome after fixation of unstable posterior pelvic ring injuries. *Clin Orthop Relat Res*. 1996;329:160–179. doi:10.1097/00003086-199608000-00020
- Denis F, Davis S, Comfort T. Sacral fractures: An important problem. Retrospective analysis of 236 cases. *Clin Orthop Relat Res*. 1988;227:67–81. PMID:3338224.
- Gibbons KJ, Soloniuk DS, Razack N. Neurological injury and patterns of sacral fractures. *J Neurosurg*. 1990;72(6):889–893. doi:10.3171/jns.1990.72.6.0889
- Keating JF, Werier J, Blachut P, Broekhuysen H, Meek RN, O'Brien PJ. Early fixation of the vertically unstable pelvis: The role of iliosacral screw fixation of the posterior lesion. *J Orthop Trauma*. 1999;13(2):107–113. doi:10.1097/00005131-199902000-00007
- McLaren AC, Rorabeck CH, Halpenny J. Long-term pain and disability in relation to residual deformity after displaced pelvic ring fractures. *Can J Surg*. 1990;33(6):492–494. PMID:2253128.
- Smith HE, Yuan PS, Sasso R, Papadopoulos S, Vaccaro AR. An evaluation of image-guided technologies in the placement of percutaneous iliosacral screws. *Spine (Phila Pa 1976)*. 2006;31(2):234–238. doi:10.1097/01.brs.0000194788.45002.1b
- Burgess AR, Eastridge BJ, Young JW, et al. Pelvic ring disruptions: Effective classification system and treatment protocols. *J Trauma*. 1990;30(7):848–856. PMID:2381002.
- Latenser BA, Gentilello LM, Tarver AA, Thalgott JS, Batdorf JW. Improved outcome with early fixation of skeletally unstable pelvic fractures. *J Trauma*. 1991;31(1):28–31. doi:10.1097/00005373-199101000-00006
- Iorio JA, Jakoi AM, Rehman S. Percutaneous sacroiliac screw fixation of the posterior pelvic ring. *Orthop Clin North Am*. 2015;46(4):511–521. doi:10.1016/j.jocl.2015.06.005
- Alvis-Miranda H, Farid-Escorcia H, Alcalá-Cerra G, Castellar-Leones S, Moscote-Salazar L. Sacroiliac screw fixation: A mini review of surgical technique. *J Craniovert Jun Spine*. 2014;5(3):110. doi:10.4103/0974-8237.142303
- Matta JM, Saucedo T. Internal fixation of pelvic ring fractures. *Clin Orthop Relat Res*. 1989;(242):83–97. PMID:2706863.
- Chip Routt ML, Kregor PJ, Simonian PT, Mayo KA. Early results of percutaneous iliosacral screws placed with the patient in the supine position. *J Orthop Trauma*. 1995;9(3):207–214. doi:10.1097/00005131-199506000-00005
- Pohlmann T, Tosounidis G, Bircher M, Giannoudis P, Culemann U. The German Multicentre Pelvis Registry: A template for an European Expert Network? *Injury*. 2007;38(4):416–423. doi:10.1016/j.injury.2007.01.007
- Naude PH, Roche S, Nortje M, Maqungo S. The safety and efficacy of percutaneous sacroiliac joint screw fixation. *SA Orthop J*. 2014;13(4):26–29. https://scielo.org.za/scielo.php?pid=S1681-150X201400400004&script=sci_abstract. Accessed September 15, 2023.
- Kim KD, Duong H, Muzumdar A, Hussain M, Moldavsky M, Bucklen B. A novel technique for sacropelvic fixation using image-guided sacroiliac screws: A case series and biomechanical study. *J Biomed Res*. 2019;33(3):208. doi:10.7555/JBR.32.20170077
- Noser H, Radetzki F, Stock K, Mendel T. A method for computing general sacroiliac screw corridors based on CT scans of the pelvis. *J Digit Imaging*. 2011;24(4):665–671. doi:10.1007/s10278-010-9327-0
- Wang JQ, Wang Y, Feng Y, et al. Percutaneous sacroiliac screw placement: A prospective randomized comparison of robot-assisted navigation procedures with a conventional technique. *Chin Med J (Engl)*. 2017;130(21):2527–2534. doi:10.4103/0366-6999.217080
- Rose P, Goldberg BA, Lindsey RW, et al. Computed tomography assessment of sacroiliac screw placement relative to the first sacral neuroforamen. *J Spinal Disord*. 2001;14(4):330–335. doi:10.1097/00002517-200108000-00008
- Chen X, Zheng F, Zhang G, et al. An experimental study on the safe placement of sacroiliac screws using a 3D printing navigation module. *Ann Transl Med*. 2020;8(22):1512–1512. doi:10.21037/atm-20-7080
- Javidmehr S, Golbakhsh MR, Siavashi B, et al. A new modified method for inserting iliosacral screw versus the conventional method. *Asian Spine J*. 2018;12(1):119–125. doi:10.4184/asj.2018.12.1.119

28. Tile M. Pelvic ring fractures: Should they be fixed? *J Bone Joint Surg Br.* 1988;70-B(1):1–12. doi:10.1302/0301-620X.70B1.3276697
29. Judet R, Judet J, Letournel E. Fractures of the acetabulum: Classification and surgical approaches for open reduction. Preliminary report. *J Bone Joint Surg Am.* 1964;46:1615–1646. PMID:14239854.
30. Kellam JF, McMurtry RY, Paley D, Tile M. The unstable pelvic fracture: Operative treatment. *Orthop Clin North Am.* 1987;18(1):25–41. PMID:3796960.
31. Noojin FK, Malkani AL, Haikal L, Lundquist C, Voor MJ. Cross-sectional geometry of the sacral ala for safe insertion of iliosacral lag screws: A computed tomography model. *J Orthop Trauma.* 2000;14(1):31–35. doi:10.1097/00005131-200001000-00007
32. Ebraheim NA, Xu R, Biyani A, Nadaud MC. Morphologic considerations of the first sacral pedicle for iliosacral screw placement. *Spine (Phila Pa 1976).* 1997;22(8):841–846. doi:10.1097/00007632-199704150-00002
33. Templeman D, Schmidt A, Freese J, Weisman I. Proximity of iliosacral screws to neurovascular structures after internal fixation. *Clin Orthop Relat Res.* 1996;329:194–198. doi:10.1097/00003086-199608000-00023
34. Collinge C, Coons D, Aschenbrenner J. Risks to the superior gluteal neurovascular bundle during percutaneous iliosacral screw insertion: An anatomical cadaver study. *J Orthop Trauma.* 2005;19(2):96–101. doi:10.1097/00005131-200502000-00005
35. Tonetti J, Carrat L, Blendea S, et al. Clinical results of percutaneous pelvic surgery: Computer-assisted surgery using ultrasound compared to standard fluoroscopy. *Comput Aided Surg.* 2001;6(4):204–211. doi:10.3109/10929080109146084

LncRNA *LINC00969* modified by *METTL3* attenuates papillary thyroid cancer progression in an m⁶A-dependent manner

Chaogang Huang^{1,B,D,F}, Ziqi Duan^{2,A,F}, Baojie Chen^{1,C,F}, Hailiang Xia^{1,E,F}, Guangxin Wang^{1,E,F}

¹ Department of General Surgery, Wuhan Third Hospital (Tongren Hospital of Wuhan University), China

² Department of General Surgery, Jiangnan University, Wuhan, China

A – research concept and design; B – collection and/or assembly of data; C – data analysis and interpretation;

D – writing the article; E – critical revision of the article; F – final approval of the article

Advances in Clinical and Experimental Medicine, ISSN 1899–5276 (print), ISSN 2451–2680 (online)

Adv Clin Exp Med. 2025;34(4):623–632

Address for correspondence

Guangxin Wang

E-mail: wangguangxin0627@163.com

Funding sources

None declared

Conflict of interest

None declared

Received on January 5, 2024

Reviewed on February 26, 2024

Accepted on May 7, 2024

Published online on August 13, 2024

Abstract

Background. The long non-coding RNA (lncRNA) *LINC00969* is involved in human disease progression, and N⁶-methyladenosine (m⁶A) modification of lncRNAs in cancer has been proven to be a key regulatory mechanism. However, our understanding of its effects and mechanisms of action in papillary thyroid carcinoma (PTC) remains limited.

Objectives. This study aimed to elucidate the role of methyltransferase-like 3 (METTL3)-induced m⁶A modification of *LINC00969* in PTC tumorigenesis.

Materials and methods. Quantitative reverse transcription polymerase chain reaction (qRT-PCR) was performed to analyze *LINC00969* and *METTL3* mRNA levels in PTC. The regulation of *LINC00969* by METTL3 was confirmed using cell function experiments, molecular biology assays and bioinformatics analysis. *LINC00969* stabilization analysis was performed to verify the regulatory roles of METTL3 and *LINC00969*.

Results. *LINC00969* expression was downregulated in PTC tissues. Increased *LINC00969* expression inhibited the invasion, growth and migration of PTC cells. *METTL3* downregulation in PTC mediated the m⁶A modification of *LINC00969*, increasing its stability. Furthermore, *METTL3* levels were downregulated in PTC, and its silencing partially reversed the inhibitory effect of *LINC00969* overexpression on PTC cell malignancy.

Conclusions. *LINC00969* overexpression inhibits PTC cell malignancy via METTL3-mediated m⁶A modification. These findings suggest that *METTL3*-m⁶A-*LINC00969* is a promising therapeutic target for PTC.

Key words: papillary thyroid cancer, long non-coding RNA, METTL3, m⁶A, *LINC00969*

Cite as

Huang C, Duan Z, Chen B, Xia H, Wang G. LncRNA *LINC00969* modified by *METTL3* attenuates papillary thyroid cancer progression in an m⁶A-dependent manner. *Adv Clin Exp Med*. 2025;34(4):623–632. doi:10.17219/acem/188367

DOI

10.17219/acem/188367

Copyright

Copyright by Author(s)

This is an article distributed under the terms of the Creative Commons Attribution 3.0 Unported (CC BY 3.0) (<https://creativecommons.org/licenses/by/3.0/>)

Background

The incidence of thyroid cancer (THCA), the most common endocrine malignancy, has increased over the past 3 decades.¹ Papillary thyroid carcinoma (PTC), the most common subtype of THCA, accounts for 80–85% of all THCA cases.² Papillary thyroid carcinoma has been documented to exhibit a favorable prognosis, with a 5-year survival rate approaching 100%.³ However, some cases of locally infiltrating PTC have a high recurrence rate.⁴ In recent years, targeted therapies, particularly small-molecule therapies targeting receptor tyrosine kinases, have been evaluated in clinical trials to improve the survival of patients with PTC presenting with local infiltration.^{2,5} Nevertheless, there is a need for further investigation into more valuable molecular targets and mechanisms for the clinical management of PTC.

With the advancement of RNA sequencing technology, scientists are increasingly focusing on a specific class of RNA molecules, namely long non-coding RNAs (lncRNAs), which are over 200 nucleotides in length and do not encode proteins.⁶ The lncRNAs play crucial roles in diverse biological processes by acting as regulators that interact with RNA, DNA and proteins.^{7,8} Studies have shown that lncRNAs regulate carcinogenesis by participating in the invasion, metastasis, differentiation, proliferation, and metabolic reprogramming of tumor cells.⁹ In PTC, a wide range of lncRNAs are involved in tumor occurrence, including lncRNA GAS8-AS1,¹⁰ LINC00671¹¹ and lncRNA ABHD11-AS1.¹² LINC00969, also known as the *MIR570* host gene, plays inconsistent roles in various human diseases. For instance, LINC00969 accelerates intervertebral disc degeneration by enhancing apoptosis in the nucleus pulposus,¹³ acts as a potential biomarker for the development of type 2 diabetes mellitus complicated by carotid atherosclerotic plaques,¹⁴ and promotes gefitinib resistance in lung cancer cells.¹⁵ These studies demonstrate that LINC00969 epigenetically regulates multiple signaling pathways and that epigenetic regulation plays an important role in many biochemical processes associated with human diseases.¹⁶ However, the effect of LINC00969 on PTC remains uncertain and requires further investigation.

N6-methyladenosine (m⁶A) is a class of dynamically reversible RNA modifications in eukaryotic mRNAs that cluster around the stop codon and 3' untranslated region.¹⁷ N6-methyladenosine regulates various cellular pathways and processes by regulating mRNA splicing, expression, decay, and translation.¹⁸ There is growing evidence of a potential link between m⁶A and cancer, with changes in m⁶A levels affecting the progression or remission of tumors, including lung,¹⁹ liver,²⁰ ovarian,²¹ and breast²² cancers. Methyltransferase-like 3 (METTL3), possessing methyltransferase activity, regulates the progression of multiple tumors, including PTC.²³ For example, *METTL3* is reported to be downregulated in PTC and to positively regulate STEAP2 levels by mediating m⁶A modification,

which in turn inhibits PTC cell malignancy.^{24,25} However, the mechanisms through which *LINC00969* and *METTL3* affect PTC require further investigation.

Objectives

This study aimed to elucidate the regulatory role of *LINC00969* in PTC development and to demonstrate the tumor-suppressive role of *METTL3* in PTC via m⁶A modification. The findings of our study broaden our understanding of the mechanisms underlying PTC development and provide valuable targets for PTC therapy.

Materials and methods

Clinical specimens

Samples from 32 patients diagnosed with PTC at Wuhan Third Hospital (Wuhan, China), including both PTC and corresponding normal tissues, were collected by surgical excision. The inclusion criteria were as follows: 1) all patients were initially diagnosed with PTC by 2 pathologists and 2) none of the patients underwent any treatment before surgery. The exclusion criteria were as follows: 1) patients who did not provide written consent and 2) patients with comorbidities such as thyroiditis and cervical lymphadenopathy. The clinical characteristics of patients with PTC is listed in Table 1. All clinical specimens were stored in a –80°C refrigerator. Prior to sample collection, all participants signed an informed consent form. The collection and use of human specimens were approved by the Ethics Committee of the Wuhan Third Hospital (approval No. KY2023-012).

Table 1. Clinical characteristics of papillary thyroid cancer patients (n = 32)

Variables		n (%)
Age [years]	<45	18 (56.3)
	≥45	14 (43.7)
Sex	male	10 (31.3)
	female	22 (68.7)
Multifocality	yes	11 (34.4)
	no	21 (65.6)
Location	left lobe	13 (40.6)
	right lobe	16 (50.0)
	bilateral	2 (6.3)
	isthmus	1 (3.1)
Tumor stage	I–II	20 (62.5)
	III–IV	12 (37.5)
Lymph node metastasis	yes	17 (53.1)
	no	15 (46.9)

Cell culture

The normal human thyroid cell line Nthy-ori-3-2 (BNCC340487) and PTC cell lines, including TPC-1 (BNCC337912) and IHH-4 (BNCC360242), were obtained from the BeNa Culture Collection (BNCC, Beijing, China). IHH-4 and TPC-1 cells were cultured in Dulbecco’s modified Eagle’s medium (DMEM; BNCC), whereas Nthy-ori-3-1 cells were cultured in Roswell Park Memorial Institute (RPMI)-1640 (BNCC). Cell supernatants were supplemented with 10% fetal bovine serum (FBS) and 1% penicillin-streptomycin and maintained at 37°C with 5% CO₂.

Cell transfection

LINC00969 or *METTL3* sequences were cloned into a pcDNA3.1 vector for overexpression of *LINC00969* or *METTL3* (*LINC00969*-OE or *METTL3*-OE; RiboBio, Wuhan, China), with blank pcDNA3.1 used as the negative control (NC-OE). In addition, RiboBio synthesized the small interfering RNAs (siRNAs) targeting *METTL3* (si-*METTL3*) and si-NC. Transfection of vector (2 µg/mL) or oligonucleotide (50 nM) was performed using Lipo6000 reagent (Beyotime Biotechnology, Shanghai, China).

qRT-PCR

A TransZol Up Plus RNA kit (TransGen Biotech, Beijing, China) was used to extract total RNA. Reverse transcription and quantitative reverse transcription polymerase chain reaction (qRT-PCR) were performed using a cDNA Synthesis Kit (Fermentas, Waltham, USA) and SYBR Green Master Mix (Takara, Shiga, Tokyo, Japan), respectively. The qRT-PCR conditions were as follows: 95°C for 30 s, followed by 40 cycles of 95°C for 5 s and 60°C for 30 s. Relative expression was determined using the 2^{−ΔΔCt} method with glyceraldehyde 3-phosphate dehydrogenase (GAPDH) as the internal reference. Primer sequences are shown in Table 2.

Table 2. Primer sequences of *LINC00969* and *METTL3* in qualitative reverse transcription polymerase chain reaction (qRT-PCR) assay

Name	Primer sequences
<i>LINC00969</i>	Forward (5′-3′): TGGTGGAAGTGAGACCGAAAT
	Reverse (5′-3′): GTGATCCGTCCCAAGACAGC
<i>METTL3</i>	Forward (5′-3′): CAAGCTGCACTTCAGACGAA
	Reverse (5′-3′): GCTTGCGTGTGGTCTTT
<i>GAPDH</i>	Forward (5′-3′): GAAGGTGAAGTCTGGAGTC
	Reverse (5′-3′): GAAGATGGTGATGGGATTTC

Nucleus and cytoplasm localization

RNA from the cytoplasm and nuclei of IHH-4 and TPC-1 cells was isolated using a Nuclear and Cytoplasmic RNA

Purification Kit (Norgen, Thorold, Canada) as described in a previous study. Quantification of *LINC00969* levels in the cytoplasm and nucleus was performed using qRT-PCR.²⁶

CCK-8 analysis

Cells (3 × 10³ cells/well) were seeded into 96-well plates, and 100 µL of DMEM medium supplemented with 10% FBS was added. Cells were incubated for 0, 24, 48, and 72 h. Each well was then supplemented with Cell Counting Kit-8 (CCK-8) reagent (10 µL; Beyotime Biotechnology), and the plates were incubated at 37°C for 1 h. Optical density at 450 nm (OD₄₅₀) was measured using a microplate reader (model 1681130; Bio-Rad, Hercules, USA).

Colony formation assay

Papillary thyroid carcinoma cells were collected, adjusted to a concentration of 2 × 10³/mL, and transferred to the corresponding 6-well plates at 1 mL per well. Once colonies had grown to the appropriate size (after approx. 14 days of cell culture), the supernatant was removed, and the cells were washed. Paraformaldehyde (4%) was added for fixation at 25°C for 10 min. Subsequently, 700 µL of crystal violet staining solution was added for a 5-min staining period. The plates were allowed to dry, and images were captured using an optical microscope (model GX53; Olympus Corp., Tokyo, Japan). The number of clones in each well was determined.

Transwell assay

Dulbecco’s modified Eagle’s medium (500 µL) containing IHH-4 and TPC-1 cells (2 × 10⁵) was added to the upper transwell insert, with or without Matrigel pre-addition for invasion or migration assays. The prepared inserts were then placed in the lower compartment with 750 µL of complete DMEM medium containing 10% FBS. Invading or migrating cells were stained with 0.1% crystal violet after 24 h of incubation. Cell counts were recorded under an optical microscope (model GX53; Olympus Corp.).

Methylated RNA immunoprecipitation assay

Methylated RNA immunoprecipitation (MeRIP) assays were conducted using the Magna MeRIP m⁶A kit purchased from Cloud-Seq Biotech (Shanghai, China). Total RNA (150 µg) extracted from cells treated with *METTL3*-OE or negative control of overexpression vector (NC-OE) was fragmented to produce fragments of 100 nucleotides or smaller. The fragmented RNA was then immunoprecipitated using magnetic beads precoated with 3 µg of anti-m⁶A antibody or anti-IgG. Finally, the immunoprecipitated RNA fragments were analyzed using qRT-PCR.²⁷

RNA stabilization assay

IHH-4 and TPC-1 cells were treated with 2 $\mu\text{g/mL}$ of the transcriptional inhibitor actinomycin D for 0, 3 and 6 h to block transcription. The cells were collected for RNA extraction, and qRT-PCR was performed to measure the LINC00969 levels.

Statistical analyses

Data expressed as mean \pm standard deviation ($\pm\text{SD}$) were analyzed using GraphPad Prism v. 9 software (GraphPad, San Diego, USA). The normality of all data was assessed using the Shapiro–Wilk test (Supplementary Table 1), and the homogeneity of variance was analyzed using either the F test or Brown–Forsythe test (Supplementary Table 2). If the data followed a normal distribution and exhibited heterogeneous variance, Student's t-test was used to compare differences between 2 groups, with significance set at $p < 0.05$. If the data did not follow a normal

distribution or heterogeneous variance or if the sample size per group was less than 20, the Mann–Whitney U test was used for 2 groups, and the Kruskal–Wallis test followed by Dunnett's post hoc test was used for multiple groups, with significance set at $p < 0.05$ (Supplementary Table 3). In addition, the data from Gene Expression Profiling Interactive Analysis (GEPIA; <http://gepia.cancer-pku.cn/index.html>) were analyzed using the R package limma.

Results

LINC00969 exhibits low expression in PTC

Gene Expression Profiling Interactive Analysis is an online tool that analyzes differentially expressed lncRNAs in THCA samples. Using GEPIA, we found that LINC00969 expression was significantly lower in 512 THCA samples compared to 337 normal samples (Fig. 1A). To confirm this

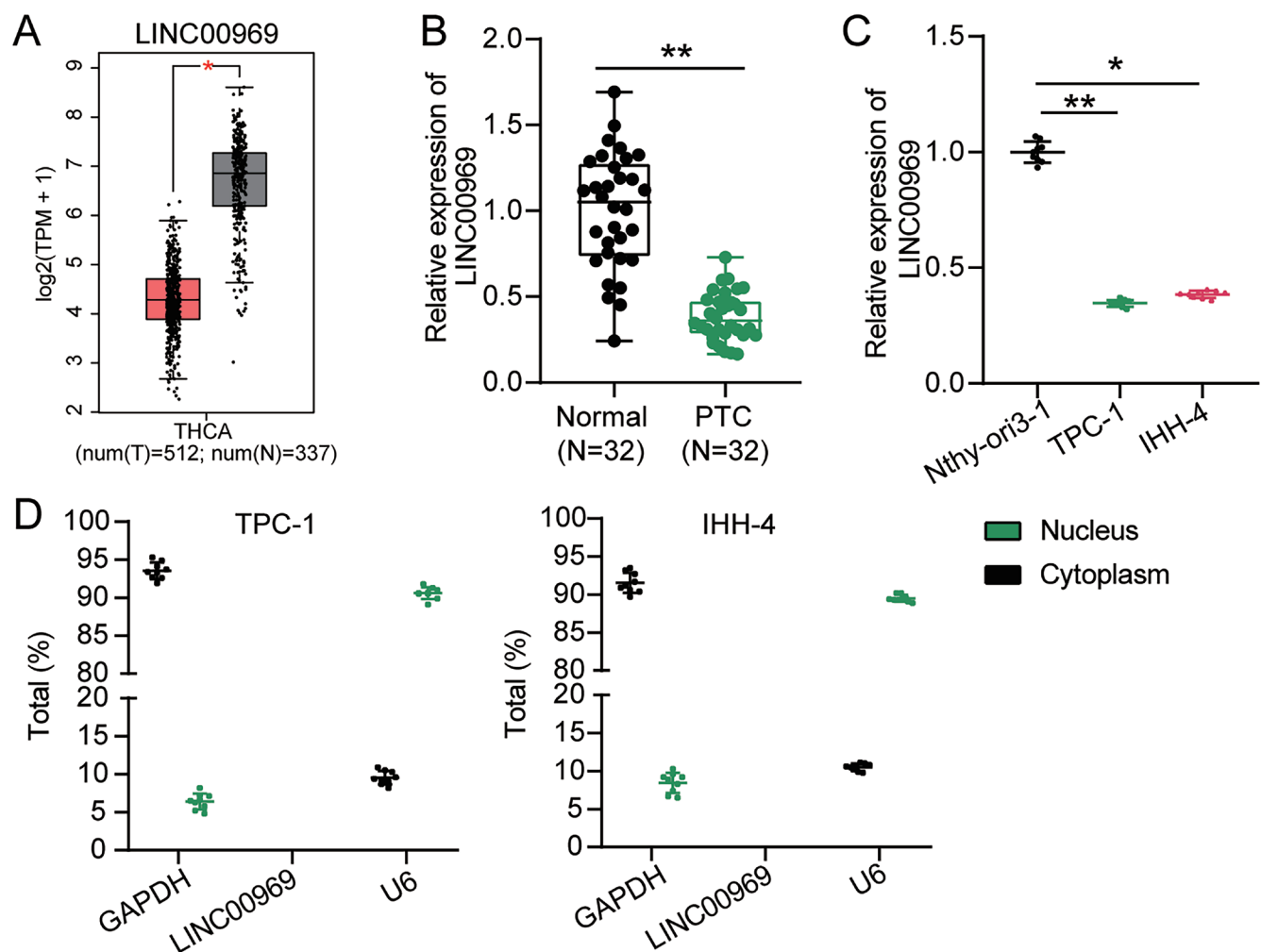


Fig. 1. LINC00969 exhibits low expression in papillary thyroid carcinoma (PTC). A. Gene Expression Profiling Interactive Analysis (GEPIA) showed the LINC00969 expression in thyroid cancer (THCA); * $p < 0.001$; B. LINC00969 expression in PTC and normal tissues was analyzed using qualitative reverse transcription polymerase chain reaction (qRT-PCR); ** $p < 0.001$; C. LINC00969 expression in Nthy-ori3-1 and PTC cell lines (IHH-4 and TPC-1) was analyzed using qRT-PCR; * $p < 0.05$, ** $p < 0.001$ vs Nthy-ori3-1; D. LINC00969 expression in the nucleus and cytoplasm of PTC cells was analyzed using qRT-PCR

finding, we collected PTC tissues and adjacent normal tissues from 32 patients with PTC and assessed *LINC00969* expression using qRT-PCR. The results showed a 70% downregulation of *LINC00969* expression in PTC tissues (Fig. 1B). Subsequently, we analyzed *LINC00969* expression in 2 PTC cell lines (TPC-1 and IHH-4) and the normal human thyroid cell line Nthy-ori-3-2 using qRT-PCR, and *LINC00969* was found to be downregulated in the PTC cell lines (Fig. 1C). Furthermore, a nuclear–cytoplasmic isolation assay was conducted to determine the subcellular localization of *LINC00969*, showing higher levels of *LINC00969* in the cytoplasm of PTC cells than in the nucleus, suggesting that *LINC00969* was enriched in the cytoplasm (Fig. 1D). Taken together, these findings suggest that *LINC00969* expression was enriched in the cytoplasm and downregulated in PTC.

***LINC00969* overexpression inhibits PTC cell malignancy**

To confirm the function of *LINC00969* in PTC, we constructed the *LINC00969* overexpression vector (*LINC00969*-OE) and its negative control (NC-OE), which were then transfected into PTC cells. Subsequently, qRT-PCR was used to detect *LINC00969* expression and verify the transfection efficiency. The results revealed a 6-fold increase in *LINC00969* expression in the *LINC00969*-OE group compared to the NC-OE group, indicating the high transfection efficiency of *LINC00969*-OE (Fig. 2A). Cell function assays were performed to analyze the effects of *LINC00969* on the proliferation, migration and invasion of PTC cells. The CCK-8 assay demonstrated an approx. 40% reduction in cell viability in the *LINC00969*-OE group (Fig. 2B). Colony formation analysis revealed that the number of colonies in the *LINC00969*-OE group decreased by nearly 70% compared to the NC-OE group (Fig. 2C). Transwell assay results showed that *LINC00969* upregulation led to approx. 62% and 70% reductions in PTC cell migration and invasion, respectively (Fig. 2D,E). These results demonstrate that *LINC00969* overexpression inhibits PTC cell malignancy.

METTL3* exhibits low expression in PTC and mediates the m⁶A modification of *LINC00969

To identify the molecular targets of m⁶A in PTC, we determined the m⁶A modification site of *LINC00969* using RMBase v2.0 (Fig. 3A). Using the GEPIA database, we found a positive correlation between *LINC00969* and *METTL3* expression in THCA, and found that *METTL3* expression was reduced in THCA (Fig. 3B,C). In our clinical samples from 32 patients with PTC, qRT-PCR analysis also showed low *METTL3* levels in PTC tissues and a positive correlation with *LINC00969* expression (Fig. 3D,E). The m⁶A modification of *LINC00969*

by *METTL3* was examined using the MeRIP assay, and the results revealed that the m⁶A levels of *LINC00969* were significantly increased following *METTL3* upregulation, indicating that *METTL3* could regulate *LINC00969* through m⁶A modification in PTC (Fig. 3F). Moreover, RNA stabilization assays revealed that *METTL3* overexpression increased the resistance of *LINC00969* to actinomycin D, indicating that *METTL3* overexpression stabilized the RNA structure of *LINC00969* (Fig. 3G). Therefore, *METTL3* downregulation in PTC could mediate the m⁶A modification of *LINC00969*, thereby stabilizing its RNA structure.

***METTL3* silencing partially reverses the malignant blockage of PTC cells caused by *LINC00969* overexpression**

Subsequently, we investigated the effects of *METTL3* combined with *LINC00969* on the biological functions of PTC cells by transfecting the *LINC00969*-OE vector and si-*METTL3* into PTC cells. The results of CCK-8 and colony formation assays showed that the decreased proliferation of PTC cells caused by *LINC00969* overexpression was increased further when *LINC00969*-OE and si-*METTL3* were co-transfected into PTC cells (Fig. 4A,B). Moreover, transwell analysis revealed that both migration and invasion of PTC cells were impaired by the transfection of *LINC00969*-OE into PTC cells; however, this inhibitory effect on migration and invasion was enhanced by co-transfection of *LINC00969*-OE and si-*METTL3* into PTC cells (Fig. 4C,D). In conclusion, *METTL3* knockdown reverses the inhibitory effects of *LINC00969* overexpression on PTC malignancy.

Discussion

In this study, we elucidated the impact of *LINC00969* on PTC cell function via the m⁶A modification of *METTL3*. We found that *LINC00969* was downregulated in PTC, and its upregulation contributed to PTC cell malignancy, thereby alleviating PTC tumorigenesis. This study also confirmed that the m⁶A modification of *LINC00969* could be induced by *METTL3*, thus enhancing the stability of *LINC00969*. *METTL3* has been shown to suppress PTC progression by mediating the m⁶A modification of *LINC00969*.

Studies have found that dysregulated lncRNAs hold great potential as biomarkers of PTC. For instance, a study published in 2021 confirmed that *LINC00671* attenuates PTC cell malignancy by interacting with LDHA and STAT3.¹¹ In 2022, another lncRNA, ABHD11-AS1, was shown to enhance PTC cell malignancy by interacting with the EPS15L1/EGFR signaling pathway.¹² These studies revealed the diverse functions of different lncRNAs in PTC. Here, we found that *LINC00969* was downregulated

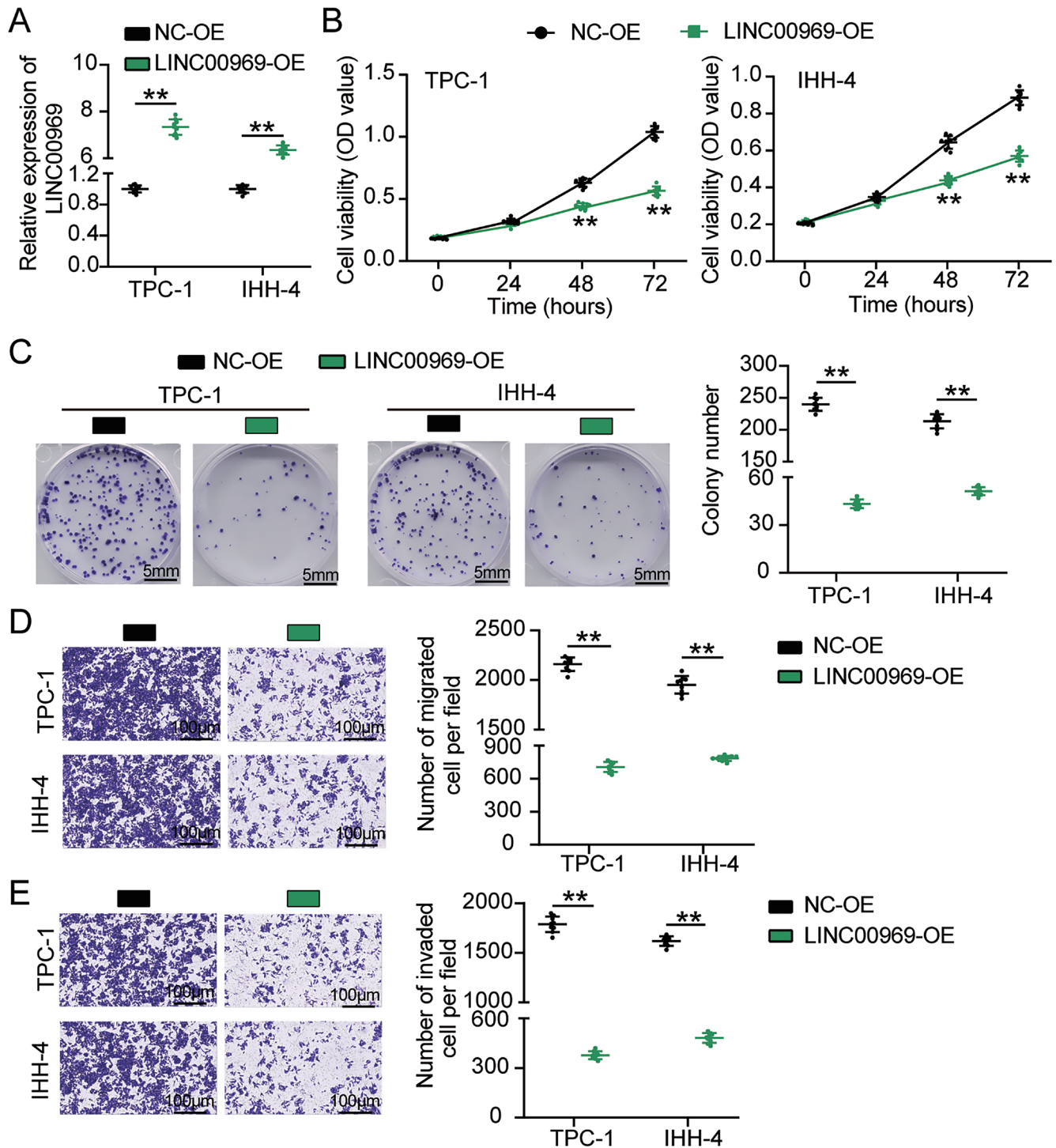


Fig. 2. Overexpression of *LINC00969* inhibits papillary thyroid carcinoma (PTC) cell malignancy. A. Qualitative reverse transcription polymerase chain reaction (qRT-PCR) revealed the *LINC00969* expression in PTC cells transfected with *LINC00969*-OE or negative control of overexpression vector (NC-OE); B,C. Cell Counting Kit-8 (CCK-8) and colony formation assays detected PTC cell proliferation following transfection with *LINC00969*-OE or NC-OE; D,E. Transwell assay detected the migration and invasion of PTC cells transfected with *LINC00969*-OE or NC-OE; **p < 0.001 vs NC-OE

OD – optical density.

in PTC. After reviewing the literature, only Dai et al.¹⁵ explored the function of *LINC00969* in lung cancer, proving that *LINC00969* promotes lung cancer progression by inhibiting cancer cell apoptosis. In contrast to the findings of Dai et al., we found that *LINC00969* repressed PTC

cell survival and metastasis, suggesting that *LINC00969* inhibited PTC progression. This is the first study to demonstrate that *LINC00969* plays different roles in different cancer types. *LINC00969* is an antitumor factor in PTC and an oncogenic factor in lung cancer.

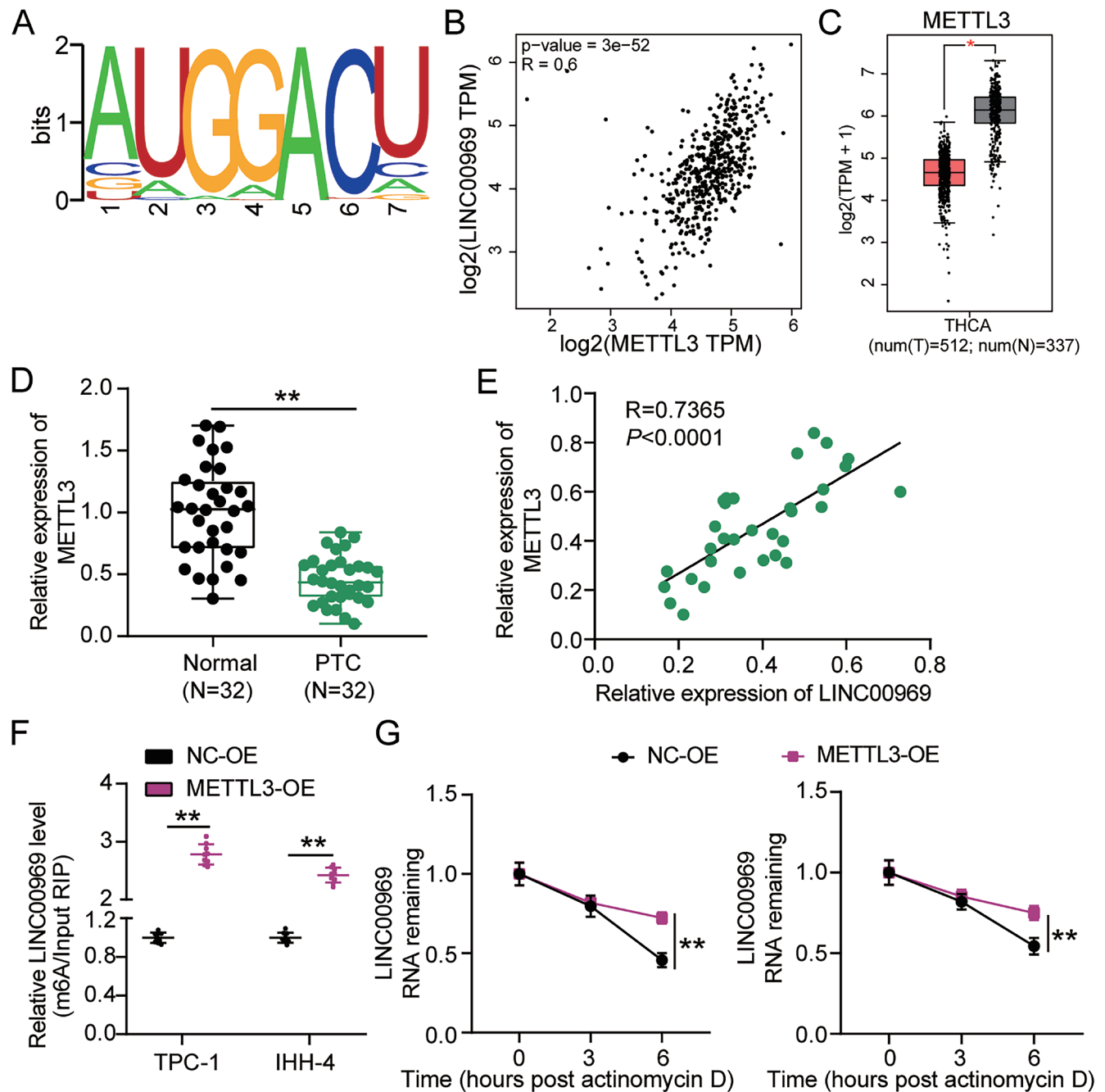


Fig. 3. *METTL3* exhibits low expression in papillary thyroid carcinoma (PTC) and mediates the m⁶A modification of *LINC00969*. A. m⁶A modification site of *LINC00969* according to RMBase v 2.0; B. Gene Expression Profiling Interactive Analysis (GEPIA) showed the correlation between *LINC00969* and *METTL3* in thyroid cancer (THCA); C. *METTL3* expression in THCA using GEPIA; D. Qualitative reverse transcription polymerase chain reaction (qRT-PCR) revealed the *METTL3* expression in PTC and normal tissues; **p < 0.001; E. Pearson's analysis was used to assess the correlation between *LINC00969* and *METTL3* in PTC samples; F. MeRIP assay detected the m⁶A modification of *LINC00969* in transfected PTC cells; **p < 0.001 vs NC-OE; G. *LINC00969* stability in transfected NPC cells; **p < 0.001

The m⁶A modifications that regulate lncRNAs have been recognized.¹⁷ Therefore, we investigated the m⁶A modification of *LINC00969* in PTC. Our research showed that *METTL3* in PTC mediates the m⁶A modification of *LINC00969*. The literature suggests that *METTL3* regulates lncRNAs to affect cancer progression. For instance, in lung cancer, *METTL3* induces m⁶A modifications that enhance the stability of *ABHD11-AS1* transcripts and are strongly associated with unfavorable patient prognosis.²⁸

Likewise, in prostate cancer, *METTL3* regulates the m⁶A modification of the lncRNA *SNHG7*, enhancing its stability and subsequently accelerating cancer glycolysis.²⁹ Furthermore, in gastric cancer, *METTL3* induces the m⁶A modification of lncRNA *THAP7-AS1* through an *IGF2BP1*-dependent pathway, which accelerates tumor development.³⁰ Previous studies have confirmed the oncogenic role of *METTL3* in cancer. However, our study is the first to provide evidence that *METTL3* is an antitumor factor

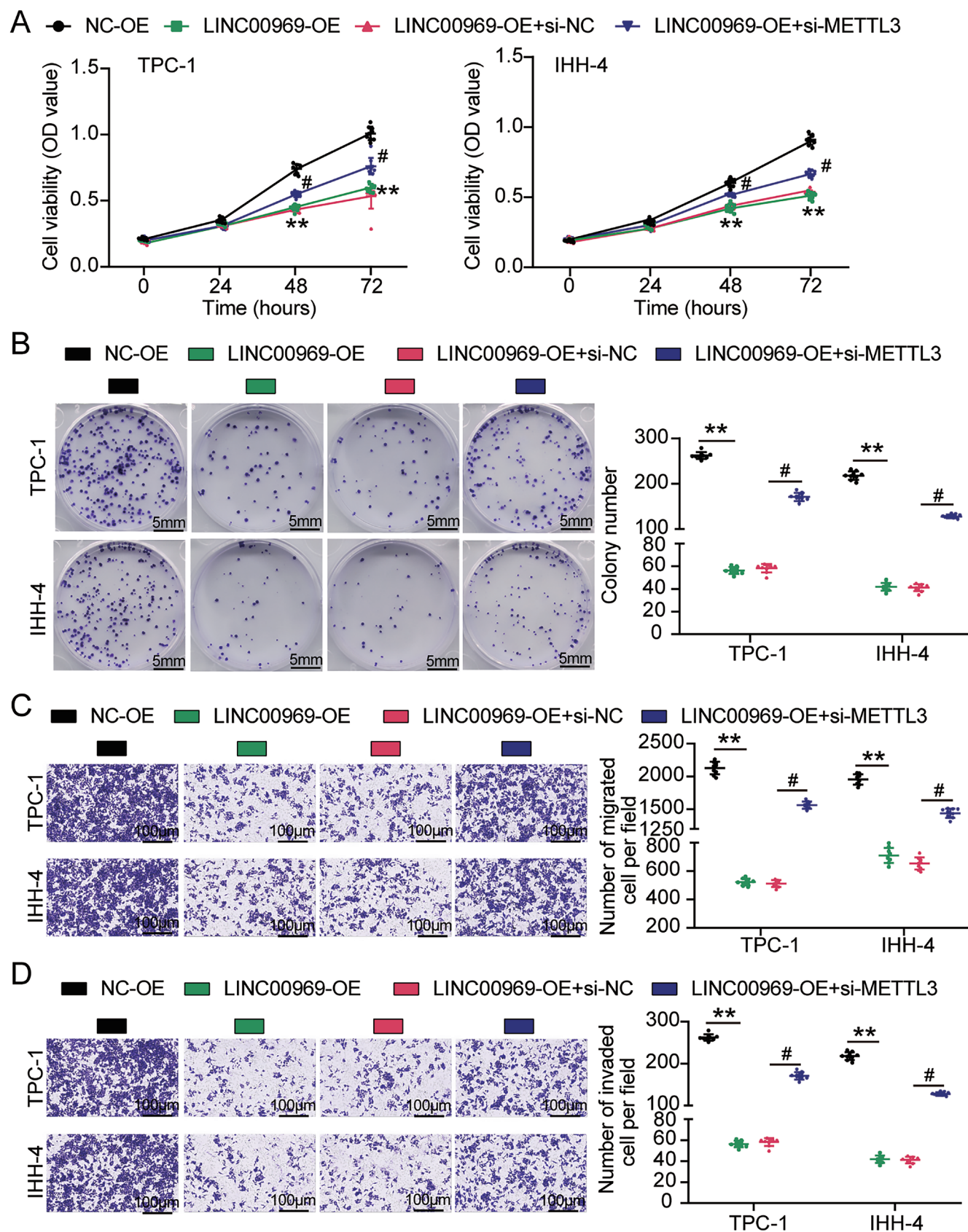


Fig. 4. Silencing of *METTL3* partially reverses the malignancy of papillary thyroid carcinoma (PTC) cells caused by *LINC00969* overexpression. A,B. Cell proliferation in transfected PTC cells was revealed using Cell Counting Kit-8 (CCK-8) and colony formation assay; C,D. Cell migration and invasion in transfected PTC cells were detected using transwell assay; ** $p < 0.001$ vs negative control of overexpression vector (NC-OE); # $p < 0.05$ vs *LINC00969*-OE + negative control of siRNA (si+NC); OD – optical density.

in PTC, showing that its downregulation in PTC and silencing promote PTC cell malignancy. Further analysis of the inhibitory effect of *METTL3* on PTC revealed that *METTL3* mediated the m⁶A modification of *LINC00969* to enhance *LINC00969* expression, thereby exerting an inhibitory effect on PTC cell malignancy. Our results align with the conventional understanding of *METTL3* as a carcinogenic factor in cancer and that the different roles and regulatory mechanisms of *METTL3* in different cancers need to be explored.

Limitations

This study elucidated the regulatory mechanism of *LINC00969* interaction with *METTL3* in PTC, but there were some limitations. First, the m⁶A modification consists of a “reader” protein, an “eraser” enzyme and a “writer” enzyme, which all play a role in regulating tumor cell malignancy in PTC.³¹ Although our study confirmed that the “writer” enzyme *METTL3* mediates m⁶A modification of *LINC00969*, we have not investigated the “reader” protein or “eraser” enzyme. Therefore, further exploration is needed to understand the roles of *LINC00969* and other m⁶A-modified proteins in PTC. Furthermore, our study collected clinical samples from only 32 patients with PTC, resulting in a small sample size that limited our ability to ascertain the clinical significance of *LINC00969* and *METTL3* in PTC. Future studies should aim to collect more extensive clinical samples to explore the relevance of *LINC00969* and *METTL3* to the histopathological phenotypes. Furthermore, the statistical analysis in our study was exploratory and did not incorporate multiple comparisons correction. Consequently, caution is warranted in interpreting the results due to the potential for uncontrolled type I error probability, which may also impact the validity of future meta-analyses. Nevertheless, this exploratory analysis provides a foundation for further research in the field.

Conclusions

This study revealed the downregulation of *LINC00969* and *METTL3* in PTC tissues and cells. Upregulation of *LINC00969* inhibited PTC proliferation, migration and invasion; however, silencing *METTL3* reversed the inhibitory effects of *LINC00969* on PTC malignancy. Further mechanistic analysis confirmed that *METTL3* mediated the m⁶A modification of *LINC00969*, stabilizing its RNA structure in PTC cells. This study presents a novel PTC regulatory mechanism based on the *METTL3/LINC00969* axis, which may provide new diagnostic or therapeutic biomarkers for PTC.

Supplementary data

The Supplementary materials are available at <https://doi.org/10.5281/zenodo.11080300>. The package includes the following files:

Supplementary Table 1. The results of normality test.

Supplementary Table 2. The results of homogeneity of variance.

Supplementary Table 3. The results of statistical analysis.


Data availability

The datasets generated and/or analyzed during the current study are available from the corresponding author on reasonable request.

Consent for publication

Not applicable.

ORCID iDs

Chaogang Huang  <https://orcid.org/0009-0002-1589-7933>
 Ziqi Duan  <https://orcid.org/0009-0007-8720-8697>
 Baojie Chen  <https://orcid.org/0009-0006-3795-6227>
 Hailiang Xia  <https://orcid.org/0009-0001-6814-2756>
 Guangxin Wang  <https://orcid.org/0009-0009-4981-3460>

References

1. Aryanpour Z, Asban A, Boyd C, et al. A single institution experience with papillary thyroid cancer: Are outcomes better at comprehensive cancer centers? *Am J Surg*. 2021;222(4):802–805. doi:10.1016/j.amjsurg.2021.02.027
2. Yang H, Liang Q, Zhang J, et al. Establishment of papillary thyroid cancer organoid lines from clinical specimens. *Front Endocrinol (Lausanne)*. 2023;14:1140888. doi:10.3389/fendo.2023.1140888
3. Bates MF, Lamas MR, Randle RW, et al. Back so soon? Is early recurrence of papillary thyroid cancer really just persistent disease? *Surgery*. 2018;163(1):118–123. doi:10.1016/j.surg.2017.05.028
4. Zhang J, Fu C, Cui K, Ma X. Papillary thyroid carcinoma with tracheal invasion: A case report. *Medicine (Baltimore)*. 2019;98(38):e17033. doi:10.1097/MD.00000000000017033
5. Fallahi P, Ferrari SM, Galdiero MR, et al. Molecular targets of tyrosine kinase inhibitors in thyroid cancer. *Semin Cancer Biol*. 2022;79:180–196. doi:10.1016/j.semcancer.2020.11.013
6. Bridges MC, Daulagala AC, Kourtidis A. LNCcation: lncRNA localization and function. *J Cell Biol*. 2021;220(2):e202009045. doi:10.1083/jcb.202009045
7. Qian X, Zhao J, Yeung PY, Zhang QC, Kwok CK. Revealing lncRNA structures and interactions by sequencing-based approaches. *Trends Biochem Sci*. 2019;44(1):33–52. doi:10.1016/j.tibs.2018.09.012
8. Li Y, Jiang T, Zhou W, et al. Pan-cancer characterization of immune-related lncRNAs identifies potential oncogenic biomarkers. *Nat Commun*. 2020;11(1):1000. doi:10.1038/s41467-020-14802-2
9. Luo J, Langer LF, Liu J. A novel role of lncRNA in regulating tumor metabolism and angiogenesis under hypoxia. *Cancer Commun (Lond)*. 2019;39(1):2. doi:10.1186/s40880-019-0348-x
10. Zhou DL, Liu Q, Xu BH, et al. lncRNA GAS8-AS1 genetic alterations in papillary thyroid carcinoma and their clinical significance. *Cancer Biomark*. 2020;29(2):255–264. doi:10.3233/CBM-191071
11. Huo N, Cong R, Sun ZJ, et al. STAT3/LINC00671 axis regulates papillary thyroid tumor growth and metastasis via LDHA-mediated glycolysis. *Cell Death Dis*. 2021;12(9):799. doi:10.1038/s41419-021-04081-0
12. Lu H, Zhu C, Chen Y, et al. lncRNA ABHD11-AS1 promotes tumor progression in papillary thyroid carcinoma by regulating EP515L1/EGFR signaling pathway. *Clin Transl Oncol*. 2022;24(6):1124–1133. doi:10.1007/s12094-021-02753-z
13. Yu L, Hao Y, Xu C, Zhu G, Cai Y. LINC00969 promotes the degeneration of intervertebral disk by sponging miR-335-3p and regulating NLRP3 inflammasome activation. *IUBMB Life*. 2019;71(5):611–618. doi:10.1002/iub.1989

14. Yu T, Xu B, Bao M, et al. Identification of potential biomarkers and pathways associated with carotid atherosclerotic plaques in type 2 diabetes mellitus: A transcriptomics study. *Front Endocrinol (Lausanne)*. 2022;13:981100. doi:10.3389/fendo.2022.981100
15. Dai J, Qu T, Yin D, et al. LncRNA LINC00969 promotes acquired gefitinib resistance by epigenetically suppressing of NLRP3 at transcriptional and posttranscriptional levels to inhibit pyroptosis in lung cancer. *Cell Death Dis*. 2023;14(5):312. doi:10.1038/s41419-023-05840-x
16. Surguchov A. α -synuclein and mechanisms of epigenetic regulation. *Brain Sci*. 2023;13(1):150. doi:10.3390/brainsci13010150
17. Ma S, Chen C, Ji X, et al. The interplay between m⁶A RNA methylation and noncoding RNA in cancer. *J Hematol Oncol*. 2019;12(1):121. doi:10.1186/s13045-019-0805-7
18. Zhang H, Shi X, Huang T, et al. Dynamic landscape and evolution of m⁶A methylation in human. *Nucl Acids Res*. 2020;48(11):6251–6264. doi:10.1093/nar/gkaa347
19. Liu J, Ren D, Du Z, Wang H, Zhang H, Jin Y. m⁶A demethylase FTO facilitates tumor progression in lung squamous cell carcinoma by regulating MZF1 expression. *Biochem Biophys Res Commun*. 2018;502(4):456–464. doi:10.1016/j.bbrc.2018.05.175
20. Chen M, Wei L, Law C, et al. RNA N6-methyladenosine methyltransferase-like 3 promotes liver cancer progression through YTHDF2-dependent posttranscriptional silencing of SOCS2. *Hepatology*. 2018;67(6):2254–2270. doi:10.1002/hep.29683
21. Liu T, Wei Q, Jin J, et al. The m⁶A reader YTHDF1 promotes ovarian cancer progression via augmenting EIF3C translation. *Nucl Acids Res*. 2020;48(7):3816–3831. doi:10.1093/nar/gkaa048
22. Wu Y, Wang Z, Han L, et al. PRMT5 regulates RNA m⁶A demethylation for doxorubicin sensitivity in breast cancer. *Mol Ther*. 2022;30(7):2603–2617. doi:10.1016/j.ymthe.2022.03.003
23. Zeng C, Huang W, Li Y, Weng H. Roles of METTL3 in cancer: Mechanisms and therapeutic targeting. *J Hematol Oncol*. 2020;13(1):117. doi:10.1186/s13045-020-00951-w
24. Hou J, Shan H, Zhang Y, Fan Y, Wu B. m⁶A RNA methylation regulators have prognostic value in papillary thyroid carcinoma. *Am J Otolaryngol*. 2020;41(4):102547. doi:10.1016/j.amjoto.2020.102547
25. Zhu Y, Peng X, Zhou Q, et al. METTL3-mediated m⁶A modification of STEAP2 mRNA inhibits papillary thyroid cancer progress by blocking the Hedgehog signaling pathway and epithelial-to-mesenchymal transition. *Cell Death Dis*. 2022;13(4):358. doi:10.1038/s41419-022-04817-6
26. Chen Z, Li Y, He K, et al. CircGPCR5A enhances colorectal cancer progress by stabilizing PPP1CA and inducing YAP dephosphorylation. *J Exp Clin Cancer Res*. 2023;42(1):334. doi:10.1186/s13046-023-02915-7
27. Fang D, Ou X, Sun K, et al. m⁶A modification-mediated lncRNA TP53TG1 inhibits gastric cancer progression by regulating CIP2A stability. *Cancer Sci*. 2022;113(12):4135–4150. doi:10.1111/cas.15581
28. Xue L, Li J, Lin Y, et al. m⁶A transferase METTL3-induced lncRNA ABHD11-AS1 promotes the Warburg effect of non-small-cell lung cancer. *J Cell Physiol*. 2021;236(4):2649–2658. doi:10.1002/jcp.30023
29. Liu J, Yuan JF, Wang YZ. METTL3-stabilized lncRNA SNHG7 accelerates glycolysis in prostate cancer via SRSF1/c-Myc axis. *Exp Cell Res*. 2022;416(1):113149. doi:10.1016/j.yexcr.2022.113149
30. Liu HT, Zou YX, Zhu WJ, et al. lncRNA THAP7-AS1, transcriptionally activated by SP1 and post-transcriptionally stabilized by METTL3-mediated m⁶A modification, exerts oncogenic properties by improving CUL4B entry into the nucleus. *Cell Death Differ*. 2022;29(3):627–641. doi:10.1038/s41418-021-00879-9
31. Zhu D, Zhou J, Zhao J, et al. ZC3H13 suppresses colorectal cancer proliferation and invasion via inactivating Ras-ERK signaling. *J Cell Physiol*. 2019;234(6):8899–8907. doi:10.1002/jcp.27551

Research status and controversy on non-small cell lung cancer stem cells

Jin Wang^{1,A,D,F}, Yunqing Chen^{2,B,C}, Chengqin Wang^{1,B,C}, Keyu Ren^{3,A,D}

¹ Department of Pathology, School of Basic Medicine, The Qingdao University, China

² Department of Pathology, The Affiliated Hospital of the Qingdao University, China

³ Department of Gastroenterology, The Affiliated Hospital of Qingdao University, China

A – research concept and design; B – collection and/or assembly of data; C – data analysis and interpretation;

D – writing the article; E – critical revision of the article; F – final approval of the article

Advances in Clinical and Experimental Medicine, ISSN 1899–5276 (print), ISSN 2451–2680 (online)

Adv Clin Exp Med. 2025;34(4):633–640

Address for correspondence

Keyu Ren

E-mail: rkyqfy@qdu.edu.cn

Funding sources

The Shandong Province Natural Science Foundation (General Program, grant No. ZR2022MH204).

Conflict of interest

None declared

Acknowledgements

The authors would like to thank Dr. Fenggang Xian for his advice.

Received on December 9, 2023

Reviewed on March 23, 2024

Accepted on April 11, 2024

Published online on November 18, 2024

Abstract

Lung cancer is a major cause of cancer-related deaths worldwide. It can be divided into 2 main types, namely non-small cell lung cancer (NSCLC) and small cell lung cancer (SCLC). Most patients with NSCLC are diagnosed at an advanced stage, and current treatments have limited success. Moreover, relapsing tumors that often appear after surgical or drug treatment are particularly difficult to treat. The existence of cancer stem cells (CSCs) has been proposed as a key factor contributing to the development of resistance to therapy, recurrence and metastasis. Targeting CSCs is a potential strategy for eradicating tumors. However, due to the tumor-type specificity and cellular plasticity, the real clinical application of lung cancer stem cells (LCSCs) has not been realized. This review details the existing phenotypic markers of LCSCs and the limitations of their identification and summarizes the roles of the tumor microenvironment (TME) and epithelial–mesenchymal transition (EMT) in the existence and maintenance of LCSCs, as well as the contribution and controversy of cellular plasticity theory on LCSCs. It is expected that future research on LCSCs can solve the present problems, and approaches targeting LCSCs may be applied in the clinic as soon as possible.

Key words: non-small cell lung cancer, cancer stem cells, epithelial–mesenchymal transition, tumor microenvironment, cellular plasticity

Cite as

Jin Wang J, Chen Y, Wang C, Ren K. Research status and controversy on non-small cell lung cancer stem cells.

Adv Clin Exp Med. 2025;34(4):633–640.

doi:10.17219/acem/187053

DOI

10.17219/acem/187053

Copyright

Copyright by Author(s)

This is an article distributed under the terms of the Creative Commons Attribution 3.0 Unported (CC BY 3.0) (<https://creativecommons.org/licenses/by/3.0/>)

Introduction

Lung cancer is a major cause of cancer-related deaths worldwide.¹ It is a heterogeneous disease that can be divided into 2 distinct pathological types: non-small cell lung cancer (NSCLC) and small cell lung cancer (SCLC), with NSCLC accounting for approx. 80–85% of all lung cancer types.^{2–4} After diagnosis, approx. 75% of patients with NSCLC have advanced diseases (stage III–IV), and the survival rate is low despite the oncological treatment of late-stage lung cancer seeing significant advances in recent years. The UK's Office for National Statistics reported that patients diagnosed with stage IV lung cancer had a 1-year survival rate of just 15–19%.⁵

In addition, relapsing tumors that often appear after surgical or drug treatment are more difficult to treat.⁶ For example, platinum-based chemotherapy was most common for advanced NSCLC, but a generation of drug-resistant tumors has proven to be a major barrier to chemotherapy efficacy.^{7–9} Although tyrosine kinase inhibitors have demonstrated significant responses in patients with advanced adenocarcinoma in recent years, almost all patients have developed drug resistance after 2–3 years of treatment.^{10,11}

Until now, the cancer stem cells (CSCs) hypothesis has been posited to be the underlying cause of relapse, metastasis and therapeutic resistance.^{12,13} On the one hand, CSCs can generate new stem cells and daughter cells that differentiate and continuously proliferate to form tumor parenchyma. Conversely, CSCs display high expression of the adenosine-triphosphate-binding cassette G2 (ABCG2), which contributes to pumping out chemotherapeutic drugs,^{14–16} leading to chemoresistance. Therefore, targeting CSCs means potential tumor eradication, and several strategies have been used in the clinical treatment of hematological malignancies and several solid tumors.^{17–19}

However, the CSCs theory has faced 2 major barriers. First, a universal CSC marker is lacking.²⁰ The specific markers to purify CSCs are still unclear because the cell surface markers used to identify CSCs vary among tumor types. Second, the mechanism by which CSCs cause the failure of therapies and the relapse is not fully understood.^{16,21–23} One likely explanation for the above controversy surrounding CSCs characterization is cellular plasticity,^{24–26} which refers to the reversible transition between a variety of cellular states, including stem cells (SCs)/non-stem cells (non-SCs), asymmetric divisions (ADs)/symmetric divisions (SDs), quiescence/proliferation, epithelial–mesenchymal transition (EMT)/mesenchymal-to-epithelial transition (MET), and drug sensitivity/drug resistance. Increasing evidence supports that CSCs represent a dynamic cellular state, in which the acquisition of stem-like traits is necessary for resistance and the promotion of tumor progression.^{27,28} Additionally, the tumor microenvironment (TME) plays an integral role in tumor progression and metastasis and is believed to support the cellular fate of CSCs.^{19,29} Thus, it is crucial to better understand

the behavior of CSCs based on their microenvironment. This understanding will aid in the development of more effective therapeutic strategies targeting CSCs.

We searched PubMed online database relevant literature until July 21, 2023, using the following search terms; “lung cancer stem cell” OR “lung cancer stemness” AND “cellular plasticity” OR “tumor microenvironment” OR “TME” OR “epithelial–mesenchymal transition” OR “EMT”. Moreover, we reviewed citations from retrieved articles to search for additional relevant studies. The retrieved studies were manually screened to assess their appropriateness for inclusion. Here, we introduced the characteristics of lung cancer stem cells (LCSCs), including their specific recognition, the interaction between LCSCs and TME, the role of EMT in acquiring stem-like phenotype, and the relationship between cellular plasticity and LCSCs. Our purpose was to summarize the existing research controversy in the LCSCs theory and to provide further direction for the study of LCSCs.

Objectives

We aimed to list the common phenotypic markers of LCSCs and summarize their limitations, reveal the relationship between LCSCs and TME and EMT, and to determine the role of cellular plasticity theory in the generation and transformation of LCSCs.

Lung cancer stem cells

Several studies have suggested that CSCs are associated with tumor heterogeneity and growth, leading to relapse and therapeutic resistance at any stage of cancer progression. The gold standard for assessing the oncogenic potential of CSCs is their ability to form transplantable tumors in immunodeficient mice. This approach has successfully confirmed the existence of CSCs in various tumor types, including brain, breast, lung, and hematological malignancies.^{30–32}

The first observation of LCSCs was published in 1982,³³ and subsequent growing evidence has confirmed that putative LCSCs can be isolated from various cell lines and tumor specimens. Lung cancer stem cells share similar properties to CSCs in other tumors: They have been associated with higher recurrence rates, radioresistance³⁴ and chemoresistance.^{35–37} Lung cancer stem cells can form stem cell spheres³⁸ and express stem-like phenotypes, including CD133, ABCG2 and ALDH1, among others.³⁹ In short, there is overwhelming evidence that stem cells exist in lung cancers.

Studies have identified CD133, CD44, CXCR4, CD166, EpCAM, CD90, and CD44 as common stemness-associated markers in lung cancers. In both NSCLC and SCLC cell lines, CD133-positive cells may generate long-term tumor spheres and differentiate into CD133-negative cells. Studies

performed *in vivo* have shown that 1×10^4 CD133-positive cells could generate tumors in immunodeficient mice. Additionally, CD133⁺ cells were found to be chemoresistant and expressed high levels of ABCG2 and other common stem cell markers, such as Oct4 or Nanog.³² Similarly, CD44-positive cells exhibited stemness properties in NSCLC cell lines.⁴⁰ CD90⁺ CSCs were also isolated from lung cancer cell lines A549 and H446,⁴¹ while cells positive for CXCR4, a chemokine receptor on the surface of hematopoietic stem cells (HSCs), can form tumor spheres *in vitro* and exhibited self-renewal capacity and radio-resistance in NSCLC.⁴² Finally, CD166⁺/CD44⁺ and CD166⁺/EpCAM⁺ lung cancer cells displayed multipotent characteristics of stem cells that can differentiate into adipogenic and osteogenic cells and express stem cell transcription factors such as Sox2 and Oct4.⁴³

The ALDH activity has also been shown to be associated with stemness traits in lung cancer cell lines. It had been reported that ALDH1-positive cells from NSCLC displayed the ability of self-renewal, proliferation potential and *in vivo* carcinogenicity. Moreover, these ALDH1-positive cells also expressed CD133 and produced resistance after treatment with commonly used chemotherapy drugs.⁴⁴ Earlier research has also demonstrated that the putative CSCs in lung cancer were able to express Oct4, Sox2, Nanog, and other core transcription factors responsible for regulating self-renewal and differentiation in embryonic stem cells, as well as CSCs.^{45,46}

However, it must be acknowledged that the expression of stem cell markers mainly depends on the source of CSCs isolation (such as primary tumors vs patient-derived xenograft tumors vs cell lines), as sometimes cell suspension culture may also cause a variety of cell surface markers. Although surface markers such as CD133 and CD44 have been successfully used to isolate CSCs, their expression is not exclusively linked to the CSC phenotype and is prone to environmental alteration.⁴⁷ Conflicting data have arisen in some settings due to the use of different markers and isolation methods, highlighting the challenges of isolating a pure CSC population.⁴⁸ For instance, CD133 was not detected at all in many lung cancer cases,^{49,50} while the expression of CD44 and ALDH display particularly strong associations with squamous cell carcinoma (SCC).^{51,52} In addition, the combined effect of these stem markers on LCSCs is not completely clear. While it has been shown that the expression of CD133 partially overlapped with that of ALDH protein in NSCLC cell lines,⁵³ there is no convincing evidence to confirm that the enrichment for 1 CSC marker also enriches the others. As these markers possibly play separate roles and represent different subgroups,⁵⁴ more powerful markers need to be identified to isolate pure CSCs in lung cancer.

Furthermore, it is being questioned whether these surface markers can accurately target CSCs. For example, CD133-negative cells in lung cancer cell lines may also cause the formation of tumors, just like CD133-positive

cells.⁵⁵ Similar results have been observed in the ALDH or SP-negative cells.^{56,57} Overall, the accuracy of currently known markers in identifying CSC populations remains uncertain, as these markers can only identify tumor gene subpopulations to varying degrees. More specific markers may be discovered in future work, and we all look forward to the emergence of real targeting markers for these cells.

Lung cancer stem cells and tumor microenvironment

There is increasing evidence that tumor biology is determined not only by the cancer cells, but also by the surrounding stromal cells and structures, known as the TME. This consists of multiple cell types that are embedded in the extracellular matrix (ECM), including immune cells, endothelial cells and cancer-associated fibroblasts (CAFs). It is now known that TME plays a vital role in the regulation of EMT and the acquisition of stem cell phenotypes.^{58,59} Moreover, it has been reported that the cytokine network established by CSCs and TME supports the upkeep of existing CSCs and promotes the generation of new CSCs. This process ultimately facilitates tumor survival, propagation and relapse.⁶⁰

One of the cellular components in the TME, CAFs, plays a critical role in promoting both the differentiation of CSCs and the dedifferentiation of non-CSCs. Cancer-associated fibroblasts increase both CD133 and CD44 expression, increase the proportion of CD133⁺ and CD44⁺ CSCs cells, and enhance the ability of metastasis and chemotherapy resistance during tumor progression. In addition, fibroblasts have a promoting effect as feeder cells on culturing LCSCs.^{61,62} It has been reported that the activation of the IGF1R signaling pathway in the presence of CAFs expressing IGF2 can induce the expression of Nanog and promote cancer stemness in NSCLC cells.⁶³ Additional research revealed that a unique subpopulation of CAFs in human NSCLC tissues expresses both CD10 and a receptor G-protein coupled receptor 77 (GPR-77), promoting the stemness properties and inducing chemoresistance by activating the NF- κ B pathway and secreting interleukin 6 (IL-6) and IL-8.⁶⁴ These findings all demonstrate that CAFs serve as a supportive niche for cancer stemness in NSCLC.

Mesenchymal stem cells (MSCs) are another important cellular component in the TME, but their precise role in tumor progression is still under debate. Research suggests that the specific effect of MSCs on tumors is dependent on the source of MSCs and tumor types.^{65,66} One study found that MSCs increase the stemness of lung cancer cells by secreting factors that activate JAK2/STAT3 pathways.⁶⁷ Another report displayed that MSCs at the primary tumor site promote the proliferation and infiltration of the malignant cells, while the metastatic site MSCs facilitate cell re-seeding.^{68,69} Non-small cell lung cancer adjacent MSCs were found to induce the expression of stem-related genes

and facilitate the formation of spheroids when tumor cells were co-incubated with them.⁷⁰

The TME also includes chronic inflammation that promotes tumor proliferation and metastasis through immunosuppression and evasion from immune surveillance. Cancer cells and CSCs create an inflammatory niche by secreting chemokines and cytokines to recruit tumor-associated macrophages (TAMs), tumor-associated neutrophils (TANs) and myeloid-derived suppressor cells (MDSCs).⁷¹ In TME, TAMs are the predominant subpopulation of immune cells, which include 2 subtypes: the classically activated M1 subtype and the alternatively activated M2 subtype. M1 macrophages may cause tumor cells to undergo lysis, promote antigen presentation and activate Th1-type cell-mediated immune responses; they mainly exert their antitumor effects by enhancing the tumor-killing ability of immune cells. In contrast, M2 macrophages may secrete immunosuppressive cytokines and promote tumor growth and metastasis.⁷² During the malignant progression in NSCLC, TAMs can also differentiate into either a tumor-inhibitory (M1) or tumor-promoting (M2) phenotype based on the influence of various stimuli.^{73,74} Tumor-associated macrophages can also activate both pro-inflammatory and anti-inflammatory pathways, which can directly inhibit or promote the cytotoxic effects of natural killer (NK) cells and CD8⁺ T lymphocytes. Additionally, TAMs can trigger Th1 immune responses and induce cytotoxic functions directed toward malignant cells by producing toxic mediators.⁷⁵ In a recent publication, a correlation study was conducted between tumor-infiltrating lymphocytes (TILs) and CSCs in tumor tissues from 12 patients with NSCLC. This research found a moderate-to-high positive linear and rank correlation between ALDH⁺ CSCs and CD3⁺ or CD8⁺ TILs. However, there was no correlation between ALDH⁺ CSCs and CD4⁺ cells.⁷⁶ Another group demonstrated that there is no correlation between CD8⁺ TILs and CD133 CSCs in surgical samples taken from 172 NSCLC patients.⁷⁷ The variation observed in these studies could be attributed to several aspects, such as the utilization of different stem-like markers (ALDH vs CD133), and the involvement of NSCLC in various stages (primary tumors vs metastasis). It has been reported that CD8⁺ T cells are crucial cytotoxic effectors in many kinds of tumors, including NSCLC. At the same time, ALDH⁺ CSCs have the potential to induce the loss of their antitumor activity through the exhaustion of CD8⁺ T cells that lost antitumor activity, or immunosuppressive CD8⁺ regulatory T cells (Tregs).⁷⁸ Furthermore, A549 cells overexpressing Oct4 were found to express higher levels of macrophage colony-stimulating factor (M-CSF), which contributed to enhanced tumor migration and increased the number of M2 macrophages. This data suggests that lung cancer cells that express Oct4 promote the polarization of M2 macrophages by upregulating the secretion of M-CSF.⁷⁹

In addition, the TME has the highest concentrations of extracellular ATP (eATP), which is mainly produced from necrotic or lytic tumor cells and stromal cells.^{80–84} Recent studies suggest that eATP can induce and regulate transcription, translation and metabolic levels of CSCs through STC1, which interacts with ATP synthesized by mitochondria.⁸⁵ Notably, the role of eATP in regulating CSCs is an area of active research and remains poorly understood.

Taken together, to better understand the emergency and maintenance of LCSCs, it is crucial to focus on the TME, which can be called the CSC niche and regulates CSCs through intercellular communication or changes in the secreted milieu. Importantly, we should know that the CSC niche is different in a variety of tumor types, which means the makeup of the CSC niche can vary significantly between tumor types, even within the same subtype of cancer. Thus, more research is needed to fully understand the complex interplay between the CSCs niche and CSCs themselves.

Lung cancer stem cells and epithelial–mesenchymal transition

A key process of invasion and metastasis, EMT, has been reported to be associated with the existence of CSCs. Epithelial–mesenchymal transition can promote epithelial cells to acquire invasive and migratory properties and become CSC-like cells. Moreover, it has also been observed that CSCs can undergo EMT⁸⁶ during radiotherapy and chemotherapy,^{87,88} in a hypoxic environment,⁸⁹ or in the process of long-term exposure to PM_{2.5}.^{90,91} Lung cancer cells can also show EMT and CSC characteristics from signaling that induces EMT, such as TGF- β , Wnt, NF- κ B, ERK/MAPK, and Notch pathways, which can promote stemness characteristics of solid tumors.^{92–94} It has been shown that the induction of EMT by TGF β -1 may increase stemness in primary lung cancer cells.⁹⁵ Moreover, when 8 different lung cancer cell lines were treated by TGF β 1, it was found that TGF β 1 signaling can not only induce EMT but also stimulate the modulation of CD133⁺ CSCs. However, the responses to TGF β 1 treatment are heterogeneous across the lung cancer cell lines. Some cell lines readily switch to a stem cell state, while others remain unresponsive. This may be caused by the ratio of expression of CDH1 (E-cadherin) to Snail2,⁹⁶ both downstream effectors of TGF β 1 signaling. Further study revealed that TGF- β signaling induces stemness through the activation of Slug and CD87 by promoter demethylation.⁹⁴ Moreover, tumor necrosis factor receptor superfamily member 19 (TNFRSF19) can inhibit TGF β downstream signal factors Smad2/3 through binding with TGF β receptor I, thus modulating stemness properties and chemotherapy resistance to gefitinib.⁹⁷ Moreover, TGF β 1 may promote cancer sphere-forming capacity, stemness traits

and chemoresistance through the expression of CXCR7.⁹⁸ In addition, other factors such as microRNAs miR-181b-5p, miR-99a, long non-coding RNAs (lncRNAs), and RNA demethylase ALKBH5 have also been revealed to modulate EMT concomitantly with the changes of stemness features in lung cancer.^{99–102} Conversely, CSCs also display some degree of EMT regulation. For example, Oct4/Nanog may regulate drug resistance and EMT change through Wnt/ β -catenin signaling activation.¹⁰³ Additionally, CD133 may induce CXCR4-mediated EMT in NSCLC.¹⁰⁴ The above studies have demonstrated the close correlation between EMT and CSCs in lung cancers, although the crosstalk mechanism between EMT and CSCs remains elusive.

Lung cancer stem cells and cellular plasticity

In general, cellular plasticity refers to the capability of a cell to change its differentiation levels or hierarchy. It can also be defined as a cell's ability to accept a new identity when faced with changes to its environment. Cellular plasticity is not limited to stem cells, as even progenitor cells, daughter cells, transient cells, and differentiation-committed cells have been found to possess this capacity. This implies that daughter cells and even fully differentiated cells can re-enter the niche to take the place of stem cells that have been lost. We now call this course neutral competition.^{105,106}

Previous investigations believed that plasticity is largely only related to CSCs because it was widely suggested that plasticity is limited to non-CSCs.³¹ However, recent research has demonstrated that non-CSCs can also supplement the CSC pool through cell plasticity in certain environmental niches, although this phenomenon is not observed in all tumor types.^{107–109} These findings highlight that CSCs are not a fixed entity in malignant tumors, but rather a state controlled by temporal and spatial characteristics.¹¹⁰ It has been revealed that transformation is also common between both CSCs and non-CSCs in lung adenocarcinoma.⁵⁴ One study demonstrated that lung cancer cells grown under standard culture conditions exhibited multidrug resistance when cultured as floating tumor spheres. However, upon re-incubation under standard culture conditions, the cells rapidly reattached and lost the acquired resistance.¹¹¹ One study revealed that dedifferentiation of lung non-CSCs into CSCs may be induced by the transcription factor HOXA5 that is mediated by oxidative stress.¹¹² A hybrid epithelial/mesenchymal phenotype could, therefore, identify tumors with a greater ability to “sense” microenvironment signals, and for this reason, lung cancer cells displaying both EMT traits may retain a high level of plasticity and could be highly reactive to convert to a stem-like state.⁹⁶ Marjanovic et al. prospectively isolated mixed program cells during lung adenocarcinoma evolution from human patient-derived

xenografts.¹¹³ These cells were defined as being in a high-plasticity cell state (HPCS). They found that the HPCS cells possess functions of both normal stem cells and CSCs, such as increased proliferation and differentiation potential. However, the *HPCS* gene expression was largely different from the common signatures in both normal stem cells and CSCs.^{105,114} Consequently, further research is required to elucidate the relationship between CSCs and HPCS.

Limitations

There is a large amount of literature on LCSCs. Unfortunately, we only summarized part of it, and the clinical application was not covered in this paper. This review catalogued the findings of pertinent research and highlighted discrepancies or deficiencies. However, the underlying mechanism remained underexplored, necessitating a more comprehensive investigation in the subsequent study.

Conclusions

In recent years, there has been a great deal of interest in the use of CSCs as a targeted antitumor strategy. Here, we concentrated on the characteristics of LCSCs, including the existing stemness phenotypes, the relationship and interaction between EMT, TME and LCSCs, as well as the role of cell plasticity theory in CSCs. As discussed, the clinical application of LCSCs will not be possible in the near future due to the present research controversy on LCSCs. On the one hand, accurate recognition of these cells requires the discovery of more specific phenotypic markers. On the other, the acquisition and maintenance of CSCs not only depend on the plasticity potential of cancer cells but also have a close relationship with the micro-environmental tumor niche. Thus, gaining a better understanding of the molecular mechanisms in CSC biology and cancer heterogeneity may help us find more effective and innovative treatment strategies.

Data availability


The datasets generated and/or analyzed during the current study are available from the corresponding author on reasonable request.


Consent for publication

Not applicable.

ORCID iDs

Jin Wang  <https://orcid.org/0009-0003-5565-2321>

Yunqing Chen  <https://orcid.org/0000-0001-9964-2537>

Chengqin Wang  <https://orcid.org/0000-0020-8863-2355>

Keyu Ren  <https://orcid.org/0000-0002-4226-0068>

References

- Leiter A, Veluswamy RR, Wisnivesky JP. The global burden of lung cancer: Current status and future trends. *Nat Rev Clin Oncol*. 2023; 20(9):624–639. doi:10.1038/s41571-023-00798-3
- Sung H, Ferlay J, Siegel RL, et al. Global cancer statistics 2020: GLOBOCAN estimates of incidence and mortality worldwide for 36 cancers in 185 countries. *CA Cancer J Clin*. 2021;71(3):209–249. doi:10.3322/caac.21660
- Zappa C, Mousa SA. Non-small cell lung cancer: Current treatment and future advances. *Transl Lung Cancer Res*. 2016;5(3):288–300. doi:10.21037/tlcr.2016.06.07
- Barta JA, Powell CA, Wisnivesky JP. Global epidemiology of lung cancer. *Ann Glob Health*. 2019;85(1):8. doi:10.5334/aogh.2419
- Blandin Knight S, Crosbie PA, Balata H, Chudziak J, Hussell T, Dive C. Progress and prospects of early detection in lung cancer. *Open Biol*. 2017;7(9):170070. doi:10.1098/rsob.170070
- Kelsey CR, Marks LB, Hollis D, et al. Local recurrence after surgery for early stage lung cancer: An 11-year experience with 975 patients. *Cancer*. 2009;115(22):5218–5227. doi:10.1002/cncr.24625
- Kryczka J, Kryczka J, Czarnecka-Chrebelska KH, Brzezińska-Lasota E. Molecular mechanisms of chemoresistance induced by cisplatin in NSCLC cancer therapy. *Int J Mol Sci*. 2021;22(16):8885. doi:10.3390/ijms22168885
- Kelland L. The resurgence of platinum-based cancer chemotherapy. *Nat Rev Cancer*. 2007;7(8):573–584. doi:10.1038/nrc2167
- Schiller JH, Harrington D, Belani CP, et al. Comparison of four chemotherapy regimens for advanced non-small-cell lung cancer. *N Engl J Med*. 2002;346(2):92–98. doi:10.1056/NEJMoa011954
- Katayama R, Shaw AT, Khan TM, et al. Mechanisms of acquired crizotinib resistance in ALK-rearranged lung cancers. *Sci Transl Med*. 2012; 4(120):120ra17. doi:10.1126/scitranslmed.3003316
- Dai J, Qu T, Yin D, et al. LncRNA LINC00969 promotes acquired gefitinib resistance by epigenetically suppressing of NLRP3 at transcriptional and posttranscriptional levels to inhibit pyroptosis in lung cancer. *Cell Death Dis*. 2023;14(5):312. doi:10.1038/s41419-023-05840-x
- Reya T, Morrison SJ, Clarke MF, Weissman IL. Stem cells, cancer, and cancer stem cells. *Nature*. 2001;414(6859):105–111. doi:10.1038/35102167
- Heng WS, Gosens R, Kruijff FAE. Lung cancer stem cells: Origin, features, maintenance mechanisms and therapeutic targeting. *Biochem Pharmacol*. 2019;160:121–133. doi:10.1016/j.bcp.2018.12.010
- Gillet J, Efferth T, Remacle J. Chemotherapy-induced resistance by ATP-binding cassette transporter genes. *Biochim Biophys Acta Rev Cancer*. 2007;1775(2):237–262. doi:10.1016/j.bbcan.2007.05.002
- Leon G, MacDonagh L, Finn SP, Cuffe S, Barr MP. Cancer stem cells in drug resistant lung cancer: Targeting cell surface markers and signaling pathways. *Pharmacol Ther*. 2016;158:71–90. doi:10.1016/j.pharmthera.2015.12.001
- Cojoc M, Mäbert K, Muders MH, Dubrovskaya A. A role for cancer stem cells in therapy resistance: Cellular and molecular mechanisms. *Semin Cancer Biol*. 2015;31:16–27. doi:10.1016/j.semcancer.2014.06.004
- Liu M, Wu H, Xu C. Targeting cancer stem cell pathways for lung cancer therapy. *Curr Opin Oncol*. 2023;35(1):78–85. doi:10.1097/CCO.0000000000000912
- Yang L, Shi P, Zhao G, et al. Targeting cancer stem cell pathways for cancer therapy. *Sig Transduct Target Ther*. 2020;5(1):8. doi:10.1038/s41392-020-0110-5
- Dzobo K, Senthebane DA, Ganz C, Thomford NE, Wonkam A, Dandara C. Advances in therapeutic targeting of cancer stem cells within the tumor microenvironment: An updated review. *Cells*. 2020;9(8):1896. doi:10.3390/cells9081896
- Abbaszadegan MR, Bagheri V, Razavi MS, Momtazi AA, Sahebkar A, Gholamin M. Isolation, identification, and characterization of cancer stem cells: A review. *J Cell Physiol*. 2017;232(8):2008–2018. doi:10.1002/jcp.25759
- Kazi JU. Mechanisms of anticancer therapy resistance: The role of cancer stem cells. *Int J Mol Sci*. 2020;21(23):9006. doi:10.3390/ijms21239006
- Konrad CV, Murali R, Varghese BA, Nair R. The role of cancer stem cells in tumor heterogeneity and resistance to therapy. *Can J Physiol Pharmacol*. 2017;95(1):1–15. doi:10.1139/cjpp-2016-0079
- Yoshida GJ, Saya H. Molecular pathology underlying the robustness of cancer stem cells. *Regen Ther*. 2021;17:38–50. doi:10.1016/j.reth.2021.02.002
- Varga J, Gretchen FR. Cell plasticity in epithelial homeostasis and tumorigenesis. *Nat Cell Biol*. 2017;19(10):1133–1141. doi:10.1038/ncb3611
- Chaffer CL, Marjanovic ND, Lee T, et al. Poised chromatin at the ZEB1 promoter enables breast cancer cell plasticity and enhances tumorigenicity. *Cell*. 2013;154(1):61–74. doi:10.1016/j.cell.2013.06.005
- Gupta PB, Pastushenko I, Skibinski A, Blanpain C, Kuperwasser C. Phenotypic plasticity: Driver of cancer initiation, progression, and therapy resistance. *Cell Stem Cell*. 2019;24(1):65–78. doi:10.1016/j.stem.2018.11.011
- Pisco AO, Huang S. Non-genetic cancer cell plasticity and therapy-induced stemness in tumour relapse: 'What does not kill me strengthens me.' *Br J Cancer*. 2015;112(11):1725–1732. doi:10.1038/bjc.2015.146
- Biddle A, Gammon L, Liang X, Costea DE, Mackenzie IC. Phenotypic plasticity determines cancer stem cell therapeutic resistance in oral squamous cell carcinoma. *EBioMedicine*. 2016;4:138–145. doi:10.1016/j.ebiom.2016.01.007
- Nayak A, Warriar NM, Kumar P. Cancer stem cells and the tumor microenvironment: Targeting the critical crosstalk through nanocarrier systems. *Stem Cell Rev Rep*. 2022;18(7):2209–2233. doi:10.1007/s12015-022-10426-9
- Al-Hajj M, Wicha MS, Benito-Hernandez A, Morrison SJ, Clarke MF. Prospective identification of tumorigenic breast cancer cells. *Proc Natl Acad Sci U S A*. 2003;100(7):3983–3988. doi:10.1073/pnas.0530291100
- Singh SK, Hawkins C, Clarke ID, et al. Identification of human brain tumour initiating cells. *Nature*. 2004;432(7015):396–401. doi:10.1038/nature03128
- Eramo A, Lotti F, Sette G, et al. Identification and expansion of the tumorigenic lung cancer stem cell population. *Cell Death Differ*. 2008;15(3):504–514. doi:10.1038/sj.cdd.4402283
- Carney DN, Gazdar AF, Bunn PA, Guccion JG. Demonstration of the stem cell nature of clonogenic tumor cells from lung cancer patients. *Stem Cells (1981)*. 1982;1(3):149–164. PMID:6294885.
- Xia P, Gou WF, Wang JJ, et al. Distinct radiosensitivity of lung carcinoma stem-like side population and main population cells. *Cancer Biother Radiopharm*. 2013;28(6):471–478. doi:10.1089/cbr.2012.1388
- Shien K, Toyooka S, Yamamoto H, et al. Acquired resistance to EGFR inhibitors is associated with a manifestation of stem cell-like properties in cancer cells. *Cancer Res*. 2013;73(10):3051–3061. doi:10.1158/0008-5472.CAN-12-4136
- Liu YP, Yang CJ, Huang MS, et al. Cisplatin selects for multidrug-resistant CD133⁺ cells in lung adenocarcinoma by activating notch signaling. *Cancer Res*. 2013;73(1):406–416. doi:10.1158/0008-5472.CAN-12-1733
- Xie M, Zhang L, He C, et al. Activation of Notch-1 enhances epithelial-mesenchymal transition in gefitinib-acquired resistant lung cancer cells. *J Cell Biochem*. 2012;113(5):1501–1513. doi:10.1002/jcb.24019
- Morrison BJ, Steel JC, Morris JC. Sphere culture of murine lung cancer cell lines are enriched with cancer initiating cells. *PLoS One*. 2012; 7(11):e49752. doi:10.1371/journal.pone.0049752
- Okudela K, Woo T, Mitsui H, Tajiri M, Masuda M, Ohashi K. Expression of the potential cancer stem cell markers, CD 133, CD 44, ALDH 1, and β -catenin, in primary lung adenocarcinoma: Their prognostic significance. *Pathol Int*. 2012;62(12):792–801. doi:10.1111/pin.12019
- Leung ELH, Fiscus RR, Tung JW, et al. Non-small cell lung cancer cells expressing CD44 are enriched for stem cell-like properties. *PLoS One*. 2010;5(11):e14062. doi:10.1371/journal.pone.0014062
- Yan X, Luo H, Zhou X, Zhu B, Wang Y, Bian X. Identification of CD90 as a marker for lung cancer stem cells in A549 and H460 cell lines. *Oncol Rep*. 2013;30(6):2733–2740. doi:10.3892/or.2013.2784
- Jung MJ, Rho JK, Kim YM, et al. Upregulation of CXCR4 is functionally crucial for maintenance of stemness in drug-resistant non-small cell lung cancer cells. *Oncogene*. 2013;32(2):209–221. doi:10.1038/ncr.2012.37
- Zakaria N, Yusoff NM, Zakaria Z, et al. Human non-small cell lung cancer expresses putative cancer stem cell markers and exhibits the transcriptomic profile of multipotent cells. *BMC Cancer*. 2015;15(1):84. doi:10.1186/s12885-015-1086-3
- Jiang F, Qiu Q, Khanna A, et al. Aldehyde dehydrogenase 1 is a tumor stem cell-associated marker in lung cancer. *Mol Cancer Res*. 2009;7(3): 330–338. doi:10.1158/1541-7786.MCR-08-0393

45. Schoenhals M, Kassambara A, Vos JD, Hose D, Moreaux J, Klein B. Embryonic stem cell markers expression in cancers. *Biochem Biophys Res Commun*. 2009;383(2):157–162. doi:10.1016/j.bbrc.2009.02.156
46. Chiou SH, Wang ML, Chou YT, et al. Coexpression of *Oct4* and *Nanog* enhances malignancy in lung adenocarcinoma by inducing cancer stem cell-like properties and epithelial–mesenchymal transdifferentiation. *Cancer Res*. 2010;70(24):10433–10444. doi:10.1158/0008-5472.CAN-10-2638
47. Miranda-Lorenzo I, Dorado J, Lonardo E, et al. Intracellular autofluorescence: A biomarker for epithelial cancer stem cells. *Nat Methods*. 2014;11(11):1161–1169. doi:10.1038/nmeth.3112
48. Quintana E, Shackleton M, Sabel MS, Fullen DR, Johnson TM, Morrison SJ. Efficient tumour formation by single human melanoma cells. *Nature*. 2008;456(7222):593–598. doi:10.1038/nature07567
49. Bertolini G, Roz L, Perego P, et al. Highly tumorigenic lung cancer CD133⁺ cells display stem-like features and are spared by cisplatin treatment. *Proc Natl Acad Sci U S A*. 2009;106(38):16281–16286. doi:10.1073/pnas.0905653106
50. Salnikov AV, Gladkikh J, Moldenhauer G, Volm M, Mattern J, Herr I. CD133 is indicative for a resistance phenotype but does not represent a prognostic marker for survival of non-small cell lung cancer patients. *Int J Cancer*. 2010;126(4):950–958. doi:10.1002/ijc.24822
51. Ko YH, Won HS, Jeon EK, et al. Prognostic significance of CD44s expression in resected non-small cell lung cancer. *BMC Cancer*. 2011;11(1):340. doi:10.1186/1471-2407-11-340
52. Moreb JS, Zucali JR, Ostmark B, Benson NA. Heterogeneity of aldehyde dehydrogenase expression in lung cancer cell lines is revealed by Aldefluor flow cytometry-based assay. *Cytometry B Clin Cytom*. 2007;72B(4):281–289. doi:10.1002/cyto.b.20161
53. Shi Y, Fu X, Hua Y, Han Y, Lu Y, Wang J. The side population in human lung cancer cell line NCI-H460 is enriched in stem-like cancer cells. *PLoS One*. 2012;7(3):e33358. doi:10.1371/journal.pone.0033358
54. Akunuru S, James Zhai Q, Zheng Y. Non-small cell lung cancer stem/progenitor cells are enriched in multiple distinct phenotypic subpopulations and exhibit plasticity. *Cell Death Dis*. 2012;3(7):e352–e352. doi:10.1038/cddis.2012.93
55. Meng X, Li M, Wang X, Wang Y, Ma D. Both CD133⁺ and CD133[−] subpopulations of A549 and H446 cells contain cancer-initiating cells. *Cancer Sci*. 2009;100(6):1040–1046. doi:10.1111/j.1349-7006.2009.01144.x
56. Ucar D, Cogle CR, Zucali JR, et al. Aldehyde dehydrogenase activity as a functional marker for lung cancer. *Chem Biol Interact*. 2009;178(1–3):48–55. doi:10.1016/j.cbi.2008.09.029
57. Akunuru S, Palumbo J, Zhai QJ, Zheng Y. Rac1 targeting suppresses human non-small cell lung adenocarcinoma cancer stem cell activity. *PLoS One*. 2011;6(2):e16951. doi:10.1371/journal.pone.0016951
58. Gao D, Vahdat LT, Wong S, Chang JC, Mittal V. Microenvironmental regulation of epithelial–mesenchymal transitions in cancer. *Cancer Res*. 2012;72(19):4883–4889. doi:10.1158/0008-5472.CAN-12-1223
59. Mani SA, Guo W, Liao MJ, et al. The epithelial–mesenchymal transition generates cells with properties of stem cells. *Cell*. 2008;133(4):704–715. doi:10.1016/j.cell.2008.03.027
60. Ravindran S, Rasool S, Maccalli C. The crosstalk between cancer stem cells/cancer initiating cells and tumor microenvironment: The missing piece of the puzzle for the efficient targeting of these cells with immunotherapy. *Cancer Microenviron*. 2019;12(2–3):133–148. doi:10.1007/s12307-019-00233-1
61. Xu Y, Hu Y, Zhou J, Zhang M. Establishing a lung cancer stem cell culture using autologous intratumoral fibroblasts as feeder cells. *Cell Biol Int*. 2011;35(5):509–517. doi:10.1042/CBI20100473
62. Shintani Y, Abulaiti A, Kimura T, et al. Pulmonary fibroblasts induce epithelial mesenchymal transition and some characteristics of stem cells in non-small cell lung cancer. *Ann Thorac Surg*. 2013;96(2):425–433. doi:10.1016/j.athoracsur.2013.03.092
63. Chen WJ, Ho CC, Chang YL, et al. Cancer-associated fibroblasts regulate the plasticity of lung cancer stemness via paracrine signalling. *Nat Commun*. 2014;5(1):3472. doi:10.1038/ncomms4472
64. Su S, Chen J, Yao H, et al. CD10⁺GPR77⁺ cancer-associated fibroblasts promote cancer formation and chemoresistance by sustaining cancer stemness. *Cell*. 2018;172(4):841–856.e16. doi:10.1016/j.cell.2018.01.009
65. Eiro N, Fraile M, Fernández-Francos S, Sánchez R, Costa LA, Vizoso FJ. Importance of the origin of mesenchymal (stem) stromal cells in cancer biology: “Alliance” or “war” in intercellular signals. *Cell Biosci*. 2021;11(1):109. doi:10.1186/s13578-021-00620-6
66. Galland S, Stamenkovic I. Mesenchymal stromal cells in cancer: A review of their immunomodulatory functions and dual effects on tumor progression. *J Pathol*. 2020;250(5):555–572. doi:10.1002/path.5357
67. Hsu HS, Lin JH, Hsu TW, et al. Mesenchymal stem cells enhance lung cancer initiation through activation of IL-6/JAK2/STAT3 pathway. *Lung Cancer*. 2012;75(2):167–177. doi:10.1016/j.lungcan.2011.07.001
68. Attar-Schneider O, Zismanov V, Drucker L, Gottfried M. Secretome of human bone marrow mesenchymal stem cells: An emerging player in lung cancer progression and mechanisms of translation initiation. *Tumor Biol*. 2016;37(4):4755–4765. doi:10.1007/s13277-015-4304-3
69. Attar-Schneider O, Drucker L, Gottfried M. The effect of mesenchymal stem cells’ secretome on lung cancer progression is contingent on their origin: Primary or metastatic niche. *Lab Invest*. 2018;98(12):1549–1561. doi:10.1038/s41374-018-0110-z
70. Yan C, Chang J, Song X, et al. Lung cancer-associated mesenchymal stem cells promote tumor metastasis and tumorigenesis by induction of epithelial–mesenchymal transition and stem-like reprogram. *Aging*. 2021;13(7):9780–9800. doi:10.18632/aging.202732
71. Kitamura T, Qian BZ, Pollard JW. Immune cell promotion of metastasis. *Nat Rev Immunol*. 2015;15(2):73–86. doi:10.1038/nri3789
72. Locati M, Curtale G, Mantovani A. Diversity, mechanisms, and significance of macrophage plasticity. *Annu Rev Pathol Mech Dis*. 2020;15(1):123–147. doi:10.1146/annurev-pathmechdis-012418-012718
73. Tang B, Wang Y, Xu W, et al. Macrophage xCT deficiency drives immune activation and boosts responses to immune checkpoint blockade in lung cancer. *Cancer Lett*. 2023;554:216021. doi:10.1016/j.canlet.2022.216021
74. Mei J, Xiao Z, Guo C, et al. Prognostic impact of tumor-associated macrophage infiltration in non-small cell lung cancer: A systemic review and meta-analysis. *Oncotarget*. 2016;7(23):34217–34228. doi:10.18632/oncotarget.9079
75. Capece D, Fischietti M, Verzella D, et al. The inflammatory microenvironment in hepatocellular carcinoma: A pivotal role for tumor-associated macrophages. *Biomed Res Int*. 2013;2013:187204. doi:10.1155/2013/187204
76. Masciale V, Grisendi G, Banchelli F, et al. Correlating tumor-infiltrating lymphocytes and lung cancer stem cells: A cross-sectional study. *Ann Transl Med*. 2019;7(22):619–619. doi:10.21037/atm.2019.11.27
77. Huang Z, Yu H, Zhang J, et al. Correlation of cancer stem cell markers and immune cell markers in resected non-small cell lung cancer. *J Cancer*. 2017;8(16):3190–3197. doi:10.7150/jca.20172
78. Kinoshita T, Kawakami Y. Interface of cancer stem cells and cancer immunity. *Ann Transl Med*. 2020;8(13):810–810. doi:10.21037/atm.2020.04.08
79. Lu CS, Shiau AL, Su BH, et al. Oct4 promotes M2 macrophage polarization through upregulation of macrophage colony-stimulating factor in lung cancer. *J Hematol Oncol*. 2020;13(1):62. doi:10.1186/s13045-020-00887-1
80. Schenk U, Westendorf AM, Radaelli E, et al. Purinergic control of T cell activation by ATP released through pannexin-1 hemichannels. *Sci Signal*. 2008;1(39):ra6. doi:10.1126/scisignal.1160583
81. De Andrade Mello P, Coutinho-Silva R, Savio LEB. Multifaceted effects of extracellular adenosine triphosphate and adenosine in the tumor–host interaction and therapeutic perspectives. *Front Immunol*. 2017;8:1526. doi:10.3389/fimmu.2017.01526
82. Grygorczyk R, Boudreault F, Ponomarchuk O, et al. Lytic release of cellular ATP: Physiological relevance and therapeutic applications. *Life*. 2021;11(7):700. doi:10.3390/life11070700
83. Moriyama Y, Hiasa M, Sakamoto S, Omote H, Nomura M. Vesicular nucleotide transporter (VNUT): Appearance of an actress on the stage of purinergic signaling. *Purinergic Signal*. 2017;13(3):387–404. doi:10.1007/s11302-017-9568-1
84. Sandilos JK, Chiu YH, Chekeni FB, et al. Pannexin 1, an ATP release channel, is activated by caspase cleavage of its pore-associated C-terminal autoinhibitory region. *J Biol Chem*. 2012;287(14):11303–11311. doi:10.1074/jbc.M111.323378

85. Song J, Qian Y, Evers M, Nielsen CM, Chen X. Cancer stem cell formation induced and regulated by extracellular ATP and stannocalcin-1 in human lung cancer cells and tumors. *Int J Mol Sci.* 2022; 23(23):14770. doi:10.3390/ijms232314770
86. Gammon L, Biddle A, Heywood HK, Johannessen AC, Mackenzie IC. Sub-sets of cancer stem cells differ intrinsically in their patterns of oxygen metabolism. *PLoS One.* 2013;8(4):e62493. doi:10.1371/journal.pone.0062493
87. Raei M, Bagheri M, Aghaabdollahian S, Ghorbani M, Sadeghi A. Ionizing radiation promotes epithelial-mesenchymal transition phenotype and stem cell marker in the lung adenocarcinoma: In vitro and bioinformatic studies. *Cell J.* 2022;24(9):522–530. doi:10.22074/cellj.2022.8403
88. Zou K, Li Z, Zhang Y, et al. β -Elemene enhances radiosensitivity in non-small-cell lung cancer by inhibiting epithelial–mesenchymal transition and cancer stem cell traits via Prx-1/NF-kB/iNOS signaling pathway. *Aging.* 2021;13(2):2575–2592. doi:10.18632/aging.202291
89. Gu X, Zhang J, Shi Y, et al. ESM1/HIF-1 α pathway modulates chronic intermittent hypoxia-induced non-small-cell lung cancer proliferation, stemness and epithelial–mesenchymal transition. *Oncol Rep.* 2020;45(3):1226–1234. doi:10.3892/or.2020.7913
90. Wei H, Liang F, Cheng W, et al. The mechanisms for lung cancer risk of PM_{2.5}: Induction of epithelial–mesenchymal transition and cancer stem cell properties in human non-small cell lung cancer cells. *Environ Toxicol.* 2017;32(11):2341–2351. doi:10.1002/tox.22437
91. Chao X, Yi L, Lan LL, Wei HY, Wei D. Long-term PM_{2.5} exposure increases the risk of non-small cell lung cancer (NSCLC) progression by enhancing interleukin-17a (IL-17a)-regulated proliferation and metastasis. *Aging.* 2020;12(12):11579–11602. doi:10.18632/aging.103319
92. Kotiyal S, Bhattacharya S. Breast cancer stem cells, EMT and therapeutic targets. *Biochem Biophys Res Commun.* 2014;453(1):112–116. doi:10.1016/j.bbrc.2014.09.069
93. Zhou P, Li B, Liu F, et al. The epithelial to mesenchymal transition (EMT) and cancer stem cells: Implication for treatment resistance in pancreatic cancer. *Mol Cancer.* 2017;16(1):52. doi:10.1186/s12943-017-0624-9
94. Kim BN, Ahn DH, Kang N, et al. TGF- β induced EMT and stemness characteristics are associated with epigenetic regulation in lung cancer. *Sci Rep.* 2020;10(1):10597. doi:10.1038/s41598-020-67325-7
95. Pirozzi G, Tirino V, Camerlingo R, et al. Epithelial to mesenchymal transition by TGF β -1 induction increases stemness characteristics in primary non small cell lung cancer cell line. *PLoS One.* 2011; 6(6):e21548. doi:10.1371/journal.pone.0021548
96. Andriani F, Bertolini G, Facchinetti F, et al. Conversion to stem-cell state in response to microenvironmental cues is regulated by balance between epithelial and mesenchymal features in lung cancer cells. *Mol Oncol.* 2016;10(2):253–271. doi:10.1016/j.molonc.2015.10.002
97. Wu L, Yu Y, Xu L, Wang X, Zhou J, Wang Y. TROY modulates cancer stem-like cell properties and gefitinib resistance through EMT signaling in non-small cell lung cancer. *Front Genet.* 2022;13:881875. doi:10.3389/fgene.2022.881875
98. Wu YC, Tang SJ, Sun GH, Sun KH. CXCR7 mediates TGF β 1-promoted EMT and tumor-initiating features in lung cancer. *Oncogene.* 2016; 35(16):2123–2132. doi:10.1038/ncr.2015.274
99. Li X, Han J, Zhu H, Peng L, Chen Z. miR-181b-5p mediates TGF- β 1-induced epithelial-to-mesenchymal transition in non-small cell lung cancer stem-like cells derived from lung adenocarcinoma A549 cells. *Int J Oncol.* 2017;51(1):158–168. doi:10.3892/ijo.2017.4007
100. Feliciano A, Garcia-Mayea Y, Jubierre L, et al. miR-99a reveals two novel oncogenic proteins E2F2 and EMR2 and represses stemness in lung cancer. *Cell Death Dis.* 2017;8(10):e3141. doi:10.1038/cddis.2017.544
101. Guo L, Sun C, Xu S, et al. Knockdown of long non-coding RNA linc-ITGB1 inhibits cancer stemness and epithelial–mesenchymal transition by reducing the expression of Snail in non-small cell lung cancer. *Thorac Cancer.* 2019;10(2):128–136. doi:10.1111/1759-7714.12911
102. Liu X, Wang Z, Yang Q, et al. RNA demethylase ALKBH5 prevents lung cancer progression by regulating EMT and stemness via regulating p53. *Front Oncol.* 2022;12:858694. doi:10.3389/fonc.2022.858694
103. Liu L, Zhu H, Liao Y, et al. Inhibition of Wnt/ β -catenin pathway reverses multi-drug resistance and EMT in Oct4⁺/Nanog⁺ NSCLC cells. *Biomed Pharmacother.* 2020;127:110225. doi:10.1016/j.biopha.2020.110225
104. Tu Z, Xie S, Xiong M, et al. CXCR4 is involved in CD133-induced EMT in non-small cell lung cancer. *Int J Oncol.* 2017;50(2):505–514. doi:10.3892/ijo.2016.3812
105. Batlle E, Clevers H. Cancer stem cells revisited. *Nat Med.* 2017;23(10): 1124–1134. doi:10.1038/nm.4409
106. Snippert HJ, Van Der Flier LG, Sato T, et al. Intestinal crypt homeostasis results from neutral competition between symmetrically dividing Lgr5 stem cells. *Cell.* 2010;143(1):134–144. doi:10.1016/j.cell.2010.09.016
107. De Sousa E Melo F, Kurtova AV, Harnoss JM, et al. A distinct role for Lgr5⁺ stem cells in primary and metastatic colon cancer. *Nature.* 2017;543(7647):676–680. doi:10.1038/nature21713
108. Shimokawa M, Ohta Y, Nishikori S, et al. Visualization and targeting of LGR5⁺ human colon cancer stem cells. *Nature.* 2017;545(7653): 187–192. doi:10.1038/nature22081
109. Chen J, Li Y, Yu TS, et al. A restricted cell population propagates glioblastoma growth after chemotherapy. *Nature.* 2012;488(7412): 522–526. doi:10.1038/nature11287
110. Rahman M, Deleyrolle L, Vedam-Mai V, Azari H, Abd-El-Barr M, Reynolds BA. The cancer stem cell hypothesis: Failures and pitfalls. *Neurosurgery.* 2011;68(2):531–545. doi:10.1227/NEU.0b013e3181ff9eb5
111. Yakisich JS, Azad N, Kaushik V, Iyer AKV. Cancer cell plasticity: Rapid reversal of chemosensitivity and expression of stemness markers in lung and breast cancer tumorspheres. *J Cell Physiol.* 2017; 232(9):2280–2286. doi:10.1002/jcp.25725
112. Saijo H, Hirohashi Y, Torigoe T, et al. Plasticity of lung cancer stem-like cells is regulated by the transcription factor HOXA5 that is induced by oxidative stress. *Oncotarget.* 2016;7(31):50043–50056. doi:10.18632/oncotarget.10571
113. Marjanovic ND, Hofree M, Chan JE, et al. Emergence of a high-plasticity cell state during lung cancer evolution. *Cancer Cell.* 2020;38(2): 229–246.e13. doi:10.1016/j.ccell.2020.06.012
114. Kreso A, Dick JE. Evolution of the cancer stem cell model. *Cell Stem Cell.* 2014;14(3):275–291. doi:10.1016/j.stem.2014.02.006

Probiotic interventions and quality of life in patients with gastrointestinal diseases: A comprehensive review

Xuejing Qiao^{1,A,D}, Haosheng Zhang^{2,B,C}, Lianmei Shan^{3,A,E,F}

¹ Department of Gastroenterology, Yantaishan Hospital, Shandong, China

² Department of Gastrointestinal Surgery, Yantaishan Hospital, Shandong, China

³ Department of General Practice, Yantaishan Hospital, Shandong, China

A – research concept and design; B – collection and/or assembly of data; C – data analysis and interpretation;

D – writing the article; E – critical revision of the article; F – final approval of the article

Advances in Clinical and Experimental Medicine, ISSN 1899–5276 (print), ISSN 2451–2680 (online)

Adv Clin Exp Med. 2025;34(4):641–658

Address for correspondence

Lianmei Shan

E-mail: shanlianmei12321@163.com

Funding sources

None declared

Conflict of interest

None declared

Received on November 20, 2023

Reviewed on April 1, 2024

Accepted on April 29, 2024

Published online on October 8, 2024

Abstract

Gastrointestinal disorders manifest through disruptions in gastrointestinal functionality accompanied by dysbiosis within the microbiome. Probiotics are considered biological agents with potential therapeutic efficacy in managing gastrointestinal pathologies by modulating the gut microbiota. Nevertheless, several hurdles, such as safety considerations, resilience to stressors, post-colonization quantifications, and evaluative modalities, may impede the adoption of probiotics for gastrointestinal disorders. Herein, we performed online research using 6 databases: Scopus, ScienceDirect, PubMed, Web of Science, Cochrane Library, and Ovid. Inclusion criteria were mostly articles published in the years 2015–2024, concerning the association between probiotics and gastrointestinal diseases. This review aimed to provide comprehensive data regarding the latest studies in this area. Additionally, this review delineates the various aspects of probiotic use, including both the positive and negative aspects, as well as the role of probiotics in immune system modulation and the prevention of various diseases. Also, we comprehensively discuss the prophylactic and supportive therapeutic role of probiotics in the management of COVID-19. Given the extensive adoption of probiotic formulations as microecological interventions for gastrointestinal disorders, a comprehensive understanding of the challenges inherent in their application and the implementation of contemporary methodologies to enhance probiotic colonization and evaluation systems are paramount for harnessing probiotics as viable biotherapeutic agents. However, there is a need for additional studies to confirm the potential role of probiotics as a suitable target in the treatment of gastrointestinal diseases.

Key words: microbiome, probiotics, gastrointestinal diseases

Cite as

Qiao X, Zhang H, Shan L. Probiotic interventions and quality of life in patients with gastrointestinal diseases: A comprehensive review. *Adv Clin Exp Med.* 2025;34(4):641–658. doi:10.17219/acem/188108

DOI

10.17219/acem/188108

Copyright

Copyright by Author(s)

This is an article distributed under the terms of the Creative Commons Attribution 3.0 Unported (CC BY 3.0) (<https://creativecommons.org/licenses/by/3.0/>)

Introduction

Probiotics, originating from the Greek term signifying “for life”, are defined by the Food and Agricultural Organization (FAO) and the World Health Organization (WHO) as “living microorganisms that, when administered in adequate quantities, confer a health advantage to the host”.¹ A substantial body of evidence from human observational studies and animal models strongly suggests the involvement of gut microbiota in various chronic human conditions, including gastrointestinal (GI) disorders, cancers, and diseases characterized by inflammatory, metabolic, cardiovascular, autoimmune, neurological, and psychiatric components, hinting at a potential pathogenic correlation.^{2,3} Given that the GI tract harbors most microbial cells in the human body, numbering in trillions, alterations in gut flora have emerged as a key mechanism in specific GI disorders.^{4,5} Probiotics are pivotal in providing substantial support against the incidence of GI diseases, such as inflammatory bowel diseases (IBD), irritable bowel syndrome (IBS), acute infectious diarrhea, antibiotic-associated diarrhea (AAD), necrotizing enterocolitis (NEC), etc. As research progressed, a paradigm emphasizing bacteria emerged, prompting a reassessment of treatment strategies for GI diseases.⁶ Probiotic microorganisms operate through diverse mechanisms, including immune reaction modulation, production of organic acids and antimicrobial agents, interaction with existing microbiota, engagement with the host, fortification of gut barrier integrity, and enzyme generation.^{7,8} This review delineates the positive and negative impacts of probiotics, their mechanisms of effect, and their influence on various GI conditions.

Objectives

The objective of this review was to substantiate the hypothesis of using probiotics as an intervention for GI diseases while providing an exhaustive compilation of contemporary research endeavors in this field.

Materials and methods

The review encompassed the utilization of 6 online databases, namely Scopus, ScienceDirect, PubMed, Web of Science, Cochrane Library, and Ovid. Most of the selected articles were published between 2015 and 2024, and focus on the role of probiotics in the prevention and treatment of GI diseases, along with their impact on the quality of life of patients. Original research articles were mostly included, resulting in the incorporation of 24 articles meeting the stipulated inclusion criteria. The data were independently cross-verified by 2 authors. The selection procedure involved the elimination of duplicate entries

and subsequent screening based on the title, abstract and full-text review, adhering to the guidelines. Furthermore, an extensive examination of the references cited in the retrieved articles and meta-analyses was conducted to identify additional relevant studies not initially captured in the primary search. The detailed selection process is delineated in Fig. 1.

Results

Regarding the preventative role of probiotics in GI diseases, they exert multifaceted effects. Probiotics demonstrate potential in inhibiting the adhesion of pathogenic bacteria, enhancing barrier functions and interacting with toll-like receptors (TLRs) present on intestinal epithelial cells and dendritic cells (DCs), thereby eliciting cytokines/chemokines to modulate T cell responses. Furthermore, probiotics generate bioactive metabolites that impact the nervous system, consequently influencing gut motility, reducing pain and participating in gut–brain interactions. Notably, probiotics possess the capability to ferment specific types of fiber, leading to increased production of short-chain fatty acids (SCFAs) like propionate, acetic acid and butyrate. Of particular significance, butyrate serves as a pivotal inflammatory modulator, exhibiting anti-inflammatory effects on intestinal epithelial cells, macrophages and leukocytes. Originating from the colonic lumen, butyrate serves as the primary energy source for colonocytes, thereby contributing to the maintenance of the epithelial barrier.⁹ Additionally, butyrate intervenes in inflammatory signaling pathways, regulating cytokine production, inhibiting histone deacetylase activity to modulate the expression of proinflammatory genes, and promoting the differentiation and expansion of regulatory T cells (Tregs). Noteworthy research findings indicate that treatment with a probiotic strain of *Lactobacillus* reduces inflammation and enhances organ survival in specific pathogen-free (SPF) mice. Moreover, probiotic mixtures have been shown to elevate mucin protein secretion and gene expression in the colons of rat.¹⁰

Definition of probiotics

Probiotics encompass microorganisms, primarily bacteria resembling the beneficial flora naturally found in the human intestinal tract.¹¹ When provided in sufficient quantities, they bestow a health advantage upon the host.¹² Nevertheless, deceased bacteria and their constituents may also demonstrate probiotic characteristics.¹³ They are obtainable without a prescription as over-the-counter (OTC) remedies or through prescribed means, and are accessible in diverse formulations such as capsules, packets or dietary supplements. While many probiotics do not require a prescription, individuals with prescription drug coverage might find an advantage, as probiotics

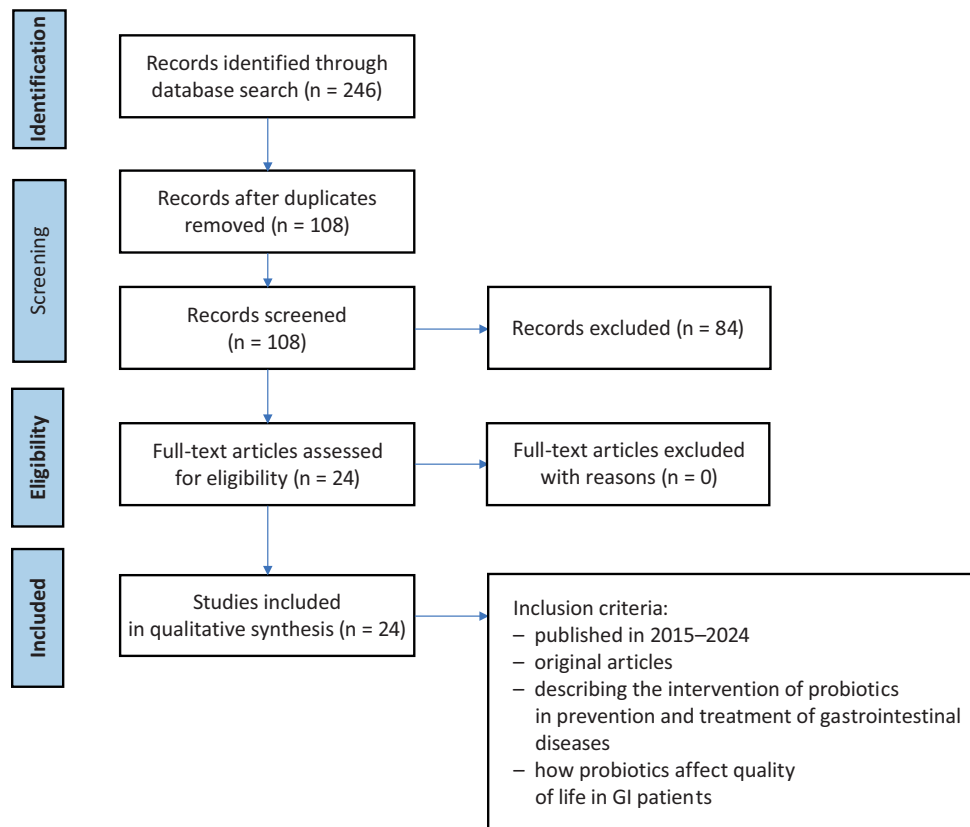


Fig. 1. Study selection process

could be covered under their plan. Extensive research has been conducted on probiotics for various GI disorders, with 1 in 5 Americans using probiotics to address digestive issues. Among the extensively studied probiotics used in humans, the prominent strains include *Lactobacillus*, *Bifidobacterium* and *Saccharomyces* species.¹¹ Moreover, these bacteria, particularly *Lactobacillus*, are commonly found in nature. *Lactobacillus*, *Bifidobacteria*, *Lactococcus*, and yeasts fall within the category of organisms considered “generally recognized as safe.” Nonetheless, there have been a few reported infections, primarily among immunocompromised patients. It is crucial to note that not all probiotics used fall under this safe category. The effectiveness and safety of probiotics need to be scientifically validated, as emphasized in recent research. Certain evidence indicates that probiotics might enhance the integrity of the gut mucosal defense action, especially by influencing intestinal epithelial cells and macrophages.¹⁴ Probiotics like *Bifidobacteria* or *Lactobacillus* have beneficial effects against influenza virus infections of the respiratory tract. Probiotics have a therapeutic effect on managing coronavirus disease-19 (COVID-19) by regulating the gut–lung axis and mucosal immune system, which can potentially have antiviral mechanisms. An adequate number of probiotics can stimulate host innate and adaptive immunities. Interestingly, intestinal bacteria can also have beneficial effects by modulating the vitamin D axis. By doing so, probiotics can protect the mucosal barrier and suppress gut mucosal inflammation.^{15,16}

Mechanisms of probiotic actions

The primary function of probiotics lies in their barrier effect, which is intricately linked to the regulation of the host microbiota. This effect establishes a defiance to colonization by impeding or hindering the presence of pathogenic bacteria. The hindrance impact operates through various mechanisms, including the obstruction of bacterial attachments and the rivalry for attachment locations. Additionally, probiotics operate as secondary agents by improving the protective capability of the intestinal lining, which relies on the tight connections between intestinal epithelial cells. They also contribute to this function by producing mucus containing antimicrobial peptides like defensins and lysozyme, as well as Paneth cells. This mucus layer acts as a shield, averting direct contact between the digestive channel and bacteria. Probiotics operate through a third mechanism, exerting an influence on the immune system. It is crucial to emphasize that over 70% of immune cells reside within the gut-associated lymphoid tissues, which are predominantly concentrated in the small intestine. Certain probiotic bacteria, notably lactobacilli, can induce either localized or systemic effects depending on their cytokine profile. It is imperative to thoroughly comprehend the mechanisms through which probiotics operate. Moreover, the properties of probiotic strains must remain unchanged throughout the production process and storage period before their use, ensuring the absence of any factors that may cause diseases.¹⁷

Each probiotic strain exerts a distinct effect, making it imperative to conduct individual assessments to determine their specific health benefits. The efficacy remains unproven because of the limitations of existing studies, such as their low quality, variations in microbiota, reactions to attempts at adjustment, and the diverse range of probiotic strains employed.¹⁸

Risk theories of probiotics usage

Numerous risk theories revolve around probiotics use. One concern involves the possibility that probiotics cause infections via translocation. Certain strains have shown the ability to either decrease or increase the movement of gut bacteria, thereby influencing this process. In addition, probiotics might produce poisonous compounds such as D-lactate during bacterial fermentation that can be a potential risk factor, leading to lactic acidosis. In cases of children with short bowel syndrome, administration of lactobacilli-rich microbiota or specific *Lactobacillus* probiotic strains has been linked to acidosis, leading to either encephalopathy or hyperventilation. Nevertheless, there have been no reported cases of lactic acidosis in healthy children. Yet another notable risk involves the exchange of antibiotic-resistance genes between typical host bacteria and probiotic strains residing in the digestive tract. This gene transfer can occur within the gut microbiota, potentially increasing bacterial diversity in the area. Probiotic strains can serve as vectors for these resistance genes, acting as either an offeror or applicant. It is recommended to select probiotic strains that do not possess acquired and potentially transferable resistance genes. Concerns arise when using probiotic strains from species that naturally carry virulence and antibiotic resistance traits, such as Enterococci or *Escherichia coli*. Genomic analyses of probiotic enterococci strains indicating the absence of virulence factors can alleviate this concern.¹⁷

Challenges of probiotic application in the treatment of gastrointestinal diseases

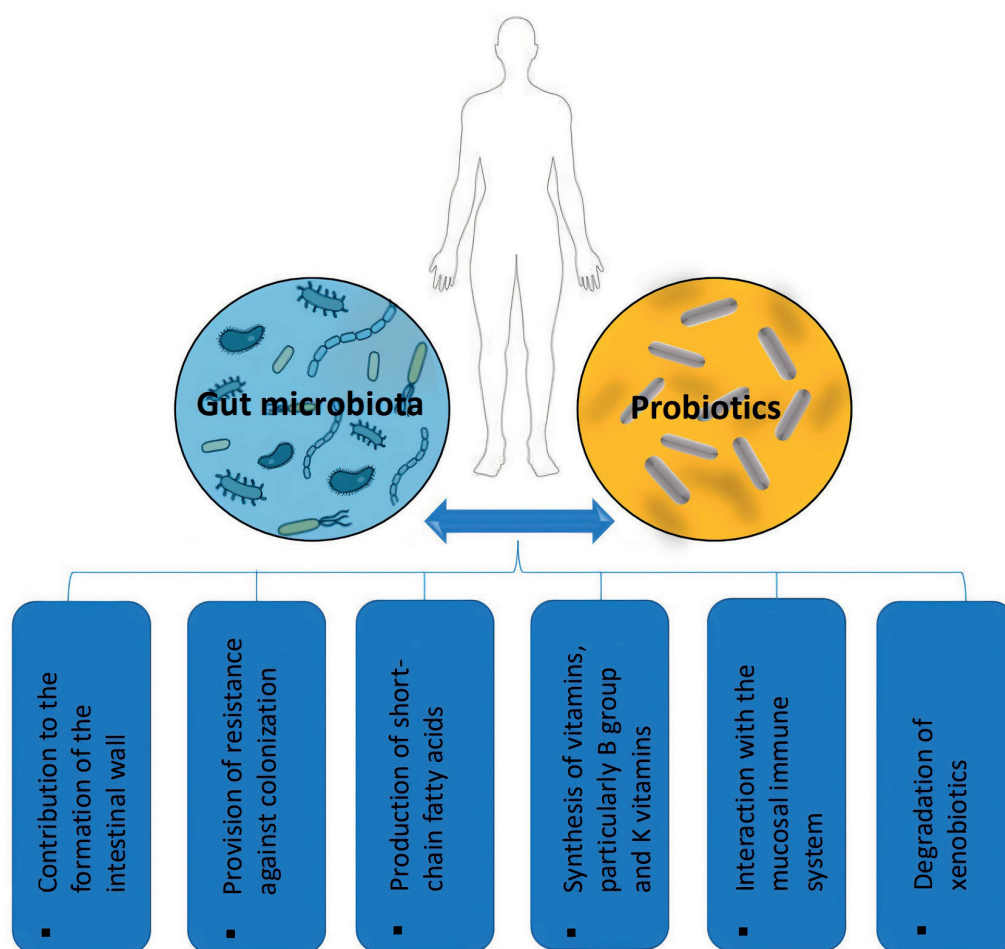
Although probiotics demonstrate considerable potential for the treatment of GI disorders, their implementation is constrained by a number of challenges.¹⁹ First, for probiotics to be deemed safe for human consumption, they must lack transferable antibiotic-resistant genes.²⁰ Consequently, the use of engineered probiotics in disease management is often restricted. Second, a minimum viable count of approx. 10^6 colony-forming units per gram (CFU/g) is necessary for probiotics to exert their beneficial effects.²¹ However, widely used probiotics such as *Lactobacillus* and *Bifidobacterium* are highly vulnerable to aerobic and high-temperature conditions. The next generation of probiotics requires an environment conducive to their viability and robustness to endure the acidic stomach and

bile environment during their transit through the GI tract. Even upon successful passage to the colon without damage, probiotics must adhere to the mucosal layer and establish effective colonization to be efficacious. Thus, formulating probiotics for targeted delivery to the intestines poses significant challenges. Bacteriocins serve as versatile agents, functioning as “colonizing peptides”, “killing peptides” and “signal peptides”, augmenting the colonizing potential of the producing strain in the gut and providing it a competitive edge over other strains. In addition, unresolved issues persist regarding probiotic quantification, encompassing on-site localization and dynamic monitoring.²² Moreover, the gut microbiota substantially influences the development and functioning of the immune system, among other physiological processes. The symbiotic relationship between the gut microbiota and the host organism offers numerous mutual benefits, as the microbiota within the host organism performs crucial functions (Fig. 2).

Positive aspects of probiotics usage

Metabolism, the barrier effect and trophic functions, recognized as pivotal aspects of intestinal physiology, constitute the primary roles of the microbiota.¹⁸ Dysbiosis, denoting bacterial imbalance, can lead to various diseases. It is widely known that the introduction of live bacteria (probiotics) or indigestible substrates (prebiotics) leads to a positive response from the microbiota, helping to prevent and even treat specific diseases. Presently, there is a widespread acknowledgment of the substantial impact of intestinal microbiota on human health, and probiotic interventions are recognized as a means to modulate this influence.¹⁷ According to the guidelines established by the WHO and the FAO, a bacterial strain can be classified as a probiotic only if it effectively reaches the targeted site in the body and withstands physiological stressors such as the acidic environment, varying pH levels in the stomach and intestines, and bile salts. Furthermore, a probiotic should demonstrate established beneficial effects on the host, be devoid of risks, and maintain its properties during both production and storage. Probiotic microorganisms can originate from diverse genera and species,²³ including yeasts like *Saccharomyces cerevisiae* and bacteria such as *Lactobacillus*, *Streptococcus*, *Enterococcus*, *Bifidobacterium*, *Propionibacterium*, *Bacillus*, and *E. coli*. These probiotics can either naturally exist in commonly consumed foods or be genetically modified for specific purposes. Notably, strains from the *Enterococcus* genus carry a heightened risk potential compared to other probiotics; although infrequent, they may cause systemic infections and antibiotic resistance in the host. Probiotic products may contain either a single strain or multiple strains.²⁴ The advantages of a probiotic formulation vary based on the specific patient demographic. Studies with limited scope have indicated heightened effectiveness

Fig. 2. The relationship between the gut microbiota and the host organism is advantageous



when utilizing probiotics sourced from diverse ethnic backgrounds. To regulate the consideration of probiotics in food, the WHO and the FAO have jointly established comprehensive guidelines. These FAO/WHO guidelines serve as the global standard for probiotic assessment. The prescribed instructions under this directive encompass the following criteria: probiotics offer several key advantages, including safeguarding against GI pathogens, enhancing immune function, reducing serum cholesterol and blood pressure levels, exhibiting anti-carcinogenic properties, and enhancing nutrient utilization and bio-availability.²⁵ These benefits are achieved through diverse mechanisms, including a decrease in intestinal pH, inhibition of pathogenic organism colonization and invasion, and modulation of the host immune response.²⁶

Probiotics' role in immune system modulation

The gut microbiota plays a pivotal role in immune system regulation through the production of molecules possessing immunomodulatory and anti-inflammatory properties. These effects result from the interactions between probiotic bacteria and various cell types, including epithelial cells, DCs, monocytes/macrophages, and lymphocytes, thereby initiating and stimulating immune

cell activity.²⁷ Probiotics fundamentally contribute to regulating the host immune response, which is categorized into innate and adaptive systems. The adaptive response involves the specific binding of B and T lymphocytes to antigens, while the innate system recognizes common structures known as pathogen-associated molecular patterns (PAMPs) shared by numerous pathogens. Pattern recognition receptors (PRRs) bind to PAMPs, triggering an initial response to pathogens. These PRRs encompass a diverse array of molecules, including transmembrane proteins like TLRs, found in various immune and non-immune cells such as B cells, natural killer cells, DCs, macrophages, fibroblast cells, epithelial cells, and endothelial cells. Additionally, PRRs encompass nucleotide-binding oligomerization domain-like receptors (NODLRs) that safeguard the cytoplasmic space. Other recognized PRRs include C-type lectin receptors, formylated peptide receptors, retinoic acid-inducible helicases, and intracellular IL-1-converting enzyme protease-activating factor.²⁸ Notably, the finely tuned regulation of the T cell subset, which is crucial for maintaining immune balance, is influenced by both the host and interacting microbes. Imbalances between effector T-helper (Th) cells and Tregs can compromise immune responses. Probiotics aid in preserving intestinal equilibrium by modulating the immune response and promoting Treg proliferation.¹³

Prebiotics

Prebiotics possess distinctive attributes: First, they resist enzymatic breakdown in the human gut and are specifically metabolized by certain genera/species of resident gut microbiota. This targeted breakdown leads to an increase in particular bacteria, providing health advantages to the host. These benefits encompass various effects, such as immune modulation characterized by elevated levels of intestinal-specific immunoglobulins and immunoregulatory interleukins, alongside a decrease in proinflammatory interleukins. In addition, prebiotics induce the production of SCFAs like acetate, propionate, butyrate, and lactate, thereby reducing the gut's pH level. This pH adjustment is crucial to preventing the colonization of acid-sensitive enteric pathogens. Notably, acetate production contributes to the synthesis of butyrate through cross-feeding, acting as a fundamental element for colonocyte function and enhancing epithelial integrity.^{29,30} Although dietary fiber found in fruits and vegetables is generally indigestible, not all varieties exhibit prebiotic effects. Certain vegetables like leeks, asparagus, chicory, garlic, and artichoke, as well as grains such as wheat, and fruits like bananas, oats and soybeans, contain compounds such as inulin, fructo-oligosaccharides and galacto-oligosaccharides (GOS). These substances serve as major prebiotic substrates. Research suggests their potential to stimulate the growth of specific colonic microbiota, potentially offering health benefits to the host.²⁹ Typically, prebiotics include dietary carbohydrates, predominantly featuring inulin-type fructans and GOS as the primary types meeting prebiotic criteria, although ongoing research explores various other carbohydrate classes in this domain.^{29,30}

Bacteriocins and other bacterial antimicrobial compounds

Numerous intestinal bacteria create antimicrobial peptides, proteins and lipoproteins to improve their dominance in particular anatomical locations. Bacteriocins, with their limited range, excel at eradicating bacteria in close proximity to the producing strain, ensuring steady colonization and thwarting intrusion from rival species. For example, *Enterococcus faecalis* strains that generate new bacteriocins can surpass strains that do not produce them. The genetic material responsible for these bacteriocins can be transferred horizontally, hinting at the possible usefulness of introducing bacteriocin-producing strains to decrease the presence of multidrug-resistant enterococci.^{31,32} Many research studies have highlighted the importance of probiotic microbes that produce bacteriocins in safeguarding food safety and packaging, especially in the fight against Gram-positive bacteria such as *Listeria*.³³ The identified bacteriocins are systematically categorized based on their design and

antimicrobial spectrum in databases such as BAGEL³⁴ and BACTIBASE³⁵ and are extensively discussed in recent reviews.^{36–38} Bacteriocins can have effects beyond direct antimicrobial activity. For instance, mice fed a high-fat diet did not experience changes in the composition of their intestinal microbiota when given *Lactobacillus plantarum* strain NCMIB8826, which produces the bacteriocin plantaricin EF. However, compared to mice fed a mutant *L. plantarum* strain lacking bacteriocin, zonulin expression increased. In vitro studies further confirmed a reduced permeability upon exposure to bacteriocin. Ongoing research is currently focused on this area³⁹ in case bacteriocins can translocate into the lamina propria and initiate systemic effects.⁴⁰

Probiotics in the prevention or treatment of different disorders

Inflammatory bowel diseases

In recent decades, there has been a noticeable upward trend in the global incidence and prevalence of inflammatory bowel diseases (IBD). Ulcerative colitis (UC) and Crohn's disease (CD) stand out as the 2 primary subtypes of IBD, with UC predominantly affecting the large bowel, and CD manifesting in any part of the GI tract. The exact etiology of UC remains a subject of substantial debate, with proposed factors including environmental influences, immune dysfunction and genetic predisposition.⁴¹ The prevailing hypothesis suggests that genetically susceptible individuals harbor abnormalities in humoral and cell-mediated immunity, leading to heightened reactivity against commensal intestinal bacteria, thereby predisposing them to colonic inflammation. The causal relationship between these abnormalities and the intense systemic inflammatory response observed in UC remains unresolved. Nevertheless, it is well-documented that patients with active UC exhibit alterations in bacterial microflora. Recent studies have highlighted considerable variability in the effects of the microbiota, particularly emphasizing the influence of a proinflammatory enterotype on mucosal integrity and disease activity.⁴² While modulation of the intestinal microbiota can be achieved through antibiotics or probiotics, antibiotic use for chronic diseases should be limited due to concerns regarding resistance, potential side effects and ecological impacts. Therefore, the use of probiotics in IBD management holds promise as a potential adjunct to current conventional therapies. A comprehensive analysis of scientific data attests to the demonstrated and confirmed efficacy of probiotics in treating various diseases. Several studies have particularly focused on the effects of probiotic blends on the enteral microbiota, particularly in cases of dysbiosis, wherein the normal concentration of beneficial bacterial flora is compromised by the presence of pathogenic bacteria.⁴³

Irritable bowel syndrome

Functional GI disorders, including ailments such as abdominal pain and irritable bowel syndrome (IBS), constitute common reasons for pediatric gastroenterologist consultations. These conditions are prevalent among school-aged children, affecting approx. 10% of this demographic, with potential regional discrepancies. For instance, IBS has been reported in 13% of children in China, 10% in the USA and 6% in Sri Lanka.⁴⁴ In contrast, IBS in adults exhibits varying prevalence rates, ranging from 6% in Africa and the Middle East to 18% in Latin America.⁴⁵ The prevalence in North America and Asia typically falls between 8% and 10%. The multifaceted etiology of IBS includes factors such as genetic predisposition, responses to life stresses and potential environmental triggers like infectious diarrhea. The Rome Criteria provides a precise definition, defining IBS as recurrent abdominal pain occurring at least once a week for over 3 months, accompanied by changes in bowel movements and stool form and/or frequency. Recent studies have highlighted an altered microbial composition in the feces of individuals with IBS. Particularly, those with diarrhea-predominant IBS exhibit a distinct microbial profile, characterized by reduced microbial diversity, diminished populations of butyrate-producing organisms (crucial for gut barrier function) and fewer methane producers (involved in gas expulsion).⁴⁶ These findings emphasize the potential role of targeted microbial interventions in managing IBS. Probiotics have been extensively investigated in numerous randomized controlled trials (RCTs) to assess their effectiveness in alleviating IBS symptoms. Ford et al.⁴⁷ conducted a comprehensive analysis encompassing 43 RCTs involving over 3,000 participants, revealing a relative risk (RR) of persistent IBS symptoms at 0.79 (95% confidence interval (95% CI): 0.70–0.89) in favor of probiotic use. Additionally, a recent review of 21 RCTs in China showcased a positive association between probiotic consumption and improved IBS symptoms, coupled with an enhancement in quality of life.⁴⁸ However, these studies presented differing conclusions. One study indicated superior outcomes with a single probiotic, while the other found similar results with both single and multi-organism probiotics. Recent RCTs have meticulously examined individual probiotics, facilitating meta-analyses that highlighted their effectiveness in individuals with IBS. Noteworthy probiotics in these analyses include *S. cerevisiae* CNCM I-385620 and *Bifidobacterium infantis* 35624.⁴⁹ The latter demonstrated efficacy specifically when incorporated into a multi-organism probiotic. Essentially, individuals with IBS exhibited a reduction in specific symptoms like flatulence, abdominal pain and constipation in response to probiotics, while discernible changes were not evident in other symptoms such as bloating or urgency. Furthermore, *Lactobacillus reuteri* showed beneficial effects in children with functional abdominal pain, leading to a decrease in episode frequencies and

pain intensity.⁵⁰ Although probiotics offer advantages for children with IBS, their impact appears relatively modest compared to alternative treatments like low-dose antidepressants.⁵¹ Several key questions persist, including the magnitude of the effect, optimal dosage, safety in vulnerable populations, and identification of the most effective probiotic species and strains.

Acute infectious diarrhea

Acute diarrhea, often caused by viruses, primarily affects children aged 6 months to 2 years. Its occurrence is closely related to water quality, sanitation and hygiene. Infants with acute diarrhea are at high risk of dehydration, a leading cause of child mortality globally, causing about 700,000 deaths annually.⁵² Probiotics, particularly *Lactobacillus rhamnosus* GG and *L. reuteri*, have been extensively studied for over 3 decades in treating acute diarrhea in children. Parker et al.⁵³ reviewed 15 studies on *L. rhamnosus* GG, finding it reduces the severity and duration of diarrhea, most effectively at doses of 10¹⁰ CFU. Their meta-analysis also showed that *L. reuteri*, at a lower dose, effectively shortens diarrhea duration by about 1 day.⁵⁴ Global efforts in hygiene, breastfeeding and rotavirus vaccination have decreased diarrhea-related deaths; however, recent refugee crises may challenge this progress. The broader effects of such measures remain a subject of interest.

Antibiotic-associated diarrhea

Antibiotics are frequently prescribed for children, with over half of those under 18 receiving at least 1 course, including commonly prescribed types like amoxicillin, azithromycin and amoxicillin/clavulanate. Antibiotic-associated diarrhea (AAD) affects approx. 11% of all children receiving antibiotics and reaches 18% among those under 2 years of age.⁵⁵ Hempel et al. conducted a meta-analysis involving 63 RCTs and 11,811 subjects, predominantly using *Lactobacillus* as the probiotic. Their findings showed a reduced risk of AAD (RR: 0.58; 95% CI: 0.50–0.68; $p < 0.001$) in individuals using probiotics. However, there was some variability in outcomes, prompting further investigation to determine the most effective probiotic regimen. A recent meta-analysis in China, encompassing 30 trials and over 7,000 participants, predominantly focusing on children and consistently containing *Bifidobacteria* strains in the probiotic, revealed a significant efficacy in preventing AAD, with an odds ratio (OR) of 0.34 (95% CI: 0.23–0.43; $p < 0.01$) for AAD occurrence among children administered *Bifidobacteria*-containing preparations, highlighting the clinical importance of such interventions.⁵⁵

Necrotizing enterocolitis

Necrotizing enterocolitis (NEC) poses a significant risk to premature infants, affecting 5–10% of those born

weighing 500–1500 g. Nearly half of these infants require surgical intervention, with mortality rates ranging between 20% and 30%. Necrotizing enterocolitis is the primary cause of short bowel syndrome in children.⁵⁶ In a 4-year multicenter trial, Warner et al. investigated the progression of microbial colonization in preterm infants and noticed disruptions occurring before NEC onset. They observed an expansion of Negativicutes in non-NEC cases. However, infants diagnosed with NEC displayed reduced Negativicutes and increased Gammaproteobacteria strains, indicating a correlation with GI dysbiosis.⁵⁷ Multiple meta-analyses corroborate the effectiveness of probiotics in preventing NEC.⁵⁸ However, determining the most effective probiotic strain remains unknown due to the variations in preparations used across studies. No studies on probiotics in preventing NEC have been completed in the USA. Safety concerns persist, with the U.S. Food and Drug Administration (FDA) categorizing probiotics similarly to vaccines. Essential preclinical and clinical trials are required to understand early-life host–bacterial interactions. Studying the immune response and microbiota impact in infants solely fed with breast milk, especially involving strains like *L. rhamnosus* GG and *L. reuteri*, holds potential. However, it is essential to exercise caution and avoid exceeding doses of 10^{10} CFU in premature neonates to mitigate the risk of bacterial translocation. Despite these safety considerations, probiotics, particularly in very low birth weight (VLBW) infants (<1,000 g), are anticipated to offer substantial preventive advantages against NEC. An initiative that introduced *L. reuteri* probiotics showcased a significant 6-fold decrease in the risk of NEC after implementation.⁵⁸

Infant colic

Colic, characterized by excessive crying and fussiness in infants, typically emerges between 3 weeks and 3 months of age, affecting up to 10% of infants. It has been associated with potential cases of child abuse and infanticide, often arising from a caregiver's attempts to alleviate the distressing crying episodes.⁵⁹ Various theories have been proposed to elucidate the origin of colic, including parental stresses, cow milk protein allergies, the 4th-trimester theory, and the inflammation-dysbiosis theory. While these theories offer insights into specific cases, dysbiosis (an imbalance in gut microbiota) and gut inflammation consistently emerge as noteworthy factors.^{60,61} Research conducted in different regions has identified alterations in the microbial composition of infants with colic. These include increased *E. coli*, reduced Lactobacilli, elevated Klebsiella, and a diminished microbial diversity.^{60,61} These findings suggest a potential link between gut microbiota and colic. Studies investigating the probiotic *L. reuteri* have shown promising results. Administered as liquid drops in sunflower oil, it demonstrated notable benefits in breast-fed infants with colic, reducing crying and fussy times. However, its effectiveness in formula-fed infants remains a subject of debate, possibly due to various factors, including differences in probiotic strains and sample sizes.^{62,63} Presently, colic is often treated with acid blockers, despite their efficacy being limited, and their potential drawbacks. The introduction of a safe and effective treatment option like *L. reuteri* represents a significant advancement in pediatric care.⁶⁴ The positive effects of probiotics on infants are mentioned in Fig. 3.

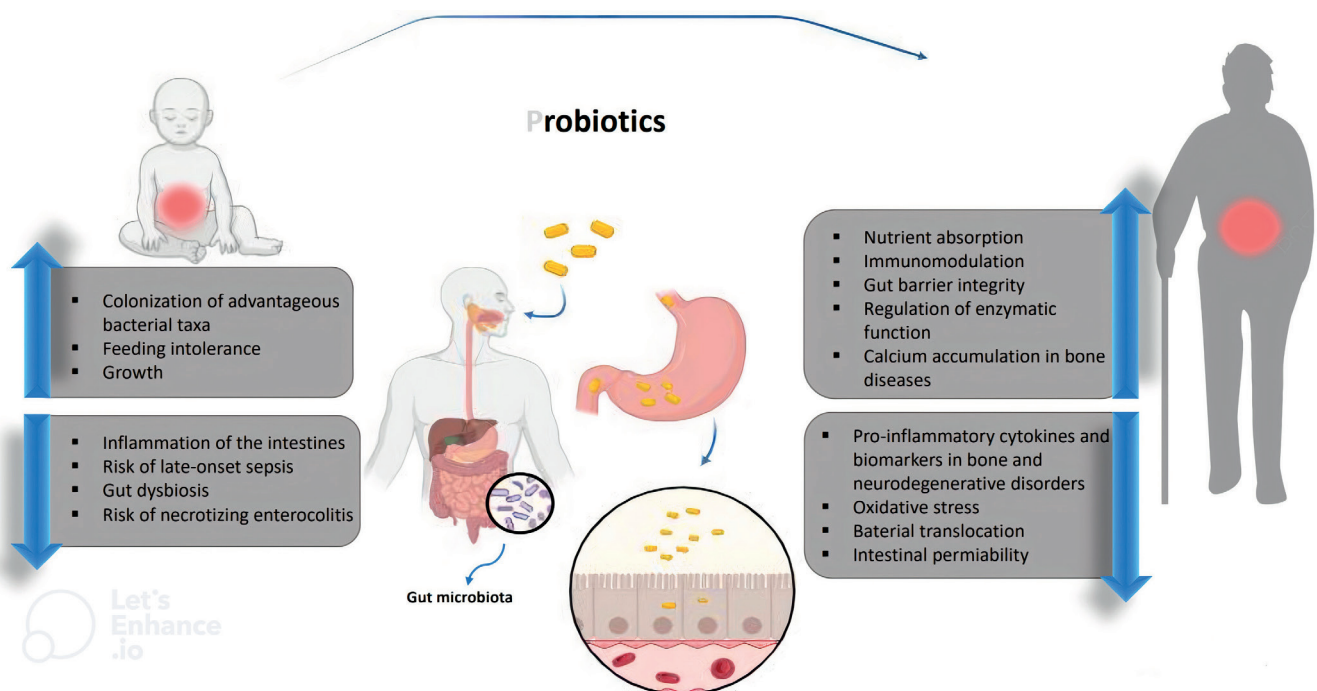


Fig. 3. The role of probiotics in infants and the elderly

Upper respiratory infections

In studies conducted at daycare centers, regular probiotic intake among healthy children demonstrated a nearly 25% decrease in absent school days.⁶⁵ Probiotics exhibit a consistent impact by promoting an immune response, resulting in heightened production of immunoglobulin A (IgA)-secreting cells in both the respiratory and GI mucosa.⁶⁶ Moreover, comprehensive analyses have affirmed the correlation between probiotics and diminished severity of symptoms, along with a shorter duration of respiratory tract infections, typically by approx. 1 day.⁶⁷

Allergic diseases

Balancing a dual role of defending against emerging organisms while tolerating nonpathogenic antigens/allergens, the immune system's primary mission is to safeguard the host. This undertaking is formidable, necessitating alliances in an ongoing battle.⁶⁸ Probiotics have emerged as a clear ally in regulating the interplay between inflammation and allergic responses. The hygiene hypothesis, supported by epidemiological data, suggests a reduced susceptibility to allergic diseases among individuals in rural and developing regions. This interest in probiotics for preventing or managing allergic conditions like asthma, eczema and food allergies has grown significantly.

However, meta-analyses revealed that probiotics may not be sufficient to prevent asthma, allergic rhinitis or food allergy onset, except for atopic dermatitis. The impact of probiotics on atopic dermatitis varies and lacks consistent demonstration across studies.⁶⁹ A recent meta-analysis involving 17 studies shows a noteworthy reduction in eczema risk for infants when both mothers and infants receive probiotic supplementation, especially a mixture of probiotics. Probiotics hold an intriguing potential as adjuncts in oral immunotherapy (OIT) for food allergies. In a recent double-blind, placebo-controlled trial, administering the probiotic *L. rhamnosus* CG MCC 1.3724 alongside peanut OIT resulted in sustained unresponsiveness in 82% of children with peanut allergies, compared to only 3.6% in the placebo group.⁷⁰ Unfortunately, despite this success, probiotics have not shown significant therapeutic efficacy in treating allergic rhinitis and asthma in RCTs.⁷¹ While ongoing clinical trial data suggest some beneficial effects of probiotics in preventing and managing allergic diseases, the evidence is not strong enough yet to support a universal recommendation for their therapeutic use. Various factors, including the specific probiotic strains tested, as well as patient-specific factors such as diet, immune responses, mucosal conditions, and emotional states, can influence probiotic functionality. Additionally, the route of administration could play a crucial role; for instance, nasal spray delivery may be more effective for allergic rhinitis, inhalation for asthma, and topical application for atopic dermatitis. Further research is imperative, particularly

in unraveling the diverse mechanisms through which probiotics contribute to immunoregulation and mucosal homeostasis.

Clostridium difficile colitis infections in hospitalized patients

Clostridium difficile colitis arises as an opportunistic infection due to disruptions in the normal gut flora induced by antibiotic administration. Antibiotics such as clindamycin, fluoroquinolones, broad-spectrum penicillin, and cephalosporin are commonly associated with this condition. The severity of *C. difficile* colitis varies, with severe cases necessitating intensive care and posing a lethal risk. Probiotics are nonpathogenic bacteria that reside in the GI system and produce lytic peptides that impede the activity of *C. difficile* toxins. Specifically, *Saccharomyces boulardii* generates a protease that inhibits the action of *C. difficile* toxins.⁷²

Prophylactic probiotics aim to establish the presence of beneficial bacteria to combat *C. difficile* overgrowth. Certain probiotics demonstrate the capacity to neutralize *C. difficile* toxins A and B, as supported by in vitro and preclinical data, conferring protective properties.⁷³ Postoperative patients are vulnerable to bacterial translocation, primarily stemming from intestinal mucosal injury, leading to gut barrier disruption, heightened intestinal permeability, microbial imbalance, and diminished immunodeficiency. This risk is particularly pertinent in abdominal surgeries for conditions like biliary cancer, pancreaticoduodenectomy and liver transplantation, predisposing patients to complications such as urinary tract infection (UTI), pneumonia, wound infection, intra-abdominal abscess, and cholangitis.^{74,75}

Administering probiotics alongside antibiotics in adult non-surgical infection patients has shown promise in reducing rates of *C. difficile* colitis. This approach holds potential for infection prevention, potentially leading to decreased morbidity, shorter antibiotic therapy durations, reduced hospital stays, and a mitigated risk in the emergence of antimicrobial resistance.^{75,76}

Probiotics in very low birth weight infants

Newborns with VLBW experience considerable neonatal morbidity and mortality, primarily linked to nosocomial infections and NEC. The multifaceted origins of these conditions involve intrinsic host factors like gestational age and underdeveloped immune responses. Moreover, environmental aspects such as enteral nutrition and exposure to a hospital environment harboring pathogen significantly influence the abnormal colonization of the GI tract and the movement of pathogenic bacteria across the fragile intestinal lining.^{77,78}

The use of *Lactobacillus acidophilus*/*Bifidobacterium infantis* probiotics has shown a noteworthy correlation

in the prevention of NEC surgery and any abdominal surgery, accompanied by a decrease in overall mortality. This hints at a potential mechanism by which probiotics may enact their effects, involving a mutual interplay between the evolving immune system and gut microbiota.⁷⁹

Prophylactic intervention involving probiotics in the context of cancer (carcinogenesis)

Colorectal cancer patients exhibit distinct gut bacteria profiles. *Bacteroides* and *Prevotella* are more prevalent, while colorectal adenoma patients have higher levels of *Dorea* spp. and fecal bacteria spp. These bacteria can produce compounds linked to carcinogenesis and tumor promotion.⁸⁰

Probiotics not only defend against infections but also possess potential anticancer properties. They play a vital role in immunomodulation and have been shown to mediate anticancer responses. Specific strains may be involved in the detection and breakdown of potential carcinogens. They also contribute to the synthesis of SCFAs, crucial for regulating cell proliferation and apoptosis. Additionally, heat-killed probiotic bacteria combined with radiation have shown promise in enhancing cancer cell immunological recognition.⁸¹

A combination of *Lacticaseibacillus rhamnosus* GG, *Bifidobacterium lactis* Bb12 and oligofructose-enriched inulin administered to colorectal cancer patients resulted in beneficial shifts in the gut microbiome. This intervention led to increased levels of advantageous bacteria and decreased levels of detrimental bacteria. *Lacticaseibacilli casei* has displayed augmented immune responses against cancer and alleviation of side effects from cancer treatments.¹³ Nevertheless, further investigation is necessary to comprehend the precise mechanisms underlying probiotic-induced anticancer effects.⁸² Potential pathways may involve the interplay between nutrition, gut microbiota and host energy metabolism, yielding diverse effects.⁸³ These effects encompass neutralizing carcinogens, fortifying intestinal barrier functions, synthesizing essential compounds, modulating immune responses, and influencing apoptosis, among other factors.⁸⁴ Exposure to *Lactobacillus* induces various biological changes, including increased levels of cytokines, interleukins, antioxidants, microbial flora, interferons, and immune cells, while simultaneously reducing factors like DNA damage, pathogens, inflammation, ulcers, tumor size, cancer-specific proteins, polyamine contents, and pro-carcinogenic enzymes.⁷⁹

In rat experiments, a combination of probiotics and celecoxib demonstrated a reduction in the expression of the proto-oncogene K-ras and an elevation in the tumor suppressor p53. This suggests a potential synergistic effect inhibiting cell growth by activating tumor suppressor genes while preserving cell activity and the cell cycle. This combined treatment likely contributed to maintaining gut integrity, enhancing the immune response, and leading

to reduced DNA damage.⁸⁵ Additionally, celecoxib's anti-inflammatory properties contributed to a decrease in colonic tumors by downregulating K-ras and upregulating p53, which can induce Bax-mediated apoptosis.^{85,86}

Additionally, DNA methylation, facilitated by differential methylation hybridization (DMH), triggers activation in the Wnt pathway. This pathway's acceleration, attributed to the increased expression of proinflammatory markers, contributes to the process of carcinogenesis. The participation of detrimental bacteria, the production of harmful metabolites, and a decrease in pro-apoptotic markers further exacerbate this progression. By administering probiotics and celecoxib, the modulation of the Wnt signaling pathway occurs along with improvements in the gut microbiome. This intervention potentially leads to decreased inflammation and heightened apoptotic markers, serving as a preventive measure against the onset of carcinogenesis.⁸⁵

Probiotics and enteral nutrition in acute pancreatitis

In cases of acute pancreatitis, a significant aspect of pathogenesis involves bacterial translocation from the stomach to necrotic pancreatic tissue. This process leads to infection of the pancreatic tissue. Preventing bacterial translocation and subsequent infection in cases of pancreatic necrosis is a key concern. To achieve this, prophylactic approaches such as antibiotics, enteral nutrition or probiotics can be used. Studies conducted in mouse models have demonstrated that administering probiotics as a pre-treatment, especially in the early stages, can effectively uphold intestinal barrier function, even in severe pancreatitis. Notably, the timing of probiotic administration plays a critical role in their efficacy. Whereas animal models have provided evidence of a correlation between probiotic timing and pancreatitis onset, it remains to be firmly established in human subjects, warranting further investigation.^{87,88}

Late-onset sepsis in preterm infants

Gram-negative bacteria, while less prevalent than their gram-positive counterparts, are linked to late-onset sepsis (LOS), marked by a more severe clinical course, higher mortality rates and increased neonatal morbidity. Late-onset sepsis can be caused by factors such as low birth weight, premature delivery or admission to the intensive care unit (ICU). Premature infants, especially those in the ICU, are susceptible to bacterial colonization. The use of antibiotics after birth and prolonged hospital stays can lead to a decrease in the diversity of microbes in the microbiome.⁸⁸ In this vulnerable population susceptible to LOS, the administration of oral probiotics may enhance the colonization of beneficial bacteria. It is important to note that the effectiveness of probiotics depends on factors like the specific strain, dosage and intended use. A recent RCT focused on preterm infants between 28

and 31 weeks of gestation and demonstrated a significant reduction in LOS incidence with a probiotic combination comprising *B. infantis*, *Streptococcus thermophiles* and *B. lactis*.⁸⁸

Necrotizing enterocolitis in preterm infants

Necrotizing enterocolitis is a condition that causes the death of intestinal tissue and is a significant contributor to neonatal mortality, affecting around 20–30% of VLBW infants, defined as those born weighing less than 1,500 g (1.5 kg). Premature neonates frequently encounter delayed and diminished colonization of the gut by probiotic organisms like Bifidobacteria and Lactobacilli. Various factors, including cesarean birth, delayed breastfeeding initiation or antibiotic treatment after birth, can lead to an imbalance favoring potentially harmful bacteria.⁸⁹ Enteral administration of probiotics has demonstrated efficacy in preventing severe NEC and reducing overall mortality in preterm infants.⁹⁰ The prophylactic use of enteral probiotics, involving the supplementation of live microbial organisms, holds promise in mitigating NEC and its associated morbidity. This is achieved through hindering bacterial migration across the mucosa, competitively excluding harmful bacteria, and enhancing the host's immune responses. Notably, probiotics containing *L. acidophilus* and *B. infantis* have shown associations with a reduced risk of NEC-related surgery, any abdominal surgery and overall mortality.⁹¹

The mechanism of probiotic action involves facilitating the establishment of beneficial microbial flora in the gut, preventing pathogenic colonization, strengthening the maturity and functionality of the gut mucosal barrier, and influencing the immune system. Typically, probiotics are administered for a duration of 2 weeks, starting either on the 1st day of life for newborns not receiving antibiotics or after the cessation of antibiotic therapy.^{91,92}

Ventilator-associated pneumonia

Ventilator-associated pneumonia (VAP) is a serious risk for patients in ICUs and can cause morbidity and mortality. Probiotics have recently emerged as a promising tool in combating VAP. The proposed mechanisms of probiotics include strengthening the intestinal barrier, increasing the production of antimicrobial peptides in host cells, regulating gut microbiota composition, and curtailing the proliferation and translocation of harmful bacteria. Multiple trials have validated the safety and efficacy of probiotics in both preventing and treating VAP among ICU patients.^{93,94}

Probiotics and their therapeutic uses

Probiotics exert their predominant therapeutic effects through their direct or indirect actions on the GI tract. Their efficacy is derived not just from interactions with

host cell mucous membranes but also from their oral intake. However, it is crucial to acknowledge that while certain probiotic microorganisms offer advantages, not all are naturally prevalent in the human gut flora. Therefore, the benefits attributed to one species might not universally apply to others⁹⁵ (Table 1).^{95–123}

In vitro and in vivo models

Bacterial growth inhibition models

There are several GI illnesses caused by common pathogens such as *E. coli*, *C. difficile*, Salmonella, *Helicobacter pylori*, Listeria, and *Candida albicans*. Traditionally, researchers have utilized in vitro methods to evaluate the potential efficacy of probiotics in inhibiting the growth of these pathogens. For example, Prasastha Ram et al. conducted studies showcasing the antibacterial and antibiofilm properties of *L. acidophilus* against multi-drug-resistant *Enterococci* *Escherichia coli* (MDR-EAEC) strains using green synthesized silver nanoparticles.¹²⁴ Ruiz et al. explored a synbiotic containing *Bifidobacterium longum* subsp. *infantis* CECT7210 and oligosaccharides, demonstrating its antimicrobial efficacy against *E. coli*, *Cronobacter sakazakii*, *Listeria monocytogenes*, and *C. difficile*.¹²⁵ Similarly, Cizeikiene and Jagelaviciute identified potential probiotic candidates like *L. acidophilus* DSM 20079, *Bifidobacterium pseudolongum* DSM 20099 and *Bifidobacterium animalis* DSM 20105 through antibacterial assays targeting various pathogenic strains.¹²⁶ In addition to pathogen growth inhibition, researchers have explored the effects of probiotics on pathogenic and host-related infection genes. *Bifidobacterium longum* JDM301 was found to inhibit *C. difficile* growth and promote clostridial toxin degradation.¹²⁷ Ghadimi et al. conducted an assessment of the probiotic effects of *B. animalis* R101-8. They evaluated the expression levels of genes linked to lipid metabolism and cytokines associated with inflammation. Their study suggested that *B. animalis* R101-8 might elevate meta-inflammation biomarkers through molecular pathways activated by proinflammatory bacteria and lipids.¹²⁶ Furthermore, the development of mathematical and genome-scale metabolic models in big data science and bioinformatics has resulted in innovative methods for assessing the functions of bacterial probiotics.^{128,129}

Models simulating intestinal microbiota in vitro

Recent advancements in batch fermentation techniques, especially those replicating the conditions of the distal colon, provide opportunities for exploring interactions between probiotics and pathogens. Several models, such as TIM-2, SHIME, ECSIM, SIMGI, PolyFermS, and EnteroMix, have been created to mimic the human intestinal microbiota.¹³⁰ Although these models were mainly

Table 1. Application of probiotics for therapeutic purposes

Disease	Definition	Etiology	Probiotic strain	Mechanism of action	Useful product	Ref.
IBD, including: (UC and CD)	Persistent inflammation of the gut mucosa. Disruption of gut barrier function/an imbalanced microbiota frequently manifest as chronic gastrointestinal mucosa inflammation.	An issue arises from the immune system's reaction to microorganisms within the natural intestinal flora. Alterations in the gut microbiota or a weakening of the mucosal barrier lead to detrimental immune reactions against the mucosa.	<i>Lactobacillus paracasei</i> L74 CBA/ <i>Streptococcus salivarius</i> / <i>Lactobacillus salivarius</i> / <i>Lactiplantibacillus plantarum</i> Lp91	Anti-inflammatory effect. Reduction in the levels of (COX-2 and TNF). Releasing large amounts of antioxidant enzymes.	fermented milk probiotic yogurt	95–101
Antibiotic-associated diarrhea	The most common adverse effect of antimicrobial therapy.	The utilization of antibiotics is considered to disrupt the natural enteric microbiota, causing a reduction in native microorganisms within the gastrointestinal system.	<i>L. rhamnosus</i> <i>L. kefir</i> <i>L. gasseri</i> F71 <i>L. gasseri</i> L1 <i>L. casei</i> <i>L. paracasei</i> <i>S. thermophilus</i> <i>L. acidophilus</i> <i>L. plantarum</i>	Initiate natural killer cell activities. Inhibit pathogen invasion and adhesion. Reinforce intestinal barrier integrity. Enhance phagocytic activities of macrophage.		99–103
HTN	HTN refers to elevated blood pressure levels, posing a significant risk factor for cardiovascular, cerebrovascular and renal diseases worldwide.	Certain gut microbial strains, and an imbalance in gut bacteria known as dysbiosis.	<i>Lactobacillus helveticus</i> / <i>Saccharomyces cerevisiae</i> / <i>Lactobacillus casei</i> (specifically, LcS)	Lowering luminal Ph. Secreting antimicrobial peptides. Inhibition of bacterial invasion. Suppression of bacterial adhesion.	fermented milk products containing specific probiotic strains (LcS)	104–106
<i>Helicobacter pylori</i> eradication	<i>Helicobacter pylori</i> is a Gram-negative, flagellated bacteria found in the stomach epithelium, causing severe side effects and disruptions in natural flora.	<i>Helicobacter pylori</i> infection leads to adverse effects and changes in stomach flora; STT declines due to complications.	<i>Lactobacillus/Bacillus subtilis</i>	Probiotics act as an antidote, inhibiting <i>Helicobacter pylori</i> through bacteriostatic and bactericidal effects, reduced cytokines, strengthened gastric defense, and immune interaction.	probiotic supplements (<i>Lactobacillus</i> , <i>Bacillus subtilis</i>)	107–110
Autoimmune and inflammatory disorders	Autoimmune diseases result from the immune system targeting the body's own cells, causing inflammation and health issues.	Molecular mimicry, self-antigen modification. Immune reactivity modulation contributes to autoimmune diseases.	Probiotics are used to treat autoimmune conditions such as RA, celiac disease, CD, and more.	Probiotics impact metabolic processes: short-chain fatty acids, tryptophan metabolism, nucleoside signaling, and histamine-2 receptor activation.	Probiotic supplements tailored for autoimmune disease.	111–113
Type 1 diabetes	Type 1 diabetes is an autoimmune disease where the immune system targets pancreatic beta-cells, causing decreased insulin production.	Genetic predispositions and environmental factors contribute to the development of type 1 diabetes. Autoantibodies and insulinitis precede β -cell decline.	Probiotic supplementation with strains like <i>Bifidobacterium longum</i> , <i>Bifidobacterium infantis</i> and <i>Lactobacillus</i> spp. shows potential in preventing autoimmune diabetes.	Probiotics reduce pro-inflammatory cytokines (IL-6, IL-1, TNF- α) and increase anti-inflammatory cytokines (TGF- β , IL-10), modulating the immune response.	Oral probiotic compounds containing specified strains can serve as preventive measures, potentially delaying or preventing autoimmune diabetes onset.	114,115
T2DM	Type 2 diabetes is a prevalent epidemic associated with obesity and gut microbiome alterations, leading to significant health and economic challenges.	Obesity, influenced by the gut microbiome, contributes to T2DM development. Altered gut microbiota affects energy extraction, inflammation, and metabolic processes.	<i>Lactiplantibacillus plantarum</i> / <i>Bifidobacterium lactis</i> / <i>Lactocaseibacillus rhamnosus</i> / <i>Lactobacillus gasseri</i> , and <i>Bifidobacterium lactis</i>	Probiotics enhance gut integrity, reduce systemic lipopolysaccharides, improve insulin sensitivity, regulate glucose, lipids, and immune responses.	Probiotic supplements containing specific strains may aid in managing T2DM by improving gut health, regulating metabolism, and modulating immune responses.	116–119

Table 1. Application of probiotics for therapeutic purposes – cont.

Disease	Definition	Etiology	Probiotic strain	Mechanism of action	Useful product	Ref.
Migraine	Recurrent severe headaches, often triggered by specific foods, accompanied by light and sound sensitivity.	Migraines linked to food triggers and inflammation; elevated IgG levels indicate food hypersensitivity.	Various strains modulating the GBA studied, specific effective strains not mentioned.	Probiotics enhance intestinal barrier function through the GBA, regulating serotonin production in the gut.	Probiotic supplements designed to improve GBA may alleviate migraines by reducing inflammation and regulating serotonin.	120
ASD	Developmental disorders characterized by challenges in social interaction, communication and repetitive behaviors.	Potential link between ASD and dysregulated gut microbiota; microbiota composition may influence ASD symptoms.	<i>Bifidobacterium</i> (<i>B. longum</i> , <i>B. breve</i> , <i>B. infantis</i> , <i>B. bifidum</i>)/ <i>Lactobacillus</i> (<i>L. acidophilus</i> , <i>L. helveticus</i> , <i>L. rhamnosus</i> , <i>L. plantarum</i>).	Probiotics regulate gut microbiota composition, enhance gut barrier integrity, modulate inflammatory pathways, and influence neurotransmission via the GBA.	Probiotic supplements containing specific strains may aid individuals with ASD by improving gut health and potentially alleviating behavioral abnormalities associated with ASD.	121–123

IBD – inflammatory bowel disease; UC – ulcerative colitis; CD – Crohn's disease; COX2 – cyclooxygenase-2; TNF – tumor necrosis factor; HTN – hypertension; LcS – *Lactobacillus casei* strain Shirota; STT – standard therapy efficacy; RA – rheumatoid arthritis; T2DM – type 2 diabetes; IgG – immunoglobulin G; ASD – autism spectrum disorder; GBA – gut–brain axis.

created to investigate the relationships among dietary functional elements, medications and the intestinal microbiota, certain studies have examined the impact of probiotics, prebiotics and synbiotics on the gut microbiota. For example, Duque et al. utilized the SHIME model and discovered that treatment with probiotics, prebiotics and synbiotics had a positive influence on the gut microbiota and metabolic activity in children with autism spectrum disorder.¹²⁹ Likewise, Marzorati et al. examined the effects of MegaSporeBiotic™, an oral probiotic made up of 5 bacillus species, on the activity and composition of gut microbiota using the SHIME model. Their results revealed an elevation in *Akkermansia muciniphila*, bifidobacteria and Firmicutes, alongside a reduction in *Lactobacillus* and Bacteroidetes during the treatment period.¹³⁰ Nevertheless, because there have been only a few studies conducted, additional research is crucial to investigate the practicality and viability of in vitro intestinal microbiota simulation models.

Animal models

Animal models are used to study the interactions between hosts, microbes and potential pathogens in controlled environments. Germ-free animals are particularly useful in these studies. These models also facilitate the retrieval of samples from distinct sections of the GI tract, a task that can be difficult in clinical trials. While mice and rats are commonly employed, alternative models such as *Caenorhabditis elegans*, honey bees, *Ciona robusta*, fruit

flies, and greater wax moths have been used to study the interactions between probiotics and pathogens. Researchers have investigated the efficacy of probiotics in mitigating pathogenic conditions in these animal models.¹³¹ For instance, Chen et al. demonstrated that certain *Lactobacillus* strains mitigated *H. pylori* colonization and associated stomach inflammation.¹³² Scalfaro et al. employed *Galleria mellonella* larvae to evaluate the antibacterial effects of *L. rhamnosus* GG and *Clostridium butyricum* MIYAIRI 588 against enteric pathogens. Their results suggested the possible usefulness of *G. mellonella* larvae as an in vivo model, complementing in vitro assays for candidate probiotic prescreening.¹³³ Despite rapid advancements in genome editing technology leading to the establishment of edited rats and mice, their application in probiotic-related research remains limited. Consequently, further investigations employing diverse animal models are crucial for advancing our understanding in this field.

Human clinical experiments

Although in vitro models and animal experiments offer simplicity, controllable experimental conditions, and lower research costs, establishing reliable evidence about the effects of probiotics on human health depends on human clinical trials. These trials have played a significant role in advancing and commercializing probiotic products. Notably, *E. coli*, comprising various strains, many of which are considered opportunistic pathogens, gained recognition as a probiotic primarily due to pivotal human clinical

trials, as seen in the case of *E. coli* Nissle 1917.¹³⁴ Researchers, such as Dronkers et al., have conducted comprehensive analyses of probiotic clinical trials. Their findings revealed that *L. rhamnosus* GG and *B. animalis* ssp. lactis BB12 are among the most extensively examined probiotic strains.¹³⁵ However, it is important to note that despite numerous clinical trials investigating probiotic benefits in GI diseases, the outcomes can be unstable and occasionally contradictory. This variation can be attributed to several factors, for instance, trial design, group size, participant features, and dosage. Therefore, meticulous consideration of probiotic selection, host population and study design is crucial in the careful planning of human clinical experiments.

Discussion

The contentious role of probiotics in various diseases has been a pivotal focus of research across different disciplines for many decades. In the present review, we evaluated the diverse positive and negative facets associated with the utilization of probiotics in addressing a spectrum of disorders, primarily those pertaining to the GI system. The prevalence of various GI disorders, including IBD, CD and UC, has spurred extensive exploration into pharmaceutical and nutritional interventions, notably probiotics, with the objective of attenuating disease progression and ameliorating associated symptoms. The integration of dietary regimens incorporating these agents has demonstrated promise in enhancing patients' quality of life and facilitating partial clinical remission.^{136–138} In the context of probiotics' influence on diverse medical conditions, emerging evidence underscores their potential to modulate respiratory immune responses by establishing a microbial interconnection between the respiratory and GI tracts. Moreover, the advantageous effects of probiotic supplementation have been noted in mitigating the frequency of allergic rhinitis episodes.⁶⁷ Additionally, probiotics have demonstrated the capacity to modulate the composition of gut microbiota, thereby ameliorating specific symptoms associated with IBS, such as flatulence, bloating and irregular bowel habits. Despite the existence of numerous pharmaceutical interventions for IBS management, probiotics have emerged as a promising adjunct, potentially regulating immune responses in IBS pathophysiology to foster intestinal homeostasis.⁴⁷ Regarding the efficacy of probiotics in addressing AAD, select strains, notably *L. rhamnosus* and *S. boulardii*, administered at a dosage of 50 CFU per day, have exhibited utility across various studies.⁵⁵ Although probiotics have recently garnered attention as a prospective intervention for combatting VAP in both adult and pediatric populations, further meticulously designed studies are requisite to ascertain their efficacy in influencing primary clinical endpoints and mortality rates.⁹⁴ Concerning NEC in preterm neonates,

investigations have indicated that supplementation with *Lactobacillus*, either alone or in combination with *Bifidobacterium*, diminishes the incidence of this grave condition.⁸⁹ The process of the current review, which emphatically studied GI disorders, encompasses the analysis of 10 articles focused on animal or cell culture studies, alongside 18 articles involving human subjects; among these, 12 included healthy controls, with only 4 involving pediatric patients. Notably, 5 studies encompassed more than 100 patients and 12 involved more than 50 patients. However, the majority of studies were based on relatively small sample sizes, thus limiting definitive evaluations. Furthermore, among the studies assessing patients with active disease, primarily with mild-to-moderate severity scores, improvements in clinical activity scores were observed in 2 out of 3 patients.^{42,43} These findings suggest the potential adjunctive use of probiotics in conjunction with conventional treatments. Nevertheless, most studies corroborated the notion that probiotics play a significant role in preventing GI diseases and are associated with improved quality of life in patients. The compiled evidence suggests that probiotics could serve as a viable component in the alleviation and prevention of GI diseases. However, the limited number of trials underscores the necessity for further research to substantiate their therapeutic benefits. Notably, probiotics exhibited efficacy in 3 out of 4 studies compared to no treatment, indicating their potential utility as an additional therapeutic option. Current data suggest the potential utility of probiotics in the prevention of various GI disorders, presenting a promising avenue for novel treatment strategies. While animal studies have contributed valuable insights, they offer a limited scope of understanding. Furthermore, no discernible differences in treatment modalities besides probiotics or sample characteristics were observed between compared groups, highlighting the potential role of probiotics as an adjunctive therapeutic option, particularly when combined with conventional treatment approaches. Notably, most trials enrolled patients with active disease, with only 5 studies examining patients with confirmed inactive disease, yielding positive results in prolonging remission and improving clinical scores in 3 instances. The most important achievement in this field is the application of probiotics in the treatment of COVID-19, which showed a therapeutic effect by regulating the gut–lung axis and mucosal immune system. These findings suggest the promising efficacy of probiotics even when compared to established therapeutic options. Nonetheless, the limited number of studies underscores the imperative for further research to validate this hypothesis.

Limitations




This review is subject to several limitations. It is essential to acknowledge that the process of comparing studies was challenging due to the observed heterogeneity among

trials regarding methodologies, including dosages and concurrent treatments administered to patients. Moreover, the majority of studies analyzed samples comprising fewer than 100 patients. While most trials did not reveal significant differences in sample characteristics and treatment options, well-designed, double-blinded, randomized clinical trials are indispensable for fully understanding the role of probiotics in GI diseases. Furthermore, the necessity for a comprehensive meta-analysis to uncover potential variations among research studies can also be regarded as a limitation. The heterogeneity of studies and the requisite sample size are critical factors in interpreting research outcomes in this field.

Conclusions

Although probiotics offer potential as therapeutic agents for treating GI diseases, several challenges may hinder their effective application. A comprehensive understanding of these challenges is essential to optimize the use of probiotics in GI conditions. This review highlights the extensive investigation of probiotics across diverse pediatric and adult GI ailments, revealing promising therapeutic prospects. Probiotics have been demonstrated to have a beneficial impact on a range of health outcomes, including the treatment of functional GI disorders, acute diarrhea and AAD, as well as the prevention of NEC in premature infants. In addition, probiotics have shown efficacy in mitigating colic in infants, reducing school absenteeism in children and potentially influencing allergic conditions, while also providing preventive benefits against infections such as *C. difficile* colitis and VAP, underscoring the versatility of probiotic interventions. Insights from various research methodologies, including in vitro studies, animal models and human clinical trials, contribute significantly to elucidating the mechanisms underlying probiotic interactions with pathogens and host systems. However, the variability in outcomes observed across studies necessitates careful consideration of factors such as probiotic strains, dosage and study design in future research endeavors. Despite these challenges, probiotics have emerged as valuable allies in promoting GI health, with ongoing investigations poised to uncover additional applications and refine their clinical use.

ORCID iDs

Xuejing Qiao  <https://orcid.org/0009-0006-6892-464x>
 Haosheng Zhang  <https://orcid.org/0009-0005-6524-1192>
 Lianmei Shan  <https://orcid.org/0009-0001-9701-8180>

References

1. Compare D, Sgammato C, Nardone OM, et al. Probiotics in gastrointestinal diseases: All that glitters is not gold. *Dig Dis*. 2022;40(1):123–132. doi:10.1159/000516023
2. Kataoka K. The intestinal microbiota and its role in human health and disease. *J Med Invest*. 2016;63(1.2):27–37. doi:10.2152/jmi.63.27
3. Cani PD. Gut microbiota: At the intersection of everything? *Nat Rev Gastroenterol Hepatol*. 2017;14(6):321–322. doi:10.1038/nrgastro.2017.54
4. Wang S, Xiao Y, Tian F, et al. Rational use of prebiotics for gut microbiota alterations: Specific bacterial phylotypes and related mechanisms. *J Funct Foods*. 2020;66:103838. doi:10.1016/j.jff.2020.103838
5. Islam F, Mitra S, Emran TB, et al. Natural small molecules in gastrointestinal tract and associated cancers: Molecular insights and targeted therapies. *Molecules*. 2022;27(17):5686. doi:10.3390/molecules27175686
6. Palumbo VD, Romeo M, Gammazza AM, et al. The long-term effects of probiotics in the therapy of ulcerative colitis: A clinical study. *Biomed Pap Med Fac Univ Palacky Olomouc Czech Repub*. 2016;160(3):372–377. doi:10.5507/bp.2016.044
7. Schmidt TSB, Raes J, Bork P. The human gut microbiome: From association to modulation. *Cell*. 2018;172(6):1198–1215. doi:10.1016/j.cell.2018.02.044
8. Parker EA, Roy T, D'Adamo CR, Wieland LS. Probiotics and gastrointestinal conditions: An overview of evidence from the Cochrane Collaboration. *Nutrition*. 2018;45:125–134.e11. doi:10.1016/j.nut.2017.06.024
9. Suez J, Zmora N, Segal E, Elinav E. The pros, cons, and many unknowns of probiotics. *Nat Med*. 2019;25(5):716–729. doi:10.1038/s41591-019-0439-x
10. Peng M, Biswas D. Short chain and polyunsaturated fatty acids in host gut health and foodborne bacterial pathogen inhibition. *Crit Rev Food Sci Nutr*. 2017;57(18):3987–4002. doi:10.1080/10408398.2016.1203286
11. Rastogi S, Singh A. Gut microbiome and human health: Exploring how the probiotic genus *Lactobacillus* modulate immune responses. *Front Pharmacol*. 2022;13:1042189. doi:10.3389/fphar.2022.1042189
12. Wilkins T, Sequoia J. Probiotics for gastrointestinal conditions: A summary of the evidence. *Am Fam Physician*. 2017;96(3):170–178. PMID:28762696.
13. Floch MH. The role of prebiotics and probiotics in gastrointestinal disease. *Gastroenterol Clin North Am*. 2018;47(1):179–191. doi:10.1016/j.gtc.2017.09.011
14. Plaza-Diaz J, Ruiz-Ojeda FJ, Gil-Campos M, Gil A. Mechanisms of action of probiotics. *Adv Nutr*. 2019;10(Suppl 1):S49–S66. doi:10.1093/advances/nmy063
15. Ben Braiek O, Smaoui S. Enterococci: Between emerging pathogens and potential probiotics. *Biomed Res Int*. 2019;2019:5938210. doi:10.1155/2019/5938210
16. Şener D, Bulut HN, Güneş Bayir A. Probiotics and relationship between probiotics and cancer types. *Bezmialem Sci*. 2021;9(4):490–497. doi:10.14235/bas.galenos.2021.5375
17. Sundararaman A, Ray M, Ravindra PV, Halami PM. Role of probiotics to combat viral infections with emphasis on COVID-19. *Appl Microbiol Biotechnol*. 2020;104(19):8089–8104. doi:10.1007/s00253-020-10832-4
18. Shen H, Zhao Z, Zhao Z, Chen Y, Zhang L. Native and engineered probiotics: Promising agents against related systemic and intestinal diseases. *Int J Mol Sci*. 2022;23(2):594. doi:10.3390/ijms23020594
19. Sanders ME, Merenstein D, Merrifield CA, Hutkins R. Probiotics for human use. *Nutr Bull*. 2018;43(3):212–225. doi:10.1111/nbu.12334
20. Guevarra R, Barraquio VL. Viable counts of lactic acid bacteria in Philippine commercial yogurts. *Int J Dairy Sci Process*. 2016;2(5):24–28. doi:10.13140/RG.2.1.4030.3764
21. Wolfe W, Xiang Z, Yu X, et al. The challenge of applications of probiotics in gastrointestinal diseases. *Adv Gut Microbiome Res*. 2023;2023:1984200. doi:10.1155/2023/1984200
22. Sanders ME, Akkermans LMA, Haller D, et al. Safety assessment of probiotics for human use. *Gut Microbes*. 2010;1(3):164–185. doi:10.4161/gmic.1.3.12127
23. Pandey KR, Naik SR, Vakil BV. Probiotics, prebiotics and synbiotics: A review. *J Food Sci Technol*. 2015;52(12):7577–7587. doi:10.1007/s13197-015-1921-1
24. Tripathi MK, Giri SK. Probiotic functional foods: Survival of probiotics during processing and storage. *J Funct Foods*. 2014;9:225–241. doi:10.1016/j.jff.2014.04.030
25. Williams NT. Probiotics. *Am J Health Syst Pharm*. 2010;67(6):449–458. doi:10.2146/ajhp090168
26. D'Amelio P, Sassi F. Gut microbiota, immune system, and bone. *Calcif Tissue Int*. 2018;102(4):415–425. doi:10.1007/s00223-017-0331-y
27. Claes AK, Zhou JY, Philpott DJ. NOD-like receptors: Guardians of intestinal mucosal barriers. *Physiology*. 2015;30(3):241–250. doi:10.1152/physiol.00025.2014

28. Hevia A, Delgado S, Sánchez B, Margolles A. Molecular players involved in the interaction between beneficial bacteria and the immune system. *Front Microbiol.* 2015;6:1285. doi:10.3389/fmicb.2015.01285
29. Wilson B, Whelan K. Prebiotic inulin-type fructans and galacto-oligosaccharides: Definition, specificity, function, and application in gastrointestinal disorders. *J Gastroenterol Hepatol.* 2017;32(Suppl 1):64–68. doi:10.1111/jgh.13700
30. Patcharatrakul T, Gonlachanvit S. Chili peppers, curcumins, and prebiotics in gastrointestinal health and disease. *Curr Gastroenterol Rep.* 2016;18(4):19. doi:10.1007/s11894-016-0494-0
31. Kommineni S, Kristich CJ, Salzman NH. Harnessing bacteriocin biology as targeted therapy in the GI tract. *Gut Microbes.* 2016;7(6):512–517. doi:10.1080/19490976.2016.1233089
32. Yang SC, Lin CH, Sung CT, Fang JY. Antibacterial activities of bacteriocins: Application in foods and pharmaceuticals. *Front Microbiol.* 2014;5:241. doi:10.3389/fmicb.2014.00241
33. Van Heel AJ, De Jong A, Montalbán-López M, Kok J, Kuipers OP. BAGEL3: Automated identification of genes encoding bacteriocins and (non-) bactericidal posttranslationally modified peptides. *Nucl Acids Res.* 2013;41(W1):W448–W453. doi:10.1093/nar/gkt391
34. Hammami R, Zouhir A, Le Lay C, Ben Hamida J, Fliss I. BACTIBASE second release: A database and tool platform for bacteriocin characterization. *BMC Microbiol.* 2010;10(1):22. doi:10.1186/1471-2180-10-22
35. Yang X, Yousef AE. Antimicrobial peptides produced by *Brevibacillus* spp.: Structure, classification and bioactivity. A mini review. *World J Microbiol Biotechnol.* 2018;34(4):57. doi:10.1007/s11274-018-2437-4
36. Garcia-Gutierrez E, Mayer MJ, Cotter PD, Narbad A. Gut microbiota as a source of novel antimicrobials. *Gut Microbes.* 2019;10(1):1–21. doi:10.1080/19490976.2018.1455790
37. Halloran K, Underwood MA. Probiotic mechanisms of action. *Early Hum Dev.* 2019;135:58–65. doi:10.1016/j.earlhumdev.2019.05.010
38. Heeney DD, Zhai Z, Bendiks Z, et al. *Lactobacillus plantarum* bacteriocin is associated with intestinal and systemic improvements in diet-induced obese mice and maintains epithelial barrier integrity in vitro. *Gut Microbes.* 2019;10(3):382–397. doi:10.1080/19490976.2018.1534513
39. Dicks LMT, Dreyer L, Smith C, Van Staden AD. A review. The fate of bacteriocins in the human gastro-intestinal tract: Do they cross the gut–blood barrier? *Front Microbiol.* 2018;9:2297. doi:10.3389/fmicb.2018.02297
40. Sandhu BK. Irritable bowel syndrome in children: Pathogenesis, diagnosis and evidence-based treatment. *World J Gastroenterol.* 2014;20(20):6013. doi:10.3748/wjg.v20.i20.6013
41. Sperber AD, Dumitrascu D, Fukudo S, et al. The global prevalence of IBS in adults remains elusive due to the heterogeneity of studies: A Rome Foundation working team literature review. *Gut.* 2017;66(6):1075–1082. doi:10.1136/gutjnl-2015-311240
42. Fan H, Du J, Liu X, et al. Effects of pentasa-combined probiotics on the microflora structure and prognosis of patients with inflammatory bowel disease. *Turk J Gastroenterol.* 2019;30(8):680–685. doi:10.5152/tjg.2019.18426
43. Steed H, Macfarlane GT, Blackett KL, et al. Clinical trial. The microbiological and immunological effects of synbiotic consumption: A randomized double-blind placebo-controlled study in active Crohn's disease. *Aliment Pharmacol Ther.* 2010;32(7):872–883. doi:10.1111/j.1365-2036.2010.04417.x
44. Pozuelo M, Panda S, Santiago A, et al. Reduction of butyrate- and methane-producing microorganisms in patients with irritable bowel syndrome. *Sci Rep.* 2015;5(1):12693. doi:10.1038/srep12693
45. Ford AC, Quigley EMM, Lacy BE, et al. Efficacy of prebiotics, probiotics, and synbiotics in irritable bowel syndrome and chronic idiopathic constipation: Systematic review and meta-analysis. *Am J Gastroenterol.* 2014;109(10):1547–1561. doi:10.1038/ajg.2014.202
46. Zhang Y, Li L, Guo C, et al. Effects of probiotic type, dose and treatment duration on irritable bowel syndrome diagnosed by Rome III criteria: A meta-analysis. *BMC Gastroenterol.* 2016;16(1):62. doi:10.1186/s12876-016-0470-z
47. Yuan F, Ni H, Asche CV, Kim M, Walayat S, Ren J. Efficacy of *Bifidobacterium infantis* 35624 in patients with irritable bowel syndrome: A meta-analysis. *Curr Med Res Opin.* 2017;33(7):1191–1197. doi:10.1080/03007995.2017.1292230
48. Weizman Z, Abu-Abed J, Binsztok M. *Lactobacillus reuteri* DSM 17938 for the management of functional abdominal pain in childhood: A randomized, double-blind, placebo-controlled trial. *J Pediatr.* 2016;174:160–164.e1. doi:10.1016/j.jpeds.2016.04.003
49. Ford AC, Quigley EMM, Lacy BE, et al. Effect of antidepressants and psychological therapies, including hypnotherapy, in irritable bowel syndrome: Systematic review and meta-analysis. *Am J Gastroenterol.* 2014;109(9):1350–1365. doi:10.1038/ajg.2014.148
50. Das JK, Bhutta ZA. Global challenges in acute diarrhea. *Curr Opin Gastroenterol.* 2016;32(1):18–23. doi:10.1097/MOG.0000000000000236
51. Szajewska H, Skórka A, Ruszczyński M, Gieruszczak-Białek D. Meta-analysis. *Lactobacillus* GG for treating acute gastroenteritis in children: Updated analysis of randomised controlled trials. *Aliment Pharmacol Ther.* 2013;38(5):467–476. doi:10.1111/apt.12403
52. Szajewska H, Urbańska M, Chmielewska A, Weizman Z, Shamir R. Meta-analysis: *Lactobacillus reuteri* strain DSM 17938 (and the original strain ATCC 55730) for treating acute gastroenteritis in children. *Benef Microbes.* 2014;5(3):285–294. doi:10.3920/BM2013.0056
53. Parker MW, Schaffzin JK, Lo Vecchio A, et al. Rapid adoption of *Lactobacillus rhamnosus* GG for acute gastroenteritis. *Pediatrics.* 2013;131(Suppl 1):S96–S102. doi:10.1542/peds.2012-14271
54. Mantegazza C, Molinari P, D'Auria E, Sonnino M, Morelli L, Zuccotti GV. Probiotics and antibiotic-associated diarrhea in children: A review and new evidence on *Lactobacillus rhamnosus* GG during and after antibiotic treatment. *Pharmacol Res.* 2018;128:63–72. doi:10.1016/j.phrs.2017.08.001
55. Hempel S, Newberry SJ, Maher AR, et al. Probiotics for the prevention and treatment of antibiotic-associated diarrhea: A systematic review and meta-analysis. *JAMA.* 2012;307(18):1959–1969. doi:10.1001/jama.2012.3507
56. Chang HY, Chen JH, Chang JH, Lin HC, Lin CY, Peng CC. Multiple strains probiotics appear to be the most effective probiotics in the prevention of necrotizing enterocolitis and mortality: An updated meta-analysis. *PLoS One.* 2017;12(2):e0171579. doi:10.1371/journal.pone.0171579
55. Warner BB, Deych E, Zhou Y, et al. Gut bacteria dysbiosis and necrotizing enterocolitis in very low birthweight infants: A prospective case-control study. *Lancet.* 2016;387(10031):1928–1936. doi:10.1016/S0140-6736(16)00081-7
58. Beghetti I, Panizza D, Lenzi J, et al. Probiotics for preventing necrotizing enterocolitis in preterm infants: A network meta-analysis. *Nutrients.* 2021;13(1):192. doi:10.3390/nu13010192
59. Zeevenhooven J, Browne PD, L'Hoir MP, De Weerth C, Benninga MA. Infant colic: Mechanisms and management. *Nat Rev Gastroenterol Hepatol.* 2018;15(8):479–496. doi:10.1038/s41575-018-0008-7
60. Harb T, Matsuyama M, David M, Hill RJ. Infant colic: What works? A systematic review of interventions for breast-fed infants. *J Pediatr Gastroenterol Nutr.* 2016;62(5):668–686. doi:10.1097/MPG.0000000000001075
61. Xu M, Wang J, Wang N, Sun F, Wang L, Liu XH. The efficacy and safety of the probiotic bacterium *Lactobacillus reuteri* DSM 17938 for infantile colic: A meta-analysis of randomized controlled trials. *PLoS One.* 2015;10(10):e0141445. doi:10.1371/journal.pone.0141445
62. Sung V, Hiscock H, Tang MLK, et al. Treating infant colic with the probiotic *Lactobacillus reuteri*: Double blind, placebo controlled randomised trial. *BMJ.* 2014;348:g2107. doi:10.1136/bmj.g2107
63. Sieczkowska A, Landowski P, Zagodzón P, Kaminska B, Lifschitz C. The association of proton pump inhibitor therapy and small bowel bacterial overgrowth in children. *Eur J Gastroenterol Hepatol.* 2017;29(10):1190–1191. doi:10.1097/MEG.0000000000000946
64. Weizman Z. The role of probiotics and prebiotics in the prevention of infections in child day-care centres. *Benef Microbes.* 2015;6(2):181–183. doi:10.3920/BM2014.0101
65. Wang Y, Li X, Ge T, et al. Probiotics for prevention and treatment of respiratory tract infections in children: A systematic review and meta-analysis of randomized controlled trials. *Medicine (Baltimore).* 2016;95(31):e4509. doi:10.1097/MD.00000000000004509
66. Daley D. The evolution of the hygiene hypothesis: The role of early-life exposures to viruses and microbes and their relationship to asthma and allergic diseases. *Curr Opin Allergy Clin Immunol.* 2014;14(5):390–396. doi:10.1097/ACI.0000000000000101

67. Zajac AE, Adams AS, Turner JH. A systematic review and meta-analysis of probiotics for the treatment of allergic rhinitis. *Int Forum Allergy Rhinol*. 2015;5(6):524–532. doi:10.1002/alr.21492
68. Tang MLK, Ponsonby AL, Orsini F, et al. Administration of a probiotic with peanut oral immunotherapy: A randomized trial. *J Allergy Clin Immunol*. 2015;135(3):737–744.e8. doi:10.1016/j.jaci.2014.11.034
69. Loke P, Orsini F, Lozinsky AC, et al. Probiotic peanut oral immunotherapy versus oral immunotherapy and placebo in children with peanut allergy in Australia (PPOIT-003): A multicentre, randomised, phase 2b trial. *Lancet Child Adolesc Health*. 2022;6(3):171–184. doi:10.1016/S2352-4642(22)00006-2
70. Rodriguez H, Miller JE. Do prophylactic probiotics prevent the incidence of *Clostridium difficile* colitis infection in hospitalized patients? *J Okla State Med Assoc*. 2019;112(1):18–19. PMID:31379393. PMCID:PMC6677267.
71. Franko J, Raman S, Krishnan N, et al. Randomized trial of perioperative probiotics among patients undergoing major abdominal operation. *J Am Coll Surg*. 2019;229(6):533–540.e1. doi:10.1016/j.jamcollsurg.2019.09.002
72. Mills JP, Rao K, Young VB. Probiotics for prevention of *Clostridium difficile* infection. *Curr Opin Gastroenterol*. 2018;34(1):3–10. doi:10.1097/MOG.0000000000000410
73. Bischoff SC, Barbara G, Buurman W, et al. Intestinal permeability: A new target for disease prevention and therapy. *BMC Gastroenterol*. 2014;14:189. doi:10.1186/s12876-014-0189-7
74. Shen NT, Maw A, Tmanova LL, et al. Timely use of probiotics in hospitalized adults prevents *Clostridium difficile* infection: A systematic review with meta-regression analysis. *Gastroenterology*. 2017;152(8):1889–1900.e9. doi:10.1053/j.gastro.2017.02.003
75. Härtel C, Pagel J, Rupp J, et al. Prophylactic use of *Lactobacillus acidophilus/Bifidobacterium infantis* probiotics and outcome in very low birth weight infants. *J Pediatr*. 2014;165(2):285–289.e1. doi:10.1016/j.jpeds.2014.04.029
76. Oncel MY, Arayici S, Sari FN, et al. Comparison of *Lactobacillus reuteri* and nystatin prophylaxis on *Candida* colonization and infection in very low birth weight infants. *J Matern Fetal Neonatal Med*. 2015;28(15):1790–1794. doi:10.3109/14767058.2014.968842
77. Johnson-Henry KC, Abrahamsson TR, Wu RY, Sherman PM. Probiotics, prebiotics, and synbiotics for the prevention of necrotizing enterocolitis. *Adv Nutr*. 2016;7(5):928–937. doi:10.3945/an.116.012237
78. Das R, Biswas S. Nutraceutical-prophylactic and therapeutic role of functional food in health. *J Nutr Food Sci*. 2016;6(4):1000527. doi:10.4172/2155-9600.1000527
79. Dasari S, Kathera C, Janardhan A, Praveen Kumar A, Viswanath B. Surfacing role of probiotics in cancer prophylaxis and therapy: A systematic review. *Clin Nutr*. 2017;36(6):1465–1472. doi:10.1016/j.clnu.2016.11.017
80. Górška A, Przystupski D, Niemczura MJ, Kulbacka J. Probiotic bacteria: A promising tool in cancer prevention and therapy. *Curr Microbiol*. 2019;76(8):939–949. doi:10.1007/s00284-019-01679-8
81. Yao D, He W, Hu Y, et al. Prevalence and influencing factors of probiotic usage among colorectal cancer patients in China: A national database study. *PLoS One*. 2023;18(9):e0291864. doi:10.1371/journal.pone.0291864
82. Molska M, Reguła J. Potential mechanisms of probiotics action in the prevention and treatment of colorectal cancer. *Nutrients*. 2019;11(10):2453. doi:10.3390/nu11102453
83. Sharaf LK, Sharma M, Chandel D, Shukla G. Prophylactic intervention of probiotics (*L. acidophilus*, *L. rhamnosus* GG) and celecoxib modulate Bax-mediated apoptosis in 1,2-dimethylhydrazine-induced experimental colon carcinogenesis. *BMC Cancer*. 2018;18(1):1111. doi:10.1186/s12885-018-4999-9
84. Qorri B, Harless W, Szewczuk MR. Novel molecular mechanism of aspirin and celecoxib targeting mammalian neuraminidase-1 impedes epidermal growth factor receptor signaling axis and induces apoptosis in pancreatic cancer cells. *Drug Des Devel Ther*. 2020;14:4149–4167. doi:10.2147/DDDT.S264122
85. van Baal MC, van Rens MJ, Geven CB, et al. Association between probiotics and enteral nutrition in an experimental acute pancreatitis model in rats. *Pancreatology*. 2014;14(6):470–477. doi:10.1016/j.pan.2014.10.002
86. Tewari VV, Dubey SK, Gupta G. *Bacillus clausii* for prevention of late-onset sepsis in preterm infants: A randomized controlled trial. *J Trop Pediatr*. 2015;61(5):377–385. doi:10.1093/tropej/fmv050
87. Dong Y, Glaser K, Speer CP. Late-onset sepsis caused by Gram-negative bacteria in very low birth weight infants: A systematic review. *Expert Rev Anti Infect Ther*. 2019;17(3):177–188. doi:10.1080/14787210.2019.1568871
88. Zbinden A, Zbinden R, Berger C, Arlettaz R. Case series of *Bifidobacterium longum* bacteremia in three preterm infants on probiotic therapy. *Neonatology*. 2015;107(1):56–59. doi:10.1159/000367985
89. Gonçalves FLL, Soares LMM, Figueira RL, Simões ALB, Gallindo RM, Sbragia L. Evaluation of the expression of I-FABP and L-FABP in a necrotizing enterocolitis model after the use of *Lactobacillus acidophilus*. *J Pediatr Surg*. 2015;50(4):543–549. doi:10.1016/j.jpedsurg.2014.07.007
90. Alfaleh K, Anabrees J. Probiotics for prevention of necrotizing enterocolitis in preterm infants. *Evid Based Child Health*. 2014;9(3):584–671. doi:10.1002/ebch.1976
91. Xie X, Lyu J, Hussain T, Li M. Drug prevention and control of ventilator-associated pneumonia. *Front Pharmacol*. 2019;10:298. doi:10.3389/fphar.2019.00298
92. Branch-Elliman W, Wright SB, Howell MD. Determining the ideal strategy for ventilator-associated pneumonia prevention: Cost-benefit analysis. *Am J Respir Crit Care Med*. 2015;192(1):57–63. doi:10.1164/rccm.201412-2316OC
93. Markowiak P, Śliżewska K. Effects of probiotics, prebiotics, and synbiotics on human health. *Nutrients*. 2017;9(9):1021. doi:10.3390/nu9091021
94. Chibbar R, Dieleman LA. The gut microbiota in celiac disease and probiotics. *Nutrients*. 2019;11(10):2375. doi:10.3390/nu11102375
95. Yadav A, Chandra, Maurya VK. Probiotics: Recent advances and future prospects. *J Plant Dev Sci*. 2017;9(11):967–975. <http://jpdscs.co.in/wp-content/uploads/2020/09/01.-Harish-Chandra-1291-corrected.pdf>.
96. De Souza MDSS, Barbalho SM, Goulart RDA, De Carvalho ADCA. The current and future role of drugs and probiotics in the management of inflammatory bowel disease. *J Biosci Med*. 2015;3(8):76–85. doi:10.4236/jbm.2015.38008
97. Zaylaa M, Alard J, Kassaa IA, et al. Autophagy: A novel mechanism involved in the anti-inflammatory abilities of probiotics. *Cell Physiol Biochem*. 2019;53(5):774–793. doi:10.33594/000000172
98. Maziade PJ, Andriessen JA, Pereira P, Currie B, Goldstein EJC. Impact of adding prophylactic probiotics to a bundle of standard preventative measures for *Clostridium difficile* infections: Enhanced and sustained decrease in the incidence and severity of infection at a community hospital. *Curr Med Res Opin*. 2013;29(10):1341–1347. doi:10.1185/03007995.2013.833501
99. Issa I, Moucari R. Probiotics for antibiotic-associated diarrhea: Do we have a verdict? *World J Gastroenterol*. 2014;20(47):17788–17795. doi:10.3748/wjg.v20.i47.17788
100. Bae JM. Prophylactic efficacy of probiotics on travelers' diarrhea: An adaptive meta-analysis of randomized controlled trials. *Epidemiol Health*. 2018;40:e2018043. doi:10.4178/epih.e2018043
101. Ling Z, Liu X, Cheng Y, et al. *Clostridium butyricum* combined with *Bifidobacterium infantis* probiotic mixture restores fecal microbiota and attenuates systemic inflammation in mice with antibiotic-associated diarrhea. *Biomed Res Int*. 2015;2015:582048. doi:10.1155/2015/582048
102. Kang Y, Cai Y. Gut microbiota and hypertension: From pathogenesis to new therapeutic strategies. *Clin Res Hepatol Gastroenterol*. 2018;42(2):110–117. doi:10.1016/j.clinre.2017.09.006
103. Borse S, Singh D, Upadhyay D, Sharma V, Nivsarkar M. Probiotic use in the management of hypertension: A new era of therapeutic management. *Indian J Health Sci Biomed Res*. 2018;11(3):207. doi:10.4103/kleuhsj.kleuhsj_3_18
104. Noce A, Marrone G, Di Daniele F, et al. Impact of gut microbiota composition on onset and progression of chronic non-communicable diseases. *Nutrients*. 2019;11(5):1073. doi:10.3390/nu11051073
105. Jung JH, Cho IK, Lee CH, Song GG, Lim JH. Clinical outcomes of standard triple therapy plus probiotics or concomitant therapy for *Helicobacter pylori* infection. *Gut Liver*. 2018;12(2):165–172. doi:10.5009/gnl17177

106. Gulzar N, Muqaddas Saleem I, Rafiq S, Nadeem M. Therapeutic potential of probiotics and prebiotics. In: Mahmoudi R, ed. *Oral Health by Using Probiotic Products*. London, UK: IntechOpen; 2019. doi:10.5772/intechopen.86762
107. Chua KJ, Kwok WC, Aggarwal N, Sun T, Chang MW. Designer probiotics for the prevention and treatment of human diseases. *Curr Opin Chem Biol*. 2017;40:8–16. doi:10.1016/j.cbpa.2017.04.011
108. Song HY, Zhou L, Liu DY, Yao XJ, Li Y. What roles do probiotics play in the eradication of *Helicobacter pylori*? Current knowledge and ongoing research. *Gastroenterol Res Pract*. 2018;2018:9379480. doi:10.1155/2018/9379480
109. Lerner A, Shoenfeld Y, Matthias T. Probiotics: If it does not help it does not do any harm. Really? *Microorganisms*. 2019;7(4):104. doi:10.3390/microorganisms7040104
110. Liu Y, Alookaran JJ, Rhoads JM. Probiotics in autoimmune and inflammatory disorders. *Nutrients*. 2018;10(10):1537. doi:10.3390/nu10101537
111. Zamani B, Golkar HR, Farshbaf S, et al. Clinical and metabolic response to probiotic supplementation in patients with rheumatoid arthritis: A randomized, double-blind, placebo-controlled trial. *Int J Rheum Dis*. 2016;19(9):869–879. doi:10.1111/1756-185X.12888
112. Rabiee MR, Babajafari S. Probiotics and diabetes: A review. *Int J Nutr Sci*. 2018;3(2):73–81. https://ijns.sums.ac.ir/article_43446_022a3ce2e69605647a3978be42055b55.pdf.
113. Mishra SP, Wang S, Nagpal R, et al. Probiotics and prebiotics for the amelioration of type 1 diabetes: Present and future perspectives. *Microorganisms*. 2019;7(3):67. doi:10.3390/microorganisms7030067
114. Kobylak N, Falalyeyeva T, Mykhalchyshyn G, Kyrienko D, Komissarenko I. Effect of alive probiotic on insulin resistance in type 2 diabetes patients: Randomized clinical trial. *Diabetes Metab Syndr*. 2018;12(5):617–624. doi:10.1016/j.dsx.2018.04.015
115. Sun Z, Sun X, Li J, et al. Using probiotics for type 2 diabetes mellitus intervention: Advances, questions, and potential. *Crit Rev Food Sci Nutr*. 2020;60(4):670–683. doi:10.1080/10408398.2018.1547268
116. Belizário JE, Faintuch J, Garay-Malpartida M. Gut microbiome dysbiosis and immunometabolism: New frontiers for treatment of metabolic diseases. *Mediators Inflamm*. 2018;2018:2037838. doi:10.1155/2018/2037838
117. Kang Y, Cai Y. The development of probiotics therapy to obesity: A therapy that has gained considerable momentum. *Hormones (Athens)*. 2018;17(2):141–151. doi:10.1007/s42000-018-0003-y
118. Xie Y, Zhou G, Xu Y, et al. Effects of diet based on IgG elimination combined with probiotics on migraine plus irritable bowel syndrome. *Pain Res Manag*. 2019;2019:7890461. doi:10.1155/2019/7890461
119. Rosenfeld CS. Microbiome disturbances and autism spectrum disorders. *Drug Metab Dispos*. 2015;43(10):1557–1571. doi:10.1124/dmd.115.063826
120. Shaaban SY, El Gendy YG, Mehanna NS, et al. The role of probiotics in children with autism spectrum disorder: A prospective, open-label study. *Nutr Neurosci*. 2018;21(9):676–681. doi:10.1080/1028415X.2017.1347746
121. El Khatib R, Karam-Sarkis D, Waligora-Dupriet AJ, Butel MJ. Could gut modulation through probiotic supplementation be beneficial in autism spectrum disorder? In: Franco-Robles E, Ramírez-Emiliano J, eds. *Prebiotics and Probiotics – Potential Benefits in Nutrition and Health*. London, UK: IntechOpen; 2020. doi:10.5772/intechopen.89375
122. Samtiya M, Puniya AK, Puniya M, Shah NP, Dhewa T, Vemuri R. Probiotic regulation to modulate aging gut and brain health: A concise review. *Bacteria*. 2022;1(4):250–265. doi:10.3390/bacteria1040019
123. Kiouisi DE, Kouroutzidou AZ, Neanidis K, Matthaios D, Pappa A, Galanis A. Evaluating the role of probiotics in the prevention and management of age-related diseases. *Int J Mol Sci*. 2022;23(7):3628. doi:10.3390/ijms23073628
124. Prasastha Ram V, Yasur J, Abishad P, et al. Antimicrobial efficacy of green synthesized nanosilver with entrapped cinnamaldehyde against multi-drug-resistant enteroaggregative *Escherichia coli* in *Galleria mellonella*. *Pharmaceutics*. 2022;14(9):1924. doi:10.3390/pharmaceutics14091924
125. Ruiz L, Flórez AB, Sánchez B, et al. *Bifidobacterium longum* subsp. infantis CECT7210 (B. infantis IM-1®) displays in vitro activity against some intestinal pathogens. *Nutrients*. 2020;12(11):3259. doi:10.3390/nu12113259
126. Cizekiene D, Jagelaviciute J. Investigation of antibacterial activity and probiotic properties of strains belonging to *Lactobacillus* and *Bifidobacterium* genera for their potential application in functional food and feed products. *Probiotics Antimicrob Proteins*. 2021;13(5):1387–1403. doi:10.1007/s12602-021-09777-5
127. Wei Y, Yang F, Wu Q, et al. Protective effects of bifidobacterial strains against toxigenic *Clostridium difficile*. *Front Microbiol*. 2018;9:888. doi:10.3389/fmicb.2018.00888
128. Ghadimi D, Nielsen A, Hassan MFY, et al. Modulation of proinflammatory bacteria- and lipid-coupled intracellular signaling pathways in a transwell triple co-culture model by commensal *Bifidobacterium animalis* R101-8. *Antiinflamm Antiallergy Agents Med Chem*. 2021;20(2):161–181. doi:10.2174/1871523019999201029115618
129. Duque ALRF, Demarqui FM, Santoni MM, et al. Effect of probiotic, prebiotic, and synbiotic on the gut microbiota of autistic children using an in vitro gut microbiome model. *Food Res Int*. 2021;149:110657. doi:10.1016/j.foodres.2021.110657
130. Marzorati M, Van den Abbeele P, Bubeck S, Bayne T, Krishnan K, Young A. Treatment with a spore-based probiotic containing five strains of *Bacillus* induced changes in the metabolic activity and community composition of the gut microbiota in a SHIME® model of the human gastrointestinal system. *Food Res Int*. 2021;149:110676. doi:10.1016/j.foodres.2021.110676
131. Anjum M, Laitila A, Ouwehand AC, Forssten SD. Current perspectives on gastrointestinal models to assess probiotic-pathogen interactions. *Front Microbiol*. 2022;13:831455. doi:10.3389/fmicb.2022.831455
132. Chen YH, Tsai WH, Wu HY, et al. Probiotic *Lactobacillus* spp. act against *Helicobacter pylori*-induced inflammation. *J Clin Med*. 2019;8(1):90. doi:10.3390/jcm8010090
133. Scalfaro C, Iacobino A, Nardis C, Franciosa G. *Galleria mellonella* as an in vivo model for assessing the protective activity of probiotics against gastrointestinal bacterial pathogens. *FEMS Microbiol Lett*. 2017;364(7):[no pages given]. doi:10.1093/femsle/fnx064
134. Zhao Z, Xu S, Zhang W, Wu D, Yang G. Probiotic *Escherichia coli* NISSLE 1917 for inflammatory bowel disease applications. *Food Funct*. 2022;13(11):5914–5924. doi:10.1039/d2fo00226d
135. Dronkers TMG, Ouwehand AC, Rijkers GT. Global analysis of clinical trials with probiotics. *Heliyon*. 2020;6(7):e04467. doi:10.1016/j.heliyon.2020.e04467
136. Bernardi S, Del Bo' C, Marino M, et al. Polyphenols and intestinal permeability: Rationale and future perspectives. *J Agric Food Chem*. 2020;68(7):1816–1829. doi:10.1021/acs.jafc.9b02283
137. Mitra S, Emran TB, Chandran D, et al. Cruciferous vegetables as a treasure of functional foods bioactive compounds: Targeting p53 family in gastrointestinal tract and associated cancers. *Front Nutr*. 2022;9:951935. doi:10.3389/fnut.2022.951935
138. Yusuf F, Fahriani M, Mamada SS, et al. Global prevalence of prolonged gastrointestinal symptoms in COVID-19 survivors and potential pathogenesis: A systematic review and meta-analysis. *F1000Res*. 2021;10:301. doi:10.12688/f1000research.52216.1